ISSN 0021-9673

VOL. 633 NOS. 1 + 2 FEBRUARY 24, 1993

COMPLETE IN ONE ISSUE

JOURNAL OF CHROMATOGRAPHY

INCLUDING ELECTROPHORESIS AND OTHER SEPARATION METHODS

ELSEVIER

JOURNAL OF CHROMATOGRAPHY

INCLUDING ELECTROPHORESIS AND OTHER SEPARATION METHODS

Scope. The *Journal of Chromatography* publishes papers on all aspects of **chromatography, electrophoresis** and related methods. Contributions consist mainly of research papers dealing with chromatographic theory, instrumental developments and their applications. The section *Biomedical Applications*, which is under separate editorship, deals with the following aspects: developments in and applications of chromatographic and electrophoretic techniques related to clinical diagnosis or alterations during medical treatment; screening and profiling of body fluids or tissues related to the analysis of active substances and to metabolic disorders; drug level monitoring and pharmacokinetic studies; clinical toxicology; forensic medicine; veterinary medicine; occupational medicine; results from basic medical research with direct consequences in clinical practice. In *Symposium volumes*, which are under separate editorship, proceedings of symposia on chromatography, electrophoresis and related methods are published.

Submission of Papers. The preferred medium of submission is on disk with accompanying manuscript (see *Electronic manuscripts* in the Instructions to Authors, which can be obtained from the publisher, Elsevier Science Publishers B.V., P.O. Box 330, 1000 AH Amsterdam, Netherlands). Manuscripts (in English; *four* copies are required) should be submitted to: Editorial Office of *Journal of Chromatography*, P.O. Box 681, 1000 AR Amsterdam, Netherlands, Telefax (+31-20) 5862 304, or to: The Editor of *Journal of Chromatography, Biomedical Applications*, P.O. Box 681, 1000 AR Amsterdam, Netherlands. Review articles are invited or proposed in writing to the Editors who welcome suggestions for subjects. An outline of the proposed review should first be forwarded to the Editors for preliminary discussion prior to preparation. Submission of an article is understood to imply that the article is original and unpublished and is not being considered for publication elsewhere. For copyright regulations, see below.

Publication. The *Journal of Chromatography* (incl. *Biomedical Applications*) has 40 volumes in 1993. The subscription prices for 1993 are:

J. Chromatogr. (incl. *Cum. Indexes, Vols. 601–650*) + *Biomed. Appl.* (Vols. 612–651):
Dfl. 8520.00 plus Dfl. 1320.00 (p.p.h.) (total *ca.* US$ 5622.75)

J. Chromatogr. (incl. *Cum. Indexes, Vols. 601–650*) only (Vols. 623–651):
Dfl. 7047.00 plus Dfl. 957.00 (p.p.h.) (total *ca.* US$ 4573.75)

Biomed. Appl. only (Vols. 612–622):
Dfl. 2783.00 plus Dfl. 363.00 (p.p.h.) (total *ca.* US$ 1797.75).

Subscription Orders. The Dutch guilder price is definitive. The US$ price is subject to exchange-rate fluctuations and is given as a guide. Subscriptions are accepted on a prepaid basis only, unless different terms have been previously agreed upon. Subscriptions orders can be entered only by calender year (Jan.–Dec.) and should be sent to Elsevier Science Publishers, Journal Department, P.O. Box 211, 1000 AE Amsterdam, Netherlands, Tel. (+31-20) 5803 642, Telefax (+31-20) 5803 598, or to your usual subscription agent. Postage and handling charges include surface delivery except to the following countries where air delivery via SAL (Surface Air Lift) mail is ensured: Argentina, Australia, Brazil, Canada, China, Hong Kong, India, Israel, Japan*, Malaysia, Mexico, New Zealand, Pakistan, Singapore, South Africa, South Korea, Taiwan, Thailand, USA. *For Japan air delivery (SAL) requires 25% additional charge of the normal postage and handling charge. For all other countries airmail rates are available upon request. Claims for missing issues must be made within six months of our publication (mailing) date, otherwise such claims cannot be honoured free of charge. Back volumes of the *Journal of Chromatography* (Vols. 1–611) are available at Dfl. 230.00 (plus postage). Customers in the USA and Canada wishing information on this and other Elsevier journals, please contact Journal Information Center, Elsevier Science Publishing Co. Inc., 655 Avenue of the Americas, New York, NY 10010, USA, Tel. (+1-212) 633 3750, Telefax (+1-212) 633 3764.

Abstracts/Contents Lists published in Analytical Abstracts, Biochemical Abstracts, Biological Abstracts, Chemical Abstracts, Chemical Titles, Chromatography Abstracts, Clinical Chemistry Lookout, Current Awareness in Biological Sciences (CABS), Current Contents/Life Sciences, Current Contents/Physical, Chemical & Earth Sciences, Deep-Sea Research/Part B: Oceanographic Literature Review, Excerpta Medica, Index Medicus, Mass Spectrometry Bulletin, PASCAL-CNRS, Pharmaceutical Abstracts, Referativnyi Zhurnal, Research Alert, Science Citation Index and Trends in Biotechnology.

US Mailing Notice. *Journal of Chromatography* (ISSN 0021-9673) is published weekly (total 52 issues) by Elsevier Science Publishers (Sara Burgerhartstraat 25, P.O. Box 211, 1000 AE Amsterdam, Netherlands). Annual subscription price in the USA US$ 4573.75 (subject to change), including air speed delivery. Application to mail at second class postage rate is pending at Jamaica, NY 11431. **USA POSTMASTERS:** Send address changes to *Journal of Chromatography*, Publications Expediting, Inc., 200 Meacham Avenue, Elmont, NY 11003. Airfreight and mailing in the USA by Publication Expediting.

See inside back cover for Publication Schedule, Information for Authors and information on Advertisements.

0021-9673/93/$06.00

This issue is printed on acid-free paper.

Printed in the Netherlands

VOL. 633, NOS. 1+2 JOURNAL OF CHROMATOGRAPHY FEBRUARY 24, 1993

CONTENTS

(Abstracts/Contents Lists published in Analytical Abstracts, Biochemical Abstracts, Biological Abstracts, Chemical Abstracts, Chemical Titles, Chromatography Abstracts, Current Awareness in Biological Sciences (CABS), Current Contents/Life Sciences, Current Contents/Physical, Chemical & Earth Sciences, Deep-Sea Research/Part B: Oceanographic Literature Review, Excerpta Medica, Index Medicus, Mass Spectrometry Bulletin, PASCAL-CNRS, Referativnyi Zhurnal, Research Alert and Science Citation Index)

(Coninued overleaf)

SHORT COMMUNICATIONS

Column Liquid Chromatography

Gas Chromatography

Electrophoresis

BOOK REVIEW

JOURNAL OF CHROMATOGRAPHY

VOL. 633 (1993)

JOURNAL of CHROMATOGRAPHY

INCLUDING ELECTROPHORESIS AND OTHER SEPARATION METHODS

ELSEVIER

AMSTERDAM — LONDON — NEW YORK — TOKYO

0021-9673/93/$06.00

Printed in the Netherlands

Journal of Chromatography, 633 (1993) 1–8
Elsevier Science Publishers B.V., Amsterdam

CHROM. 24 733

Chromatography Classic

History of a theory

Torvard C. Laurent

Department of Medical and Physiological Chemistry, University of Uppsala, Biomedical Center, Box 575, S-751 23 Uppsala (Swede

(Received October 26th, 1992)

ABSTRACT

The article "A theory of gel filtration and its experimental verification" was published in *Journal of Chromatography* in 1964. One its authors gives an account of the origin of the work.

INTRODUCTION

The Editor asked me to describe the background of the paper "A theory of gel filtration and its experimental verification" which was published almost three decades ago by Johan Killander and myself in the *Journal of Chromatography* [1]. The title and the summary of the paper are shown in Fig. 1. The Editor also asked if I could give an explanation for the apparent impact of the paper as measured by its citation frequency. On this matter I can only speculate.

The research that led to that paper was not at all primarily aimed at the clarification of a chromatographic process. As so many times before, the results arose from the interaction between scientists from different fields at the right time and the right place, Uppsala.

When our paper was written, I had been working in the Department of Medical Chemistry at the University of Uppsala for 2 years. I had earlier received basic training in medicine in Stockholm, but I never went into practice after medical school. Instead, I was recruited to research which led to a doctorate in chemistry at the Karolinska Institute and postdoctoral work at the Retina Foundation in Boston, MA, USA. Research positions were scar at Swedish Universities but fortunately I received a appointment as investigator in ophthalmic biochen istry at the Medical Research Council and moved Uppsala in 1961 at the age of 30.

HYALURONAN —A HIGH-MOLECULAR MASS POL SACCHARIDE IN CONNECTIVE TISSUE

Dr. Endre A. Balazs, my first research teache raised my interest in hyaluronan, a carbohydra component of connective tissue, and this compour has since been a life-long subject of my curiosity [2 The space between the cells in the connective tissue filled by a matrix, which is composed of differe types of macromolecules, among them a family polysaccharides. These have linear structures an contain, with one exception, alternating residues uronic acid and hexosamine. One of them is hyalu ronan (previously called hyaluronic acid). It has high molecular mass (10^6–10^7) and is found as major component of soft tissues such as skii umbilical cord, the vitreous body of the eye and join fluid.

During the 1950s, work in different laboratorie especially by Dr. Alexander G. Ogston (Fig. 2) i

0021-9673/93/$06.00

A THEORY OF GEL FILTRATION AND ITS EXPERIMENTAL VERIFICATION

TORVARD C. LAURENT AND JOHAN KILLANDER

Department of Medical Chemistry and Department of Clinical Chemistry at the University Hospital, University of Uppsala, Uppsala (Sweden)

(Received December 17th, 1963)

SUMMARY

The separation by gel filtration of molecules varying in size is explained as a steric exclusion of solutes from the gel phase.

The volume available for a solute in the gel phase can be determined from the elution volume, the void volume and the total volume of the gel column. It has been calculated for a number of proteins and dextran fractions and for various dextran gels from data given in the literature as well as from some new data. The values were used to test the hypothesis that the exclusion takes place from a three-dimensional random network of straight polymer fibers distributed in the gel. The experimental data were found to verify the hypothesis.

The experimentally determined available volumes in the gel phase for three proteins are approximately the same as the available volumes in dextran solutions, having the same polymer concentrations as the gels. Therefore there seems to be no essential difference between the exclusion phenomenon in a polymer gel and in a polymer solution.

J. Chromatog., 14 (1964) 317–330

Fig. 1. Title and summary of the paper in *Journal of Chromatography*, 14 (1964) 317–330.

Oxford, Dr. Endre Balazs in Boston and myself in Stockholm, clarified that hyaluronan behaves as a large extended and hydrated coil structure in solution [3]. It can be calculated but also shown experimentally that entanglement of the individual molecules must occur already at concentrations of the order of 1 mg/ml. At higher concentrations the solution can be regarded as a continuous mesh of polymer chains. It became a challenge in the late 1950s and early 1960s to describe the physiological functions of such networks in physical chemical terms, *e.g.*, in lubrication, water homeostasis, regulation of transport and distribution of plama proteins (for a review see, *e.g.*, ref. 4).

Much of this work was carried out in Ogston's and our laboratories. In both places we approached the problems with a very similar picture of the hyaluronan network in mind. Ogston was intrigued by the question of how much space could be occupied in the network by other molecules, such as proteins, and deduced mathematically the volume available for a spherical particle with a given diameter in a space occupied by a random network of rods of given length and diameter [5]. Ogston and Phelps [6] then measured the exclusion of proteins from hyaluronan compartments by means of equilibrium dialysis and tried to apply the theoretical relationship to the experimental data, although without immediate success. It was later shown that theory and experiment in fact fitted excellently [7]. I was myself studying the physical resistance to transport of globular particles through hyaluronan networks by measuring diffusion and sedimentation and found evidence that the networks acted as filters

Fig. 2. Photographs of some of the workers mentioned in the text, taken approximately at the time when gel filtration was developed. (Left to right) Top row, Arne Tiselius, who suggested the name "gel filtration", Björn Ingelman, who synthesized the first dextran gels, and Alexander G. Ogston, who derived mathematically the excluded fraction for spherical particles in a system of randomly distributed fibres; middle row, Jerker Porath and Per Flodin, wo described the technique of gel filtration; bottom row, Johan Killander, after having received his doctorate, and the author, who collaborated on the theory. (The photographs were kindly supplied by Drs. B. Ingelman, J. Killander and A. G. Ogsten, Mrs. I. Johansson and Mr. B. Ejdesjö.)

or sieves [8]. Thus, within the connective tissue field, steric interaction between proteins and linear polysaccharide chains was well established.

DEXTRAN —A POLYSACCHARIDE USED AS A PLASMA SUBSTITUTE [9]

At the beginning of this century, Uppsala was a centre of protein research. The Svedberg, Professor of Physical Chemistry, had built the ultracentrifuge and shown that proteins are molecules of defined molecular masses. His pupil, Arne Tiselius, developed electrophoresis into an important tool for separating and characterizing proteins. In 1938 a Chair of Biochemistry was created for Tiselius, and he surrounded himself with a number of enthusiastic collaborators from Sweden and elsewhere.

Two young scientists, Björn Ingelman and Anders Grönwall, worked in the same room of the crowded department. Ingelman, studying for his Ph. D., was asked in 1940 to enter a project, supported by the Swedish Sugar Industry, on the macromolecular composition of sugar beet extracts in the hope that one would find proteins, pectin or other products, which could be of use in food production. In one extract he was able to identify by ultracentrifugation a new component which turned out to be a bacterial polysaccharide produced by *Leuconostoc mesenteroides* infecting some of the batches. It was soon identified as a polyglucose, already known as dextran, of very high molecular mass. Anders Grönwall had a medical degree from the University of Lund. He had studied the electrophoretic properties of proteins in Lund and protein solubility at the Carlsberg laboratories in Copenhagen when he became employed by Tiselius in 1942 to work on the chemical composition of tuberculin and its antibodies. Grönwall was thus well oriented in immune techniques.

In order to develop a simple analytical method for dextran, which could be used to identify infected beet extracts, Ingelman tried to raise antibodies against dextran in two rabbits but was unsuccessful. This was a key experiment. Owing to the scientific interaction between Ingelman and Grönwall it was soon realized that the non-immunogenic dextran probably could be a useful plasma substitute, for which there was a great need during World War II. Already in 1943 the two scientists entered into an agreement with the drug firm Pharmacia in Stockholm to develop the idea. Within a few years dextran became a pharmaceutical product. Pharmacia grew and moved to Uppsala in 1950, no doubt owing to the close ties with the Department of Biochemistry.

An immediate consequence of the success of dextran as a plasma substitute and the presence of Pharmacia in Uppsala was a boost in research in both the physical chemistry and the physiology of polymers. Björn Ingelman became Research Direc-

tor at Pharmacia. Dr. Kirsti Granath from the Physical Chemistry Department was recruited to Pharmacia as head of the Polymer Physical Chemical Unit and her well characterized dextran fractions were used in laboratories all over the world. Anders Grönwall was appointed Professor of Clinical Chemistry (and later Hospital Director) at the University Hospital in Uppsala, where research on haemodynamics and infusion therapy flourished.

GEL FILTRATION—A NEW TECHNIQUE TO SEPARATE MOLECULES ACCORDING TO SIZE

Arne Tiselius received the 1948 Nobel Prize in Chemistry for his work on electrophoresis and chromatography, and this increased the fame of biochemistry in Uppsala. At the beginning of the 1950s Per Flodin and Jerker Porath joined Tiselius's department and worked on the zone electrophoretic separation of proteins on a preparative scale on vertical columns of starch gels [10]. During these experiments they made unpublished observations that chromatography on starch columns could separate molecules according to size [11], but similar observations were also made by others [12,13]. There were, however, practical problems in using starch. A breakthrough for utilizing this observation in a new technique came when Flodin was employed at Pharmacia in 1954 and worked with Björn Ingelman.

Already in the 1940s Ingelman had cross-linked dextran with epichlorohydrin and obtained gels[a]. Flodin supplied Porath with a granulated dextran gel from Phamacia to be used as column material in zone electrophoresis. Porath soon observed that this dextran gel had properties that were superior to those of starch gels in separating molecules according to size. When a mixture of compounds of different molecular sizes was chromatographed on a gel column, the substances emerged according to size with the largest molecules first. A new product and a new technique had been born. The observations were published by Porath and Flodin in *Nature* in 1959 under the title "Gel filtration: a method for desalting and group separation" [14]. The name "gel filtration" was suggested by Arne Tiselius (see ref. 15).

Pharmacia soon manufactured dextran gels of various porosities that could be used for the separation of molecules in different size intervals. They were named Sephadex G-10, G-15, G-50, G-75, G-100, G-150 and G-200, where the number stands for the water regain, *e.g.*, Sephadex G-10 takes up 1 g of water and Sephadex G-200 20 g of water per gram of dextran. Soon other types of gels, such as agar (agarose) [16,17] and polyacrylamide [18] gels, were also employed. The impact that gel filtration had on the development of biochemistry is well known.

Jerker Porath succeeded Arne Tiselius as Professor of Biochemistry in Uppsala in 1968. He is now retired but continues to be a major contributor to biochemical separation techniques, *e.g.*, immobilized metal ion affinity chromatography. Per Flodin worked in industry for a while before he was appointed to a Chair in Polymer Technology in Gothenburg.

IMPACT OF PROTEIN CHEMISTRY ON CLINICAL SCIENCE

It was as late as 1926 that Svedberg and Fåhreus by means of ultracentrifugation described for the first time a protein, haemoglobin, as a homogeneous molecular entity with a defined molecular mass. In the following decades research efforts in many laboratories were aimed at finding techniques to isolate and purify individual proteins and Svedberg's and Tiselius's laboratories made major contributions. The greatest impact of this work was seen in medicine where pure proteins were required for diagnosis and treatment. Purification of plasma proteins, including immunoglobulins, enzymes, peptide hormones and toxins, was carried out in laboratories all over Uppsala.

Johan Killander was engaged in graduate work at Anders Grönwall's Department of Clinical Chemistry at the beginning of the 1960s when the new technique of gel filtration emerged. He was especially concentrating his work on the purification of immunoglobulins. Already in 1962 there was an important paper by Flodin and Killander in which

[a] The former Executive Director of Pharmacia, Elis Göth, told me that Björn Ingelman once came into his office to show him a jelly on a dish. Göth asked what it was and Ingelman replied that it was cross-linked dextran. Göth asked what Ingelman was going to use it for and Ingelman answered, "No idea"!

they demonstrated that plasma proteins can be separated into three major peaks by chromatography on Sephadex G-200 [19]. Subsequently, Killander refined his purifications by combining gel filtration with other techniques such as zone electrophoresis and ion-exchange chromatography and he reported a considerable purification of several plasma proteins.

A THEORY OF GEL FILTRATION

Thus, at the beginning of the 1960s in Uppsala, a powerful new product and technique had emerged in the Biochemistry Department, Pharmacia had great interests in polymer chemistry and manufactured the Sephadex products, scientists in many fields were interested in polymer–protein interactions and their biological implications and the scientific community was rather small and most people involved knew each other personally. It was natural that somebody in this community would search for a theory that described the gel filtration process quantitatively.

One obstacle was psychological. The name "gel filtration" implies that the molecules are passing a filter, *i.e.*, that large molecules should be retarded and small ones should pass through the pores of the filter. Similarly, the term molecular sieving [18], which also was used for this chromatographic process, implies that the molecules pass a sieve. At the time many persons really believed that it was a filtration effect, even if it then was a paradox that large molecules emerged first. Steere and Ackers [20,21] explained the phenomenon in terms of restricted diffusion of large molecules in gel pores.

That the phenomenon was due to an exclusion of molecules from the gel grains, however, was apparent to many investigators [13,22–24]. This was also reflected in alternative names given to the technique such as exclusion chromatography [23] and gel permeation chromatography [24]. Personally, I have in later papers used the term gel chromatography to avoid any misinterpretations [25]. However, in 1964 there was a lack of a simple steric model to quantitatively account for the results in terms of exclusion, although various attempts had been or were being made [22,26].

Being well acquainted with Ogston's [5] calculations of steric exclusion of spheres in a system of randomly distributed rods, it was obvious that we should try to use this model to explain the exclusion from gel grains in the gel chromatographic process. Fig. 3 depicts the principle of the model. As Johan Killander had accumulated a large amount of data on the chromatographic behaviour of proteins on dextran gels, we engaged in a collaboration. He had observed that some proteins, *e.g.*, serum albumin and hemoglobin, with similar molecular mass, separated well by gel filtration and he was looking for a theoretical explanation.

Our modified version of Ogston's eqn. 5 was

$$K_{av} = \exp[-\pi L(r_s + r_r)^2]$$

where K_{av}[a] is the fraction of the total gel volume which is available to a spherical protein, L is the total concentration of fibre in the gel expressed in cm fibre per cm^3 gel, r_s is the radius of the protein (the Stokes radius) and r_r is the radius of the fibres. K_{av} can be calculated from the chromatogram by the simple relationship

$$K_{av} = \frac{V_e - V_0}{V_t - V_0}$$

where V_e, V_0 and V_t are the elution volume of the

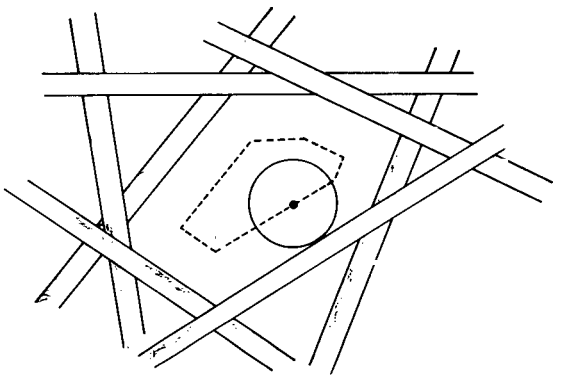

Fig. 3. Demonstration of steric exclusion of a spherical object from a random network of rigid fibres. The centre of the sphere can only move within a volume (available volume; dashed area) which is at a distance from the fibres corresponding to the radius of the sphere. The excluded volume for the centre of the sphere is thus much larger than the volume of the fibres themselves and increases with increasing size of the sphere.

[a] In the designation K_{av} for the partition coefficient, "av" stands for *available*. I regret that we used this designation since it has been a common misunderstanding that "av" stands for *average*.

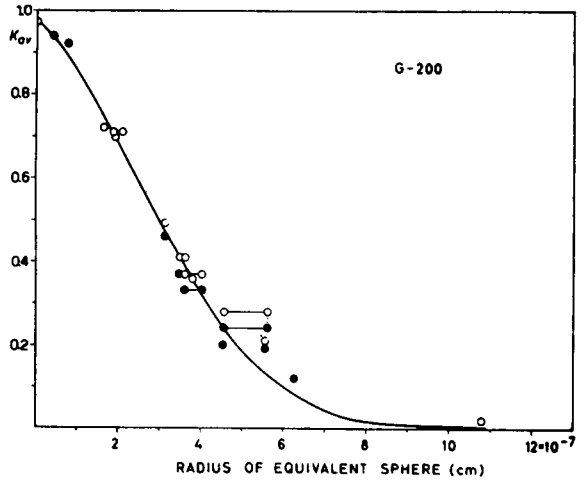

Fig. 4. The available fraction (K_{av}) for a number of proteins chromatographed on Sephadex G-200 plotted as a function of the Stokes radius. The line is the function predicted by Ogston's equation assuming a value of L of $1.6 \cdot 10^{12}$. (Taken from *J. Chromatogr.*, 14 (1964) 317.)

compound and the void volume and total volume of the column, respectively.

Using our own and literature data, we calculated K_{av} for a number of proteins and carbohydrate fractions chromatographed on Sephadex G-25, G-50, G-75, G-100 and G-200. We chose compounds for which we also could obtain the diffusion coefficients. The diffusion data were used to calculate r_s, the Stokes radius, *i.e.*, the radius of a sphere that has the same diffusion coefficient as the compound. The parameter r_r, the radius of the fibre, had to be estimated but the value was not very critical for the calculations. The dextran chain is coiled and branched and it is therefore shorter and thicker than a stretched linear polysaccharide. We assumed r_r to be 0.7 nm. This value and the calculated L values for the various gels (see below) gave a total volume of dextran per ml that corresponded to the known concentrations of dextran in the various Sephadexes.

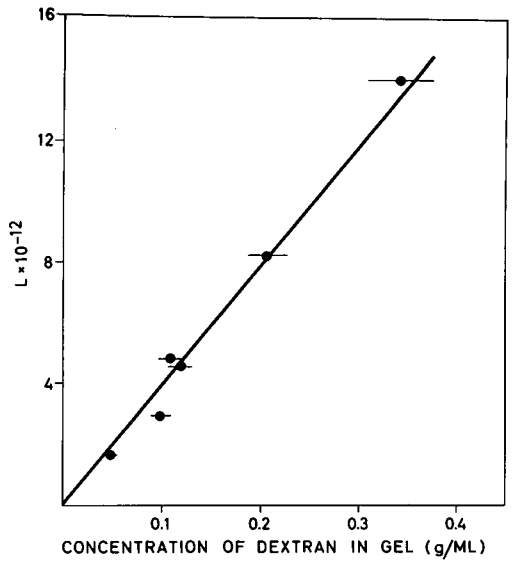

Fig. 5. Experimentally obtained values of L for various Sephadex gels plotted *versus* the dextran concentrations of the gels. As predicted by theory there is a linear relationship. (Taken from *J. Chromatogr.*, 14 (1964) 317.)

When K_{av} was plotted against r_s (an example is shown in Fig. 4), the data followed an S-shaped curve similar to what Ogston's equation predicted. A theoretical curve could be adjusted to the experimental points by choosing the right L value. When the L values obtained for the different gels were plotted against their known concentrations, the relationship was linear, as expected (Fig. 5). For example, in a gel of concentration 0.1 g/ml, L was found to be $4 \cdot 10^{12}$ cm/cm^3. Using the r_r value of $7 \cdot 10^{-8}$ cm one can calculate that the volume occupied by the dextran would be 0.063 ml/ml. As the partial specific volume of dextran is 0.61 g/ml this fits with the concentration 0.1 g/ml. The L value found was 4–5 times shorter than the length of a single stiff linear polysaccharide chain, and this was ascribed to branching and coiling of the dextran molecule.

The success in describing the gel chromatographic data as exclusion of spheres from a simple three-dimensional meshwork of stiff fibres gave a rationale for using chromatography on gels to determine the hydrodynamic size of various compounds, *e.g.*, proteins. The method has subsequently been used for this purpose by numerous workers. It can also be used in the opposite way, however, *i.e.*, to characterize the structure of the gel. When I cross-linked hyaluronan and chromatographed proteins on the gels they had the exclusion properties expected for an unbranched stiff linear polysaccharide network [7]. Results from chromatography on agarose gels corresponded to gel structures that were much more compact [27]. Polyacrylamide gels [28] and elastin networks [29] were also characterized in this way.

To follow up the gel chromatographic studies, my

younger brother and I, with the help of our father, our elder brother and our brother-in-law, built an electrical analogue computer to describe the process [30]. With this machine we could predict the shape of the chromatogram as a function of column length, flow-rate, sample volume and partition coefficient of the compound. This work gave me as much enjoyment as the paper on the theory, but I doubt that it has ever been cited by anyone.

An important observation, which strengthened our conclusion that the gel chromatographic process is based on exclusion from a polysaccharide network and not from structures formed by the cross-linking, came from independent studies with dextran and hyaluronan in solution [7,31,32]. When the exclusion properties of the polysaccharides in solution were determined by independent methods, such as equilibrium dialysis, osmometry and solubility studies, results identical with the chromatographic data were obtained.

Since our paper appeared three decades ago, gel chromatographic techniques have been highly refined, the analytical results have become much more accurate and numerous other papers on the theoretical basis of gel chromatography have been published. By today's standards our approach may look simple, but the basic idea of steric exclusion from the gel matrix at least at slow flow-rates seems still to be valid.

Neither Johan Killander nor I continued to work on chromatographic techniques. Johan Killander defended his thesis "Separation of immunoglobulins and some other plasma proteins by gel filtration" on April 21st, 1964 [33]. Our joint paper was included as part of the thesis. He later became Head Doctor in Clinical Chemistry at one of the major hospitals in Stockholm. I myself continued to work on physiological aspects of connective tissue and later on the metabolism of hyaluronan and I am still working in the same department in Uppsala.

HYPOTHESES ON THE REASON WHY THE THEORY MADE AN IMPACT

Why did our paper become a citation classic? I have not looked up the citations so I really do not know why it was cited. My suggestions are therefore purely hypothetical.

First, the practical concept of separating molecules according to size, which was presented in the paper by Porath and Flodin [14], was of immediate and tremendous importance to biological sciences. There was a need for understanding the process. The term "gel filtration" had created confusion among the users. The presentation of a simple steric model, which could visually and quantitatively explain the phenomenon in terms of exclusion, made the process understandable and could with advantage be used in teaching.

Second, there was a need for simple techniques to determine the molecular size of proteins and the theory gave a rationale for using gel chromatography. It complemented gel electrophoretic techniques, which were developed at about the same time.

Third, the paper promoted the "concept of exclusion", which is important not only for chromatographic techniques but also in understanding physiological and biochemical reactions.

Very often so-called "citation classics" describe the details of a useful technique (the Lowry paper on protein determinations in 1951 had been cited 205 000 times up to 1990). When *Current Contents* identified our paper as among the most cited of those published in the 1960s, its Editor drew the conclusion that the publication was a technique paper. It should be clear from the above description that this is not so, but I must admit that I am slightly worried that the scientific community may have made the same misinterpretation as the Editor of *Current Contents*. The technique was developed by Porath, Flodin and Ingelman. Further, A. G. Ogston must be credited for the concept of exclusion from a three-dimensional network of rods.

REFERENCES

1 T. C. Laurent and J. Killander, A theory of gel filtration and its experimental verification, *J. Chromatogr.*, 14 (1964) 317–330.
2 T. C. Laurent and J. R. E. Fraser, Hyaluronan, *FASEB J.*, 6 (1992) 2397–2404.
3 T. C. Laurent, Structure of hyaluronic acid, in E. A. Balazs (Editor), *Chemistry and Molecular Biology of the Intercellular Matrix*, Academic Press, London, 1970, pp. 703–732.
4 W. D. Comper and T. C. Laurent, Physiological function of connective tissue polysaccharides, *Physiol. Rev.*, 58 (1978) 255–315.
5 A. G. Ogston, The spaces in a uniform random suspension of fibres, *Trans. Faraday Soc.*, 54 (1958) 1754–1757.

6 A. G. Ogston and C. F. Phelps, The partition of solutes between buffer solutions and solutions containing hyaluronic acid, *Biochem. J.*, 78 (1961) 827–833.
7 T. C. Laurent, The interaction between polysaccharides and other macromolecules, 9, The exclusion of molecules from hyaluronic acid gels and solutions, *Biochem. J.*, 93 (1964) 106–112.
8 T. C. Laurent and A. Pietruszkiewicz, The effect of hyaluronic acid on the sedimentation rate of other substances, *Biochim. Biophys. Acta*, 49 (1961) 258–264.
9 A. Lundgren, Dextran som blodplasmasubstitut, in T. Frängsmyr (Editor), *Vetenskap och Läkemedel*, Almqvist & Wiksell International, Uppsala, 1987, pp. 113–164.
10 P. Flodin and J. Porath, Zone electrophoresis in starch columns, *Biochim. Biophys. Acta*, 13 (1954) 175–182.
11 J.-C. Janson, On the history of the development of Sephadex, *Chromatographia*, 23 (1987) 361–369.
12 B. Lindqvist and T. Storgårds, Molecular-sieving properties of starch, *Nature*, 175 (1955) 511–512.
13 G. H. Lathe and C. R. J. Ruthven, The separation of substances and estimation of their relative molecular sizes by the use of columns of starch in water, *Biochem. J.*, 62 (1956) 665–674.
14 J. Porath and P. Flodin, Gel filtration: a method for desalting and group separation, *Nature*, 183 (1959) 1657–1659.
15 P. Flodin, Methodological aspects of gel filtration with special reference to desalting operations, *J. Chromatogr.*, 5 (1961) 103–115.
16 A. Polson, Fractionation of protein mixtures on columns of granulated agar, *Biochim. Biophys. Acta*, 50 (1961) 565–567.
17 S. Hjertén, Chromatographic separation according to size of macromolecules and cell particles on columns of agarose suspensions, *Arch. Biochem. Biophys.*, 99 (1962) 466–475.
18 S. Hjertén and R. Mosbach, "Molecular-sieve" chromatography of proteins on columns of cross-linked polyacrylamide, *Anal. Biochem.*, 3 (1962) 109–118.
19 P. Flodin and J. Killander, Fractionation of human serum proteins by gel filtration, *Biochim. Biophys. Acta*, 63 (1962) 403–410.
20 R. L. Steere and G. K. Ackers, Restricted-diffusion chromatography through calibrated columns of granulated agar gel; a simple method for particle-size determination, *Nature*, 196 (1962) 475–476.
21 G. K. Ackers, Molecular exclusion and restricted diffusion processes in molecular-sieve chromatography, *Biochemistry*, 3 (1964) 723–730.
22 J. Porath, Some recently developed fractionation procedures and their application to peptide and protein hormones, *Pure Appl. Chem.*, 6 (1963) 233–244.
23 K. O. Pedersen, Exclusion chromatography, *Arch. Biochem. Biophys.*, Suppl. 1 (1962) 157–168.
24 J. C. Moore, Gel permeation chromatography. I. A new method for molecular weight distribution of high polymers, *J. Polym. Sci., Part A2*, (1964) 835–843.
25 T. C. Laurent, On the theoretical aspects of gel chromatography, in T. Gerritsen (Editor), *Modern Separation Methods of Macromolecules and Particles*, Wiley-Interscience, 1969, pp. 199–218.
26 P. G. Squire, A relationship between the molecular weights of macromolecules and their elution volumes based on a model for Sephadex gel filtration, *Arch. Biochem. Biophys.*, 107 (1964) 471–478.
27 T. C. Laurent, Determination of the structure of agarose gels by gel chromatography, *Biochim. Biophys. Acta*, 136 (1967) 199–205.
28 J. S. Fawcett and C. J. O. R. Morris, Molecular-sieve chromatography of proteins on granulated polylacrylamide gels, *Sep. Sci.*, 1 (1966) 9–26.
29 M. Partridge, Diffusion of solutes in elastin fibers, *Biochim. Biophys. Acta*, 140 (1967) 132–141.
30 T. C. Laurent and E. P. Laurent, An electrical analogy to the gel filtration process, *J. Chromatogr.*, 16 (1964) 89–98.
31 T. C. Laurent and A. G. Ogston, The interaction between polysaccharides and other macromolecules. 4. The osmotic pressure of mixtures of serum albumin and hyaluronic acid, *Biochem. J.*, 89 (1963) 249–253.
32 T. C. Laurent, The interaction between polysadcharides and other macromolecules. 5. The solubility of proteins in the presence of dextran, *Biochem. J.*, 89 (1963) 253–257.
33 J. Killander, Separation of immunoglobulins and some other plasma proteins by gel filtration, *Acta Univ. Ups., Abstr. Uppsala Diss. Med.*, 13 (1964) 1–16.

Journal of Chromatography, 633 (1993) 9–23
Elsevier Science Publishers B.V., Amsterdam

CHROM. 24 749

Review

Analysis of carotenoids by high-performance liquid chromatography and supercritical fluid chromatography

E. Lesellier* and A. Tchapla

Letiam, IUT Orsay, Plateau du Moulon, B.P. 127, 91403 Orsay (France)

C. Marty

Département SA, Ensia, 1 Avenue des Olympiades, 91305 Massy (France)

A. Lebert

Département GIA, Ensia 1, Avenue des Olympiades, 91305 Massy (France)

(First received January 16th, 1992; revised manuscript received October 28th, 1992)

ABSTRACT

The first part of this paper describes the chemical structures and the importance of carotenoids for health. Sample preparation for extracting the carotenoids from fruits and vegetable matrices is detailed in terms of pre-extraction treatment (enzyme inactivation, addition of antioxidants and acid neutralizers), extraction conditions with solvents or supercritical fluids and saponification. In the second part, HPLC and SFC separation methods are described. The efficiencies of different inorganic packings (silica, magnesium oxide, calcium hydroxide, alumina), bonded silica packings (cyano, octadecyl) and chiral phases (cellulose, cyclodextrins) are discussed. The choice of an appropriate method depending on the type of pigment to be separated (xanthophylls, catotenes, *cis–trans* isomers) is discussed. The effects of the mobile phase (specific interactions, hydrogen bonding) and of the stationary phase (nature and type of linkage: monofunctional or polyfunctional, end-capping of residual silanols) on the solute retention are reported and explained on the basis of the differences between the chemical structures of the pigments.

CONTENTS

* Corresponding author.

0021-9673/93/$06.00

1. INTRODUCTION

Because of their wide distribution in the plant and animal kingdoms, carotenoids are one of the main classes of natural pigments. They are found in a large number of fruits and vegetables (oranges, tomatoes, carrots, spinach, sweet potatoes, pumpkins), in spices and herbs (paprika, parsley, alfalfa) and in leaves, where their presence is masked by chlorophylls until autumn. They are also found in some animal products (eggs, butter, milk), and some seafoods.

Their basic structure is composed of eight isoprene units. The structural formula of all carotenoids is derived from that of lycopene, starting with different structural modifications [1]. The presence of oxygenated groups on this chain and ring closure at the extremes, and the partial dehydrogenation of the chain or its scission, define the structure of carotenoids, which makes it possible to divide them into two classes: (1) carotenes or hydrocarbon carotenoids, composed of only carbon and hydrogen, whose major components in foods are lycopene and α- and β-carotene (Fig. 1); and (2) xanthopylls or oxygenated carotenoids, which bear the following functions on their extremity or terminal ring: epoxy, carbonyl, hydroxyl ester or acids such as cryptoxanthin, the major pigment of citrus fruits, lutein or zeaxanthin present in green vegetables, or capsorubin and capsanthin the major pigments of paprika (Fig. 2).

The presence of numerous conjugated double bonds (eleven in β-carotene and zeaxanthin and ten in α-carotene and lutein) explains the intense colour of these molecules. Carotenoids can also be classified on the basis of the colour of the pigments: yellow-orange pigments such as β-carotene, lutein and zeaxanthin, whose absorbance maximum is about 450 nm; and red pigments such as cryptoxanthin, capsorubin and capsanthin, which have one or two oxygenated groups conjugated with the double bonds of the hydrocarbon chain and whose absorbance maximum is around 480 nm. This property is widely used in the food industry to increase the colour of a preparation. The pigments may be synthetic (β-carotene, β-apo-carotenal) or natural. Natural pigments are used as extracts or as dehydrated powders.

Carotenoids with a β-ionone terminal ring have provitamin A activity. Thus, β-carotene is the first vitamin A precursor, while α and γ-carotenes and cryptoxanthin have lower provitamin activity. Finally, it has been reported that β-carotene has antineoplastic activity, not only at the stage of onset of the disease [2] but also on existing tumours [3]. These properties depend to a great extent on the stereochemical structure of the pigments. In fresh plant tissues, carotenoids are generally present in the most stable structural form, all-*trans*, where all the double bonds are in the *trans* configuration [4–6]. The other forms are due to the *trans–cis* isomerization of the double bonds. This may involve a double bond (positions 7, 9, 13, 15, 13′, 9′) (Fig. 3) to form a mono-*cis* isomer or more rarely may occur on two double bonds and lead to the formation of a di-*cis* isomer. Chemically, this results in a disturbance of conjugation which has two effects of the visible spectrum: a hypochromic effect [7,8] and hypsochromic effect [7–9], causing degradation of the colour of the product and decreased provitamin activity.

In addition, *cis* isomers of carotenoid pigments are less stable to light [10] and can oxidize more rapidly than the *trans* compounds.

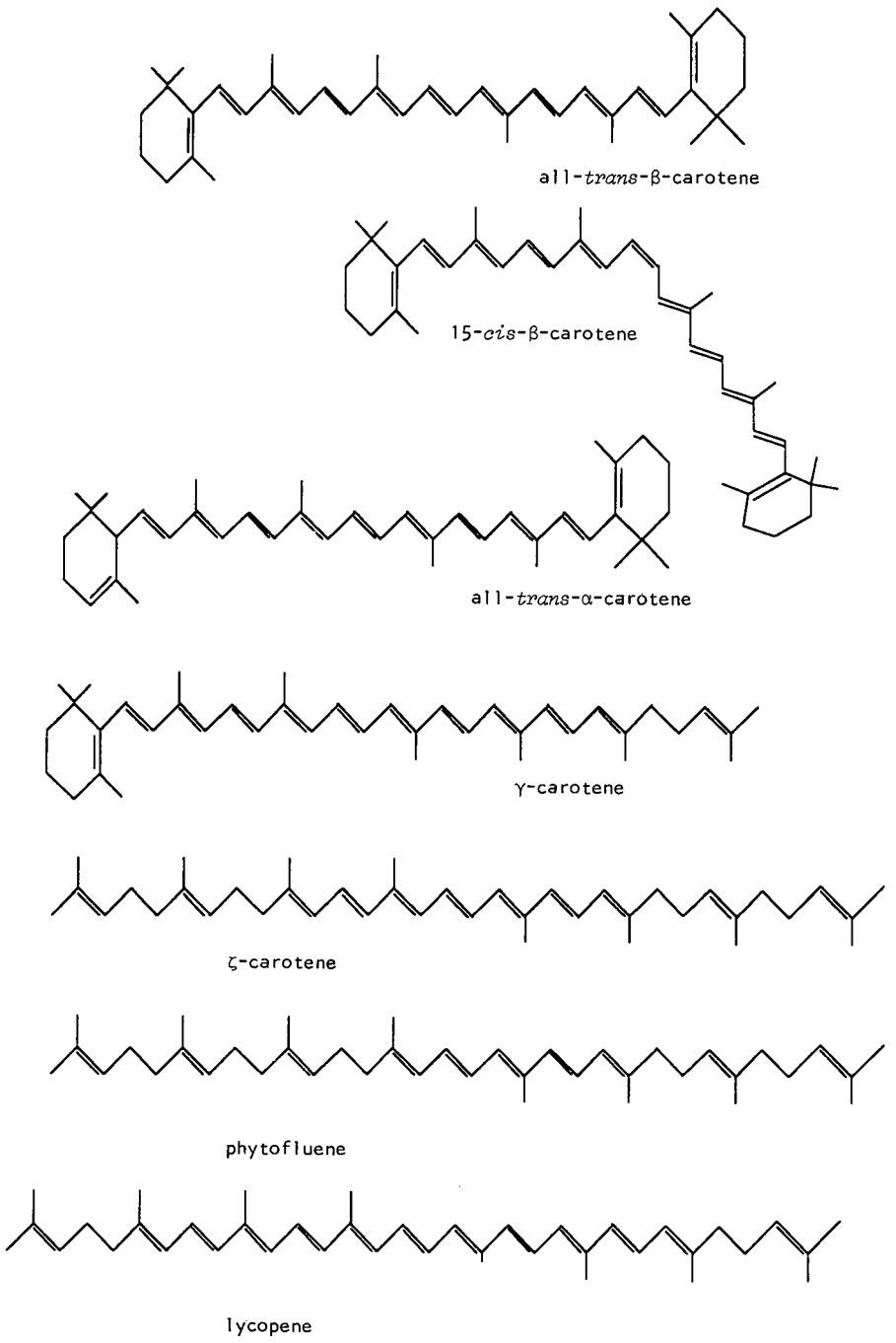

Fig. 1. Structures of some carotenes.

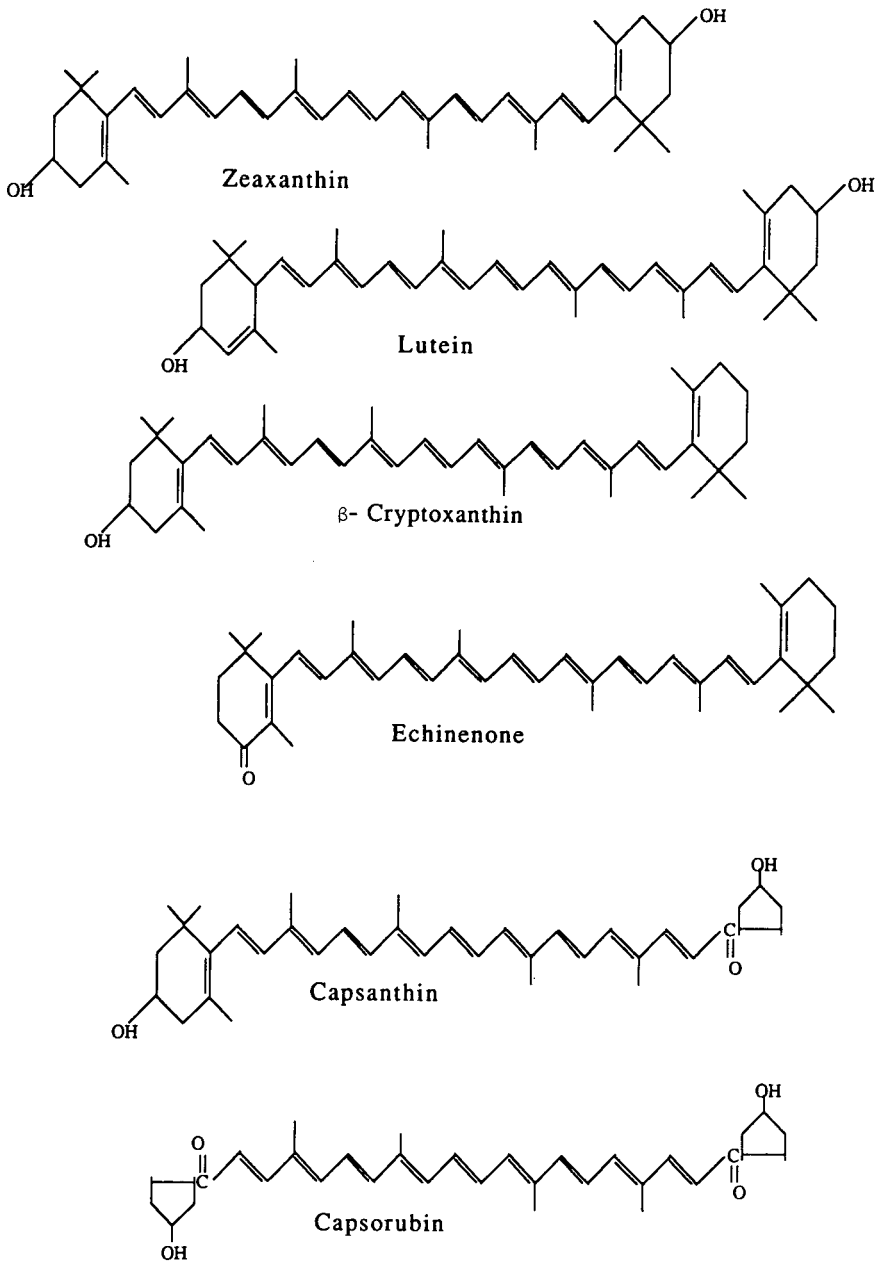

Fig. 2. Structures of some xanthophylls.

The importance of the constituents, in terms not only of colour but also nutrition, explains why many research groups are attempting to characterize and determine these pigments, especially stereoisomers that have different properties.

In this paper we describe and compare the techniques for the extraction and separation of carotenoid pigments in fruits and vegetables.

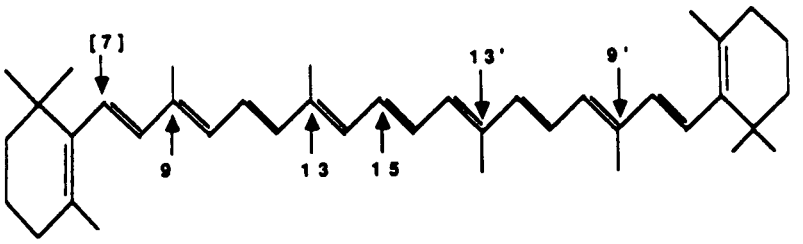

Fig. 3. Positions of isomerization for β-carotene.

2. SAMPLE PREPARATION

The lability of these unsaturated compounds is such that all operations must be conducted with special precautions (low temperature, attenuated light). Other factors can also favour structural modifications of the pigments in the sample, such as solubilization of carotenoids, presence of acids or enzymatic oxidation. This is why pretreatments are sometimes used to prevent or to minimize the degradation of carotenoid pigments during their extraction.

2.1. Pre-extraction treatments

2.1.1. Enzyme inactivation

In order to inactivate enzyme systems, such as lipoxygenase and peroxidase, vegetables are blanched before extraction. Daood and Biacs [11] reported the presence of lipoxygenase in paprika, particularly in the seeds, a portion of which is ground with the product. This enzyme has considerable denaturing activity towards the non-exterified pigments of paprika [12]. These enzymes have also been detected in green peas. Blanching in water for 90 s was required to destroy it [13].

2.1.2. Addition of antioxidants and acid neutralizers

Lipid oxidation activity in carrots has been reported [14,15]. The addition of antioxidants as butylhydrosylanisole (BHA) inhibits lipoxygenase [16]. Pinsky *et al.* [17], however, were unable to detect this activity, but did show the presence of antioxidant compounds in the root.

In order to limit pigment oxidation, antioxidants such as hydroquinone can be added to the sample [15]. Similarly, 2,6-di-*tert.*-butylhydroxytoluene [butylated hydroxytoluene (BHT)] is added to the diethyl ether used for extraction in order to inhibit the formation of peroxides. To the same end, Reeder and Park [18] proposed washing the diethyl ether with an aqueous solution of sodium hydrogensulphite ($NaHSO_3$).

The action of acids on the bleaching of carotenoids can ultimately cause the total decoloration of the pigment solution [7]. The isomerization of all-*trans*-β-carotene has also been observed in the presence of concentrated hydrochloric acid [7]. The solution is therefore made basic by adding 1% of magnesium carbonate ($MgCO_3$) [14] in order to neutralize acids released during extraction. This has also been recommended by the Association of Official Analytical Chemists (AOAC) [19].

2.2. Extraction conditions

The isomerization of carotenoid pigments begins as soon as they are solubilized and cannot be prevented by storing solutions in the cold. Zechmeister [7] reported that it depends on the solvent: the rate of β-carotene isomerization is greater in apolar than in polar solvents. This explains why extraction should be done as rapidly as possible.

In addition to precautions related to changing the pigment medium and to their contact with other substances during extraction, a large number of parameters have been taken into account in establishing extraction protocols: the nature of plant tissues, *i.e.*, fibrous (carrots) or relatively non-fibrous (citrus); the form in which the pigments are present, *i.e.*, free, esterified or complexed with matrix proteins; the chemical structure of different carotenoids together in the same extract; and the state of the product to be analysed, *e.g.*, fresh tissues with a high water content or dehydrated tisues.

We shall successively distinguish the extraction operations as a function of the type of sample.

2.2.1. Extraction with solvents

2.2.1.1. Fresh tissues. Regardless of the product being studied, the chronology of the steps in the extraction of carotenoid pigments is identical; the operational differences depend on the product.

Sample size depends on the occasionally non-homogeneous distribution of pigments in tissues and on their pigment content, variable from one to another. This size is virtually the same for carrots (2–20 g) [20–22], persimmon or papaya (10 g) [23] and fresh paprika (2–10 g) [12,24]. The volume of citrus juice extracted is 20–100 ml [18,19].

For sample preparation, tissues are generally mixed for several minutes alone, with water [4] or an organic solvent [5,21–23]. For juices, mixing is replaced with centrifugation [6], filtration [18,19] or even a prefractionation on an alumina column [26].

The principal extraction solvents, acetone, light petroleum, *n*-hexane, diethyl ether and tetrahydrofuran, have been used alone or in binary mixtures. The simultaneous presence of polar and non-polar solvents in an extraction mixture leads to the total recovery of pigments [5,20,23,24,27,28]. The AOAC recommends using acetone–*n*-hexane (60:40). Bauernfeind [29] indicated that the use of diethyl ether enabled te most highly polar compounds to be extracted into the organic phase, which otherwise could have been solubilized in the aqueous phase.

Grinding the residue is applied. Extraction is considered to be complete when the filtrates are colourless. The residue can be ground manually in methanol [21] and then extracted with acetone. It is important to grind samples to facilitate access of solvent to pigments located inside tissues and to break cell structures containing them (chloroplasts). This may be done at the beginning of the extraction if the tissues in question are fibrous, *e.g.*, carrots.

2.2.1.2. Dried tissues. The concentration of pigments resulting from the elimination of water is high (around tenfold for carrots); hence the sample size is smaller than with fresh tissues: 0.5–2 g for paprika powder [12,30,31] and about 1 g for dehydrated carrots [21].

As a result of their compact and solid nature, it is often necessary to saponify dry tissues before extraction [21,28] in order to increase the contact surface between the extraction solvent and pigments. The tissues are then extracted in the same way as fresh tissues.

2.2.2. Extraction with supercritical fluid

Supercritical CO_2 behaves as an non-polar solvent and solubilizes hydrocarbons. It has been used for the extraction and separation of carotenoids. One advantage of using it for extraction is that its residues in food extracts are not toxic, in contrast to organic extraction solvents.

The polarity of CO_2, related to its density, is determined by the pressure and temperature. Favati *et al.* [32] used this property to extract lutein or β-carotene selectively from a protein concentrate of alfalfa leaves (Fig. 4).

The solubility parameter of CO_2 (calculated ac-

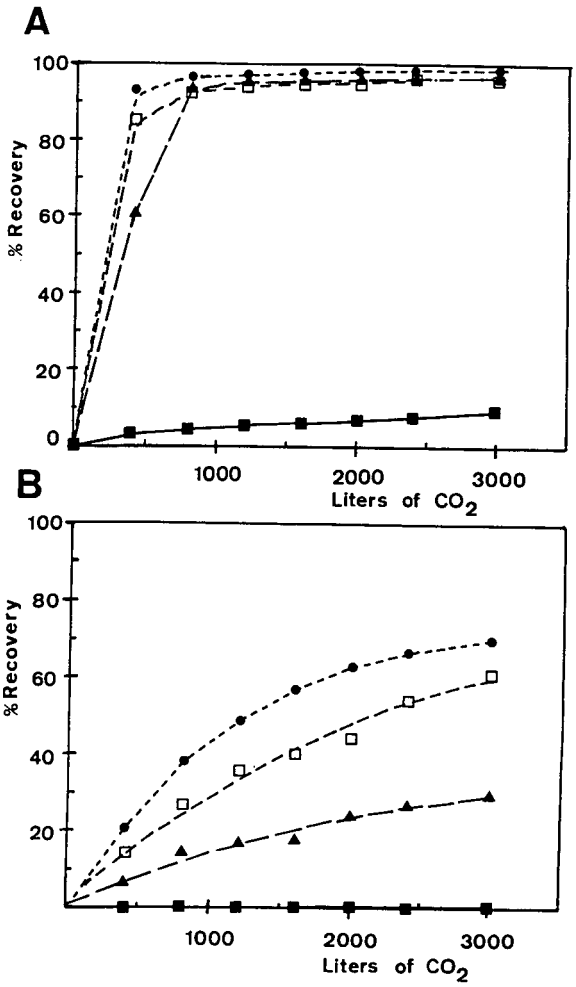

Fig. 4. Effect of pressure on the extraction of pigments as function of total CO_2 used. Temperature = 40°C. (a) β-Carotene; (b) lutein. Pressure: ■ = 10; ▲ = 30; □ = 50; ● = 70 MPa. From ref. 32.

cording to the equation of Giddings *et al.* [33]) was very close to that of β-carotene for pressures from 5 to 7 MPa and was close to that of lutein for 7 MPa. The stability of the pigments extracted under supercritical conditions was not studied. Yamagushi *et al.* [34], however, reported the degradation of astaxanthin esters extracted from shrimp at 80°C, which was apparently favoured by high extraction pressures (25 MPa).

Once the pigments have been extracted, chromatographic fractionation of the untreated extract is used for the subsequent identification and assay of the carotenoids.

2.3. Saponification

Saponification is carried out with the deal aim of eliminating chlorophylls that interfere in the spectrophotometric assay of carotenes and of releasing esterified xanthophylls [35]. This is done before or after extraction, depending on the nature of the plant material containing the pigments. For citrus fruits, saponification is done before extraction, whereas for more fibrous vegetables, in which pigments are not directly accessible, saponification is done after extraction. Methanolic sodium or potassium hydroxide (10–30%) is added to the pigment extract and the mixture is stirred either in an open container or under reflux for various time periods. Saponification itself can cause the aldo-condensation of β-8′-apo-carotenal with a ketone function [19]. A decrease in the carotenoid content has also been reported for extracts of squash [36], citrus [6], paprika [37] or broccoli [38].

This treatment is superfluous for a large number of plants containing carotenes as a major pigment, which by definition do not have esterifiable groups (carrots, tomatoes, pumpkin, sweet potatoes). In addition, these plants are relatively poor in lipids and thus saponification does not change the carotene content [22,25], nor does it cause the appearance of additional α- and β-carotene isomers [5].

In the light of this, most workers have chosen to avoid saponification, because even when justified, it can lead to degradation of the pigments being studied.

3. SEPARATION

The chemical diversity of carotenoids (polar and non-polar) or their similarity (positional isomers, *trans–cis* isomers and diastereoisomers) increase the problem of selecting a separation method, which is often a delicate step.

The instability of carotenoids towards heat and their low volatility make it difficult to use gas chromatography for analysis [39]. The less drastic operating conditions of liquid chromatography explain why this method is more widely used to analyse heat-sensitive components such as carotenoids. Numerous studies of the separation of carotenoids by HPLC have been performed. The large number of chromatographic parameters does not always lead to a clear understanding of the mechanisms governing separations. Therefore, it is the influence of these parameters related to the chemical strucure of pigments that we shall attempt to discern, particularly, with certain more complex separations.

3.1. High-performance liquid chromatography

3.1.1. Chromatography on inorganic supports

Historically, the first separations of carotenes were done by adsorption chromatography [40,41]. This method is generally adapted to the separation of certain isomers and compounds with different functional groups. The first nomenclature of *trans–cis* isomers was based on their retention in adsorption chromatography (neo A, neo B, all-*trans*, W, V, U) [42].

Four different adsorbents can been used [41]. Their capacity to separate different component is related to their polarity. In general, the main types of supports and the classes or compounds separated can be summarized as follows: silica is highly polar and very efficient for fractionating oxygen-containing pigments; magnesium oxide has intermediate polarity and can separate xanthophylls into several fractions (although with less resolution than silica) and carotenes (lycopene, α- and β-carotenes); calcium hydroxide is the phase with the lowest polarity and is better suited to the purification of the stereoisomers of carotenes, especially those of β-carotene; and the polarity of alumina depends on the degree of its activation state [43] and it can be used for separations of all carotenes: neutral alumina with activity 1 for fractionating *trans–cis* isomers, alumina with activity 2–3 inactivated by 4% water for oxygenated xanthophylls or alumina with activity 4 (inactivated by 10% of water).

Carotenes lacking oxygenated functions are eluted first. This shows their reduced affinity for these adsorbents. The retention of carotenes is apparently governed by interactions between the π-electrons of the pigments and the polar adsorbents. It depends both on the number of double bonds in the pigment and the accessibility to the stationary phase. Thus, increasing the number of double bonds increases the retention time while cyclization of the extremity of the hydrocarbon chain reduces it. Similarly, conjugation favours the retention of carotenes [44]. The decrease in conjugation sometimes competes with accessibility of the double bond, particularly in the separation of α- and β-carotenes; the retention time of α-carotene is lower than that of β-carotene. Xanthophylls are eluted later, in an order that depends on the functions they bear: monohydroxy, followed by dihydroxy.

The elution order of *trans–cis* isomers depends on the pigments, but is always related to the localization of the *cis* double bond, which increases or decreases interactions between the pigment and the stationary phase.

Results obtained with β-carotene show that the shift of the *cis* bond from the extremity (9-*cis*) towards the middle of the molecule (15-*cis*) decreases the retention of the compound [8,9,45,46]. As π interactions appear to be responsible for the retention

TABLE 1

ANALYTICAL CONDITIONS FOR THE SEPARATION OF CAROTENOID PIGMENTS BY NORMAL-PHASE CHROMATOGRAPHY

(i) = Isocratic elution; (g) = gradient elution.

Carotenoid	Origin	Stationary phase	Mobile phase	Flow-rate (ml/min)	Ref.
α- and β-carotenes, cryptoxanthin	Orange juice	Basic alumina, silica	(g) Benzene–hexane (37.5:62.5) (g) THF–*n*-hexane (16.6:83.3)	2 2	18
α- and β-carotenes, α- and β-cryptoxanthin	Orange juice	Magnesium oxide	(g) Acetone–hexane	3.5	19
Lycopene, α- and β-carotenes	Tomato	Magnesium oxide	(g) A = acetone–benzene (90:10), B = hexane, (A:B) = 2:98 → 100:0	–	55
All-*trans*-β-carotene, 8 *cis* isomers, α-carotene	Standard	Alumina	(i) *n*-Hexane	–	9
cis–trans-β-carotene, 9 *cis* isomers	Standard	$Ca(OH)_2$	(i) Acetone–*n*-hexane (0.5:99.5)	1	8
17 oxidized compounds of β-carotene	Extract of extruded starch	Silica	(i) *n*-hexane–diethyl ether (95:5)	2	54
cis–trans isomers of 1,2-epoxy-1,2-dihydrolycopene	Standard	Silica	(i) *n*-Hexane–TBME–NN-diisoPEamine[a] (100:4:0.1)	1.4	60
Dihydroxyxanthophylls, *cis–trans* isomers of lutein, diastereo-isomers of lutein	Standard	Silica	(g) *n*-Hexane–methanol (99.9:0.1), acetone = 0 → 40%	1.25	61
cis–trans α- and β-carotene	Vegetables, sweet potatoes	$Ca(OH)_2$	(i) Acetone–hexane (3:97)	0.9	62
β-Carotene and xanthopylls	Sea sediments	Silica	(g) Acetone–hexane (1:99 → 75:25)	1	63
β-Carotene, ζ-carotene, phytoene, neurosporene, lycopene	Standard	Silica	(i) CH_3CN–hexane (0.12:99.8)	2	64
cis–trans isomers of neurosporene	Cellular	$Ca(OH)_2$	(i) Benzene–*n*-hexane (15:85)	2	45

[a] TBME = *tert.*-butylmethyl ether; PE = propylethyl.

of carotene, this shift of the *cis* double bond probably decreases the accessibility of π electrons to the adsorbent.

With xanthophylls such as astaxanthin [47] or canthaxanthin [48], on the other hand, the elution order is reversed. In this instance, retention is governed by the interactions between the hydroxyl groups and the adsorbents, which decrease when the *cis* double bond shifts towards the extremity.

Thin-layer chromatography [5,21,49,50–54] and open-column chromatography [20;28,29,55–59] have been widely employed. These methods are currently used in preliminary studies for the prefractionation of complex mixtures, or to prepare larger amounts of standards.

The main advantages of HPLC are easier quantification of products and speed of analysis, which with carotenoids reduces photochemical or oxidative degradation. These analyses are carried out on those supports classically used for pigment separation on open columns or on thin layers (Table 1). HPLC is generally carried out under isocratic conditions [4,8,9,44].

Fiksdhal *et al.* [61] reported the purification of xanthophylls and also certain *trans–cis* isomers and diastereoisomers of lutein 3′-ethyl ether. Nakazoe [64] reported the separation of two positional isomers, lutein (3,3′-hydroxy-β-carotene) and zeaxanthin (3,3′-hydroxy-α-carotene) on a column of Li-Chrosorb Si 100 with water–acetone as eluent. α- and β-carotenes have been separated on all the adsorbents cited except silica [19,44,61]. Rhodes *et al* [44] fractionated several carotenes on this adsorbent (phytoene, phytofluene, ζ-carotene, neurosporene and lycopene) as a result of the presence of 0.12% of acetonitrile in hexane mobile phase.

The properties of the supports used, combined with the efficiency of HPLC, explain the excellent results obtained in the separation of positional or *trans–cis* isomers. Thus, Vecchi *et al.* [9] isolated all-*trans*-β-carotene and eight of its isomers (Fig. 5). Tsukida *et al.* [8] separated nine *cis* isomers of all-*trans*-β-carotene on calcium hydroxide. They also demonstrated the formation of the 7-*cis* isomer, which was thought to be sterically impossible from a theoretical point of view. Using the same adsorbent, Chandler and Schwartz [4] fractionated the *trans–cis* isomers of α- and β-carotenes but noted a lack of resolution between the all-*trans* and *cis* isomers of α-carotene.

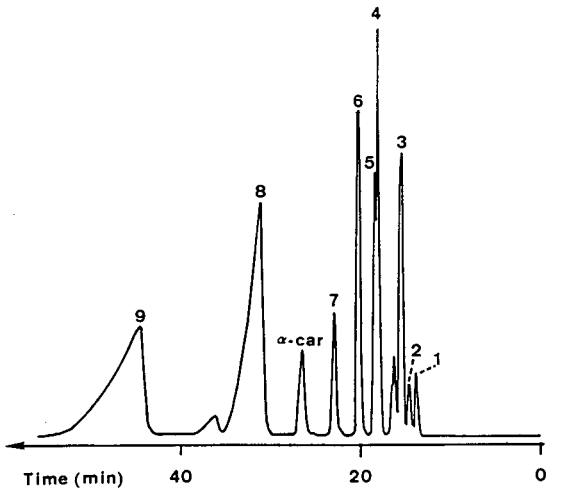

Fig. 5. Separation of nine stereoisomers of β-carotene by HPLC. Stationary phase, alumina; mobile phase, hexane; temperature, 19°C. 1 = 13,13′-di-*cis*-; 2 = 9,13,13′-tri-*cis*-; 3 = 9,13′-di-*cis*-; 4 = 15-*cis*-; 5 = 9,13-di-*cis*-; 6 = 13-*cis*-; 7 = 9,9′-di-*cis*-; 8 = all-*trans*-; 9 = 9-*cis*-. From ref. 9.

In general, the analytical conditions of adsorption chromatography, such as strict control of the water content in the mobile phase, which necessitates considerable control of the apparatus [9], the use of two different columns to separate xanthophylls and carotene [18] and the very long equilibration times between two injections make this technique difficult to use routinely with crude extracts.

3.1.2. Chromatography on bonded silica packings

An alternative is the use of silica bonded with functional groups, which presents a number of advantages: the interactions occurring in reversed-phase separations are different from those encountered in adsorption chromatography and will therefore have less impact on the structural modification of solutes; rapid equilibration of columns, permitting a change in composition in preliminary or optimization studies; the activity of the adsorbent is slightly modified by the water content of the mobile phase; and adsorption of impurities present in solvents or in samples on the stationary phase has little effect on the reproducibility of the results.

Satisfactory results have been obtained with cyano groups, particularly in the separation of enantiomers or of *trans–cis* isomers of xanthophylls [54,65–69].

Hydrocarbon chains are widely used for the separation of carotenoids. Octadecyl chains (C_{18}) are preferred to ethyl (C_2) or octyl (C_8) because of their greater hydrophobic interactions with carotenoid pigments. Elution solvents used are acetonitrile, methanol, water, methylene chloride, chloroform

TABLE 2

ANALYTICAL CONDITIONS FOR THE SEPARATION OF CAROTENOID PIGMENTS BY REVERSED-PHASE CHROMATOGRAPHY

(i) = Isocratic elution; (g) = gradient elution.

Carotenoid	Origin	Stationary phase	Mobile phase	Flow-rate (ml/min)	Ref.
Provitamin A compounds	Tomato	Partisil ODS 5	(i)CH_3CN–$CHCl_3$	2	70
Xanthophylls, carotenes	Spinach	Sil 60-RP 18	(g) CH_3OH–CH_3CN (25:75), H_2O 80 → 100%	1	59
α- and β-carotenes	Carrot, sweet potatoes	Partisil ODS 5	(i) CH_3CN–THF–H_2O (85:12.5:2.5)	2	22
α- and β-carotenes	Fruits, vegetables	μBondapak C_{18}	(i) CH_3CN–$CHCl_3$ (98:2)	1	27
Xanthophylls α- and β-carotenes	Human plasma	Zorbax ODS	(i) CH_3CN–CH_3OH–CH_2Cl_2 (70:10:20)	1	71
α- and β-carotenes, mixture of *cis* isomers	Plants	μBondapak C_{18}	(i) CH_3CN–CH_3OH–$CHCl_3$ (47:47:6)	2	5
5 carotenes	Standards	Ultrasphere ODS	(g) CH_3CN–H_2O (90:10), 2-propanol 30 → 55%	0.66	72
Canthaxanthin, β-cryptoxanthin, α- and β-carotenes, isomers of β-carotene	Standards	Vydax 201,	(i) Many solvent systems (i) CH_3OH–CH_3CN–THF:	1	73
		Vydac 218,	(40:52:8)	1	
		Nova-Pak,	(40:52:8)	1	
		Zorbax ODS	(35:50:15)	1	
Neoxanthin, vialaxanthin, lutein, carotenes	Berries of grapes	Brownlee RP-18	(g) $(CH_3)_2CO$–H_2O (50:50) $(CH_3)_2CO$ 50 → 100%	1	74
Neoxanthin, violaxanthin, β-carotene	Alfalfa	Zorbac ODS, Hypersil ODS, Nova-Pak, Spherisorb ODS	(i) Ethyl acetate–CH_3CN (75:25 → 97:3)	1.6	75
β-Cryptoxanthin, α- and β-carotenes	Orange	Zorbax ODS	(i) CH_3CN–CH_2Cl_2–CH_3OH (65:25:10)	1	6
α- and β-carotenes, 9- and 15-*cis*-β-carotene	Fruits, vegetables	Vydac 218 TP 54	(i) CH_3OH–CH_3CN–THF (40:56:4)	1	76
β-Cryptoxanthin, α- and β-all-*trans* and-*cis* isomers β-carotene	Orange	Vydac 218 TP	(i) CH_3OH–$CHCl_3$ (94:6)	1	77
All-*trans*-neoxanthin, violaxanthin, lutein, β-carotene	Green vegetables	Microsorb	(g) CH_3OH–CH_3CN–CH_2Cl_2–hexane	0.5	38
α- and β-carotenes, non-apreno-β-carotene	Yellow plants	Brownlee RP 18	(i) CH_3OH–CH_3CN–CH_2Cl_2	1	78
α- and β-*trans*–*cis*-carotene	Standards	Vydac 201 TP	(g) CH_3OH 5 min, CH_3OH–$CHCl_3$ (94:6)	1	79
α- and β-*trans*–*cis*-carotene, lycopene	Carrot	Brownlee Spheri 5 ODS	(i) CH_3CN–CH_3OH–CH_2Cl_2 (63:27:10)	1	80
α- and β-carotenes, lutein, zeaxanthin	Standards	Brownlee RP 18	(i) CH_3CN–CH_3OH (85:15)	1.8 → 3.5	81
Carotene and xanthophylls	Barley	Hypersil	(g) THF–H_2O 50:50 → 100:0	1	82
Xanthopylls	Standards	Nova-Pak	(i) H_2O–CH_3CN–$CHCl_3$ (2:83:15)	1	83

and tetrahydrofuran, in binary or ternary mixtures, with isocratic or gradient elution (Table 2). All the results obtained with these stationary phases show that the order of elution depends on the hydrophobicity of pigments. Xanthophylls are more polar than carotenes, which are the least retained. The replacement of an alcohol function (neoxanthin) by an epoxy function (violaxanthin) increases the retention of the pigment, as does the esterification of xanthophylls. Monoesterified pigments are eluted first, followed by diesters [12,24,30,36]. If the same basic xanthophylls are considered, the elongating fatty acid chain length of esters increases the retention time of the compounds [36].

The retention times of carotenes are higher than those of xanthophylls, with lycopene being the first eluted. The elution order of α- and β-carotenes, on the other hand, is the same as that in adsorption chromatography [70,77].

Work done on the separation of *trans–cis* isomers of α- and β-carotenes has shown that the retention time of the *cis* isomer is greater than that of all-*trans* compound [73,79,80]. This has also been observed for canthaxanthin isomers [48,84].

3.1.2.1. Effect of the mobile phase. The presence of water in the mobile phase is the prime discriminating factor for the chromatographic system used. Braumann and Grimme [59] and Bushway and Wilson [22] reported separations done with low water contents, whereas Ruddat and Will [72] fractionated five standard carotenes (lycopene, α-, γ- and β-carotene and β-zeacarotene) and lutein from zeaxanthin in 25 min.

Other workers used only organic solvents in the mobile phase [70,71,73,76,81]. Thus, Nelis and De Leenheer [71] developed a system for separating carotenoids with a ternary mixture in a non-aqueous reversed phase (NARP) (Fig. 6). This avoids peak deformation and partial precipitation of the compounds on the column, and polar xanthophylls (lutein) and non-polar carotenoids (lycopene, α- and β-carotene) can be separated in the same analysis in less than 30 min [71]. Finally, this technique permitted the study of esterified xanthophylls, which could not be investigated by adsorption chromatography because of the strongly hydrophobic nature of the hydrocarbon chains of fatty acids.

The choice of organic solvents is dictated primarily by the eluent strength and the solubility of pigments. The specific properties of each solvent enable the results to be optimized. The presence of methanol (5–10%) masks residual silanol groups which interact with xanthophylls [75] or even with the double bonds of carotenes [80]. Thus, the presence of alcohol in the mobile phase leads to decreased selectivity between lutein and zeaxanthin which can cause an inversion of the elution order of the compounds, with zeaxanthin eluting first with an alcohol-free mobile phase [82,85], and lutein eluting first when alcohol is present [72,83,86,87].

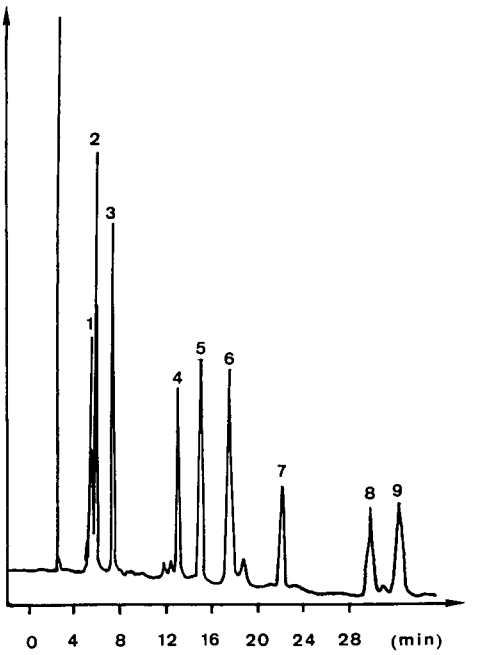

Fig. 6. Separation of a standard mixture of nine carotenoids by NARP-LC. Column, Zorbax ODS (250 × 4.6 mm I.D.); mobile phase, acetonitrile–methylene chloride–methanol (70:20:10, v/v/v); flow-rate, 1 ml min^{-1}; detection, 450 nm. 1 = Lutein; 2 = zeaxanthin; 3 = canthaxanthin; 4 = β-cryptoxanthin; 5 = echinenone; 6 = lycopene; 7 = torulene; 8 = α-carotene; 9 = β-carotene. From ref. 71.

In addition, the existence of π–π interactions between the double bonds of pigments and acetonitrile has been shown [80]. These interactions initially favour the solubility of carotenes in the mobile phase [80].

3.1.2.2. Characteristics of stationary phases. Lauren and McNaughton [75] investigated the effect of certain characteristics of C_{18}-bonded stationary phases on the separation of carotenes and xantho-

TABLE 3

EFFECT OF THE TYPE OF C_{18} COLUMN PROPERTIES ON THE SEPARATION OF α- AND β-*TRANS–CIS* ISOMERS

E = End-capped; NE = non-end-capped; M = monofunctional bonded silica; P = polyfunctional bonded silica; H = high (11%); L = low (7–8%).

Stationary phase	Carbon loading	E/NE	Type of bonded phase	Pore diameter of silica (Å)	CH_3OH in eluent (%)	Non-polar modifier in eluent (%)	Resolution (R_s) of α- and β-carotene	Resolution (R_s) of β-carotene *cis–trans* isomers	Ref.
Zorbax ODS	H	NE	M	70	<10	CH_2Cl_2 25	<1.25	–	6
Zorbax ODS	H	NE	M	70	<10	CH_2Cl_2 20	>1.25	–	71
Vydax 201 TP	L	NE	P	300	>10	THF 8	>1.25	>1.25	73
Zorbax ODS	H	NE	M	70	>10	THF 15	>1.25	<1.25	73
Vydax 218 TP	L	E	P	300	>10	THF 8	>1.25	>1.25	73
Vydac 201 TP	L	NE	P	300	>10	THF 8	>1.25	>1.25	79
Brownlee RP 18	–	E	M	80	10	CH_2Cl_2 10	>1.25	<1.25	80
Brownlee Spheri 5 ODS	–	E	P	80	10	CH_2Cl_2 10	>1.25	>1.25	80

phylls. They include the extent of bonding, varying from 7 to 11% (low and high density), and the degree of end-capping of residual silanol groups. The results showed that the optimum separation of a mixture of carotenes and xanthophylls was obtained with a non-end-capped bonded silica with a high bonding density (Zorbax ODS). Matus and Ohmacht [86] also observed an increased resolution of xanthophylls on non-end-capped columns. However, the retention of carotenes was decreased.

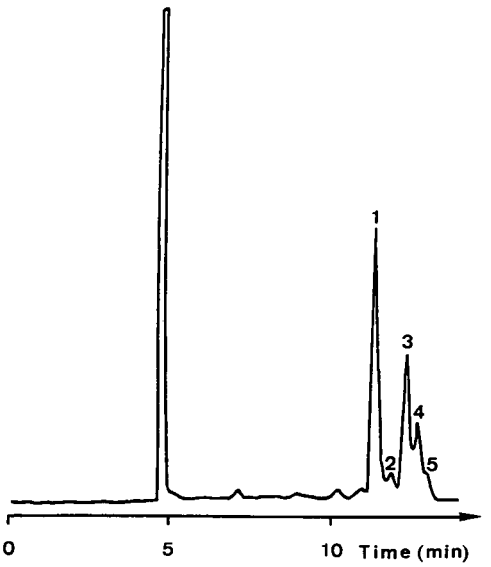

Fig. 7. HPLC separation of *cis–trans* isomers of β-carotene on a polyfunctional column. Column, Vydac 218 TP 54 (250 × 4.6 mm I.D.); mobile phase, acetonitrile–methanol–tetrahydrofuran (40:52:8, v/v/v); flow-rate, 1.0 ml min^{-1}; detection, 450 nm. 1 = All-*trans*-β-carotene; 2 = unknown; 3 = neo-U β-carotene; 4 = neo-B β-carotene; 5 = unknown. From ref. 73.

However, end-capping does not seem to affect the separation of *trans–cis* isomers of β-carotene (Table 3). Bushway [73,76] used different Vydac C_{18} columns to separate all-*trans*-β-carotene from its *cis* isomers (Fig. 7). All-*trans*-α- and -β-carotenes were not separated simultaneously, because of interference between the *cis* isomers of α-carotene and all-*trans*-β-carotene.

Using a Vydac C_{18} (201 TP) column, Quackenbush and Smallidge [77] were the first to report the separation of α-carotene from all-*trans*-β-carotene and from *cis*-β-carotenes. More recently, Quackenbush [79] reported the separation of all-*trans*-α- and -β-carotenes from their *cis* isomers by gradient elution, which improved the resolution between the compounds.

Lesellier *et al.* [80] reported the same separation under isocratic conditions using a column of Brownlee Spheri-5 ODS in NARP-LC. They showed that the type of bonding (mono- or polyfunctional) was very important for the separation of these compounds, both in HPLC [80] and in supercritical fluid chromatography (SFC) [88], where 22

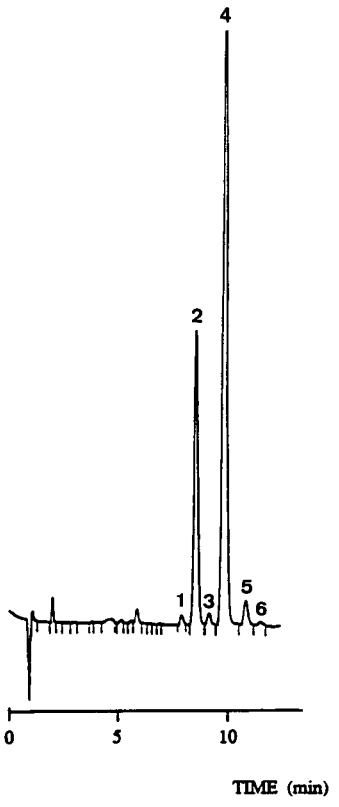

Fig. 8. Separation of a carrot extract by supercritical fluid chromatography. Column, Ultrabase UB 225 (250 × 4.6 mm I.D.); mobile phase, CO_2–methanol–acetonitrile (85:0.75:14.25, v/v/v); pressure, 15 MPa; temperature, 22°C; flow-rate, 3.0 ml/min; detection, 450 nm. 1 = γ- or ζ-all-*trans*-carotene; 2 = all-*trans*-α-carotene; 3 = *cis*-α-carotenes; 4 = all-*trans*-β-carotene; 5 = *cis*-β-carotene; 6 = *cis*-β-carotene. From ref. 96.

columns were tested. The use of a polyfunctional column is preferable for obtaining this separation. It is probable that the "network" structure of this phase was responsible for the separation, which can be explained in terms of flatness or non-flatness between compounds of identical chemical composition, as observed with polyaromatic hydrocarbons [89].

These compounds can, however, be fractionated with monofunctional columns at low temperature, although this is impossible at room temperature [80,90]. The temperature decrease should influence the conformation of hydrocarbon chains of the stationary phase and their mobility.

Monofunctional columns such as Ultrasphere ODS [84] and Zorbax ODS [48] enable *trans–cis* isomers of keto-carotenoids to be separated under the usual conditions.

Reversed-phase chromatography is well suited to the routine analysis of carotenoid pigments, regardless of the mixture being studied. Particular attention should be paid to the type of bonding, which can lead to considerable difference in the results.

3.1.3. Chromatography on chiral phases

This type of phase was first developed to separate optical isomers and is beginning to be used for the analysis of carotenoids. Moaka and co-workers [91,92] used cellulose supports (Chiracel OD) to separate the *trans–cis* isomers or diastereoisomers of carotenoids hydroxylated in position 2 or 4. A cyclodextrin support was used to fractionate lutein and zeaxanthin. The interactions between the hydroxy groups of carotenoids and the glucose molecules located at the periphery of the cyclodextrin cavity explain these results [93]. All-*trans*-β-carotene is also separated from the 15-*cis* isomer on cyclodextrin, but not from all-*trans*-α-carotene [93].

3.2. Supercritical fluid chromatography

Already used to extract pigments, CO_2 is also used in SFC for their separation. The relatively low critical temperature of CO_2 (31°C) enables heat-sensitive compounds such as carotenoids to be separated. It can be used equally well with capillary columns and packed columns. The first separation of α- and β-carotenes with packed columns in SFC was reported in 1968 by Giddings *et al.* [94]. More recently, Gere [95] separated lycopene and α- and β-carotenes in 5 min. He also fractionated a paprika oleoresin in 15 min and showed that the red pigments were eluted before carotene.

The simultaneous SFC separation of *trans–cis*-α- and -β-carotenes [88,96] has been achieved. Separations were more satisfactory than in NARP-LC [80] because two additional compounds could be separated, including one *cis* isomer of β-carotene (Fig. 8). The analogy between the separation mechanisms of these two techniques has been observed, in addition to the importance of π–π interactions [97]. Schmitz *et al.* [98] separated the *trans–cis* isomers of α- and β-carotenes on capillary columns. The results are very encouraging in terms of separation and gain in analysis time.

4. CONCLUSIONS

Progress in the analysis of carotenoid pigments during the last few years is due primarily to the introduction of new methods, such as NARP-LC, SFC and multi-wavelength on-line detection by coupling HPLC and photodiode-array spectrophotometry. Also, the more detailed understanding of pigment–stationary phase–mobile phase interactions and of the structures of stationary phases has enabled more complex separations to be carried out.

This understanding is of fundamental importance, as the diversity of stationary phases is constantly increasing (polymerization of linkages, mixed bonded phases) and will probably lead to highly efficient separations, provided that the choice of mobile phase and stationary phase parameters is optimized as a function of the pigments studied.

REFERENCES

1 T. W. Goodwin, *The Biochemistry of the Carotenoids*, Chapman & Hall, London, 1980.
2 D. E. Ong and F. Chytil, in G. D. Aurbach (Editor), *Vitamins and Hormones*, Vol. 40, Academic Press, New York, 1983, p. 105.
3 R. C. Moon and L. M. Itri, in M. B. Sporn, A. B. Roberts and D. S. Goodman (Editors), *The Retinoids*, Vol. 2, Academic Press, New York, 1984, p. 327.
4 L. A. Chandler and J. S. Schwartz, *J. Food Sci.*, 52 (1987) 669.
5 J. S. Schwartz and M. Patroni-Killiam, *J. Agric. Food Chem.*, 33 (1985) 1160.
6 J. F. Fischer and R. L. Rousseff, *J. Agric. Food Chem.*, 34 (1986) 985.
7 L. Zechmeister, *Fortschr. Chem. Org. Naturst.*, 18 (1959) 223.
8 K. Tsukida, K. Saiki, T. Takii and Y. Koyana, *J. Chromatogr.*, 245 (1982) 359.
9 M. Vecchi, G. Englert, R. Maurer and V. Meduna, *Helv. Chim. Acta*, 64 (1981) 2746.
10 L. Zechmeister, *Cis–Trans Isomeric Carotenoids, Vitamin A and Arylpolyenes*, Academix Press, New York, 1962.
11 H. G. Daood and P. A. Biacs, *Acta Aliment.*, 15 (1986) 319.
12 P. A. Biacs, H. G. Daood, A. Pavisa and F. Hajdu, *J. Agric. Food Chem.*, 52 (1987) 1071.
13 K. S. Rhee and B. M. Watts, *J. Food Sci.*, 2 (1966) 675.
14 K. S. Rhee and B. M. Watts, *J. Food Sci.*, 2 (1966) 664.
15 A. K. Balock, K. A. Buckle and R. A. Edwards, *J. Food Technol.*, 12 (1977) 285.
16 K. S. Rhee and B. M. Watts, *J. Food Sci.*, 2 (1966) 669.
17 A. Pinsky, G. Grossman and M. Trop, *J. Food Sci.*, 2 (1971) 571.
18 S. K. Reeder and G. L. Park, *J. Assoc. Off. Anal. Chem.*, 58 (1975) 595.
19 I. Stewart, *J. Assoc. Off. Anal. Chem.*, 60 (1977) 132.
20 A. T. Ogunlesi and C. Y. Lee, *Food Chem.*, 4 (1979) 311.
21 A. K. Balock, K. A. Buckle and R. A. Edwards, *J. Chromatogr.*, 39 (1977) 149.
22 R. J. Bushway and A. M. Wilson, *Can. Inst. Food Sci. Technol. J.*, 15 (1982) 165.
23 T. Philip and T. S. Chen, *J. Food Sci.*, 53 (1988) 1720.
24 G. K. Gregory, T. S. Chen and T. Philip, *J. Food Sci.*, 52 (1987) 1071.
25 P. W. Simon and X. Y. Wolff, *J. Agric. Food Chem.*, 35 (1987) 1017.
26 G. Calabro, G. Micali and P. Curro, *Essence Deriv. Agrum.*, 48 (1978) 359.
27 Y. P. Hsieh and M. Karel, *J. Chromatogr.*, 259 (1983) 515.
28 W. Horwitz (Editor), *Official Methods of Analysis of the Association of Official Analytical Chemists*, AOAC, Washington, D.C., 12th ed., 1975, pp. 821–823.
29 J. C. Bauernfeind, *Carotenoids as Colorants and Vitamin A Precursors—Technological and Nutritional Applications*, Academic Press, New York, 1981.
30 C. Fisher and J. A. Kocis, *J. Agric. Food Chem.*, 35 (1987) 55.
31 E. Malchev, U. Ioncheva, S. Tanchev and K. Kalpakchieva, *Nährung*, 26 (1982) 415.
32 F. Favati, J. W. King, J. P. Friedrich and K. Eskins, *J. Food Sci.*, 53 (1988) 1532.
33 J. C. Giddings, M. N. Myers, L. McLaren and R. A. Keller, *Science*, 162 (1968) 67.
34 K. Yamagushi, M. Murakami, H. Nakano, S. Konosu, T. Kokura, H. Yamamoto, M. Kosaka and K. Hata, *J. Agric. Food Chem.*, 34 (1986) 904.
35 R. Huet, *Fruits*, 34 (1979) 479.
36 K. Khachik and G. R. Beecher, *J. Agric. Food Chem.*, 36 (1988) 929.
37 M. Baranyai, Z. Matus and J. Szabolcs, *Acta Aliment.*, 11 (1981) 309.
38 F. Khachik, G. R. Beecher and F. Whittaker, *J. Agric. Food Chem.*, 34 (1986) 603.
39 R. F. Taylor and M. Ikawa, *Methods Enzymol.*, 67 (1980) 233.
40 E. Lederer, *Chromatographie en Chimie Organique et Biololgique*, Vol. 2, Masson, Paris, 1959.
41 E. Lederer, *Chromatographie en Chimie Organique et Biologique*, Vol. 1, Masson, Paris, 1959.
42 L. Zechmeister and A. L. le Rosen, *J. Am. Chem. Soc.*, 64 (1942) 2755.
43 H. Brockmann and H. Schrodder, *Chem. Ber.*, 74 (1941) 73.
44 S. H. Rhodes, A. G. Netting and B. V. Milborrow, *J. Chromatogr.*, 442 (1988) 412.
45 N. Katayama, H. Hashimoto and Y. Koyama, *J. Chromatogr.*, 519 (1990) 221.
46 Y. Koyama, M. Hosomi, A. Miyata, H. Hashimoto and S. A. Reames, *J. Chromatogr.*, 439 (1988) 417.
47 M. Vecchi, E. Glinz, V. Meduna and K. Schiedt, *J. High Resolut. Chromatogr. Chromatogr. Commun.*, 10 (1987) 348.
48 H. J. C. F. Nelis, M. M. Z. Van Steenberge, M. F. Lefevere and A. P. De Leenheer, *J. Chromatogr.*, 353 (1986) 295.
49 K. Randerath, *Chromatographie sur Couche Mince*, Gautier-Villard, Paris, 1971.
50 B. H. Chen, S. H. Yang and L. H. Han, *J. Chromatogr.*, 543 (1991) 147.

51 M. T. Winkler and M. Kiszel-Richter, *Acta Aliment.*, 1 (1972) 47.
52 A. E. Purcell, *Anal. Chem.*, 30 (1958) 1049.
53 G. W. Francis and M. Isaken, *J. Food Sci.*, 53 (1988) 979.
54 M. H. Daurade-le Vagueresse and M. Bounias, *Chromatographia*, 31 (1991) 5.
55 M. Cabibel, F. Lapize and P. Ferry, *Sci Aliment.*, 1 (1981) 489.
56 M. D. Nutting, H. J. Neuman and J. R. Wagner, *J. Sci. Food Agric.*, 21 (1970) 197.
57 J. P. Sweeney and M. A. Marsh, *J. Am. Diet. Assoc.*, 59 (1971) 238.
58 C. Marty and C. Berset, *J. Food Sci.*, 53 (1988) 1880.
59 T. Braumann and L. H. Grimme, *Biochim. Biophys. Acta*, 637 (1981) 8.
60 M. Kamber and H. Pfamder, *J. Chromatogr.*, 295 (1984) 295.
61 A. Fiksdahl, J. T. Mortensen and S. Liaaen-Jensen, *J. Chromatogr.*, 157 (1978) 111.
62 L. A. Chandler and S. J. Schwartz, *J. Agric. Food Chem.*, 36 (1988) 129.
63 S. K. Hajibrahim, P. J. C. Tibbette, C. D. Watts, J. R. Maxwell, G. Eglinton, H. Colin and G. Guiochon, *Anal. Chem.*, 50 (1978) 319.
64 J. Nakazoe, *Nippon Suisan Gakkaishi*, 48 (1982) 1007.
65 M. Vecchi, G. Englert and H. Mayer, *Helv. Chim. Acta*, 65 (1982) 1050.
66 G. Englert and M. Vecchi, *J. Chromatogr.*, 235 (1982) 197.
67 P. Ruedi, *Pure Appl. Chem.*, 57 (1985) 793.
68 R. Ohmacht, G. Toth and G. Voight, *J. Chromatogr.*, 395 (1987) 609.
69 F. Khachik, G. R. Beecher and M. B. Goli, *Pure Appl. Chem.*, 63 (1991) 71.
70 M. Zakaria, K. Simpson, P. R. Brown and A. Krstulovic, *J. Chromatogr.*, 176 (1979) 109.
71 H. J. C. F. Nelis and A. P. De Leenheer, *Anal. Chem.*, 55 (1983) 270.
72 M. Ruddat and O. H. Will, *Methods Enzymol.*, 111 (1985) 189.
73 R. J. Bushway, *J. Liq. Chromatogr.*, 8 (1985) 1527.
74 A. Razungles, *Ph.D. Thesis*, Ecole Nationale Superieure Agronimique de Montpellier (ENSAM), Montpellier, 1985.
75 D. R. Lauren and D. E. McNaughton, *J. Liq. Chromatogr.* 9 (1986) 2013.
76 R. J. Bushway, *J. Agric. Food Chem.*, 34 (1986) 409.
77 F. W. Quackenbush and R. L. Smallidge, *J. Assoc. Off. Anal. Chem.*, 69 (1986) 767.
78 K. Khachik and G. R. Beecher, *J. Agric. Food Chem.*, 35 (1987) 732.
79 F. W. Quackenbush, *J. Liq. Chromatogr.*, 10 (1987) 643.
80 E. Lesellier, C. Marty, C. Berset and A. Tchapla, *J. High Resolut. Chromatogr. Chromatogr. Commun.*, 12 (1989) 447.
81 B. Olmedilla, F. Granado, E. Rojas-Hidalgo and I. Blanco, *J. Liq. Chromatogr.*, 13 (1990) 1455.
82 R. K. Juhler and R. P. Cox, *J. Chromatogr.*, 508 (1990) 232.
83 L. A. Mejia, E. Hudson, E. Gonzalez De Mejia and F. Vazquez, *J. Food Sci.*, 53 (1988) 1448.
84 S. T. Mayne and R. S. Parker, *J. Agric. Food Chem.*, 36 (1988) 48.
85 C. A. Bailey and B. H. Chen, *J. Food Sci.*, 54 (1989) 584.
86 Z. Matus and R. Ohmacht, *Chromatographia*, 30 (1990) 318.
87 A. M. Gilmore and H. Y. Yamamoto, *J. Chromatogr.*, 543 (1991) 137.
88 E. Lesellier, M. R. Pechart, A. Tchapla, C. R. Lee and A. M. Krstulovic, *J. Chromatogr.*, 557 (1991) 59.
89 L. C. Sander and S. A. Wise, *J. High Resolut. Chromatogr. Chromatogr. Commun.*, 11 (1988) 383.
90 L. C. Sander and N. E. Craft, *Anal. Chem.*, 62 (1990) 1545.
91 T. Moaka and T. Marsuno, *J. Chromatogr.*, 482 (1989) 189.
92 T. Moaka, A. Arai, M. Shimizu and T. Matsuno, *Comp. Biochem. Physiol.*, 83 (1986) 121.
93 A. M. Stalcup, H. L. Jin, D. W. Armstrong, P. Mazur, F. Derguini and K. Nakanishi, *J. Chromatogr.*, 499 (1990) 627.
94 J. C. Giddings, L. McLaren and M. N. Myers, *Science*, 159 (1968) 197.
95 D. R. Gere, *Application Note AN 800-5*, Hewlett-Packard, Avondale, PA, 1983.
96 M. C. Aubert, C. R. Lee, A. M. Krstulovic, E. Lesellier, M. R. Pechart and A. Tchapla, *J. Chromatogr.*, 557 (1991) 47.
97 A. Tchapla, S. Heron and E. Lesellier, *Spectra 2000*, 158 (1991) 42.
98 H. H. Schmitz, W. E. Artz, C. L. Poor, J. M. Dietz and J. W. Erdman, Jr., *J. Chromatogr.*, 479 (1989) 261.

Journal of Chromatography, 633 (1993) 25–30
Elsevier Science Publishers B.V., Amsterdam

CHROM. 24 765

Extra-column band broadening in high-temperature open-tubular liquid chromatography

G. Liu*

Southwest Research Institute of Chemical Industry, P.O. Box 445, Chengdu 610041 (China)

L. Svenson, N. Djordjevic and F. Erni

Analytical Research and Development, Sandoz Pharma AG, CH-4002 Basle (Switzerland)

(First received August 21st, 1992; revised manuscript received November 16th, 1992)

ABSTRACT

In the development of high-efficiency split high-temperature open-tubular liquid chromatographic systems, the study of the extra-column band broadening and the "cold-point" effect is of great importance. For a rectangular sample plug of volume V_{inj}, $\sigma^2_{inj} = 0.181\ V^2_{inj}$ if the peak width at half-height is used in the column efficiency calculations. In a split system, the contribution of the connection tube between the split tee-piece and the sample valve to the observed peak variance can be calculated with the Taylor equation and the known splitting ratio. As this tube also performes as a preheating tube, a Perkin-Elmer serpentine tube is recommended from considerations of the heating efficiency and the resistance to mass transfer. In order to obtain a higher sensitivity, an external small volume Z-shaped cell was used in series with the on-column cell. The results show that a large decrease in efficiency occurs at the low-temperature column outlet outside the oven. If the Z-shaped cell is connected to the column with a very narrow-bore tube (half of the column I.D.) and the connection is made inside the column oven, higher selectivity could be obtained with little efficiency loss.

INTRODUCTION

In the development of high-efficiency open-tubular liquid chromatographic (OT-LC) systems, the study of the extra-column band broadening is of great importance. Although many studies have been published on the different extra-column effects and equations have been proposed for calculating individual extra-column variances [1–9], few, if any, have discussed the extra column band broadening in a split OT-LC system. In addition, the validity of the theoretical calculation for use under high-temperature conditions (above the normal boiling points of solvents) has not so far been proved.

In addition to the commonly discussed extra-column factors, such as the sample size, the connection tube and the detector cell volume, the "cold-point" effect is another source of band broadening in high-temperature (HT) OT-LC [10]. This not only reduces the column efficiency itself, also causes much greater band broadening in the connection tubes.

This paper discusses the contributions of the sample volume and the connection tube to the overall band broadening in an HT-OT-LC system. The influence of the "cold-point" effect is also discussed.

EXPERIMENTAL

The same experimental set-up as in previous work [10] was used except that a 10 mm × 25 μm I.D. Z-shaped cell (LC Packings, Amsterdam, Netherlands) was inserted between the column outlet and the flow restriction tube (Fig. 1). The column outlet (outside the oven) was 4 cm long and the cell inlet tube was 40 cm long. The cell and its hold-

* Corresponding author.

0021-9673/93/$06.00

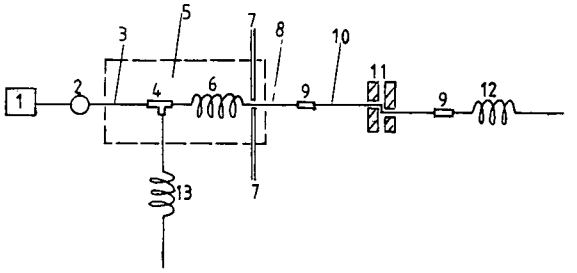

Fig. 1. Experimental set-up. 1 = Solvent pump; 2 = sample valve; 3 = preheating tube; 4 = split tee-piece; 5 = column oven; 6 = chromatographic column; 7 = optical fibres and on-column cell, 8 = column outlet piece; 9 = zero-dead volume unions; 10 = inlet tube of the Z-shaped cell; 11 = Z-shaped cell and holder; 12 = restriction tube; 13 = split tube.

er were placed in a Kontron (Watford, UK) Model 430 UV detector. For the study of the influences of the sample size and the connection tube, signals from the on-column cell were used. For the study of the "cold-point" effect, signals from both the on-column cell and the Z-shaped cell were used.

SB-Methyl-100 and SB-Octyl-50 open-tubular capillary columns were obtained from Lee Scientific (Salt Lake City, UT, USA), fused-silica capillaries from Polymicro Technologies (Phoenix, AZ, USA) and a stainless-steel serpentine tube from Perkin-Elmer (Norwalk, CT, USA). Acetonitrile and methanol were HPLC grade solvents from Rathburn (Walkerburn, UK) and chlorobenzenes of with different Cl substitutions were HPLC test substances from Aldrich-Chemie (Steinheim, Germany). Other chemicals were of analytical-reagent grade from Fluka (Buchs, Switzerland). All chemicals were used as received.

RESULTS AND DISCUSSION

The total peak variance, σ^2, is the sum of the column variance and all independent extra-column variances:

$$\sigma^2 = \sigma_c^2 + \sigma_d^2 + \sigma_t^2 + \sigma_{inj}^2 + \sigma_s^2 \quad (1)$$

where σ_c^2 is the column variance, σ_d^2 is the variance caused by the detector cell volume, σ_t^2 is the variance caused by the preheating tube, σ_{inj}^2 is the variance caused by the injected sample volume and σ_s^2 is the contribution of all other factors, such as dead volumes between connections, electrical response delay and column end flow patterns.

The influence of the "cold-point" effect on the overall band broadening cannot be expressed as a separate term in eqn. 1. Its contribution is indicated by the increase in the σ_c^2 and σ_t^2 values.

In our system with on-column UV detection, the cell dead volume is in the range 0.2–0.4 nl, depending on the column diameter. The contribution of σ_d^2 to the observed peak dispersion is negligible. Also, σ_s^2 can be made insignificant through a proper choice of electronic devices and through the application of high-quality, zero-dead-volume fittings. Hence, σ_t^2 and σ_{inj}^2 are the only extra-column variances that should be studied carefully.

Influence of sample size

The contribution of the sample size to the total peak variance depends on the sample profile and the method by which the column efficiency is measured. In most instances the sample profile can be considered as a rectangular plug, but there are different ways of measuring column efficiency.

The peak variance σ^2 can be calculated from the eluting peak profile with the computerized second momentum method [5]. For this method, the volume variance of a rectangular sample plug of volume V_{inj} is $V_{inj}^2/12$. As Kirkland *et al.* [5] have pointed out, σ^2 obtained with the second momentum method cannot reflect the real separation quality of seriously skewed peaks. This method is not commonly used.

For a Gaussian peak, the standard deviation σ can be measured from the half-width at 0.607 of the peak height. In this instance, the contribution of a rectangular sample plug of volume V_{inj} is given by $\sigma_{inj}^2 = 0.25\ V_{inj}^2$ or $\sigma_{inj} = 0.5\ V_{inj}$ [6]. This method is rarely used in practice.

As the peak width at half-height, $\Delta V_{1/2}$, is critical in determining resolution, the column efficiency derived from $\Delta V_{1/2}$ is commonly used and σ^2 is calculated from the measured plate number (n) and the known retention volume (V_0). Here, σ_{inj}^2 has to be determined in the following way.

If the influence of the sample size only is considered, *i.e.*, $\sigma^2 = \sigma_{inj}^2$, then

$$n = 5.54\ (V_0/\Delta V_{1/2})^2 = (V_0/\sigma)^2 = (V_0/\sigma_{inj})^2 \quad (2)$$

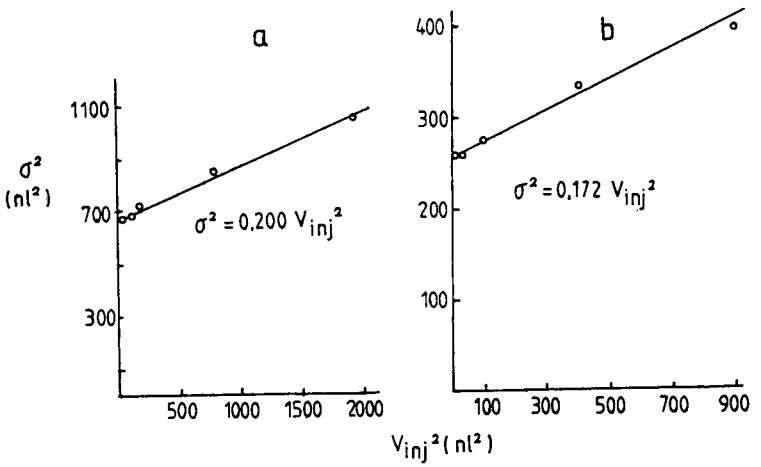

Fig. 2. σ^2 *vs.* V_{inj}^2 plot. (a) column 8.4 m × 0.051 mm I.D. SB-Octyl-50, 100°C, u = 0.27 cm/s; (b) column 1.2 m × 0.051 mm I.D. SB-Methyl-100, 22°C, u = 0.33 cm/s.

For a rectangular sample plug,

$$\Delta V_{1/2} = V_{inj} \quad (3)$$

From eqns. 2 and 3, we obtain

$$\sigma_{inj}^2 = V_{inj}^2/5.54 = 0.181 V_{inj}^2 \quad (4)$$

To prove this relationship, different volumes of acetophenone in methanol were injected into the methanol mobile phase under the same chromatographic conditions. For each injection, the plate number (n) was measured and the peak variance (σ^2) was calculated. Calculated σ^2 values were then plotted against V_{inj}^2 (Fig. 2). The slope of this plot equals the proportionality constant of eqn. 4. The experiments were repeated at 22 and 100°C, and the slope values obtained were 0.171 and 0.200, respectively. As the experimental values approximate the theoretical value of 0.181, eqn. 4 must give a correct description of the influence of the sample size in HT-OT-LC.

If a 20% efficiency loss is the acceptable limit, it can be calculated that a 9.6-nl injection volume is allowed for a 1.2 m × 0.05 mm I.D. column and a 35-nl volume can be used for a 16-m column.

Influence of the connection tube

In our HT-OT-LC system, a connection tube (preheating tube) was inserted between the sample valve and the split tee-piece (Fig. 3). Unlike room-temperature OT-LC, where the connection tube is always cut as short as possible, the connection tube in HT-OT-LC must have a certain size so as to provide enough residence time for the cold liquid (mobile phase and sample) to be heated up. In this instance, the contribution of the connection tube to the overall band broadening must be taken into consideration.

The volume variance in the connection tube, σ_{tube}^2, can be calculated with the Taylor equation:

$$\sigma_{tube}^2 = \pi d_t^4 F l_t / 384 D_m \quad (5)$$

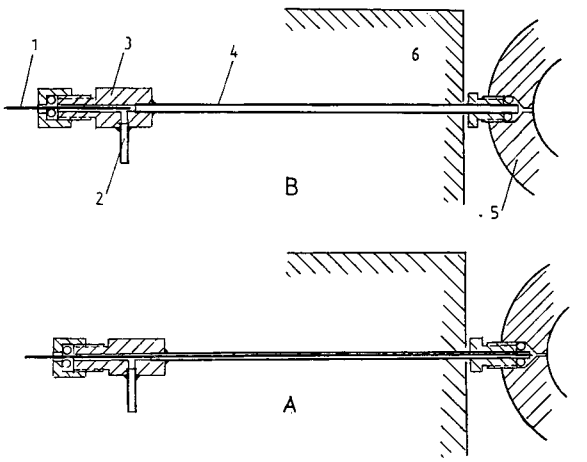

Fig. 3. Column inlet position. 1 = Capillary column; 2 = split outlet; 3 = split tee-piece; 4 = connection tube; 5 = sample valve; 6 = column oven.

where d_t is the inner diameter of the connection tube (cm), l_t is its length (cm), F is the mobile phase flow-rate (ml/s) and D_m is the diffusivity of the solute in the mobile phase. In a split OT-LC system, however, we are interested only in the contribution of the connection tube to the observed peak dispersion (σ_t^2). This can be derived as follows.

As the time variance at the end of the connection tube and the time variance at the inlet of the capillary column should be the same, we have

$$\sigma_t^2/F_c^2 = \sigma_{tube}^2/F^2$$

$$\sigma_t^2 = \sigma_{tube}^2 (F_c/F)^2 = \sigma_{tube}^2 / (SR)^2 \quad (6)$$

where F_c is the flow-rate through the column and $SR = F/F_c$ is the splitting ratio.

To prove the correctness of eqns. 5 and 6 under HT-OT-LC conditions, a piece of 12 cm × 0.52 mm I.D. stainless-steel tubing was used as the connection tube and the following experiments were carried out. First, the column inlet was pushed directly to the sample valve outlet (Fig. 3A) and the peak variance (σ_A^2) was measured. As there was no connection tube, the measured value was the sum of all other variances except σ_t^2. The column inlet was then withdrawn to the position shown in Fig. 3B and the peak variance was measured again (σ_B^2). The contribution of the connection tube, σ_t^2, can be obtained as the difference between σ_B^2 and σ_A^2,

$$\sigma_t^2 = \sigma_B^2 - \sigma_A^2 \quad (7)$$

The experiments were repeated at different column temperatures and different mobile phase flow-rates. The results are given in Table I, where the experimentally obtained σ_t^2 values are compared with the theoretical values calculated from eqns. 5 and 6, using known values for d_t, l_t, D_m, F and SR.

At room temperature, the agreement between the experimental and the theoretical values was acceptable, but at 100°C the experimental values were always higher than the theoretical values. This must be due to the insufficient heating of the sample in the connection tube. The real D_m value of the solute was much lower than that expected for 100°C, resulting in a much higher band broadening in the tube. Considering the heating efficiency and the resistance to mass transfer, a Perkin-Elmer 40 cm × 0.2 mm I.D. serpentine tube was used as the connection tube.

"Cold-point" effect

Above we have seen that insufficient heating of the sample causes a decrease in the overall efficiency. This is the so-called "cold-point" effect. As was

TABLE I

PEAK VARIANCE CAUSED BY THE CONNECTION TUBE

Column, 85 cm × 0.075 mm I.D. fused silica; mobile phase, methanol; test sample, acetophenone in methanol.

Column temperature (°C)	Flow-rate (ml/min)	σ_A^2 (nl^2)	σ_B^2 (nl^2)	σ_t^2 (nl^2)	σ_t (nl)	σ_t^a (nl)
100	1.00	873.0	1137.3	264.3	16.26	15.31
	0.60	564.1	748.7	184.6	13.59	11.63
	0.40	468.7	635.5	166.8	12.91	9.84
	0.30	436.3	565.5	129.2	11.37	8.57
	0.20	427.8	500.4	72.6	8.52	7.18
	0.10	569.5	622.2	52.7	7.26	5.34
22	0.30	709.7	903.7	194.0	13.93	15.75
	0.20	544.3	729.1	184.8	13.59	12.97
	0.10	426.8	491.2	64.4	8.03	9.22
	0.07	417.3	490.0	72.7	8.55	7.87
	0.05	456.6	488.7	32.1	5.66	6.50

[a] Theoretical values.

shown previously [10], the efficiency loss caused by the "cold-point" effect in the inlet region can be made insignificant if a serpentine tube is used as the connection tube and is separately heated to a few degrees higher than the column oven temperature.

Sometimes, a Z-shaped UV cell outside the column oven was used in order to obtain a higher sensitivity. The sensitivity of the LC Packings cell was 10–20 times higher than that of our on-column cell (a window on the 50 μm I.D. capillary column). However, in this instance, a large efficiency loss resulted owing to the "cold-point" effect (Table II).

The volume of the Z-shaped cell is about 5 nl and its contribution to the overall band broadening is negligible. The efficiency loss mainly arises from the extra band broadening in the column outlet and/or in the Z-shaped cell inlet tube. Several conclusions could be drawn from the data in Table II. First, k' values measured with the Z-shaped cell are smaller than those with the on-column cell. This is due to the 40-cm long inlet tube of the Z-shaped cell. There is no stationary phase in this tube, so the average k' values must decrease. The second fact is that the efficiency loss of the slightly retained solute, 1,4-dichlorobenzene, did not change with the column temperature. This means that the inlet tube of the Z-shaped cell itself does not give rise to a noticeable "cold-point" effect. As this tube is very narrow (25 μm I.D.), extra band broadening in this tube, even at a much lower temperature, is very small (see eqn. 5). The 15–18% efficiency loss must come from the connection between the column outlet piece and the Z-shaped cell inlet tube.

The most important finding is that the efficiency loss of the more retained pentachlorobenzene increases rapidly with increasing column temperature. This is explained as the result of the additional retention of the solute on the stationary phase in the low-temperature column outlet. Solute diffusivity in the stationary phase decreases rapidly with decreasing temperature, resulting in very large band broadening. This additional retention became noticeable when the column temperature was raised to 200°C. Here, the k' value of pentachlorobenzene on the Z-shaped cell became larger than that on the on-column cell. We noticed that column bleeding often leads to very thick films at the column outlet. This is why the 4-cm long column outlet created such a large "cold-point" effect. Fig. 4 shows the chromatograms of a chlorobenzene mixture, obtained with the Z-shaped cell and the on-column cell. Broadening of the pentachlorobenzene band is clearly seen with the Z-shaped cell. As the column was operated at a much higher flow-rate than optimum, the column efficiency was relatively low.

In future work, connection between the column outlet and the Z-shaped cell inlet will be made inside the column oven. In this way, the high sensitiv-

TABLE II

INFLUENCE OF THE "COLD-POINT" EFFECT

Column, 19.5 m × 51 μm I.D. SB-Methyl-100; mobile phase, acetonitrile–water (50:50).

Column temperature (°C)	Detector	1,4-Dichlorobenzene		Pentachlorobenzene	
		k'	n	k'	n
22	On-column	0.1627	37270	0.5722	11330
	Z-shaped	0.1622	30780	0.5691	8610
	%[a]	−0.31	−17.4	−0.54	−24.0
100	On-column	0.08625	143000	0.2791	62270
	Z-shaped	0.08588	120500	0.2785	28580
	%[a]	−0.43	−15.7	−0.21	−54.1
200	On-column	0.03468	815400	0.07933	616300
	Z-shaped	0.03465	683100	0.08077	176000
	%[a]	−0.12	−16.2	+0.93	−71.4

[a] % = 100 $(k'_Z - k'_{oc})$ or 100 $(n_Z - n_{oc})/n_{oc}$, where the subscript oc refers to the on-column cell and Z to the Z-shaped cell.

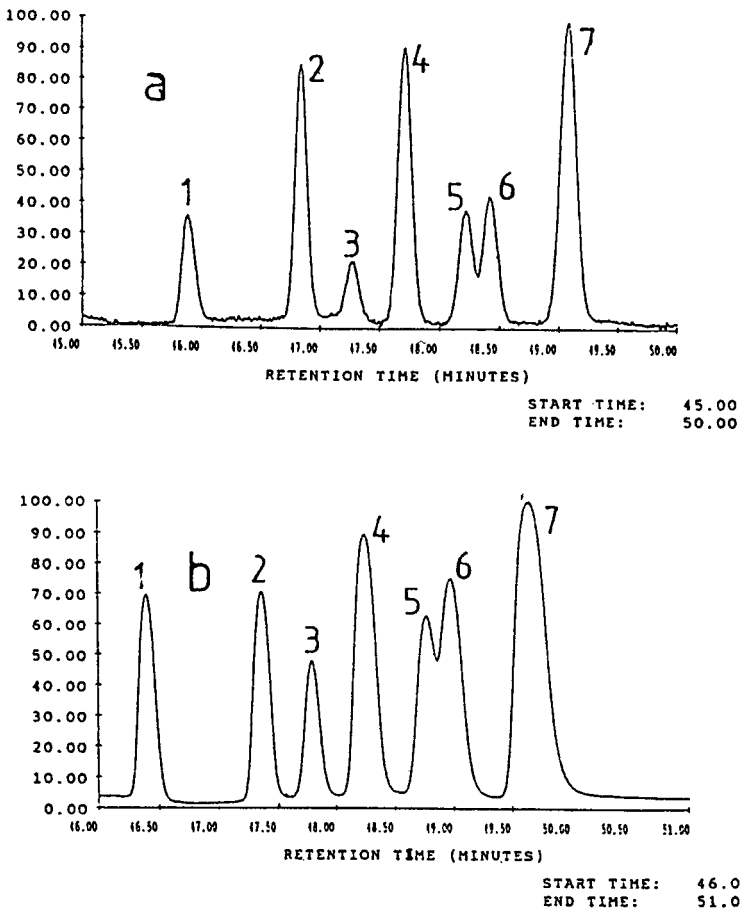

Fig. 4. Chromatograms of a chlorobenzene mixture. Column, 19.5 × 51 μm I.D. SB-Methyl-100, 200°C, mobile phase, acetonitrile–water (50:50), u = 0.584 cm/s; UV detection at 210 nm. (a) On-column cell; (b) Z-shaped cell. Peaks: 1 = tropolone; 2 = benzene; 3 = 1,4-dichlorobenzene; 4 = 1,2,4-trichlorobenzene; 5 = 1,3,5-trichlorobenzene; 6 = 1,2,4,5-tetrachlorobenzene; 7 = pentachlorobenzene.

ity of the Z-shaped cell could be utilized with little efficiency loss.

REFERENCES

1 G. Taylor, *Proc. R. Soc. London, Ser. A*, 219 (1953) 186.
2 G. Taylor, *Proc. R. Soc. London, Ser. A*, 225 (1954) 473.
3 J. C. Sternberg, *Adv. Chromatogr.*, 2 (1966) 205.
4 K. P. Hupe, R. J. Jonker and G. Rozing, *J. Chromatogr.*, 285 (1984) 253.
5 J. J. Kirkland, W. W. Yau, H. J. Stoklosa and C. H. Dilks, Jr., *J. chromatogr. Sci.*, 15 (1977) 303.
6 H. H. Laner and G. P. Rozing, *Chromatographia*, 14 (1981) 641.
7 K. W. Freebairn and J. H. Knox, *Chromatographia*, 19 (1984) 37.
8 J. H. Knox and M. T. Gilbert, *J. Chromatogr.*, 186 (1979) 405.
9 A. Mainz and W. Simon, *J. Chromatogr.*,, 387 (1987) 187.
10 G. Liu, N. Djordjevic and F. Erni, *J. Chromatogr.*, 592 (1992) 239.

Journal of Chromatography, 633 (1993) 31–41
Elsevier Science Publishers B.V., Amsterdam

CHROM. 24 708

Effects of molecular structure on the log k'_w index and linear S–log k'_w correlation in reversed-phase high-performance liquid chromatography

Nong Chen*, Yukui Zhang and Peichang Lu

National Chromatographic Research and Analysis Center, Dalian Institute of Chemical Physics, Chinese Academy of Sciences, 116011 Dalian (China)

(First received July 14th, 1992; revised manuscript received October 20th, 1992)

ABSTRACT

The log k'_w index in the retention equation log k' = log k'_w − $S\varphi$ in reversed-phase high-performance liquid chromatography was systematically studied as a function of molecular structure parameters. The log k'_w index or the "hydrophobic index", which was observed to be nearly constant for a specific solute on the particular column system, was quantitatively correlated with the solvatochromic parameters of the solutes. The coefficients in the correlation of the log k'_w index in methanol–water and acetonitrile–water mixtures with solvatochromic parameters of the solutes were systematically investigated and were found to be consistent with the results of using solvatochromic comparison method. A linear relationship between S and log k'_w was obtained only when two or three of the solute parameters are constant and solute volume varies. The linear relationship between S and log k'_w for structurally related compounds were systematically described. The parameters of the correlation equations referring to various reversed-phase columns with different carbon loadings were compared.

INTRODUCTION

The popularity of reversed-phase high-performance liquid chromatography (RP-HPLC) can be attributed to the development of chemically stable, microparticulate bonded phases [1–4]. The most prevalent type of RP-HPLC column packing is prepared by reacting uniform silica gel particles with an alkylchlorosilane; the reaction with trimethylchlorosilane (TMCS) was followed to eliminate the residual silanols. The molecular organization of highly densely bonded phases resembles that of biomembranes and may be used as a model system to study quantitative structure–retention relationships (QSRR). There have been many studies on increasing the bonding density [2–4], as orginally described by Szabo *et al.* [2] using dimethylamino leaving groups. The steric constraints made further increases in high bonding densities extremely difficult, but this steric hindrance was reduced by Golding *et al.* [3] through the use of dihydrochlorosilane [3].

Despite the enormous popularity of RP-HPLC, there is a lack of understanding of the solute retention mechanism. Such an understanding ultimately requires a sufficiently detailed description of the relationships between retention and various mobile and stationary phase variables. As the rigorous theoretical study of retention mechanisms is very complicated, it is more practical to approximate the retention behaviour of a solute by using empirical relationships. In RP-HPLC, there is ample evidence that the chemical bonded phase (CBP) structure depends also on the nature of the organic modifier [4]. The organic component of the mobile phase is sorbed by the CBP and alters its properties. These alterations are not significant in methanol–water and acetonitrile–water mixtures.

* Corresponding author.

0021-9673/93/$06.00

In RP-HPLC, the mobile phase effects can be separated from stationary phase effects by using the linear relationship between the retention values and the composition of the mobile phase. The linear approximation of the relationship between the logarithm of the capacity factors (log k') and the composition of the mobile phase (φ) has found considerable applications [5–8], and can be described by

$$\log k' = \log k'_w - S\varphi \quad (1)$$

where k' is the capacity factor, φ is the volume fraction of strong solvent in binary mobile phase, k'_w is the extrapolated value of the capacity factor in pure water and S is the negative of the slope of the plot. Eqn. 1 was derived from the hydrophobic interaction model using the thermodynamic method combined with empirical relationships [7].

The slope of the log k' *vs* φ plot is determined by the mobile phase effects, whereas the intercepts of the linear plots are determined mainly by the properties of the stationary phases and solvent water [7,8]. Both parameters are functions of solute molecular structural parameters [7].

The solute distribution in RP-HPLC appears to approach that of partition between two bulk liquid phases, and therefore the capacity factor in RP-HPLC has been used to describe quantitatively the partition coefficient measured in the *n*-octanol–water system (log P). The capacity factor in RP-HPLC has been extensively used as a hydrophobic parameter [9–23]. The retention parameter log k' over a certain concentration range of the mobile phase has been correlated with the classical *n*-octanol–water partition coefficient log P but, in view of the fact that log k' values vary with the volume fraction of the strong solvent, in some instances, different conclusions can be reached owing to a cross-over of peaks at different compositions of the mobile phase.

Many attempts have been made to use the extrapolated k' value (log k'_w) as a hydrophobic index [9–19]. It has been found that log k'_w has some advantage over the isocratic k' [20]. The log k'_w value plays an important role in understanding the hydrophobic interactions of the solute and stationary phase. The log k'_w index or the "hydrophobic index" is an intrinsic property of the solute on a particular column. The extrapolated log k'_w of a specific solute for pure water as the eluent should be constant for a given stationary phase, independent of the organic modifier used in mixtures with water, but the reported parameter log k'_w obtained by extrapolation of eqn. 1 depends on the nature of the organic modifier present in the aqueous mobile phase. Much effort has been directed at making liquid chromatographic systems mimic the conventional *n*-octanol–water system [20–23].

Log k'_w is a function of molecular structure parameters. There have been few studies to explore the effects of molecular structure parameters on log k'_w [20–23]. Many studies have shown that there was a better relationship between log k'_w and log P for structurally related compounds [9–23]. Other studies have found that log k'_w has the property of additivity [20–23], as expressed by

$$\tau_i = \log k'_{w(j)} - \log k'_{w(i)} \quad (2)$$

where j and i differ in a substitutent, but non-additivity has been found for multi-substituted intra- and intermolecular hydrogen-bonding solutes.

In several other studies, log k'_w has been found empirically to be linearly correlated with S (eqn. 1) [24–26], but there is a lack of understanding of the quantitative relationship between log k'_w and solute parameters. Therefore systematic studies on the relationship between log k'_w and structural parameters need to be established.

In previous papers, S or the "hydrophilic index" has been observed to be nearly constant for a specific solute even when column systems with different C_{18} packing materials are used [7,8]. The solvatochromic parameters are widely used molecular structural parameters for characterizing the size, the dipolarity/polarizability interactions and hydrogen bonding interactions of the solute in an aqueous mobile phase [27–32]. The S index has been quantitatively correlated with the solvatochromic parameters of the solutes [8].

In this work, the quantitative correlation of the log k'_w index with the solvatochromic parameters of the solutes was studied and the coefficients in the correlation of log k'_w in methanol–water and acetonitrile–water mixtures with the solvatochromic parameters were investigated through the use of the solvatochromic comparison method. The linear relationships between S and log k'_w are also systematically described for structurally related compounds.

EXPERIMENTAL

The experimental results utilized in this paper were taken from papers by Hammers *et al.* [13], Hafkenscheid and Tomlinson [33], Hanai and Hubert [34,35], Harnisch *et al.* [36] and Petrovic and Lomic [37,38], which gave an exact description of the chromatographic conditions employed. All data were processed with a BASIC program on AST-286 micro-computer.

RESULTS AND DISCUSSION

Log k'_w mainly describes the difference in free-energy change between the solute and a weak solvent and between the solute and a hydrocarbonaceous ligand, as is shown by the following equation [7]:

$$\log k'_w = \log \phi + (\Delta G^0_{A,C} - \Delta G^0_{A,L})/RT \quad (3)$$

where $\Delta G^0_{A,C}$ and $\Delta G^0_{A,L}$ are the non-electrostatic solute–weak solvent and solute–ligand free-energy change, respectively, R is the gas constant, T is the absolute column temperature and ϕ is the phase ratio.

The non-electrostatic free-energy change consists of the Van der Waals interactions [ΔG^0(van)] and hydrogen-bonding interactions [ΔG^0(H)]. These interactions can be characterized by the solvatochromic parameters. The molecular solute Van der Waals volume is measured by the solvatochromic parameter V_2, the solute dipolarity/polarizability is measured by the solvatochromic parameter, π_2 and the solvatochromic parameters α_2 and β_2 measure the solute hydrogen-bond donor (HBD) acidity and hydrogen-bond acceptor (HBA) basicity, respectively [27–32]. Accordingly, the distribution or partition between a pair of solvents takes the form

$$SP = SP_0 + mV_2/100 + d\pi_2 + b\beta_2 + a\alpha_2 \quad (4)$$

where SP denotes solvent-dependent properties, V_2, π_2, β_2 and α_2 characterize the solutes, and the m, d, b and a coefficients characterize the solvent water and the quasi-liquid-like stationary phase.

As the solvent complementary to solute HBA basicity is solvent HBD acidity, for the energetically homogeneously distributed bonded phases the property of the bonded phase that complements the solute's ability to accept a hydrogen bond (β) is the ligand's ability to donate a hydrogen bond (α). The chemical property of water or the quasi-liquid-like bonded phase that complements the solute molar volume is its cohesive energy taken as δ^2, the square of the Hildebrand solubility parameter.

In RP-HPLC, log k'_w, which mainly characterizes the partitioning between water and the quasi-liquid-like bonded phase, can be quantitatively correlated with the solvatochromic parameters. Therefore, according to the solvatochromic comparison method, we have the following equation:

$$\log k'_w = SP_0 + mV_2/100 + d\pi_2 + b\beta_2 + a\alpha_2 \quad (5)$$

where

$$m = f(\delta^2_C - \delta^2_L) \quad (6)$$

$$d = g(\pi_L - \pi_C) \quad (7)$$

$$b = h(\alpha_L - \alpha_C) \quad (8)$$

$$a = l(\beta_L - \beta_C) \quad (9)$$

where δ_C and δ_L are the solubility parameters for water and hydocarbonaceous ligands, respectively, π_L, β_L and α_L are solvatochromic parameters for ligands, π_C, β_C and α_C are solvatochromic parameters for water and f, g, h and l are constants. In eqn. 5, the magnitude of the coefficient m denotes the difference in solubility parameters of water and hydrocarbonaceous ligands and d denotes the difference in dipolarity/polarizability parameters between ligands and water, the coefficient b shows the difference in hydrogen donor ability of the bonded ligands and water and a shows the difference in hydrogen acceptor ability of the ligands and water. The solvatochromic and solubility parameters for C_{18} bonded ligand and water are given in Table I.

TABLE I

SOLUBILITY AND THE SOLVATOCHROMIC PARAMETERS FOR C_{18} BONDED PHASE AND WATER

Solubility and solvatochromic parameters taken from refs. 20 and 27.

Parameter	C_{18}	Water
π	0.01	1.09
β	0.00	0.18
α	0.00	1.17
δ (cal/ml)$^{1/2}$	8.00	23.4

TABLE II

VALUES OF SOLVATOCHROMIC PARAMETERS AND COMPARISON OF THE EXPERIMENTAL LOG k'_w VALUES WITH CALCULATED VALUES FOR VARIOUS AROMATICS

Column, LiChrosorb RP-C_{18}; eluent, methanol–water. Log k'_w values taken from ref. 13 and solvatochromic parameters from ref. 27.

Compound	$V_2/100$	π_2	β_2	α_2	Log k'_w (exp.)	Log k'_w (calc.)[a]	Δ
Benzene	0.491	0.59	0.10	0	2.11	2.25	0.14
Toluene	0.592	0.55	0.11	0	2.74	2.82	0.08
1,2-Dimethylbenzene	0.668	0.51	0.12	0	3.19	3.23	0.04
1,3-Dimethylbenzene	0.668	0.51	0.12	0	3.30	3.23	−0.07
1,4-Dimethylbenzene	0.668	0.51	0.12	0	3.29	3.23	−0.06
1,3,5-Trimethylbenzene	0.769	0.47	0.13	0	3.90	3.79	−0.11
1,2,3,4-Tetramethylbenzene	0.867	0.43	0.15	0	4.20	4.30	0.10
1,2,3,5-Tetramethylbenzene	0.867	0.43	0.15	0	4.26	4.30	0.04
Pentamethylbenzene	0.965	0.39	0.17	0	4.70	4.81	0.11
Hexamethylbenzene	1.063	0.35	0.19	0	5.30	5.31	0.01
Ethylbenzene	0.668	0.53	0.12	0	3.27	3.22	−0.05
n-Propylbenzene	0.769	0.51	0.12	0	3.97	3.81	−0.16
n-Butylbenzene	0.867	0.49	0.12	0	4.57	4.37	−0.20
Naphthalene	0.753	0.70	0.15	0	3.48	3.51	0.03
Fluorene	0.960	1.18	0.22	0	4.26	4.20	−0.06
Phenanthrene	1.015	0.80	0.20	0	4.54	4.78	0.24
Anthracene	1.015	0.80	0.20	0	4.73	4.78	0.05
Pyrene	1.156	0.90	0.25	0	5.10	5.35	0.25
Biphenyl	0.92	1.18	0.20	0	4.17	4.05	−0.12
Bibenzyl	1.116	1.10	0.22	0	4.92	5.13	0.21
Fluorobenzene	0.520	0.62	0.07	0	2.28	2.51	0.23
Chlorobenzene	0.581	0.71	0.07	0	2.80	2.81	0.01
Bromobenzene	0.624	0.79	0.06	0	2.90	3.05	0.15
1,2-Dichlorobenzene	0.671	0.80	0.03	0	3.36	3.41	0.05
1,3-Dichlorobenzene	0.671	0.75	0.03	0	3.49	3.44	−0.05
1,4-Dichlorobenzene	0.671	0.70	0.03	0	3.43	3.47	0.04
1,2,3-Trichlorobenzene	0.761	0.85	0	0	3.95	4.01	0.06
1,2,4-Trichlorobenzene	0.761	0.75	0	0	4.03	4.06	0.03
1,3,5-Trichlorobenzene	0.761	0.70	0	0	4.26	4.09	−0.17
1,2,3,4-Tetrachlorobenzene	0.851	0.80	0	0	4.53	4.55	0.02
1,2,3,5-Tetrachlorobenzene	0.851	0.80	0	0	4.66	4.55	−0.11
1,2,4,5-Tetrachlorobenzene	0.851	0.70	0	0	4.65	4.60	−0.05
Pentachlorobenzene	0.941	0.75	0	0	5.25	5.08	−0.17
Hexachlorobenzene	1.031	0.70	0	0	5.90	5.62	−0.28
2-Chloroaniline	0.652	0.83	0.40	0.25	1.89	1.81	−0.08
3-Chloroanaline	0.652	0.78	0.40	0.31	1.90	1.91	0.01
4-Chloroaniline	0.653	0.73	0.40	0.31	1.92	1.94	0.02
3-Chlorophenol	0.626	0.77	0.23	0.69	2.29	2.23	−0.06
4-Chlorophenol	0.626	0.72	0.23	0.67	2.27	2.26	−0.01
Aniline	0.562	0.73	0.50	0.26	1.05	1.09	0.04
Phenol	0.536	0.72	0.33	0.61	1.27	1.42	0.15
Benzyl alcohol	0.634	0.99	0.52	0.39	1.39	1.25	−0.14
Benzaldehyde	0.606	0.92	0.44	0	1.74	1.55	−0.19
Benzonitrile	0.590	0.90	0.37	0	1.83	1.72	−0.11
Nitrobenzene	0.631	1.01	0.30	0	1.91	2.14	0.23
Acetophenone	0.690	0.90	0.49	0.04	2.02	1.85	−0.17
Anisole	0.639	0.73	0.32	0	2.23	2.26	0.03
Methyl benzoate	0.736	0.75	0.39	0	2.44	2.55	0.11
N,N-Dimethylaniline	0.752	0.90	0.43	0	2.57	2.43	−0.14

[a] Log $k'_w = (0.113 \pm 0.12) + (5.69 \pm 0.13)V_2/100 - (0.51 \pm 0.11)\pi_2 - (3.50 \pm 0.15)\beta_2 - (0.37 \pm 0.12)\alpha_2$; $n = 49$; $R = 0.995$; S.D. = 0.133.

The log k'_w values reported by Hammers *et al.* [13] for 49 solutes whose solvatochromic parameters are known are given in Table II together with values of $V_2/100$, π_2, β_2 and α_2.

The correlation of log k'_w index and the solvatochromic parameters for 49 solutes in methanol–water mixtures was also established; the correlation according to eqn. 5 is as follows:

$$\log k'_w = (0.113 \pm 0.12) + (5.69 \pm 0.13)\, V_2/100 - (0.51 \pm 0.11)\pi_2 - (3.50 \pm 0.15)\beta_2 - (0.37 \pm 0.12)\alpha_2$$
$$n = 49;\ R = 0.995;\ \text{S.D.} = 0.133 \qquad (10)$$

In this and all regression equations that follow, n is the number of data points in the regression, R is the regression coefficient and S.D. is the standard deviation. It is seen that the goodness of the statistical fit of the data to eqn. 10 is excellent. The calculated log k'_w values for 49 compounds according to eqn. 10 are listed in Table II. For comparison, we also listed the correlation of the S index with the solvatochromic parameters for these 49 solutes, as shown in the equation

$$S = (1.09 \pm 0.14) + (4.55 \pm 0.15)V_2/100 - (0.252 \pm 0.13)\pi_2 - (2.50 \pm 0.17)\beta_2 + (0.0948 \pm 0.15)\alpha_2$$
$$n = 49;\ R = 0.987;\ \text{S.D.} = 0.156 \qquad (11)$$

It can be seen in eqns. 10 and 11 that the chief factors that control log k'_w and S are solute size and hydrogen bond basicity, less important factors are the polarizability/dipolarity and hydrogen bond acidity of the solute and the contributions of α to log k'_w and S is not very significant. This reveals that the predominant mechanism of retention in RP-HPLC is the hydrophobic expulsion of the solute from the aqueous mobile phase, and therefore log k'_w is often referred to as the "hydrophobic index", indicating the hydrophobicity of the solute, and S is often referred to as the "hydrophilic index", $-S$ revealing the hydrophilicity of the solute. The coefficients m, d, b and a in eqn. 10 have the expected signs. As the value of the solubility parameter for water is greater than for a C_{18} phase (see Table I), and the dipolarity of water ($\pi_C = 1.09$) is higher than that of C_{18} ligands ($\pi_L = 0.01$), m has a positive and d a negative sign. As C_{18} ($\beta_L = 0$) is less basic than water ($\beta_C = 0.18$), then a is negative, whereas as water is a stronger HB acid ($\alpha_C = 1.17$) than C_{18} ($\alpha_L = 0.00$), b is negative.

The correlation of log k'_w and the solvatochromic parameters for 27 solutes was also elucidated (see Table III). The following equations were obtained by least-square regression for log k'_w and S:

$$\log k'_w = (0.60 \pm 0.10) + (5.14 \pm 0.11)V_2/100 - (0.95 \pm 0.12)\pi_2 - (3.52 \pm 0.19)\beta_2 - (0.068 \pm 0.09)\alpha_2$$
$$n = 27;\ R = 0.997;\ \text{S.D.} = 0.10 \qquad (12)$$

$$S = (1.55 \pm 0.11) + (4.13 \pm 0.12)V_2/100 - (0.52 \pm 0.14)\pi_2 - (2.36 \pm 0.21)\beta_2 + (0.25 \pm 0.10)\alpha_2$$
$$n = 27;\ R = 0.993;\ \text{S.D.} = 0.12 \qquad (13)$$

The calculated log k'_w values for 27 compounds are also given in Table III.

Table IV shows the results of another example for seventeen compounds in methanol–water mixtures.

Table V gives the experimental log k'_w values and the calculated values for 32 solutes in acetonitrile–water mixtures based on the relationship between log k'_w and the solvatochromic parameters. The resulting regression equations for log k'_w and S are

$$\log k'_w = (1.12 \pm 0.12) + (3.08 \pm 0.17)V_2/100 - (0.82 \pm 0.09)\pi_2 - (3.02 \pm 0.36)\beta_2 - (1.52 \pm 0.53)\alpha_2$$
$$n = 32;\ R = 0.987;\ \text{S.D.} = 0.13 \qquad (14)$$

$$S = (1.88 \pm 0.12) + (1.79 \pm 0.17)V_2/100 - (0.47 \pm 0.07)\pi_2 - (1.55 \pm 0.35)\beta_2 - (2.06 \pm 0.51)\alpha_2$$
$$n = 32;\ R = 0.975;\ \text{S.D.} = 0.13 \qquad (15)$$

On comparing the pairs of eqns. 10 and 11, 12 and 13, and 14 and 15, it can be seen that the signs of the coefficients in eqns. 10, 12 and 14 are almost the same as those in eqns. 11, 13 and 15, except for the terms whose coefficients are not very significant, which implies that the magnitude of log k'_w increases with increase in the size of the solute, whereas $-S$ decreases with increasing solute size; increasing hydrogen bonding interaction results in a large decrease in log k'_w and a large increase in $-S$ when other conditions remain the same, which are widely consistent with the practical observations that when other factors are equal, more polar or strong hydrogen bonding interactions will decrease the k' values, whereas increasing the size of the solute leads to an increase in k'. Therefore, when two or three solute parameters are equal, there is a general trend that as the solute becomes increasingly hydrophobic, log

TABLE III

VALUES OF SOLVATOCHROMIC PARAMETERS AND COMPARISON OF EXPERIMENTAL LOG k'_w VALUES WITH CALCULATED VALUES FOR VARIOUS COMPOUNDS

Column, Hypersil-ODS; eluent, methanol–water; phosphate buffer was used when applied to ionizable compounds. Log k'_w values taken from ref. 33 and solvatochromic parameters from ref. 27.

Compound	$V_2/100$	π_2	β_2	α_2	Log k'_w (exp.)	Log k'_w (calc.)[a]	Δ
4-Nitrophenol	0.676	1.15	0.32	0.82	1.77	1.81	0.04
4-Nitroaniline	0.702	1.25	0.48	0.42	1.30	1.31	0.01
Benzene	0.491	0.59	0.10	0	2.05	2.22	0.17
Toluene	0.592	0.55	0.11	0	2.59	2.74	0.15
Chlorobenzene	0.581	0.71	0.07	0	2.72	2.67	−0.05
Nitrobenzene	0.631	1.01	0.30	0	1.93	1.84	−0.09
Phenol	0.536	0.72	0.33	0.61	1.35	1.48	0.13
Aniline	0.562	0.73	0.50	0.26	0.98	1.03	0.05
Benzoic acid	0.650	0.74	0.40	0.59	1.86	1.80	−0.06
p-Xylene	0.668	0.51	0.12	0	3.18	3.14	−0.04
4-Chlorotoluene	0.679	0.67	0.08	0	3.32	3.18	−0.14
4-Nitrotoluene	0.729	0.97	0.31	0	2.46	2.35	−0.11
p-Cresol	0.634	0.68	0.34	0.58	1.90	1.99	0.09
p-Toluidine	0.660	0.69	0.51	0	1.53	1.55	0.02
p-Toluic acid	0.748	0.70	0.41	0.59	2.40	2.31	−0.09
1,4-Dichlorobenzene	0.671	0.70	0.03	0	3.33	3.29	−0.04
4-Nitrochlorobenzene	0.721	1.01	0.26	0	2.42	2.44	0.02
4-Chlorophenol	0.626	0.72	0.23	0.67	2.22	2.29	0.07
4-Chloroaniline	0.653	0.73	0.40	0.31	1.82	1.84	0.02
4-Chlorobenzoic acid	0.740	0.74	0.36	0.63	2.63	2.40	−0.23
1,3,5-Trimethylbenzene	0.769	0.47	0.13	0	3.75	3.66	−0.09
1,2,4,5-Tetramethylbenzene	0.867	0.43	0.15	0	4.12	4.13	0.01
Naphthalene	0.753	0.70	0.15	0	3.28	3.29	0.01
Phenanthrene	1.015	0.80	0.20	0	4.30	4.36	0.06
Anthracene	1.015	0.80	0.20	0	4.45	4.36	−0.09
Pyrene	1.156	0.90	0.25	0	4.69	4.82	0.13
Perylene	1.415	1.0	0.30	0	5.82	5.88	0.06

[a] $\log k'_w = (0.603 \pm 0.10) + (5.14 \pm 0.11)V_2/100 - (0.945 + 0.12)\pi_2 - (3.517 \pm 0.19)\beta_2 - (0.068 \pm 0.09)\alpha_2$; $n = 27$; $R = 0.997$; S.D. = 0.104.

k'_w and S will become increasingly positive and, in contrast, as the solute becomes more hydrophilic and more polar, log k'_w and S will decrease.

Hence it can be concluded that for a given RP-HPLC column system, it is possible to obtain a linear relationship between S and log k'_w if two or three structural parameters (π_2, β_2, α_2) are equal or close and V_2 varies. These compounds are often called structurally related. Homologues and non-polar and structurally related polar compounds belong to solutes of this kind. For non-polar compounds such as polynuclear aromatic hydrocarbons (PAHs), the solvatochromic parameters π_2, β_2 and α_2 are almost identical, and therefore, from eqn. 5, it can be seen that linear relationships between log k'_w and S and the Van der Waals volume of the solute can be obtained, which results in a linear S–log k'_w correlation for PAHs. The dependence of S on log k'_w for PAHs in methanol–water eluent is demonstrated in Fig. 1.

Table VI shows the experimental log k'_w values and values calculated from the Van der Waals volume for some PAHs in methanol–water mixtures.

For homologous series, it is strictly observed that

TABLE IV

EXPERIMENTAL LOG k'_w VALUES AND CALCULATED VALUES FOR SEVENTEEN SOLUTES IN METHANOL-WATER MIXTURES

Column, LiChrosorb C_{18} with a surface coverage of 0.255 mmol/g; eluent, methanol–water (methanol from 10 to 60%, v/v). Log k'_w values taken from refs. 37 and 38 and solvatochromic parameters from ref. 27.

Compound	$V_2/100$	π_2	β_2	α_2	Log k'_w (exp.)	Log k'_w (calc.)[a]	Δ
Acetophenone	0.690	0.90	0.49	0.04	1.43	1.55	0.12
p-Cresol	0.634	0.68	0.34	0.58	1.40	1.52	0.12
Benzyl alcohol	0.634	0.99	0.52	0.39	0.95	0.85	−0.10
Phenol	0.536	0.72	0.33	0.61	0.86	0.82	−0.04
Aniline	0.562	0.73	0.50	0.26	0.80	0.64	−0.16
Benzene	0.491	0.59	0.10	0	1.48	1.54	0.06
Toluene	0.592	0.55	0.11	0	2.15	2.25	0.10
Ethylbenzene	0.668	0.53	0.12	0	2.87	2.77	−0.10
n-Propylbenzene	0.769	0.51	0.12	0	3.54	3.50	−0.04
n-Butylbenzene	0.867	0.49	0.12	0	4.20	4.20	0
Pentane	0.553	−0.08	0	0	2.72	2.73	0.01
Hexane	0.648	−0.04	0	0	3.40	3.38	−0.02
Heptane	0.745	−0.02	0	0	4.08	4.05	−0.03
Octane	0.842	0.01	0	0	4.74	4.72	−0.02
1-Butanol	0.499	0.40	0.45	0.33	0.57	0.55	−0.02
1-Pentanol	0.593	0.40	0.45	0.33	1.19	1.21	0.02
1-Hexanol	0.690	0.40	0.45	0.33	1.80	1.90	0.10

[a] $\log k'_w = (-1.23 \pm 0.16) + (7.07 \pm 0.23)V_2/100 - (0.70 \pm 0.10)\pi_2 - (2.95 \pm 0.20)\beta_2 - (0.44 \pm 0.15)\alpha_2$; $n = 17$; $R = 0.998$; S.D. = 0.09.

their solvatochromic parameters π_2, β_2 and α_2 are equal and only V_2 varies, and V_2 can be written as a linear function of the number of methylene groups [8]. Therefore, linear dependences of log k'_w on n_c for homologues are found, which leads to an excellent linear S–log k'_w correlation (see Fig. 2).

For homologues, the insertion of a methylene group into a compound gives a constant change in log k'_w, as can be seen from Tables VII and VIII. The average contribution of a methylene group to log k'_w is almost constant. The average contribution of a methylene group to log k'_w for alkylbenzenes is defined by

$$\Delta\log k'_w\,(CH_2) = [\log k'_w\,(n\text{-alkylbenzene}) - \log k'_w\,(\text{benzene})]/n_c \qquad (16)$$

The calculated log k'_w values obtained by using the linear relationships between log k'_w and n_c are also given in Tables VII and VIII.

For structurally related polar compounds whose solvatochromic parameters π_2, β_2 and α_2 are almost the same, a linear S–log k'_w correlation (LSLC) can be derived and LSLC analysis can be suggested as a measure of the structural similarity of compounds. Fig. 3 illustrates the linear S–log k'_w correlations for chloro-substituted benzenes in methanol–water mixtures. For these compounds, the solvatochromic parameters π_2, β_2 and α_2 are almost identical (see Table II). Details of LSLC analysis will be discussed elsewhere.

Table IX gives the coefficients m, d, b and a on four different C_{18} packings with surface coverages ranging from 0.255 to 0.699 mmol/g. These coefficients are approximately equal on the four columns, showing the characteristic constants of water and the C_{18} used, whereas the SP_0 values increase with increasing surface coverage of the C_{18} bonded phases, which resulted in a simplified linear log k'_w–

TABLE V

VALUES OF SOLVATOCHROMIC PARAMETERS AND COMPARISON OF THE EXPERIMENTAL LOG k'_w VALUES WITH CALCULATED VALUES FOR VARIOUS AROMATICS

Column, Develosil-ODS; eluent, acetonitrile–water (acetonitrile from 60 to 95%, v/v). Log k'_w values taken from ref. 34 and solvatochromic parameters from ref. 27.

Compound	$V_2/100$	π_2	β_2	α_2	Log k'_w (exp.)	Log k'_w (calc.)[a]	Δ
Benzene	0.491	0.59	0.10	0	1.83	1.85	0.02
Naphthalene	0.753	0.70	0.15	0	2.34	2.42	−0.12
Biphenyl	0.92	1.18	0.20	0	2.71	2.39	−0.32
Fluorene	0.960	1.18	0.22	0	2.78	2.45	−0.33
Phenanthrene	1.015	0.80	0.20	0	2.87	2.99	0.12
Anthracene	1.015	0.80	0.20	0	2.76	2.99	0.23
Pyrene	1.156	0.90	0.25	0	2.94	3.19	0.15
Toluene	0.592	0.55	0.11	0	2.13	2.16	0.03
Ethylbenzene	0.668	0.53	0.12	0	2.43	2.38	−0.05
n-Propylbenzene	0.769	0.51	0.12	0	2.77	2.71	−0.06
Isopropylbenzene	0.769	0.51	0.12	0	2.69	2.71	0.02
n-Butylbenzene	0.867	0.49	0.12	0	3.11	3.03	−0.08
Chlorobenzene	0.581	0.71	0.07	0	2.12	2.12	0.00
1,2-Dichlorobenzene	0.671	0.80	0.03	0	2.35	2.44	0.09
1,3-Dichlorobenzene	0.671	0.75	0.03	0	2.48	2.48	0.00
1,4-Dichlorobenzene	0.671	0.70	0.03	0	2.45	2.53	0.08
1,2,4-Trichlorobenzene	0.761	0.75	0	0	2.76	2.85	0.09
1,3,5-Trichlorobenzene	0.761	0.70	0	0	2.93	2.89	−0.04
1,2,3,4-Tetrachlorobenzene	0.851	0.80	0	0	2.98	3.09	0.11
1,2,3,5-Tetrachlorobenzene	0.851	0.80	0	0	3.14	3.09	−0.05
1,2,4,5-Tetrachlorobenzene	0.851	0.70	0	0	3.12	3.17	0.05
Pentachlorobenzene	0.941	0.75	0	0	3.42	3.40	−0.02
Hexachlorobenzene	1.031	0.70	0	0	3.75	3.73	−0.02
Bromobenzene	0.624	0.79	0.06	0	2.18	2.22	0.04
Iodobenzene	0.671	0.81	0.05	0	2.34	2.35	0.01
Butyl alcohol	0.499	0.40	0.45	0.33	0.46	0.47	0.01
Pentyl alcohol	0.593	0.40	0.45	0.33	0.76	0.76	0.00
Hexyl alcohol	0.690	0.40	0.45	0.33	1.07	1.06	−0.01
n-Pentane	0.553	−0.08	0	0	2.81	2.89	0.07
n-Hexane	0.648	−0.04	0	0	3.18	3.15	−0.03
n-Heptane	0.745	−0.02	0	0	3.55	3.43	−0.12
n-Octane	0.842	0.01	0	0	3.91	3.71	−0.20

[a] Log $k'_w = (1.12 \pm 0.12) + (3.08 \pm 0.17)V_2/100 - (0.82 \pm 0.09)\pi_2 - (3.02 \pm 0.36)\beta_2 - (1.52 \pm 0.53)\alpha_2$; $n = 32$; $R = 0.987$; S.D. = 0.13.

TABLE VI

COMPARISON OF EXPERIMENTAL LOG k'_w VALUES [LOG k'_w (exp.)] WITH THOSE CALCULATED [LOG k'_w (calc.)] FROM THE SOLVATOCHROMIC PARAMETERS FOR SOME PAH COMPOUNDS

Column, YWG-C_{18}; eluent, methanol–water (methanol from 60 to 90%, v/v). For experimental conditions, see ref. 7.

Compound	$V_2/100$	Log k'_w (exp.)	Log k'_w (calc.)[a]	Δ
Benzene	0.49	2.05	2.06	0.01
Naphthalene	0.75	3.03	3.06	0.03
Biphenyl	0.92	3.70	3.72	0.02
Phenanthrene	1.01	4.04	4.07	0.03
Anthracene	1.01	4.17	4.07	−0.10
Chrysene	1.25	5.06	4.99	−0.07
p-Terphenyl	1.38	5.40	5.49	0.09

[a] Log $k'_w = (0.17 \pm 0.10) + (3.85 \pm 0.10)V_2/100$; $n = 7$, $R = 0.998$, S.D. = 0.03.

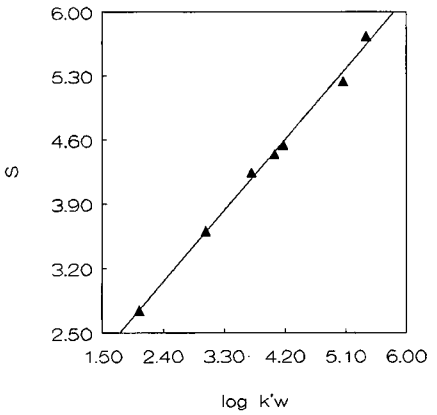

Fig. 1. Linear relationship between S and log k'_w for some PAHs in methanol–water on YWG-C_{18}. Conditions as in Table VI.

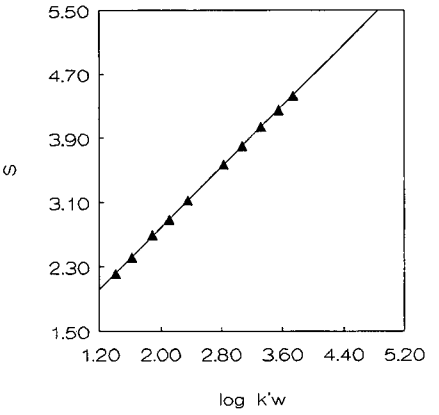

Fig. 2. Linear relationship between S and log k'_w for alkylbenzenes in acetonitrile–water mixtures. Conditions as in Table VIII.

TABLE VII

EXPERIMENTAL LOG k'_w VALUES [LOG k'_w (exp.)], Δ LOG $k'_w(CH_2)$ AND CALCULATED VALUES [LOG k'_w (calc.)] FOR *n*-ALKYLBENZENES IN METHANOL–WATER SYSTEM

Column, SIL-X-5-C_{18}; eluent, methanol–water (methanol from 60 to 95%, v/v). Log k'_w values taken from ref. 36.

Compound	n_c	Log k'_w (exp.)	Δ log k'_w (CH_2)	Log k'_w (calc.)[a]	Δ
Benzene	0	2.39	–	2.39	0
Toluene	1	3.03	0.64	2.98	−0.05
Ethylbenzene	2	3.54	0.58	3.58	0.04
Propylbenzene	3	4.17	0.59	4.17	0
Butylbenzene	4	4.76	0.59	4.77	0.01
Hexylbenzene	6	5.95	0.59	5.96	0.01
Octylbenzene	8	7.15	0.60	7.15	0
Decylbenzene	10	8.36	0.60	8.34	−0.02

[a] Log k'_w = (2.39 ± 0.02) + (0.60 ± 0.003)n_c; n = 8; R = 0.9999; S.D. = 0.004.

TABLE VIII

EXPERIMENTAL LOG k'_w VALUES [LOG k'_w (exp.)], ΔLOG $k'_w(CH_2)$ AND CALCULATED VALUES [LOG k'_w (calc.)] FOR *n*-ALKYLBENZENES IN ACETONITRILE–WATER SYSTEM

Column, YMC-phenyl; eluent, acetonitrile–water (acetonitrile from 50 to 80%, v/v). Log k'_w values recalculated from ref. 35.

Compound	n_c	Log k'_w (exp.)	ΔLog $k'_w(CH_2)$	Log k'_w (calc.)[a]	Δ
Benzene	0	1.41	–	1.41	0.00
Toluene	1	1.62	0.21	1.64	0.02
Ethylbenzene	2	1.89	0.24	1.88	−0.01
Propylbenzene	3	2.11	0.23	2.12	0.01
Butylbenzene	4	2.36	0.24	2.35	−0.01
Hexylbenzene	6	2.83	0.24	2.83	0.00
Heptylbenzene	7	3.07	0.24	3.06	−0.01
Octylbenzene	8	3.32	0.24	3.30	−0.02
Nonylbenzene	9	3.55	0.24	3.54	−0.01
Decylbenzene	10	3.74	0.23	3.77	0.03

[a] Log k'_w = (1.41 ± 0.01) + (0.237 ± 0.002)n_c; n = 10; R = 0.9999; S.D. = 0.003.

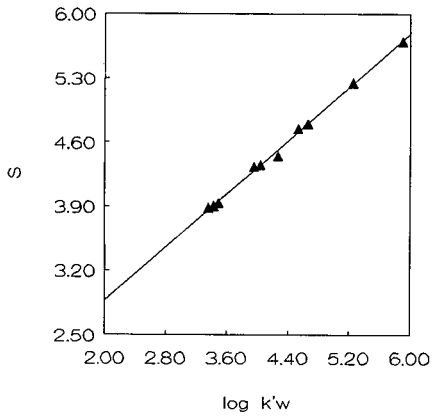

Fig. 3. Linear relationship between S and log k'_w for chlorosubstituted benzenes in methanol–water mixtures. Conditions as in Table II.

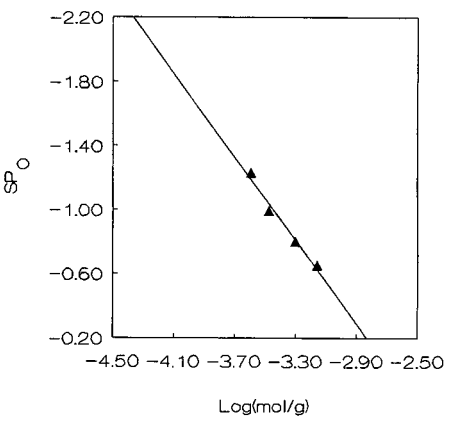

Fig. 4. Linear relationship between SP_0 and the logarithm of the surface coverage of C_{18} packings. For details, see Table IX.

log k'_w relationship for column pairs in RP-HPLC. As the phase ratio can be written as the ratio of the volume of the bonded ligands to that of the mobile phase [37,38], a linear relationship between SP_0 and the logarithm of the surface coverage can be obtained (see Fig. 4).

In conclusion, log k'_w in the retention equation log $k' = \log k'_w - S\varphi$ in RP-HPLC can be calculated by using the solvatochromic parameters. The coefficients in the correlation of log k'_w with the solvatochromic parameters of the solutes are determined mainly by the properties of water and the quasi-liquid-like chemical bonded phases.

When two or three of the solute parameters are constant and V_2 varies, a linear relationship between S and log k'_w was obtained. The parameter SP_0 in the correlation equation referring to the various reversed-phase columns with different carbon loadings was linearly correlated with the logarithm of the surface coverage.

TABLE IX

COEFFICIENTS OF SP_0, m, d, b AND a ON DIFFERENT COLUMNS PACKED WITH VARIOUS C_{18} PACKING MATERIALS WITH SURFACE COVERAGES RANGING FROM 0.255 TO 0.690 mmol/g

Log k'_w values for regression taken from refs. 37 and 38. The compounds used for the regression were acetophenone, *p*-cresol, benzyl alcohol, phenol, aniline, benzene, toluene, ethylbenzene, *n*-propylbenzene, *n*-butylbenzene, pentane, hexane, heptane, octane, 1-butanol, 1-pentanol and 1-hexanol.

C_{18} coverage (mmol/g)	SP_0	m	d	b	a	R	n
0.255	−1.23 ±0.16	7.07 ±0.23	−0.70 ±0.10	−2.95 ±0.20	−0.44 ±0.15	0.998	17
0.335	−0.99 ±0.16	6.97 ±0.23	−0.74 ±0.10	−2.92 ±0.20	−0.51 ±0.15	0.998	17
0.499	−0.80 ±0.16	6.93 ±0.22	−0.64 ±0.10	−2.96 ±0.20	−0.53 ±0.15	0.998	17
0.690	−0.65 ±0.16	6.95 ±0.23	−0.63 ±0.10	−2.94 ±0.20	−0.54 ±0.15	0.998	17

REFERENCES

1 J. G. Dorsey and K. A. Dill, *Chem. Rev.*, 89 (1989) 331.
2 K. Szabo, N. Le Ha, P. Schneider, P. Zeltmer and E. sz. Kováts, *Helv. Chim. Acta*, 67 (1984) 2128.
3 R. D. Golding, A. J. Barry and M. F. Burke, *J. Chromatogr.*, 384 (1987) 105.
4 D. E. Martire and R. E. Boehm, *J. Phys. Chem.*, 87 (1983) 1045.
5 B. L. Karger, J. R. Gant, A. Hartkopf and P. H. Weiner, *J. Chromatogr.*, 128 (1976) 65.
6 J. W. Dolan, J. R. Gant and L. R. Snyder, *J. Chromatogr.*, 165 (1979) 31.
7 N. Chen, Y. Zhang and P. Lu, *J. Chromatogr.*, 603 (1992) 35.
8 N. Chen, Y. Zhang and P. Lu, *J. Chromatogr.*, 606 (1992) 1.
9 T. Braumann, G. Weber and L. H. Grimme, *J. Chromatogr.*, 261 (1983) 329.
10 T. Hanai, *J. High Resolut. Chromatogr. Chromatogr. Commun.*, 6 (1983) 20.
11 T. Braumann, *J. Chromatogr.*, 373 (1984) 191.
12 J. L. G. Thus and J. C. Kraak, *J. Chromatogr.*, 320 (1985) 271.
13 W. E. Hammers, G. J. Meurs and G. L. de Ligny, *J. Chromatogr.*, 247 (1982) 1.
14 H. A. Cooper and R. J. Hurtubise, *J. Chromatogr.*, 360 (1986) 313.
15 P. Jandera, *J. Chromatogr.*, 352 (1986) 91.
16 N. El Tayar, H. van de Waterbeemd and B. Testa, *J. Chromatogr.*, 320 (1985) 305.
17 M. J. M. Wells and C. R. Clark, *J. Chromatogr.*, 284 (1984) 319.
18 A. Opperhuizen, T. L. Sinnige, J. M. D. van der Steen and O. Hutzinger, *J. Chromatogr.*, 388 (1987) 51.
19 P. M. Sherblom and R. P. Eganhouse, *J. Chromatogr.*, 454 (1988) 37.
20 R. Kaliszan, *Quantitative Structure Chromatographic Retention Relationships*, Wiley, New York, 1987.
21 D. Reymond, G. N. Chung, J. M. Mayer and B. Testa, *J. Chromatogr.*, 391 (1987) 97.
22 T. M. Jefferies, *J. Chromatogr.*, 185 (1979) 197.
23 K. Miyake, N. Mizuno and T. Terada, *J. Chromatogr.*, 439 (1988) 227.
24 L. R. Snyder, M. A. Quarry and J. L. Glajch, *Chromatographia*, 24 (1987) 33.
25 K. Valko, *J. Liq. Chromatogr.*, 10 (1987) 1663.
26 N. Chen, Y. Zhang and P. Lu, *J. Liq. Chromatogr.*, 15 (1992) 1523.
27 M. J. Kamlet, R. M. Doherty, M. H. Abraham, Y. Marcus and R. W. Taft, *J. Phys. Chem.*, 92 (1988) 5244.
28 J. H. Park, J. W. Carr, M. H. Abraham, R. W. Taft, R. W. Doherty and M. J. Kamlet, *Chromatographia*, 25 (1988) 373.
29 R. W. Taft, M. H. Abraham, G. R. Famini, R. M. Doherty, J. L. M. Abboud and M. J. Kamlet, *J. Pharm. Sci.*, 74 (1985) 807.
30 P. W. Carr, R. M. Doherty, M. J. Kamlet, R. W. Taft, W. Melander and Cs. Horváth, *Anal. Chem.*, 58 (1986) 2674.
31 D. E. Leahy, P. W. Carr, R. S. Pearlman, R. W. Taft and M. J. Kamlet, *Chromatographia*, 21 (1980) 473.
32 P. C. Sadek, P. W. Carr, R. M. Doherty, M. J. Kamlet and M. H. Abraham, *Anal. Chem.*, 57 (1985) 2971.
33 T. L. Hafkenscheid and C. Tomlinson, *J. Chromatogr. Sci.*, 24 (1986) 307.
34 T. Hanai and J. Hubert, *J. Chromatogr.*, 290 (1984) 197.
35 T. Hanai and J. Hubert, *J. Chromatogr.*, 291 (1984) 81.
36 M. Harnisch, H. J. Mockel and G. Schulze, *J. Chromatogr.*, 282 (1983) 315.
37 S. M. Petrovic and S. M. Lomic, *J. Liq. Chromatogr.*, 12 (1989) 59.
38 S. M. Petrovic and S. M. Lomic, *Chromatographia*, 27 (1989) 378.

Journal of Chromatography, 633 (1993) 43–56
Elsevier Science Publishers B.V., Amsterdam

CHROM. 24 743

Model building for the prediction of initial chromatographic conditions in pharmaceutical analysis using reversed-phase liquid chromatography

T. Hamoir, B. Bourguignon and D. L. Massart*

Pharmaceutical Institute, Vrije Universiteit Brussel, Laarbeeklaan 103, B-1090 Brussels (Belgium)

H. Hindriks

Analytical R&D Laboratories, Organon International BV, P.O. Box 20, 5340 BH Oss (Netherlands)

(First received February 5th, 1992; revised manuscript received October 8th, 1992)

ABSTRACT

The development of a first guess expert system in HPLC requires a rough estimate of retention properties. This paper investigates the extent to which the simplest possible descriptor, namely the total number of carbons in a molecule, can be used. For this purpose, experimental data acquired after investigation of this parameter on the retention behaviour of various acidic, basic and neutral compounds, for a mobile phase composed of methanol–phosphate buffer and a LiChrosorb CN column, were employed. The usefulness of the descriptor log P (calculated according to Rekker's fragment system) was also studied. Similar models were derived for both descriptors. Subsequently these models were used for the selection of initial chromatographic conditions. Both models were compared through a PRESS value. The regression equation including the descriptor log P was found to be more appropriate for the present purpose.

INTRODUCTION

Expert systems, an important application of artificial intelligence (AI), are becoming increasingly important in the field of analytical chemistry, particularly RPLC. Such computer systems contain the experts' chemical knowledge and can be applied by analytical chemists less experienced in the field. One of the possible functions of an RPLC expert system is the selection of initial chromatographic conditions. For this aim simple heuristics can be applied, as was performed in the expert system LABEL by considering the number of carbons in the solute(s). A molecule with a number of carbon atoms smaller than 10, for instance, was considered by LABEL to be non-hydrophobic [1]. The total number of carbons in a molecule is, of course, only a very rough indication of the polarity of a compound. Still, in the field studied (drugs with $M_r < 1500$) the approach used in LABEL [1] worked fairly well. A model for retention prediction would certainly be more convenient. Different approaches to retention prediction can be followed. A first point to be considered is whether to apply gradient elution or whether to use isocratic conditions in the final procedure. Certainly gradient elution is necessary if the retention range of the solutes is too wide. Moreover, the application of gradient elution presents some advantages, such as providing information on early- and late-eluting peaks for unknown samples, which under isocratic conditions can be lost owing to elution in the solvent peak or disappearance in the baseline, respectively. The gradient elution method is then best developed

* Corresponding author.

0021-9673/93/$06.00

as proposed by Dolan *et al.* [2], Chaminade [3] and Heinisch *et al.* [4].

Drylab and other such programs can also use the gradient results to predict optimum isocratic conditions. Often this works very well. However, sometimes one would like to develop the method using only isocratic elutions, as such an approach provides a better idea of peak shapes to be expected under those conditions. It is then necessary to have a good estimate of the solvent strength required to avoid unnecessary experimentation.

Several retention models have already been introduced for the prediction of retention in RPLC. However, these models are restricted to those cases where Martin's equation [5] applies, *i.e.*, to closely related compounds [6–14], and are therefore not applicable to a wide range of pharmaceutical compounds. The parameters should be simple and obtainable without additional experimentation. The most evident parameters to be included are the total number of carbons in the molecule, n_c, and the percentage of organic modifier in the mobile phase. A second descriptor will be considered, namely the log P value of the compound, which reflects the hydrophobic character of the molecule. Numerous publications have already described reasonable relationships between log $P_{o/w}$ of congeneric drugs and reversed-phase chromatographic retention data. The approach of Valko [15], however, was found to be applicable to structurally heterogeneous compounds. This approach was incorporated in a commercially available computer program to suggest HPLC eluent systems [16]. Recently, Kaliszan and Osmialowski [17] investigated the correlation between the chemical structure of structurally unrelated compounds and their retention on a polybutadiene-coated alumina column. The relationship between log k' extrapolated to pure water as the eluent (log k'_w) and log P, calculated by the fragmental method of Hansch and Leo [18], was found to be fairly satisfactory, considering the wide diversity of the structure. As the intention is to predict a mobile phase composition by computerized techniques, a computable descriptor is required. This is the case with log P, as it can be calculated by using the Hansch–Leo fragment system or the Rekker fragment system [19,20]. The latter method has been found to give a fairly good description of the hydrophobicity of more complex molecules [21]. Log P, calculated with Rekker's method, will therefore also be used as descriptor. Log P values can also be determined experimentally [22–24]. A database of experimental log P values, from which a first guess expert system would extract the value(s), seems an attractive approach. However, the insufficient availability of such values is an important problem with regard to our purposes and therefore not applicable in practice. The quality of the calculated log P values according to Rekker is not very good and better methods are available. However, we do not want lengthy and difficult calculations and the best possible log P values, as we only want to predict acceptable starting conditions that will be optimized in a later stage. Our purpose is therefore to investigate whether the relatively easy to obtain Rekker log P values are so much better than n_c that it is worth the trouble of performing log P calculations.

The aim of this study was to investigate whether it is feasible to derive a model for the retention prediction of a very diverse set of pharmaceutical compounds with the simple descriptors given, and subsequently to demonstrate the feasibility of the equation to determine initial chromatographic conditions. The quality of the prediction is expected to be superior using the descriptor log P. It should be stressed again that, in practice, chromatographers work in several steps. The initial guess is followed by an optimization of the separation and the aim is therefore not to obtain the best possible prediction, but a prediction good enough to guess with acceptable accuracy conditions for a first try.

THEORETICAL

The retention of the members of a homologous series has been described by Czok and Engelhardt [25] using an equation with four parameters:

$$\log k' = A_1 X_m + B_1 n_c + C_1 n_c X_m + D_1 \quad (1)$$

where X_m and n_c represent the percentage organic modifier in the mobile phase and the number of carbons in a homologous series, respectively. The quadratic dependence of log k' *versus* the percentage of organic modifier in a binary mobile phase, on the one hand, and the number of carbons in a homologous series, on the other, was shown by Schoenmakers [26] and Bogusz and Aderjan [27], respectively.

If quadratic terms are also included, the following equation is obtained:

$$\log k' = A_2X_m + B_2n_c + C_2n_cX_m + D_2X_m^2 + E_2n_c^2 + F_2 \quad (2)$$

By investigating whether the coefficients differ significantly from zero, the eventual equations can be obtained.

On the basis of previously published results [1], such equations can be derived for the descriptor n_c not only for homologous series, but also for a broader range of compounds and for the descriptor log P. It is the intention to investigate whether such equations permit the extent of retention of a specific compound as a function of the percentage of organic modifier to be predicted.

EXPERIMENTAL

High-performance liquid chromatography

The chromatographic system was a Varian 5000, equipped with a Rheodyne injector (sample loop 100 μl). The stationary phase was LiChrosorb cyanopropyl (particle size 5 μm; Merck) (250 × 4.0 mm I.D. column) and the mobile phase was mixtures of methanol and phosphate buffer (pH 3, ionic strength $u = 0.05$). The flow-rate was set at 1.0 ml/min. Detection was performed with a Perkin-Elmer LC 90 variable-wavelength UV detector at 254 μm and an attenuation of 0.05 a.u.f.s. Chromatograms were recorded with a Varian CDS 401 data system. All measurements were performed at 25°C in triplicate. The capacity factors, log k'_i, were determined as defined by

$$\log k' = (t_r - t_0)/t_0 \quad (3)$$

The dead time of the system, t_0, was determined as the first distortion of the baseline after injection of methanol.

Standards and reagents

All drugs were of pharmaceutical purity. Stock solutions of 500 μl/ml in methanol were preserved at 4°C. Dilutions to the final injected concentrations were prepared freshly daily. Methanol, phosphoric acid, sodium phosphate and disodium phosphate, of analytical-reagent grade, were purchased from Merck. Purified water was obtained with a Milli-Q water purification system (Millipore). Buffers (ionic strength 0.05) were prepared using phosphoric acid, sodium phosphate and disodium phosphate. The pH of the buffers was adjusted to the final value by using an Orion Research 501 digital ionalyser and the electrodes were calibrated with standard buffer solutions (pH 3.00 and 7.00; Merck). Prior to use, the buffers were filtered through a membrane filter (0.2 μm).

Molecular descriptors

Retention data were correlated with the following molecular descriptors: n_c, which was obtained from the empirical formula; experimentally determined log $P_{o/w}$ values, taken from the literature; and calculated log P values, making use of Rekker's hydrophobic fragmental system.

The following equation is used for the calculation of log P values:

$$\log P = \sum_i a_n f_n \quad (4)$$

where f is the hydrophobic fragmental constant, the lipophilicity contribution of a constituent part of a structure to the total lipophilicity, and a is a numerical factor indicating the incidence of a given fragment in the structure.

Statistics

Statistical analysis of the retention data was performed with the Statistical Package for Social Sciences (SPSS) [28]. This program runs on an IBM PC or compatible computers. The orthogonal regression program was written in our laboratory. It is written in Basic and runs on an Apple II computer.

RESULTS AND DISCUSSION

First the usefulness of both descriptors was examined with literature data. As it is our intention to use the eventual model for the prediction of first guess conditions for structurally unrelated compounds, only data sets corresponding to this description were studied. Hafkenscheid and Tomlinson [29] investigated the relationship between experimental log P values of strongly basic compounds ($pK_a > 7.5$) and reversed-phase liquid chromatographic capacity factors (log k') of partially ionized solutes using an aqueous methanol mobile phase. Good correlations (multiple $R = 0.974$) were obtained after correction for ionization effects. This, however, required a

knowledge of the mobile phase pH and solute pK_a values (both under aqueous and mobile phase conditions). As the pK_a will often not be known to the chromatographer, we studied the same relationship without taking into account ionization effects. At pH 4.0 a good correlation was obtained (multiple $R = 0.944$). The equation was also found highly significant ($p < 0.00005$). At pH 7.0 similar results were obtained (multiple $R = 0.863$ and $p < 0.00005$). By using the descriptor n_c instead of log P, less satisfactory results were found, as expected. At pH 4.0 a correlation of 0.413 and a significance level of 0.0404 were obtained for the equation. At pH 7.0 similar results were derived (multiple $R = 0.547$ and $p = 0.0038$).

De Biasi and Lough [30] studied the suitability of retention data of non-ionized organic bases ($pK_a > 7$) for the estimation of the lipophilicity characteristics on a styrene–divinylbenzene stationary phase. A correlation coefficient of 0.906 was obtained for the relationship between log k' and experimentally determined log P values. The equation was found to be significant at $p = 0.0001$. Similar results were obtained when we used the calculated log P values (multiple $R = 0.843$ and $p = 0.0043$). When we replaced log P with n_c, a correlation coefficient of 0.632 and a significance level of 0.0276 were obtained for the equation. These results demonstrate that the descriptor log P is indeed more suitable than n_c for retention prediction purposes. The descriptor n_c can be used, but one must be aware that this is a very rough descriptor of a drug's polarity. As our purpose is not to obtain the best prediction, which would certainly require extensive structural information, but rather an acceptable prediction, the suitability of n_c for retention prediction purposes will be investigated further in this paper.

Most of the retention prediction studies were performed on reversed-phase C_{18} columns. Our laboratory has several years of experience with the LiChrosorb cyanopropyl (CN) column. It has been shown that most drug analyses can be carried out with this type of column [31]. This study was therefore performed with the LiChrosorb CN column. The presence of residual silanol sites on the surface of such a chemically bonded alkylsilica stationary phase plays an important role. The retention behaviour of a solute then becomes the result not only of a partition process between the stationary and the mobile phase (comparable to the log P value of a solute), but also of adsorption on the residual silanol sites. These silanophilic interactions therefore have to be eliminated either by the use of additives in the mobile phase, such as propylamine, or by the use of buffers [32,33]. Recently, polymeric columns, based for example on styrene–divinylbenzene polymers, were introduced. On such a type of column the silanophilic interactions are non-existent. However, polymeric columns suffer from a low plate number in comparison with traditional columns [34]. In this study, the LiChrosorb CN column was used in combination with a buffered mobile phase,

TABLE I

CHROMATOGRAPHIC DATA FOR THE ACIDIC COMPOUNDS ON A LICHROSORB CN COLUMN WITH THE MOBILE PHASE METHANOL–PHOSPHATE BUFFER: (A) 10:90, (B) 30:70 AND (C) 50:50

No.	Compound	Empirical formula	pK_a	Log P (exp.)	Log P (calc.)	Log k'		
						A	B	C
1	Salicylic acid	$C_7H_6O_3$	3.0	2.26	1.28	−0.069	−0.292	−0.398
2	Nipasol	$C_{10}H_{12}O_3$	8.4	3.04	2.70	0.399	−0.054	−0.309
3	Furosemide	$C_{12}H_{11}ClN_2O_5S$	3.9	−0.83	1.47	0.611	0.084	−0.280
4	Chlorthalidone	$C_{14}H_{11}ClN_2O_4S$	9.3	2.82	0.54	0.254	−0.169	−0.352
5	Flufenamic acid	$C_{14}H_{10}F_3NO_2$	3.9	5.62	3.91	1.360	0.553	−0.112
6	Bumetanide	$C_{17}H_{20}N_2O_5S$	N.A.[a]	N.A.	2.63	0.832	0.170	−0.245
7	Diethylstilbestrol	$C_{18}H_{20}O_2$	10.9	5.07	5.79	1.228	0.352	−0.239
8	Sulindac	$C_{20}H_{17}FO_3S$	4.7	3.01	3.81	1.145	0.371	−0.158

[a] N.A. = Not available.

TABLE II

CHROMATOGRAPHIC DATA FOR THE BASIC COMPOUNDS ON A LICHROSORB CN COLUMN WITH THE MOBILE PHASE METHANOL–PHOSPHATE BUFFER: (A) 10:90, (B) 30:70 AND (C) 50:50

No.	Compound	Empirical formula	pK_a	Log P (exp.)	Log P (calc.)	Log k'		
						A	B	C
9	Amphetamine	$C_9H_{13}N$	9.9	1.76	1.96	−0.332	−0.403	−0.391
10	Triamterene	$C_{12}H_{11}N_7$	6.2	0.98[1]	–	0.113	−0.177	−0.297
11	Metoclopramide	$C_{14}H_{22}ClN_3O$	9.4	2.62	1.95	0.432	−0.037	−0.219
12	Diazepam	$C_{16}H_{13}ClN_2O$	3.4	2.80	2.95	0.755	0.277	−0.119
13	Triflupromazine	$C_{18}H_{19}F_3N_2S$	9.3	5.19	5.08	1.409	0.652	0.021
14	Mianserin	$C_{18}H_{20}N_2$	6.5	3.36	3.48	0.597	0.367	−0.062
15	Amitriptyline	$C_{20}H_{23}N$	9.4	5.04	5.55	1.136	0.490	0.000
16	Aprindine	$C_{22}H_{30}N_2$	10.0	4.76	5.92	0.346	0.086	−0.043
17	Mebeverine	$C_{25}H_{35}NO_5$	N.A.[a]	N.A.	6.27	1.175	0.402	−0.036

[a] N.A. = Not available.

and more specifically a phosphate buffer because, according to Wang and Lien [35], for acidic and neutral solutes this buffer appears to give partition coefficients closer to the values obtained with the *n*-octanol–water system than other buffers, such as acetate and hydrogencarbonate buffers.

The type of organic modifier also affects RPLC retention behaviour. The organic modifier methanol has been shown to interfere the least with the hydrophobic partition mechanism in RPLC among commonly used organic solvents, such as acetonitrile and tetrahydrofuran (THF) [36–39]. For this reason, an aqueous methanol mobile phase was used for this structure–retention study. The role of methanol may be much more active, owing to its interaction with surface silanols. Using methanol as solvent in a first guess study is compatible with optimization using the solvent strength, where acetonitrile and THF are introduced at a later stage. In fact, any solvent can be used initially using relationships from the literature that allow estimates of equivalent %B values for different solvents B to achieve the same retention time [26].

The investigation of the influence of the number

TABLE III

CHROMATOGRAPHIC DATA FOR THE NEUTRAL COMPOUNDS ON A LICHROSORB CN COLUMN WITH THE MOBILE PHASE METHANOL–PHOSPHATE BUFFER: (A) 10:90, (B) 30:70 AND (C) 50:50

No.	Compound	Empirical formula	Log P (exp.)	Log P (calc.)	Log k'		
					A	B	C
18	Phenacetin	$C_{10}H_{13}NO_2$	1.58	1.87	0.147	−0.177	−0.319
19	Pentoxifylline	$C_{13}H_{18}N_4O_3$	0.29	−1.67	0.179	−0.152	−0.277
20	Griseofulvin	$C_{17}H_{17}ClO_6$	2.18	1.16	0.882	0.225	−0.174
21	Testosterone	$C_{19}H_{28}O_2$	3.32	3.95	0.763	0.143	−0.210
22	Methyltestosterone	$C_{20}H_{30}O_2$	3.36	4.47	0.810	0.202	−0.180
23	Triamcinolone	$C_{21}H_{27}FO_6$	1.16	−3.08	0.120	−0.183	−0.346
24	Progesterone	$C_{21}H_{30}O_2$	3.87	4.43	N.A.[a]	0.372	−0.101
25	Betamethasone	$C_{22}H_{29}FO_5$	1.94	−0.93	0.400	−0.035	−0.289

of carbons in the molecule, log P and the percentage of organic modifier (methanol) in the mobile phase on the retention was carried out with 25 pharmaceutical compounds of various polarities. Molecules with different numbers of carbons and also different functional groups or acidic–basic properties were selected. The chromatographic data are listed in Tables I, II and III for acidic, basic and neutral compounds, respectively.

Prior to the application of multiple regression techniques, a comparison was made between linear and orthogonal regression. The linear (multiple) regression techniques assume that the error exists only in the y direction (response). In fact, both descriptors are only indications of the hydrophobicity of a molecule and are therefore also subject to error. In such a situation orthogonal regression techniques [40], which are equivalent to determining the first principal component (PC1) of a matrix consisting of i rows (objects) and two columns (variables), are preferred. The results, including the slope and intercept, for the set of acidic compounds and a mobile phase composed of methanol–phosphate buffer (10:90), are listed in Table IV. The difference in the results obtained between the two regression techniques is clearly small. Similar results were found for the other chromatographic conditions (30 and 50% methanol) and also for the set of basic and neutral compounds. Further investigation was therefore restricted to the more usual multiple regression analysis.

Multiple regression analysis is a frequently used statistical method to study the relationships among variables. The aim is to describe a dependent variable by a set of independent variables, more specifically to investigate the following linear relationship:

$$Y_i = \sum_{j=1}^{k} \beta_j X_{ij} + e_i \quad (5)$$

where Y_i represents the dependent variable, X_1 to X_k the different independent variables and e_i the residuals. The regression coefficients β_j are estimated by multiple linear regression. The most commonly used measure of the goodness of fit of the model is R^2 or its square root, called the multiple R. The adjusted R^2, however, reflects best the goodness of fit of the model in the population [28]. For the validation of linear models the F-statistic and its corresponding

TABLE IV

COMPARISON OF LINEAR *VERSUS* ORTHOGONAL REGRESSION FOR THE RELATIONSHIP LOG k' *VERSUS* THE DESCRIPTORS n_c AND LOG P (CALCULATED) FOR THE ACIDIC COMPOUNDS

The mobile phase was methanol–phosphate buffer (10:90).

Parameter	Linear regression		Orthogonal regression	
	n_c	Log P	n_c	Log P
Slope	0.0919	0.2389	0.0924	0.2431
Intercept	−0.5657	−0.0443	−0.5729	−0.0577

significance level p are available. These are described in most textbooks on regression analysis. Different procedures can be applied for the selection of appropriate variables, *i.e.*, stepwise regression, forward selection and backward elimination. Stepwise regression analysis is the most commonly used procedure. Less frequently used are the other two procedures, which need not result in the same equation. However, as stepwise regression investigates the significance of previously entered variables, which is not the case for the other two procedures, the stepwise technique is to be preferred.

Multiple regression was carried out by first considering the dependent variable log k' and the independent variables n_c, X_m, the interaction term and the quadratic terms.

The regression equation (eqn. 6) was derived for the acidic compounds by stepwise regression analysis (values of p-to-enter and p-to-remove 0.05 and 0.10, respectively). The regression coefficients are accompanied by the 95% confidence intervals according to the t-test. The number of data points (n), the standard deviation of the residuals (s), the multiple correlation coefficient (Mult. R), the adjusted R^2, the calculated F-value of the derived equation and its significance level (p) are also presented.

In eqn. 6, the retention is related to the number of carbons in the molecule on the one hand and the interaction between the percentage of organic modifier in the mobile phase and the number of carbons on the other. Both parameters were found to be significant at $p < 0.00005$. The quadratic terms and

$$\log k' = 0.1048\ (\pm 0.0271)n_c - 1.7694 \cdot 10^{-3}\ (\pm 0.4099 \cdot 10^{-3})n_c X_m - 0.5308\ (\pm 0.3524) \quad (6)$$

$n = 24$; $s = 0.2297$; Mult. $R = 0.9094$; Adj. $R^2 = 0.8105$; F(eqn.) = 50.19; $p < 0.00005$

$$\log k' = 0.0521\ (\pm 0.0250)n_c - 0.0198\ (\pm 0.0072)X_m - 0.0578\ (\pm 0.4926) \quad (7)$$

$n = 27$; $s = 0.2954$; Mult. $R = 0.8239$; Adj. $R^2 = 0.6521$; F(eqn.) = 25.36; $p < 0.00005$

$$\log k' = -0.0176\ (\pm 0.0061)X_m + 0.6226\ (\pm 0.2124) \quad (8)$$

$n = 23$; $s = 0.2269$; Mult. $R = 0.7953$; Adj. $R^2 = 0.6150$; F(eqn.) = 36.15; $p < 0.00005$

$$\log k' = 0.0249\ (\pm 0.0181)n_c - 0.0215\ (\pm 0.0050)X_m + 0.3978\ (\pm 0.3297) \quad (9)$$

$n = 47$; $s = 0.2738$; Mult. $R = 0.8080$; Adj. $R^2 = 0.6371$; F(eqn.) = 41.37; $p < 0.05$

$$\log k' = -9.9935 \cdot 10^{-3}\ (\pm 0.0108)X_m + 0.2995\ (\pm 0.1156)\log P - 5.2776 \cdot 10^{-3}\ (\pm 3.3843 \cdot 10^{-3})X_m \log P + 0.1029\ (\pm 0.3692) \quad (10)$$

$n = 24$; $s = 0.2073$; Mult. $R = 0.9305$; Adj. $R^2 = 0.8457$; F(eqn.) = 43.01; $p < 0.00005$

$$\log k' = -0.0149\ (\pm 0.0116)X_m + 0.0361\ (\pm 0.0187)\log P^2 - 3.0943 \cdot 10^{-3}\ (\pm 2.9687 \cdot 10^{-3})X_m \log P + 0.4519\ (\pm 0.3475) \quad (11)$$

$n = 21$; $s = 0.2622$; Mult. $R = 0.8932$; Adj. $R^2 = 0.7621$; F(eqn.) = 22.35; $p < 0.00005$

$$\log k' = -0.0198\ (\pm 0.0074)X_m + 0.1269\ (\pm 0.0652)\log P + 0.3518\ (\pm 0.3536) \quad (12)$$

$n = 27$; $s = 0.3042$; Mult. $R = 0.8121$; Adj. $R^2 = 0.6312$; F(eqn.) = 23.25; $p < 0.00005$

$$\log k' = 0.3352\ (\pm 0.0871)X_m - 5.1533 \cdot 10^{-3}\ (\pm 1.7315 \cdot 10^{-3})X_m \log P + 0.4067\ (\pm 0.2532) \quad (13)$$

$n = 24$; $s = 0.2414$; Mult. $R = 0.8729$; Adj. $R^2 = 0.7392$; F(eqn.) = 33.60; $p < 0.00005$

$$\log k' = -0.0182\ (\pm 4.76 \cdot 10^{-3})X_m + 0.0520\ (\pm 0.0283)\log P + 0.5811\ (\pm 0.1672) \quad (14)$$

$n = 23$; $s = 0.1763$; Mult. $R = 0.8880$; Adj. $R^2 = 0.7674$; F(eqn.) = 37.30; $p < 0.00005$

$$\log k' = -8.6645 \cdot 10^{-3}\ (\pm 8.1355)X_m + 0.2903\ (\pm 0.1237)\log P - 4.6905 \cdot 10^{-3}\ (\pm 3.4548 \cdot 10^{-3})X_m \log P + 0.0415\ (\pm 0.2826) \quad (15)$$

$n = 23$; $s = 0.1391$; Mult. $R = 0.9355$; Adj. $R^2 = 0.8554$; F(eqn.) = 44.37; $p < 0.00005$

also the term taking into account the pure effect of the percentage of organic modifier in the mobile phase were found to be insignificant. Initially the latter was introduced in the regression equation ($p < 0.00005$), but in a final step this variable was removed ($p = 0.8277$). The introduction of the interaction term in the equation was expected, because the change in log k' by changing the percentage of organic modifier depends on the number of carbons in the molecule (Fig. 1). This is true also for the basic and neutral compounds (Figs. 2 and 3).

About 80% of the model was explained by means of the selected parameters, which was considered satisfactory taking the diversity of the pharmaceutical compounds into account.

For the set of basic compounds the regression equation (eqn. 7) was obtained by stepwise regression (value of p-to-enter and p-to-remove 0.05 and 0.10, respectively). In comparison with eqn. 6, the term $n_c X_m$ was substituted by X_m. The latter term and the term n_c were found to be significant at $p < 0.00005$ and $p = 0.0002$, respectively.

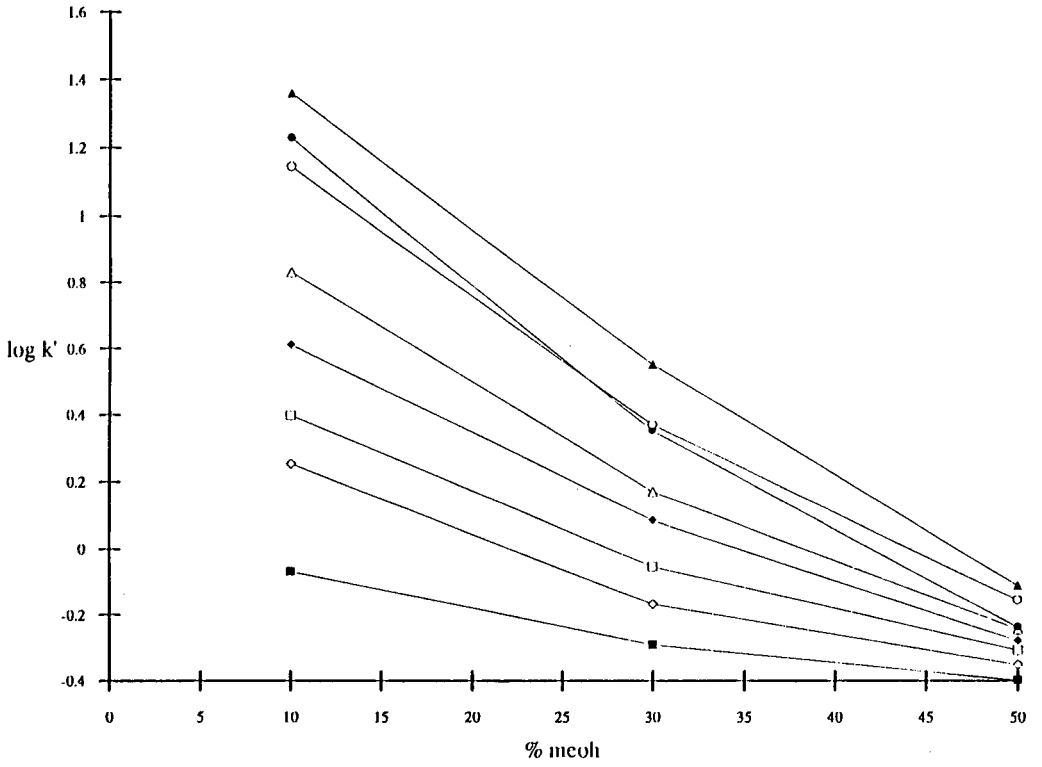

Fig. 1. Plot of log k' *versus* the volume percentage of methanol (meoh) with phosphate buffer (pH 3, $u = 0.05$) for acidic compounds. ■ = Salicylic acid; □ = nipasol; ◆ = furosemide; ◇ = chlorthalidone; ▲ = flufenamic acid; △ = bumetanide; ● = diethylstilbestrol; ○ = sulindac.

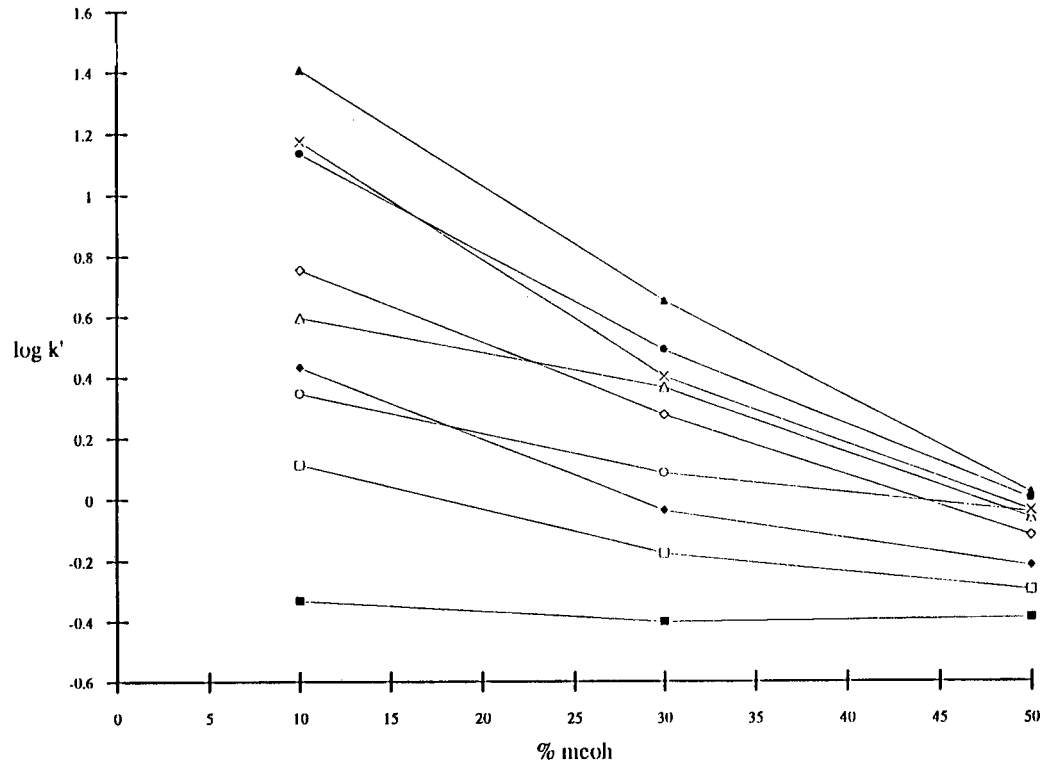

Fig. 2. Plot of log k' *versus* the volume percentage of methanol with phosphate buffer (pH 3, $u = 0.05$) for basic compounds. ■ = Amphetamine; □ = triamterene; ◆ = metoclopramide; ◇ = diazepam; ▲ = triflupromazine; △ = mianserin; ● = amitriptyline; ○ = aprindine; × = mebeverine.

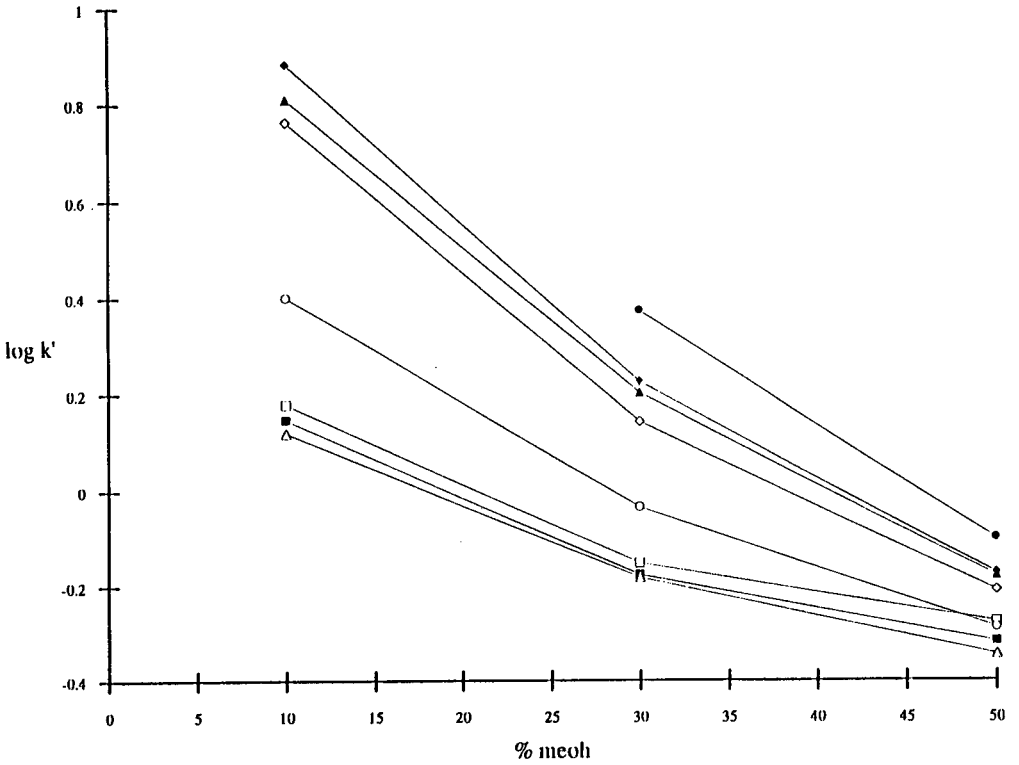

Fig. 3. Plot of log k' *versus* the volume percentage of methanol with phosphate buffer (pH 3, $u = 0.05$) for neutral compounds. ■ = Phenacetin; □ = pentoxifylline; ◆ = griseofulvin; ◇ = testosterone; ▲ = methyltestosterone; △ = triamcinolone; ● = progesterone; ○ = betamethasone.

For the neutral compounds eqn. 8 was derived by stepwise regression analysis (value of p-to-enter and p-to-remove 0.05 and 0.10, respectively). The only significant factor ($p < 0.00005$) is the volume percentage of organic modifier. The number of carbons in the molecule and the interaction term were found to be insignificant with p-values of 0.1145 and 0.8871, respectively, probably because the diversity in polarity for the set of neutral compounds studied was insufficient or that the dispersion of the results is too high.

The mobile phase consisted of a methanol–phosphate buffer (pH 3). At this pH most of the acidic molecules are present in non-ionic form, which is also the case for the neutral compounds. Therefore, the neutral and acidic compounds were considered together (eqn. 9). By stepwise regression the percentage of organic modifier ($p < 0.00005$) and the number of carbons in the molecule ($p = 0.0081$) were introduced into the regression equation. The interaction term was found to be insignificant ($p = 0.1676$).

In a second step, the usefulness of the descriptor log P, calculated according to Rekker's fragment system, was investigated. Regarding the application of Rekker's method, several problems were encountered. For the compound triamterene the contribution of the pteridine fragment was unavailable. As further division of this fragment would lead to a serious underestimation of the log P value, the experimental value was used. The application of Rekker's method to steroid compounds (testosterone, methyltestosterone, triamcinolone, progesterone and betamethasone) would certainly result in an overestimation of the log P value. For this reason, the log P values were calculated by using the experimental log P value of desoxycorticosterone ($\log P_{exp.} = 2.80$) as representative of the base structure of such compounds and also taking into account the Rekker fragment values for the differ-

ences in functional groups. As the experimental log P values were available for most compounds, these were also used for comparison with the calculated values (Tables I, II and III).

For the set of acidic compounds the regression equation (eqn. 10) was derived by stepwise regression analysis (value of p-to-enter and p-to-remove 0.05 and 0.10, respectively). In eqn. 10, the retention is related to X_m ($p = 0.0681$), log P ($p < 0.00005$) and the interaction term ($p = 0.0040$); the quadratic terms were found to be insignificant. The latter is in accordance with eqn. 1.

Similar results were obtained with the experimental log P values (eqn. 11). However, log P was not included in the regression equation ($p = 0.9437$), but rather its quadratic form ($p = 0.0008$). The terms X_m and the interaction term were found to be significant at $p = 0.0145$ and $p = 0.0420$, respectively.

For the set of basic compounds eqn. 12 was obtained by stepwise regression analysis (value of p-to-enter and p-to-remove 0.05 and 0.10, respectively). In eqn. 12, in comparison with the set of acidic compounds, the interaction term was found to be insignificant ($p = 0.0854$).

With the experimental log P values (eqn. 13), X_m ($p = 0.8022$) was replaced with the interaction term ($p < 0.00005$). The term log P was found to be significant at $p < 0.00005$.

For the neutral compounds, similar results to those for the basic compounds were derived (eqn. 14). The interaction term was found to be insignificant at $p = 0.0677$. In comparison with eqn. 8 the descriptor log P was introduced into the regression equation. This resulted in a change in R^2 of 0.1560, which was found to be significant at $p = 0.0010$. The term X_m was found to be significant at $p < 0.00005$.

Here also different results were obtained with the experimental log P values (eqn. 15). The interaction term was also found to be significant ($p = 0.0104$). The other terms, X_m, log P and the interaction term, were found to be significant at $p = 0.0380$, $p = 0.0001$ and $p = 0.0104$, respectively.

Comparison of the results obtained with the experimental log P values on the one hand and the log P values, calculated according to Rekker's fragment system, on the other demonstrates that the calculated descriptor log P values can be used instead of the experimental values.

Cross-validation of the model

Many regression analyses study only the estimation of coefficients and the quality of the fit. It is necessary, however, also to validate regression methods and to investigate how good the prediction is. This requires cross-validation. Cross-validation of a model is performed by leaving out each molecule in turn from the data set, by computing the regression equation without the molecule in question and then predicting the retention for the same molecule. This approach is called the leave-one-out method (LOOM). The predicted (estimated) value is then compared with the experimental (observed) value through a PRESS (prediction error sum of squares) value:

$$\text{PRESS} = \sum_i [y_{(i)} - \hat{y}_{(i)}]^2 \tag{16}$$

where $y_{(i)}$ and $\hat{y}_{(i)}$ represent the experimental value and the predicted value after the LOOM, respectively. PRESS is used to assess the predictive performance of the model. The model that produces the lowest PRESS value is preferred [41,42].

From the chromatographic point of view, the accuracy of the selection of initial chromatographic conditions with the model is most interesting. For this purpose eqns. 6 and 7 were rearranged as follows:

$$X_m = \frac{\log k' - An_c - C}{Bn_c} \tag{17}$$

$$X_m = \frac{\log k' - An_c - C}{B} \tag{18}$$

The following equations were derived for the model including the descriptor log P for acidic and basic (neutral) compounds, respectively:

$$X_m = \frac{\log k' - B \log P - D}{A + C \log P} \tag{19}$$

$$X_m = \frac{\log k' - B \log P - C}{A} \tag{20}$$

The cross-validation was hence performed by comparing the percentage of organic modifier required to obtain a given k', predicted by eqns. 17–20 and an experimental value. The latter was calculated by interpolation using the slopes and intercepts derived for the relationship of log k' *versus* X_m for

each compound. The k' values were selected to obtain a percentage of organic modifier situated in the investigated area, *i.e.*, between 10 and 50% methanol. The same k' values, together with the cross-validation regression coefficients and either the number of carbons in the molecule or the calculated log P value were used to predict the percentage of organic modifier from eqns. 17–20. These results are given in Tables V and VI. For amphetamine no interpolated value was obtained because of the very low retention of this molecule ($k' < 0.5$). For trifluprómazine and flufenamic acid, which exhibit a very high retention ($k' > 20$) for a mobile phase containing a small amount of the organic modifier (10% methanol), the prediction was unsatisfactory in comparison with the other molecules. Similar results, but less pronounced, were obtained with the descriptor log P. For aprindine less satisfactory results were also found. These molecules, except amphetamine, were designated as outliers on a statistical basis. Such values certainly influence the quality of the prediction. However, outliers can also be considered as containing a lot of information and, bearing in mind the purpose of this study, these values were taken into account.

The same strategy was used to determine the quality of the prediction for the neutral compounds. For the determination of the percentage of organic modifier from eqns. 18 and 20, the cross-validation regression coefficients for the set of acidic and

TABLE V

ABSOLUTE DIFFERENCES BETWEEN THE INTERPOLATED VALUE (I) AND THE PERCENTAGE OF ORGANIC MODIFIER PREDICTED BY THE MODEL INCLUDING THE DESCRIPTOR n_c (II) OR CALCULATED LOG P (III) FOR ACIDIC COMPOUNDS

Compound	k'	Methanol (%)			|II − I|	|III − I|
		I	II	III		
Salicylic acid	0.5	36	47	48	11	12
Nipasol	0.5	48	46	50	2	2
	1.0	31	29	38	2	7
Furosemide	0.5	50	48	47	2	3
	1.0	36	34	29	2	7
	3.0	15	11	0	4	15
Chlorthalidone	0.5	44	51	44	7	0
	1.0	24	39	18	15	6
Flufenamic acid	1.0	46	36	40	10	6
	3.0	33	15	24	18	9
	5.0	27	6	16	21	11
Bumetanide	0.5	51	52	50	1	1
	1.0	39	42	37	3	2
	3.0	22	27	17	5	5
	5.0	13	19	7	6	6
Diethylstilbestrol	0.5	50	52	55	2	5
	1.0	42	43	49	1	7
	3.0	29	27	38	2	9
	5.0	23	20	33	3	10
	10.0	15	10	27	5	12
Sulindac	1.0	44	45	41	1	3
	3.0	29	32	25	3	4
	5.0	20	26	17	6	3
	10.0	13	17	7	4	6

TABLE VI

ABSOLUTE DIFFERENCES BETWEEN THE INTERPOLATED VALUE (I) AND THE PERCENTAGE OF ORGANIC MODIFIER PREDICTED BY THE MODEL INCLUDING THE DESCRIPTOR n_c (II) OR CALCULATED LOG P (III) FOR BASIC COMPOUNDS

Compound	k'	Methanol (%)			|II − I|	|III − I|
		I	II	III		
Amphetamine	0.5	N.A.[a]	42	49	N.A.	N.A.
Triamterene	0.5	46	45	39	1	7
	1.0	17	30	25	13	8
Metoclopramide	1.0	34	34	30	0	4
Diazepam	1.0	44	39	35	5	9
	3.0	22	14	11	8	11
Trifluprómazine	1.0	50	43	49	7	1
	3.0	36	16	23	20	13
	5.0	30	4	10	26	20
Mianserin	1.0	49	44	39	5	10
	3.0	17	20	14	3	3
Amitriptyline	1.0	49	49	54	0	5
	3.0	32	24	28	8	4
	5.0	24	12	16	12	8
Aprindine	1.0	43	59	61	16	18
Mebeverine	1.0	47	71	61	24	14
	3.0	31	45	35	14	4
	5.0	24	33	23	9	1
	10.0	14	17	7	3	7

[a] N.A. = Not available.

TABLE VII

ABSOLUTE DIFFERENCES BETWEEN THE INTERPOLATED VALUE (I) AND THE PERCENTAGE OF ORGANIC MODIFIER PREDICTED BY THE MODEL INCLUDING THE DESCRIPTOR n_c (II) OR CALCULATED LOG P (III) FOR THE NEUTRAL MOLECULES

Compound	k'	Methanol (%)			|II − I|	|III − I|
		I	II	III		
Phenacetin	0.5	45	55	50	10	10
	1.0	20	32	39	12	19
Pentoxifylline	0.5	49	53	44	4	5
	1.0	23	35	28	12	5
Griseofulvin	1.0	43	38	34	5	9
	3.0	25	16	5	9	20
Testosterone	1.0	40	39	44	1	4
	3.0	20	20	16	0	4
	5.0	11	11	3	0	8
Methyltesto-sterone	1.0	41	40	45	1	4
	3.0	22	22	17	0	5
	5.0	13	13	4	0	9
Triamcinolone	1.0	18	42	24	24	6
Progesterone	1.0	46	39	44	7	2
	3.0	26	23	18	3	8
	5.0	16	15	5	1	11
Betamethasone	1.0	31	42	29	11	2

neutral compounds were used. These results are given in Table VII.

Through a PRESS value the predictive performance of the model was assessed and the most appropriate descriptor selected. From the results in Table VIII it can be concluded that the descriptor log P should be preferred to n_c. On the basis of these results and also the literature results the descriptor log P should be preferred.

TABLE VIII

PRESS VALUES FOR THE MODEL INCLUDING THE DESCRIPTOR n_c OR CALCULATED LOG P FOR THE SET OF ACIDIC, BASIC AND NEUTRAL COMPOUNDS

Group	PRESS	
	n_c	Log $P_{calc.}$
Acidic compounds ($n = 24$)	1468	1289
Basic compounds ($n = 18$)	2744	1701
Neutral compounds ($n = 17$)	1268	1439

TABLE IX

MEAN OF THE ABSOLUTE DIFFERENCES BETWEEN THE INTERPOLATED VALUE AND THE PERCENTAGE OF ORGANIC MODIFIER PREDICTED BY THE MODEL INCLUDING THE DESCRIPTOR LOG P (CALCULATED)

Group	Mean methanol content ± S.D. (%)
Acidic compounds ($n = 24$)	6 ± 4
Basic compounds ($n = 18$)	8 ± 5
Neutral compounds ($n = 17$)	8 ± 5

As the mobile phase consisted of methanol–phosphate buffer (pH 3), the ionization effects certainly play an important role. This is most certainly so for the basic compounds, which resulted in less satisfactory results for this type of compound in comparison with the acidic compounds. Other workers have also found that basic compounds cause problems [43]. Corrections for ionization effects are possible [29], but very impractical with regard to our purpose. Apart from ionization effects, stationary phase effects are likely to play an important role with basic compounds.

The results for the selection of initial chromatographic conditions are presented in Table IX as the mean (and standard deviation) of the absolute differences between the interpolated and the predicted value for the descriptor log P. The initial chromatographic conditions to obtain a certain k' will be under- or overestimated within a range of 6–8% methanol, which from the chromatographic point of view is satisfactory as a first guess, considering the diversity of molecular structures investigated. With the equation including the descriptor n_c, the range varied from 6 to 10% methanol but with a larger standard deviation of the mean prediction error.

CONCLUSIONS

The parameter log P, calculated according to the Rekker fragment system, has been found to be the

most suitable descriptor for the prediction of initial chromatographic conditions. The model, including the parameter log P, can cover a wide composition range (organic modifier contents between 10 and 50%) to predict a capacity factor situated between 1 and 10. However, in some instances, the prediction was less satisfactory. A source of error causing this bad prediction is the calculation of the log P values. Steric effects, for instance, cannot be taken into account. Hence, calculated log P values are certainly limited in their ability to predict retention as a function of the percentage of organic modifier in the mobile phase. However, it was necessary for this approach. Some suggestions are available in the literature for improving the prediction of log P values. However, our purpose was not to obtain the best prediction, but an acceptable one. Moreover, the regression results with the experimental log P values were very similar to these with the calculated log P values, indicating the possibility of applying the latter values for retention prediction and also the prediction of initial chromatographic conditions. Hence, log P values calculated according to Rekker seem sufficient for our purposes.

In the near future the retention prediction model will be incorporated into a first guess expert system. On the basis of the log P value of a compound the initial solvent composition can be predicted once the desired capacity factor has been defined. In some instances, however, Rekker's method is not applicable. The experimental log P can then be used, provided that this value is available. If not, the conditions can still be predicted on the basis of the total number of carbons in the molecule, *i.e.*, the retention model including the descriptor n_c will also be incorporated in the first guess expert system. The sample can, on the other hand, also contain different solutes of interest. In such a case, the average log P value of the compounds will be used to select the first guess.

ACKNOWLEDGEMENT

This work was financially supported by Fonds voor Geneeskundig en Wetenschappelijk Onderzoek (FGWO).

REFERENCES

1 M. De Smet, G. Musch, A. Peeters, L. Buydens and D. L. Massart, *J. Chromatogr.*, 485 (1989) 237.
2 J. W. Dolan, D. C. Lommen and L. R. Snyder, *J. Chromatogr.*, 485 (1989) 91.
3 P. Chaminade, *Ph. D. Thesis*, University of Paris-Sud, Paris, 1992.
4 S. Heinisch, J. L. Rocca and M. Kolosky, *Chromatographia*, 29 (1990) 483.
5 L. R. Snyder and J. J. Kirkland, *Introduction to Modern Liquid Chromatography*, Wiley-Interscience, New York, 1979.
6 P. Jandera, *Chromatographia*, 19 (1984) 101.
7 P. Jandera, *J. Chromatogr.*, 314 (1984) 13.
8 P. Jandera, *J. Chromatogr.*, 352 (1986) 91.
9 P. Jandera, *J. Chromatogr.*, 352 (1986) 111.
10 K. Jinno, M. Yamagami and M. Kuwajima, *Chromatographia*, 25 (11) (1988) 974.
11 K. Jinno, *A Computer-Assisted Chromatography System*, Hüthig, Heidelberg, 1990.
12 H. A. Cooper and R. J. Hurtubise, *J. Chromatogr.*, 360 (1986) 313.
13 S. F. Y. Li and H. K. Lee, *Chromatographia*, 25 (1988) 515.
14 R. M. Smith and C. M. Burr, *J. Chromatogr.*, 485 (1989) 325.
15 K. Valko, *J. Liq. Chromatogr.*, 7 (1984) 1405.
16 *EluEx 1.0*, CompuDrug Chemistry, Budapest, 1991.
17 R. Kaliszan and K. Osmialowski, *J. Chromatogr.*, 506 (1990) 3.
18 C. Hansch and A. Leo, *Substituent Constants for Correlation Analysis in Chemistry and Biology*, Wiley, New York, 1979.
19 R. F. Rekker, *The Hydrophobic Fragmental Constant —Its Derivation and Application*, Elsevier, Amsterdam, 1977.
20 R. F. Rekker and H. M. de Kort, *Eur. J. Med. Chem. Chim. Ther.*, 14 (1979) 479.
21 R. E. Koopmans and R. F. Rekker, *J. Chromatogr.*, 285 (1984) 267.
22 Y. C. Martin, *Quantitative Drug Design*, Marcel Dekker, New York, 1978.
23 T. Braumann, *J. Chromatogr.*, 373 (1986) 191.
24 R. S. Tsai, N. El Tayar, B. Testa and Y. Ito, *J. Chromatogr.*, 538 (1991) 119.
25 M. Czok and H. Engelhardt, *Chromatographia*, 27 (1989) 5.
26 P. J. Schoenmakers, *Optimization of Chromatographic Selectivity*, Elsevier, Amsterdam, 1st ed., 1986.
27 M. Bogusz and R. Aderjan, *J. Chromatogr.*, 435 (1988) 43.
28 *SPSS/PC for the IBM PC/XT, Release 1.0*; SPSS, Chicago, 1984, Ch. 17.
29 T. L. Hafkenscheid and E. Tomlinson, *J. Chromatogr.*, 292 (1984) 305.
30 V. De Biasi and W. J. Lough, *J. Chromatogr.*, 353 (1986) 279.
31 M. De Smet, G. Hoogewijs, M. Puttemans and D. L. Massart, *Anal. Chem.*, 56 (1984) 2662.
32 D. Chan Leach, M. A. Stadalius, J. S. Berus and L. R. Snyder, *LC · GC Int.*, 1, No. 5 (1988) 22.
33 J. W. Dolan, *LC · GC Int.*, 2, No. 7 (1989) 18.
34 R. Vervoort, H. Hindriks, M. Vrieling and F. Maris, *18th International Symposium on Chromatography, Amsterdam, 1990*, abstract Mo-P-092.
35 P. Wang and E. J. Lien, *J. Pharm. Sci.*, 69 (1980) 662.

36 N. Tanaka, G. Goodell and B. L. Karger, *J. Chromatogr.*, 158 (1978) 233.
37 T. Braumann, G. Werber and L. H. Grimme, *J. Chromatogr.*, 261 (1983) 329.
38 B. L. Karger, J. R. Gant, A. Hartkopf and P. H. Wiener, *J. Chromatogr.*, 128 (1976) 65.
39 A. Bechalany, A. Tsantili-Kakoulidou, N. El Tayar and B. Testa, *J. Chromatogr.*, 541 (1991) 221.
40 J. Mandel, *The Statistical Analysis of Experimental Data*, Wiley, New York, 1964.
41 F. Mosteller and J. W. Tukey, *Data Analysis and Regression*, Addison-Wesley, 1977.
42 G. H. Golub, M. Heath and G. Wakba, *Technometrics*, 21 (1979) 215.
43 J. A. Lewis, D. C. Lommen, W. D. Raddatz, J. W. Dolan and L. R. Snyder, *J. Chromatogr.*, 592 (1992) 183.

Journal of Chromatography, 633 (1993) 57–63
Elsevier Science Publishers B.V., Amsterdam

CHROM. 24 715

Application of chemometrically processed chromatographic data for pharmacologically relevant classification of antihistamine drugs

René Gami-Yilinkou, Antoni Nasal and Roman Kaliszan*

Department of Biopharmaceutics and Pharmacodynamics, Medical Academy of Gdańsk, Gen. J. Hallera 107, 80-416 Gdańsk (Poland)

(Received July 16th, 1992)

ABSTRACT

For a set of 22 drugs known to modify physiological effects of endogenous histamine, high-performance liquid chromatographic (HPLC) retention data were determined employing two reversed-phase columns, seven compositions of methanol–buffer eluent and three pH values (acidic, neutral and alkaline) of the buffer. Logarithms of capacity factors, normalized to 100% buffer eluent (log k'_w), were determined by extrapolation of the respective data in five HPLC systems studied. Chemometric analysis of the 5 × 22 matrix of log k'_w data obtained in five HPLC systems for 22 drug solutes allowed the extraction of two main principal components which accounted for 96% of total data variance. The distribution of individual drugs on the plane determined by the two first principal component axes forms the patterns, which are in excellent agreement with the established pharmacological classification of the structurally diverse compounds studied. It was demonstrated that systematic information extracted by chemometric analysis of behaviour of solutes in diverse HPLC systems has direct relevance to the pharmacological properties of the solutes. The approach developed here should facilitate the preselection of drug candidates, at the same time reducing the costs and the use of laboratory animals.

INTRODUCTION

Dynamic, non-destructive processes involved in chromatographic separations resemble the essential processes at the basis of drug action (except for metabolism). The analogy is especially relevant with reversed-phase high-performance liquid chromatography (RP-HPLC), as hydrophobic–hydrophilic equilibria determine both chromatographic distribution and the penetration of a drug within a living system, in addition to its affinity to a receptor.

Until recently, the applications of RP-HPLC in medicinal chemistry and molecular pharmacology concentrated on the determination of convenient scales of drug hydrophobicity [1]. Much effort has been devoted to producing an RP-HPLC system mimicking the common reference hydrophobicity scale which is provided by the octanol–water partition system [2]. However, it must be realised that what is measured as the hydrophobicity of solutes depends on the partition system employed [3]. Different hydrophobicity scales reflect some "phobia" of solutes towards the aqueous phase but this "phobia" depends considerably on the environment. There is no single, unique, universal, continuous, unequivocally defined and pharmacologically distinguished hydrophobicity scale. Consequently, there is no justification to prefer information on properties of drug solutes provided by an individual RP-HPLC system over information gained from measurements performed in another chromatographic system [4].

We assume that systematic information extracted from diverse RP-HPLC retention data can be more appropriate for the prediction of the net effects of complex pharmacokinetic and pharmacodynamic processes than information based on an individual

* Corresponding author.

0021-9673/93/$06.00

one-dimensional hydrophobcity scale. To extract systematic information from diverse (yet usually highly intercorrelated) sets of data, the multivariate chemometric methods of data analysis must be applied.

Factorial methods of analysis of chromatographic data have been successfully employed for the classification of solutes and/or chromatographic systems according to their physico-chemical properties (*e.g.*, refs. 5 and 6). Combining the normal-phase thin-layer chromatographic and other physico-chemical data for amino acids, Wold *et al.* [7] applied the approach to determine the pharmacological activity of a series of peptides. Recently, we subjected to principal component analysis a large set of RP-HPLC data previously determined for a series of eighteen imidazoline derivative drugs of various pharmacological activity [8]. The grouping of these agents according to retention behaviour correlated surprisingly well with their established pharmacological classification. As the approach offers the potential of facilitating the search for new drugs, at the same time reducing the costs and the use of laboratory animals, we further tested its validity. Here, the results are reported of principal component analysis of several RP-HPLC hydrophobicity parameters determined for a series of drugs known to affect the biological activity of histamine.

EXPERIMENTAL

Materials

The following drugs were chromatographed after dissolution in the mobile phase: anatazoline hydrochloride (a gift from Polfa, Warsaw, Poland), burimamide (Smith Kline & French, Welwyn Garden City, UK), chloropyramine hydrochloride (a gift from Polfa, Kraków, Poland), cimetidine (a gift from Polfa, Rzeszów, Poland), cinnarizine (a gift from Polfa, Warsaw, Poland), dimethindene maleate (a gift from Zyma, Munich, Germany), diphenhydramine hydrochloride (a gift from Polfa, Kraków, Poland), disodium cromoglycate (a gift from Lek, Ljubljana, Slovenia), famotidine (a gift from Polfa, Starogard, Poland), isothipendyl hydrochloride (a gift from ASTA Pharma, Frankfurt, Germany), ketotifen fumarate (a gift from Polfa, Warsaw, Poland), khellin (Fluka, Buchs, Switzerland), mepyramine maleate (a gift from Rhône-Poulenc, Dagenham, UK), metiamide (Smith Kline & French), nizatidine (a gift from Lilly France, Saint-Cloud, France), pheniramine hydromaleate (a gift from Hoechst, Frankfurt, Germany), pizotifen maleate (a gift from Sandoz, Nürnberg, Germany), promethazine hydrochloride (a gift from Polfa, Jelenia Góra, Poland), ranitidine hydrochloride (a gift from Polfa, Starogard, Poland), roxatidine acetate hydrochloride (a gift from Albert-Roussel Pharma, Wiesbaden, Germany), tripelenamine hydrochloride (a gift from Teva Pharmaceutical Industries, Petah Tiqva, Israel) and tymazoline hydrochloride (a gift from Polfa, Warsaw, Poland).

A Suplex pKb-100 deactivated hydrocarbon-bonded silica column (15 cm × 4.6 mm (I.D.) (particle size 5 μm) was purchased from Supelco (Bellefonte, PA, USA) and a Unisphere-PBD polybutadiene-encapsulated alumina column (10 cm × 4.6 mm (I.D.) (partice size 8 μm) from Biotage, (Charlottesville, VA, USA).

Deuteromethanol (CH_3O^2H) was purchased from IBJ (Swierk, Poland).

Apparatus

The chromatographic system consisted of a Model L-6200A pump, a Model L-4250 UV–VIS detector and a Model D-2500 chromato-integrator (all from Merck–Hitachi, Vienna, Austria). The experiments were carried out using a flow-rate of 1 ml/min and the columns were thermostated at 22°C.

Chromatographic conditions

Chromatography was carried out polycratically using eluents with following proportions (v/v) of methanol to buffer: 80:20, 70:30, 60:40, 50:50, 40:60, 30:70 and 20:80. Buffers of pH 2.20, 7.40 and 11.40 were prepared by adding 0.2 *M* NaOH to a solution of 0.04 *M* CH_3COOH, 0.04 *M* H_3PO_4 and 0.04 *M* H_3BO_3.

Capacity factors were calculated assuming a constant dead volume of the column. The dead volumes were determined by measuring signals of deuteromethanol (CH_3O^2H) chromatographed with neat methanol (CH_3OH) [9].

Logarithms of capacity factors (log k') for individual solutes chromatographed in a given chromatographic system were regressed against the volume fraction of methanol in the eluent. The linear

part of the relationship was extrapolated to a hypothetical capacity factor corresponding to 0% of methanol (100% buffer) in the mobile phase. The resulting retention parameters, normalized to pure buffer, log k'_w, were subjected to further analysis.

Chemometric analysis

A 5 × 22 matrix of log k'_w parameters determined in five HPLC systems for 22 solutes was subjected to statistical analysis by the principal component method [10]. A standard, commercially available statistical package was employed, run on a personal computer.

RESULTS AND DISCUSSION

Structural formulae of the compounds studied are given in Fig. 1. There are two main pharmacological groups represented by the drugs analysed [11]. One group are classified as classical antihistaminics (antiallergics) which are antagonists of the type H_1 of histamine receptor. The second large group are antiulcerative drugs which block the type H_2 of histamine receptor. Ketotifen, sodium cromoglycate and khellin are used for the prophylaxis of bronchial asthma. Pizotifen is an antimigraine drug and cinnarizine is recommended for improving the brain blood circulation.

All the drugs are assumed to modify somehow the effects of endogenous histamine. The hypothesis on the structural similarity of the drugs to one of the two energetically favoured conformations of histamine [12] and the rational design of H_2-antagonists [13] imply differences in the physico-chemical properties of the compounds. If these differences could be measured by convenient HPLC methods then the procedure of preselection of potential drug candidates could be greatly facilitated.

Measurements of chromatographic retention were performed at neutral and acidic pH when employing the Suplex pKb-100 hydrocarbon-bound silica column. The chemical stability of the Unisphere-PBD polybutadiene-encapsulated alumina column allowed retention measurements at acidic, neutral and alkaline pH. As the compounds studied are mostly organic bases their retention at pH 2.20 on the silica-based column was low and several solutes (**2**, **4**, **9**, **14**, **15** and **19** in Fig. 1) were excluded from the stationary zone in the whole range of eluent composition studied. However, these compounds were retained using the alumina-based column also operated at pH 2.20. On the other hand, exclusion of some solutes **4**, **8** and **15**) was observed with the alumina based column at pH 11.40. Well measurable retention data were obtained on both columns at pH 7.40. With the alumina-based column only acidic cromoglycate was excluded.

Very good linearity of the relationship of log k' *versus* methanol concentration in the eluent was observed for the most of the solutes when chromatographed at pH 7.40 and 11.40 in a wide eluent composition range (see Fig. 2 for illustration). The linearity range was limited to the higher buffer concentrations for most of the compounds chromatographed at acidic pH. The number of the highest consecutive concentrations of the buffer used to extrapolate linearly log k' data to log k'_w is given in Table I together with the respective log k'_w values. For excluded solutes a value of -1 was assumed for chemometric analysis.

The log k'_w data in Table I indicate that typical H_2-antagonists are generally less retained than H_1-antagonists. However, relative ordering of the agents differs in all five RP-HPLC systems studied. Hence, specific properties of individual chromatographic systems affect the specific retention of a given solute.

Differences in the properties of solutes which manifest themselves in a systematic manner may be of relevance for their diverse pharmacological behaviour. To check this hypothesis, the data matrix in Table I was subjected to principal component analysis (PCA). PCA is a statistical procedure aimed at the reduction of the dimensionality of data space but providing concentration of systematic information previously dispersed over many variables in a few common abstract factors [10].

The PCA of the log k'_w data in Table I yielded two main factors accounting together for about 96% of the variance. The first principal component accounted for 90.3% of the total variance and the second for 5.7% of the variance. The loadings (weights) of the two main principal components by the five variables of the chromatographic analysis (Fig. 3) indicate that the first factor ($W1$) is loaded mostly by retention data determined at pH 7.40 on Suplex pKb-100 and at pH 11.40 on Unisphere-PBD. In both instances one can presume an effec-

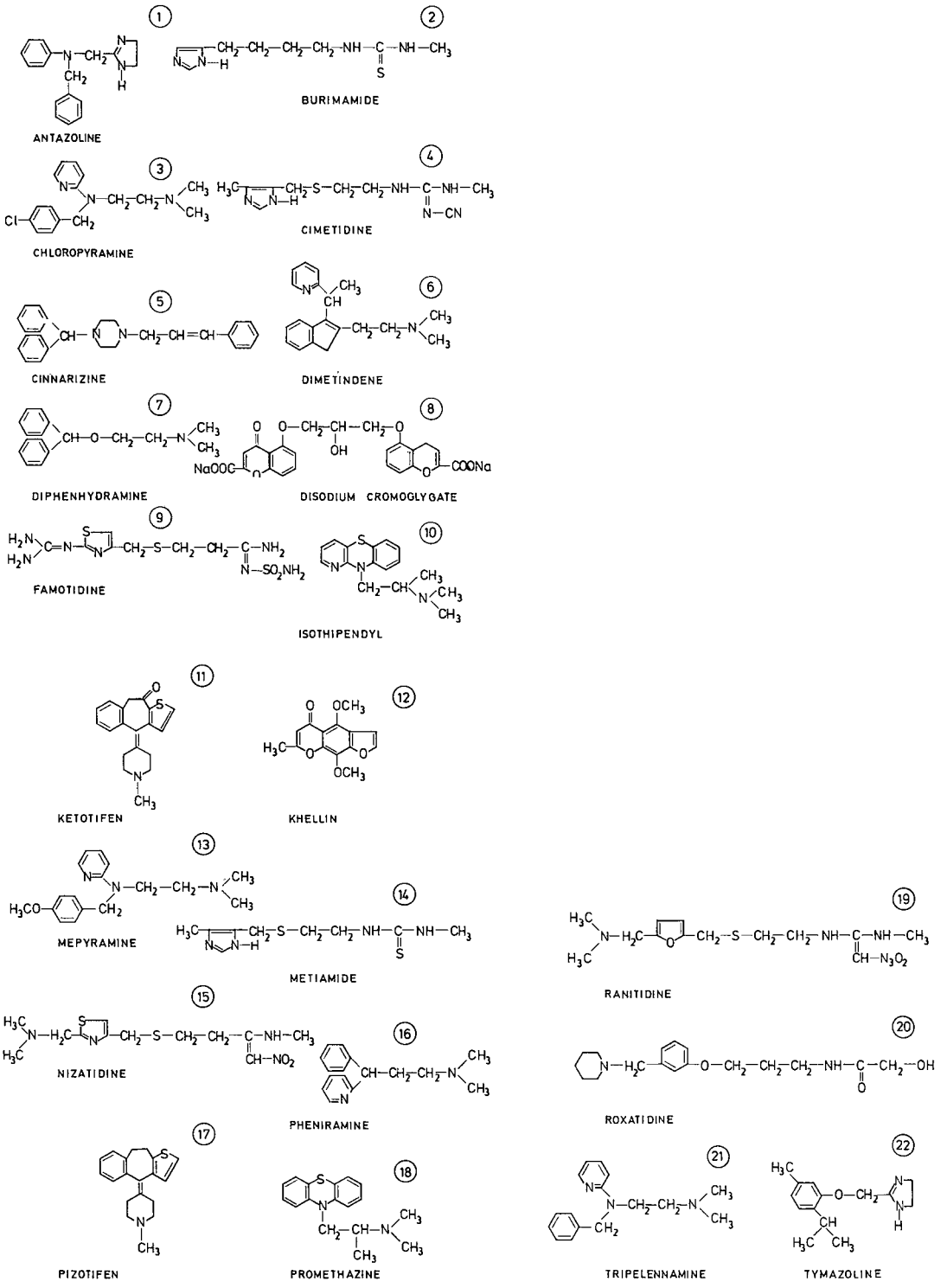

Fig. 1. Structural formulae of drug solutes studied.

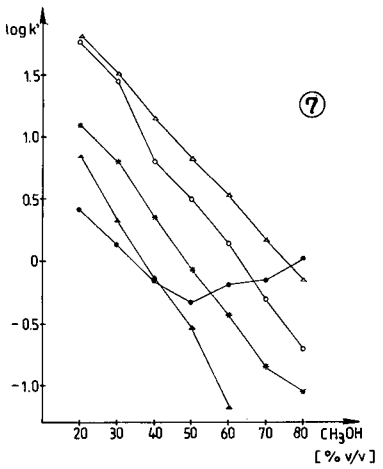

Fig. 2. Typical relationships between logarithms of capacity factors (log k') and percentage (v/v) of methanol in eluent for diphenhydramine chromatographed in five HPLC systems: △ = Suplex pKb-100, pH 7.40; ○ = Unisphere-PBD, pH 7.40; * = Unisphere-PBD, pH 11.40; ▲ = Suplex pKb-100, pH 2.20; ● = Unisphere-PBD, pH 2.20.

tive suppression of specific, polar solute–stationary phase interactions due to the suppression of the ionization of the solutes and deactivation of the stationary phase support material. Thus, $W1$ is postulated to extract information on abilities of the solutes to take part in the molecular-size-related, nonspecific, dispersive intermolecular interactions. The second principal component ($W2$) is loaded mostly by retention data determined on alumina-based Unisphere-PBD column at acidic and neutral pH. $W2$ can be assumed to reflect the abilities of the fully or partially ionized basic solutes to participate in structurally specific, polar (ionic, dipole–dipole, dipole–induced dipole, charge-transfer) intermolecular interactions.

Principal component object (solute) scores were calculated for individual compounds. The positions of the drugs on the plane determined by the two first principal component axes (PC1 and PC2) are displayed in Fig. 4. There are two clear clusters of sol-

TABLE I

LOGARITHMS OF CAPACITY FACTORS OF DRUG SOLUTES EXTRAPOLATED TO PURE BUFFER AS THE MOBILE PHASE (LOG k'_w) FROM FIVE HPLC SYSTEMS

Number of mobile phase concentrations used for linear extrapolation is denoted by n. For excluded solutes log $k'_w = -1$ was assumed.

No.[a]	Suplex pKb-100				Unisphere-PBD					
	pH 2.20		pH 7.40		pH 2.20		pH 7.40		pH 11.40	
	log k'_w	n	log k'_w	n	log k'_w	n	log k'_w	n	log k'_w	n
1	1.8063	4	2.4829	6	0.8102	4	1.8797	7	1.7027	6
2	−1		1.0777	6	−0.6040	3	0.4621	5	−1.0041	3
3	1.2718	5	3.0857	5	0.9504	4	2.9227	6	2.4413	4
4	−1		1.4185	4	0.5141	3	0.100	2	−1	
5	3.6665	5	4.5896	4	2.7722	4	4.8184	5	4.5332	4
6	1.4333	6	2.8009	6	0.7147	4	2.2400	7	1.9607	6
7	1.8521	5	2.4835	6	0.8999	4	2.6170	6	1.9383	6
8	−1.0800	2	2.2643	6	1.3939	5	−1		−1	
9	−1		0.8113	7	0.3027	3	0.4189	6	−0.7400	2
10	2.0595	5	2.9256	6	1.3740	4	2.4681	7	2.5455	6
11	1.6011	6	2.8090	5	1.2823	4	2.4950	7	1.8976	5
12	2.4974	6	2.3777	7	0.6595	6	0.6738	5	0.5587	6
13	0.2599	3	2.3865	6	0.5465	4	2.0513	7	0.4622	4
14	−1		1.1579	7	0.3997	3	0.3706	4	−0.3768	4
15	−1		1.1229	7	0.3294	4	0.5500	2	−1	
16	0.4443	5	1.8109	7	0.1825	4	1.1495	6	1.1568	5
17	2.4328	6	3.7361	4	1.9797	4	3.5771	5	3.1903	5
18	2.2227	6	3.7144	4	1.7941	3	3.4184	6	3.0831	6
19	−1		1.2764	6	0.3019	4	0.3320	5	−1.1445	4
20	−1.2500	2	1.3134	7	−0.5500	2	0.5392	7	0.8782	4
21	0.7102	5	2.3295	6	0.4458	4	1.9938	7	1.6395	6
22	1.7398	6	2.2431	6	0.8952	4	2.1513	6	1.6954	6

[a] Solutes are numbered as in Fig. 1.

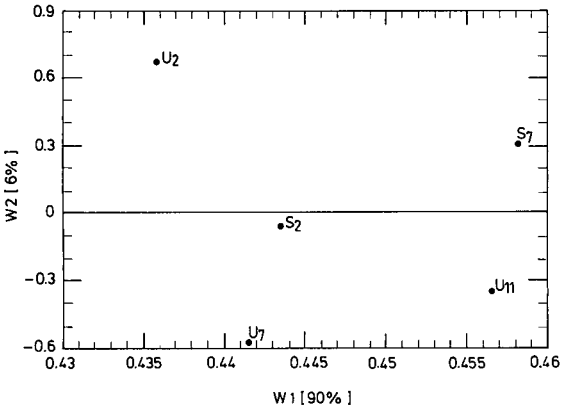

Fig. 3. Two-dimensional scatter plot of two first principal component weights, *W*1 and *W*2, due to the individual HPLC system employed: S_7 = Suplex pKb-100, pH 7.40; U_{11} = Unisphere-PBD, pH 11.40; S_2 = Suplex pKb-100, pH 2.20; U_7 = Unisphere-PBD, pH 7.40; U_2 = Unisphere-PBD, pH 2.20.

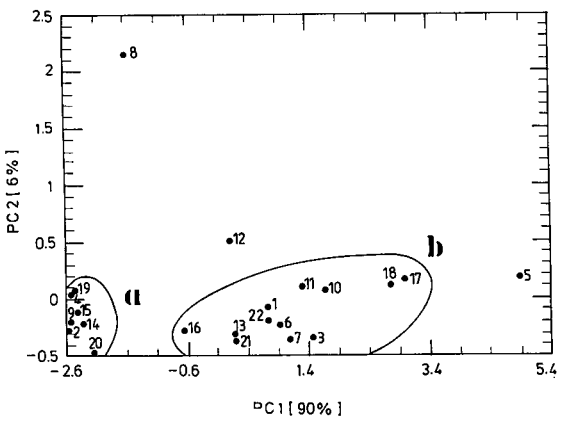

Fig. 4. Two-dimensional scatter plot of scores by individual drug solutes in two first principal components, PC1 and PC2.

utes in Fig. 4 and three solutes show distinctive chromatographic behaviour. Undoubtedly, compounds **2**, **4**, **9**, **14**, **15**, **19** and **20** form a compact cluster **a** of drugs unequivocally classified as antagonists of the H_2 type of histamine receptor [11,14–16]. This is in spite of evident diversity of chemical structures within the group of H_2-antagonists studied.

Among twelve compounds forming cluster **b** there are ethylendiamine derivatives (**3**, **13** and **21**), imidazoline derivatives (**1** and **22**), phenothiazine derivatives (**10** and **18**), an oxyethylamine derivative (**7**), an arylalkylamine derivative (**16**) and an indene derivative (**6**). All these are classified and employed clinically as typical antagonists of H_1 receptor [11, 17, 18]. To the cluster **b** belong also ketotifen (**11**) and pizotifen (**17**). Although the clinical indication for ketotifen is prophylaxis of bronchial asthma and for pizotifen it is migraine, both ketotifen [19] and pizotifen [20] are reported to possess antagonistic activity towards H_1-type histamine receptors.

Compounds **8** and **12** clearly do not belong to cluster **a** nor **b**. Khellin (**12**) is a miolytic agent [21] and its derivative, disodium cromoglycate (**8**), decreases the liberation of histamine which accompanies the antigen-antibody reaction [22]. None of the drugs is known to interfere with the H_1 or H_2 receptors.

Cinnarizine (**5**) could perhaps be included in cluster **b**. This drug has diverse sites of actions, including some antihistaminic properties [23]. Central effects ascribed to the drug are certainly connected with its high hydrophobicity (and thus brain barrier permeation), as is reflected by a high PC1 score.

The data discussed above demonstrate the applicability of the chemometrically processed retention data, generated in diverse HPLC systems, for predicting the pharmacological classification of drug solutes. As representative sets of reliable HPLC data can readily be obtained for large series of compounds, the approach developed here appears suitable for the preselection of drugs and other substances with a given, required property.

ACKNOWLEDGEMENTS

Support for this research by the Komitet Badań Naukowych, Warsaw, Poland (Project No. 408319101) is gratefully acknowledged. One of the authors (R. G.-Y.) acknowledges receipt of a scholarship from the Polish Ministry of Health and Social Welfare.

REFERENCES

1 R. Kaliszan, *Quantitative Structure–Chromatographic Retention Relationships*, Wiley, New York, 1987, pp. 279–295.

2 R. Kaliszan, *Quant. Struct.–Act. Relat.*, 9 (1990) 83.
3 R. Kaliszan, *Anal. Chem.*, 64 (1992) 619A.
4 R. Kaliszan, *Adv. Chromatogr.*, 34 (1993) in press.
5 J. F. K. Huber, C. A. M. Meijers and J. A. R. J. Hulsman, *Anal. Chem.*, 44 (1972) 111.
6 K. Szymoniak and J. Chrétien, *J. Chromatogr.*, 404 (1987) 11.
7 S. Wold, L. Eriksson, S. Hellberg, J. Jonsson, M. Sjöström, B. Skagerberg and C. Wikström, *Can. J. Chem.*, 65 (1987) 1814.
8 R. Gami-Yilinkou and R. Kaliszan, *J. Chromatogr.*, 550 (1991) 573.
9 J. H. Knox and R. Kaliszan, *J. Chromatogr.*, 349 (1985) 211.
10 J. R. Llinas and J. M. Ruiz, in G. Vernin and M. Chanon (Editors), *Computer Aids to Chemistry*, Ellis Horwood, Chichester, 1986, pp. 200–256.
11 W. B. Bowman and M. J. Rand, *Textbook of Pharmacology*, Blackwell, Oxford, 1980.
12 L. B. Kier, *J. Med. Chem.*, 11 (1968) 441.
13 J. W. Black, W. A. M. Duncan and G. J. Durant, *Nature*, 236 (1972) 385.
14 D. M. Campoli-Richards and S. P. Clissold, *Drugs*, 32 (1986) 197.
15 A. H. Price and R. N. Brodgen, *Drugs*, 36 (1988) 521.
16 D. Murdoch and D. McTavish, *Drugs*, 42 (1991) 240.
17 L. Wexler, *Curr. Ther. Res.*, 4 (1962) 306.
18 B. G. Katzung (Editor), *Basic and Clinical Pharmacology*, Appleton & Lange, Norwalk, CT, 1987.
19 U. Martin and D. Römer, *Arzneim.-Forsch.*, 28 (1978) 770.
20 A. K. Dixon, R. C. Hill, D. Roemer and G. Scholtysik, *Arzneim.-Forsch.*, 27 (1977) 1968.
21 G. Schoff and G. Faucon, *Arch. Int. Pharmacodyn.*, 145 (1963) 213.
22 R. N. Brogden, T. M. Speight and G. S. Avery, *Drugs*, 7 (1974) 164.
23 T. Godfraind, *Br. J. Pharmacol.*, 62 (1978) 376P.

Journal of Chromatography, 633 (1993) 65–72
Elsevier Science Publishers B.V., Amsterdam

CHROM. 24 750

On-line immunochemical detection in liquid chromatography using fluorescein-labelled antibodies

H. Irth*, A. J. Oosterkamp, W. van der Welle, U. R. Tjaden and J. van der Greef

Division of Analytical Chemistry, Leiden/Amsterdam Center of Drug Research, University of Leiden, P.O. Box 9502, 2300 RA Leiden (Netherlands)

(First received September 29th, 1992; revised manuscript received November 12th, 1992)

ABSTRACT

A postcolumn immunochemical detection system for on-line coupling to HPLC is described. The effluent from a reversed-phase LC column is mixed with fluorescein-labelled antibodies that are added via a mixing union. Antigenic analytes react with the antibodies to form strongly fluorescent immunocomplexes. In a second step, free antibodies are removed prior to fluorescence detection via passage through a small column packed with an antigen-bound support. The performance of the immunochemical reaction system was investigated using digoxin and its metabolites as analytes and fluorescein-labelled Fab fragments of polyclonal anti-digoxigenin as immunoreagent. This system tolerates up to 95% methanol or 45% acetonitrile in the LC eluent, allowing the separation of digoxin and its metabolites. The immunoreaction sequence is in equilibrium after *ca.* 1 min resulting in peak broadening comparable to that in standard postcolumn derivatization systems. The detection limits obtained for digoxin and digoxigenin after separation on a C_{18} column are 200 and 50 fmol, respectively. The applicability of the method is demonstrated for the bioanalysis of digoxin and digoxigenin. Owing to the high selectivity of the immunodetection system, sample pretreatment can be reduced to deproteination and dilution of plasma and urine samples. Detection limits in both matrices (100-μl injections) are $1 \cdot 10^{-9}$ *M* for digoxigenin and $4 \cdot 10^{-9}$ *M* for digoxin.

INTRODUCTION

The inherent selectivity of biospecific interactions is widely exploited in affinity chromatographic separations and immunoassays [1,2]. Immunoaffinity sorbents have found application in the selective preconcentration of low- and high-molecular-mass compounds [3–10] in combination with liquid chromatography. Immunoassays, on the other hand, have revolutionized many fields of clinical chemistry and biochemistry especially in the form of radioimmunoassays (RIA). Although highly sensitive, immunoassays suffer from cross-reactivity, *i.e.*, the reactions of the antibodies with more than one analyte, leading to erroneous results. Consequently, HPLC is frequently employed in a fractionation step prior to the immunoassay [11–14].

The on-line coupling of liquid chromatography with an immunoassay would overcome this problem in an elegant way by combining the high separation power and ease of automation of HPLC with the selectivity and sensitivity of immunoassays. Several approaches have been described to perform continuous-flow immunoassays in the form of a postcolumn reaction detection system, most of them being based on sequential addition immunoassay (SAIA). Cassidy *et al.* [15] developed a kinetically controlled immunoassay based on the sequential addition of antibody, sample and label on a protein A column, performing immunoassays for albumin and transferrin in under 1 min. Another continuous-flow competitive assay involving enzyme-labelled antibodies was described by Mattiasson *et al.* [16]. This system was coupled to a size-exclusion column allowing the monitoring of horseradish peroxidase. A different approach was used

* Corresponding author.

0021-9673/93/$06.00

by Kusterbeck *et al.* [17], who developed a detection technique based on a displacement reaction between ^{125}I- or fluorescein-labelled 2,4-dinitrophenyl (DNP)-insulin and DNP-containing analytes.

The sequential nature makes SAIA techniques unsuitable candidates for on-line coupling to liquid chromatographic systems, since it does not allow the continuous monitoring of the LC effluent. In this paper we report the on-line coupling of reversed-phase liquid chromatography with a fluoroimmunoassay using fluorescein-labelled antibodies. The immunoassay is performed in a postcolumn derivatization system and is entirely based on association reactions of antibodies with analytes (antigens) eluting from the analytical column. Owing to the generally high reaction rate of association reactions between antibodies and antigens, the peak broadening obtained in this system is comparable to that with standard postcolumn derivatization systems in liquid chromatography. By using antibodies labelled with fluorescein, detection limits in the nanomolar range are obtained. The selectivity of the method is demonstrated by the determination of antigens in virtually untreated plasma and urine samples.

EXPERIMENTAL

Chemicals and supports

Digoxin, digoxigenin and bovine serum albumin (BSA) were purchased from Sigma (St. Louis, MO, USA), sodium metaperiodate, sodium tetrahydroborate, sodium hydrogensulphite and Tween 20 from Merck (Darmstadt, Germany) and all organic solvents (analytical-reagent grade) from J.T. Baker (Deventer, Netherlands). Immunoaffinity-purified fluorescein-labelled Fab fragments of polyclonal anti-digoxigenin (Fab-DIG) and blocking solution consisting of a casein hydrolysate were obtained from Boehringer Mannheim (Mannheim, Germany). The immunoreagent solution was prepared by dissolving Fab-DIG ($1.3 \cdot 10^{-9} M$) in phosphate-buffered saline (PBS) (pH 7.5) and adding 0.5% of Tween 20.

Amino-silica was synthesized according to a procedure described by Ernst-Cabrera and Wilchek [18] using Nucleosil Si-100 (10 nm pore size) (Macherey–Nagel, Düren, Germany). Affi-Prep HZ and aminoethyl Bio-Gel P-100 were purchased from Bio-Rad Labs. (Richmond, CA, USA), Fractogel TSK AF from Merck and Carbolink hydrazide from Pierce (Rockford, IL, USA).

Synthesis of antigen-bound supports

Digoxin (100 mg) was suspended in 10 ml of ethanol and 10 ml of 0.1 *M* sodium metaperiodate solution were dropwise added in the dark with stirring. After 30 min the excess of metaperiodate was titrated with 1 *M* sodium hydrogensulphite solution until disappearance of the brown colour. After addition of 5 ml of saturated ammonium sulphate solution, the ethanol phase was recovered and used without further treatment for the synthesis of digoxin-bound supports.

Binding of digoxin to amino supports. Amounts of 200 mg of the respective amino supports (amino-silica, aminoethyl Bio-Gel P-100, Fractogel TSK AF) were suspended in 10 ml of potassium carbonate buffer (100 m*M*, pH 9.5), 10 ml of the ethanolic solution of oxidized digoxin were added dropwise and the mixture was stirred for 2 h at room temperature. Then 10 ml of sodium tetrahydroborate solution (15 mg/ml) were added and the reaction was allowed to proceed for 1 h. The digoxin support obtained was washed with 200 ml of dimethyl sulphoxide–water (50:50, v/v), 500 ml of distilled water and 200 ml of PBS and stored at 4°C.

Binding of digoxin to hydrazide supports. Affi-Prep HZ and Carbolink hydrazide-activated supports were suspended in 10 ml of acetate buffer (100 m*M*, pH 5.5), 10 ml of the ethanolic solution of oxidized digoxin were added dropwise and the mixture was stirred for 2 h at room temperature. No reduction of the hydrazone was carried out. The digoxin supports produced in this way were washed according the procedure described for amino supports.

Blocking of the derivatized supports with a casein hydrolysate in order to reduce non-specific binding was carried out according to the manufacturer's procedure. In the final system, Tween 20 was added to the immunoreagent solution to prevent non-specific binding.

HPLC system

All experiments were carried out in an LC system consisting of a Kratos-ABI (Ramsey, NJ, USA) Spectroflow 400 pump, a Kontron (Zürich, Swit-

zerland) MSI 660 autosampler, a 100 × 3.0 mm I.D. stainless-steel separation column packed with 5-μm Nucleosil ODS (Macherey–Nagel) and a Kontron SFM 23 fluorescence detector (excitation wavelength 488 nm, emission wavelength 514 nm). The LC mobile phase was acetonitrile–water (30:70, v/v) pumped at a flow-rate of 0.25 ml/min. The immunoreagent pump was a Pharmacia (Uppsala, Sweden) P3500 used at a flow-rate of 0.5 ml/min. Mixing of the eluent with the immunoreagent solution was performed by using an inverted Y-type low-dead volume mixing union. The reaction coil (volume 600 μl) consisted of 0.3 mm I.D. PTFE tubing; the reaction was performed at 20°C. A 10 × 3.0 mm I.D. column slurry packed with Carbolink hydrazide-coupled digoxin was used to bind free antibodies.

Pretreatment of urine and plasma samples

Blank and spiked urine samples were diluted 1:1 with water and filtered through a 2-μm membrane filter. The filtrate was injected into the LC system. Blank and spiked plasma samples (1 ml) were deproteinated with acetonitrile (1.5 ml). After centrifugation for 15 min the supernatant was injected into the LC system.

RESULTS AND DISCUSSION

Design of the postcolumn immunodetection system

In contrast to immunoassays, where the immunoreaction is usually carried out in batch, on-line coupling to an LC system requires fast reaction times in order to minimize extra-column band broadening. Consequently, only those immunoassays that have reaction times of the order of minutes rather than hours should be considered. Therefore, all assays that are based partly or entirely on the dissociation of immunocomplexes can be excluded. The postcolumn immunodetection system (for the principle, see Fig. 1) presented here is based on the kinetically fast association of fluorescein-labelled antibodies with antigenic analytes. In a first step, the antibodies are added to the LC effluent via a mixing union. Antigenic analytes react with the antibodies to form strongly fluorescent immunocomplexes in concentrations proportional to the analyte concentration. In a second step the excess of free antibodies is removed prior to fluorescence detection via passage through a small column packed with an antigen-bound support (see Fig. 1).

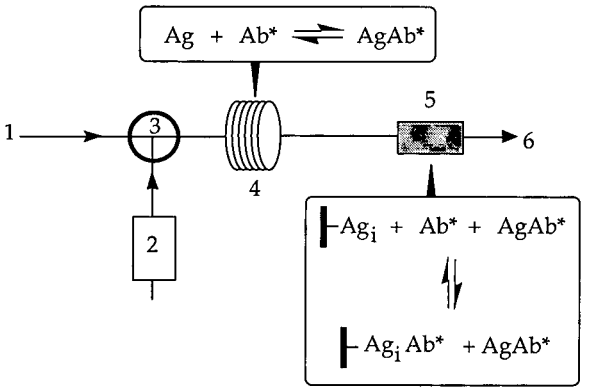

Fig. 1. Scheme of the immunodetection system. 1 = Effluent from analytical column; 2 = immunoreagent pump; 3 = mixing union; 4 = reaction coil; 5 = immobilized-antigen column; 6 = to fluorescence detector. Ag = antigen; Ab* = fluorescein-labelled antibody; AgAb* = immunocomplex; Ag$_i$ = immobilized antigen.

We investigated the performance of such a reaction scheme using the fluorescein-labelled Fab fragments of anti-digoxigenin antibodies (Fab-DIG). The Fab fragments which have a molecular mass of *ca.* 45 000 are labelled with 2–3 mol of fluorescein per mol of Fab fragment according to manufacturer's specifications. These Fab-DIG antibodies are highly cross-reactive with all compounds possessing the genin moiety of the original immunogenic cardenolide, *e.g.*, digoxin (for structure, see Fig. 2) and its metabolites [19].

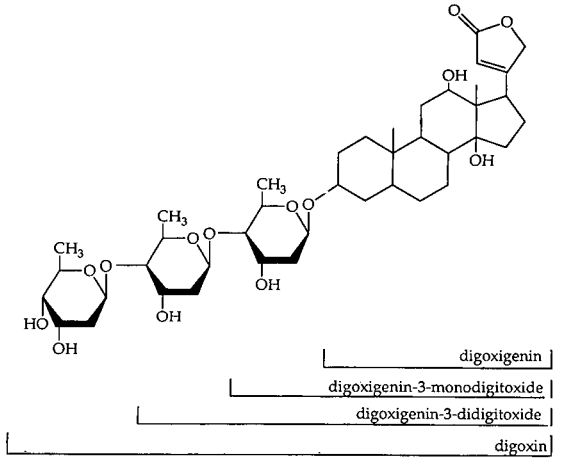

Fig. 2. Structure of digoxin and its metabolites.

Synthesis of an antigen-bound support

The separation step of the postcolumn immunoassay prior to fluorescence detection can be performed by exploiting the physico-chemical differences of free and bound antibodies. A possible difference in molecular mass or charge between free and bound antibodies could be exploited by membrane-based separation systems or ion exchangers, respectively. The most universal means of separation, however, is the implementation of a solid support or a membrane to which the antigen is immobilized while still being reactive towards the antibodies. The synthesis of such an immunoaffinity support or membrane for low-molecular-mass antigens can be performed in a similar manner to the way in which the hapten is bound to a carrier protein to induce the production of antibodies.

With anti-digoxigenin antibodies, digoxin instead of digoxigenin was bound to silica gel, agarose or polymeric supports. Digoxin is highly cross-reactive towards anti-digoxigenin antibodies compared with digoxigenin (manufacturer's specification) and provides an ideal spacer group if it is bound via its hydrophilic carbohydrate moiety. After oxidation of the vicinal OH groups with sodium metaperiodate, the resulting aldehyde groups were bound to supports functionalized with either amino or hydrazide groups. Binding to amino supports requires the subsequent reduction of the Schiff base with sodium tetrahydroborate to obtain a stable bonding. The hydrazones formed in the reaction with hydrazide supports are stable even without further reduction. The highest surface loading of digoxin was obtained for Affigel-Hz, Carbolink hydrazide and aminoethyl Bio-Gel P-100 and ranged from 5 to 10 μmol/g dry support.

In addition to a high surface loading with digoxin, a low degree of non-specific binding is a crucial requirement since non-specific binding would result in the removal of both free antibodies and immunocomplexes and, thus, in an increase in detection limits. All the supports investigated except Carbolink hydrazide exhibited a high degree of non-specific binding (higher than 60%) that could not be suppressed by blocking of the supports with casein hydrolysate or Tween 20. The agarose-based Carbolink hydrazide, however, provided virtually no non-specific binding (lower than 2%) whereas 75% of the fluorescent antibodies present in the polyclonal antiserum were retained. Changes in the flow-rate did not influence the binding of the antibodies, indicating that the background fluorescence is caused by either inactive antibodies or other protein impurities and not by slow association kinetics.

Optimization of parameters affecting the immunoreaction

Organic modifier and pH. Most reversed-phase liquid chromatographic eluents contain organic modifiers such as methanol or acetonitrile and separations are carried out mostly at pH values between 2 and 8. As immunoreactions normally take place in buffered aqueous media at approximately neutral pH, the effects of different concentrations of methanol or acetonitrile and different pH values on the detector response were tested. All experiments were carried out using flow-injection analysis (FIA) at a mixing ratio of 1:2 between the LC eluent and immunoreagent solution.

Fig. 3 (representing organic modifier concentrations after mixing) shows that methanol and acetonitrile influence the immunoreaction in different ways. Whereas up to 95% methanol could be tolerated in the LC eluent (corresponding to *ca.* 32% after mixing), acetonitrile concentrations higher than 45% (15% after mixing) caused a considerable decrease in antibody binding to the immobilized-digoxin support. However, with these maximum concentrations of organic modifier most com-

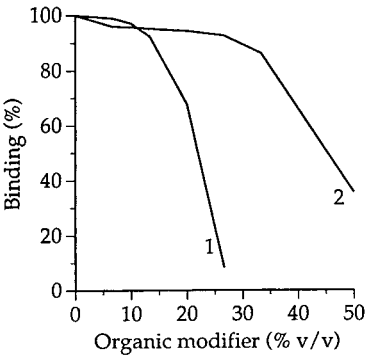

Fig. 3. Influence of organic modifier on the binding to the immobilized-digoxin column. 1 = Acetonitrile; 2 = methanol. 100% response refers to the binding obtained with PBS in both LC eluent and immunoreagent solution. All data (n = 3) were acquired in the flow-injection mode. For other conditions, see Experimental.

pounds of interest can still be chromatographed on a C_{18} stationary phase. Further, it was found that the immunoreaction was unaffected by pH changes in the range 5–8. By employing a strong buffer in the immunoreagent solution (usually PBS of pH 7.5) it is therefore possible to operate the LC column at pH values ranging from 2 to 11 without affecting the immunoreaction.

Reaction time and concentration of Fab-DIG. The reaction rate of the association reaction between Fab-DIG and analytes and the dimensions of the postcolumn reaction system are the most important factors that contribute to extra-column band broadening and therefore determine the sensitivity of the analytical method. The amount of immunocomplex formed during the immunoreaction depends on the reaction rate of the association, the concentration of Fab-DIG employed and the mass transport of the reaction detection system. As the reaction rate constant for the association reaction of digoxin with anti-digoxin, $k_a = 10^7$ l mol^{-1}s^{-1} [20], is extremely high, the latter two parameters mainly determine the performance of the postcolumn immunodetection system. Fig. 4 shows the dependence of the detector response on the reaction time using a Fab-DIG concentration of $1.3 \cdot 10^{-9}$ *M*. The stage of equilibrium is reached after *ca.* 1 min, which demonstrates that immunoreactions of this type are well suited for postcolumn reaction detection systems even at extremely low antibody concentrations. At higher Fab-DIG concentrations the gain in response was counterweighted by the increase in noise caused by the non-binding fraction of Fab-DIG.

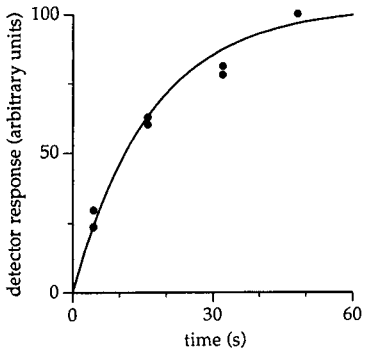

Fig. 4. Influence of the reaction time on detector response. All data (n = 3) were acquired in the flow-injection mode. For other conditions, see Experimental.

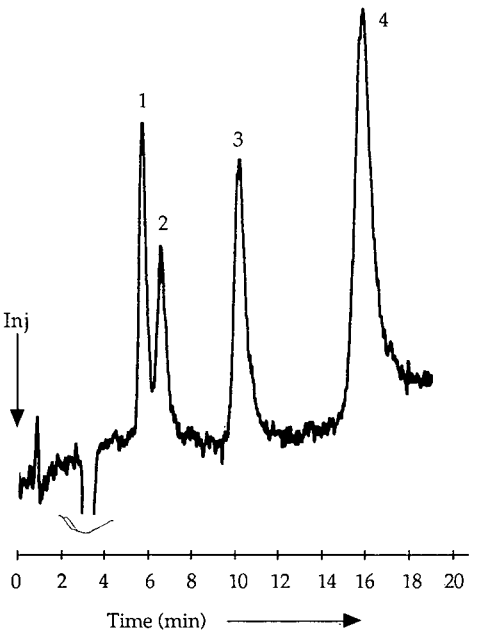

Fig. 5. Chromatogram obtained from the hydrolysis of digoxin (10^{-8} *M*) after 30 min at 37°C and pH 3. 1 = Digoxigenin; 2 = digoxigenin-3-monodigitoxide; 3 = digoxigenin-3-didigitoxide; 4 = digoxin. Injection volume, 100 μl; for other conditions, see Experimental.

Coupling to a reversed-phase LC system

Fig. 5 shows a chromatogram obtained from a hydrolysate mixture of digoxin using fluorescence detection after postcolumn immunochemical reaction. The hydrolysis was carried under the conditions described by Sonobe *et al.* [21]. All degradation products of digoxin, digoxigenin-3-didigitoxide, digoxigenin-3-monodigitoxide and digoxigenin are antigenic towards Fab-DIG and can therefore be monitored with the immunoreaction system. The additional band broadening of the digoxin peak caused by the introduction of a mixing piece, reaction coil and immobilized-digoxin column (reaction coil volume 600 μl; column dimensions 10 × 3.0 mm I.D.) prior to the fluorescence detector amounted to $\sigma^2 = 111$ s^2 compared to $\sigma^2 = 270$ s^2 for the same chromatographic system using UV detection. The separation efficiency in terms of plate numbers decreases from $N = 2610$ for a direct detection system to $N = 1850$ for the postcolumn reaction system. As the reaction kinetics of the antibody–antigen reaction are very fast (see Fig. 4), the band

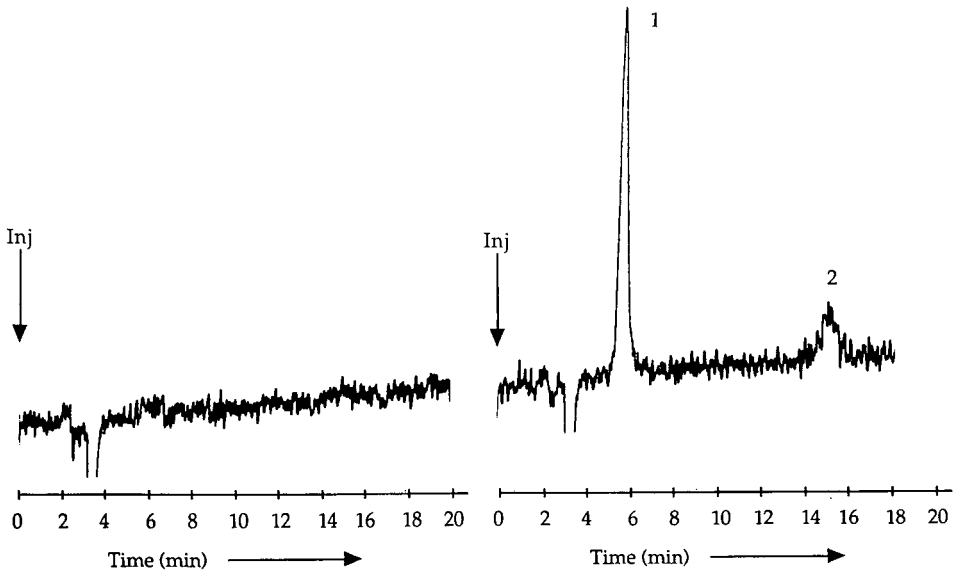

Fig. 6. Chromatograms of (left) blank plasma and (right) plasma spiked with (1) $4 \cdot 10^{-9}$ *M* digoxigenin and (2) $4 \cdot 10^{-9}$ *M* digoxin. Injection volume, 100 μl; for other conditions, see Experimental.

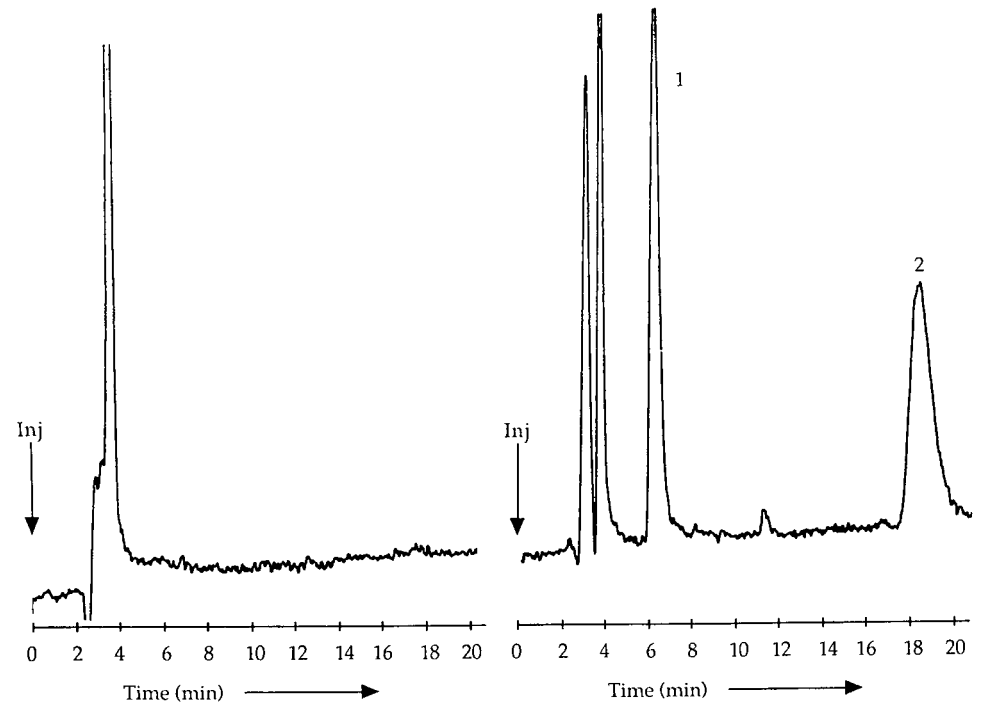

Fig. 7. Chromatograms of (left) blank urine and (right) urine spiked with (1) 10^{-8} *M* digoxigenin and (2) 10^{-8} *M* digoxin. Injection volume, 100 μl; for other conditions, see Experimental.

broadening mainly originates from the design of the reaction detection system. This decrease in separation efficiency, however, is compensated for by the enormous gain in selectivity as the analysis of plasma and urine samples demonstrates (see below). The organic modifier content of the LC mobile phase, *i.e.*, 30% acetonitrile, caused no loss in sensitivity as it is well below the critical value of 45%.

Analytical data

The detection limits (signal-to-noise ratio = 3) for digoxin and digoxigenin amounted to 200 and 50 fmol, respectively (Fab-DIG concentration 1.3 n*M*; injection volume 100 μl). Although these detection limits are higher than those obtained with RIA, they compare favourably with all those methods that determine both compounds simultaneously. The relative standard deviation for 20-μl injections of 100 fmol of digoxigenin was less than 2.0% (n = 7). The detector response was linear (r = 0.998, n = 4) between 50 and 1000 fmol of digoxigenin. The relatively small linear range can be attributed to the fact that the Fab-DIG concentration used is in the same order of magnitude as the analyte concentration (which is usually the case in most immunoassays). Owing to this rather low Fab-DIG concentration, the immobilized-digoxin column could be used without regeneration for at least 500 injections before breakthrough of Fab-DIG occurred.

Applicability to the determination of digoxin and digoxigenin in urine and plasma

The selectivity of the immunochemical reaction detection system was tested by determining digoxin and digoxigenin in biological matrices such as plasma or urine. Sample pretreatment consisted of filtration and 1:1 dilution for urine and deproteination using acetonitrile and centrifugation for plasma. The chromatograms in Figs. 6 and 7 representing blank and spiked plasma and urine, respectively, demonstrate the high selectivity and sensitivity of immunochemical reaction detection. Virtually no interferences were observed in the analysis of plasma samples, whereas chromatograms deriving from urine samples exhibited a single peak eluting with the void volume which possibly derives from cross-reactive steroid components of urine. Both digoxin and digoxigenin can be determined in urine and plasma with detection limits of $4 \cdot 10^{-9}$ and $1 \cdot 10^{-9}$ *M*, respectively (injection volume 100 μl).

CONCLUSIONS

The incorporation of an immunochemical reaction using fluorescein-labelled antibodies in a post-column reaction detection system is a promising way to improve both the selectivity and sensitivity of liquid chromatographic systems. Long incubation times characteristic of immunoassays can be avoided by employing solely association reactions. In this way the benefits of immunoassays, high sensitivity and selectivity, can be combined with the separation power of LC, avoiding the tedious collection of fractions characteristic for off-line systems.

The method presented here requires that (preferably fluorescent) labelled antibodies and an immobilized-antigen support are available. The labelling of antibodies with fluorescent labels has been extensively described [22]. The production of an antigen-bound support requires synthetic work which, in the case of low-molecular-mass antigens, can be performed in a similar way as the synthesis of hapten carriers used for the production of antibodies. High-molecular-mass antigens such as peptides or proteins might be coupled directly to activated supports via free amino groups. In order to reduce background fluorescence, non-binding labelled antibodies should be removed as far as possible. The immunoaffinity purification of polyclonal antisera using the antigen-bound support as chromatographic stationary phase is currently under investigation. In addition to regenerating the immobilized antigen column, this procedure should lead to the recovery of a homogeneous antibody fraction with high specificity.

The choice of antibodies, *i.e.*, monoclonal *vs.* polyclonal, obviously influences the selectivity and sensitivity of the analytical method in addition to the range of compounds that can be determined. Highly specific monoclonal antibodies with high binding constants are preferable if only a small number of structurally similar antigens are to be determined. Polyclonal antibodies may find application in metabolic screening procedures for drugs, for example, thus helping to identify antigenic metabolites.

The selectivity of the immunochemical detection system was demonstrated by the determination of digoxin and digoxigenin in virtually untreated bi-

ological matrices. Currently the coupling of the present method with on-line solid-phase extraction is being investigated, which should lead to a further decrease in detection limits.

REFERENCES

1 A. F. Bergold, D. A. Hanggi, A. J. Muller and P. W. Carr, in Cs. Horváth (Editor), *High-Performance Liquid Chromatography —Advances and Perspectives,* Vol. 5, Academic Press, San Diego, 1988, p. 57.
2 J. P. Gosling, *Clin. Chem.*, 36 (1990) 1408–1427.
3 A. Farjam, G. J. de Jong, R. W. Frei, U. A. Th. Brinkman, W. Haasnoot, A. R. M. Hamers, R. Schilt and F. A. Huf, *J. Chromatogr.*, 452 (1988) 419–433.
4 C. van de Water and N. Haagsma, *J. Chromatogr.*, 411 (1987) 415–421.
5 B. B. Johansson, *J. Chromatogr.*, 381 (1986) 107–113.
6 R. G. Glencross, S. A. Abeywardene, S. J. Corney and H. S. Morris, *J. Chromatogr.*, 223 (1981) 193–197.
7 G. C. Davis, M. B. Hein and D. A. Chapman, *J. Chromatogr.*, 366 (1986) 171–189.
8 Y. Murai, M. Ohno, M. Konishi and G. Kominami, *J. Chromatogr.*, 597 (1992) 201–205.
9 L. J. Janis, A. Grott, F. Regnier and S. J. Smith, *J. Chromatogr.*, 476 (1989) 235–244.
10 L. J. Janis and F. Regnier, *Anal. Chem.*, 61 (1989) 1901–1906.
11 E. Gelpi, I. Ramis, G. Hotter, G. Bioque, O. Bulbena and J. Roselló, *J. Chromatogr.*, 492 (1989) 223–250.
12 S. J. Vetticaden, W. H. Barr and L. A. Beightol, *J. Chromatogr.*, 383 (1986) 187–193.
13 S. Harajiri, G. Wood and D. M. Desiderio, *J. Chromatogr.*, 575 (1992), 213–222.
14 E. Gelpi, *Trends Anal. Chem.*, 4 (1985) XII.
15 S. A. Cassidy, L. J. Janis and F. E. Regnier, *Anal. Chem.*, 64 (1992) 1973–1977.
16 B. Mattiasson, M. Nilsson, P. Berdén and H. Håkanson, *Trends Anal. Chem.*, 9 (1990) 317.
17 A. W. Kusterbeck, G. A. Wemhoff, P. T. Charles, D. A. Yeager, R. Bredehorst, C.-W. Vogel and F. S. Ligler, *J. Immunol. Methods*, 135 (1990) 191–197.
18 K. Ernst-Cabrera and M. Wilchek, *J. Chromatogr.*, 397 (1987) 187–196.
19 H. Flasch, N. Heinz and R. Petersen, *Arzneim.-Forsch.*, 27 (1977) 649–653.
20 T. W. Smith and K. M. Skubitz, *Biochemistry*, 14 (1975) 1496.
21 T. Sonobe, S. Hasumi, T. Yoshino, Y. Kobayashi, H. Kawata and T. Nagai, *J. Pharm. Sci.*, 69 (1980) 410–413.
22 E. Harlow and D. Lane, *Antibodies, A Laboratory Manual,* Cold Spring Harbor Laboratory, Cold Spring Harbor, 1988 p. 354.

Journal of Chromatography, 633 (1993) 73–80
Elsevier Science Publishers B.V., Amsterdam

CHROM. 24 753

Chiral resolution of enantiomers of asymmetric cobaltacarboranes with a monoatomic bridge between ligands by liquid chromatography on a β-cyclodextrin column

Jaromír Plešek and Bohumír Grüner*

Institute of Inorganic Chemistry of the Czechoslovak Academy of Sciences, 250 68 Řež near Prague (Czechoslovakia)

Tomáš Vaněk and Hana Votavová

Institute of Organic Chemistry and Biochemistry, Czechoslovak Academy of Sciences, 166 10 Prague 6 (Czechoslovakia)

(First received September 18th, 1992; revised manuscript received November 12th, 1992)

ABSTRACT

The HPLC resolution on a β-cyclodextrin column is reported of thirteen enantiomeric pairs of racemates of the type 6,6′-μ-R-E(1,7-$C_2B_9H_{10})_2$-2-Co with oxygen, sulphur and nitrogen bridges (E) and with a variety of R substituents differing in size and electronic properties along with structural factors influencing the capacity factors, selectivity and resolution of individual compounds. A semi-preparative method for chiral separations of these racemates is described and circular dichroism (CD) spectra of several pure enantiomers are presented. The CD spectra indicate the same absolute configurations of all enantiomers eluted first or last independent of the nature of the bridging atom and the size of the bridge substituting group R.

INTRODUCTION

Covalently bonded β-cyclodextrin chiral stationary phases (CSPs) have been widely used for the resolution of enantiomers of organic chiral compounds [1–5]. The separation of several metallocene derivatives on this type of CSP has also been described [6]. Both studies of the intercalation complexes of metallocenes with cyclodextrins [7–9] and the investigation of the separation mechanism of selected enantiomers on β-cyclodextrin columns [10–12] suggest that the inclusion process of the solute with the cyclodextrin hydrophobic cavity along with additional interactions (hydrogen bonding, steric, etc.) with hydroxyl groups on the rim of the cyclodextrin cavity are responsible for the enantiomer discrimination.

Recent studies in this laboratory have shown the efficiency of covalently linked β-cyclodextrin CSPs for the HPLC resolution of the first eleven enantiomeric pairs of chiral deltahedral carborane derivatives [13,14]. In this investigation, of four protochiral metallaborane derivatives tested, only one pair of enantiomers was successfully resolved.

Another structural type of metallacarborane complex suitable for HPLC resolution of enantiomers on β-cyclodextrin columns [15] is the monoatomic bridge cobaltacarboranes of the type 6,6′-μ-R-E(1,7-$C_2B_9H_{10})_2$-2-Co (Fig. 1). The constitutions of the first two representatives of this series have been determined by multinuclear NMR

* Corresponding author.

0021-9673/93/$06.00

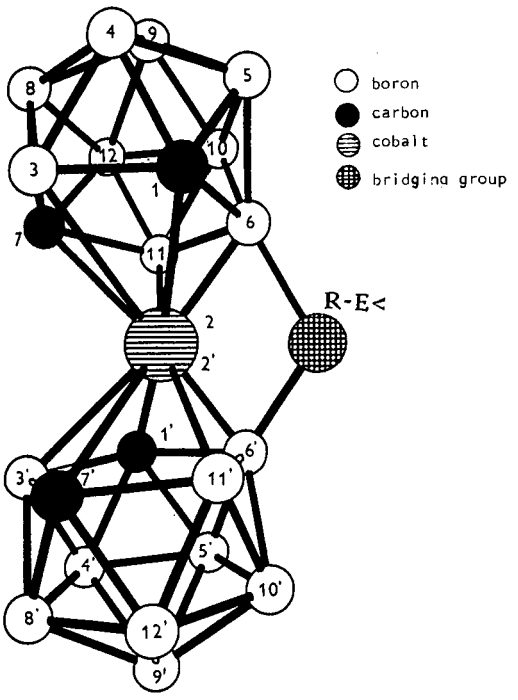

Fig. 1. Structure of the asymmetric metallaboranes of the 6,6′-μ-R-E(1,7-$C_2B_9H_{10})_2$-2-Co (E = O, S, N) type. Terminal hydrogens are omitted for clarity.

spectroscopy and confirmed by resolution of enantiomers [16].

Both of the above-mentioned sulphur-bridged species are just examples of a large family of potentially available compounds of this type because of the possible variation of the bridge substituent and the bridging atom itself. The main structural features will remain essentially the same for all members of this family, *e.g.*, the rigid helical arrangement of both ligands with consequent protochirality without any individual chiral centre joined to a single atom. Moreover, the charge non-equivalence of C–H and B–H vertices at the circumference of both pentagonal ligand planes renders the molecule strongly quadrupolar in the area adjacent to the central cobalt atom. The known hydrophobicity of large deltahedral *closo* frameworks is another interesting and general feature of such species.

Such features are entirely different from conventional organic compounds. The chiral resolution of these unique cobaltacarborane compounds might reveal some additional factors essential for chiral resolution on β-cyclodextrin CSPs.

EXPERIMENTAL

Column

A stainless-steel (250 × 8 mm I.D.) HPLC column was slurry packed with β-cyclodextrin CSP having a high cyclodextrin loading (carbon content 9%). Synthesis of the CSP with β-cyclodextrin directly bonded on the spherical silica support (Separon SGX, 7 μm; Tessek, Prague, Czechoslovakia) was made according to the previously described procedure [15]. The void volume of the β-cyclodextrin column was determined according to the literature method [2].

Apparatus

The chromatographic equipment consisted of a pulseless dual-piston high-pressure VCR 40 pump (Development Workshops, Czechoslovak Academy of Sciences, Prague, Czechoslovakia), a Rheodyne (Cotati, CA, USA) Model 7125 sampling valve with 10- or 200-μl loops, an LCD 2040 variable-wavelength (190–560 nm) UV spectrophotometric detector (Laboratory Instruments, Prague, Czechoslovakia), a Servogor 2s line recorder (Brown Boveri, Germany), and a CI 100 integrator (Laboratory Instruments).

Chemicals, sample preparation and detection

Deionized water was used for the preparation of aqueous–organic mobile phases. All other chemicals were of analytical-reagent grade (Lachema Brno, Czechoslovakia). Methanol was distilled before use. Eluents were filtered through a 0.45 μm filter and briefly degassed under vacuum.

All deltahedral borane compounds (**1–13**, Tables I and II) were prepared in the Boron Chemistry Group of the Institute of Inorganic Chemistry, Czechoslovak Academy of Sciences. The syntheses and properties of the still not reported zwitterionic compounds 6,6′-μ-R-S(1,7-$C_2B_9H_{10})_2$-2-Co (**2–8;** R = ethyl, *n*-propyl, isopropyl, allyl, *n*-butyl, methoxycarbonylmethyl, *n*-hexyl), 6,6′-μ-R_1,R_2-N(1,7-$C_2B_9H_{10})_2$-2-Co (**11,** R_1 = R_2 = H; **12,** R_1 = methyl, R_2 = H; **13,** R_1 = R_2 = methyl) and 6,6′-μ-Me-O(1,7-$C_2B_9H_{10})_2$-2-Co (**10**) will be the subject of a separate paper [17]. The synthesis and

properties of the 6,6′-μ-Me-S(1,7- $C_2B_9H_{10})_2$-2-Co (**1**) and its parent $S^{(-)}$ < (**9**) bridged anion have been reported recently [16].

Special attention was paid to ensure the purity of the individual protochiral positional isomers used in this study. The purity of all species was checked by ^1H (at 500 MHz) and ^{11}B (at 160 MHz) NMR and mass spectrometry.

Samples were prepared as methanolic solutions of concentration 1.0 mg/ml. Before injection all samples were filtered through a 0.45-μm PTFE microfilter (Tessek).

The sulphur and oxygen bridge compounds (**1–10**, Tables I and II) were detected at 290 nm and the analogous nitrogen bridge compounds (**11–13**, Table II) at 280 nm.

Circular dichroism spectra

The solutions of enantiomers (see *Semipreparative separations*) accumulated from twelve successive injections of 40 μl of the solution of the given racemate (concentration 1.0 mg/ml) were evaporated to dryness under vacuum, the residue was dissolved in 4 ml of methanol and the resulting solutions were used directly for circular dichroism (CD) spectral measurements.

CD spectra were recorded on an Auto Dichrographe MarkV instrument (Jobin Yvon, France). The instrument is driven by a microcomputer (Silex, France) loaded with our own software. The measurements were performed in quartz cells with an optical path length of 1 or 0.1 cm. The spectra are computer averages over 2–3 instrument scans and the intensities are presented in arbitrary units.

RESULTS AND DISCUSSION

The zwitterionic S-bridge compounds used in this study are summarized in Table I together with their retention data in 85% and 78% aqueous methanol, selectivity (α) and resolution (R_s). The k' and R_s values of these compounds indicate the usual retention behaviour observed on β-cyclodextrin CSPs by varying the organic modifier content in the mobile phase (studied in the range 70–90%) [1,2,14]. The high methanol content necessary for elution gave evidence of a strong hydrophobic interaction of these compounds with β-cyclodextrin CSPs. However, the more hydrophilic (because of its charge) parent anion [6,6′-μ-S(1,7-$C_2B_9H_{10})_2$-2-Co]$^-$ (**9**, Table II) could be resolved only in mobile phases with lower methanol concentrations (50–60%). In the series of zwitterrionic substituted sulphur compounds (**1–8**, Table I), the effect of increasing the substituent size is generally to decrease the capacity factors (k'). Maximum resolution was obtained with the ethyl-substituted compound, which was followed by a decreasing trend as the size of the

TABLE I

CAPACITY FACTORS (k'), SELECTIVITY (α) AND RESOLUTION (R_s) OF ENANTIOMERS OF COMPOUNDS OF THE 6,6′-μ-R-S(1,7-$C_2B_9H_{10})_2$-2-Co TYPE ON A DIRECTLY BONDED β-CYCLODEXTRIN (7 μm) COLUMN (250 × 8 mm I.D.) USING AQUEOUS–METHANOLIC MOBILE PHASES

R	No.	85% Methanol[a]			78% Methanol[b]		
		k_1'[c]	α	R_s	k_1'[c]	α	R_s
Me	**1**	7.50	1.17	1.08	16.11	1.19	1.05
Et	**2**	5.92	1.20	1.87	12.0	1.31	2.06
n-Pr	**3**	4.42	1.12	1.41	7.89	1.16	1.47
i-Pr	**4**	4.21	1.11	1.33	7.06	1.17	1.50
CH_2=CH-CH_2	**5**	4.67	1.12	1.27	7.72	1.15	1.42
n-Bu	**6**	3.58	1.10	1.05	6.50	1.09	1.13
$MeOCOCH_2$	**7**	4.25	1.10	1.0	7.67	1.13	1.22
n-Hex	**8**	3.0	1.09	0.94	5.85	1.07	0.7

[a] Flow-rate 1.2 ml/min.

[b] Flow-rate 1.6 ml/min.

[c] k_1' = Capacity factor of the first-eluting enantiomer.

substituent increased. However, for substituents up to *n*-butyl or methylacetyl, relatively good resolutions ($R_s > 1$) were still obtained.

The separation is exemplified by Fig. 2. The poor R_s value for the methyl derivative **1** was not the result of selectivity, which was almost as good as that of the ethyl derivative, but rather to the peak broadening. Therefore, the methyl derivative **1** seems to follow to some extent the behaviour of the parent anion with a relatively high α value and extensively broadened peaks. Comparison of the chromatographic behaviour of series of compounds with a three-carbon chain as the substituent group (**3–5**) revealed only slight differences in capacity factors and resolution values. Also, no substantial enhancement of resolution was observed for **7** with a more hydrophilic methylacetate substituent. The correlation of decreasing capacity factors with increasing size of the substituent groups would be consistent with increasing disruption of the intercalation process between the hydrophobic carborane part of the compounds and the cyclodextrin cavity as the size of the side substituents bonded to the rigid molecule increases.

TABLE II

CAPACITY FACTORS (k'), SELECTIVITY (α) AND RESOLUTION (R_s) OF ENANTIOMERS OF COMPOUNDS OF THE 6,6′-μ-R-E(1,7-$C_2B_9H_{10})_2$-2-Co (E = O,S) AND 6,6′-μ-R_2-N(1,7-$C_2B_9H_{10})_2$-2-Co TYPE ON A DIRECTLY BONDED β-CYCLODEXTRIN (7 μm) COLUMN (250 × 8 mm I.D.) IN AQUEOUS–METHANOLIC MOBILE PHASES

Flow-rate, 1.6/min.

Bridge	No.	k_1'[a]	α	R_s	MeOH (%)
S(⁻)<	**9**	8.0	1.37	0.85	55
MeO<[b]	**10**	4.0	1.72	1.30	56
H_2N<	**11**	7.33	1.12	0.95	75
MeHN<	**12**	7.83	1.16	1.06	78
Me_2N<	**13**	7.67	1.23	1.47	85

[a] k_1' = Capacity factor of the first-eluting enantiomer.
[b] Demethylation occurs, enantiomers are eluted as [6,6′-μ-O< (1,7-$C_2B_9H_{10})_2$-2-Co]⁻ anions.

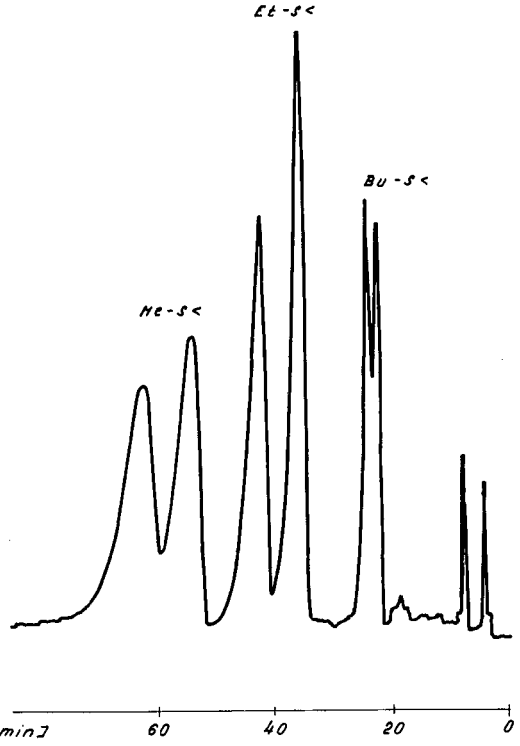

Fig. 2. Separation of the enantiomers of the zwitterionic species of the 6,6′-μ-R-S(1,7-$C_2B_9H_{10})_2$-2-Co type with BuS<, EtS< and MeS< bridges. Column, β-cyclodextrin (250 × 8 mm I.D.); mobile phase, 80% aqueous methanol; flow-rate 1.2 ml/min; detection, UV at 290 nm; sensitivity, 0.04 a.u.f.s.

Additionally, three compounds with nitrogen (**11–13**) and one with oxygen (**10**) monoatomic bridges can also be resolved on this type of CSP. Table II summarizes their retention data, selectivity and resolution achieved using the optimum mobile phase composition for each compound. The separation of the enantiomers of three zwitterionic nitrogen bridge compounds, the parent [6,6′-μ-H_2N (1,7-$C_2B_9H_{10})_2$-2-Co (**11**) and its monomethyl and dimethyl derivatives (**12** and **13**), is depicted in Fig. 3. The retention and selectivity trends in this series of nitrogen-bridged compounds can be clearly seen from Table II and Fig. 3. The strength of interaction with β-cyclodextrin increases with the degree of nitrogen alkylation similarly to the selectivity and resolution. The R_s values for the Me_2N<-bridged compound **13** were generally better than those for the corresponding methylated sulphur-bridged compound **1**. The worst α and R_s values were obtained for the parent H_2N< compound (**11**) with acidic hydrogens on the nitrogen bridge. The compound with an MeO< bridge (**10**) exhibited surprisingly low hydrophobicity, as can be seen from

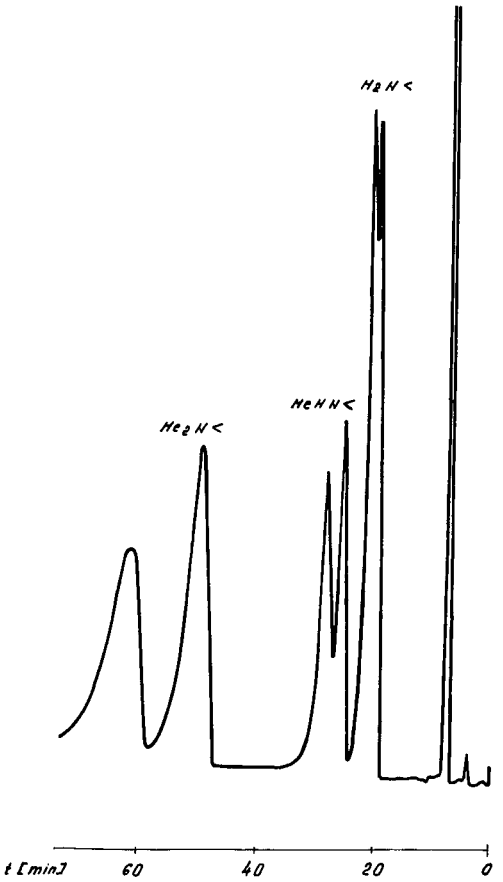

Fig. 3. Separation of the enantiomers of the zwitterionic $H_2N<$ (**11**), MeHN< (**12**) and $Me_2N<$ (**13**) bridged compounds of the 6,6′-μ-R_2-N(1,7-$C_2B_9H_{10})_2$-2-Co type. Chromatographic conditions as in Fig. 2, except for detection at 280 nm.

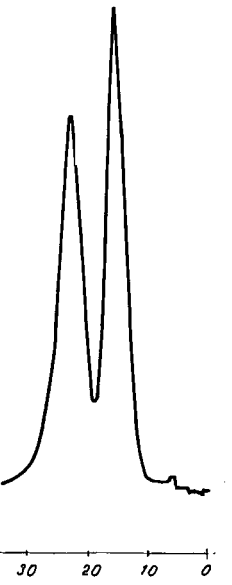

Fig. 4. Separation of the enantiomers of 6,6′-μ-Me-O(1,7-$C_2B_9H_{10})_2$-2-Co (**10**). Conditions as in Fig. 2, except for methanol concentration 60%.

the low organic modifier content used for its elution (Table II). Additionally, it was proved that the demethylation to the anion with a bare oxygen bridge took place during the chromatographic process and the enantiomers were eluted as the respective conjugate acids. An example of such a separation is given in Fig. 4. As with the sulphur-bridged anion (**9**), compound **10** gives a high selectivity value, but the decrease in resolution is apparent by extensive band broadening.

It is noteworthy that no bridge substituent is needed for a successful resolution of this class of compounds, as shown by examples of the separation of parent compounds with $S^{(-)}<$, $O^{(-)}<$ and $H_2N<$ bridges (**9, 10** and **11**). In these species, similarly as in **13**, the primary coordination sphere around the bridging atom is not chiral; however, the whole molecules are helically twisted (Fig. 1). Therefore, for the successful resolution of enantiomers of **1–13** on β-cyclodextrin columns, only general asymmetry of these molecules is essential. Therefore, no distinct monoatomic chiral centres need be present.

Semi-preparative separations

The successful resolution of species **1–7, 10, 12** and **13** with resolution values better than 1 led us to develop a semi-preparative procedure for the accumulation of pure enantiomers in amounts sufficient for the measurement of their circular dichroism spectra and for X-ray diffraction studies aimed at determinating absolute configurations. Therefore, a study of the dependence of the capacity factors and resolution values on the sample loading was performed on the 250 × 8 mm I.D. column used throughout this work.

The results for the allyl-S<-bridged compound (**5**) for two mobile phase compositions are shown in Table III. In the mobile phase with a lower metha-

TABLE III

EFFECT OF SAMPLE LOADING ON THE CAPACITY FACTORS (k') AND THE RESOLUTION (R_s) OF THE ENANTIOMERS OF 6,6'-μ-ALLYL-S(1,7-$C_2B_9H_{10}$)$_2$-2-Co (**5**)

Column, β-cyclodextrin (7 μm) (250 × 8 mm I.D.); mobile phase, A = 77% and B = 83% aqueous methanol; flow-rate, 1.6 ml/min; detection, UV at 290 nm; injections, 1–200 μl of methanolic solution of concentration 1 mg/ml.

Injection volume (μl)	Mobile phase A				Mobile phase B			
	k'_1	k'_2	α	R_s	k'_1	k'_2	α	R_s
1	10.10	11.55	1.15	1.45	5.25	5.81	1.11	1.31
5	10.0	11.33	1.13	1.30	5.25	5.75	1.10	1.28
10	9.33	10.63	1.14	1.17	5.25	5.81	1.11	1.25
20	9.11	10.32	1.13	1.10	5.25	5.75	1.10	1.25
40	8.55	9.66	1.13	1.05	5.25	5.75	1.10	1.20
50	8.22	9.33	1.14	0.96	5.25	5.75	1.10	1.20
80	8.0	8.88	1.11	0.77	5.13	5.68	1.11	1.06
100	7.91	8.62	1.09	0.65	5.13	5.68	1.11	0.87
200	–	–	–	–	5.06	5.45	1.08	0.72

nol content (77%), it is apparent that both k' and R_s have decreased relatively rapidly with increasing loading of the sample (from 1.0 to 100 μg). In contrast, with a mobile phase with a methanol content of 83%, the k' values have been less affected and the R_s values decreased less sharply with increasing sample loading. Therefore, it seems that the observed decreases in R_s can be attributed to kinetic factors (poor mass transport in mobile phases with limited solubility of solutes) rather than to a true overloading of the stationary phase. From these results it follows that the mobile phases with higher methanol contents are to be preferred for preparative applications, thus permitting the separation of a large amount of sample with a single injection (*ca.* 80 μg).

Collection of the eluent from the start up to the upper quarter of the descending part of the first peak afforded the faster moving enantiomer in nearly 100% purity. The fraction collected from the

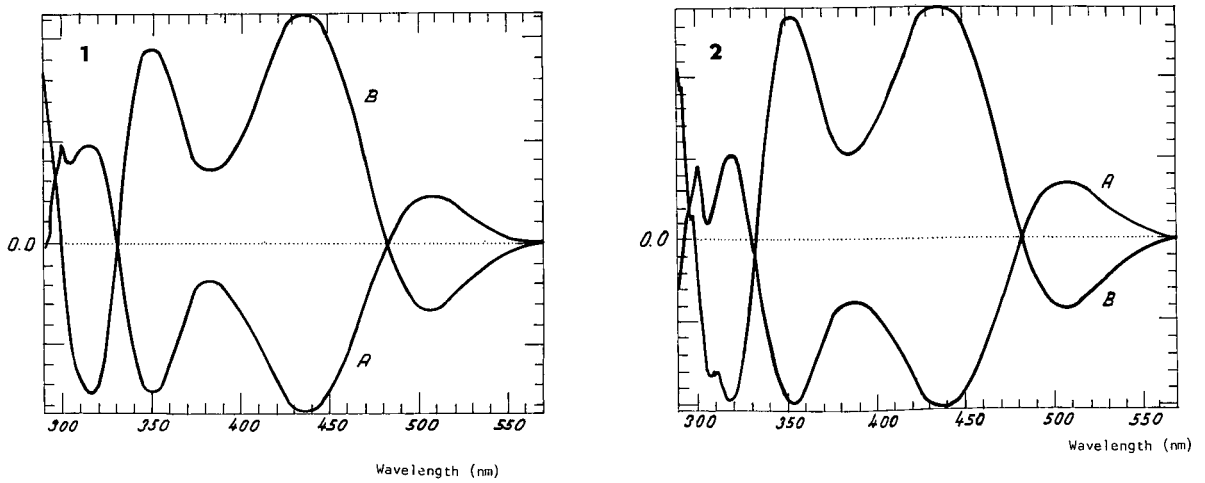

Fig. 5. CD spectra (wavelength range 300–580 nm) of the enantiomers of compounds **5** and **7**. (1) 6,6'-μ-allyl-S(1,7-$C_2B_9H_{10}$)$_2$-2-Co enantiomers; (2) 6,6'-μ-MeOCOCH$_2$-S(1,7-$C_2B_9H_{10}$)$_2$-2-Co enantiomers. Curves A and B represent the first- and second-eluting enantiomers, respectively.

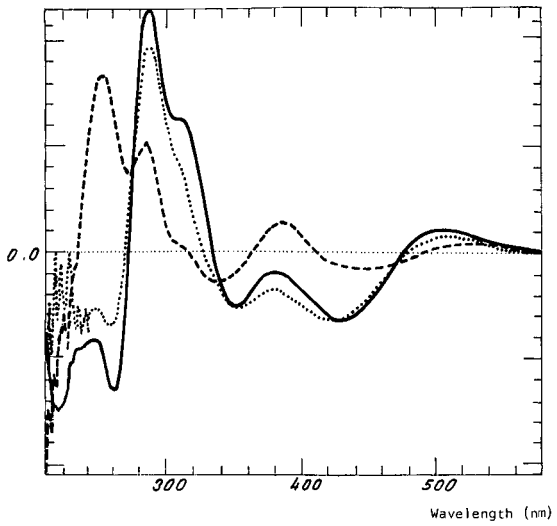

Fig. 6. CD spectra of the first-eluting enantiomers of (dashed line) [6,6′-μ-S(1,7-$C_2B_9H_{10})_2$-2-Co]$^-$ (**9**), (dotted line) [6,6′-μ-O(1,7-$C_2B_9H_{10})_2$-2-Co]$^-$ (**10**) and (solid line) 6,6′-μ-Me_2-N(1,7-$C_2B_9H_{10})_2$-2-Co.

maximum of the second peak throughout its descending part contained the second enantiomer in 96–97% purity. The optical purity of the both enantiomers was determined by the HPLC method under discussion.

Following this procedure, about 25 μg of each enantiomer can be isolated from single injections.

Circular dichroism spectra

CD spectra of the first- and second-eluted enantiomers of **1, 4, 5, 7, 9** and **13** prepared according to the scheme described above, exhibit very similar characteristics. The CD spectra of the enantiomers of **1, 4, 5** and **7** with a substituted sulphur bridge are almost identical, differing only in the intensities of the Cotton effects. Fig. 5 exemplifies the CD spectra of the first- and second-eluted enantiomers of **5** and **7**. Similar patterns of CD curves are also exhibited by the parent sulphur- and oxygen-bridged anions (**9** and **10**). CD spectra of their first-eluted enantiomers are depicted in Fig. 6 together with the spectrum of the first-eluting enantiomers of the $Me_2N<$-bridged compound. It can be seen that the orientations of the Cotton curves of these enantiomers are also very similar; only the positions of the Cotton effects are shifted to lower or higher wavelengths.

The close similarities of the CD spectra suggest the same absolute configurations of the enantiomers eluted as the first and second peaks, respectively, for all the compounds studied.

CONCLUSIONS

β-Cyclodextrin CSPs have proved to be efficient for the resolution of enantiomers of a variety of deltahedral carborane and metallaborane species, as demonstrated by the present study and by the results reported previously [13,14,16]. So far, 25 enantiomeric pairs of boron chiral species have been resolved on a β-cyclodextrin column and therefore the number of resolved chiral boranes known before their introduction (about 20) [18] has been more than doubled.

In addition to the study of the enantiomeric discrimination of the above species by use of a β-cyclodextrin HPLC column, the practical application of such knowledge for preparative purposes has proved possible, enabling us to isolate pure enantiomers in amounts sufficient for subsequent studies of their properties, *e.g.*, CD measurements and possibly for the determination of their structures by X-ray diffraction analysis.

ACKNOWLEDGEMENTS

Financial support from the Czechoslovak Academy of Sciences (grant No. 43 203) is highly appreciated. The authors are grateful to Mrs. P. Marková for technical assistance, Dr. Z. Plzák for technical support and Dr. B. Štíbr for helpful discussions of the text.

REFERENCES

1 R. A. Menges and D. W. Armstrong, in S. Ahuja (Editor), *Chiral Separations by Liquid Chromatography*, American Chemical Society, Washington, DC, 1991, p. 68.
2 W. L. Hinze, T. E. Riehl, D. W. Armstrong, W. DeMond, A. Alak, and T. Ward, *Anal. Chem.*, 57 (1985) 237.
3 D. W. Armstrong, Y. I. Han and S.H. Han, *Anal. Chim. Acta*, 208 (1988) 275.
4 S. H. Han, Y. I. Han and D. W. Armstrong, *J. Chromatogr.*, 441 (1988) 376.
5 T. J. Ward and D. W. Armstrong, *J. Liq. Chromatogr.*, 9 (1986) 407.

6 D. W. Armstrong, W. DeMond and B. P. Czech, *Anal. Chem.*, 57 (1985) 481.
7 R. Breslow, G. Trainor and A. Veno, *J. Am. Chem. Soc.*, 105 (1983) 2739.
8 W. J. LeNoble, S. Sristava, R. Breslow and G. Trainor, *J. Am. Chem. Soc.*, 105 (1983) 2745.
9 A. Harda and S. Takahashi, *J. Chem. Soc., Chem. Commun.*, 645 (1984)
10 E. N. Arnold, T. S. Lillie and T. S. Beesley, *J. Liq. Chromatogr.*, 12 (1989) 337.
11 R. D. Armstrong, T. J. Ward, N. Pattabiraman, C. Benz and D. W. Armstrong, *J. Chromatogr.*, 414 (1987) 192.
12 A. W. Coleman, G. Tsoucaris, H. Parrot, G. Galons, M. Miocque, B. Perly, N. Keller and P. Charpin, *J. Chromatogr.*, 450 (1988) 175.
13 J. Plešek, B. Grüner and P. Maloň, *Collect. Czech. Chem. Commun.*, in press.
14 J. Plešek, B. Grüner and P. Maloň, *J. Chromatogr.*, 626 (1992) 197.
15 T. Vaisar, T. Vaněk and E. Smolková-Keulemansová, *Eur. Pat.*, 891 215 26.1 (1988); *Czech. Pat. Appl.*, 7640 (1988).
16 J. Plešek, B. Grüner and H. Votavová, *Collect. Czech. Chem. Commun.*, in press.
17 J. Plešek, J. Holub, B. Grüner and J. Fusek, in preparation.
18 J. Plešek, S. Heřmánek and B. Štíbr, *Pure Appl. Chem.*, 63 (1991) 399.

Journal of Chromatography, 633 (1993) 81–87
Elsevier Science Publishers B.V., Amsterdam

CHROM. 24 762

Direct high-performance liquid chromatographic resolution of 2-aryl- and 2-heteroarylpropionic acids on a chiral stationary phase containing the N,N′-dinitrobenzoyl derivative of (1*R*,2*R*)-diaminocyclohexane

F. Gasparrini*, D. Misiti, C. Villani and M. Pierini

Dipartimento di Studi di Chimica e Tecnologia delle Sostanze Biologicamente Attive, Università "La Sapienza", Piazzale A. Moro 5, 00185 Rome (Italy)

F. La Torre

Istituto Superiore di Sanità, Laboratorio di Chimica del Farmaco, Viale Regina Elena 299, 00185 Rome (Italy)

(First received June 10th, 1992; revised manuscript received November 18th, 1992)

ABSTRACT

Racemic mixtures of eight non steroidal anti-inflammatory agents (derivatives of arylpropionic acids) were separated as 1-naphthalenemethylamides by HPLC on a chiral stationary phase containing the N,N′-3,5-dinitrobenzoyl derivative of (1*R*,2*R*)-diaminocyclohexane as chiral selector. Ibuprofen N,N-diethylamide, *n*-hexylamide and benzylamide and naproxen *n*-hexylamide and benzylamide were also resolved with chromatographic separation factors comparable to those obtained for the corresponding 1-naphthalenemethylamides; however, the latter derivatives showed significantly greater capacity factors (k'). The α values ranged from 1.10 to 1.83 and the k' values from 1.88 to 18.40 on a 250 × 4.0 mm I.D. stainless-steel column using *n*-hexane–2-propanol as the mobile phase.

INTRODUCTION

Analytical and preparative chromatographic methods for the separation of enantiomeric drugs are of great importance in the development of new therapeutic principles. The use of chromatographic systems (mainly HPLC and TLC) for monitoring enantiomeric purity has grown considerably in recent years [1–3]; in fact, the enantiomers of drugs may differ not only in their pharmacological properties but also in their side effects [4].

The optical resolution of a racemate may be achieved by reaction of the enantiomers with an enantiomerically pure reagent; the mixture of diastereoisomers is then separated on traditional columns. The formation of diastereoisomeric derivatives can introduce undetected errors arising from optically impure reagents, racemization of the reagents during the derivatization or different rates of formation of the diastereoisomers. These drawbacks can be avoided by means of direct liquid chromatographic separation of enantiomers after the formation of diastereoisomeric derivatives with a chiral selector in the mobile phase or by the use of chiral stationary phases (CSPs).

Arylpropionic acids are an important class of non-steroidal anti-inflammatory agents widely used for the relief of acute and chronic rheumatoid arthritis and osteoarthritis. Owing to a stereogenic

* Corresponding author.

0021-9673/93/$06.00

centre they exist as enantiomers, displaying pharmacokinetic stereoselectivity both *in vitro* and *in vivo*. The (*S*)-enantiomers of this class of compounds have a consistently higher pharmacological activity than (*R*)-enantiomers; further, the (*R*)-(−)-enantiomers of ibuprofen and naproxen were found to be converted *in vivo* into the corresponding (*S*)-(+)-enantiomers [5–8]. However, only naproxen and flunoxaprofen are administered as the resolved (*S*)(+)-enantiomer.

Several chromatographic methods for the resolution of arylpropionic acids have been developed. A series of anti-inflammatory agents were resolved as amides and anilides on a chiral stationary phase composed of (*R*)-N-(3,5-dinitrobenzoyl)phenylglycine or a variant of this chiral selector covalently bonded to the silica [9,10]. The effects of the mobile phase modifiers and four derivatizing reagents were investigated for the separation of enantiomers of ibuprofen and α-methoxyphenylacetic acid on a Pirkle column and on cellulose triphenylcarbamate coated on macroporous silica [11]. A chiral recognition model was proposed, involving interaction between amide derivatives of ibuprofen and the chiral selector contained in a Pirkle column [10]. Enantiomers of ibuprofen in biological fluids were resolved as amide derivatives on a Pirkle column [12,13]. Anionic drugs were separated without any derivatization on a chiral α_1-acid glycoprotein column (Enantiopac), and the effects of mobile phase additives and pH on the chiral resolution were also investigated [14]. Ibuprofen was separated as an amide derivative on a chiral stationary phase obtained by reacting γ-mercaptopropyl silica with quinine [15]. Acetylquinine chemically bonded to silica was used as a chiral selector in reversed-phase chromatography for the separation of naproxen derivatives [16]. Racemic mixtures of arylpropionic acids were resolved as diastereoisomeric derivatives of 1-phenylethylalanine [17] or 1-aminoethyl-4-dimethylaminonaphthalene using a normal-phase system [18]; enantiomers of naproxen [8] and ibuprofen in serum [19] were separated by means of a silica column after derivatization with chiral reagents. Diastereoisomeric derivatives of tiaprofenic acid [20] were resolved on a reversed-phase column after extraction from human plasma and urine. Derivatives of several non steroidal anti-inflammatory agents with optically active amines were separated as diastereoisomers by using TLC [21] or GC methods [22,23].

In this paper we describe the resolution of a series of racemic anti-inflammatory agents as amides using a chiral column containing the N,N′-3,5-dinitrobenzoyl derivative of (*R*,*R*)-1,2-diaminocyclohexane (DACH) as a chiral selector covalently bonded to a siliceous matrix [24,25].

EXPERIMENTAL

Apparatus

Chromatography was performed with a Waters (Milford, MA, USA) HPLC apparatus consisting of two Model 510 delivery systems, a U6K injector and a Model 481 variable-wavelength UV detector; chromatographic data were collected and processed on a Waters Model 840 data station.

Materials

HPLC-grade solvents were purchased from Merck (Darmstadt, Germany), 2-ethoxy-1-ethoxycarbonyl-1,2-dihydroquinoline (EEDQ), N,N-diethylamine, *n*-hexylamine and benzylamine from Fluka (Buchs, Switzerland) and 1-napthalenemethylamine from Aldrich-Chemie (Steinheim, Germany). Racemic pure acids (ketoprofen, flurbiprofen, fenoprofen, tiaprofenic acid, suprofen and ibuprofen) were extracted from pharmaceutical preparations: racemic naproxen and Br-naproxen [26] and the (*S*)-enantiomers [96% enantiomeric excess (e.e.)] were supplied by Zambon (Milan, Italy) and racemic flunoxaprofen and the (*S*)-enantiomer (96% e.e.) by Ravizza (Milan, Italy). Ibuprofen enriched in the (*S*)-enantiomer was obtained as described by Nicoll-Griffith *et al.* [13].

Amide derivatives of α-methylarylacetic acids were prepared by two different procedures, as follows.

Method A. This was used for ibuprofen, ketoprofen, fenoprofen and flurbiprofen 1-naphthalenemethylamides and ibuprofen *n*-hexylamide, benzylamide and N,N′-diethylamide.

In a typical run, ibuprofen (1.03 g, 5 mmol) was dissolved in 1.0 ml of thionyl chloride and refluxed for 2 h; the excess of thionyl chloride was removed under reduced pressure, then 5 ml of dry benzene were added to the residue and the solution was evaporated under reduced pressure; 1.1 g (98%) of acid chloride was obtained as a yellowish oil.

To a solution of the acid chloride (1.1 g, 4.9 mmol) in 10 ml of chloroform, 1-napthalenemethylamine (0.78 g, 4.9 mmol) and triethylamine (0.7 ml, 4.9 mmol) were added dropwise; after 1 h at room temperature, the solution was washed with 1 *M* HCl (2 × 10 ml), 1 *M* NaOH (2 × 10 ml) and brine (2 × 10 ml) and dried over anhydrous sodium sulphate. Filtration and evaporation afforded 1.3 g of 1-naphthalenemethylamide (75%).

Method B. This was used for flunoxaprofen, naproxen, Br-naproxen and tiaprofenic acid 1-naphthalenemethylamide and naproxen benzylamide and *n*-hexylamide.

To a solution of naproxen (0.23 g, 1 mmol) in 5 ml of dry tetrahydrofuran (THF), EEDQ (0.25 g, 1 mmol) was added; the mixture was stirred at room temperature for 2 h and then 1-naphthalenemethylamine (0.15 g, 1 mmol) was added. After 4 h at room temperature, the THF was removed under reduced pressure and the residue dissolved in diethyl ether. Work-up of the crude product (see method A) afforded 0.31 g of the desired amide (85%).

Chiral stationary phase

The preparation of the chiral stationary phase and the evaluation of the kinetic performance of the columns have been reported previously [24,25]. The structure of the CSP is shown in Fig. 1.

For this work a 250 × 4.0 mm I.D. stainless-steel column, packed with (*R,R*)-DACH-DNB CSP (LiChrosorb Si 100, 5 μm), was used. The elution order of ibuprofen, flurbiprofen, flunoxaprofen, naproxen and bromonaproxen derivatives was determined by injection of samples enriched in one enantiomer of known configuration.

RESULTS AND DISCUSSION

The racemic acids were converted into substituted amides as shown in Fig. 2; this manipulation allowed us to include in the structure of the analytes additional interaction sites complementary with the CSP, namely the secondary amide group and the electron-rich naphthalene ring; the latter, a strong UV-absorbing chromophore, is also useful in the enantiomeric trace analysis of solutes (*e.g.*, ibuprofen) with low UV molar absorptivities.

No detectable isomerization was observed during the conversion of naproxen, Br-naproxen, flunoxaprofen and ibuprofen, enantiomerically enriched (96% e.e.), into substituted amides with methods A and B. Chromatographic results are given in Table

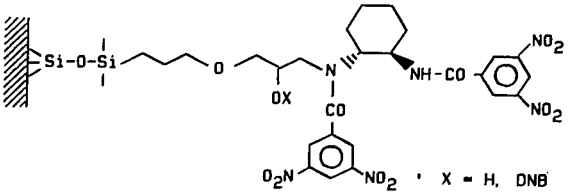

Fig. 1. Structure of the chiral stationary phase.

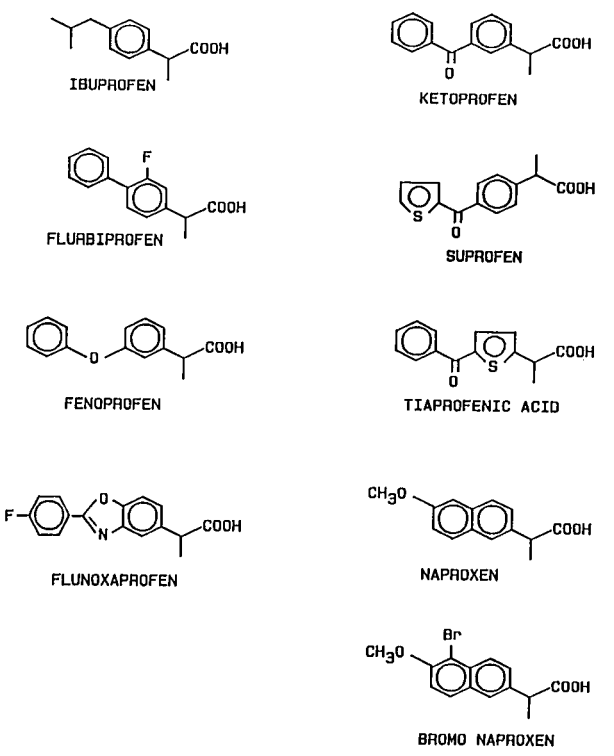

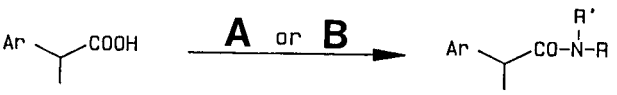

Fig. 2. Structures of racemic acids and derivatization procedures. A = $SOCl_2$, amine, Et_3N. B = EEDQ, amine. R = n-C_6H_{13}, $PhCH_2$, 1-naphthyl-CH_2, R′ = H; R = R′ = ethyl.

TABLE I

CHROMATOGRAPHIC RESULTS

CSP: (*R,R*)-DACH-DNB LiChrosorb Si 100, 5 μm. All compounds were eluted at a flow-rate of 2 ml/min at 25°C. UV detection at 280 nm.

Compound	Acid	Derivative	k'^a	α^b	R_s	2PA[c] (%)	First-eluted isomer
1	Ibuprofen	N,N'-Diethylamide	2.00	1.11	1.0	5	*S*
2	Ibuprofen	*n*-Hexylamide	2.59	1.16	1.2	10	*S*
3	Ibuprofen	Benzylamide	7.21	1.20	1.4	10	*S*
4	Ibuprofen	1-Naphthalenemethylamide	1.88	1.26	1.0	40	*S*
5	Flurbiprofen	1-Naphthalenemethylamide	2.98	1.27	1.2	40	*S*
6	Fenoprofen	1-Naphthalenemethylamide	3.34	1.27	1.2	40	n.d.[d]
7	Flunoxaprofen	1-Naphthalenemethylamide	4.66	1.46	1.9	40	*S*
8	Ketoprofen	1-Naphthalenemethylamide	6.06	1.23	1.1	40	n.d.
9	Suprofen	1-Naphthalenemethylamide	9.88	1.10	0.6	40	n.d.
10	Tiaprofenic acid	1-Naphthalenemethylamide	10.22	1.83	2.7	40	n.d.
11	Naproxen	*n*-Hexylamide	2.22	1.47	1.5	40	*S*
12	Naproxen	Benzylamide	6.37	1.49	2.2	40	*S*
13	Naproxen	1-Naphthalenemethylamide	18.40	1.49	2.0	40	*S*
14	Br-naproxen	1-Naphthalenemethylamide	18.02	1.55	2.1	40	*S*

[a] Capacity factor for the first-eluted enantiomer.
[b] Enantioselectivity factor.
[c] Percentage of 2-propanol in *n*-hexane in the mobile phase.
[d] Not determined.

I. The α-values range from 1.10 to 1.83 using *n*-hexane–2-propanol as the mobile phase; slightly different selectivities and lower retentions were observed using a ternary mobile phase containing both dichloromethane and 2-propanol as polar modifiers (see Table II and Fig. 3). Owing to the efficiency of the chiral column, all the examined compounds were completely resolved; for compound **9**, partial resolution was obtained as a result of low stereoselectivity and pronounced peak tailing.

TABLE II

CHROMATOGRAPHIC RESULTS

CSP: (*R,R*)-DACH-DNB LiChrosorb Si 100, 5 μm. All compounds were eluted at a flow-rate of 2 ml/min at 25°C. UV detection at 280 nm. All compounds as 1-napthalenemethylamide derivatives.

Compound	Acid	k'^a	α^b	R_s	Eluent[c]	First-eluted isomer
4	Ibuprofen	1.76	1.21	1.1	A	*S*
5	Flurbiprofen	2.54	1.41	1.5	A	*S*
7	Flunoxaprofen	2.00	1.34	1.3	B	*S*
10	Tiaprofenic acid	2.92	2.08	3.7	B	n.d.[d]
13	Naproxen	4.11	1.49	2.0	B	*S*

[a] Capacity factor for the first-eluted enantiomer.
[b] Enantioselectivity factor.
[c] A = *n*-hexane–dichloromethane–2-propanol (60:20:20); B = *n*-hexane–dichloromethane–2-propanol (50:25:25).
[d] Not determined.

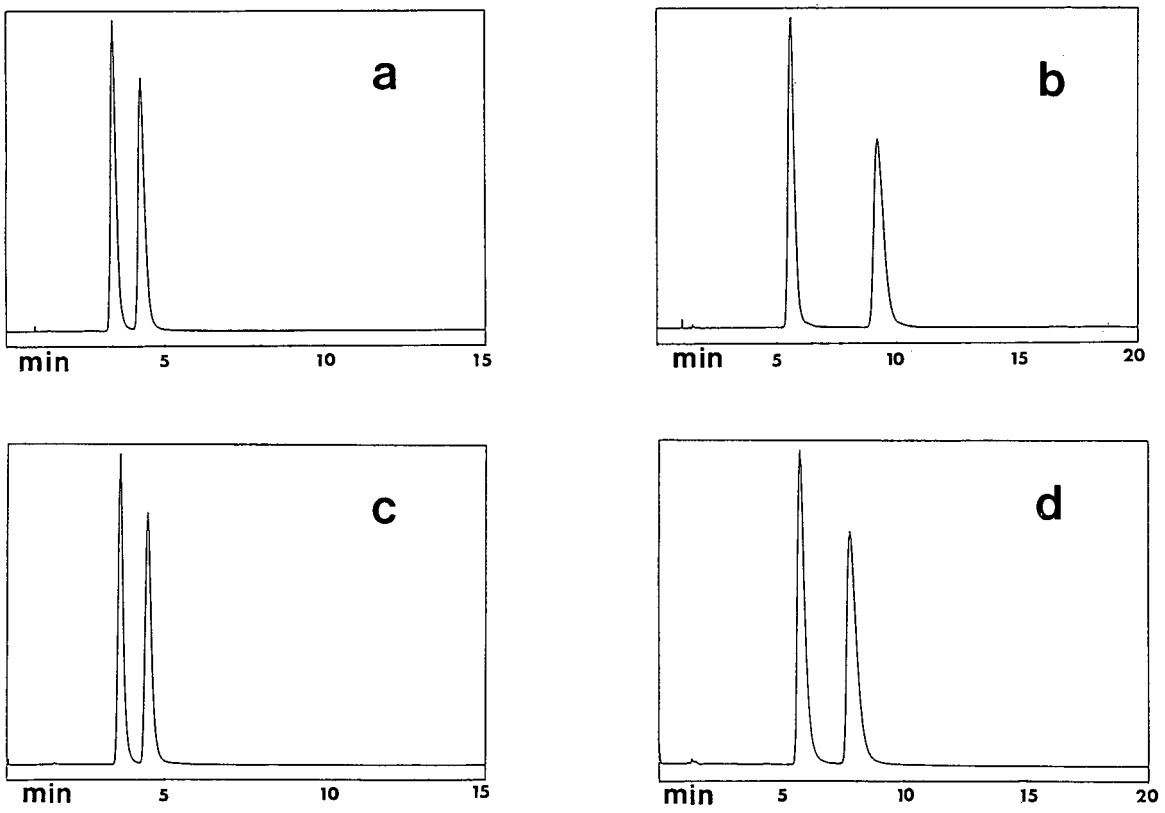

Fig. 3. Resolution of racemic acids as 1-naphthalenemethylamides on (*R,R*)-DACH-DNB CSP. (a) Ibuprofen; (b) tiaprofenic acid; (c) flunoxaprofen; (d) naproxen. UV detection at 280 nm; other chromatographic conditions as in Table II.

Solute structure and stereoselectivity

Both retention and enantioselectivity show a significant dependence on the nature of the aromatic groups arranged around the stereogenic centre of the analytes; in the series of 1-naphthalenemethylamides the capacity factors (k') increase with increasing ability of the acid-derived aryl substituent to act as a π-donor and a similar trend is observed for the α values.

As far as the carboxylic group transformation is concerned, the data in Table I clearly show that the nature of the amine employed has little effect on the chiral recognition ability of the CSP towards different derivatives of the same acid; the chromatographic separation factors for the *n*-hexylamides and benzylamides of ibuprofen and naproxen are comparable to those noted for the corresponding 1-naphthalenemethylamides; however, the latter derivatives show significantly greater capacity factors.

Tertiary amide derivatives of ibuprofen and naproxen are also resolved with similar α values and reduced retentions in comparison with the secondary amide derivatives; these results indicate that both hydrogen bonding (between the N–H amide proton of the secondary amides and the CSP) and dipole stacking (tertiary amides) are operative during the chiral recognition process.

The elution order is constant for all the amides of ibuprofen, flurbiprofen, flunoxaprofen, naproxen and Br-naproxen, the (*R*)-enantiomers being those most retained on the (*R,R*)-DACH-DNB CSP; the same elution order has been reported by several workers for the resolution of amides of ibuprofen, naproxen, benoxaprofen, fenoprofen on a Pirkle (*R*)-phenylglycine-derived CSP [9,11,27]. From the above observations, at least two extreme possible mechanisms of resolution can be outlined: for solutes obtained from amines lacking π-basic groups,

chiral recognition occurs through a π–π interaction between the DNB groups of the CSP and the aryl (or heteroaryl) substituent of the analytes, together with dipole stacking and/or hydrogen bonding of amide dipoles; in the case of amides prepared from amines containing adequate π-basic groups (*i.e.*, 1-naphthalenemethylamine), the dominant π–π interaction is established between the dinitrobenzoyl group of the stationary phase and the aryl group derived from the amine.

These two mechanisms can be operated simultaneously for compounds containing two aryl groups of comparable π-basicity (compounds **3**, **13** and **14**); the high retentions observed for these analytes, especially **13** and **14**, can be accounted for the assumption of multiple interaction sites and modes with the stationary phase.

The broad selectivity of the (*R*,*R*)-DACH-DNB towards different derivatives of the same acid can be exploited to design "flexible" analytical methods capable of detecting a low concentration of a single enantiomer even in complex matrices. For example, the resolution of ibuprofen can be carried out after its conversion into a secondary amide using either amines containing an aromatic group or aliphatic amines: in the first instance, the two enantiomers corresponding to the ibuprofen derivatives are well separated from the impurities arising from the derivatization step, allowing the sample to be injected directly without any work-up. Moreover, the sensitivity of the chromatographic method is greatly enhanced by the additional UV-absorbing group introduced in the analyte structure. On the other hand, the use of aliphatic amines as derivatizing agents results in the formation of secondary amides that are still well resolved on the CSP but show lower capacity factors, which lead to reduced analysis times.

The precision and accuracy of the stereoselective chromatographic methods based on DACH-DNB CSP can also be improved by switching from one enantiomeric form of the chiral selector to the other [both the (*R*,*R*) and the (*S*,*S*) versions of the CSP, as well as the racemic version, have been prepared and evaluated] [25]. This technique is successfully employed when a low level of a single enantiomer has to be determined in the presence of a large excess of the other; by choosing the appropriate chirality of the CSP, the trace isomer can be positioned in the chromatogram before the major constituent, thus allowing more precise and accurate quantification.

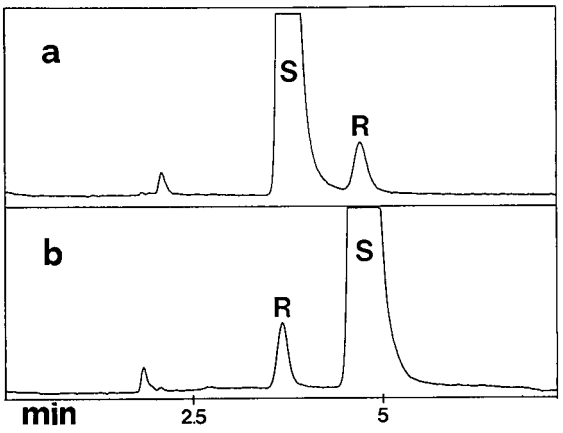

Fig. 4. Optical purity determination on two columns of opposite chirality; (a) (*R*,*R*)-DACH-DNB column; (b) (*S*,*S*)-DACH-DNB column. Sample: (*S*)-flunoxaprofen as 1-naphthalenemethylamide. UV detection at 293 nm; other conditions as in Table II.

An example is shown in Fig. 4: six replicate injections of (*S*)-flunoxaprofen-1-naphthalenemethylamide containing a small amount of the (*R*)-isomer gave a mean value for the trace enantiomer of 2.64 ± 0.03% using the (*S*,*S*) column (minor enantiomer eluting first) and 2.68 ± 0.08% using the (*R*,*R*) column.

ACKNOWLEDGEMENT

This work was supported by CNR–Progetto Finalizzato Chimica Fine II.

REFERENCES

1 M. Zief and L. J. Crane (Editors), *Chromatographic Chiral Separations*, Marcel Dekker, New York and Basle, 1988.
2 A. M. Krstulovic (Editor), *Chiral Separations by HPLC: Applications to Pharmaceutical Compounds*, Ellis Horwood, Chichester, 1989.
3 S. G. Allenmark, *Chromatographic Enantioseparations: Methods and Applications*, Ellis Horwood, Chichester, 1988.
4 E. J. Ariens, *Med. Res. Rev.*, 6 (1986) 451.
5 D. G. Kaiser, G. J. Vangiessen, R. J. Reischer and W. J. Wechter, *J. Pharm. Sci.*, 65 (1976) 269.
6 J. Caldwell, A. J. Hutt and S. Fournel-Gigleux, *Biochem. Pharmacol.*, 37 (1988) 105.
7 F. Jamali, *J. Drug Metab. Pharmacokinet.*, 13 (1988) 1.
8 J. Goto, N. Goto and T. Nambara, *J. Chromatogr.*, 239 (1982) 559.

9 I. W. Wainer and T. D. Doyle, *J. Chromatogr.*, 284 (1984) 117.
10 W. H. Pirkle and J. E. McCune. *J. Chromatogr.*, 471 (1989) 271.
11 D. M. McDaniel and G. Snider, *J. Chromatogr.*, 404 (1987) 123.
12 D. A. Nicoll-Griffith, *J. Chromatogr.*, 402 (1987) 179.
13 D. A. Nicoll-Griffith, T. Inaba, B. K. Tang and W. Kalov, *J. Chromatogr.*, 428 (1988) 103.
14 G. Schill, I. W. Wainer and S. A. Barkan, *J. Chromatogr.*, 365 (1986) 73.
15 C. Bertúcci, C. Rosini, D. Pini and P. Salvatori, *J. Pharm. Biomed. Anal.*, 5 (1987) 171.
16 C. Pettersson and C. Gioeli, *J. Chromatogr.*, 398 (1987) 247.
17 J. M. Maître, G. Boss and T. Testa, *J. Chromatogr.*, 299 (1984) 397.
18 J. Goto, N. Goto, A. Hikichi, T. Nishimaki and T. Nambara, *Anal. Chim. Acta*, 120 (1980) 187.
19 A. Avgerinos and A. J. Hutt, *J. Chromatogr.*, 415 (1987) 75.
20 R. Mehvar, F. Jamali and F. M. Pasutto, *J. Chromatogr.*, 425 (1988) 135.
21 P. Slégel, G. Vereczkey-Donath, L. Ladanyi and M. Toth-Lauritz, *J. Pharm. Biomed. Anal.*, 5 (1987) 665.
22 N. N. Singh, F. M. Pasutto, R. T. Coutts and F. Jamali, *J. Chromatogr.*, 378 (1986) 125.
23 B. Blessington, N. Crabb, S. Karkee and A. Northage, *J. Chromatogr.*, 469 (1989) 183.
24 F. Gasparrini, D. Misiti, C. Villani, F. La Torre and M. Sinibaldi, *J. Chromatogr.*, 457 (1988) 235.
25 F. Gasparrini, D. Misiti, C. Villani and F. La Torre, *J. Chromatogr.*, 539 (1991) 25.
26 C. Giordano, G. Castaldi, S. Cavicchioli and M. Villa, *Tetrahedron*, 45 (1989) 4243.
27 W. H. Pirkle and J. E. McCune, *J. Chromatogr.*, 469 (1989) 67.

Journal of Chromatography, 633 (1993) 89–96
Elsevier Science Publishers B.V., Amsterdam

CHROM. 24 748

Direct high-performance liquid chromatographic separation of the enantiomers of diltiazem hydrochloride and its 8-chloro derivative on a chiral ovomucoid column

Hiroyuki Nishi*, Norio Fujimura, Hiroshi Yamaguchi and Tsukasa Fukuyama

Analytical Chemistry Research Laboratory, Tanabe Seiyaku Co., Ltd., 16–89, Kashima 3-chome, Yodogawa-ku, Osaka 532 (Japan)

(First received October 12th, 1992; revised manuscript received November 9th, 1992)

ABSTRACT

A direct enantiomeric separation of diltiazem hydrochloride and its related compounds was investigated by using an ovomucoid bonded chiral stationary phase. The enantiomers of diltiazem hydrochloride, the 8-chloro derivative of diltiazem (clentiazem maleate) and their desacetyl forms were resolved with a mobile phase of acetonitrile–0.02 *M* phosphate buffer (pH 6.0) according to the retention mechanism of reversed-phase liquid chromatography. The effects of mobile phase composition on the retention and the enantioselectivity, the effects of sample capacity on the retention time, theoretical plate number, peak height and peak area were investigated. The chromatographic conditions chosen for the separation permitted the separation of these enantiomers within 20 min. The determination of the antipode in the drug substances and those in tablets was also successfully achieved at levels down to *ca.* 0.1% by the area-percentage method.

INTRODUCTION

The desired pharmacological effect of a drug is often associated with only one of the enantiomers and the antipode may have different potencies, pharmacological activities and/or side-effects [1,2]. It is very important to characterize the pharmacological effects and the pharmacokinetics of the enantiomers of the drug in order to elucidate whether therapeutic benefits can be obtained by the use of only one enantiomer. The antipode, which has no or undesired pharmacological effects, can be regarded as one of impurities from the quality aspect. Such studies require techniques that permit the separation of the enantiomers.

High-performance liquid chromatography (HPLC) is suitable for such a purpose. Generally, there are two methods for the chromatographic separation of enantiomers: the indirect diastereomeric method using a chiral derivatization reagent, followed by separation on a non-chiral column [3], or direct chromatographic separation on a chiral column. During the last few years, interest in the direct separation of the enantiomers has increased and a number of chiral stationary phases have been prepared and some of them are now commercially available [4,5]. Especially bonded proteins such as bovine serum albumin (BSA) and α_1-acid glycoprotein (AGP) as a chiral selector have great enantioselectivity for solutes with widely different structures [6,7].

Diltiazem hydrochloride [(+)-(*S*,*S*)-form], 1,5-benzothiazepine derivative, is a representative calcium antagonist along with nifedipine and verapamil and is widely used as an antianginal and antihypertentive drug [8]. The 8-chloro derivative of diltiazem [(+)-(*S*,*S*)-form] is a new 1,5-benzothiazepine calcium antagonist that is currently being evaluated as clentiazem maleate. The calcium antagonist action of clentiazem is 2–10 times as potent as that of diltiazem is vascular smooth muscles and lasts longer [9–12].

* Corresponding author.

0021-9673/93/$06.00

Enantiomers of diltiazem hydrochloride were first chromatographically resolved by the indirect method using two kinds of chiral reagents [13,14]. Recently, a direct chiral separation was successfully achieved by using a chiral stationary phase such as Chiralcel OC or OF (Daicel, Tokyo, Japan) in normal-phase HPLC [15,16]. This paper describes the direct reversed-phase HPLC separation of the enantiomers of diltiazem hydrochloride, the 8-chloro derivative of diltiazem and their desacetyl forms on recently developed ovomucoid chiral stationary phase [17–19]. The effects of pH, ionic strength of the buffer and organic solvents (species and content) on the retention and enantioselectivity of the solutes were studied. The effects of sample capacity on the retention time, theoretical plate number, peak height and peak area were also investigated. The separation of the enantiomers was achieved within 20 min according to the reversed-phase HPLC retention mechanism. The method permitted the determination of the optical purity of the drug at levels down to *ca.* 0.1% by the area-percentage method. It was found that the structure of these solutes significantly affects their enantioselectivity.

EXPERIMENTAL

Apparatus

The chromatographic system consisted of a Shimadzu (Kyoto, Japan) LC-3A pump, a Rheodyne Model 7125 injector with a 20-μl loop, a Shimadzu CTO-2A column oven and a Shimadzu SPD-2A variable-wavelength UV detector. A Shimadzu SPD-M6A photodiode-array detector was used to monitor the UV spectra of the peaks. The chromatograms were recorded on a Shimadzu Chromatopac CR5A. An Ultron ES-OVM ovomucoid chiral column (150 mm × 4.6 mm I.D.), in which ovomucoid is chemically bonded to aminopropylsilica gel of particle size 5 μm, was purchased from Shinwakako (Kyoto, Japan).

Chemicals and materials

Racemic diltiazem hydrochloride (DIL), the 8-

Solute	R_1	R_2
Diltiazem hydrochloride (DIL)	H	$COCH_3$
Desacetyl diltiazem (DIL-OH)	H	H
8-Chloro derivative (CHL)	Cl	$COCH_3$
Desacetyl 8-chloro derivative (CHL-OH)	Cl	H

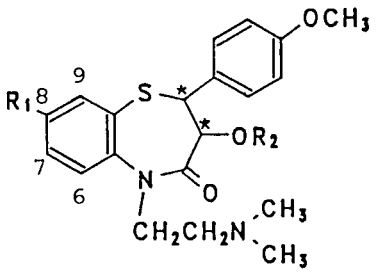

* asymmetric carbon atom

Fig. 1. Structures of diltiazem and related compounds.

chloro derivative of diltiazem (clentiazem maleate) (CHL) and their desacetyl forms and their (+)-(*S*,*S*)-enantiomers were obtained from the research laboratory of Tanabe Seiyaku (Osaka, Japan). The 6-, 7- and 9-chloro derivatives of diltiazem were also used to investigate the enantioselectivity of the column. The structures are shown in Fig. 1. These solutes were dissolved in acetonitrile–water (1:1) at a concentration of *ca.* 0.2 mg/ml. The drug substances for optical purity testing were dissolved in acetonitrile–water (1:1) at 2 mg/ml. Acetonitrile of HPLC grade and ethanol and methanol of analytical-reagent grade were purchased from Katayama Kagaku (Osaka, Japan). Water was purified with a Millipore RO-60 water system (Nihon Millipore, Tokyo, Japan). All other reagents and solvents were of analytical-reagent grade from Katayama Kagaku.

Chromatographic conditions

The separation was carried out at a flow-rate of 1.0 ml/min and a column temperature of 40°C. The wavelength of detection was 240 nm, which is around the UV absorption maximum of the solutes. The mobile phase were prepared by mixing a 0.02 *M* phosphate buffer solution with an organic solvent. The pH of the buffer was adjusted to specified values by using dilute phosphoric acid (*ca.* 5%) or 0.2 *M* sodium hydroxide solution. The mobile phases were passed through a membrane filter of 0.45-μm pore size (Fuji Photo Film, Tokyo, Japan) prior to use. The injection volume was fixed at 5 μl.

RESULTS AND DISCUSSION

Effect of organic solvents

Different organic solvents such as methanol, ethanol and acetonitrile were used to regulate the retention and the enantioselectivity. The results using 0.02 *M* phosphate buffer (pH 6.0) and each organic solvent are summarized in Table I. The sample loading was 1 μg each in a 5-μl injection. Methanol was the most effective organic solvent for the enantioselectivity. With the use of methanol or ethanol, the (+)-enantiomer of the 8-chloro derivative of diltiazem did not elute within 35 min whereas its (−)-enantiomer eluted at *ca.* 6 min. This is not acceptable from the separation aspect, although these conditions are suitable for preparative purposes. The separation of the enantiomers was then optimized by using acetonitrile as the organic solvent.

The effect of the concentration of acetonitrile was investigated with a 0.02 *M* phosphate buffer (pH 6.0). The results with acetonitrile at concentrations of 10% and 20% are summarized in Table II and those with 15% acetonitrile in Table I. The retention times of the solutes increased with a decrease in the acetonitrile content. The resolution (R_s) and separation factor (α) were improved with an increase in the retention times. The same results were obtained with other organic solvents.

Effect of buffer pH

The retention of ionic solutes on protein bonded phases generally varies with changes in pH [6,7].

TABLE I

EFFECT OF ORGANIC SOLVENT ON RETENTION AND ENANTIOSELECTIVITY

Mobile phase: organic solvent–0.02 *M* phosphate buffer (pH 6.0)

Solute	Methanol (35%)				Ethanol (25%)				Acetonitrile (15%)			
	k' (−)	k' (+)	α	R_s	k' (−)	k' (+)	α	R_s	k' (−)	k' (+)	α	R_s
DIL	1.62	8.11	5.00	8.26	1.82	3.31	1.82	2.81	1.39	2.78	2.00	3.80
DIL-OH	1.85	4.48	2.42	7.27	1.99	2.69	1.35	1.98	1.41	2.01	1.43	2.35
CHL	2.68	20<[a]	–	–	2.40	20<[a]	–	–	2.29	18.59	8.10	8.79
CHL-OH	2.60	15.58	5.98	11.45	2.56	6.33	2.40	6.33	1.94	3.86	1.99	4.70

TABLE II

EFFECT OF ACETONITRILE CONCENTRATION ON RETENTION AND ENANTIOSELECTIVITY

Mobile phase: acetonitrile–0.02 *M* phosphate buffer (pH 6.0).

Solute	20%				10%			
	$k'(-)$	$k'(+)$	α	R_s	$k'(-)$	$k'(+)$	α	R_s
DIL	1.05	1.40	1.33	1.57	2.80	12.23	4.37	7.99
DIL-OH	1.12	1.33	1.19	0.97	2.13	4.78	2.24	6.03
CHL	1.31	5.04	3.84	6.48	3.84	20<[a]	–	–
CHL-OH	1.34	1.85	1.38	1.98	3.52	15.42	4.35	8.51

[a] Not eluted within 35 min.

This can be interpreted by the charges generated in the protein, through the electrostatic interaction. For comparison, the retention of the solutes was investigated with 0.02 *M* phosphate buffer of pH 4.0, and the results are summarized in Table III. The sample loading was 1 μg each in a 5-μl injection. The concentration of the organic solvent required for their elution at a capacity factor of *ca.* 1 was lower than that at pH 6.0. This can be interpreted by the increase in electrostatic repulsion between the protein and the solute from the isoelectric point of the solutes of *ca.* 7 [20] and that of the ovomucoid of 3.9–4.3 [17]. The enantioselectivity at pH 4.0 was much improved by an increase in the retention of the (+)-enantiomers compared with that of the (−)-enantiomers, resulting in larger separaton factors and long analysis times. From the standpoint of analysis time and appropriate k' value ($1 < k' < 10$), a buffer of pH 6.0 was selected.

Effect of ionic strength

The effect of the ionic strength on the retention and the enantioselectivity was investigated using a mobile phase of phosphate buffer (pH 6.0)–acetonitrile (88:12) and diltiazem and its desacetyl form as test samples (1 μg each). The results are summarized in Table IV. The separation factors gradually decreased with an increase in ionic strength, owing to the decrease in retention. However, the effect is not very large and is not important for the chiral recognition and hydrophobic interaction.

The final composition of the mobile phase established through the investigation of the effects of these parameters was 0.02 *M* phosphate buffer (pH 6.0)–acetonitrile (88:12) for diltiazem hydrochloride and (82:18) for the 8-chloro derivative of diltiazem, clentiazem maleate. Typical chromatograms are shown in Figs. 2 and 3. The UV spectra of the enantiomers of diltiazem hydrochloride monitored by using the photodiode-array detector are shown in Fig. 4. Each peak gave the same spectrum and the maximum absorption at around 240 nm.

Effect of solute structure on enantioselectivity

The effect of solute structure on the enantioselec-

TABLE III

EFFECT OF pH BUFFER ON RETENTION AND ENANTIOSELECTIVITY

Mobile phase: 0.02 *M* phosphate buffer (pH 4.0)–organic solvent.

Solute	Methanol (20%)				Acetonitrile (5%)			
	$k'(-)$	$k'(+)$	α	R_s	$k'(-)$	$k'(+)$	α	R_s
DIL	0.23	2.38	10.37	3.17	0.43	3.75	8.79	6.79
CHL	0.46	17.52	38.26	7.86	1.33	20<[a]	–	–

[a] Not eluted within 35 min.

TABLE IV

EFFECT OF IONIC STRENGTH ON RETENTION AND ENANTIOSELECTIVITY

Mobile phase: phosphate buffer (pH 6.0)–acetonitrile (88:12).

Solute	Ionic strength											
	10 m*M*				20 m*M*				40 m*M*			
	$k'(-)$	$k'(+)$	α	R_s	$k'(-)$	$k'(+)$	α	R_s	$k'(-)$	$k'(+)$	α	R_s
DIL	3.37	8.77	2.60	6.01	2.96	7.63	2.58	6.41	2.59	6.63	2.56	6.18
DIL-OH	3.03	4.93	1.62	4.46	2.66	4.24	1.59	4.29	2.36	3.47	1.47	3.58

tivity was investigated using 0.02 *M* phosphate buffer (pH 6.0)–acetonitrile (82:18). The results are summarized in Table V. The retention time of the (+)-enantiomer of the 8-chloro derivative was the largest among the five solutes tested, those of the others being similar to each other. The 8-chloro derivative also eluted last among these solutes using ion-pair chromatography and an ODS column [20] and using micellar electrokinetic chromatography [21]. These results indicate that 8-substituted diltiazem acquires a very hydrophobic nature owing to the substitution at the 8-position. This hydrophobic nature probably leads to dramatic improvements in enantioselectivity through hydrophobic interaction and/or hydrogen bonding.

Effect of sample capacity

The effects of the amount of sample on the retention time (t_R), theoretical plate number (N), peak height (h) and peak area (A) were investigated using diltiazem as a sample with an injection volume of 5

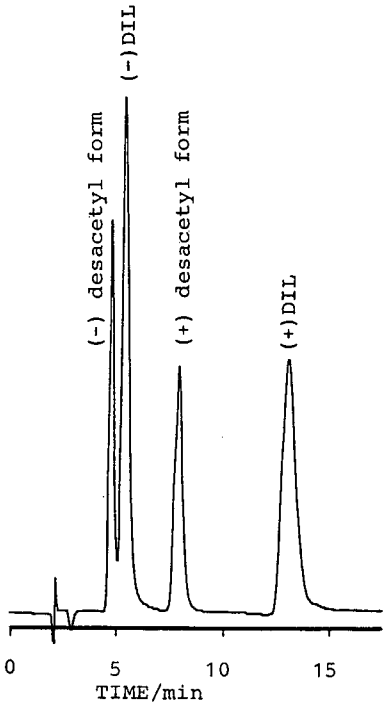

Fig. 2. Chiral separation of the enantiomers of diltiazem hydrochloride (DIL) and its desacetyl form.

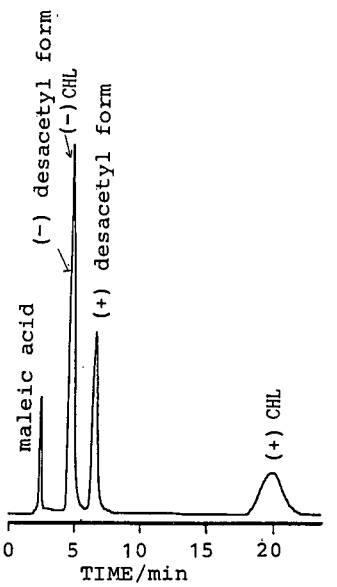

Fig. 3. Chiral separation of the enantiomers of the 8-chloro-derivative of diltiazem (clentiazem; CHL) and its desacetyl form.

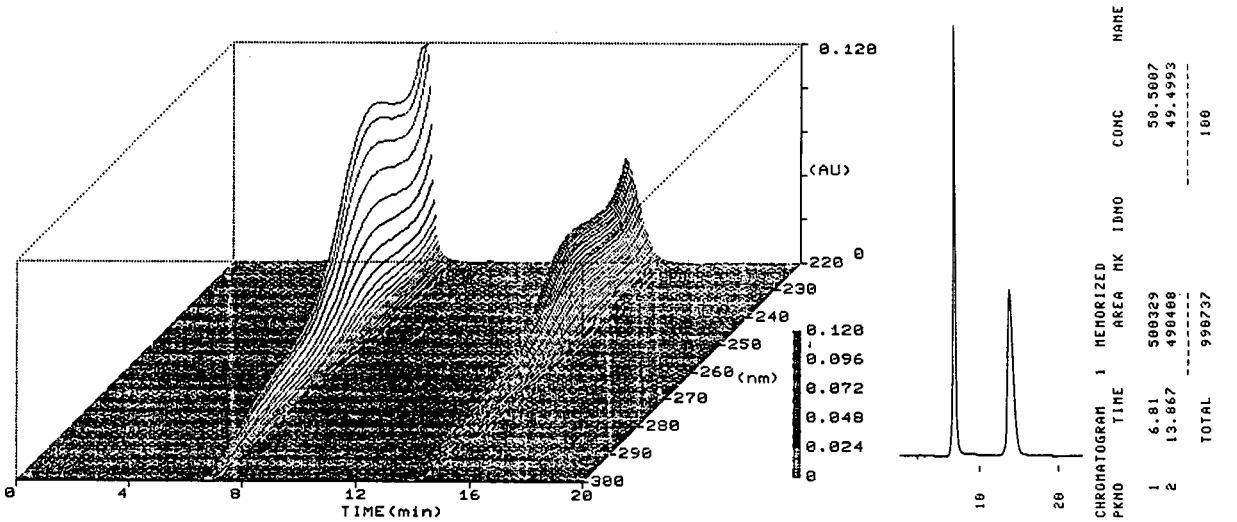

Fig. 4. UV spectra of the enantiomers of diltiazem hydrochloride obtained with the photodiode-array detector.

μl. The results are shown in Figs. 5 and 6. N and t_R decreased with increase in the amount of sample. A tenfold increase in the amount of diltiazem (1–10 μg) resulted in a 10% decrease in t_R and a *ca.* 70% decrease in N. The peak areas, however, showed good linearity over the tested range with a correlation coefficient (r) of 0.9999. This permits the optical purity testing of the enantiomer by the area-percentage method.

Application to the optical purity testing

The linearity of the response of the (−)-enantiomer of diltiazem was investigated over the concentration range 0.1–2.0% (w/w). The total amount of diltiazem injected was 10 μg with a 5-μl injection volume. The result is shown in Fig. 7. The graph is a straight line that passes through the origin over the tested range with r = 0.9998, slope =

TABLE V

EFFECT OF SAMPLE STRUCTURE ON RETENTION AND ENANTIOSELECTIVITY

Mobile phase: 0.02 M phosphate–buffer (pH 6.0)–acetonitrile (82:18).

Solute	k' (−)	k' (+)	α
9-Chloro	2.18	2.63	1.21
8-Chloro	2.37	10.75	4.54
7-Chloro	−[a]	2.36	−
6-Chloro	1.78	2.38	1.34
Diltiazem	2.28	3.38	1.48

[a] Not examined.

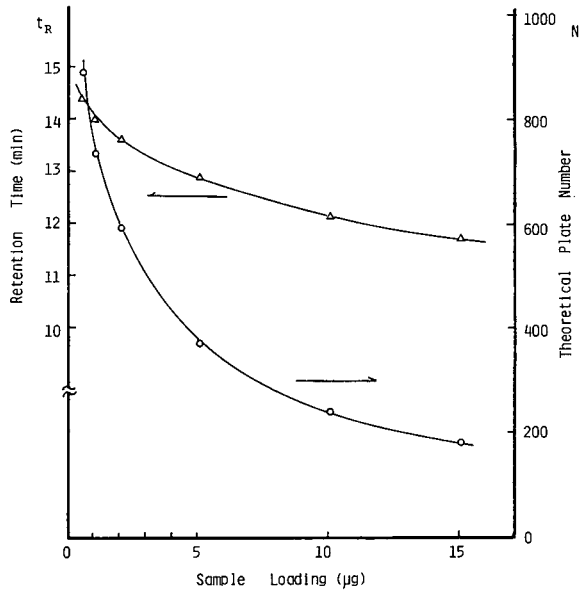

Fig. 5. Effects of sample loading on retention times and theoretical plate numbers.

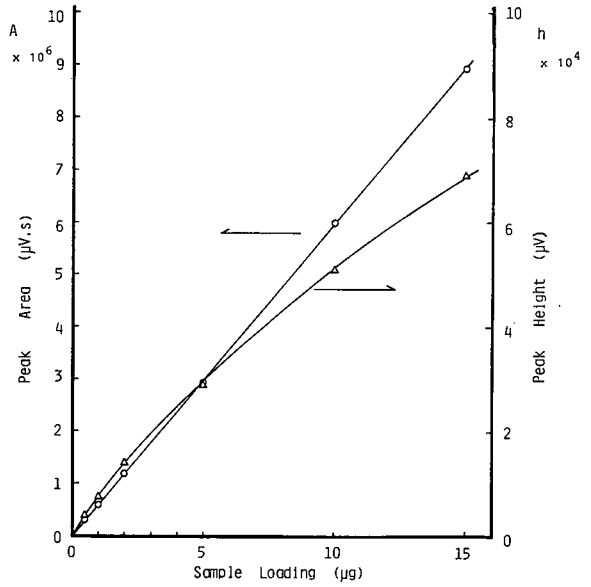

Fig. 6. Effects of sample loading on peak heights and peak areas.

1.017 and intercept = −0.003. The method was then applied to the optical purity testing of diltiazem drug substances and tablets and the 8-chloro derivative drug substances. The results are summarized in Table VI. Diltiazem in tablets was extracted

TABLE VI

RESULTS OF OPTICAL PURITY TESTING

Sample	Lot	Concentration (%)	
		(−) Enantiomer	(+)-Desacetyl form
DIL drug substances	TA1	ND[a]	0.07
	TA2	ND	0.07
	TA3	ND	0.08
	FE1	ND	ND
	FA1	ND	0.16
DIL tablets (30 mg)	TA1	ND	0.19
	TO1	ND	1.98
CHL drug substances	520	ND	0.06
	530	ND	0.07
	540	ND	0.07
	810	0.68	0.05
	820	0.25	0.07

[a] Not detected.

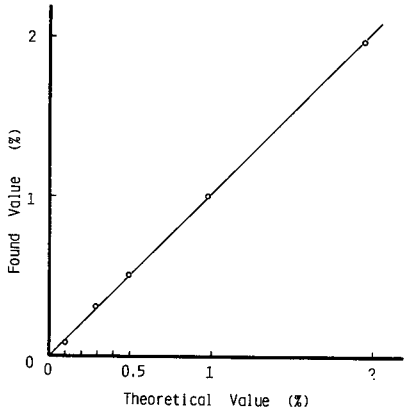

Fig. 7. Linearity of response of the (−)-enantiomer of diltiazem hydrochloride.

from the matrix using methanol–0.02 *M* hydrochloride solution (1:1). The extract solution was then filtered through the membrane filter and the filtrate was injected directly into the HPLC column. Typical chromatograms of optical purity testing are shown in Fig. 8.

CONCLUSIONS

The enantiomers of diltiazem hydrochloride, its 8-chloro derivative and their desacetyl forms were succesfully separated on an ovomucoid chiral column in the reversed-phase HPLC mode. The retention and enantioselectivity were optimized through the pH of buffer solutions and the type and concentration of organic solvent. The chromatographic conditions chosen permitted enantiomeric separation within 20 min. The good linearity of the peak area *versus* sample amount plot permitted the optical purity determination of small amounts of the antipode at levels down to *ca.* 0.1%. This column will be applied to the other pharmaceuticals owing to its wide enantioselectivity.

ACKNOWLEDGEMENTS

The authors are grateful to Dr. H. Inoue (organic chemistry research laboratory of Tanabe Seiyaku) and Dr. T. Sato, head of the analytical chemistry research laboratory, for their critical reading of the manuscript and useful discussions.

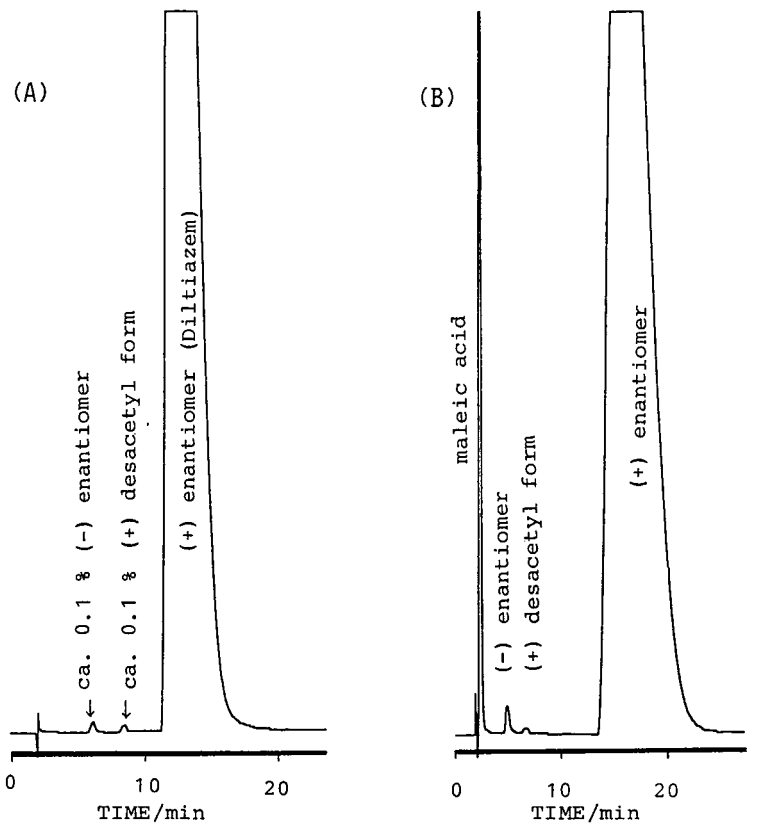

Fig. 8. Typical chromatogram fo optical purity testing of (A) drug substances of diltiazem spiked with *ca.* 0.1% (−)-enantiomer and *ca.* 0.1% of the (+)-desacetyl form and (B) drug substance of the 8-chloro derivative of diltiazem.

REFERENCES

1 E. J. Ariëns, in E. J. Ariëns, W. Soudijn and P. Timmermans (Editors), *Stereochemistry and Biological Activity of Drugs*, Blackwell, Oxford, 1983, pp. 11–32.
2 D. E. Drayer, in I. W. Wainer and D. E. Drayer (Editors), *Drug Stereochemistry*, Marcel Dekker, New York, Basle, 1988, pp. 209–226.
3 K. Imai, *Adv. Chromatogr.*, (1987) 223.
4 R. Dappen, H. Arm and V. R. Meyer, *J. Chromatogr.*, 373 (1986) 1.
5 D. Armstrong, *Anal Chem.*, 59 (1987) 84A.
6 S. Allenmark, *Chiral Separation by HPLC*, Ellis Horwood, Chichester 1989, pp. 286–311.
7 J. Hermansson, *Trends Anal. Chem.*, 8 (1989) 251.
8 M. Chaffman and R. N. Brogden, *Drugs*, 29 (1986) 387.
9 K. Kikkawa, S. Murata and T. Nago, *Arzneim.-Forsch.*, 38 (1988) 526.
10 S. Murata, K. Kikkawa, H. Yabana and T. Nago, *Arzneim.-Forsch.*, 38 (1988) 521.
11 H. Narita, S. Murata, H. Yabana, K. Kikkawa, Y. Sugawara, Y. Arimoto and T. Nagao, *Arzneim.-Forsch.*, 38 (1988) 515.
12 H. Inoue, M. Konda, T. Hashiyama, H. Otsuka, K. Takahashi, M. Gaino, T. Date, K. Aoe, M. Takeda, S. Murata, H. Narita and T. Nagao, *J. Med. Chem.*, 34 (1991) 675.
13 R. Shimizu, K. Ishii, N. Tsumagari, M. Tanigawa, M. Matsumoto and I. T. Harrison, *J. Chromatogr.*, 253 (1982) 101.
14 R. Shimizu, T. Kakimoto, K. Ishii, Y. Fujimoto, H. Nishi and N. Tsumagari, *J. Chromatogr.*, 357 (1986) 119.
15 K. Ishii, K. Banno, T. Miyamoto and Kakimoto, *J. Chromatogr.*, 564 (1991) 338.
16 *Chiralcel and Chiralpak*, Diacel, Tokyo, 1991.
17 T. Miwa, M. Ichikawa, M. Tsuno, T. Hattori, T. Miyakawa and M. Kayano, Y. Miyake, *Chem. Pharm. Bull.*, 35 (1987) 682.
18 T. Miwa, T. Miyakawa, M. Kayano and Y. Miyake, *J. Chromatogr.*, 408, (1987) 316.
19 J. Iredale, A. F. Aubry and I. Wainer, *Chromatographia*, 31 (1991) 329.
20 Y. Hirota, K. Ishii, Y. Shiba, R. Honjyo and H. Nishi, unpublished data.
21 H. Nishi, T. Fukuyama, M. Matsuo and S. Terabe, *J. Chromatogr.*, 515 (1990) 233.

Journal of Chromatography, 633 (1993) 97–103
Elsevier Science Publishers B.V., Amsterdam

CHROM. 24 780

Separation of Beraprost sodium isomers using different cyclodextrin stationary phases

Thomas A. Walker

Pharmaceutical and Analytical Sciences, Marion Merrell Dow Inc., P.O. Box 9627, Kansas City, MO 64134 (USA)

(First received October 15th, 1992; revised manuscript received November 24th, 1992)

ABSTRACT

The separation of isomers present in a new prostacyclin analogue (Beraprost sodium) on several different cyclodextrin stationary phases was investigated. Beraprost sodium, which contains six chiral centers, is a mixture of four isomers; two diastereomers each containing a pair of enantiomers. The cyclodextrin stationary phases used included: α-, β- and γ-cyclodextrins as well as several derivatized β-cyclodextrins. The mobile phase variables that were found to affect the chiral separation were: type and concentration of organic modifier, type and concentration of buffer, the cation and anion associated with the buffer, mobile phase pH, preparation of the mobile phase, and column temperature. The cyclodextrin stationary phases that were found to separate all four isomers were: the acetylated β-cyclodextrin (Cyclobond I AC) and the *para*-toluoyl ester-derivatized β-cyclodextrin (Cyclobond I PT). The selectivities of the isomers were better on the Cyclobond I AC column than on the Cyclobond I PT column. Therefore the Cyclobond I AC column was used to determine what effect each mobile phase variable had on isomer retention and resolution. Calibration curves were done for the four isomers and the correlation coefficients determined using UV detection. Plots of log peak area *versus* concentration of each isomer provided correlation coefficients of 0.998 or better. Detection limits of 75 ng/ml and quantitation limits of 500 ng/ml of each isomer were found.

INTRODUCTION

Cyclodextrins have been described as chiral, doughnut-shaped molecules composed of multiple glucose residues that are connected end-to-end in closed rings via α-1,4-glycosidic linkages [1,2]. The glucose residues are locked in the chair conformation and its orientation is constrained by the cyclic linkage so that the esterified oxygens and 3,5-hydrogens line the hole of the doughnut which creates a relatively hydrophobic core. Hydroxyl groups on the second, third and fifth carbon atoms of each glucose residue face the edges and outside of the doughnut. These hydroxyl groups produces a relatively hydrophilic rim and outer surface. Each of the glucose residues contains five carbons that are chiral. Hydrophobic molecules can bind to the cyclodextrins by entering the central hydrophobic cavity to form "inclusion complexes". Retention of the molecule depends on its size and any substituent groups that are on the molecule. The molecule must fit into the cyclodextrin cavity in order to be retained and separated from an enantiomer [1,2]. Interactions between the secondary hydroxyl groups and the enantiomers must take place for resolution to occur. Differences in the stability of the inclusion complexes that are formed for each isomer must also be great enough to allow the enantiomers to be resolved [3].

Prostacylin (PGI_2), which was discovered in 1976 [4], was found to be an inhibitor of platelet aggregation and had potent vasodilating properties [5]. This has lead to investigating its use for atherosclerosis [6], diabetes [7] and uremia [8]. The major problem with PGI_2 has been its instability in acidic or neutral aqueous solutions. The half-life of PGI_2 in an aqueous solution at pH 7.0 and 25°C is about 2 min [9]. Since PGI_2 is unstable, research has been on-

0021-9673/93/$06.00

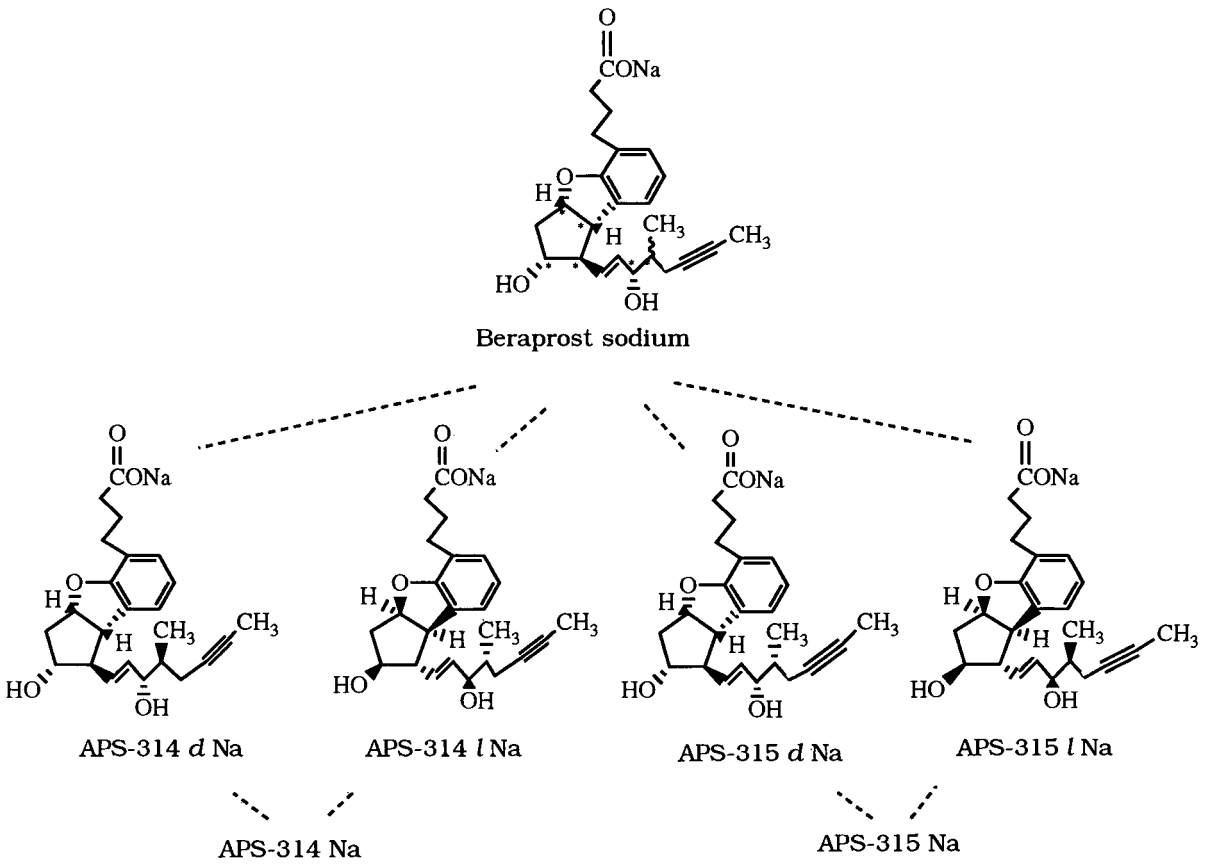

Fig. 1. The chemical structure of Beraprost sodium and the four isomers.

going to produce an analog that is more stable yet maintains the same anti-platelet and vasodilating properties.

The compound used in this study, Beraprost sodium {Sodium (1*R**,2*R**,3*aS**,8*bS**)-2,3,3*a*,8*b*-tetrahydro-2-hydroxy-1-[(*E*)-(3*S**,4*RS*)-3-hydroxy-4-methyl-1-octen-6-ynyl]-1*H*-cyclopenta[*b*]benzofuran-5-butyrate}, is a prostacylin analogue that is significantly more stable in aqueous solutions and maintains the same properties as those found for the orginal prostacylin [10–14]. Beraprost sodium (Fig. 1) is composed of two diastereomers with each diastereomer containing a pair of enantiomers. The ability to separate and quantitate the isomers present in a racemic mixture is important in pharmaceutical products, especially in terms of both bulk drug and formulation stability and purity [15].

This paper will discuss the separation of the isomers present in Beraprost sodium using different cyclodextrin stationary phases. The two stationary phases that were able to separate all four isomers were the acetylated β-cyclodextrin (Astec Cyclobond I AC) and the *para*-toluoyl ester-derivatized β-cyclodextrin (Astec Cyclobond I PT). The mobile phase parameters that had an affect on the chiral separation were identified and studied. The acetylated β-cyclodextrin stationary phase was used to determine the effect that the different mobile phase variables had on the separation of the isomers and was also used to optimize the Beraprost sodium isomer separation.

EXPERIMENTAL

Instrumentation

The instrumentation used in this study includes a

Spectra-Physics IsoChrom HPLC pump, Spectra-Physics Model 8810 autosampler, Spectra-Physics Model 100 variable-wavelength UV-visible detector, and a Spectra-Physics ChromJet integrator. The stationary phases that were studied included: a 250 × 4.6 mm I.D. Astec Cyclobond I AC column (acetylated β-cyclodextrin), a 250 × 4.6 mm I.D. Astec Cyclobond I column (β-cyclodextrin), a 250 × 4.6 mm I.D. Astec Cyclobond I RSP column (*R,S*-hydroxypropyl ether substituent), a 250 × 4.6 mm I.S. Astec Cyclobond I SN column (*S*-naphthylethyl carbamate substituent), a 250 × 4.6 mm I.D. Astec Cyclobond I RN column (*R*-naphthylethyl carbamate substituent), a 250 × 4.6 mm I.D. Astec Cyclobond I DMP column (3,5-dimethylphenyl carbamate substituent), a 250 × 4.6 mm I.D. Astec Cyclobond I PT column (*para*-toluoyl ester substituent), a 250 × 4.6 mm I.D. Astec Cyclobond III (α-cyclodextrin) and a 250 × 4.6 mm I.D. Astec Cyclobond II column (γ-cyclodextrin) all purchased from Astec (Whippany, NJ, USA). Injection sizes of 50 μl were used for all of the studies except for the calibration data where 100-μl injections were used. A 1.0 ml/min flow-rate was used for all studies. A detection wavelength of 282 nm was used throughout the study.

Chemicals

Trimethylamine, tripropylamine, tributylamine and triethanolamine were purchased from Aldrich (St. Louis, MO, USA). Ammonium hydroxide, triethylamine, acetic acid, formic acid, nitric acid, sulfuric acid and tartaric acid were purchased from Mallinckrodt (Paris, KY, USA). HPLC-grade acetonitrile, methanol, ethanol and isopropanol were purchased from Burdick & Jackson (Muskegon, MI, USA).

RESULTS AND DISCUSSION

The major mobile phase parameters that were found to affect isomer retention and selectivity on the acetylated β-cyclodextrin column were: preparation of the mobile phase, type and concentration of organic modifier, type and concentration of buffer, mobile phase pH, type of cation and the type of

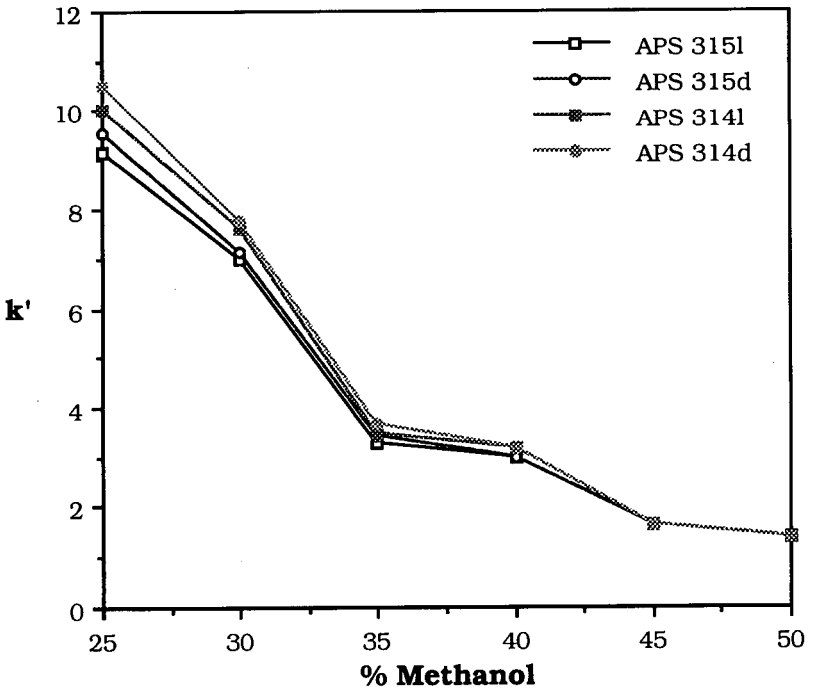

Fig. 2. The effect of methanol concentration using a mobile phase composed of 0.05% triethylamine (v/v), pH 3.5 adjusted with acetic acid.

anion present in the mobile phase, and column temperature. Each of these mobile phase parameters was studied and the effect that each had on the separation and selectivity of the Beraprost sodium isomers was determined.

Mobile phase preparation

Preparation of the mobile phase was found to influence the retention and resolution of the Beraprost sodium isomers. The mobile phase must be prepared so that the base (*i.e.*, triethylamine) is accurately measured first and then the buffer pH adjusted with an appropriate acid (*i.e.*, acetic acid). The isomer separation was not successful if an acid was measured out and then the buffer pH adjusted with a base. All of the studies done were prepared with the base being accurately measured out and then the pH of the buffer solution adjusted using an appropriate acid.

Organic modifier

Retention and resolution of the isomers were found to decrease as the concentration of organic modifier was increased. Methanol provided the best separation for the four isomers while very little or no resolution of the isomers was observed when stronger organic modifiers, such as acetonitrile, ethanol and isopropanol were used. Fig. 2 shows the relationship between the concentration of methanol and isomer retention. Resolution of the isomers was the best when the mobile phase was composed of 25% methanol. Higher concentrations of methanol resulted in loss of resolution. The isomers were more highly retained at lower concentrations of methanol, however, signicant band broadening and poor resolution occurred.

Mobile phase pH

The β-cyclodextrin stationary phases have a pH range of 3.5 to 7.0. If the mobile phase pH is lower than 3.5 or higher than 7.0, column life can rapidly decrease. Fig. 3 shows the effect that mobile phase pH had on isomer retention. At pH 5.0, the diastereomers were separated, however the enantiomers were not resolved whereas at pH 3.5 the enantiomers were resolved although not baseline re-

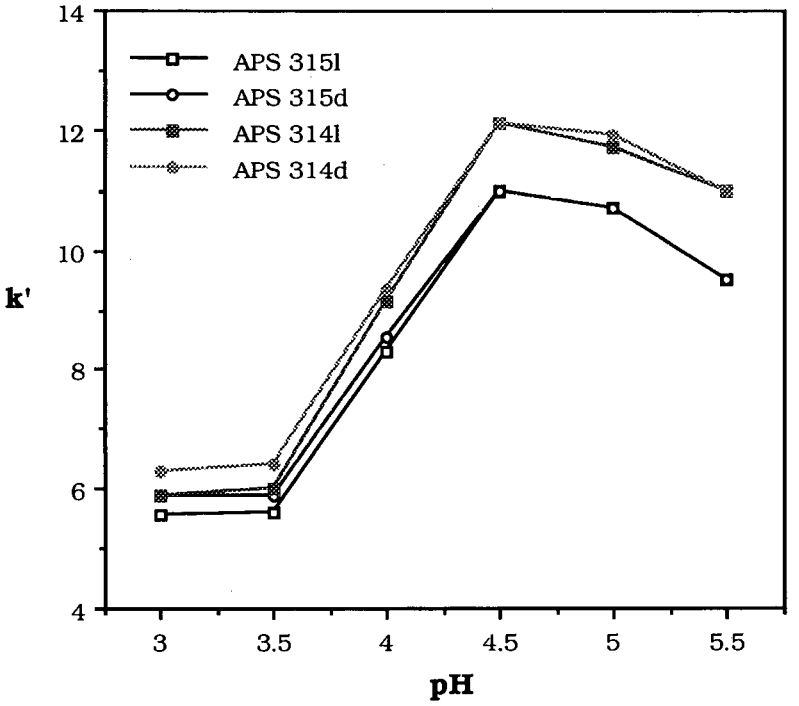

Fig. 3. The effect of mobile phase pH using a mobile phase composed of 0.05% triethylamine (v/v), the pH adjusted with acetic acid and 30% methanol.

solved. It is interesting to note that as the mobile phase pH was increased, resolution between the diastereomers increased while resolution between the enantiomers decreased.

Buffer concentration

Table I shows the results that were obtained when the concentration of buffer (triethylamine) in the mobile phase was increased. Isomer retention, resolution and selectivity decreased as the concentration of buffer was increased. It has been reported that as the concentration of triethylamine in the mobile phase was increased, a corresponding decrease in analyte retention was observed as well as an increase in the efficiency of the separation [16]. The decrease in analyte retention and the improvement in efficiency may be attributed to the triethylamine binding to the silanol groups on the silica backbone and/or sites on the β-cyclodextrin functional group.

Effect of cations and anions

The cation used in the mobile phase as part of the buffer was also studied to determine what effect it might have on the chiral separation. The following amine modifiers were studied: ammonia, trimethylamine, triethylamine, tripropylamine, tributylamine, and triethanolamine. Table II shows the affect that each cation had on isomer retention. When triethanolamine, triethylamine or ammonia were used in the mobile phase, the four isomers were resolved. However, the best resolution was observed when triethylamine was used.

Several inorganic and organic anions were studied to determine what effect the different anions would have on the separation. The five different anions that were studied were; sulfate, nitrate, tartrate, formate and acetate. Table III shows how the different anions affected isomer retention. Acetate provided the best resolution for the isomers. Formate also separated the isomers, however peak shape was not acceptable. The other anions did not adequately separate the isomers; poor peak shape and poor selectivities typically were observed.

TABLE I

EFFECT OF BUFFER CONCENTRATION ON ISOMER RETENTION

Mobile phase: methanol–triethylamine, pH 3.5 (adjusted with acetic acid) buffer (25:75, v/v).

Triethylamine (%)	Capacity factor (k')			
	APS 315*l*	APS 315*d*	APS 314*l*	APS 314*d*
0.01	14.8	15.0	16.4	16.6
0.02	11.2	11.6	12.4	12.8
0.04	10.3	10.7	11.3	11.8
0.05	9.4	9.8	10.3	10.8
0.075	9.6	9.9	10.5	10.9
0.10	7.7	8.1	8.3	8.9
0.20	5.8	6.2	6.2	6.8
0.50	3.1	3.3	3.3	3.6

TABLE II

EFFECT OF DIFFERENT CATIONS ON THE CHIRAL SEPARATION

Mobile phase: methanol–0.05% cation, pH 3.5 (adjusted with acetic acid) buffer (30:70, v/v).

Cation	Capacity factor (k')			
	APS 315*l*	APS 315*d*	APS 314*l*	APS 314*d*
Triethylamine	6.7	7.0	7.2	7.6
Tributylamine	9.4	9.5	10.2	10.5
Ammonia	10.5	11.1	11.4	12.4
Triethanolamine	11.5	12.0	12.7	13.4
Tripropylamine	15.5	15.9	17.1	17.7
Trimethylamine	17.5	17.7	19.3	19.8

TABLE III

EFFECT OF DIFFERENT ANIONS ON THE CHIRAL SEPARATION

Mobile phase: methanol–0.05% NH_4, pH 3.4 (adjusted with appropriate acid) buffer (30:70, v/v).

Anion	Capacity factor (k')			
	APS 315*l*	APS 315*d*	APS 314*l*	APS 314*d*
Acetate	9.7	10.1	10.5	11.2
Sulfate	9.6	10.4	10.4	11.4
Tartrate	9.8	10.5	10.5	11.5
Nitrate	9.8	10.1	10.6	11.2
Formate	11.7	12.0	12.8	13.4

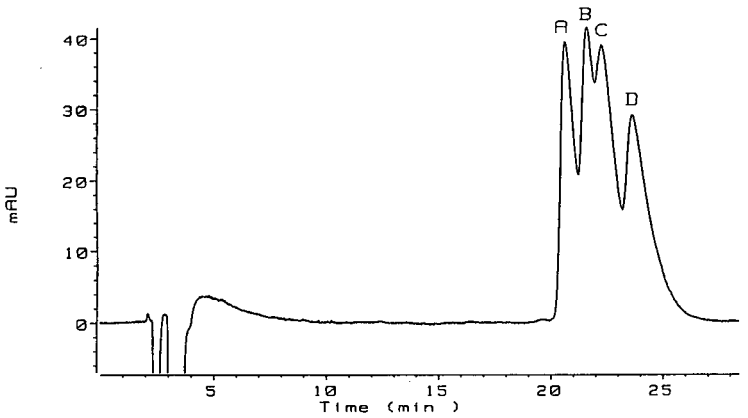

Fig. 4. The separation of the Beraprost sodium isomers: a mobile phase composed of methanol–0.05% (v/v) triethylamine, pH 3.5 adjusted with acetic acid) buffer (25:75, v/v). Peaks: A = APS 315*l*; B = APS 315*d*; C = 314*l*; D = APS 314*d*.

Temperature

The effect of temperature over the range of 0 to 30°C was studied. As the column temperature is lowered, kinetic rates are decreased and interactions between the isomers and the stationary phase are slowed down. As the column temperature was decreased isomer retention was found to increase. (The mobile phase concentration of organic modifier was adjusted so that the isomers would elute within 30 min.) However, no significant differences were observed for the resolution and retention of the isomers at the different temperatures. Therefore, a column temperature of 30°C was used.

Separation

Fig. 4 shows the separation of the four isomers on the acetylated β-cyclodextrin column with a mobile phase consisting of 0.05% (v/v) triethylamine, a pH of 3.5 adjusted with acetic acid and methanol–water (25:75). The column temperature was maintained at 30°C.

Quantitation

Calibration curves and detection limits were determined for the isomers. Isomer standards were prepared that covered a range of 0.049 μg/ml to 98.9 μg/ml. Linear calibration curves of log peak area *versus* ppm of isomer were obtained for 100-μl injections. The correlation coefficients obtained were greater than 0.998 for all four isomers. A detection limit of 75 ng/ml and a limit of quantitation of 500 ng/ml for each isomer was found.

CONCLUSIONS

The separation of the four isomers present in Beraprost sodium was studied using different derivatized and underivatized cyclodextrin stationary phases. The cyclodextrin stationary phases that were found to separate all four isomers were: the acetylated β-cyclodextrin (Cyclobond I AC) and the *para*-toluoyl ester-derivatized β-cyclodextrin (Cyclobond I PT). The mobile phase parameters that influenced the separation were identified and studied. The preparation of the mobile phase was also found to influence the isomeric separation. Calibration data were obtained for each isomer. Detection limits for each isomer were found to be 75 ng/ml with a quantitation limit of 500 ng/ml.

REFERENCES

1 D. W. Armstrong, *J. Liq. Chromatogr.*, 7, Suppl. 2 (1984) 353.
2 D. W. Armstrong and W. DeMond, *J. Chromatogr. Sci.*, 22 (1984) 411.
3 W. J. Lough, *Chiral Liquid Chromatography*, Chapman & Hall, New York, 1989, Ch. 8.
4 S. Moncada, R. J. Gryglewski, S. Bunting and J. R. Vane, *Nature*, 263 (1976) 663.
5 S. Moncada and J. R. Vane, *J. Med. Chem.*, 23 (1980) 591.
6 A. Dembinska-Kiec, T. Gryglewski, A. Zmuda and R. J. Gryglewski, *Prostaglandins*, 14 (1977) 1025.
7 M. Johnson, H. E. Harrison, A. T. Raferty and J. B. Elder, *Lancet*, i (1979) 325.
8 K. Silberbauer, H. Sinzinger and M. Winter, *Artery*, 4 (1978) 554.
9 F. Hirayama, M. Kurihara and K. Uekama, *Int. J. Pharm.* 35 (1987) 193.

10 K. Ohno, H. Nagase, K. Matsumoto, H. Nishiyama and S. Nishio, *Adv. Prostaglandin Thromboxane Leukotrine Res.*, 15 (1985) 279.
11 T. Umetsu, T. Murata, Y. Tanaka, E. Osada and S. Nishio, *Jpn. J. Pharmacol.*, 43 (1987) 81.
12 S. Nishio. H. Matsuura, N. Kanai, Y. Fukatsu, T. Hirano, N. Nishikawa, K. Kameoka and T. Umetsu, *Jpn. J. Pharmacol.*, 47 (1988) 1.
13 N. Toda, *Cardiovascular Drug Review*, 6, No. 3 (1988) 222.
14 K. Nogimori, N. Kajikawa, S. Nishio and N. Yajima, *Prostaglandins*, 37(2) (1989) 205.
15 W. De Camp, *Chirality*, 1 (1989) 2.
16 D. W. Armstrong, T. J. Ward, R. D. Armstrong and T. E. Beesley, *Science*, 232 (1986) 1132.

Journal of Chromatography, 633 (1993) 105–110
Elsevier Science Publishers B.V., Amsterdam

CHROM. 24 751

High-performance liquid chromatographic determination of sulphadiazine and trimethoprim in Chinook salmon muscle tissue

Michael S. Gentleman and Helen M. Burt

Department of Pharmaceutical Sciences, University of British Columbia, 2146 East Mall, Vancouver, B.C. V6T 1Z3 (Canada)

David D. Kitts

Department of Food Sciences, University of British Columbia, 6650 N.W. Marine Drive, Vancouver, B.C. V6T 1Z4 (Canada)

Keith M. McErlane*

Department of Pharmaceutical Sciences, University of British Columbia, 2146 East Mall, Vancouver, B.C. V6T 1Z3 (Canada)

(First received August 4th, 1992; revised manuscript received November 12th, 1992)

ABSTRACT

A sensitive high-performance liquid chromatographic (HPLC) analytical procedure was developed for the quantitative determination of sulphadiazine (SDZ) and trimethoprim (TMP) in Chinook salmon muscle tissue. SDZ and TMP were extracted from salmon muscle tissue using solid-phase extraction, and the extract was subsequently subjected to separate HPLC assay for each of the drugs. An Ultrasphere octadecylsilyl ion-pair column (250 × 4.6 mm I.D.) was used for both assays. A mobile phase of methanol–0.05 *M* phosphate buffer pH 2.5 (17:83), with ultraviolet detection at 280 nm was used for the SDZ assay. A mobile phase of acetonitrile–0.05 *M* phosphate buffer pH 2.5 (5:95), with ultraviolet detection at 224 nm was used for the TMP assay. The calibration curves for both assays in Chinook salmon tissue were linear over the concentration range of 0.1 to 10 μg/g for SDZ (r^2 = 0.9990) and 0.1–15 μg/g for TMP (r^2 = 0.9996). The minimum detectable quantities in Chinook salmon muscle tissue for both SDZ and TMP were 0.1 μg/g at signal-to-noise ratios of 10:1. The average recoveries for the drugs from Chinook salmon muscle tissue were 63% for SDZ and 42% for TMP.

INTRODUCTION

The ocean net-pen culture of Chinook salmon (*Oncorhynchus tshawtschya*) represents an important component of the finned-fish aquaculture industry. As with terrestrial animal husbandry, control of infectious disease is an important requirement for successful growing of stock to marketable size. Administration of antibacterial drugs to fish, either prophylactically or therapeutically, is commonly used to control infection. The choice of the antibacterial agent depends on the identity of the pathogen, however, most such xenobiotics exhibit a broad spectrum of antibacterial activities. The drug product Tribrissen (Burroughs Wellcome, Kirkland, Canada) classified therapeutically as a potentiated sulphonamide, is a commonly used broad-spectrum antibacterial agent. Tribrissen is a mixture of sulphadiazine (SDZ) and trimethoprim (TMP) in a fixed-dose combination of 5:1. Both SDZ and TMP interfere with bacterial growth by inhibiting the folic acid biosynthetic pathway synergistically. In order to ensure that acceptable levels of SDZ and TMP occur in Chinook salmon muscle

* Corresponding author.

0021-9673/93/$06.00

following adequate depletion times, selective and sensitive assays for SDZ and TMP are required.

Both SDZ and TMP have been previously determined in fish tissue. McCarthy *et al.* [1] measured SDZ in rainbow trout muscle using the colorimetric Bratton–Marshall reaction and TMP in the same samples utilizing a microbiological bioassay procedure. These techniques gave sensitivities of approximately 1 ppm for both drugs which exceeded the acceptable residue level for most antibacterial agents in farmed fish muscle. Both techniques were also non-selective, since non-analytes commonly present in the fish extracts contributed to the values measured. Bergsjo and Sognen [2], analyzed TMP in muscle tissue of rainbow trout using a microbiological bioassay procedure that had a sensitivity of approximately 0.5 μg/g, also considered inadequate for residue depletion studies. Tissue concentrations of SDZ have been determined in rat muscle, liver and kidney at a sensitivity of greater than 0.1 μg/g using radioisotope-labeled SDZ and liquid scintillation spectrophotometry by Woolley and Sigel [3]. Concentrations of SDZ have also been determined in rat liver and chicken liver by an assay incorporating extraction into ethyl acetate followed by thin-layer chromatography of the extract [4]. Quantitation was achieved by fluorescamine derivatization of SDZ followed by densitometric scanning. The sensitivity of this assay was approximately 0.1 μg/g, however there was substantial variability in SDZ measurements. Jacobsen [5], using a sensitive and selective HPLC assay reported a sensitivity of 0.01 ppm for TMP extracted from rainbow trout muscle tissue that was suitable for residue depletion studies in rainbow trout. These studies can not be completely extrapolated to salmon since cultivated salmon muscle tissue has a higher lipid content than rainbow trout muscle tissue [6]. Lipids can be a limiting factor in the efficiency of TMP extraction by reported liquid–liquid techniques [7,8], due to the large amount of co-extracted endogenous material associated with the tissue matrix. Solid-phase extraction methods offer an attractive alternative for sample preparation since drugs can be preferentially bound to a solid matrix and subsequently selectively eluted prior to chromatographic analysis [4]. The aim of this research was to utilize solid-phase extraction in the development of sensitive and specific HPLC assays for SDZ and for TMP in Chinook salmon muscle tissue.

EXPERIMENTAL

Chemicals and reagents

SDZ, TMP and salbutamol (SAL) were obtained from Sigma (St. Louis, MO, USA), *p*-toluenesulphonamide (PTS) was obtained from Matheson Coleman & Bell (Los Angeles, CA, USA). Phosphoric acid (H_3PO_4) 85% was obtained from Fisher (Fair Lawn, NJ, USA). HPLC-grade solvents were obtained from BDH Chemicals (Vancouver, Canada). Purified water was produced using a Milli-Q water purification system from Millipore (Mississauga, Canada).

Apparatus

The HPLC system consisted of a Beckman Model 100A solvent metering system (Palo Alto, CA, USA), a Rheodyne Model 7125 sample injection valve (Berkeley, CA, USA) equipped with a 20-μl loop, a Gilson Model HM Holochrome variable wave-length detector (Villiers, FRA) attached to a Hewlett-Packard Model 3390A integrator (Avondale, PA, USA). Ultraviolet detection was at 224 nm for the TMP assay and at 280 nm for the SDZ assay. The HPLC column for both assays was an Ultrasphere octadecylsilyl ion-pair 5-μm column (250 × 4.6 mm I.D.) from Beckman. A NewGuard holder equipped with an RP-18 cartridge (15 × 3.2 mm I.D.) (Brownlee, Santa Clara, CA, USA) was used as a guard column. The mobile phase for the SDZ assay consisted of acetonitrile–0.05 *M* phosphate buffer pH 2.5 (5:95) delivered isocratically at 1.0 ml/min. The mobile phase for the TMP assay consisted of methanol–0.05 *M* phosphate buffer pH 2.5 (17:83) delivered isocratically at 1.0 ml/min. Filtration of the mobile phase prior to use was accomplished using an HPLC solvent filtration apparatus (Kontes, Vineland, NJ, USA) and FP Vericel 47 mm, 0.45-μm membrane filters (Gelman, Ann Arbor, MI, USA).

Preparation of standard solutions and reagents

All standard solutions were prepared with HPLC-grade solvents, and all solutions were stored at 4°C until required for use.

A stock solution of TMP was prepared by dissolving 50 mg of TMP in 100 ml of acetonitrile to yield a concentration of 500 μg/ml. This solution was diluted with acetonitrile to produce solutions

with final TMP concentrations of 1, 5, 10, 50 and 100 μg/ml.

A stock solution of SDZ was prepared by dissolving 50 mg of SDZ in 100 ml of methanol to yield a concentration of 500 μg/ml. This solution was diluted with acetonitrile to produce solutions with final SDZ concentrations of 1, 5, 10, 50 and 100 μg/ml.

A stock solution of PTS was prepared by dissolving 10 mg of PTS in 100 ml of acetonitrile to yield a concentration of 100 μg/ml. A stock solution of SAL was prepared by dissolving 10 mg of SAL in 50 ml of methanol to yield a concentration of 200 μg/ml. The internal standard solution was prepared by adding 100 ml of the PTS stock solution to 50 ml of the SAL stock solution and diluting the resulting solution to 100 ml with acetonitrile to yield final concentrations of PTS 10 μg/ml and SAL 100 μg/ml.

Chinook salmon muscle tissue

Farmed Chinook salmon of approximately 1.5 to 2 kg total body weight were obtained from an ocean net-pen farm site where they had been grown out on a standard salmon aquaculture diet. They were maintained free of drugs for at least 120 days prior to being obtained for analysis. Fish were killed by cranial fracture and edible muscle tissue samples were removed and stored frozen at −20°C until required for analysis.

Sample preparation and extraction procedure

Chinook salmon muscle tissue samples (5 g) were minced with a scalpel to form cubes approximately 1 mm on each side. The samples were transferred quantitatively to 150 × 18 mm test tubes and 9 ml acetonitrile, 0.5 ml internal standard solution and 0.5 ml drug solution were added. The samples were homogenized for 1 min at medium speed using a Brinkmann (Rexdale, Canada) Polytron Model PT 10/35 homogenizer. The samples were centrifuged for 10 min at 1500 *g* in a Beckman GP centrifuge equipped with a GH-3.7 swing-head rotor. The supernatants were decanted to 125 × 16 mm test tubes. Acetonitrile (10 ml) was added to each of the tissue pellets which were then homogenized and centrifuged as before. The supernatants from the first and second extraction of each sample were combined and the tissue pellet was discarded. The organic extracts were evaporated under a stream of dry nitrogen in a 37°C water bath to a residual volume of 0.5 to 1 ml. At this stage the extracts comprised an aqueous phase and a semi-solid phase which consisted primarily of lipids and lipid-soluble orange pigments. The volumes were adjusted to 2 ml with purified water and the extracts were vortex-mixed for 1 min. The samples were then centrifuged for 10 min as before, to cause the semi-solid phase to coalesce. Following centrifugation, the aqueous portions of the extracts were passed through activated C_{18} Sep-Pak solid-phase extraction cartridge assemblies (Waters, Mississauga, Canada). The cartridge assemblies consisted of two 400-mg cartridges connected in series. The cartridges were wetted by passing through 3 ml of methanol, and then equilibrated to the aqueous phase by passing through 5 ml of water. The eluate from loading the muscle tissue extracts to the cartridges was discarded. The drugs were subsequently eluted from the cartridges with 5 ml of methanol and the eluate was collected and evaporated to dryness under a stream of dry nitrogen in a 37°C water bath. The dried extract was dissolved in 0.5 ml of methanol and vortex-mixed prior to HPLC analysis.

Calibration curves, assay precision, and recovery

Calibration curves were prepared by taking 5-g samples of Chinook salmon muscle tissue and adding 0.5 ml of the prepared solutions of either SDZ or TMP to yield final drug concentrations of 0.1, 0.5, 1.0, 5.0 and 10.0 μg/g tissue. In addition, 0.5 ml of the internal standard solution was added to each of these samples to yield final concentrations of SAL 10 μg/g of tissue or PTS 1 μg/g of tissue. The samples were then prepared for analysis as described in the extraction procedure.

Intra-assay variability was determined in control Chinook salmon muscle tissue by preparing and analyzing 6 extracts containing SDZ at a concentration of 0.1 μg/g of tissue and TMP at a concentration of 0.4 μg/g tissue in one day.

Inter-assay variability was determined in control Chinook salmon muscle tissue by preparing and analyzing extracts containing SDZ at 0.1, 5 and 10 μg/g (n = 5 at each concentration) and extracts containing TMP at 0.2, 2 and 10 μg/g (n = 5 at each concentration). These extracts were prepared and analyzed over a period of several days to test for

day-to-day precision and variability in the assays.

Recoveries of SDZ and TMP from Chinook salmon muscle tissue were determined by adding 0.5, 2.5, 5, 25 and 50 μg of SDZ and TMP to 5-g samples of muscle tissue (0.1, 0.5, 1, 5 and 10 μg/g, respectively) and carrying out the extraction and analysis as described. Identical quantities of SDZ and TMP in solution were also analyzed directly using the HPLC methods described. The recoveries were determined by comparison of the peak areas (average of 3 injections) of the tissue extracts with those (average of 3 injections) of the corresponding drug solution (*i.e.* 10 μg/ml drug solution corresponds to 1 μg/g tissue extract).

RESULTS AND DISCUSSION

Representative chromatograms of a control salmon muscle tissue extract and extract containing SDZ with the internal standard, SAL, are presented in Fig. 1. The calibration curve for SDZ extracted from Chinook salmon muscle gave a linear relationship over the concentration range of 0.1–10 μg/g of SDZ ($y = 1.994x + 0.085$; $r^2 = 0.9990$).

Representative chromatograms of a control salmon muscle tissue extract and extract containing TMP with the internal standard, PTS, are presented in Fig. 2. The calibration curve for TMP extracted from Chinook salmon muscle tissue gave a linear relationship over the concentration range of 0.1–15 μg/g ($y = 0.702x + 0.0015$; $r^2 = 0.9996$).

The intra-assay relative standard deviation (R.S.D.) was 9.1% for SDZ and 4.7% for TMP, as shown in Table I. The precision of the extraction method for SDZ was determined at three different concentrations over a period of several days and the resulting inter-assay R.S.D.s are presented in Table II. This procedure was also performed for TMP and the resulting data are presented in Table II.

Both assays employed an initial solvent extraction of the drugs from muscle tissue, followed by a purification of the primary extract by retention and subsequent elution of the drugs from a solid-phase extraction cartridge. The average recoveries were 63% for SDZ and 42% for TMP (Table III).

Initial experiments were undertaken to develop a single extraction procedure and chromatographic method for the simultaneous recovery and analysis of SDZ and TMP, using PTS as an internal standard. However, SDZ with a UV absorption maximum at approximately 280 nm, and TMP with a UV absorption maximum at approximately 224 nm, did not allow for detection at a common wave-

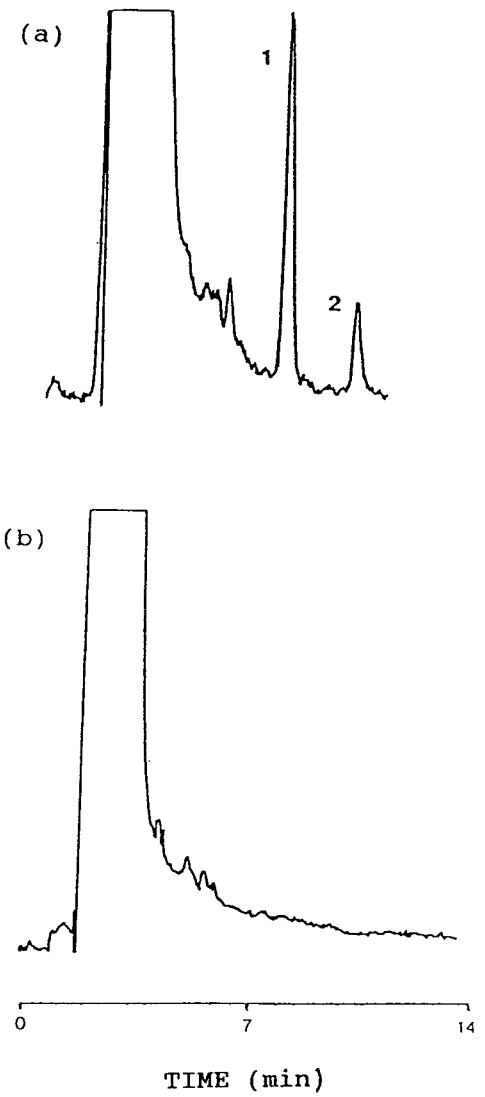

Fig. 1. Chromatogram of (a) a Chinook salmon muscle tissue extract spiked with 0.1 μg/g sulphadiazine and 10 μg/g salbutamol and (b) a control Chinook salmon muscle tissue extract. Chromatographic conditions: column, Ultrasphere I.P. 5 μm (25 cm × 4.6 mm I.D.); mobile phase, acetonitrile–0.05 *M* phosphate buffer pH 2.5 (5:95); HPLC flow-rate, 1.0 ml/min; ultraviolet detection wavelength, 280 nm. Peaks: 1 = salbutamol; 2 = sulphadiazine.

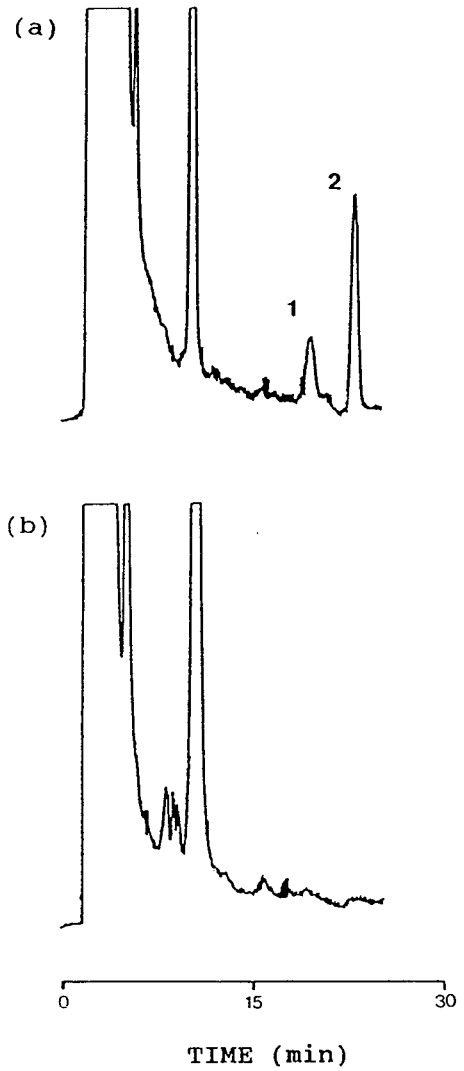

Fig. 2. Chromatogram of (a) a Chinook salmon muscle tissue extract spiked with 0.1 μg/g trimethoprim and 1 μg/g *p*-toluenesulphonamide and (b) a control Chinook salmon muscle tissue extract. Chromatographic conditions: column, Ultrasphere I.P. 5 μm (25 cm × 4.6 mm I.D.); mobile phase, methanol–0.05 *M* phosphate buffer pH 2.5 (17:83); HPLC flow-rate, 1.0 ml/min; ultraviolet detection wavelength, 224 nm. Peaks: 1 = trimethoprim; 2 = *p*-toluenesulphonamide.

length with adequate sensitivities for both drugs. Accordingly, two separate chromatographic procedures were developed. TMP was analyzed at 224 nm using PTS as the internal standard. SDZ was analyzed at 280 nm, however since PTS exhibited

TABLE I

INTRA-ASSAY VARIABILITY OF SULPHADIAZINE AND TRIMETHOPRIM IN CHINOOK SALMON MUSCLE TISSUE

Extract No.	SDZ/I.S. area ratio	TMP/I.S. area ratio
1	0.126	0.292
2	0.120	0.291
3	0.114	0.292
4	0.111	0.317
5	0.105	0.296
6	0.134	0.324
Mean area ratio	0.118	0.302
S.D.	0.011	0.014
R.S.D. (%)	9.1	4.7

TABLE II

INTER-ASSAY VARIABILITY OF SULPHADIAZINE AND TRIMETHOPRIM IN CHINOOK SALMON MUSCLE TISSUE

Sulphadiazine		Trimethoprim	
Sample concentration (μg/g)	R.S.D. (%)	Sample concentration (μg/g)	R.S.D. (%)
0.1	5.9	0.2	10.4
5.0	3.3	2.0	7.8
10.0	4.9	10.0	4.7

TABLE III

RECOVERY OF SULPHADIAZINE AND TRIMETHOPRIM FROM CHINOOK SALMON MUSCLE TISSUE

Sample concentration (μg/g)	Recovery (%)	
	Sulphadiazine	Trimethoprim
0.1	73	39
0.5	61	44
1.0	69	43
5.0	56	43
10.0	57	47
Mean	63	42

poor absorbance at this wavelength, SAL was selected as internal standard.

Preliminary extraction methods based on liquid–liquid extraction procedures outlined in the literature [4,5,7,8] resulted in low recoveries and substantial chromatographic interferences from co-extracted endogenous substances. Since cultivated salmon muscle tissue contains substantial quantities of lipid material, the low recoveries and chromatographic interferences were felt to be at least partially due to lipid constituents in the salmon muscle. The extraction procedure was modified to reduce the final extract to a small volume, with drugs predominantly isolated in the aqueous phase. The extracts at this stage still exhibited significant interference with the chromatographic analysis due to co-extracted endogenous materials. Incorporation of a solid-phase extraction cartridge protocol [9] improved the chromatographic appearance of the extracts, and permitted concentration of the extracts which enhanced the sensitivity of detection.

The method outlined in this study incorporates a single extraction procedure using two internal standards to satisfy detection requirements and provides analytical control of extraction variations from sample to sample. While the recoveries of SDZ and TMP were 63% and 42%, respectively, the sensitivity of the assay allows for quantitation of SDZ and TMP at 0.1 μg/g. While the recoveries are not as efficient as those previously reported in rainbow trout [1,2,5], attempts to increase the recovery led to increased co-extraction of endogenous materials which interfered with the chromatography. Similar observations with extraction of the combination of sulphadimethoxine and ormetoprim from Chinook salmon muscle tissue have been reported [9].

In summary, the methods reported in this study enable the quantitation of trimethoprim and sulphadiazine to 0.1 μg/g in Chinook salmon muscle tissue. Further research to incorporate these methods for Tribrissen analysis in pharmacokinetic studies in Chinook salmon are certainly warranted.

REFERENCES

1 D. H. McCarthy, J. P. Stevenson and A. W. Salsbury, *Aquaculture*, 4 (1974) 299.
2 T. Bergsjo and E. Sognen, *Acta Vet. Scand.*, 22 (1980) 18.
3 J. L. Woolley and C. W. Sigel, *Drug Metab. Dispos.*, 7 (1979) 94.
4 C. W. Sigel, J. L. Woolley and C. A. Nichol. *J. Pharm. Sci.*, 64 (1975) 973.
5 M. Jacobsen, *J. Fish Dis.*, 12 (1989) 29.
6 J. A. Nettleton and J. Exler, *J. Food Sci.*, 57 (1992) 257.
7 D. Lichtenwalner, B. Suh, B. Lorber and A. Sugar, *Antimicrob. Agents Chemother.*, 16 (1979) 579.
8 L. Nordholm and L. Dalgaard, *J. Chromatogr.*, 233 (1982) 427.
9 J. A. Walisser, H. M. Burt, T. A. Valg, D. D. Kitts and K. M. McErlane, *J. Chromatogr.*, 518 (1990) 179.

Journal of Chromatography, 633 (1993) 111–118
Elsevier Science Publishers B.V., Amsterdam

CHROM. 24 773

High-performance liquid chromatographic separation and electrochemical detection of penicillins

Eric Kirchmann☆ and Lawrence E. Welch*

Department of Chemistry, Knox College, Galesburg, IL 61401 (USA)

(First received September 1st, 1992; revised manuscript received November 16th, 1992)

ABSTRACT

A reversed-phase high-performance liquid chromatography method used to determine penicillins is described. A C_{18} stationary phase is used in conjunction with mixed solvent systems containing acetate buffer, methanol, and acetonitrile in various proportions. An isocratic separation is illustrated, but usage of a gradient program varying the composition of the organic modifier gives better performance. Detection is accomplished using pulsed amperometric detection to indirectly monitor the penicillins. The detection limit for ampicillin is $4 \cdot 10^{-7}$ *M*.

INTRODUCTION

Penicillins are the most popular class of antimicrobial agents, used to fight off a wide range of bacterial infections [1]. Even though they are widely used, the incidence of oversensitive reactions may be as high as 10%, with symptoms ranging from skin rashes to, in rare cases, fatal episodes of anaphylaxis [2]. Because of their widespread use in fields such as pharmaceuticals, health care, research, and regulation, the analysis of penicillins is relevant and has many practical applications. Veterinarians find penicillins to be useful for fighting bacterial infections in various domesticated animals [3,4]. This can lead to the transfer of penicillins to milk and meat products by and from the animals. Although the amounts are small, this is a serious matter due to the aforementioned potential for severe allergic response, even in small doses. This hypersensitivity insures that methods for monitoring penicillins in food products must have very low detection limits [5]. The Food and Drug Admninistration has recently unveiled plans for a nationwide screening of milk for several drugs, including penicillins, so there is a demand for this type of methodology [6].

Most of the current methods use high-performance liquid chromatography (HPLC) coupled with a variety of detectors. Taking advantage of the carboxylate group of the penicillins, some early separations employed anion-exchange HPLC in alkaline solution [7,8]. Recent work has focused on reversed-phase HPLC on C_8 [9–12] and C_{18} columns [1,5,13–15]. The chromatographic efficiency of the reversed phase separations are superior, and the more moderate pH values minimize penicillin degradation. Others have used ion pair separations on C_{18} columns [13,16].

The most common detection mode is absorbance spectrophotometry in the ultraviolet (UV) region [1,5,13–16]. The absorbance maxima are just outside the vacuum UV range, resulting in excitation wavelengths in the range of 200–230 nm. Detection limits have been measured as low as 0.1 to 0.5 μg/ml [1,10,15] for direct determinations. Due to the large number of compounds displaying absorbance at these same wavelengths, peak overlap can be problematic for complex biological samples. Application

* Corresponding author.
☆ Present address: School of Medicine, Washington University, St. Louis, MO 63110, USA.

0021-9673/93/$06.00

of higher excitation wavelengths (254 nm typically) will improve selectivity, but limited sensitivity is displayed due to lower absorptivity [7,8,17].

Various indirect methods and derivatization schemes have been examined to improve detection. Besada and Tadros [18] oxidized the penicillins with potassium iodate, then monitored the amount of iodine formed colorimetrically. Morelli [19] oxidized the penicillins with ammonium vanadate, monitoring the amount of blue vanadium(IV) produced spectrophotometrically. A similar procedure using ammonium molybdate has also been published [20]. Kok *et al.* [21] monitored the penicillins indirectly by oxidizing them with electrogenerated bromine followed by subsequent measurement of the amount of Br_2 in excess. Several studies have formed mercuric mercaptides of penicillins by pre- [22,23] or post-column [24] addition of imidazole and mercury(II) chloride coupled with a reversed-phase separation. Derivatization of the penicillins with *o*-phthaldialdehyde [23,25] can produce fluorescent derivatives, although this is limited to only the species that have a primary amine group on their side chain. Reported detection limits range from 0.5 to 1 μg/ml. Amoxicillin can be determined with fluorescence spectroscopy following electrochemical oxidation [26] to 50 ng/ml levels. This method is limited solely to amoxicillin, which has an electroactive phenol group in its side chain.

Voltammetric detection methods have been investigated in several previous studies, leading one group to conclude that the penicillins, "do not contain a polarographically reducible or oxidizable functional group" [27]. Due to, "the general lack of suitable oxidative and/or reductive properties," another group [28] has photolytically derivatized the penicillins with a UV flashlamp to allow electrochemical detection. Musch *et al.* [29] have reported penicillin detection using constant potential (d.c.) amperometric detection at a glassy carbon working electrode. Recent work in this research group [30,31] has shown that penicillins can be monitored with good sensitivity on gold and platinum electrodes using pulsed amperometric detection [32,33]. Electrode fouling problems were minimized due to the built-in cleaning mechanism of pulsed amperometric detection. This work sought to couple this detection scheme with a chromatographic separation that could speciate the various penicillins.

EXPERIMENTAL

Materials and reagents

All penicillins were purchased from Sigma (St. Louis, MO, USA). Reagent-grade acetic acid from Fisher (Pittsburgh, PA, USA) and sodium acetate from Baker (Phillipsburg, NJ, USA) were used to produce acetate buffer solutions. HPLC-grade acetonitrile and methanol from Fisher were used as mobile phase organic modifiers. Water was distilled and deionized before use as a solvent. All mobile phases were vacuum filtered through an Alltech (Deerfield, Ill, USA) 0.2-μm nylon filter and sonicated before use. Samples were filtered through nylon 0.45-μm syringe tip filters before injection into the HPLC system. Standard solutions were prepared in either the chromatographic solvent or water.

Chromatographic apparatus

A Waters (Milford, MA, USA) 625 Gradient LC System was used for all HPLC work. A standard flow-rate of 2.0 ml/min was used for most applications. The pump was run in "silk mode", a Waters feature designed to reduce pump noise. The injection loop had a volume of 50 μm.

A 10-μm μBondapak C_{18} Radial-Pak cartridge (Waters) was employed as the chromatographic stationary phase. The cartridge had an internal diameter of 8 mm and a length of 100 mm. The cartridge was housed in a Waters 8 × 10 Radial-Pak compression module. All separations were done at ambient laboratory temperature (*ca.* 20 ± 2°C).

Electrochemical detection used the Waters 464 pulsed electrochemical detector. For all experiments, a thin-layer cell was utilized that had a block with dual gold electrodes in the series configuration. The upstream element was used as the working electrode, while the downstream electrode served as the counter electrode for a majority of this work. The stainless-steel block opposing the dual gold electrodes was tested as an alternative counter electrode; no significant difference in performance was noted. The detector was configured in the floating ground mode throughout this project to minimize detector noise. This served to ground the detector at a virtual point rather than to the chassis of the instrument. The thin-layer cell used a Ag/AgCl reference electrode. A time constant of 0.5 s was used for

d.c. amperometric detection; 1250 mV was the optimum potential setting. Many different pulsed amperometric detection waveforms were used; details are given in the following section. A majority of the data was collected with a Gateway (N. Sioux City, SD, USA) 386SX computer using a Keithley MetraByte (Taunton, MA, USA) Chrom-1AT interface board.

RESULTS AND DISCUSSION

Previous work [30] has demonstrated the applicability of pulsed amperometric detection for penicillin quantitation in a flowing liquid stream. By adapting an HPLC scheme followed by pulsed amperometric detection we sought to allow separation and speciation of the common penicillins without interference from other sample matrix components. Upon addition of a C_{18} HPLC column to the flow injection analysis system used previously, some modification was needed. The prior solvent, 0.2 *M* acetate buffer (pH 4.7), provided a proper pH to insure the chemical stability of the penicillins, was compatible with a silica-based C_{18} resin, and provided electrolyte for electrochemical detection.

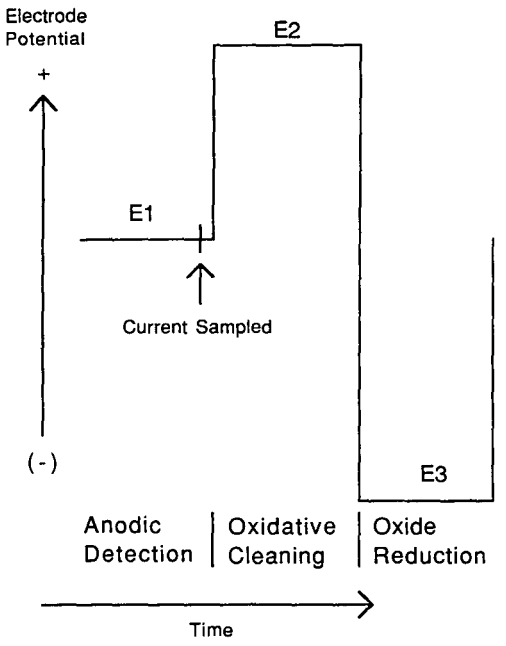

Fig. 1. Pulsed amperometric detection waveform schematic.

However, when penicillin solutes were dissolved in the acetate mobile phase and passed through a μBondapak C_{18} column, the penicillins were not recovered from the column.

By the addition of an organic modifier and by shifting from 0.2 to 0.02 *M* acetate buffer, the mobile phase was made less polar, which enabled penicillin recovery from the C_{18} column. Methanol and acetonitrile were chosen as organic modifiers since both had been used previously for penicillin separations on C_{18} columns [5,34] and both had been used successfully with pulsed amperometric detection [35–38]. Finding the proper mobile phase composition involved compromising detector performance, which was best at high concentrations of aqueous buffer, for the sake of optimizing HPLC performance, as increased organic modifier concentrations improved peak shapes and reduced retention times. The best combination was in the range of 70% (v/v) aqueous buffer and 30% organic modifier (hereafter designated 70:30).

Detector performance had been optimized previously [30] for use with the 0.2 *M* acetate buffer solvent. With the modification in solvent composition for use as a chromatographic mobile phase, reoptimization of the pulsed amperometric detection waveform was necessary. In particular, the addition of organic modifier causes a significant alteration of electrochemical response. As was discussed previously [30], either "direct" or "indirect" detector response can be obtained depending on the pulsed amperometric detection waveform that was chosen. In brief, direct detection refers to an increase in the anodic current resulting from oxidation of the analyte. Indirect detection refers to a suppression of the anodic background current in the absence of significant current from analyte oxidation. The adsorbed analyte occupies space on the electrode surface, attenuating the signal from the surface-dependent residual formation of gold oxide. The analyte will not be significantly oxidized during indirect detection due to slow kinetics. By adjusting the pulsed amperometric detection waveform (Fig. 1) one can convert negative response from indirect detection to positive response from direct detection. Increasing the overpotential (*i.e.* increasing *E*1) can accelerate the reaction rate of penicillin oxidation [30] to produce positive peaks. In some cases, by sampling the current after a long time delay at the *E*1 potential, it

TABLE I

PULSED AMPEROMETRIC DETECTION WAVEFORM VARIATION WITH SOLVENT COMPOSITION

Indirect pulsed amperometric detection, 0.2 *M* acetate buffer	Indirect pulsed amperometric detection, 0.02 *M* acetate–organic modifier (70:30)	Direct pulsed amperometric detection, 0.2 *M* acetate buffer	Direct pulsed amperometric detection, 0.02 *M* acetate–organic modifier
*E*1 = 1100 mV	*E*1 = 1300 mV	*E*1 = 1500 mV	*E*1 = 1500 mV
*T*1 = 0.200 s	*T*1 = 0.167 s	*T*1 = 0.333 s	*T*1 = 1.333 s
*E*2 = 1600 mV	*E*2 = 1500 mV	*E*2 = 1600 mV	*E*2 = 1600 mV
*T*2 = 0.167 s	*T*2 = 0.167 s	*T*2 = 0.167 s	*T*2 = 0.167 s
*E*3 = −200 mV	*E*2 = −200 mV	*E*3 = −200 mV	*E*2 = −200 mV
*T*3 = 0.167 s	*T*3 = 0.333 s	*T*3 = 0.167 s	*T*3 = 0.333 s

is possible to observe positive peaks at potentials where penicillin oxidation occurs very slowly.

Both direct and indirect detection were observed in 0.2 *M* acetate buffer solvent [30], but the *S/N* ratio was vastly superior using direct pulsed amperometric detection. However, adapting a 70:30 acetate buffer–organic modifier solvent led to much slower penicillin oxidation kinetics than seen with the 0.2 *M* acetate buffer solvent. A much greater overpotential was needed to produce positive response with a 70:30 solvent, and the noise present under these conditions hindered the performance of direct pulsed amperometric detection waveforms. The *S/N* response of the indirect pulsed amperometric detection waveforms was better for mobile phases containing organic modifier. Optimization of both waveforms with 70:30 solvents and subsequent comparison clearly showed that indirect pulsed amperometric detection was superior to direct pulsed amperometric detection. Hence, indirect detection was used throughout the balance of this work when pulsed amperometric detection was employed. D.c. amperometric waveforms were also investigated and found to be clearly inferior to pulsed amperometric detection in all cases. See Table I for a compilation of pulsed amperometric detection waveforms.

Nine common penicillins (Table II) were obtained with the intention of resolving each using HPLC. Various different aqueous–organic (70:30) phases were examined for the job. For further studies of penicillin retention times two of the best 70:30 mobile phases were selected: acetonitrile–methanol–0.02 *M* acetate buffer) (20:10:70) and (25:5:70).

TABLE II

RETENTION TIMES FOR PENICILLINS IN SELECTED MOBILE PHASES

Flow-rate: 2 ml/min. Mobile phase: acetonitrile–methanol–acetate buffer.

Penicillin	Retention time at 20:10:70 (min)	*k'* Value 20:10:70	Retention time at 25:5:70 (min)	*k'* Value 25:5:70
Amoxicillin (Amox)	1.97	0.15	1.78	0.11
Amphicillin (Amp)	2.38	0.40	2.03	0.26
Methicillin (Meth)	4.58	1.66	3.18	0.98
Penicillin (Pen) G	6.35	2.73	3.94	1.43
Penicillin V	9.62	4.62	5.35	2.34
Oxacillin (Oxa)	12.57	6.35	6.62	3.11
Cloxacillin (Cloxa)	19.27	10.25	9.80	5.07
Nafcillin (Naf)	25.03	13.64	12.28	6.62
Dicloxacillin (Dicloxa)	38.02	21.30	18.11	10.32

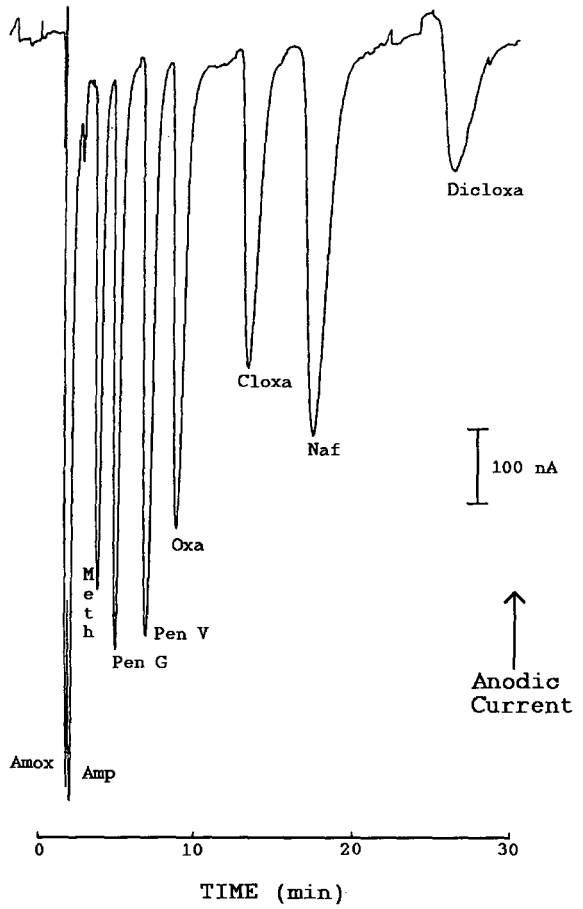

Fig. 2. Isocratic separation of nine penicillins. Mobile phase was acetonitrile–methanol–0.02 *M* acetate buffer (22.5:7.5:70), 2 ml/min. Indirect waveform (Table I). Penicillin concentrations = 1 m*M*.

Trials with the two organic modifiers had shown that acetonitrile had greater eluting strength than methanol, so it was expected that retention times would be shorter with 25:5:70. Retention times and k' values for the penicillins with the two solvents are given in Table II. The data in Table II might suggest that the 25:5:70 solvent should function well, with k' values all differing and under 10.5. However, the early eluting peaks are not well resolved. Amoxicillin and ampicillin (1.78 and 2.03 min, respectively) are so close together that they practically coelute. In 20:10:70, the resolution of the early peaks was improved. Unfortunately, the separation took over 35 min at a 2 ml/min flow-rate. Thus, 25:5:70 mobile phase is too strong, while 20:10:70 is too weak. For an isocratic separation, an intermediate strength mobile phase was needed.

To produce a mobile phase intermediate in strength to the previous two, a 22.5:7.5:70 solvent was chosen for an isocratic separation (see Fig. 2). This separation gave k' values better than the other two mobile phases used in the retention time study. All nine penicillins were eluted in less than 30 min, and the earliest peaks were less cramped than the 25:5:70 retention times. Despite the improvement, amoxicillin and ampicillin were still not adequately resolved (resolution = 0.29). To improve upon their separation, gradient elution was the obvious choice. This would allow usage of a weaker solvent early in the separation to allow improved resolution of the low k' peaks, with a gradient to a stronger solvent to minimize retention of the later-eluting peaks.

The marriage of gradient elution and electrochemical detection has proven troublesome in previous work [35,36]. After experimentation with many different gradients, it became clear that any gradient that significantly changed the percent organic modifier would cause a large baseline shift. Hence, the simple concept of increasing the percentage of organics over the course of a run was eliminated. An alternative was to produce a solvent program that maintained the same total percentage of organic modifier, but changed its composition. Because acetonitrile was a stronger eluent for these analytes than methanol, it was hypothesized that the overall eluting strength of the mobile phase could be controlled by changing the amounts of the two organics relative to each other. In this manner,

TABLE III

OPTIMIZED GRADIENT PROGRAM FOR PENICILLIN SEPARATION

Flow-rate 2 ml/min.

Time (min)		Solvent (acetonitrile–methanol–acetate buffer)
0		15:10:75
	Linear Ramp	
15		30:0:70
	Isocratic Hold	

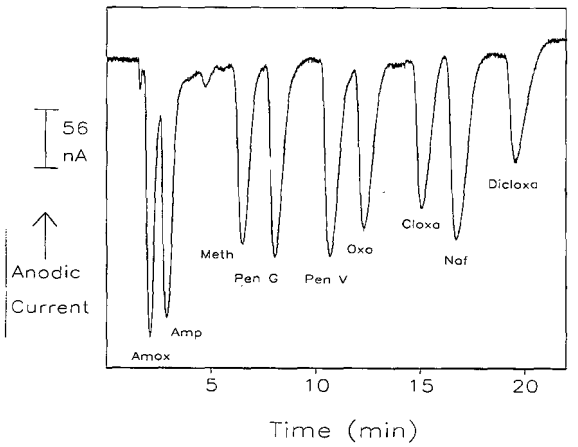

Fig. 3. Gradient separation of nine penicillins. Gradient program is given in Table III. Indirect pulsed amperometric detection waveform (Table I). Penicillin concentrations = 1 m*M*.

solvent strength could be altered while minimizing any baseline offset.

To satisfactorily separate amoxicillin and ampicillin, a slight change in the 70:30 buffer to organic ratio was necessary. The separation of these two penicillins was achieved by starting the gradient at 15:10:75, a 75:25 ratio of buffer to organic. This slight alteration in the buffer to organic ratio was small enough to avoid the baseline shifting problems. Consequently, the gradient ran from 75 to 70% acetate buffer. The exact specifications of the best gradient are detailed in Table III. A chromatogram obtained using this gradient is shown in Fig. 3. From this figure, it can be seen that all nine penicillins were well separated with only a minor baseline perturbation. The problematic amoxicillin–ampicillin duo had a resolution measurement of 1.05 with this gradient, as compared to a value of 0.29 in the isocratic trial from Fig. 2. An additional point to note is that the separation was done in twenty minutes, around a ten minute improvement over the isocratic separation above.

To allow the application of this methodology for quantitative work, the relationship between detector response (anodic current) and concentration must be understood. As was expected from previous work [39,40], pulsed amperometric detection current *vs.* concentration (*I vs. C*) response was non-linear when plotted over a wide concentration range. However, response was linear at low concentrations. The loss of calibration curve linearity can be aptly illustrated and the concentration at which the non-linear behaviour begins shown by a special type of calibration plot. Normalized peak area is plotted *vs.* log concentration, where the normalization process uses statistics from a modified linear regression fit [40] of the linear portion of the *I vs. C* plot.

$$\text{Normalized peak area} = \frac{(\text{peak area} - y\ \text{intercept})}{\text{slope} \cdot \text{concentration}}$$

This plot can be seen in Fig. 4. Ideal linear behavior would result in all normalized peak areas equaling one. All of the points at lower concentrations are within + or − 10% relative deviation from this ideal value. At $3.5 \cdot 10^{-4}$ *M* the plot exits this region; this concentration is designated as the upper limit of linear *I vs. C* behavior. Above this concentration, one must either employ a non-linear calibration curve or dilute samples to reach the linear response region. Using the optimized gradient program on the μBondapak C_{18} column, the detection limit for ampicillin was found to be $4 \cdot 10^{-7}$ *M*. (0.2 μg/ml).

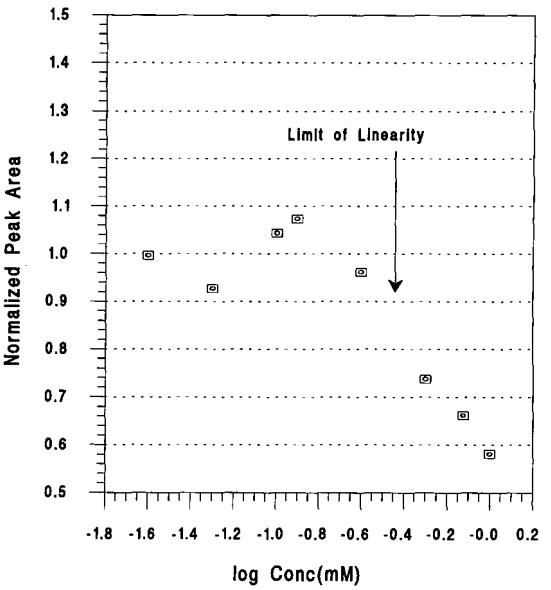

Fig. 4. Normalized calibration curve for ampicillin. 0.9 and 1.1 represent 10% relative deviation from linearity. Mobile phase was acetonitrile–methanol–0.02 *M* acetate buffer (15:10:75), 2 ml/min. Indirect pulsed amperometric detection waveform (Table I).

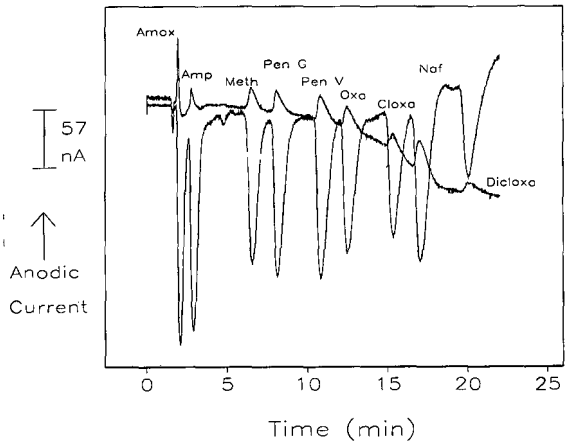

Fig. 5. A comparison of direct and indirect pulsed amperometric detection. Trace with peaks pointing upward is direct pulsed amperometric detection (Table I). Trace with peaks pointing downward is indirect pulsed amperometric detection (Table I). Both were run with 1 m*M* penicillin concentrations and the gradient from Table III.

The response to all of the other penicillins was within a factor of 2 of that for ampicillin.

As noted earlier, the pulsed amperometric detection waveform was optimized for negative response, which was used throughout this study. An alternative waveform optimized to produce positive response will also function for this separation (see Fig. 5). As expected, the *S/N* ratio for the direct pulsed amperometric detection waveform was poorer than with the indirect pulsed amperometric detection waveform. Nevertheless, the selectivities of the two waveforms are different, and it is conceivable that the direct pulsed amperometric detection waveform might be superior in the presence of interfering components during application work.

CONCLUSIONS

Pulsed amperometric detection can provide sensitive detection for penicillins following HPLC as long as one carefully matches the detector waveform with the chromatographic mobile phase. When *ca.* 30% organic modifier was added to an aqueous solvent for chromatographic purposes, slowed electrochemical kinetics required a waveform adjustment. Rather than increasing the detection potential to provide overpotential, better *S/N* was achieved by monitoring the penicillins indirectly by measuring their suppression of the background anodic current from the mobile phase. This type of detection gave non-linear *I vs. C* response just as would be expected for positive pulsed amperometric detection. Despite the overall non-linearity, linear behavior extends nearly three concentration decades above the detection limit.

Although an isocratic separation of the penicillins was feasible, gradient elution produced superior resolution and shorter analysis times. The application of a solvent program that kept the percent organic modifier constant while varying the modifier composition was a major step forward. Attempts to alter solvent strength by the traditional methods of increasing the percentage of the organic modifer all resulted in an unacceptable shift in baseline response. This shift can be attributed to enhanced irreversibility of the electrochemical reactions due to slowed kinetics as the solvent polarity and the ionic strength decreased. By exchanging acetonitrile for methanol, one can keep the ionic strength constant while changing the polarity by only a minimal amount. This served to minimize baseline perturbation as solvent strength was increased.

The detection limits observed for the penicillins were on par with the best values reported using direct UV absorbance. The application of a pulsed coulometric detection system in future studies should provide enhancement of the *S/N* observed with pulsed amperometric detection, giving electrochemical detection a clear edge over direct spectrophotometry. The selectivity of pulsed amperometric detection should also be an advantage that will be borne out in future application work.

ACKNOWLEDGEMENTS

This research was supported by an award from Research Corporation. The generous donation of equipment from the Waters Chromatography division of the Millipore Corporation is acknowledged with gratitude. Additional financial support was provided by the PEW Midstates Math and Science Consortium, which is funded by the PEW Charitable Trusts. Special thanks to Bill LaCourse and Jim Oberholtzer.

REFERENCES

1 F. Jehl, P. Birckel and H. Monteil, *J. Chromatogr.*, 413 (1987) 109.
2 A. G. Gilman, L. S. Goodman and A. Gilman, *The Pharmacological Basis of Therapeutics*, Macmillan, New York, 6th ed., 1980, p. 1147.
3 J. Jarp, H. P. Bugge and S. Larsen, *Vet. Rec.*, 124 (1989) 630.
4 P. A. Okewole, E. M. Uche, I. L. Oyetunde, P. S. Odeyemi and P. B. Dawal, *Lab. Anim.*, 23 (1989) 275.
5 W. A. Moats, *J. Chromatogr.*, 507 (1990) 177.
6 K. Schneider, *Chicago Tribune*, Dec. 28 (1990) Section 1, p. 5.
7 K. Tsuji and J. H. Robertson, *J. Pharm. Sci.*, 64 (1975) 1542.
8 J. M. Blaha, A. M. Knevel and S. L. Hem, *J. Pharm. Sci.*, 64 (1975) 1384.
9 F. W. Teare, R. H. Kwan, M. Spino and S. M. Macleod, *J. Pharm. Sci.*, 71 (1982) 938.
10 T. L. Lee and M. A. Brooks, *J. Chromatogr.*, 306 (1984) 429.
11 T. B. Vree, Y. A. Hekster, A. M. Baars and E. van der Kleijn, *J. Chromatogr.*, 145 (1978) 496.
12 H. H. W. Thijssen, *J. Chromatogr.*, 183 (1990) 339.
13 A. M. Lipczynski, *Analyst*, 112 (1987) 411.
14 W. A. Moats, *J. Chromatogr.*, 317 (1984) 311.
15 A. Marzo, M. Monti, M. Ripamonti, E. A. Martelli and M. Picari, *J. Chromatogr.*, 507 (1990) 235.
16 H. Terada and Y. Sakabe, *J. Chromatogr.*, 348 (1958) 379.
17 Y. Murai, T. Nakagawa, K. Yamaoka and T. Uno, *Chem. Pharm. Bull.*, 29 (1981) 3290.
18 A. Besada and N. Tadros, *Mikrochim. Acta*, 2 (1987) 225.
19 B. Morelli, *Anal. Lett.*, 20 (1987) 141.
20 B. Morelli and M. Mariani, *Anal. Lett.*, 20 (1987) 1429.
21 W. T. Kok, J. J. Havax, W. H. Voogt, U. A. T. Brinkman and R. W. Frei, *Anal. Chem.*, 57 (1985) 2580.
22 M. E. Rogers, M. W. Adlard, G. Saunders and G. Holt, *J. Liq. Chromatogr.*, 6 (1983) 2019.
23 M. E. Rogers, M. W. Adlard, G. Saunders and G. Holt, *J. Chromatogr.*, 297 (1984) 385.
24 D. Westerlund, J. Carlqvist and A. Theodorsen, *Acta Pharm. Suec.*, 16 (1979) 187.
25 M. E. Rogers, M. W. Adlard, G. Saunders and G. Holt, *J. Chromatogr.*, 257 (1983) 91.
26 H. Mascher and C. Kikuta, *J. Chromatogr.*, 506 (1990) 517.
27 J. A. Squella and L. J. Nunez-Vergara, *J. Electroanal. Chem.*, 130 (1981) 361.
28 C. M. Selavka, I. S. Krull and K. Bratin, *J. Pharm. Biomed. Anal.*, 4 (1986) 83.
29 G. Musch, M. DeSmet and D. L. Massart, *J. Chromatogr.*, 348 (1985) 97.
30 L. Castello, E. Kirchmann and L. E. Welch, *Electroanalysis*, in press.
31 P. Fairbank, L. Castello and L. E. Welch, in preparation.
32 S. Hughes and D. C. Johnson, *Anal. Chim. Acta*, 132 (1981) 11.
33 D. C. Johnson and W. R. LaCourse, *Anal. Chem.*, 62 (1990) 589A.
34 G. T. Briguglio and C. A. Lau-Cam, *J. Assoc. Off. Anal. Chem.*, 67 (1984) 228.
35 L. E. Welch, W. R. LaCourse, D. A. Mead, D. C. Johnson and T. Hu, *Anal. Chem.*, 61 (1989) 555.
36 L. E. Welch and D. C. Johnson, *J. Liq. Chromatogr.*, 13 (1990) 1387.
37 W. R. LaCourse, W. A. Jackson and D. C. Johnson, *Anal. Chem.*, 61 (1989) 2466.
38 A. Ngoviwatchai and D. C. Johnson, *Anal. Chim. Acta*, 215 (1988) 1.
39 T. Z. Polta and D. C. Johnson, *J. Electroanal. Chem.*, 209 (1986) 159.
40 D. C. Johnson, *Anal. Chim. Acta*, 204 (1988) 1.

Journal of Chromatography, 633 (1993) 119–128
Elsevier Science Publishers B.V., Amsterdam

CHROM. 24 732

High-performance liquid chromatographic–mass spectrometric analysis of *cis*-dichlorodiamineplatinum–DNA complexes using an ionspray interface

R. Da Col and L. Silvestro*

Respharma Pharmacological Research srl, Via Belfiore 57, 10125 Turin (Italy)

C. Baiocchi and D. Giacosa

Dipartimento di Chimica Analitica, Università di Torino, Via P. Giuria 5, 10125 Turin (Italy)

I. Viano

Istituto di Farmacologia e Terapia Sperimentale, Facoltà di Medicina, Università di Torino, Via P. Giuria 13, 10125 Turin (Italy)

(Received September 2nd, 1992)

ABSTRACT

An efficient RP-HPLC separation technique was used in combination with mass spectrometric detection with an ionspray ionization source to analyse complexes between nucleosides and *cis*-dichlorodiamineplatinum(II). Conventional detection techniques (UV and atomic absorption spectrometry) were also used as starting points for the setting-up of this HPLC–MS approach. The method was developed using complexes obtained either by reaction of free deoxynucleosides with *cis*-dichlorodiamineplatinum or by reaction *in vitro* of DNA samples with the same drug. DNA samples before HPLC–MS were completely depolymerized by digestion with nuclease P1 and alkaline phosphatase, in order easily to separate and determine the complexes formed. The sensitivity obtained makes this technique very suitable for future application in biological studies. The detection level, defined as the detector response with a signal-to-noise ratio of 2, corresponds to 2 pmol injected. In DNA samples treated with *cis*-dichlorodiamineplatinum, a series of *cis*-dichlorodiamineplatinum–deoxynucleoside complexes not previously described were also detected.

INTRODUCTION

Several platinum derivatives have cytotoxic acitivity. Among others, *cis*-dichlorodiamineplatinum (II) (CDDP) is one of the most effective drugs in cancer therapy [1] and the theory of its mechanism of action suggests that DNA is its main intracellular target [2]. NMR studies of the *in vitro* reaction between CDDP and DNA have shown [3] that deoxyguanosine (dGua) and deoxyadenosine (dAde) are the nucleosides involved in the adduct formation. Fig. 1 shows the structures of the possible complexes.

The sensitivity of the NMR technique was far too inadequate, however, to study *in vivo* situations. In fact, in order to reach an adequate sensitivity for the study of DNA platination in biological samples, mainly alkaline elution [4], atomic absorption spectrometry (AAS) [5] and immunochemical techniques [6] have been used.

The biological effects of platinum derivatives are different and depend on the structure of the complexes with nucleosides that can be formed. None of

* Corresponding author.

0021-9673/93/$06.00

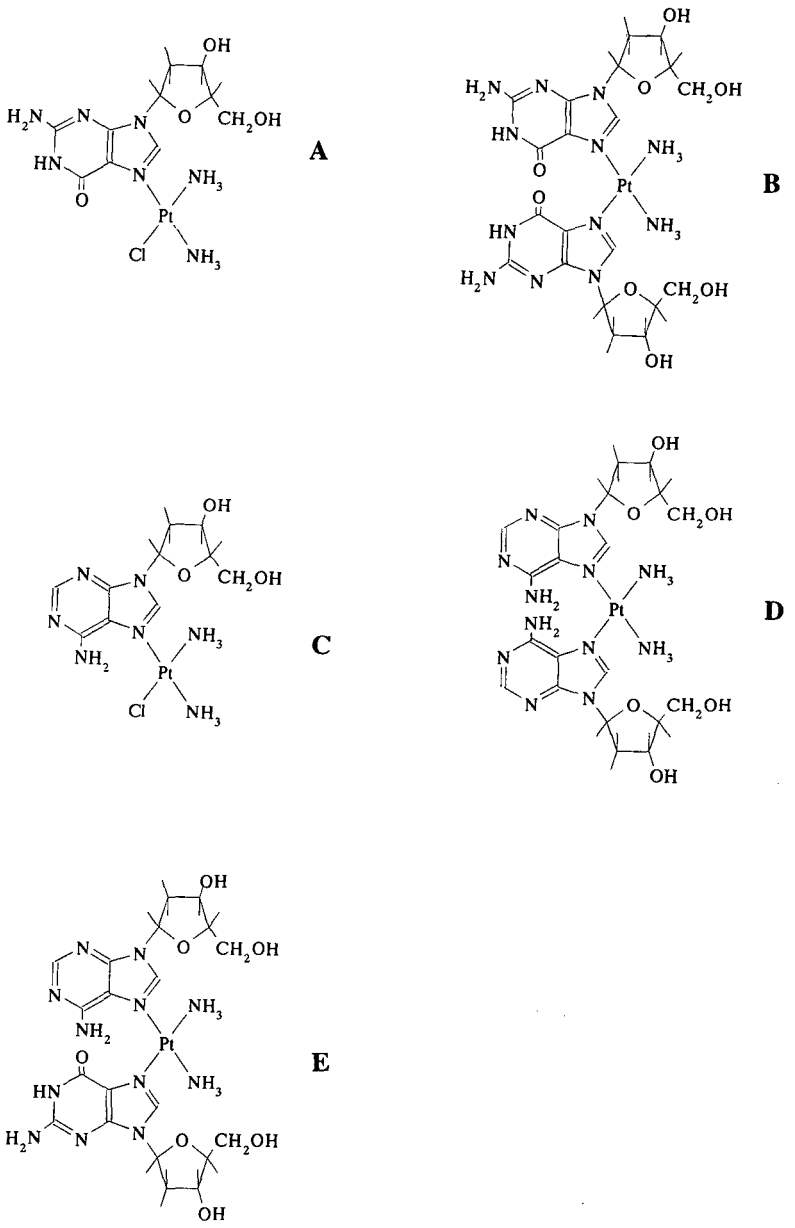

Fig. 1. Structures of the known nucleoside–CDDP complexes. A = dGua–CDDP; B = dGua–CDDP–dGua; C = dAde(N-7)–CDDP; D = dAde–CDDP–dAde; E = dGua–CDDP–dAde.

the aforementioned techniques, except the immunochemical type, allow a complete identification of the complexes present in the cells. Unfortunately, the immunochemical techniques are not of general application because they are tailored for the specific platinum compound under study, so they cannot be easily adapted to investigate different platinum derivatives with different antigenic properties. Since, at present, one of the main tasks of pharmacological research is to carry out studies on new cytotoxic

anticancer drugs, there is a need for a technique of general applicability and high sensitivity.

Mass spectrometry (MS) is a sensitive technique that is able to provide relevant structural information and, at the same time, flexible enough to be used in many different analytical situations. Therefore, in combination with an efficient separation mode, it may play an important role in extending to biological samples the study of the interactions between nucleosides and platinum compounds. The aim of this work was to check the possibilities of this technique by studying under *in vitro* conditions the products of the reaction between CDDP and DNA.

The efficiency of reversed-phase HPLC for the separation of the various complexes of CDDP with nucleosides has already been reported [7]. In previous work [8] we adopted, in the analysis of such complexes, an HPLC–MS technique using a plasma thermospray interface, but poor results were obtained. In this study we have combined a microbore RP-HPLC separation procedure and mass spectrometric detection with a pneumatically assisted ionspray ionization source, particularly suitable for polar compounds. In this way we obtained structural information about various CDDP–nucleoside complexes of different stoichiometry and composition. Structures already known were confirmed and at the same time some evidence for the presence of new complexes was obtained.

EXPERIMENTAL

Chemicals

All the reagents of the purest grade available and HPLC-grade acetonitrile were purchased from Fluka, except nuclease P1, which was obtained from Pharmacia. Ultrapure water was prepared with a Milli-Q purification system (Millipore).

Synthesis of nucleoside–CDDP complexes

To obtain complexes of CDDP with dGua and dAde, 10.0 μmol of each nucleoside were reacted separately for 24 h at 37°C in the dark with an equimolar amount of CDDP in 2.5 ml of distilled water. To synthesize the complexes of CDDP with both nucleosides (dGua–CDDP–dAde), 5.0 μmol each of the two nucleosides were combined and made react with 1.0 μmol of CDDP, dissolved in 2.5 ml of water, for 24 h at 37°C in the dark.

Synthesis of platinated DNA

A 1.0-mg amount of extractive DNA from calf thymus was incubated for 24 h at 37°C in the dark dissolved in 2.5 ml of distilled water containing 1.0 mg of CDDP.

Chromatographic separations

Separations were performed with an Applied Biosystems Model 140A syringe pump HPLC system and a Perkin-Elmer ISS-101 autosampler. UV detection was performed at 260 nm with an Applied Biosystems 1000S diode-array detector and the data were treated with a Varian 4270 computing integrator. When necessary, fraction collections were performed using a FRAC 100 fraction collector (Pharmacia). Separations were performed with a reversed-phase column [Hypersil MOS, 5 μm, 25 cm × 1 mm I.D. (Shandon)]. The mobile phase was 0.05 *M* ammonium acetate buffer (pH 4.0) (solvent A) and methanol–0.1 *M* acetate buffer (pH 4.0) (50:50) (solvent B). The elution conditions adopted were as follows: after 10.0 min of isocratic condition elution with 100% A, a linear gradient was started with a slope of 2.0% B min^{-1} up to 10% B and then 3.33% B min^{-1} up to 60% B, this final composition being maintained for 25.0 min. The flow-rate was 50 $\mu l/min^{-1}$. The samples were collected with the fraction collector just after injection in 30 fractions for 60 min.

Atomic absorption spectrometric assay

Platinum determinations by AAS were performed with a Varian SpectraAA 10 atomic absorption spectrometer equipped with a Varian GTA 96 graphite furnace. Aliquots (20.0 μl) were injected into the graphite tube and vaporized at 2700°C after ashing at 1200°C in a nitrogen atmosphere.

Enzymatic degradation of DNA samples

To the DNA samples after the reaction with CDDP were added solid NaCl up to a final concentration of 0.1 *M* and subsequently 2.5 volumes of cold ethanol. The resulting solution was kept overnight at −20°C in order to obtain complete precipitation of DNA. DNA pellets, recovered by centrifugation (20 min at 10 000 *g* in Corex tubes), before enzymatic treatment were dried under vacuum. Depolymerization of DNA was achieved by treating the samples, dissolved in 50.0 m*M* sodium acetate

buffer (pH 6.0) containing 3.0 m*M* $ZnCl_2$, with nuclease P1 (5 U for 1 mg of DNA) for 6 h at 37°C. To remove terminal phosphate groups the samples were then basified, by addition of 50.0 m*M* Tris–HCl buffer (pH 10.55) containing 3.0 m*M* $MgCl_2$, and 5 U (for 1 mg of DNA) of alkaline phosphatase were added and the incubation was continued at 37°C for 12 h. After these treatments, enzymes and residual undigested materials were removed from nucleosides by ultrafiltration with an Ultrafree-MC 10K NMWL (Millipore) with a molecular mass cut-off of 10 000 operated in a fixed-angle centrifuge (3000 *g* for 45 min).

Mass spectrometry

Mass spectra were acquired using a Perkin-Elmer–Sciex API III triple quadrupole tandem mass spectrometer equipped with an ionspray atmospheric pressure ionization source. The mobile phase flow was introduced, without splitting, to the source. Mass spectra were acquired in the positive-ion mode scanning, in a range including the expected molecular masses of nucleoside–CDDP complexes.

RESULTS

The first step in this work was a detailed HPLC study with different detection system (UV, AAS, MS) of the products of the reaction between CDDP and dGua and dAde free nucleosides.

The chromatographic separation and determination with UV detection of the products of the reaction between deoxyguanosine and CDDP is illustrated in Fig. 2. The higher peak at t_R = 11.3 min (peak 2) corresponds to the unreacted deoxyguanosine, as confirmed by injection of a pure standard of the nucleoside. The assignment of the peaks eluting at t_R = 9.7 min (peak 1) and 14.9 min (peak 3) was performed by MS detection (Fig. 2B and C). Their MS peaks corresponded to *m/z* values typical of the protonated molecular ions $[M + H]^+$ of the complexes CDDP–dGua (Fig. 1A) and dGua–CDDP–dGua (Fig. 1B). In complete agreement with these results, platinum was detected by AAS in the fractions collected from the same peaks (data not shown).

In Fig. 3 are summarized analogous results obtained analyzing the products of the reaction of de-

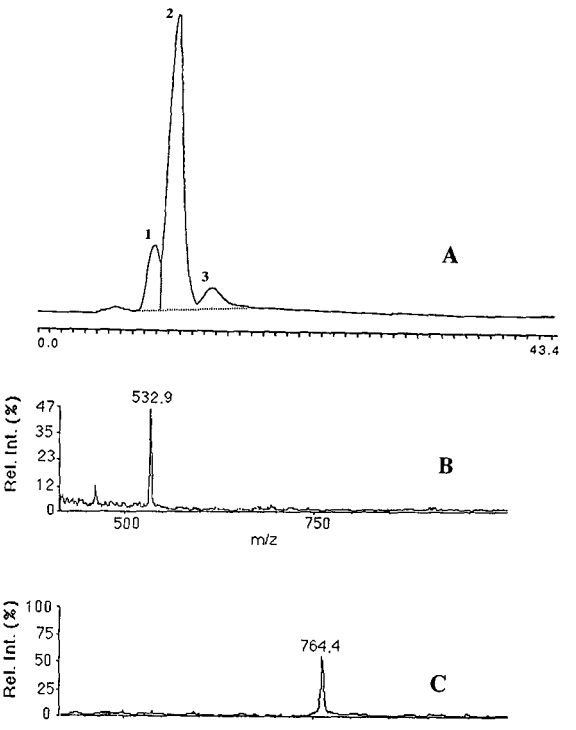

Fig. 2. (A) RP-HPLC separation with UV detection at 260 nm of a standard mixture of dGua–CDDP complexes. For chromatographic conditions, see Experimental. 1 = dGua–CDDP; 2 = free dGua; 3 = dGua–CDDP–dGua. (B) Mass spectrum of peak 1. (C) Mass spectrum of peak 3.

oxyadenosine with CDDP. The free nucleoside, as confirmed by injecting the pure standard, elutes at t_R = 18.5 min (peak 3). The first two eluting peaks in Fig. 3A (t_R = 13.3 and 14.9 min), analysed by MS (spectra reported in Fig. 3B and C), were identified as dAde–CDDP complexes, on the basis of the presence of *m/z* values corresponding to the masses of the protonated molecular ions. However, both peaks show identical mass spectra owing to the possibility of *cis*-CDDP coordinating with the nitrogen atom in either position 7 or 1 of the dAde molecule, as already proposed by Wenclawiak *et al.* [7] (Fig. 1C shows one of the possible structures). For the same reason, three different types of dAde–CDDP–dAde complex (one of them is depicted in Fig. 1D) are formed, eluting at t_R = 36.6 min (peak 4), 37.5 min (peak 5) and 38.9 min (peak 6) with identical mass spectra, exhibiting the most relevant peak at

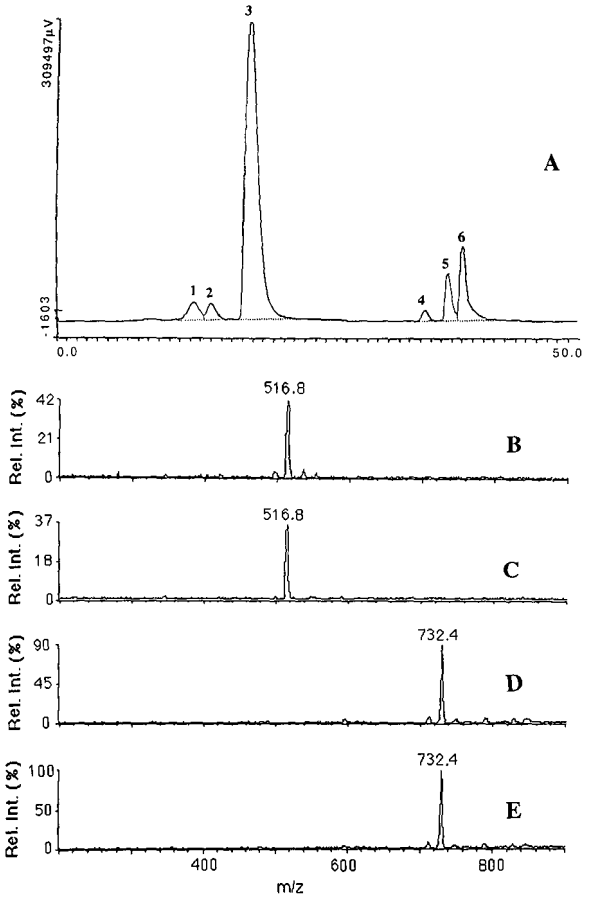

Fig. 3. (A) RP-HPLC separation with UV detection at 260 nm of a standard mixture of dAde–CDDP complexes. Chromatographic conditions as in Fig. 2. 1, 2 = dAde–CDDP complexes differing in the N atom involved in the coordination; 3 = free dAde; 4, 5, 6 = dAde–CDDP–dAde complexes differing in the N atoms involved in the coordination (N-1–N-1, N-7–N-1, N-7–N-7). (B,C) Mass spectra obtained from peaks 1 and 2; (C,D,E) Mass spectra obtained from peaks 4, 5 and 6.

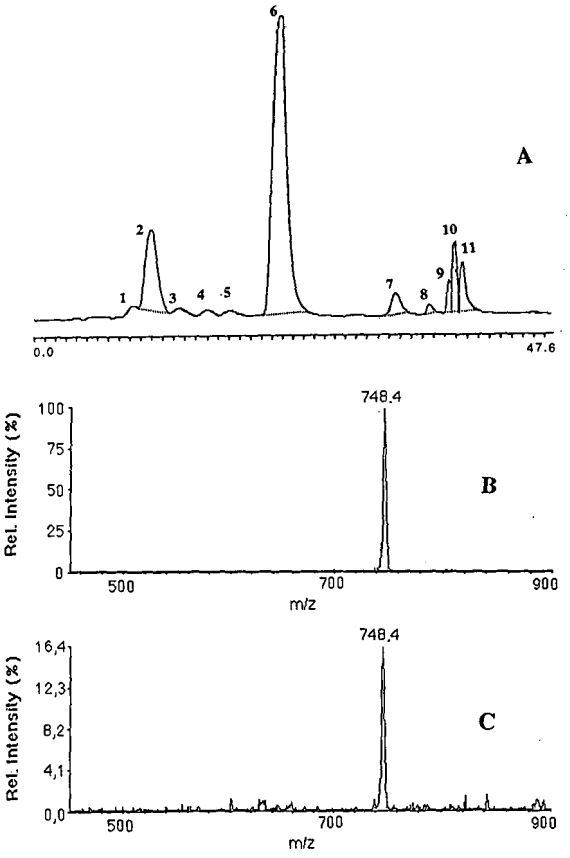

Fig. 4. (A) RP-HPLC separation with UV detection at 260 nm of the products of the reactions of dGua, dAde and CDDP. Chromatographic conditions as in Fig. 2. 1 = dGua–CDDP; 2 = free dGua; 3 = dGua = dGua–CDDP–dGua; 4 = dAde(N-1)–CDDP; 5 = dAde(N-7)–CDDP; 6 = free dAde(N-1)–CDDP-dGua; 8 = dAde(N-1)–CDDP–dAde(N-1); 9 = dAde(N-1)–CDDP–dAde(N-7); 10 = dAde(N-7)–CDDP–dGua; 11 = dAde (N-7)–CDDP–dAde(N-7). (B,C) Mass spectra of peaks 7 and 10.

the m/z value corresponding to the mass of the $[M + H]^+$ ion (Fig. 3D and E for peaks 5 and 6, respectively). As before, the AAS results (data not shown) obtained from fractions collected during this separation are in agreement with the proposed interpretation.

Fig. 4 shows the results obtained after reaction of both nucleosides with CDDP. In the UV trace (Fig. 4A) are present the chromatographic peaks previously observed and identified either as nucleoside–CDDP complexes or free nucleosides. The MS data (spectra not reported) supported this interpretation. In addition, two new peaks containing platinum (confirmed by AAS) were observed at t_R = 33.6 min (peak 7) and 38.8 min (peak 10) and identified as dAde–CDDP–dGua mixed complexes differing in the nitrogen atom (N-1 or N-7) of dAde involved in the complexation (Fig. 1E shows one of the possible cases) on the basis of the corresponding mass spectra (Fig. 4B and C) showing relevant signals at the m/z value corresponding to the $[M + H]^+$ ion.

The next step was an analogous chromatographic

study of the products of the *in vitro* reaction between CDDP and intact DNA in order to verify the type and number of complexes formed and to compare them to those examined previously.

Fig. 5A shows the separation of the digestion products obtained from a pure DNA sample and monitored by UV detection. Four large peaks can be observed at retention times comparable to deoxycitydine, deoxyguanosine, thymidine and deoxyadenosine. The slight shifts in the observed retention times are probably due to co-elution problems. Fig. 5B reports the UV trace of the chromatographic separation of the products obtained after reaction of the pure intact DNA sample with CDDP. The four major peaks corresponding to the free nucleosides are still present, but there is a decrease in those corresponding to dGua and dAde, clearly owing to their reaction with CDDP. By comparing the peak areas of the two separations it was calculated that 85.3% and 36.5% of dGua and dAde, respectively, have reacted. Some of the peaks corresponding to the complexes whose formation was previously assessed were hidden by the peaks of deoxycitydine and thymidine and several of the adducts involving dAde were not found. On the other hand, new peaks undetected in the preceding study can be observed, eluting at very long retention times.

In Fig. 5C are reported the results, obtained by AAS, for platinum contents in the fractions collected during the chromatographic run of the same sample. As expected, platinum was found in the fractions corresponding to the retention times of dGua–CDDP, dGua–CDDP–dGua and dGua–CDDP–dAde. However, large amounts of platinum were unexpectedly found either in a fraction corresponding to the elution time of dAde or in the group of the later eluting peaks, suggesting the formation of nucleoside–CDDP complexes of unknown structure.

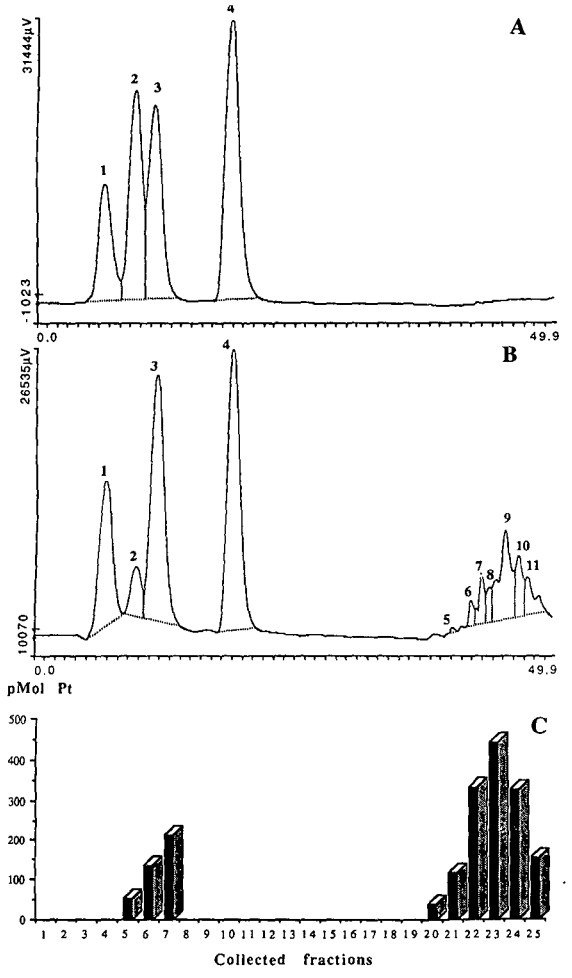

Fig. 5. (A) RP-HPLC separation with UV detection at 260 nm of a standard mixture of (1) deoxycitydine, (2) deoxyguanosine (3) thymidine and (4) deoxyadenosine. (B) Chromatographic separation under the same conditions as above of the products of reaction between pure intact DNA and CDDP. (C) Pt contents determined by AAS of the fractions collected during the run of chromatogram B.

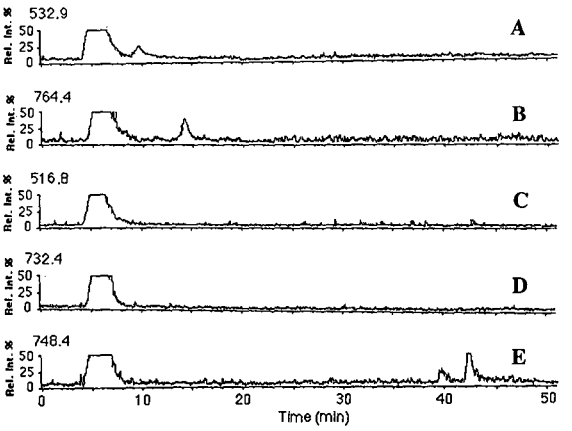

Fig. 6. Chromatogram of Fig. 5B retraced by MS detection with single-ion monitoring at the *m/z* values corresponding to the protonated ions of (A) dGua–CDDP (532.9), (B) dGua–CDDP–dGua (764.4), (C) dAde–CDDP (515.8), (D) dAde–CDDP–dAde (732.4) and (E) dAde–CDDP–dGua (748.4).

The chromatogram in Fig. 5B was retraced, with MS detection, in a number of chromatograms detected at the *m/z* values corresponding to the protonated ions of dGua–CDDP, dAde–CDDP, dGua–CDDP–dGua, dAde–CDDP–dAde and dGua–CDDP–dAde. Such reconstructed chromatograms are shown in Fig. 6. All of the traces exhibit a large peak, eluting at the void volume of the column, corresponding to ions produced by ionization of salts present in the sample. The chromatograms in Fig. 6A and B, detected at the *m/z* values of dGua–CDDP and dGua–CDDP–dGua molecular ions, respectively, show peaks with the expected retention times. In traces C and D, corresponding to ion monitoring of dAde–CDDP and dAde–CDDP–dAde complexes, respectively, no peaks can be detected according to previous studies which had already shown that these types of complexes are hardly formed in platinated DNA. Trace E, corresponding to the monitoring of dGua–

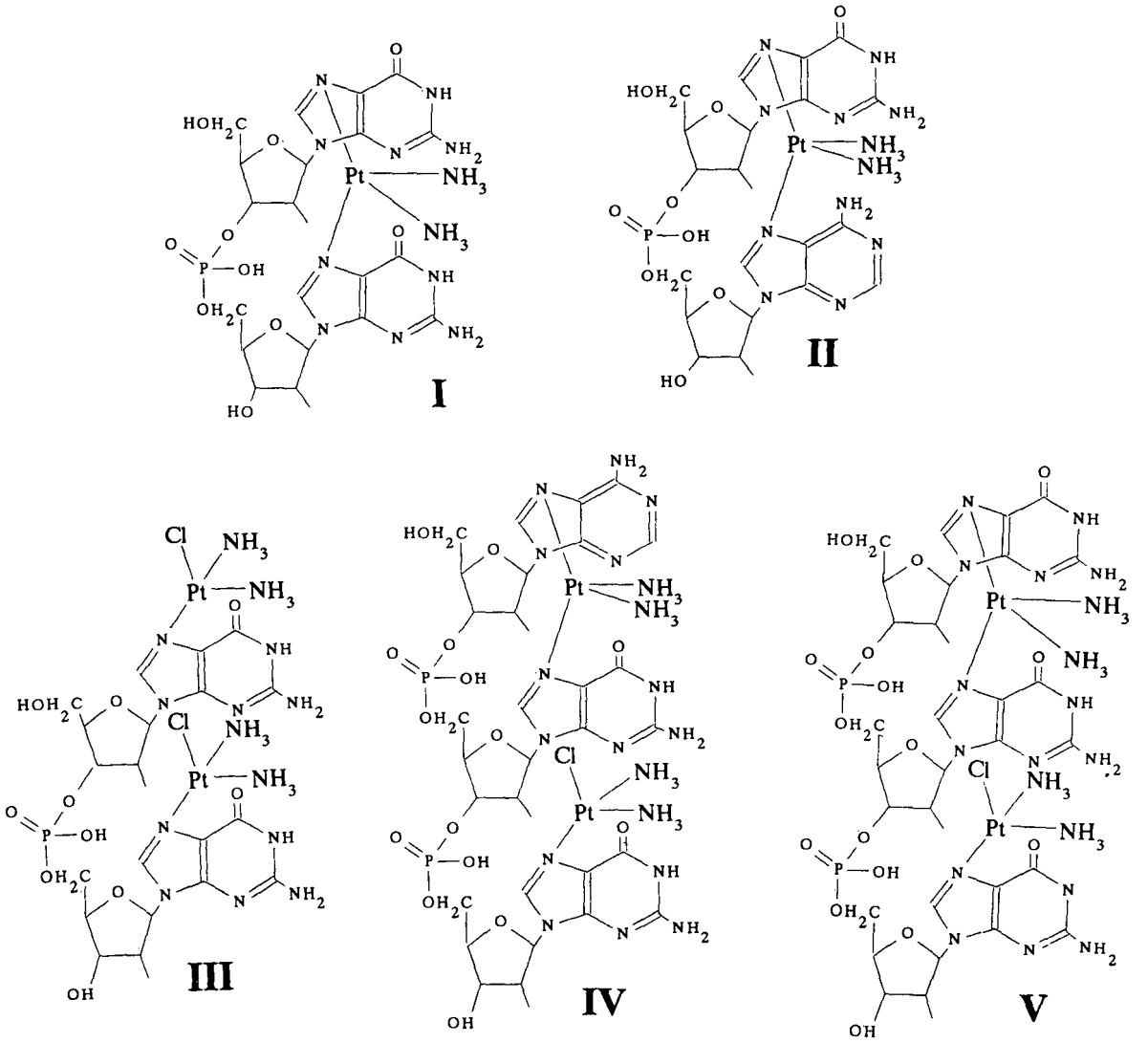

Fig. 7. Structures of possible nucleoside–CDDP complexes proposed in order to explain the presence of the last-eluting peaks of Fig. 5B containing platinum.

CDDP–dAde molecular ion, clearly shows a peak at the expected retention time along with a larger peak at a retention time corresponding to one of the later eluting substances of unknown structure.

Fig. 7 illustrates some proposed structures of possible nucleoside–CDDP complexes which could correspond to the last-eluting peaks. The formation of such molecules may be hypothesized as a consequence of the steric hindrance exerted by adjacent nucleoside–CDDP complexes on the phosphorus bonds, not allowing correct cleavage by nuclease P1. In particular, the complex

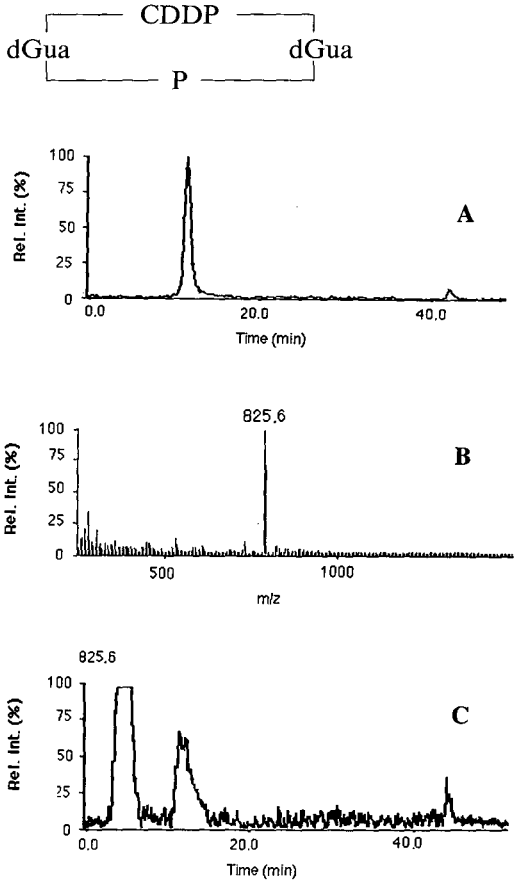

Fig. 8 (A) Chromatographic profile with MS detection (total ion current) of the products or reaction between dGua–P–dGua and CDDP. (B) Mass spectrum of the first peak of chromatogram A. (C) Chromatogram A retraced with single-ion monitoring at the m/z value corresponding to the $[M + H]^+$ ion from the complex

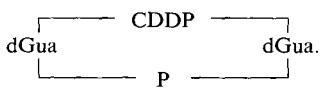

where –P– indicates the phosphorus bonds between the carbohydrates of the nucleosides (I, Fig. 7) is a structure already proposed [9]. We did not find this type of complex before because its formation is impossible in the reaction of free nucleosides with CDDP.

To elucidate this aspect better, 1.0 mg of synthetic dGua–P–dGua (Sigma, Rochester, NY, USA) was reacted with 1.0 mg of CDDP under the same conditions as reported for the nucleoside–CDDP reaction. In Fig. 8A is presented the chromatographic trace obtained in the total ion current mode for the product of this reaction under the same HPLC–MS conditions as described earlier. Platinum amounts were detected by AAS (data not shown) mainly in the second large peak (t_R = 12.1 min) and much less in the peak at 43.3 min. Fig. 8B shows the mass spectrum obtained from the peak at 12.1 min, characterized by an intense signal at m/z corresponding to the $[M + H]^+$ ion. As expected, in the reconstructed chromatogram at m/z 825.6 (Fig. 8C), corresponding to the complex

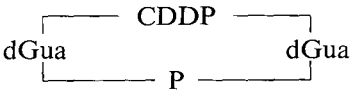

present in the DNA samples, two peaks are observed at retention times of 12.3 and 43.4 min, respectively.

As regards the last-eluting peaks in the chromatogram with UV detection in Fig. 5B, whose identification remained undefined at that stage of the study, an examination of their mass spectra was

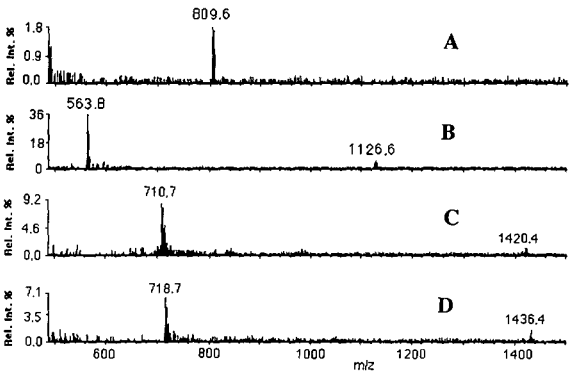

Fig. 9. Mass spectra of some of the later eluting peaks in the chromatogram in Fig. 5B. See text for explanations.

accomplished with the aim of finding significant mass spectral peaks compatible with the structures proposed in Fig. 7 (II–V). Fig. 9A shows the mass spectrum of the peak at t_R = 44.2 min. It is characterized only by an ion at m/z 809.6 corresponding to the protonated ion of the complex

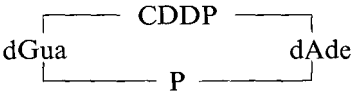

(II, Fig. 7). Also in this instance we tried to prepare such a type of complex starting from dGua–P–dAde as described previously for dGua–P–dGua. The chromatographic analysis of the product of this reaction gave several peaks whose mass spectra were similar to that reported in Fig. 9A.

The mass spectrum illustrated in Fig. 9B (peak at t_R = 47.1 min) includes two relevant ions that seem to be singly and doubly charged ions derived from the same molecule; the m/z values correspond to the hypothetical complex (III, Fig. 7) formed by two dGua–CDDP linked by a phosphorus bond. We could not obtain this type of complex from the synthetic dinucleotide and therefore we could not verify this hypothesis definitively.

The spectra presented in Fig. 9C (peak at t_R = 47.8 min) and D (peak at t_R = 48.9 min) are again characterized by mass spectral peaks due to singly and doubly charged ions. The molecular masses calculated from these two spectra may be related to complexes made up of a sequence of three nucleosides, two dGua and one dAde (M_r = 1435.4) or three dGua (M_r = 1419.4) with intact phosphorus bonds and two molecules of CDDP (IV and V, Fig. 7). Further reasonable interpretations in terms of mass spectral analysis could not be obtained. About fifteen peaks can be observed in the UV trace between 40 and 50 min and at present we can propose an interpretation for only five of them.

DISCUSSION

The conditions adopted for the chromatographic analysis provided separations of limited resolution (Fig. 5A and B). Peaks of thymidine, dGua, dGua–CDDP, dAde–CDDP,

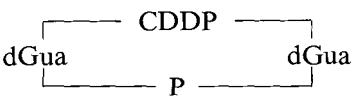

and dGua–CDDP–dGua elute very closely, without a complete separation. However, with MS detection, the separation was good enough to obtain a reliable identification and determination of the different CDDP–nucleoside complexes and nucleosides. In fact, as regards the quantitative aspect, analyses performed with single-ion monitoring at the m/z values in Fig. 6 gave a limit of detection, defined as the detector response with a signal-to-noise ratio of 2, of 2 pmol injected for each of the complexes of defined structure analysed alone or in a DNA digestion.

By analysing the products of the reaction of free nucleosides with CDDP, all of the expected complexes were identified, and also those involving deoxyadenosine that cannot be formed by reaction inside DNA. The results achieved for DNA reacted with CDDP confirmed the findings obtained by other workers [7]; moreover, an interesting series of peaks corresponding to complexes not yet described were also found.

These results do not conflict with previous studies, as most of these complexes seems to be always dGua–and/or dAde–CDDP complexes, even if with much more complicated structures, owing to a linkage of the constituents in sequences resistant to enzyme degradation.

It is worth noting that the reaction between synthetic dGua–P–dGua and CDDP produced two products having the same mass spectra but very different chromatographic properties (Fig. 8A–C). No attempts have made to interpret these results, which seem suggest the existence of two isomers.

Some peaks could be characterized, because their mass spectra were not interpretable with reasonable combinations of CDDP, nucleosides and phosphoric acid molecules. Under our experimental conditions (molecular mass exclusion limit of the ultrafiltration step = 10 000, presence of proteic materials coming from several sources), complexation between CDDP and protein fragments may not be excluded and DNA–CDDP–protein or amino acid–CDDP complexes have been extensively described in other studies.

If these more complex structures are really present in the cells, it is possible that they can play a relevant role in determining the biological effects of CDDP because, as they are resistant to the action of nuclease P1, they can be more resistant also to the

action of the enzymes involved in the mechanisms of DNA repair. Experiments on DNA extracted from cells treated with CDDP will be necessary in order really to understand the role of these complexes. Moreover, other techniques such as NMR spectroscopy, must be used to clarify their structures.

The sensitivity of the present procedure is very satisfactory and, by comparison with the results of other workers regarding the amount of nucleoside–CDDP complexes present in cells treated with CDDP, may well be considered suitable for the analysis of biological samples. In conclusion, we believe that the present HPLC–MS analysis under the proposed conditions is a promising technique for chemical and biological studies on platinum drug–DNA interactions.

REFERENCES

1 B. Rosenberg, *Cancer (Philadelphia)*, 55 (1985) 2309.
2 J. A. Howle and G. Gale, *Biochem. Pharmacol.*, 19 (1970) 2757.
3 A. M. J. Fichtinger-Schepman and J. L. Van der Veer, *Biochemistry*, 24 (1985) 707.
4 B. A. Teicher and S. A. Holden, *Cancer Res.*, 47 (1987) 388.
5 A. M. J. Fichtinger-Schepman and P. H. M. Lohman, *Carcinogenicity of Alkylating Cytostatic Drugs (IARC Scientific Publication*, No. 78), IARC, Lyon, 1986, p. 83.
6 A. M. J. Fichtinger-Schepman and A. T. Van Oosterom, *Cancer Res.*, 47 (1987) 3000.
7 B. Wenclawiak, W. Kleibohmer and B. Krebs, *J. Chromatogr.*, 296 (1984) 395.
8 L. Silvestro, C. Baiocchi, D. Giacosa, R. Ferro, C. Dianzani and I. Viano, in P. Periti and T. Mazzei (Editors), *Atti XVI Congresso Società Italiana di Chemioterapia (Firenze)*, II Sedicesimo, Firenze, 1989, pp. 563–565.
9 G. A. P. Hospers and N. H. Mulder, *Cancer Res.*, 48 (1988) 6803.

Journal of Chromatography, 633 (1993) 129–133
Elsevier Science Publishers B.V., Amsterdam

CHROM. 24 714

High-performance liquid chromatographic determination of aluminium and iron(III) in solar salt in the form of their 1-phenyl-3-methyl-4-benzoyl-5-pyrazolone chelates

Yoshifumi Akama* and Aijun Tong

Department of Chemistry, Faculty of Science and Engineering, Meisei University, Hodokubo, Hino, Tokyo 191 (Japan)

(First received February 26th, 1992; revised manuscript received October 23rd, 1992)

ABSTRACT

Aluminium and iron(III) ions in solar salts were separated and simultaneously determined in the form of their 1-phenyl-3-methyl-4-benzoyl-5-pyrazolone (PMBP) chelates by HPLC. Four imported solar salt samples were subjected to this investigation. The samples were dissolved in dilute nitric acid with heating. An aliquot of the solution was pipetted and adjusted to pH 3 with acetate buffer, then 10 ml of 0.02 *M* PMBP–methanol solution were added. The chelates obtained were dissolved in dioxane and 10 μl were injected and analysed by HPLC. The determinations were completed within 20 min and the recoveries of each metal were satisfactory. Divalent metal ions did not interfere under the same chromatographic conditions.

INTRODUCTION

A knowledge of the presence of various trace metals in sodium chloride samples is important for the quality control of salt. Therefore, the determination of trace metals in such samples is of great value [1–3]. Interference by NaCl is often troublesome in the analysis of solar salt for trace metals, and the latter are usually separated and concentrated by liquid–liquid extraction and by coprecipitation techniques and subsequently determined by a variety of methods. The major advantage of the coprecipitation technique is that a large volume of sample solution can be used in the concentration of desired elements. In this study we applied the coprecipitation technique to the concentration of aluminium and iron in solar salt samples.

The high-performance liquid chromatographic (HPLC) separation and determination of metals in the form of chelates is gaining increasing popularity and many chelating agents have been introduced [4–8]. The ligands used need to have such properties as a high reaction ability with most metals, formation of stable chelates over a wide pH range and formation of chelates with high molar absorptivities in the UV or visible region.

In previous studies, 1-phenyl-3-methyl-4-benzoyl-5-pyrazolone (PMBP) was used for the group extraction and separation of trace metals with subsequent atomic absorption spectrometric analysis [9–11]. PMBP is an excellent complexing agent of metals owing to the high reactivity and stability of its complex. It satisfies well the conditions for the prederivatization of metal ions for HPLC determination. The chromatographic behaviour and simultaneous determination of Al and In have been published previously [12–14]. These methods would be of value especially for the selective separation of In in Al and Ga.

In this paper, the use of PMBP as a precolumn derivatizing agent for the mutual separation and determination of Al and Fe(III), which had been concentrated by PMBP coprecipitation, by HPLC in imported solar salt samples is reported.

* Corresponding author.

0021-9673/93/$06.00

EXPERIMENTAL

Apparatus and reagents

The analytical HPLC system consisted of a Japan Spectroscopic (JASCO) Model 880-PU pump and Model 875-UV spectrophotometric detector and a Rheodyne Model 7125 injector with a 20-μl injection loop. The recorder was a CR4A Chromatopak (Shimazu). A Chemcosorb 5-ODS-UH column (250 × 4.6 mm I.D.) was used throughout. The PMBP chelates of Al and Fe(III) were synthesized as described previously [12] and their composition was found by elemental analysis to be 1:3 (metal: PMBP). The purities were found to be *ca.* 94% for Al–PMBP and 100% for Fe–PMBP.

All solvents and reagents were of analytical-reagent grade.

Al and Fe(III) stock standard solutions were prepared by dissolving 21.5 and 22.2 mg of Al– and Fe(III)–PMBP, respectively, in dioxane and diluting to 25 ml with dioxane, giving a concentration of $1 \cdot 10^{-3}$ *M* for each metal. The solutions were mixed to make a $2.5 \cdot 10^{-5}$ *M* solution of Al or Fe by appropriate dilution with dioxane. Dioxane was chosen as the solvent for dissolution of the chelates because it is more efficient than other solvents such as acetonitrile and methanol.

Procedure

Chromatographic separations were carried out at room temperature using pure acetonitrile as the mobile phase at a flow-rate of 1.0 ml min^{-1}. An aliquot of the solution was injected with a 20-μl loop injection in all instances. The spectrophotometric detector was set at 245 nm.

Application

The proposed method was applied to the determination of Al and Fe(III) in solar salt samples imported from Australia and Mexico. A sample of about 40 g was dissolved on a thermostated hotplate (100°C) in 150 ml of water containing 5 ml of concentrated nitric acid, then the solution was diluted to 200 ml with distilled water. A 20-ml aliquot of the sample solution was pipetted into a 100-ml beaker and the pH was adjusted to about 3 with 1 *M* sodium acetate. A 10-ml volume of 0.02 *M* PMBP solution in methanol was then added, and the solution was heated to 90°C while being stirred on a water-bath for about 1 h. The precipitate was filtered off, washed with water and finally dissolved in and diluted to 25 ml with dioxane. A 10-μl aliquot of the sample solution was injected into the chromatograph and the determination of the two metals was carried out with the dioxane solution of pure chelates as a standard. Then 1 ml of a standard solution containing 14 and 30 μg of Al and Fe, respectively, was added to the 20 ml of salt solution and treated as above. The recoveries of the two metals were calculated.

RESULTS AND DISCUSSION

The absorption spectra of Al– and Fe(III)–PMBP chelates were measured in dioxane solution. Both Al– and Fe(III)–PMBP chelates exhibit maximum absorption at 245 nm, as shown in Fig. 1. The molar absorptivities of Al– and Fe(III)–PMBP chelates in dioxane at 245 nm were found to be $5.4 \cdot 10^4$ and $7.4 \cdot 10^4$ dm^3 mol^{-1} cm^{-1}, respectively, making them suitable for trace analysis by HPLC because of the excellent sensitivities. In this study, 245 nm was chosen as the detection wavelength.

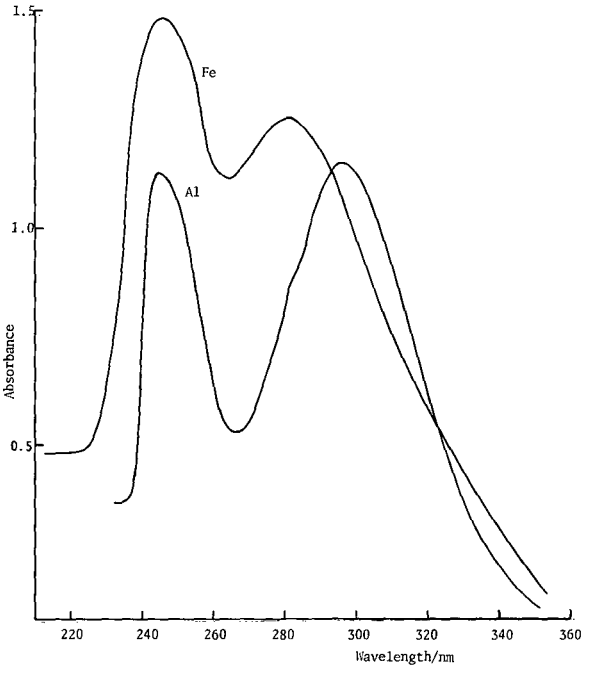

Fig. 1. UV spectra of PMBP chelates in dioxane. $Al(PMBP)_3$ and $Fe(PMBP)_3$ concentrations, $2.0 \cdot 10^{-5}$ *M*.

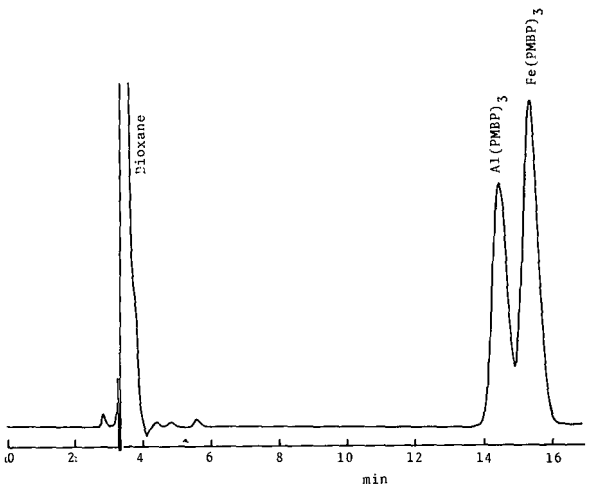

Fig. 2. Chromatograms of Al– and Fe–PMBP chelates with pure acetonitrile as the mobile phase. $Al(PMBP)_3$ and $Fe(PMBP)_3$ concentrations, $2.5 \cdot 10^{-5}$ *M*.

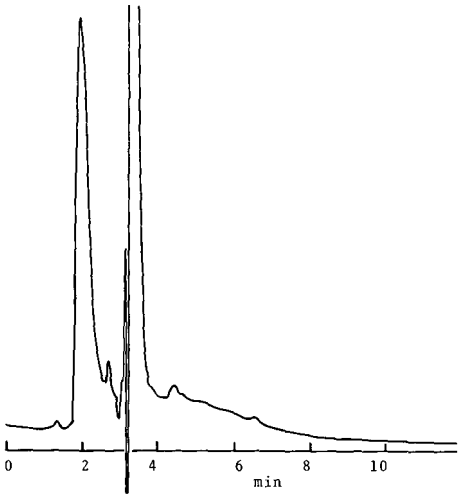

Fig. 3. Chromatogram of Al– and Fe–PMBP chelates with methanol as the mobile phase. $Al(PMBP)_3$ and $Fe(PMBP)_3$ concentrations $2.5 \cdot 10^{-5}$ *M*.

In the initial studies using acetonitrile as the mobile phase, a good separation of Al– and Fe(III)–PMBP chelates (eluted in that order) was obtained, as shown in Fig. 2. Pure acetonitrile was found to be the most suitable mobile phase for the separation of these two chelates in the investigated organic solvents (methanol, ethanol and water–actonitrile).

When pure methanol was used as the mobile phase, the peaks of the Al– and Fe(III)–PMBP chelates disappeared and a new peak was observed before the dioxane peak, as shown in Fig. 3. With ethanol, the two elements were also not separated and co-eluted with dioxane. This appearance of a new peak before the dioxane peak and lack of retention are due to ionization in the column, the charged species of the chelates passing through the column without distribution to the stationary phase. We did not pursue this point further because the aim of this study was to determine the Al and Fe under optimum conditions.

The effect of the water content in acetonitrile on the separation of the chelates was investigated in the range of 0–10% (v/v). The retention time of each chelate increased with increasing of water content in the acetonitrile, and some dissociation of the Fe–PMBP chelate was also observed. The elution of the two chelates took longer than 1 h and no peaks were observed for the Al– and Fe(III)–PMBP chelates; some new peaks, most of which overlapped with the dioxane peak, were observed before and after the dioxane peak when acetonitrile containing $> 10\%$ (v/v) of water was used as the mobile phase. These results suggest that the complexes were decomposed in the column by water. Dissociation of the chelate is presumably due to the hydrolysis of these chelates in the chromatographic process.

Fig. 4 shows the results of an attempt to separate PMPB chelates of Al, Fe(III), Mn(II), Zn, Ni, Co (II) and Pb using pure acetonitrile as the mobile phase. The peaks for the Al and Fe(III) chelates were well resolved, whereas for the other chelates co-eluted immediately behind the dioxane peak, indicating that the other metals do not interfere in the presence of a tenfold molar excess. The retentions of the chelates mainly depend on the charge of the central metal ion and on the molecular size of the chelate; hence there would be no difficulty in the mutual separation of di- and trivalent cations.

Fig. 5 shows the calibration graphs obtained for the Al– and Fe(III)–PMBP chelates. The linearity of both graphs is good in the metal concentration ranges $0–5 \cdot 0^{-5}$ *M* with a 10-μl injection. The detection limits, defined as the concentrations where the peak height was three times the background, were *ca.* 13 and 28 μg/l for Al and Fe, respectively when the injection volume was 20 μl. The precision

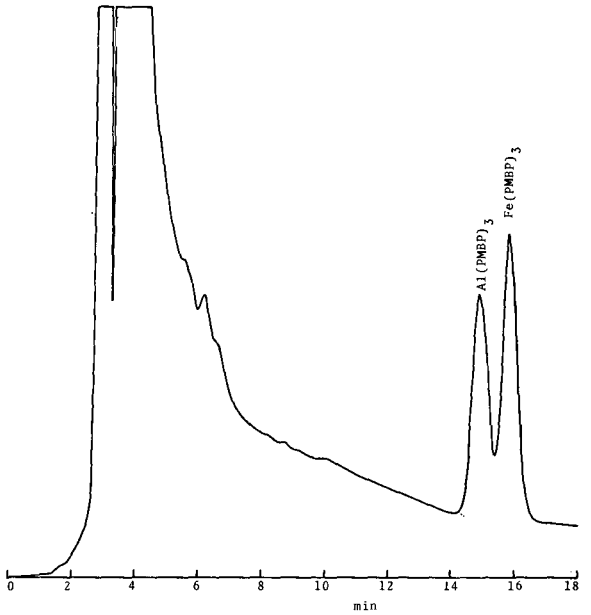

Fig. 4. Chromatogram of metal–PMBP chelates with acetonitrile as the mobile phase. Al– and Fe–PMBP chelate concentrations, $2.5 \cdot 10^{-5}$ *M*; Mn–, Co–, Ni–, Pb– and Zn–PMNB chelate concentrations, $2.5 \cdot 10^{-4}$ *M*.

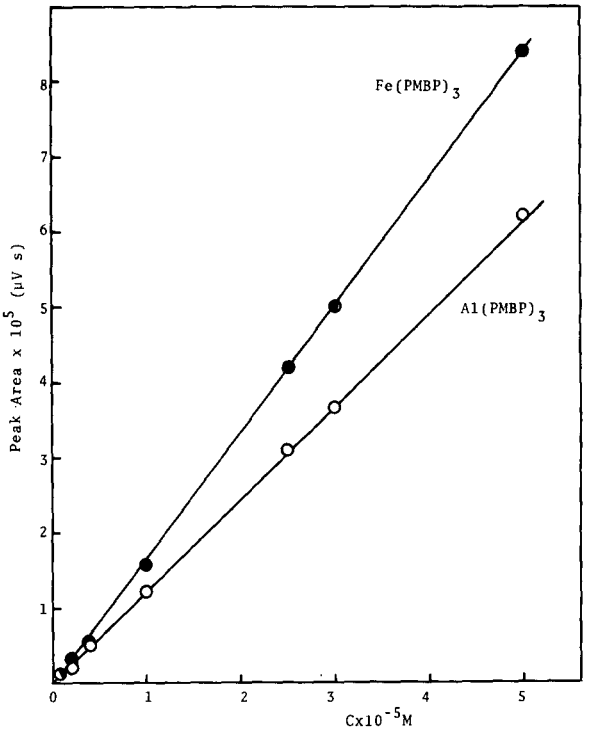

Fig. 5. Calibration graphs for Al– and Fe–PMBP chelates.

of the peak height was excellent for five determinations of $2.5 \cdot 10^{-5}$ M Al and Fe, with relative standard deviations of 1.5% for Al and 1.0% for Fe.

A solar salt sample was dissolved (as described in the *Application* section) and the proposed method was applied to the determination of Al and Fe(III). The contamination of the solar salt with Al and Fe may be mainly caused by traces of soil and rust from the chemical tanker. The Al and Fe(III) levels in the soil probably vary with the method used for the dissociation of the salt; however, in this study, the salt sample was dissociated as described above. Fig. 6 shows a chromatogram for the solar salt sample. The larger peak preceding the Al– and Fe(III)–PMBP chelate peaks is due to the excess of PMBP; this peak did not affect the separation of these chelates.

The results for the determination of Al and Fe (III) in four solar salt samples by the proposed method are given in Table I. The results of recovery tests are also given. The recoveries of Al and Fe(III) added to the sample were 88.0–95.3 and 92.0–99.7%, respectively.

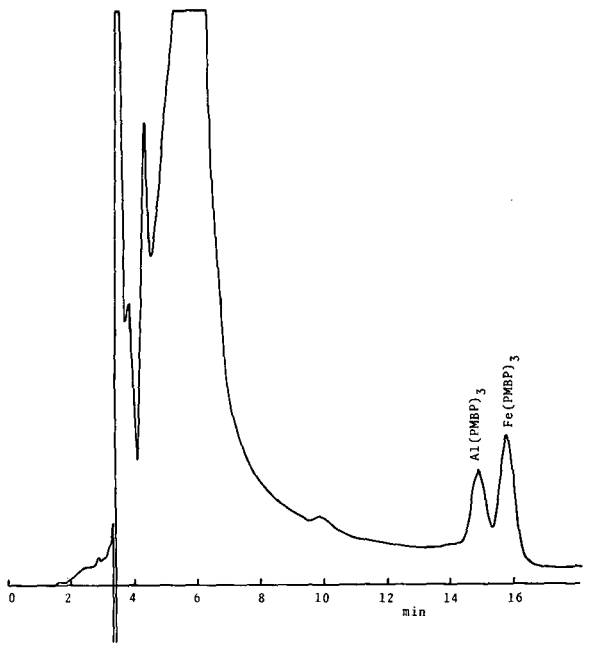

Fig. 6. Chromatogram obtained for solar salt sample.

TABLE I

ANALYTICAL RESULTS FOR Al AND Fe IN SOLAR SALTS

Results are averages of two determinations.

Sample[a]	Taken (g)	Element	Added (μg)	Found (μg)	Found in salt (ppm)	Recovery (%)
SA1	3.85	Al	0.0	6.3	1.6	
		Fe	0.0	17.6	4.6	
		Al	15.0	20.3		93.3
		Fe	30.0	47.5		99.7
SA2	3.93	Al	0.0	4.8	1.2	
		Fe	0.0	9.5	2.4	
		Al	15.0	18.0		88.0
		Fe	30.0	38.3		96.0
SA3	3.91	Al	0.0	5.1	1.3	
		Fe	0.0	7.1	1.8	
		Al	15.0	19.4		95.3
		Fe	30.0	37.0		99.6
SM	3.93	Al	0.0	4.7	1.2	
		Fe	0.0	13.8	3.5	
		Al	15.0	18.0		88.7
		Fe	30.0	41.4		92.0

[a] SA1 = Australian salt (date of sampling, July 1988); SA2 = Australian salt (date of sampling, April 1989); SA3 = Australian salt (date of sampling, January 1989); SM = Mexican salt (date of sampling, December 1989).

CONCLUSIONS

Al– and Fe(III)–PMBP chelates can be well separated on an ODS column with pure acetonitrile as the mobile phase. Divalent metals did not interfere under the same chromatographic conditions. The proposed method was applied to the determination of the two metals in imported solar salts. The recoveries and the precision of the determination were satisfactory, indicating that the method would be capable of the simultaneous determination of Al and Fe(III) in samples containing some divalent elements.

ACKNOWLEDGEMENT

This research was supported by a grant from The Salt Science Research Foundation (Grant No. 9110).

REFERENCES

1 K. Akatsuka and I. Atsuya, *Fresenius' Z. Anal. Chem.*, 329 (1988) 453.
2 P. Burba and P. G. Willmer, *Fresenius' Z. Anal. Chem.*, 329 (1988) 539.
3 C. Cheng, T. Akagi and H. Haraguchi, *Anal. Chim. Acta*, 198 (1987) 173.
4 R. C. Gurira and P. W. Carr, *J. Chromatogr. Sci.*, 20 (1982) 416.
5 L. H. Lajunen, E. Eijarvi and T. Kenakkala, *Analyst*, 109 (1984) 699.
6 K. Ohashi, S. Iwai and M. Horiguchi, *Bunseki Kagaku*, 31 (1982) E285.
7 S. Ichinoki and M. Yamazaki, *Anal. Chem.*, 57 (1985) 2219.
8 D. A. Roston, *Anal. Chem.*, 56 (1984) 241.
9 Y. Akama, T. Nakai and F. Kawamura, *Bunseki Kagaku*, 25 (1976) 496.
10 A. Tong, Y. Akama and S. Tanaka, *Bull. Soc. Sea Water Sci.*, 42 (1988) 59.
11 Y. Akama, A. Tong, S. Ishima and M. Kajitani, *Anal. Sci.*, 8 (1992) 41.
12 A. Tong, Y. Akama and S. Tanaka, *J. Chromatogr.*, 478 (1989) 408.
13 Y. Akama and A. Tong and S. Tanaka, *Chem. Lett.*, (1989) 963.
14 Y. Akama and A. Tong, *Anal. Sci.*, 7 (1991) 745.

Journal of Chromatography, 633 (1993) 135–142
Elsevier Science Publishers B.V., Amsterdam

CHROM. 24 769

Cyclodextrin stationary phases for the gas–solid chromatographic separation of light hydrocarbons

Evidence for multiple retention mechanisms

G. L. Reid, III, C. A. Monge, W. T. Wall and D. W. Armstrong*

Department of Chemistry, University of Missouri, Rolla, MO 65401 (USA)

(First received July 16th, 1992; revised manuscript received October 29th, 1992)

ABSTRACT

Cyclodextrin, bonded to silica gel and used as a gas–solid chromatographic (GSC) stationary phase provides a practical and efficient means for separating a wide variety of volatile C_1–C_7 hydrocarbons at ambient to elevated temperatures. Conditioning the columns at high temperature (300°C) for several hours increased efficiency and resolution. The adsorption of these light hydrocarbons involves multiple retention mechanismns. For unsaturated hydrocarbons, the cyclodextrin GSC column can act as a polar stationary phase analogous to silica gel. However, for saturated hydrocarbons, it acts as a non-polar phase. Evaluation of the columns and an analogous silica gel column with hydrocarbon standards is reported. Capacity factors and chromatograms are presented for compounds analyzed on these GSC stationary phases.

INTRODUCTION

Gas–solid chromatography (GSC) is a widely used technique for the separation of light hydrocarbons and a variety of other gases. Compared with gas–liquid chromatography (GLC), GSC stationary phases have comparatively larger surface areas [1] and strong adsorption properties which result in excessive retention times and band broadening for most large molecules. For the GLC separation of lower-molecular-mass hydrocarbons (C_1–C_4), small partition coefficients at room temperature make for necessarily long columns [2]. Packed columns, and more recently, porous-layer open-tubular (PLOT) or support-coated open-tubular (SCOT) [3–5] columns are preferred for the separation of a wide range of gaseous and volatile molecules. Molecular sieves [6,7], alumina and silica gel [8–11], porous polymers [12–16], charcoal [17–19] and other more novel GSC stationary phases, including charge-transfer complexes [20], ammonium tungstosilicate [21] and metal complexes (for a review, see ref. 22) have been cited as separating light hydrocarbons. Elution order for adsorption columns vary by stationary phase polarity [23]. Hydrocarbons are separated by boiling point on non-polar columns, while on polar stationary phases, compounds containing triple bonds are more strongly retained than compounds with double bonds, which, in turn, are more strongly retained than saturated compounds.

Smolková-Keulemansová [24] first used native and methylated cyclodextrins as stationary phase coatings for packed gas chromatographic columns. She found evidence for inclusion complex formation while focusing on somewhat higher boiling point hydrocarbons and geometric isomers. Presently, many researchers are reporting the use of amorphous derivatized cyclodextrins as chiral stationary phases for GLC [25–28]. Cyclodextrins are

* Corresponding author.

0021-9673/93/$06.00

cyclic oligosaccharides. They are composed of D(+)-glucopyranose units and are linked by α-(1,4) bonds. The three most common cyclodextrins, α, β and γ, are differentiated by the number of glucopyranose subunits (6,7 and 8, respectively). The cyclized glucopyranose units form a conical shaped structure, with secondary hydroxyls (12 for α-cyclodextrin) surrounding the wider end, and primary hydroxyls (6 for α-cyclodextrin) opposite. The top and bottom of the structure are polar, due to the hydroxyl groups, while the interior of the cavity is apolar. The internal diameter of α and β-cyclodextrin's cavities are approximatley 4.5 and 7 Å, respectively, and molecules with appropriate sizes can form a host/guest inclusion complex.

Mechanistic studies involving cyclodextrins [29,30] and derivatized cyclodextrins [31] have cited multiple retention mechanisms. Dipersive forces are responsible for the separation of aliphatic hydrocarbons [32]. Inclusion complexes of α-cyclodextrin and many lower hydrocarbons (methane, ethylene, propane and butane) in solution are formed when high positive pressures of these gases are maintained over an aqueous solution of cyclodextrin [33]. The crystalline complexes are very stable for long periods of time and contain 0.6–1.2 mol of gas per mol of cyclodextrin. Similiarly, crystalline complexes are formed for the noble gases krypton and xenon (0.34 and 0.85 mol of gas per mol of cyclodextrin, respectively) [34]. Lower noble gases (helium, neon and argon) do not to form inclusion complexes with α-cyclodextrin.

EXPERIMENTAL

Instrumentation

A Hewlett-Packard (Avondale, PA, USA) 5890 Series II gas chromatograph equipped with a packed column injection port, flame ionization detector, and a liquid nitrogen cryogenic coolant system was utilized in this study. The injector and detector were set at 200°C. The oven temperature program was 30°C for 2 min, then increasing at 7.5°C/min to 200°C. The program was terminated with the last eluting peak. Data collection was accomplished with a Hewlett-Packard 3396B Series II integrator. Helium was used as the carrier gas for all separations, with a flow-rate of approximately 10 ml/min. The dead (or void) time for the columns was measured with repetitive injections of hydrogen (150 μl). This large volume of hydrogen appeared to give a small peak before methane even with a flame ionization detector. Hamilton gas-tight syringes were used for all injections.

Stationary phases

Stationary phases were obtained from Advanced Separation Technologies (Whippany, NJ, USA). All separations were accomplished on 40-μm silica supports (preparative HPLC supports). The stationary phases were: Cyclobond I (CBI), Cyclobond I Acetylated (CBI AC), Cyclobond III (CBI-II), Cyclobond III Acetylated (CBIII AC), silica gel, silica gel containing the 6–10 atom epoxy-terminated linkage [35,36] used to bond cyclodextrin to silica gel (Epoxy) and β-cyclodextrin directly bonded to silica gel (contains a higher stationary phase loading than CBI) (HIGH). In the case of HIGH, there was no epoxy-terminated linkage chain. The modified β-cyclodextrin was directly attached to the silica via a "Si–O–C" linkage. All bonded stationary phases were made from the same base silica gel to which the epoxy-terminated linkage chain had been attached. The only exception to this, as noted above, was for "HIGH" which used the same silica gel, but no linkage chain. The acetylated stationary phases were made by taking a portion of the native cyclodextrin bonded phase and reacting them with acetic anhydride. Consequently the size, pore distribution and surface area of the different stationary phases were as close as experimentally feasible. Stationary phases were packed into 91 cm × 0.21 cm inner diameter (I.D.) stainless-steel tubing (Supelco, Bellefonte, PA, USA). All columns were dry packed, while tapping or vibrating the column to ensure tight packing. Approximately 1.5 g of stationary phase were packed into each column.

The stationary phases were activated at 280–300°C for several hours before testing commenced. Conditioning removes water and any residual solvent remaining from the cyclodextrin/epoxy bonding procedure. It was observed that better efficiency occurred after conditioning (Fig. 1).

Chemicals

Reagents were obtained from Aldrich (Milwaukee, WI, USA): 1,3-butadiene, 1-butene, *cis*-2-butene, cyclopentane, 2,2-dimethylbutane, 2,3-di-

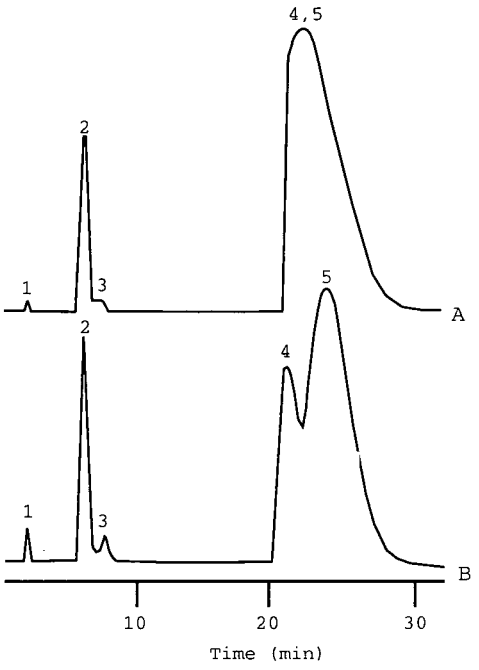

Fig. 1. Chromatogram of gas from a butane lighter. Column is 30 cm × 0.21 cm I.D. packed with 20-μm β-cyclodextrin stationary phase. (A) chromatogram prior to temperature conditioning; (B) same column conditioned at 300°C for several hours. Temperature is 50°C. Peaks: 1 = ethane; 2 = propane; 3 = propene; 4 = isobutane; 5 = butane.

methylbutane, 2,3-dimethylpentane, 2-methylpentane, 2-methylpropene (or isobutylene) and *trans*-2-butene; Matheson Gas (East Rutherford, NJ, USA): propylene; Phillips Petroleum (Bartlesville, OK, USA): 2,2-dimethylpropane; Scott Specialty Gases (Plumsteadville, PA, USA): (1000 ppm C_1–C_6 *n*-alkanes (can mix 236), 100 ppm C_2-C_6 olefins (can mix 222), 10 ppm C_2-C_4 alkynes (can mix 30), 10 ppm branched paraffins (can mix 2), 10 ppm, C_4 + isomers (can mix 55) and hydrogen (can 108). Liquids were sampled via headspace analysis, and gases were sampled directly from containers or gas sampling bulbs. Approximately 2 μl of headspace above liquids were injected into the gas chromatograph. Gas mixture injection volumes varied with the concentration of the blend. Successively lower amounts of the above alkane, olefin and alkyne mixtures were injected (until the detection limit was reached) to verify that there was no significant effect of concentration on retention at the analyte levels used in this study.

RESULTS AND DISCUSSION

Six GSC stationary phases, along with silica gel (for comparison), were evaluated in terms of retention and separation characteristics of light hydrocarbons. The stationary phases consisted of three native and two derivatized (acetylated) cyclodextrins in addition to silica gel covered with the epoxy terminated linkage chain but no cyclodextrin.

In general, native cyclodextrin columns produced longer retention times (larger capacity factors, k') than the analogous acetylated cyclodextrin columns, with the directly bonded β-cyclodextrin (HIGH) having the largest capacity factors. Every solute tested had a longer retention time on the directly bonded β-cylodextrin column than any other stationary phase. The data in Table I (k' values, arranged by stationary phase and by each component's boiling point) indicates that compounds are not always eluted in order of their boiling points. Table II lists three series of analytes composed of n-alkanes, 1-alkenes and 1-alkynes. Table II shows that for all columns, compounds in a family (*i.e.*, ethane, ethylene, acetylene) containing triple bonds are retained longer than those with double bonds, which, in turn are adsorbed more strongly than compounds with only single bonds (*i.e.*, the elution order for this series of compounds is the same when analyzed on either cyclodextrin or silica gel columns). The trend observed when comparing the data from the silica gel column to the cyclodextrin phases is the silica gel column had the smallest capacity factors for saturated compounds, but the k' between silica gel and the directly bonded β-cyclodextrin columns became similar as unsaturation was introduced into a compound series (*i.e.*, propane, propene and propyne). This is indicated in Table III (also Figs. 2 and 3) which lists the ratio of capacity factors between silica gel and directly bonded β-cyclodextrin stationary phases (HIGH) for a series of compounds. Figs. 2 and 3 plot the capacity factors of *n*-alkanes, 1-alkenes and 1-alkynes for the silica gel and directly bonded β-cyclodextin stationary phases. Figs. 2 and 3 show the capacity factors for three families of compounds. Fig. 4 gives a comparison of the *n*-alkane capacity

TABLE I

COMPARISON OF LIGHT HYDROCARBON CAPACITY FACTORS (k') BY STATIONARY PHASE AND BOILING POINT (°C)

Hydrocarbons	B.p. (°C)	k'						
		Silica	Epoxy[a]	CBIII[b]	CBIIIAC[c]	CBI[d]	HIGH[e]	CBIAC[f]
Hydrogen	−252.8	0.00	0.00	0.00	0.00	0.00	0.00	0.00
Methane	−161.4	0.69	0.70	0.85	0.83	0.85	0.92	0.76
Ethene	−103.7	7.03	5.20	5.90	5.33	6.12	8.33	4.68
Ethane	−88.6	3.87	4.12	5.37	5.13	5.43	6.42	4.67
Acetylene	−84.0	11.58	8.85	9.20	8.77	9.35	12.01	7.70
Propene	−47.7	15.28	12.96	14.27	13.28	14.47	17.25	12.37
Propane	−42.1	9.68	10.15	12.35	11.79	12.47	14.29	11.18
Propyne	−23.2	23.26	19.27	19.87	18.77	20.06	23.55	17.29
Isobutane	−11.7	14.99	15.45	17.91	17.37	18.10	20.15	16.56
Isobutylene	−6.9	21.86	19.11	20.65	19.85	20.86	24.14	18.68
Bútene	−6.3	20.78	18.47	20.65	19.85	20.86	23.47	18.68
1,3-Butadiene	−4.4	22.68	19.57	21.40	20.71	21.72	25.32	19.45
Butane	−0.5	15.90	16.46	19.02	18.25	19.23	21.55	17.55
trans-2-Butene	0.9	22.20	19.64	21.32	20.54	21.52	24.56	19.36
cis-2-Butene	3.7	22.20	19.64	21.32	20.54	21.52	24.56	19.36
1-Butyne	8.1	27.45	23.48	24.35	23.47	24.55	28.41	22.06
2,2-Dimethylpropane	9.5	19.29	19.59	22.05	21.60	22.24	24.28	20.69
2-Butyne	27.0	31.78	27.22	27.84	26.63	27.99	32.29	24.97
2-Methylbutane	27.9	20.61	21.18	23.85	23.25	24.10	26.62	22.32
1-Pentene	30.1	24.86	23.39	25.45	24.52	25.70	28.93	23.55
Pentane	36.1	21.23	21.87	24.59	23.76	24.87	27.56	22.98
Cyclopentane	49.3	21.34	22.15	24.89	24.47	25.07	27.09	23.69
2,2-Dimethylbutane	49.7	24.59	25.04	27.70	27.24	27.93	30.37	26.24
2,3-Dimethylbutane	58.0	25.06	25.65	28.45	27.89	28.73	31.44	27.02
2-Methylpentane	60.3	25.25	25.93	28.74	28.16	29.02	31.96	27.15
3-Methylpentane	63.3	25.25	25.93	28.74	28.16	29.02	31.96	27.15
Hexene	63.5	29.01	27.86	30.13	29.25	30.43	34.80	28.25
Hexane	69.0	25.79	26.55	29.40	28.58	29.72	32.94	27.75
2,3-Dimethylpentane	89.8	29.20	29.87	33.12	32.50	33.52	38.01	31.45

[a] Epoxy-terminated 6–10 atom linkage connecting cyclodextrin (CD) to silica gel.
[b] CBIII is native α-CD bonded to silica gel.
[c] CBIIIAC is acetylated α-CD bonded to silica gel.
[d] CBI is native β-CD bonded to silica gel.
[e] HIGH is a high-density surface coverage of β-CD directly bonded to silica gel (2–3 times more coverage than CBI).
[f] CBIAC is acetylated β-CD bonded to silica gel.

factors. Due to similar retention characteristics between the cyclodextrin and silica gel columns, it would appear that under these separation conditions, the underivatized cyclodextrin stationary phases tested can be considered polar (at least for unsaturated compounds).

A compound-by-compound comparison of stationary phases shows that alkanes are not as strongly retained on silica gel columns as on cyclodextrin stationary phases (Tables I and III). In fact, the retention of saturated compounds on the silica gel column was less than any other column tested. This retention behavior is in contrast to that for unsaturated analytes. When cyclodextrin is bonded to sil-

TABLE II

COMPARISON OF LIGHT HYDROCARBON CAPACITY FACTORS (k') BY FAMILY

See Table I or text for indications of phases.

Hydrocarbons	B.p. (°C)	k'						
		Silica	Epoxy	CBIII	CBIIIAC	CBI	HIGH	CBIAC
Ethane	−88.6	3.87	4.12	5.37	5.13	5.43	6.42	4.67
Ethene	−103.7	7.03	5.20	5.90	5.33	6.12	8.33	4.68
Acetylene	−84.0	11.58	8.85	9.20	8.77	9.35	12.01	7.70
Propane	−42.1	9.68	10.15	12.35	11.79	12.47	14.29	11.18
Propene	−47.7	15.28	12.96	14.27	13.28	14.47	17.25	12.37
Propyne	−23.2	23.26	19.27	19.87	18.77	20.06	23.55	17.29
Butane	−0.5	15.90	16.46	19.02	18.25	19.23	21.55	17.55
1-Butene	−6.3	20.48	18.56	20.29	19.31	20.51	23.47	18.38
1-Butyne	8.1	27.45	23.48	24.35	23.47	24.55	28.41	22.06

ica gel, the retention times of non-polar non-polarizable saturated hydrocarbons increase. When the cyclodextrin density on the surface of the silica gel is increased (as with the directly bonded β-cyclodextrin stationary phase), the retention times of these alkanes show a further increase. The interaction of alkanes with cyclodextrin must involve a non-polar portion of the stationary phase and that interaction very likely occurs in the cyclodextrin's cavity.

From the previously discussed results, it appears that there may be two different retention mechanisms for light hydrocarbons on cyclodextrin stationary phases in GSC. Clearly the retention of unsaturated compounds, particulary those with triple bonds, are nearly identical on the directly bonded β-cyclodextrin column (HIGH) and silica gel column. When the linkage chain and cyclodextrin are bonded to silica gel, the number of free silanol

TABLE III

RATIO OF CAPACITY FACTORS FOR COMPOUNDS CHROMATOGRAPHED ON DIRECTLY BONDED β-CD AND SILICA GEL STATIONARY PHASES

HIGH is a high-density surface coverage of β-CD directly bonded to silica gel (2–3 times more coverage than CBI).

Hydrocarbons	B.p. (°C)	$\frac{k'_{HIGH}}{k'_{silica\ gel}}$
Ethane	−88.6	1.66
Ethene	−103.7	1.18
Acetylene	−84.0	1.04
Propane	−42.1	1.48
Propene	−47.7	1.13
Propyne	−23.2	1.01
Butane	−0.5	1.36
1-Butene	−6.3	1.15
1-Butyne	8.1	1.04

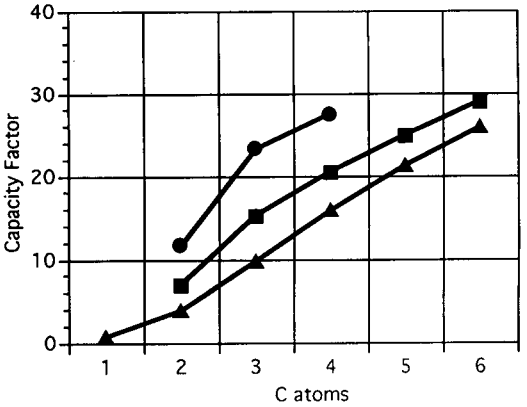

Fig. 2. Comparison of *n*-alkane (▲), 1-alkene (■) and 1-alkyne (●) capacity factors on a silica gel column by degree of unsaturation and number of carbon atoms in a compound. Temperature program: 30°C for 2 min, ramp at 7.5°C/min to 200°C. Column is 91 cm × 0.21 cm I.D. packed with 40-μm stationary phase.

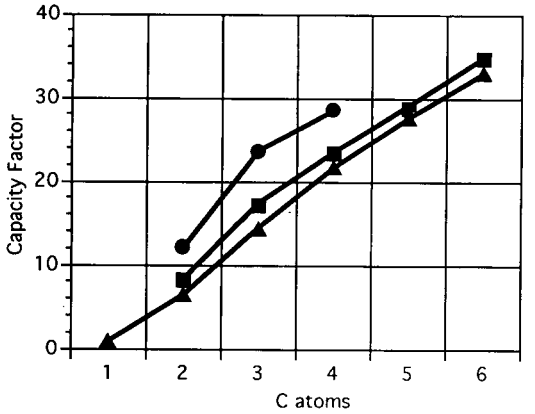

Fig. 3. Comparison of *n*-alkane (▲), 1-alkene (■) and 1-alkyne (●) capacity factors on a directly bonded β-cyclodextrin column by degree of unsaturation and number of carbon atoms in a compound. Temperature program: 30°C for 2 min, ramp at 7.5°C/min to 200°C. Column is 91 cm × 0.21 cm I.D. packed with 40-μm stationary phase.

groups is greatly reduced. Indeed, the stationary phase that retained unsaturated compounds the least was the one that had only the linkage chain attached to the silica gel (*i.e.*, "Epoxy" in Tables I and II). However, native cyclodextrins have a plethora of free hydroxyl groups. It is likely that the retention of unsaturated compounds on the native cyclodextrin phases is due to the cyclodextrin-hydroxyl groups, just as in the silica gel case, it is through the silanol groups. However, in the retention of saturated hydrocarbons, an option exists with the cyclodextrin phases that does not exist with silica gel. Retention in a relatively apolar cavity is the most likely explanation for the enhanced retention of saturated hydrocarbons on cyclodextrin stationary phases. No analogous retention mechanism exists on underivatized silica gel.

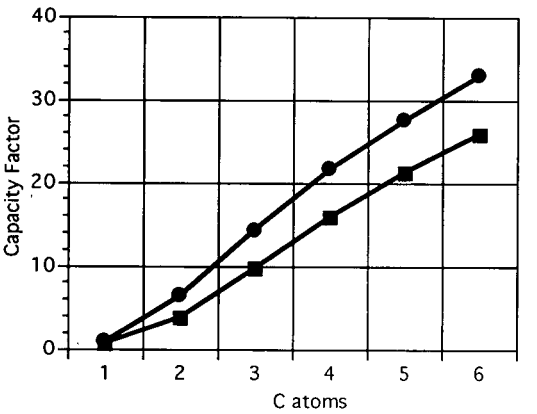

Fig. 4. Comparison of *n*-alkane capacity factors on directly bonded β-cyclodextrin (●) and silica gel (■) columns. Temperature program: 30°C for 2 min, ramp at 7.5°C/min to 200°C. Columns are 91 cm × 0.21 cm I.D. packed with 40-μm stationary phase.

Smolková *et al.* [30] reported the measurement of a wide range of sorbates from 50 to 80°C on α- and β-cyclodextrin. Two compounds, *n*-pentane and *n*-hexane are common to this study. Smolková *et al.* reported a 50–100 factor increase in the adjusted retention time of *n*-pentane on α-cyclodextrin over β-cyclodextrin. This was attributed to the tighter inclusion complex formed in α-cyclodextrin's cavity. Under the conditions of this study, there was little difference in retention times for compounds tested on α and β-cyclodextrin stationary phases. At the higher elution temperatures of this study, a tight inclusion complex may play a less dominant role in retention. Berthod *et al.* [31] reported a strong mechanistic temperature dependence in derivatized cyclodextrin liquid stationary phases. Indeed, the same compound could have different retention mechanisms at different temperatures, and these mechanisms are determined on a case-by-case basis.

Smolková-Keulemansová *et al.* [29] reported large differences in the retention times of isomers (branched versus straight chained compounds) on α-, but not β-cyclodextrin. This was attributed to the cavity size; the branched isomer was prohibited by size from entering α-cyclodextrin's cavity, and hence was less retained than the straight chain isomer, which could form an inclusion complex. In our studies, the elution order of branched and straight-chain aliphatic isomers occurred by boiling point. The elution order of these isomers on silica gel and non-polar stationary phases are also by boiling point. However, our studies were done at considerably higher temperatures and generally with smaller analytes. Despite these differences, we arrived at essentially the same conclusion as Smolková-Keulemansová *et al.* [29] for the saturated hydrocarbons, particularly at lower temperatures (*i.e.*, that inclusion complexation plays a significant role in retention).

In the present study, acetylating cyclodextrins re-

sulted in a decreased stationary phase polarity (by derivatizing hydroxyl groups) compared to native cyclodextrin. Compounds chromatographed on acetylated cyclodextrin stationary phases had shorter retention times than the same compound analyzed on the analogous native cyclodextrin phase. Table IV lists the capacity factor ratios for compounds analyzed on native and acetylated cyclodextrin stationary phases.

The bonding of the epoxy-terminated linkage to silica gel support could modify the support in two ways. First, the epoxy linkage should decrease the silica gel support's polarity (modification of a polar surface with a less polar appendage). For saturated hydrocarbons, the elution time is slightly higher on the epoxy column than on the silica gel support, but the retention times are still smaller than those obtained on any cyclodextrin stationary phase. If one assumes that alkanes are retained more on non-polar phases and less on polar stationary phases, under these experimental conditions, then the epoxy phase would appear to have a polarity between that of the silica gel and the cyclodextrin-bonded stationary phases.

Bonding cyclodextrin to the polar silica gel support modifies the silica gel's surface polarity. This modification of the surface polarity changes adsorption behavior. The phenomenon of differing adsorption between cyclodextrins and silica gel leads to gas mixtures separable on cyclodextrin but not on silica gel. Fig. 5 shows chromatograms obtained on the directly bonded β-cyclodextrin and silica gel stationary phases. The directly bonded β-cyclodextrin phase separates C_1–C_6 *n*-alkanes

TABLE IV

RATIO OF CAPACITY FACTORS FOR COMPOUNDS CHROMATOGRAPHED ON NATIVE AND ACETYLATED CYCLODEXTRIN STATIONARY PHASES

See Table I or text for indications of phases.

Hydrocarbons	$\frac{k'_{\alpha\text{-CD}}}{k'_{\text{AC-}\alpha\text{-CD}}}$	$\frac{k'_{\beta\text{-CD}}}{k'_{\text{AC-}\beta\text{-CD}}}$
Methane	1.02	1.12
Ethane	1.05	1.16
Propane	1.05	1.12
Butane	1.04	1.10
Pentane	1.03	1.08
Hexane	1.03	1.07
Ethylene	1.11	1.31
Propylene	1.07	1.17
1-Butene	1.05	1.12
1-Pentene	1.04	1.09
1-Hexene	1.03	1.08
Acetylene	1.05	1.21
Propyne	1.06	1.16
1-Butyne	1.04	1.11
2-Butyne	1.05	1.12
2,2-Dimethylpropane	1.02	1.08
2-Methylbutane	1.03	1.08
2,2-Dimethylbutane	1.02	1.06
2-Methylpentane	1.02	1.07
3-Methylpentane	1.02	1.07
Isobutane	1.03	1.10
Isobutylene	1.04	1.12
trans-2-Butene	1.04	1.11
cis-2-Butene	1.04	1.11
1,3-Butadiene	1.03	1.12
Cyclopentane	1.02	1.06
2,3-Dimethylbutane	1.02	1.06
2,3-Dimethylpentane	1.02	1.07

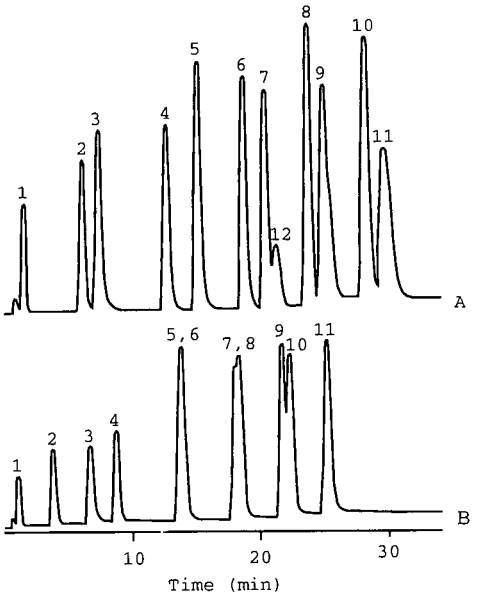

Fig. 5. Chromatogram of C_1–C_6 *n*-alkanes and C_2–C_6 1-alkenes. Temperature program: 30°C for 2 min, ramp at 7.5°C/min to 200°C. Columns are 91 cm × 0.21 cm I.D. packed with 40-μm stationary phase. (A) With the directly bonded β-cyclodextrin stationary phase; (B) with a silica gel stationary phase. Peaks: 1 = methane; 2 = ethane; 3 = ethene; 4 = propane; 5 = propene; 6 = butane; 7 = butene; 8 = pentane; 9 = pentene; 10 = hexane; 11 = hexene; 12 = impurity.

from C_2–C_6 1-alkenes but an analogous silica gel column does not completely resolve all peaks.

Cyclodextrin bonded to silica gel allows for different adsorption behaviors in regard to light hydrocarbons. A dual retention mechanism seems to be a factor in the separation of these compounds. Alkanes appear to be retained through an interaction with the apolar cavity, while unsaturated molecules can interact with the cavity and/or through the hydroxyl groups on the top and bottom of the cyclodextrin molecules. Separation of geometric isomers is inadequate at the high temperature and conditions of this study. However, these compounds are effectively resolved by GLC on the derivatized cyclodextrin phases [27]. New approaches are being tested to improve the generality and selectivity of the cyclodextrin columns for the GSC separation of other volatile compounds and gases.

ACKNOWLEDGEMENT

Support of this work by the Department of Energy, Office of Basic Science (DE FG02 88ER13819) is gratefully acknowledged.

REFERENCES

1 C. F. Poole and S. A. Schuette, *Contemporary Practice of Chromatography*, Elsevier, Amsterdam, New York, 1984, p. 72.
2 A. B. Littlewood, *Gas Chromatography —Principles, Techniques, and Applications*, Academic Press, New York, 1970, p. 429.
3 L. S. Ettre and J. E. Purcell, *Adv. Chromatogr.*, 10 (1974) 1.
4 R. G. Mathews, J. Torres and R. D. Schwartz, *J. Chromatogr.*, 199 (1980) 97.
5 W. Schneider, J. C. Frohne and H. Bruderreck, *J. Chromatogr.*, 155 (1978) 311.
6 N. Brenner and V. J. Coates, *Nature*, 181 (1958) 1401.
7 B. T. Whitman, *Nature*, 182 (1958) 391.
8 S. A. Greene, M. L. Moberg and E. M. Wilson, *Anal. Chem.*, 28 (1956) 1369.
9 S. A. Greene and H. Pust, *Anal. Chem.*, 29 (1957) 1055.
10 H. N. Morrow and K. B. Buckley, *Petrol. Refiner.*, 36 (1957) 157.
11 J. J. Kirkland, *Anal. Chem.*, 35 (1963) 129.
12 O. L. Hollis, A. Zlatkis and L. S. Ettre (Editors), *Advances in Gas Chromatography 1965*, Preston Technical Abstracts, Evanston, IL, 1966, p. 56.
13 O. L. Hollis, *Anal. Chem.*, 38 (1966) 309.
14 O. L. Hollis and W. V. Hayes, *J. Gas Chromatogr.*, 4 (1966) 235.
15 W. F. Wilhite and O. L. Hollis, *J. Gas Chromatogr.*, 6 (1968) 84.
16 C. N. Jones, *Anal. Chem.*, 39 (1967) 1858.
17 H. W. Patton, J. S. Lewis and W. I. Kaye, *Anal. Chem.*, 27 (1955) 170.
18 S. Ohksoshi, Y. Fujita, and T. Kwan, *Shokubai*, 15 (1958) 1.
19 N. H. Ray, *J. Appl. Chem.*, 4 (1954) 21.
20 O. K. Guja and J. Janák, *J. Chromatogr.*, 68 (1972) 325.
21 V. S. Nayak and R. N. Pandey, *J. Chromatogr. Sci.*, 28 (1990) 617.
22 W. Szczepaniak, J. Nawrocki and W. Wasiak, *Chromatographia*, 12 (1979) 559.
23 A. B. Littlewood, *Gas Chromatography —Principles, Techniques, and Applications*, Academic Press, New York, 1970, p. 431.
24 E. Smolková-Keulemansová, *J. Chromatogr.*, 251 (1982) 17.
25 W. Y. Li, H. L. Jin and D. W. Armstrong, *J. Chromatogr.*, 509 (1990) 303.
26 V. Schuring and H. P. Nowotny, *J. Chromatogr.*, 441 (1988) 155.
27 D. W. Armstrong, W. Li, C. D. Chang and J. Pitha, *Anal. Chem.*, 62 (1990) 914.
28 W. A. Konig, R. Krebber and P. Mischnick, *J. High Resolut. Chromatogr.*, 12 (1989) 732.
29 E. Smolková-Keulemansová, L. Feltl and S. Krýsl, *J. Inclusion Phenomena*, 3 (1985) 183.
30 R. Smolková, H. Králová, S. Krýsl and L. Feltl, *J. Chromatogr.*, 241 (1982) 3.
31 A. Berthod, W. Li and D. W. Armstrong, *Anal. Chem.*, 64 (1992) 873.
32 J. Szejtli, *Cyclodextrin Technology*, Kluwer, Dordrecht, Boston, MA, 1988, p. 418.
33 F. Cramer and F. M. Henglein, *Angew. Chem.*, 68 (1956) 649.
34 F. Cramer and F. M. Henglein, *Chem Ber.*, 90 (1957) 2572.
35 D. W. Armstrong, *US Pat.*, 4 359 399 (1985).
36 D. W. Armstrong and W. Demond, *J. Chromatogr. Sci.*, 22 (1984) 411.

Journal of Chromatography, 633 (1993) 143–149
Elsevier Science Publishers B.V., Amsterdam

CHROM. 24 770

Cyclodextrin stationary phases for the gas–solid chromatographic separation of inorganic gases

G. L. Reid, III, W. T. Wall and D. W. Armstrong*

Department of Chemistry, University of Missouri, Rolla, MO 65401 (USA)

(First received August 18th, 1992; revised manuscript received October 29th, 1992)

ABSTRACT

Cyclodextrins linked to silica gel are used as gas–solid chromatographic stationary phases. They provide an effective means for separating a wide variety of gases. Evaluation of different cyclodextrin columns and the analogous silica gel support column with inorganic gas standards is reported. Separation selectivities and efficiencies differ between silica gel and the cyclodextrin phases. Capacity factors and chromatograms are presented for these gas–solid chromatographic stationary phases. The native cyclodextrin stationary phases appear to retain gases via at least two different retention mechanisms.

INTRODUCTION

Gas-solid chromatography (GSC) is a technique used for the separation of gases and compounds with low boiling points. Packed columns, and more recently, porous-layer open-tubular (PLOT) or support-coated open-tubular (SCOT) [1–3] columns are preferred for the separation of these highly volatile materials. Many GSC stationary phases, including molecular sieves [4–6], alumina [7], silica gel [8,9], porous polymers [10] and charcoal [11,12] have been cited as separating inorganic gases. For the separation of argon, oxygen and nitrogen, molecular sieves [13–15] and porous polymers [16,17] are widely used. Several review articles have summarized the separation of inorganic gases on many different stationary phases [18–21]. Generally, gas–liquid chromatographic (GLC) stationary phases have limited applicability in the analysis of compounds such as H_2, O_2, N_2, CO and Ar due to the low solubility of these gases in liquid phases [19].

One of the problems associated with the analysis of a wide range of gases is the non-universality of columns. A column that is ideal for one separation may be completely useless for another (*e.g.* molecular sieves easily separate oxygen, nitrogen and argon, but irreversibly retain carbon diodixe and water [21]). The usual solution to this problem is to use several different types of columns.

The cyclodextrin molecule has been reported to be able to form stable complexes with gases. Inclusion complexes of α-cyclodextrin with oxygen and carbon dioxide are formed when the gases are held at high pressure for several days over an aqueous solution of cyclodextrin. The cyclodextrin–guest crystalline complexes are stable for long periods of time. α-Cyclodextrin complexes 0.3 mol of oxygen and 1.4 mol of carbon dioxide per mole of cyclodextrin [22]. Carbon monoxide, unlike carbon dioxide, does not form an inclusion complex with α-cyclodextrin. Similarly, lower noble gases (helium, neon and argon) do not form inclusion complexes with α-cyclodextrin, whereas the larger members of the group (krypton and xenon) do when under high pressure [23]. GSC separation of a wide range of low-molecular-mass (C_1–C_7) hydrocarbons using cyclodextrin-bonded phases recently has been reported [24].

Cyclodextrins previously have been used as coat-

* Corresponding author.

0021-9673/93/$06.00

ings for chromatographic stationary phases [25]. Presently, many researchers are reporting the use of amorphous derivatized cyclodextrins as GLC chiral stationary phases [26–30].

Cyclodextrins are cyclic oligosaccharides composed of D(+)-glucopyranose units which are linked by α-(1,4) bonds. The cyclized glucopyranose units form conical structures, with secondary hydroxyls (12 for α-CD) surrounding the wider end and the primary hydroxyls (6 for α-CD) on the opposite end. The top and bottom of the structure are polar, due to the hydroxyl groups, while the interior of the cavity is non-polar. α-, β- and γ-cyclodextrins are differentiated by the number of glucopyranose subunits (6, 7 and 8, respectively) in the structure. The internal diameter of α and β-cyclodextrin's cavity are 4.5 and 7 Å, respectively, and molecules of suitable size can form inclusion complexes. Many recent mechanistic studies involving chromatographic separations on cyclodextrin and derivatized cyclodextrin stationary phases have cited multiple retention mechanisms [24,31–33]. Depending on the chromatographic conditions and the nature of the analyte, either inclusion complexation or external adsorption with the cyclodextrin moiety can contribute to retention and separation.

EXPERIMENTAL

Instrumentation

A Hewlett-Packard (Avondale, PA, USA) 5890 Series II gas chromatograph equipped with a packed column injection port, thermal conductivity detector, and a liquid nitrogen cryogenic coolant system was utilized in this study. The injector and detector were set at 200°C. The oven temperature program, unless otherwise noted, was 30°C for 1 min, then increasing at 10°C/min to 180°C. The temperature was held at 180°C until the last component eluted (which was determined from prior experiments). Data collection was accomplished with a Hewlett-Packard 3396B Series II integrator. Helium was used as the carrier gas for all separations, with a flow-rate of approximately 20 ml/min. The void time for all columns was measured with repetitive injections of (150 μl) hydrogen. The void time is the time required for an unretained component to elute. Hamilton gas-tight syringes were used for all injections.

Stationary phases

Stationary phases were obtained from Advanced Separation Technologies (Whippany, NJ, USA). All separations were accomplished on 40-μm silica supports (preparative HPLC supports). The stationary phases were: Cyclobond II (CBI), Cyclobond I Acetylated (CBI AC), Cyclobond III (CBI-II), Cyclobond III Acetylated (CBIII AC), silica gel, silica gel containing the 6–10 atom epoxy-terminated linkage [34,35] used to bond cyclodextrin to silica gel (Epoxy) and β-cyclodextrin directly bonded to silica gel (HIGH) which contains a higher stationary phase loading than CBI. Cyclobond I (CBI) is the β-cyclodextrin-bonded phase and Cyclobond III (CBIII) is the α-cyclodextrin-bonded phase. Stationary phases were packed into 91 cm × 2.1 mm I.D. stainless-steel tubing (Supelco, Bellefonte, PA, USA). All columns were prepared by dry packing, using tapping or vibrating to ensure a compact bed. Approximately 1.5 g of stationary phase were loaded into each 3-ft. column. The columns were activated at 280–300°C for several hours before use commenced. Conditioning removes water and any residual solvent remaining from the cyclodextrin/epoxy bonding procedure. As long as there is no oxygen in the flow stream the cyclodextrin stationary phases appear to be stable at high temperatures.

Chemicals

Gases were obtained from LIF-O-GEN (Cambridge, MD, USA): oxygen; MG Industries (Valley Forge, PA, USA): ethylene oxide and nitrogen dioxide; Scott Specialty Gases (Plumsteadville, PA, USA): carbon dioxide, carbon monoxide, carbonyl sulfide, hydrogen, hydrogen sulfide, nitrous oxide, sulfur dioxide and sulfur hexafluoride; Spectra Gases (Newark, NJ, USA): krypton and neon. Gases were sampled directly from cylinders or from gas sampling bulbs. Approximately 2–5 μl of gas were injected into the gas chromatograph.

RESULTS AND DISCUSSION

Six cyclodextrin GSC stationary phases, along with the silica gel support for comparison, were evaluated in terms of retention and separation characteristics of selected inorganic gases. Several "families" (*i.e.*, noble, nitrogen containing, sulfur based, etc.) of gases were chosen in order to evaluate the

TABLE I

COMPARISON OF INORGANIC GAS CAPACITY FACTORS (k') BY STATIONARY PHASE AND ELUTION ORDER ON SILICA GEL

Gases	k'						
	Silica	Epoxy[a]	CBIII[b]	CBIIIAC[c]	CBI[d]	HIGH[e]	CBIAC[f]
Hydrogen	0.00	0.00	0.00	0.00	0.00	0.00	0.00
Nitrogen	0.32	0.27	0.30	0.27	0.38	0.43	0.27
Carbon monoxide	0.49	0.36	0.39	0.38	0.48	0.64	0.39
Krypton	0.69	0.76	0.94	0.94	1.13	1.42	0.82
Nitrogen dioxide[g]	1.12	0.95	0.89	0.98	1.01	1.00[i]	0.82
Sulfur hexafluoride	3.81	3.28	4.42	4.23	5.01	7.89	3.80
Nitrous oxide	5.70	4.77	5.07	4.75	5.58	6.95	4.41
Carbon dioxide	6.32	4.94	5.01	4.69	5.47	7.03	4.40
Carbonyl sulfide	8.67	7.66	9.20	8.74	10.04	12.28	8.25
Ethylene oxide	9.86	9.55	11.58	11.19	12.71	16.46	10.95
Hydrogen sulfide	10.44	8.23	8.97	8.44	9.64	12.17	8.19
Sulfur dioxide	21.55[h]	16.87	16.21	15.84	16.79	19.29	15.92

[a] Epoxy-terminated 6–10 atom linkage connecting cyclodextrin (CD) to silica gel.
[b] CBIII is native α-CD bonded to silica gel.
[c] CBIIIAC is acetylated α-CD bonded to silica gel.
[d] CBI is native β-CD bonded to silica gel.
[e] HIGH is a high-density surface coverage β-CD on silica gel (2–3 times more coverage than CBI).
[f] CBIAC is acetylated β-CD directly bonded to silica gel.
[g] Chromatographed isothermally at 135°C.
[h] Elution occured only when final temperature of temperature program was 200°C.
[i] The first of two peaks past the air peak was used as the NO_2 peak.

TABLE II

RATIO OF INORGANIC GAS CAPACITY FACTORS OBTAINED ON CYCLODEXTRIN STATIONARY PHASES *VERSUS* SILICA GEL

See Table I or text for indications of phases.

Inorganic gases	$\frac{k'_{Epoxy}}{k'_{Silica}}$	$\frac{k'_{CBIII}}{k'_{Silica}}$	$\frac{k'_{CBIIIAC}}{k'_{Silica}}$	$\frac{k'_{CBI}}{k'_{Silica}}$	$\frac{k'_{HIGH}}{k'_{Silica}}$	$\frac{k'_{CBIAC}}{k'_{Silica}}$
Nitrogen	0.84	0.93	0.86	1.19	1.35	0.84
Carbon monoxide	0.74	0.79	0.77	0.99	1.31	0.79
Krypton	1.09	1.35	1.35	1.63	2.05	1.18
Nitrogen dioxide	0.85	0.79	0.87	0.90	0.89	0.73
Sulfur hexafluoride	0.86	1.16	1.11	1.32	2.07	1.00
Nitrous oxide	0.84	0.89	0.83	0.98	1.22	0.77
Carbon dioxide	0.78	0.79	0.74	0.87	1.11	0.70
Carbonyl sulfide	0.88	1.06	1.01	1.16	1.42	0.95
Ethylene oxide	0.97	1.17	1.14	1.29	1.67	1.11
Hydrogen sulfide	0.79	0.86	0.81	0.92	1.17	0.78
Sulfur dioxide	0.78	0.75	0.74	0.78	0.90	0.74

overall applicability of these stationary phases. Table I lists the gases used in this investigation. Capacity factors (k') for the compounds are listed by stationary phase and by the elution order on silica gel. This table shows that the gases chromatographed in this study were all more strongly adsorbed on β-cyclodextrin (CBI) than α-cyclodextrin (CBIII), with the high-surface-density β-cyclodextrin (HIGH) giving the greatest retention (of the cyclodextrin phases). Native cyclodextrin stationary phases retained the gases more than the corresponding acetylated cyclodextrin stationary phase. The epoxy silanized silica gel generally showed the least retention for the analytes in this study.

Table II lists the capacity factor ratios of the gases analyzed on the epoxy and cyclodextrin column *versus* the silica gel column. Values less than one indicate that the chromatographed compound had a longer retention time on the silica gel column, while values greater than one indicate that the analyte gases were more strongly retained on the cyclodextrin-derivatized silica gel.

In general, the silica gel column showed greater retention for the more polar gases and those with multiple bonds (*e.g.*, inorganic oxides). All cyclodextrin-based columns tended to retain the non-polar, symmetrical gases or those with only single bonds (*e.g.*, sulfur hexafluoride, krypton, ethylene oxide) to a greater extent. Clearly, the native cyclodextrin stationary phases were significantly different from their peracetyl-derivatized analogues. This is particularly evident for the high-coverage, directly bonded stationary phase (*i.e.*, HIGH). These stationary phases seemed to retain polar gases and with multiple bonds as much (or more in some cases) as silica gel. However, unlike silica gel, cyclodextrins also retained the less polar molecules. Most likely, the explanation for this lies with cyclodextrins' ability to retain molecules via at least two different mechanisms [24]. Analytes such as krypton and ethylene oxide tend to form inclusion complexes with cyclodextrin under these experimental conditions, while the more polar oxides tend to be retained by surface adsorption to the hydroxyl group (as in silica gel).

Often there are selectivity differences between silica gel and cyclodextrin based stationary phases. For example, cyclodextrin phases retain ethylene oxide considerably more than hydrogen sulfide, while the opposite elution order was found for silica gel. Table III shows that the separation factor for ethylene oxide and hydrogen sulfide is 0.94 on silica gel, which increases on the epoxy column to 1.16, and stabilizes between 1.29 (CBI) and 1.35 (directly bonded β-cyclodextrin, HIGH) on the cyclodextrin columns. To a much smaller extent, nitrous oxide is eluted slightly later than carbon dioxide on cyclodextrin phases, while again, the opposite elution order occurs with silica gel.

Variations in the size of separation factors between classes of columns (silica gel, epoxy and cyclodextrins) also are observed. The separation factor (α) for carbonyl sulfide and carbon dioxide on silica gel is 1.37, which increases to 1.55 on the epoxy column and fluctuates between 1.75 on the directly bonded β-cyclodextrin (HIGH) column

TABLE III

RATIO OF INORGANIC GAS SEPARATION FACTORS ARRANGED BY STATIONARY PHASE

Stationary phase[a]	$\frac{k'_{\text{Ethylene oxide}}}{k'_{\text{Hydrogen sulfide}}}$	$\frac{k'_{\text{Carbonyl sulfide}}}{k'_{\text{Carbon dioxide}}}$	$\frac{k'_{\text{Carbon dioxide}}}{k'_{\text{Nitrous oxide}}}$
Silica gel	0.94	1.37	1.11
Epoxy	1.16	1.55	1.03
CBI	1.29	1.84	0.99
CBI AC	1.33	1.86	0.99
CBIII	1.32	1.84	0.98
HIGH	1.35	1.75	0.99
CBIII AC	1.34	1.87	1.00

[a] See Table I or text for indication of phases.

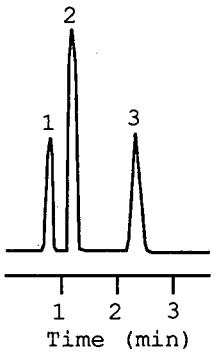

Fig. 1. Isothermal GSC separation of a three-component noble gas mixture at 25°C on the directly bonded β-cyclodextrin (HIGH) stationary phase. Peaks: 1 = neon; 2 = argon; 3 = krypton.

and 1.87 on the acetylated α-cyclodextrin column (CBIII AC) (Table III). The acetylated cyclodextrins, while having smaller capacity factors, effectively retain the same separation factors (α) as the native cyclodextrins for many of the compounds in this study.

Fig. 1. shows the selectivity of the directly bonded β-cyclodextrin column (HIGH) for the noble gases. Neon, argon and krypton are all more than baseline resolved at 25°C and in under 3 min. Fig. 2 displays the separation of hydrogen, nitrogen, carbon monoxide and ethylene oxide on directly bonded β-cyclodextrin at three different initial temperatures of 20, 0 and −20°C. The first peak, hydrogen, produces a negative signal since it has a higher

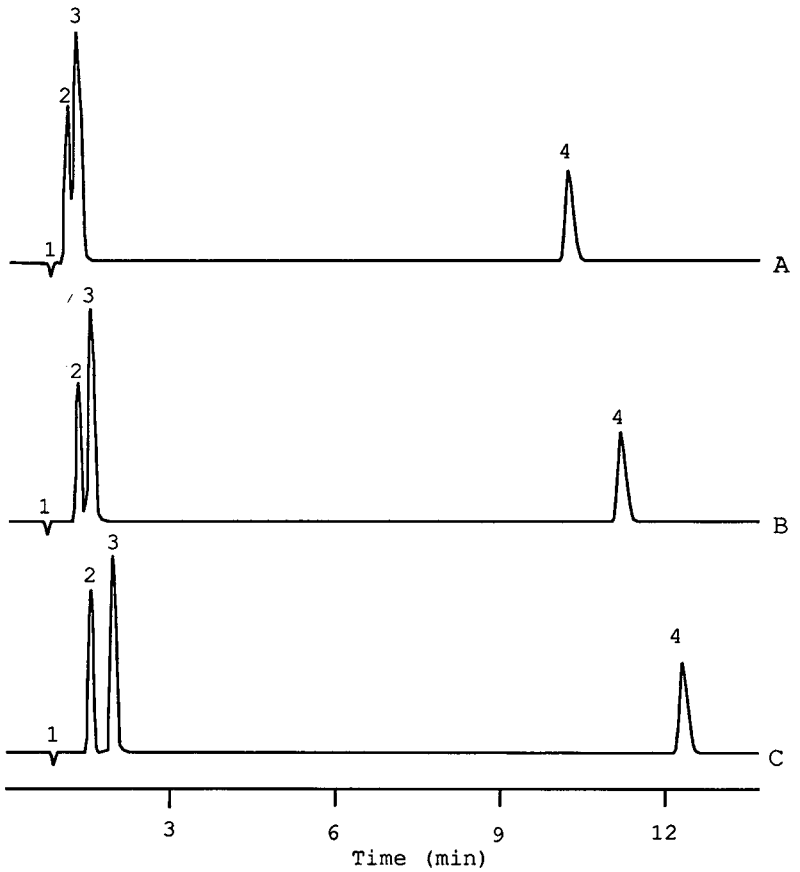

Fig. 2. GSC of a four-component gas mixture on directly bonded β-cyclodextrin. (A) initial temperature 20°C; (B) initial temperature 0°C; (C) initial temperature −20°C. The temperature program was: initial temperature for 2 min and ramp at 10°C/min until ethylene oxide eluted. Peaks: 1 = hydrogen (negative peak); 2 = nitrogen; 3 = carbon monoxide; 4 = ethylene oxide.

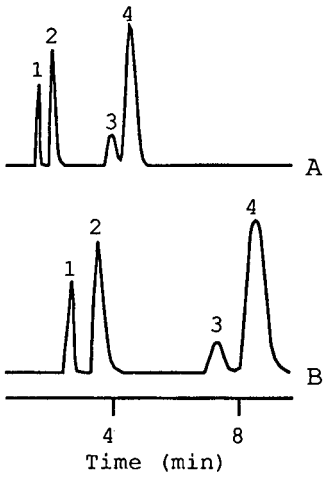

Fig. 3. Isothermal GSC separation of a four-component gas mixture on directly bonded β-cyclodextrin stationary phase. (A) −30°C; (B) −50°C. Peaks: 1 = nitrogen; 2 = carbon monoxide; 3 = methane; 4 = krypton.

thermal conductivity than the helium carrier gas. This separation is commercially important and currently requires two separate columns [36]. Fig. 3 presents the isothermal separation of nitrogen, carbon monoxide, methane and krypton (elution order) at temperatures of −30 and −50°C. These separations can be achieved closer to or at room temperature with the use of a longer column. The elution order of krypton and methane on a molecular sieve 5A column is the opposite of that obtained on the directly bonded β-cyclodextrin phase [18].

Fig. 4B shows an unusual chromatogram obtained for nitrogen dioxide when analyzed on the directly bonded β-cyclodextrin column, compared with the same compound chromatographed on silica gel (Fig. 4A) or any other column used in this study. Why this particular column produces two overlapping peaks for nitrogen dioxide while all other columns produce a single peak is unknown. Rechromatographing either peak from the HIGH column on a silica gel column gives a single nitrogen dioxide peak. It appears that the peak overlapping with nitrogen dioxide may be dinitrogen tetraoxide. However, we have no good explanation as yet for its appearance under these particular conditions.

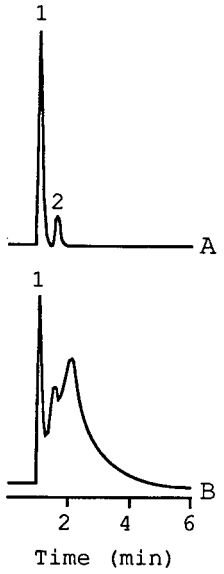

Fig. 4. Isothermal (135°C) GSC separation of nitrogen dioxide. (A) On silica gel; (B) on the directly bonded β-cyclodextrin stationary phase (HIGH). Note that the two overlapping peaks are obtained for nitrogen dioxide only on HIGH. Peaks: 1 = nitrogen; 2 = nitrogen dioxide.

Cyclodextrin bonded to a silica gel support and used as a GSC stationary phases is shown to be useful in the separation of many inorganic gases. Unique selectivities for some compounds have been observed. The selectivity differences between silica gel and the cyclodextrin phases can be attributed partially to modified support polarity. In addition, the native cyclodextrin moiety allows for both polar interactions with the hydroxyl groups and non-polar interactions with the cavities. Continued research on cyclodextrins as GSC stationary phases will very likely provide a more selective and widely useful column for the separation of gases and volatile compounds. We are now attempting to perfect an equivalent open-tubular capillary column for these separations.

ACKNOWLEDGEMENT

Support for this work by the Department of Energy, Office of Basic Sciences (Grant DE FG02 99ER13819) is gratefully acknowledged.

REFERENCES

1 L. S. Ettre and J. E. Purcell, *Adv. Chromatogr.*, 10 (1974) 1.
2 R. G. Mathews, J. Torres and R. D. Schwartz, *J. Chromatogr.*, 199 (1980) 97.

3 W. Schneider, J. C. Frohne and H. Bruderreck, *J. Chromatogr.*, 155 (1978) 311.
4 R. Berry, in M. Van Swaay (Editor), *Gas Chromatography 1962*, Butterworths, London, 1963, pp. 321–334.
5 R. Aubeau, L. Champeix and J. Reiss, *J. Chromatogr.*, 6 (1961) 209.
6 J. E. Purcell, *Nature*, 201 (1964) 1321.
7 J. King and S. W. Benson, *Anal. Chem.*, 38 (1966) 261.
8 S. A. Greene, *Anal. Chem.*, 31 (1959) 480.
9 J. N. Murray and J. B. Doe, *Anal. Chem.*, 37 (1965) 941.
10 O. L. Hollis, *Anal. Chem.*, 38 (1966) 309.
11 J. Janák, *Collect. Czech. Chem. Comm.*, 19 (1954) 917.
12 D. H. Smith and E. Clark, *Proc. Soil Science Soc. Am.*, 24 (1960) 111.
13 E. I. Obermiller and R. W. Freedman, *J. Gas Chromatogr.*, 3 (1965) 242.
14 B. D. Gunter and B. C. Musgrave, *J. Gas Chromatogr.*, 4 (1966) 162.
15 G. W. Heylmun, *J. Gas Chromatogr.*, 3 (1965) 82.
16 O. L. Hollis, *Anal. Chem.*, 38 (1966) 309.
17 G. E. Pollock, *J. Chromatogr. Sci.*, 24 (1986) 173.
18 J. C. MacDonald, *Inorganic Chromatographic Analysis*, Wiley, New York, 1985, pp. 233–238.
19 G. Guiochon and C. Pommier, *Gas Chromatography in Inorganics and Organometallics*, Ann Arbor Sci. Publ., Ann Arbor, MI, 1973, pp. 79–115.
20 A. B. Littlewood, *Gas Chromatography —Principles, Techniques and Applications*, Academic Press, New York, 1970, pp. 420–429.
21 R. S. Juvet, Jr. and F. Zado, in J. C. Giddings and R. A. Keller (Editors), *Adv. Chromatogr.*, 1 (1965) 250–278.
22 W. Lautsch, H. Rauhut, W. Grimm and W. Broser, *Z. Naturforsch.*, 126 (1957) 307.
23 F. Cramer and F. M. Henglein, *Chem. Ber.*, 90 (1957) 2572.
24 G. L. Reid, III, C. A. Monge, W. T. Wall and D. W. Armstrong, *J. Chromatogr.*, 633 (1993) 135.
25 E. Smolková-Keulemansová, *J. Chromatogr.*, 251 (1982) 17.
26 W. Y. Li, H. L Jin and D. W. Armstrong, *J. Chromatogr.*, 509 (1990) 303.
27 D. W. Armstrong, W. Li, A. M. Stalcup, J. I. Seeman, H. V. Secor and R. R. Izac, *Anal. Chim. Acta.*, 234 (1990) 365.
28 D. W. Armstrong, W. Li, C. D. Chang and J. Pitha, *Anal. Chem.*, 62 (1990) 914.
29 W. A. Konig, R. Krebber and P. Mischnick, *J. High Resolut. Chromatogr.*, 12 (1989) 732.
30 V. Schurig and H. P. Nowotny, *J. Chromatogr.*, 509 (1990) 303.
31 E. Smolková-Keulemansová, L. Feltl and S. Krýsl, *J. Inclusion Phenomena*, 3 (1985) 183.
32 E. Smolková, H. Králová, S. Krýsl and L. Feltl, *J. Chromatogr.*, 241 (1982) 3.
33 A. Berthod, W. Li and D. W. Armstrong, *Anal. Chem.*, 64 (1992) 873.
34 D. W. Armstrong, *US Pat.*, 4 359 399 (1985).
35 D. W. Armstrong and W. Demond, *J. Chromatogr. Sci.*, 22 (1984) 411.
36 Larry A. Spino, Shell Oil Company, personal communication.

Journal of Chromatography, 633 (1993) 151–162
Elsevier Science Publishers B.V., Amsterdam

CHROM. 24 790

Spectrum, multi-element selectivity and elemental response of a linear sulfur emitter in flame photometry☆

Walter A. Aue* and Xun-Yun Sun

Department of Chemistry, Dalhousie University, Halifax, Nova Scotia B3H 4J3 (Canada)

(First received August 14th, 1992; revised manuscript received November 24th, 1992)

ABSTRACT

Although the luminescence from sulfur compounds in the flame photometric detector (FPD) is dominated by the S_2 main-system bands (of about quadratic response), it contains as well a *linear* emitter whose "spectrum" could be recorded in the 600 to 850 nm region. In this region sulfur chemiluminescence is a first-order process and varies, if at all, by a factor of less than two in elemental response (sulfur equivalency) among several structurally diverse compounds. The single-channel selectivity of linear sulfur against other FPD-active elements —B, C and H, Sn, Pb, N, P, As, Se, Cr, Mn, Fe, Ru and Os— was measured for a band at *ca.* 750 nm (as well as for a wider 600 to 850 nm range), and was compared with the selectivity of S_2 for its commonly monitored band at 394 nm (as well as for the total 300–850 nm photomultiplier range). The IUPAC detection limit ($S/\sigma = 3$) of linear sulfur is $2 \cdot 10^{-13}$ mol S/s and its linear range spans four orders of magnitude. Overall, the new linear mode seems preferable to the conventional quadratic one; and it appears competitive with other methodologies of organosulfur detection. A speculative discussion of inter-element selectivity, mainly as it relates to spectral features, is appended, at the reviewer's request.

INTRODUCTION

During a study of response ratios in a dual-channel flame photometric detector (FPD) we chanced upon a linear sulfur emitter [1]. Since it attracted some interest, a more detailed assessment of its spectral and analytical properties appears warranted.

Such an assessment poses a few experimental questions: What is the spectrum of the linear emission? Can it be attributed to one or more of the many known sulfur systems? And —given that the search for the linear spectrum is successful— can that knowledge be used to improve selectivity *vis-à-vis* other elements that luminesce in the FPD? Indeed, what are the interelemental selectivities at some well-chosen and typical conditions? How do they compare with similar selectivities for S_2? Do structurally different compounds produce *different* responses per gram of sulfur? If so, how large is the effect in the linear as compared to the conventional (quadratic) mode? Finally, when most of the above questions have been answered, which analytical mode is likely to emerge as the "better" one for the flame photometry of sulfur compounds? And if that is to be the linear mode, how would it compare with other methods of linear sulfur detection in chromatographic effluents?

The first question —as any first question about a newly recognized emitter— must obviously be directed at its spectrum and, subsequently, its chemical nature. Two aspects make the quest for the linear sulfur spectrum particularly difficult.

On one hand —and common to all elements responding in the FPD— the spectrum of the emitter has to be determined under typical operating conditions. Otherwise, analytical relevance may be lost [2,3]. That means making do with the low spectral

* Corresponding author.

☆ Part of Ph.D. Thesis of X.-Y. S.

0021-9673/93/$06.00

resolution imposed by a feeble luminescence; it also means remaining within the linear (or, in the case of S_2, quadratic) range of analyte concentration.

On the other hand —and peculiar to sulfur— the S_2 bands arise from a *second*-order reaction [4,5]. Hence they tend to overwhelm any first-order luminescence at those high analyte concentrations that (see above) have to be used for spectral assignments. The S_2 main system stretches from the ultraviolet to the red [5,6] and is extremely prominent in the feeble, cool, and hydrogen-rich flame of the FPD. Optimizing the conditions for the competitive linear emission detracts but little from that prominence. Still, the need is urgent to define if not the chemical nature so at least the spectral distribution of the linear emitter in order to optimize analytical performance.

Analytical performance also motivates the second question of this study, *i.e.* how selective linear sulfur behaves *vis-à-vis* other important FPD elements, and how those selectivities compare with similar data from quadratic sulfur. *Linear* sulfur behaviour allows response relationships to other elements to be described by single numbers (selectivity ratios), which remain valid as long as both elements stay within their respective linear ranges. Quadratic sulfur behaviour does not lend itself to so simple a description: full calibration curves would be required for a complete picture. Yet, even an approximate indication of relative response intensities might prove valuable for the analyst.

That brings up the question under what conditions selectivity ratios should be measured to be of maximum analytical value. Quadratic sulfur response is traditionally determined using a 394 nm interference filter [7,8]. In some of our own work (*e.g.* ref. 9) we have preferred to use the FPD "open", *i.e.* free of spectral discrimination beyond the response profile of the photomultiplier tube. Recently we compared some main-group [3] and transition [10] elements on that basis. In this study we shall use the open mode again for quadratic sulfur, but only as an appurtenance to the traditional measurement at 394 nm.

A spectrally "open" measurement is not possible for linear sulfur (the S_2 bands would overwhelm it at the required high analyte concentration) but it *is* possible to measure a relatively large part of the spectrum, *i.e.* the region transmitted by a 600 nm long-pass (cut-on) filter. To narrow that range down to one band (belonging to the linear sulfur emitter, one hopes), a filter centered at 750 nm is used. As in measurements dealing with quadratic sulfur, the obvious analytical trade-off should occur between selectivity and sensitivity. In order to be fair to both methods of sulfur determination, each is individually optimized. In particular, the quadratic sulfur mode uses the quartz chimney, the linear mode does not. Also, the detector flows differ significantly.

The last major question about the analytical performance of sulfur in the flame photometric detector is one of long standing: Do the molecular surroundings of sulfur in analyte molecules influence its response? Differently put: Does one nanogram of sulfur always produce the same luminescent intensity regardless of the type of functional group that carries it into the flame? Can the response of sulfur compounds be represented solely by the amount of sulfur they contain? Is there (at least in theory) just *one* calibration curve for *all* sulfur compounds?

In the conventional FPD determination of sulfur via the S_2 bands, the situation is complicated by the much discussed experimental evidence that the exponent "n" of the correlation between the amount and the luminescence of sulfur —in other words the slope of the log/log calibration curve— varies from about 1 to about 2.3. (Note, however, that *most* compounds are reported having n values around the "theoretical" 2.0, *i.e.* between about 1.8 and 2.2 [4]). If n varies, then the determination of response on a "per gram sulfur" basis will depend on the amounts in which these compounds are injected for the measurement. The convenient but hypothetical assumption of a truly quadratic sulfur response has allowed "response corrections" to be used in a variety of literature studies; those notwithstanding, the question of sulfur equivalency (and exponent variability) still remains to be settled to everybody's satisfaction [4]. (Note that the term "quadratic", as used in this and other papers from our group, indicates a simple square function ($n = 2$); it is *not* derived from the "quadratic equation" with its additional constant and linear terms.)

A further complication arises from the fact that slowly eluting sulfur (or selenium or tellurium) residues from column and detector "linearize" the

lowest part of the calibration curve [11]. The variability of n among most calibration curves, and its frequent approach to unity in their lower regions, are probably the dominating causes for discrepancies found in the literature. However, the questionable purity of some purchased sulfur compounds or their tendency to sorb on metal surfaces and prematurely decompose, as well as the different levels of quenching wrought by variable concentrations of hydrocarbonaceous and other species originating both from the analyte itself and from the (temperature-dependent) column bleed, all add to the experimental difficulties involved in deciding whether the response of sulfur in the FPD does or does not depend on molecular structure.

Yet, a structure-*in*dependent sulfur response would obviously be of great analytical value. The experimental difficulties encountered in defining sulfur equivalency are greatly reduced when, instead of the S_2 band, a linear emitter is monitored. Then n is unity and, of course, does not vary —though compound purity and premature decomposition, as well as internal and external quenching, still may. If only for its analytical utility, a simple investigation of the structure–response relationship of sulfur compounds is therefore clearly called for.

EXPERIMENTAL

An 18-year old and somewhat worn Shimadzu Model 4 (GC-4BMPF) gas chromatograph with dual-channel FPD was used for this study with a 4-year old packed column (100 × 0.3 cm I.D. borosilicate, 5% OV-101 on Chromosorb W, 100–120 mesh) under a nitrogen flow of 20 ml/min. The two photomultipliers were conventional Hamamatsu R-374 tubes (nominal range 180 to 850 nm, maximum yield at 420 nm).

The "*linear*" sulfur mode used flows of 500 ml/min hydrogen and 40 ml/min air, a 600-nm longpass or a 750-nm wideband filter (the latter of bandpass 40 nm), and no quartz chimney. The "*quadratic*" (conventional) sulfur mode used flows of 50 ml/min hydrogen and 40 ml/min air, a 394-nm interference filter (of bandpass 11 nm), or no filter at all. Also, the commercial quartz chimney was kept in place.

(Note that optimal conditions may vary considerably from detector to detector: for instance, the linear-sulfur mode in our much younger but detector-wise quite similar model 8 single-channel Shimadzu GC–FPD worked best with 100–200 ml/min hydrogen, 20–30 ml/min air, and a 620 or 640 nm

TABLE I

AMOUNTS OF COMPOUNDS USED FOR DETERMINING SELECTIVITY RATIOS

Group	Element	Compound[a]	Formula	Amount injected (ng)			
				Quadratic		Linear	
				394 nm	Open	600 nm long pass	750 nm wideband
3A	B	*o*-Carborane	$1,2\text{-}H_2C_2B_{10}H_{10}$	50	50	2000	2000
4A	C	Dodecane	$n\text{-}C_{12}H_{26}$	2000	2000	1000	3000
4A	Sn	Tetrabutyltin	$(n\text{-}C_4H_9)_4Sn$	0.5	0.5	2	100
4A	Pb	Tetraethyllead	$(C_2H_5)_4Pb$	200	200	2	10
5A	N	Tributylamine	$(n\text{-}C_4H_9)_3N$	2000	2000	1000	5000
5A	P	Tributylphosphite	$(n\text{-}C_4H_9O)_3P$	20	20	5	20
5A	As	Triphenylarsine	$(C_6H_5)_3As$	50	50	2	10
6A	Se	Diphenylselenide	$(C_6H_5)_2Se$	5	5	100	1000
6B	Cr	Chromiumhexacarbonyl	$(CO)_6Cr$	50	50	1	10
7B	Mn	MMT[b]	$C_5H_4CH_3Mn(CO)_3$	30	30	2	10
8B	Fe	Ferrocene	$(C_5H_5)_2Fe$	20	20	2	10
8B	Ru	Ruthenocene	$(C_5H_5)_2Ru$	1	0.2	3	30
8B	Os	Osmocene	$(C_5H_5)_2Os$	5	2	3	3
6A	S	Thianaphthene	C_8H_6S	3	3	3	10

[a] All compounds except last one tested against thianaphthene.
[b] MMT = Methylcyclopentadienyl manganese tricarbonyl.

long-pass filter [12]. FPDs from other manufacturers could be expected to show even greater variation in optimum settings.)

For spectral measurements, one of the FPD channels was replaced by a Jarrell-Ash Model 82-415 quarter-meter monochromator with a 1180 grooves/mm grating blazed for 500 nm, and equipped with the same Hamamatsu R-374 photomultiplier tube as the regular FPD channel. When necessary, an order-sorting filter was inserted. Spectral measurements were conducted either by automatic scanning of a constant stream of carbonyl sulfide introduced into the flame via the hydrogen line; or by small manual advances of the wavelength drive after each of a larger number of injections of di-*tert*.-butyldisulfide.

All analytes were used "as received". Table I charts them according to FPD-active element and lists the amounts in which the compounds were injected for the determination of selectivity ratios. (Knowing the injected amounts is important only for elements whose response is *non*-linear; all others were injected well within their linear ranges.)

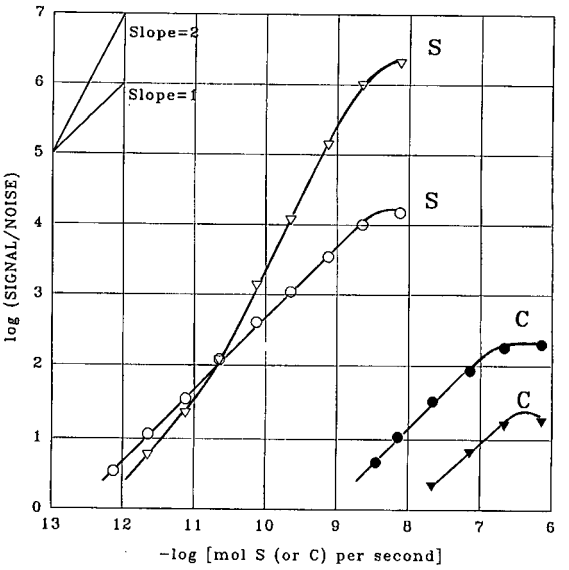

Fig. 1. Calibration curves of thianaphthene ("S", open symbols) and dodecane ("C", closed symbols) in a dual-channel FPD. The flow conditions are those of the "linear mode" (see Experimental). ○,● = Channel 1, 600-nm longpass filter; ▽,▼ = Channel 2, 394-nm (11 nm bandpass) filter.

RESULTS AND DISCUSSION

Sulfur spectrum

There is little doubt that the emission monitored for the linear sulfur mode is *not* the commonly observed S_2 main system [6]. We feel obliged to make this point here because, under particular circumstances, S_2 can indeed produce a linear calibration curve. For instance, a sulfur-containing analyte will respond linearly when superimposed on a massive sulfur background [11]. Also, the S_2 emission will become linear if all (or a constant percentage) of analyte sulfur is converted to S_2^* [5,13]. And, though highly unlikely, it is nevertheless theoretically possible that S_2 could be produced by two different mechanisms: one with second-order, the other with first-order characteristics. Furthermore, beyond the strong, ubiquitous S_2 main system ($B^3\Sigma_u^- - X^3\Sigma_g^-$, 240–711 nm), there also occur (in different sources) three weak, overlapping S_2 systems in the far red and infrared [6]. Much of the remote possibility that main-system S_2 should be responsible for the observed effect can be ruled out by simultaneously observing both quadratic and linear behaviour. Experimentally this is easily achieved by using *both* channels of the dual-channel FPD. The results of such an experiment are plotted in Fig. 1.

Fig. 1 shows the familiar quadratic response of sulfur and, measured from the very same analyte peaks in the second FPD channel, the new linear response. The flow conditions for this experiment are those that favor the linear (but do not prevent the quadratic) emission: primarily a high hydrogen flow in the absence of the conventional quartz chimney. One channel monitors the commonly used S_2 band at 394 nm; the other the red plus adjoining infrared region from about 600 to 850 nm. (Also shown in Fig. 1 are the calibration curves of a standard alkane, which we shall discuss later in the context of selectivity ratios).

The response measured with the conventional 394-nm interference filter displays the typical behaviour attributed to S_2: a mostly quadratic (slope 2) calibration curve with an almost linear (slope 1) section at its base. In contrast, the response simultaneously measured with a 600-nm longpass filter is purely linear. It spans about four orders of magnitude (depending on the definition used for detecta-

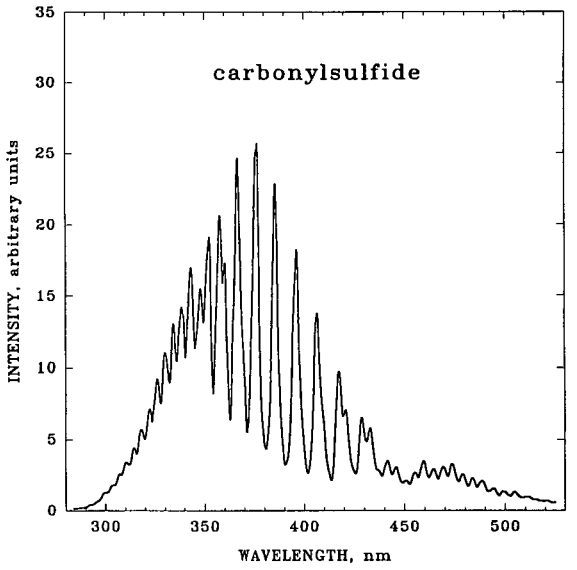

Fig. 2. S_2 luminescence (obtained from continuous introduction of COS) in the "quadratic mode" (see Experimental for conditions). Bandpass *ca.* 6.7 nm.

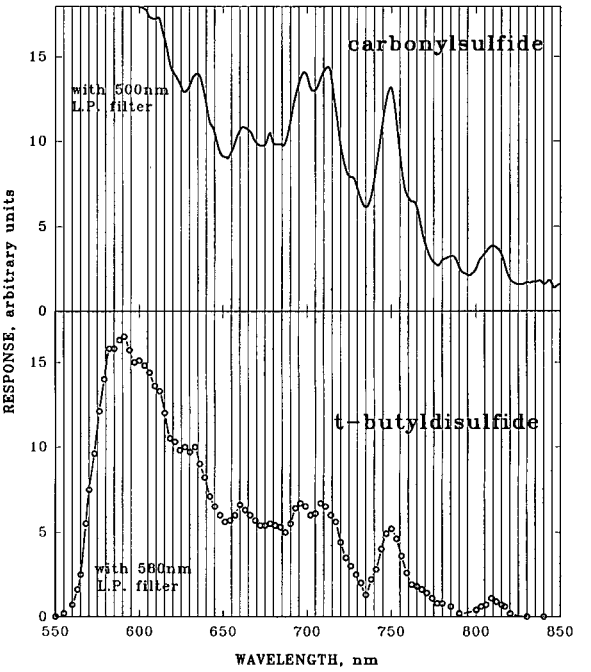

Fig. 3. Luminescence obtained by continuous introduction of COS (above) and repeated injection of (*tert.*-$C_4H_9)_2S_2$ (below) in the "linear mode" (see Experimental for conditions). Bandpass *ca.* 6.7 nm; 500-nm (above) and 580-nm (below) longpass (L.P.) filters are used for order sorting.

bility) and bends off, likely for good spectrochemical reasons, at the same analyte level as the S_2 emission. Under this set of conditions, the *linear* response is the stronger of the two in the low-concentration range.

While the calibration curves of Fig. 1 establish the likely presence of an emitter other than S_2, the most direct evidence for this emitter would be its spectrum. However, that is difficult to obtain in the presence of S_2. Fig. 2 displays these repeatedly shown bands as they appear in our FPD under "conventional" (see Experimental) conditions. This spectrum makes it clear why the linear sulfur emission has remained hidden for so long: on the chosen intensity scale, no further emissions appear beyond 520 nm (except for the S_2 bands in second order, of course).

Even without the quartz chimney, at a higher hydrogen flow, and with an order-sorting filter, it is difficult if not impossible to recognize and define the linear emitter. Fig. 3 shows the crucial region —on the top in automatic scanning, on the bottom in manual injection mode. The latter was used for a spectrally confirmative replication, for a clearer definition of possible continua, and for the circumvention of any conceivable background features. The automatic mode represents conventional spectroscopic procedure; the manual approach mimics chromatographic practice. Fortunately, the two produce very similar spectra.

The emitter they represent remains unknown; none of the common emission systems of sulfur [6] could be unambiguously assigned to it. (Note, however, that the 0,0i and 0,0ii heads of the "infrared and far red" S_2 systems lie at 751, 743, 710 and 698 nm [6], *i.e.* quite close to the position of the protuberances shown in Fig. 3.) The spectra of Fig. 3 must also include some outliers of the main-system S_2 bands and, for this and other reasons, even the spectral distribution of the new linear emission remains vague. A 600-nm cut-on filter will produce a purely linear calibration curve; a 550-nm cut-on filter will come close to that. The most pronounced —though, response-wise, not very important— feature of Fig. 3 is the band located at *ca.* 750 nm. That it belongs to a linear sulfur emitter is supported by the fact that, as seen through a 750-nm filter of 40

nm bandpass, the band yields *linear* calibration curves for sulfur analytes. The same is the case for the "doublet" at *ca.* 700 nm, as seen through a filter of 70 nm bandpass.

Sulfur selectivity

With the 750-nm wideband filter just mentioned, sensitivity should be clearly lower but selectivity generally higher than with, say, a 600 nm cut-on filter. To determine the selectivity of sulfur against other FPD-active elements in the "linear" mode is interesting and indeed necessary; we have done that for both optical conditions. Note, however, that all selectivity ratios are *single*-channel values. Improvements of one to three orders of magnitude can be easily achieved by *dual*-channel differential operation [10]. It is furthermore possible to use the CONDAC algorithm [3] for obtaining apparent specificity for linear sulfur (as well as for any other FPD-active element).

It is also interesting, as well as conducive to an assessment of the two techniques, to determine the selectivity ratios of sulfur against other FPD-active elements in the *quadratic* mode, and to compare these numbers with those of the linear mode. To remain analytically relevant, such a comparison needs to be carried out with each mode under its own, individually *S/N*-optimized conditions. Yet the comparison will still be restricted in application: it applies only to *one* level of sulfur (see Table I). Higher sulfur levels increase, lower sulfur levels decrease the single-value selectivity ratios in the quadratic mode. (Very rough estimates of the selectivity ratios at higher or lower levels of sulfur can be obtained by assuming response to be proportional to the square of the sulfur concentration; however, as previously discussed, the exponential factor often differs from the ideal value of 2 and, furthermore, often approaches 1 in the low concentration range of the "quadratic" calibration curve.)

TABLE II

MOLAR SELECTIVITY OF SULFUR AGAINST OTHER ELEMENTS IN TWO FPD RESPONSE MODES

The selectivity of sulfur against element X, $S_{S/X}$, is calculated as

$$S_{S/X} = \frac{R_{(S)}}{R_{(X)}} \cdot \frac{\text{mol X/s}}{\text{mol S/s}}$$

where $R_{(S)}$ is the peak height response at unit attenuation of thianaphthene, and $R_{(X)}$ is the same for a compound of element X (see injection amounts from Table I); while mol X/s and mol S/s are the molar flows per second at peak apex of element X and sulfur.

Group	Element (X)	Quadratic sulfur mode[a]		Linear sulfur mode[b]	
		394 nm	Open[c]	600 nm long pass	750 nm wideband
3A	B	$6 \cdot 10^2$	$2 \cdot 10^2$	$3 \cdot 10^3$	$> 10^4$
4A	C	$2 \cdot 10^4$	$2 \cdot 10^4$	$1 \cdot 10^{3d}$	$6 \cdot 10^{3d}$
4A	Sn	0.1	0.05	0.03	0.7
4A	Pb	$2 \cdot 10^2$	$4 \cdot 10^1$	0.07	0.1
5A	N	$7 \cdot 10^2$	$1 \cdot 10^2$	$1 \cdot 10^{2d}$	$1 \cdot 10^{2d}$
5A	P	$1 \cdot 10^1$	0.1	0.2	0.5
5A	As	3	4	0.05	0.1
6A	Se	8	6	7	$5 \cdot 10^1$
6B	Cr	$3 \cdot 10^1$	2	0.05	0.1
7B	Mn	$2 \cdot 10^1$	7	0.08	0.2
8B	Fe	5	5	0.09	0.2
8B	Ru	0.4	0.09	0.2	1
8B	Os	6	0.3	0.08	0.1

[a] 50 ml/min H_2, 40 ml/min air and 22 ml/min carrier N_2; with quartz chimney; Hamamatsu R-374 photomultiplier tube.
[b] 500 ml/min H_2, 40 ml/min air and 22 ml/min carrier N_2; without quartz chimney; Hamamatsu R-374 photomultiplier tube.
[c] No optical filter used.
[d] Inverted peak.

Although the quadratic sulfur mode has been in use around the world for several decades, published information on sulfur selectivity ratios is largely restricted to the selectivity of sulfur *versus* carbon (really: *versus* the particular hydrocarbon that serves as a carbon standard in the selectivity ratio measurement). Recently, selectivity ratios of sulfur against various other elements were reported [3], but these values pertain to open (filter-less) operation at a generalized (as opposed to a sulfur-optimized) set of conditions. Thus the values of Table II may be helpful to users not only of the linear but also of the quadratic sulfur mode.

With the above caveats in mind, we can now examine the compilation of experimentally determined selectivity ratios in Table II —first for each mode on its own, then for the two modes in comparison. Those of the conventional quadratic mode show the expected higher selectivity conferred by the 394-nm narrow-band interference filter (*versus* open, *i.e.* filter-less operation) in all but three cases. However, the increase in selectivity —which comes at some decrease in sensitivity— is small (a factor of 5 on average). This is in agreement with earlier data on the generally minor improvement interference filters bring to FPD selectivity [3,9,10].

For obvious reasons the linear sulfur mode cannot be run "open", *i.e.* it cannot be observed unless a filter cuts off most of the S_2 bands. Still, analogous comments can be made about the comparison of the nominal 730–770 nm range monitored through the 750-nm wideband interference filter, with the much wider 600–850 nm range admitted by the 600-nm longpass filter and the red-extended R-374 photomultiplier tube. Not surprisingly, the increase in selectivity owing solely to optical discrimination is smaller in the linear than in the quadratic mode.

Perhaps more important than these *intra*modal relationships is the *inter*modal confrontation of linear with quadratic sulfur. The linear mode shows selectivity ratios that are better in three, about equal in two, and worse in eight cases. This seems reasonable if one considers the decidedly greater intensity of the S_2 emission overall. At higher sulfur levels than those used for Table II, the selectivity ratios of the quadratic mode would increase, tilting the comparison still further in its favor. An advantage of the linear mode, on the other hand, is that the response of hydrocarbons is generally negative (peaks are inverted), thereby providing a qualitative distinction between compounds that contain sulfur and those that contain only carbon and hydrogen. (It may be noted that in the comparison with selenium, the S/Se selectivity ratios depend strongly not only on the injected amount of sulfur but also on the injected amount of the — similarly quadratic — selenium analyte.)

Sulfur equivalency

Another seeming advantage of the linear mode is the very minor (if at all existing) dependence of the response of sulfur on the structure of its compounds. Obviously, any intrinsic dependence of organosulfur peak size on analyte concentration or retention time (as it occurs strongly and predictably in the quadratic mode) can be ruled out. Differences observed between the sensitivities of various compounds are thus directly attributable to differences in photon yield per sulfur atom (absent impurity, degradation and quenching effects, of course).

Fig. 4 shows the linear calibration curves of seven disparate sulfur compounds, plotted on a "peak area *vs.* gram sulfur" basis. The responses vary (*i.e.* they differ vertically in the graph) by a factor of less

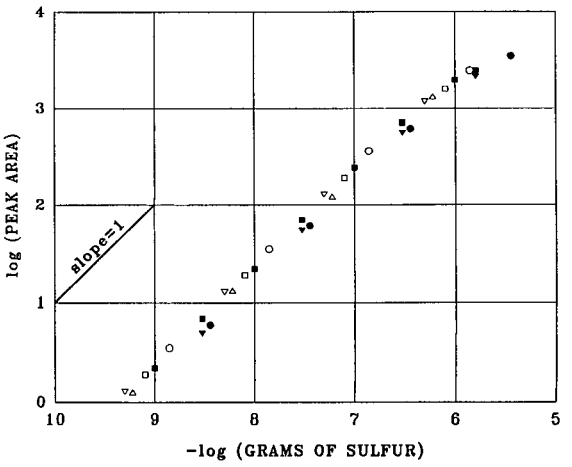

Fig. 4. Calibration curves for seven sulfur compounds in the "linear mode". ○ = Thianaphthene; △ = *n*-octylsulfide; ■ = *n*-hexylsulfide; □ = dibenzothiophene; ▼ = 1-dodecanethiol; ▽ = phenylsulfide; ● = di-*tert.*-butyldisulfide. Conditions: 600-nm longpass filter; R-374 photomultiplier tube; 500 ml/min H_2, 40 ml/min air; no chimney.

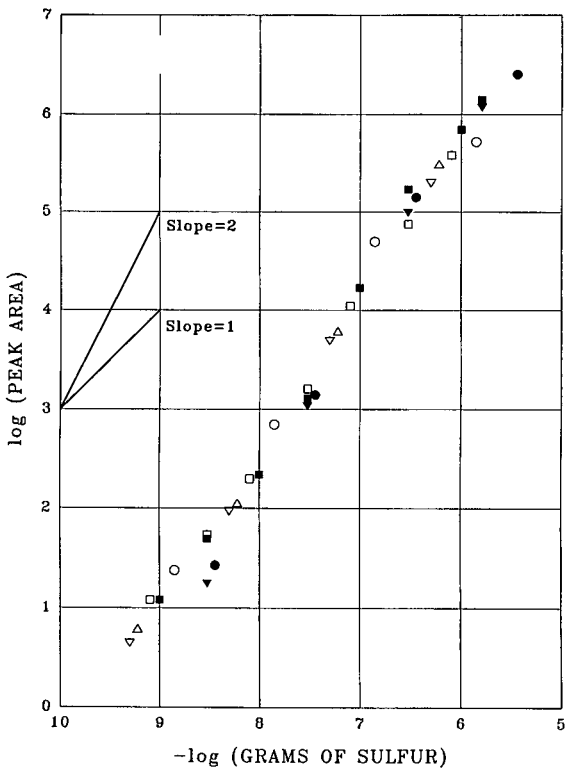

Fig. 5. Calibration curves for seven sulfur compounds in the "quadratic mode". Symbols as in Fig. 4. Conditions: 394-nm interference filter; R-374 photomultiplier tube; 50 ml/min H_2; 40 ml/min air; with chimney.

than two, over an analyte concentration range of more than three orders of magnitude. Given (a) the experimental error band (injection, flow and temperature control, etc.) for each individual sulfur compound; (b) the always possible and often present perturbations caused by premature decomposition, irreversible absorption, or lacking purity of the analyte; and (c) the likely quenching that occurs internally (by analyte carbon) or externally (by column bleed and/or co-eluting compounds); a factor of two seems small enough for sulfur response to be considered *in*dependent of molecular structure. A similar factor of two is, for instance, apparent in the two newest instrumental contenders for linear organosulfur determination; each of which is nevertheless considered "a specific detector for sulfur present in different molecular forms" [14]. For purposes of analytical response estimates, therefore, a rough sulfur equivalency can be assumed for the linear mode. Note, however, that the range of compounds tested in this study is limited, and that its present conclusion should remain open to future re-evaluation.

What about sulfur equivalency in the *quadratic* mode? Fig. 5 exhibits the "quadratic" calibration curves of the compounds used for producing the earlier Fig. 4. *Response* among the seven analytes varies here by a factor of just less than five. That seems clearly more than the factor of two for the linear mode. However, while analytically relevant, this comparison is not fair. A quadratic emitter will, per definition, respond to any structure-related difference in the *second* power. Hence, a mechanistically fairer approach will use the *square root* of the response or, more simply, the *amount* of sulfur involved. If this is done, the variation in sulfur equivalency of the quadratic mode that may be attributed to *structural* factors is only slightly larger than a factor of two, *i.e.* it appears to correspond to the like variation of the linear mode.

If such narrow variation should prove typical of a more extensive and variegated future roster of sulfur compounds, it would suggest that the *quadratic* mode may be independent of molecular structure as well. (Note that this study is unable to identify the linear emitter, and that the literature remains uncertain even about the basics of the quadratic response mechanism [4,5,15]. It could, for instance, be possible that both modes start from the same species, *e.g.* H_2S, S, etc. Ergo, if the linear mode is really structure-independent, so could be the quadratic one.) Sulfur equivalency in the quadratic mode was indeed credibly claimed a long time ago [16], but evidence to the contrary has since amassed [4] and appears to have been accepted.

Sulfur performance

Minimum detectable flows of linear sulfur can be read off the (extrapolated) calibration curve of Fig. 1, since the ordinate is based on signal/noise measurements (where noise is the peak-to-peak baseline fluctuation, with drift and outliers excluded). The detectability measurement most common to chromatography calls for $S/N = 2$ (*i.e.* $\log [S/N] = +0.3$ on our scale); while the IUPAC-recommended detection limit of $S/\sigma = 3$ (where σ is the standard variation of the baseline noise) lies for our experi-

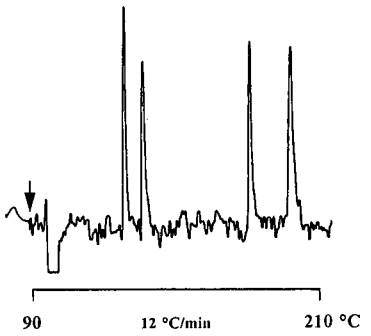

Fig. 6. Temperature-programmed separation of four sulfur compounds near their detection limit in the "linear mode". In order of elution: 3 ng di-*tert.*-butyldisulfide, 3 ng benzo[*b*]thiophene (thianaphthene), 4 ng diphenylsulfide, 4 ng dibenzothiophene.

ments at approximately $S/N = 0.5$ (*i.e.* $\log [S/N] = -0.3$ [2]). The detection limits for the optimized linear mode are larger by about a factor of five than those for the optimized quadratic mode. {For the quadratic sulfur mode in various FPDs, Dressler [8] cites a range of minimum detectabilities ($S/N = 2$) of $2 \cdot 10^{-12}$ to $5 \cdot 10^{-11}$ g S/s}. The detection limits for the linear mode are also larger, by about an order of magnitude, than those reported about a side-by-side comparison of the Hewlett-Packard atomic emission detector (AED) and the Sievers Research sulfur chemiluminescence detector (SCD) [14].

A more practical, visual assessment of detectability can be provided by the actual chromatography of some sulfur compounds near their detection limit in a temperature-programmed separation. Such a chromatography is shown in Fig. 6. (Note that it uses a 1-m packed column; capillary columns should do much better.)

The linear range of the new sulfur mode is approximately 4 orders of magnitude (depending on the definition used for the detection limit). For comparison, the linearity of the SCD is generally four, that of the AED five orders of magnitude [14]. As shown in Fig. 4, the linear sulfur response in the FPD is independent of analyte structure within a factor of 2, similar to the behaviour of SCD and AED [14]. Remember, however, that our study sampled only seven different sulfur analytes.

As far as we can tell, the linear sulfur response in our FPD has remained approximately constant since we started investigating it a year or so ago. However, we did not carry out special studies of long-term (or short-term) reproducibility; in part owing to the reputation —well deserved, in our opinion— of the FPD as a reliable and stable workhorse. (One might add that it is also inexpensive compared to some of the newer instrumentation: our recently purchased gas chromatograph with single-channel FPD came at < US$ 10 000.)

Preliminary experiments indicate that the linear sulfur mode suffers significantly less from quenching by co-eluting hydrocarbons than does the quadratic mode. However, the problem of quenching is a complex one and will be dealt with in a separate manuscript; we mention it here only because it can constitute a major factor in evaluating detector performance.

A much-cited review of sulfur determination in the FPD concludes that further research into the S_2 mode should be encouraged, but that "the development of a simple and sensitive sulfur-selective detector with a linear response should receive even higher priority" [4]. The new linear sulfur mode may well meet those requirements. Although its sensitivity is at present somewhat lower than that of the quadratic mode, that disadvantage may be more than compensated by its other advantages, in particular its uncompromised linearity.

NOTE ADDED IN REVISION

One of the reviewers of this manuscript requested that we "provide some discussion with regard to the selectivities [of the linear sulfur mode], since some of these markedly differ from the quadratic mode." We are pleased to oblige, although to do so will force us to rely heavily on speculation.

There are several problems to bear in mind when discussing the selectivity ratios of Table II. That their values depend on the *amount* of sulfur (or selenium) in the quadratic mode has already been mentioned. The problems of comparing kinetically different emitters and vastly different linear ranges are persuasively illustrated by Fig. 1. Selectivity ratios (in logarithmic, *i.e.* order-of-magnitude form) are represented by the horizontal (or vertical) distances between two corresponding log–log calibration curves. Obviously, they are constant only if measured exclusively between two *straight* lines of the *same* slope.

The next problem concerns absolute signal inten-

sity: sulfur response is considerably more intense in the quadratic than in the linear mode. Furthermore, the two modes differ strongly in their flow conditions, hence also in flame and excitation characteristics. This applies not only to sulfur, but also to all the other elements with which sulfur is being compared. At present there exists no logical framework that would be capable of predicting whether an element will chemiluminesce, or to what extent and where in which type of a flame. Theories of chemiluminescent flame excitation, few as they are, are often derived by necessity from experimental hindsight and speculative analogy.

The numerical values of selectivity ratios depend on the sometimes arbitrary choice of conditions at which they are measured. In the present case the conditions are based on the *maximum S/N ratio* for sulfur in the two modes, with further choices based on their characteristic spectral distributions (the bands at 394 and 750 nm). Yet, if one were to base the conditions on the *maximum selectivity ratio* for pairs of sulfur with each of the other elements, the flow conditions and related spectral distributions of *both* elements would have to be taken into account. For instance, the origin, shape and behaviour of spectral features of the "other" element would have to be considered as well: it is far easier to improve selectivity by focussing on, say, the element with the strong atomic line or the one whose response varies conspicuously with changes in flow, than on the one with the prominent continuum or the one whose response ignores changes in flow. Not that we propound to carry out *selectivity* optimization (except, perhaps, for the "important" sample that cannot be dealt with by any other means), but mentioning it helps us to draw attention to the many parameters and choices that hide behind those deceptively simple numbers known as selectivity ratios.

It is obvious from the above considerations that what is mainly left to speculate on is the effect of spectral distributions on selectivity ratios. The spectrum of quadratic sulfur (S_2) is well known; the "spectrum" of linear sulfur has been measured (Fig. 3). However, the spectra of other elements have not; at least not, as demanded by the present context, *at the conditions of the linear sulfur mode.* FPD spectra are difficult to determine under analytically relevant conditions, particularly when the emitters are weak. Also, FPD spectra can change drastically with flame conditions. It is therefore not surprising that uncritical reference to literature spectra measured under different conditions —sometimes conditions in the FPD that yield the highest *S/N* ratio not for sulfur but for the particular element with which it is being compared, or even conditions in other excitation sources— can prove highly misleading.

To rely on literature spectra thus requires a leap of faith, *i.e.* it implies (sometimes correctly but often in error) that spectral distribution does not change significantly with changes in flow conditions. Yet, with the tenuous nature of this implication being understood, we shall attempt (as requested) to comment on the selectivity of linear sulfur *vis-à-vis* other elements; and further, to compare it to the behaviour of quadratic sulfur as listed in Table II.

In the cases of boron and selenium, the linear sulfur mode shows the much better selectivity, presumably because the dominant FPD spectra (BO/BO_2 [3] and Se_2 [17]) do not stretch beyond 600 nm. A similar though not as clear-cut case can be made for tin. The main spectra relevant to the quadratic sulfur mode (the blue luminescence of tin on quartz, and SnOH [18]) do not extend beyond 600 nm. The dominant FPD spectrum in the red is due to SnH, with its strongest band at 610 and a much weaker one at 690 nm [6,19].

The (inverted) peaks of carbon/hydrogen and nitrogen found under the conditions of the linear sulfur mode represent *decreases* in emission, *i.e.* they are due to a quenching of the background luminescence. The spectral distribution and origin of the luminescent background in the >600 nm region is unknown and could, furthermore, contain "memory" components both significant in intensity and variable in time. (Some of this background is evident from a comparison of the two spectra of Fig. 3 in the >800 nm region.) In the quadratic sulfur mode, in contrast, C/H and N peaks represent *increases* in emission. The FPD emission spectra resulting from aliphatics, aromatics, oxygenates [2] and nitrogen compounds [3] have been measured (though not identified) at different conditions. Both stretch, however weakly, beyond 600 nm, and must then obviously dip below the zero intensity level at longer wavelengths. Thus we are dealing with a mixture of emission and quenching spectra in that region, which makes the selectivity ratios of the two

modes neither easily predictable nor directly comparable.

(Parenthetically it may be added that, as Fig. 1 illustrates, measurement of selectivity against carbon, or other elements of weak response and short linear range, can lead to an inappropriately high result if the injected amount of carbon exceeds its linear range. The more appropriate way to increase selectivity ratios is to use a *dual*-channel FPD for annulling the response of carbon, or of other elements, by differential operation [10]; or to have the CONDAC algorithm deny unwanted elements access to the chromatogram [3].)

In the cases of lead, arsenic, chromium, manganese, iron and osmium, the selectivity ratios of the linear sulfur mode are quite noticeably worse than even those of the *open* (filterless) quadratic mode. In part this is due to the considerably higher intensity of the S_2 bands. But it also strongly suggests that the listed elements do produce sizeable emissions between 600 and 850 nm. Indeed, the FPD spectra of chromium [2] and osmium [20] contain strong continua in the far red and near infrared. Also, noteworthy red/infrared emissions emanate from lead under conditions of the linear sulfur mode; these are currently under investigation [21]. We have no like information on the FPD spectra of iron [22] or manganese [23], since these metals were unfortunately measured with a photomultiplier restricted to wavelengths below about 650 nm. The only surprise, in view of the well-known As continuum [ref. 3 and references cited therein], comes from the apparently sizable response of arsenic above 600 nm.

The case of ruthenium, an unusually sensitive element, — seems different from that of the other transition metals. Its dominant features are molecular bands (of RuH?) at 484 and 528 nm, while several (much weaker) atomic lines appear in the 350 to 400 nm range (ref. 24; *cf.* discussion in ref. 2). We have no spectral information beyond the nominal 650 nm upper limit of the photomultiplier, but the selectivity ratios suggest only minor ruthenium emission activity in that region.

That leaves to the last the case of phosphorus, the second-most important FPD analyte. The selectivity measurement of quadratic sulfur against phosphorus at 394 nm is the highest of the four taken, not surprisingly so in light of the well-documented S_2 and HPO systems. The major HPO band appears at 526 nm; however, the whole HPO spectrum stretches from 460 to 680 nm [25] and often rests on a "white" continuum with strong components in the green and red [5]. This could account for the unexpectedly poor selectivity ratios of the linear sulfur mode against phosphorus.

Any further discussion of the selectivity ratios of quadratic and linear sulfur against the roster of other FPD-active elements must await the determination of the latters' spectra at the precise conditions of these two analytical modes and, still farther away, a better understanding of the chemistry and excitation/quenching processes in the FPD flame. Until then, the selectivity ratios of Table II are best understood as condition-dependent, empirical data of mainly analytical (as opposed to spectrochemical) value.

Our reviewer also requested that "the detection limit should have numerical values in the text". Certainly such numbers facilitate comparison with other methods of chromatographic organosulfur analysis. We therefore established separately the minimum detectable quantity of sulfur by using isothermal chromatography of the standard analyte thianaphthene (benzothiophene), and by following the IUPAC-recommended criterion $S/\sigma_N = 3$ via an algorithm that determined σ_N, the standard deviation of the baseline noise, by a least-squares fit to a normal (Gaussian) distribution. The result was $2 \cdot 10^{-13}$ mol sulfur per second. For easy comparison with values arrived by other commonly used definitions, that value translates into $6 \cdot 10^{-12}$ g S/s or $2.5 \cdot 10^{-11}$ g thianaphthene/s; or, at the $S/N_{p\text{-}t\text{-}p} = 2$ limit (where $N_{p\text{-}t\text{-}p}$ is the peak-to-peak baseline noise, with drift and spikes excluded), $7 \cdot 10^{-13}$ mol S/s or $2 \cdot 10^{-11}$ g S/s or $1 \cdot 10^{-10}$ g thianaphthene/s. Fig. 7 shows the 2 ng peak of thianaphthene (of 8 s peak width at half height) that was used for this evaluation of sulfur detectability in the linear mode; together with a sizable stretch of baseline fluctuations and their approximation by a Gaussian curve.

ACKNOWLEDGEMENT

This study was supported by NSERC operating grant A-9604. We appreciate the assistance of C. H. Warren and B. Millier in obtaining the Gaussian fit shown in Fig. 7.

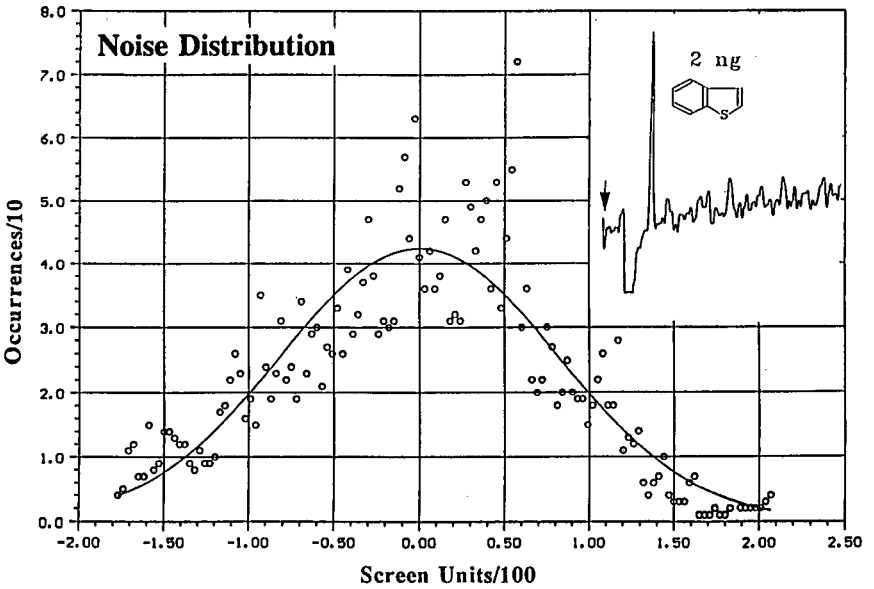

Fig. 7. Typical peak of 2 ng thianaphthene in the linear mode near the detection limit, and least-squares Gaussian fit of the baseline fluctuation.

REFERENCES

1 B. Millier, X.-Y. Sun and W. A. Aue, presented at the *75th Canadian Institute of Chemistry Conference, Edmonton, June 1992.*
2 X.-Y. Sun, B. Millier and W. A. Aue, *Can. J. Chem.*, 70 (1992) 1129.
3 W. A. Aue, X.-Y. Sun and B. Millier, *J. Chromatogr.*, 606 (1992) 73.
4 S. O. Farwell and C. J. Barinaga, *J. Chromatogr. Sci.*, 24 (1986) 483.
5 P. T. Gilbert, in R. Mavrodineanu (Editor), *Analytical Flame Spectroscopy*, Philips Technical Library/Macmillan, London, 1969, pp. 181–376.
6 R. W. B. Pearse and A. G. Gaydon, *The Identification of Molecular Spectra*, Chapman & Hall, London, 4th ed., 1976.
7 S. Kapila, D. O. Duebelbeis, S. E. Manahan, in R. M. Harrison and S. Rapsomanikis (Editors), *Environmental Analysis Using Chromatography Interfaced with Atomic Spectroscopy*, Ellis Horwood, Chichester, 1989.
8 M. Dressler, *Selective Gas Chromatographic Detectors (Journal of Chromatography Library*, Vol. 36), Elsevier, Amsterdam, 1986, pp. 133–160.
9 W. A. Aue and C. R. Hastings, *J. Chromatogr.*, 87 (1973) 232.
10 W. A. Aue, B. Millier and X.-Y. Sun, *Can. J. Chem.*, 70 (1992) 1143.
11 W. A. Aue and C. G. Flinn, *J. Chromatogr.*, 158 (1978) 161.
12 N. B. Lowery, unpublished Ph.D. work, 1992.
13 Y.-Z. Tang, *Ph.D. Thesis*, Dalhousie University, Halifax, 1987.
14 S. E. Eckert-Tilotta, S. B. Hawthorne and D. J. Miller, *J. Chromatogr.*, 591 (1992) 313.
15 S. V. Olesik, L. A. Pekay and E. A. Paliwoda, *Anal. Chem.*, 61 (1989) 58.
16 M. Maruyama and M. Kakemoto, *J. Chromatogr. Sci.*, 16 (1978) 1.
17 C. G. Flinn and W. A. Aue, *J. Chromatogr.*, 153 (1978) 49.
18 C. G. Flinn and W. A. Aue, *Can. J. Spectrosc.*, 25 (1980) 141.
19 C. G. Flinn and W. A. Aue, *J. Chromatogr.*, 186 (1979) 299.
20 X.-Y. Sun and W. A. Aue, *Mikrochim. Acta*, I (1990) 1.
21 J. A. Gebhardt, unpublished Ph.D. work, 1992.
22 X.-Y. Sun and W. A. Aue, *J. Chromatogr.*, 467 (1989) 75.
23 W. A. Aue, B. Millier and X.-Y. Sun, *Anal. Chem.*, 62 (1990) 2453.
24 X.-Y. Sun and W. A. Aue, *Can. J. Chem.*, 67 (1989) 897.
25 B. Gutsche and R. Herrmann, *Dtsch. Lebensm.-Rundsch.*, 67 (1971) 243.

Journal of Chromatography, 633 (1993) 163–168
Elsevier Science Publishers B.V., Amsterdam

CHROM. 24 764

Evaluation of series-coupled gas chromatographic capillaries of different polarities

Application to the resolution of problem pairs of constituents in Algerian cypress essential oil

N. Chanegriha and A. Baaliouamer*

Université des Sciences et de la Technologie Houari Boumediene, Institut de Chimie, Laboratoire d'Analyse Organique Fonctionnelle, B.P. 32 El Alia, Bab-Ezzouar, Algiers (Algeria)

(First received July 6th, 1992; revised manuscript received November 16th, 1992)

ABSTRACT

The inability of capillary columns used in GC, GC–MS and GC–Fourier transform IR spectrometry to provide complete resolution of all components of complex mixtures such as essential oils has often been reported. By connecting fused-silica capillary columns of different polarity in series and by changing the temperature programme gradient or the column sequence, a more efficient separation system is obtained. Retention indices of some previously unresolved constituent pairs were calculated and an application to the analysis of cypress essential oil is reported.

INTRODUCTION

Algerian cypress (*Cupressus sempervirens* Linnaeus = *Cupressus fastigiata* De Condolle) essential oil [1] offers some difficulties for the capillary gas chromatographic (GC) separation of pairs of constituents such as limonene–1,8-cineole and 1,8-cineole–β-phellandrene (OV-101 capillary column, GC–MS on FFAP capillary column). To solve this problem, we coupled two capillary columns in series. The analytical use of serially coupled GC columns (packed or capillary) has been the subject of considerable study [2–12]). The advantages of this technique [10] over other techniques such as parallel and mixed-phase capillary columns are the use of just one injector and one detector and the possibility of changing the polarity of the linked columns. However, it must be noted that this method is efficient only if the difference in polarity of the two columns is high [13].

*Corresponding author.

EXPERIMENTAL

Instruments

The gas chromatograph used was a Hewlett-Packard Model 5730A with a flame ionization detector and an HP 3390 integrator. Two WCOT fused-silica columns with grafted phases were used, nominally 25 m × 0.22 mm I.D., manufactured by Chrompack (Middelburg, Netherlands): a low-polarity (NON) CP-Sil 5 CB (dimethylsiloxane, equivalent to OV-101, film thickness 0.11 μm) and a high-polarity (POL) CP-Wax 57 CB (polyethylene glycol, equivalent to Carbowax 20M, film thickness 0.21 μm). They were linked by a Swagelok 1/16, Ref. 2053 (Supelco, Gland, Switzerland).

0021-9673/93/$06.00

Chromatographic conditions

The columns had different optimum flow-rates as determined by the Van Deemter curve when connected in different orders: CP-wax 57 CB–CP-sil 5 CB (POL → NON) 0.36 ml/min and CP-Sil 5 CB–CP-Wax 57 CB (NON → POL) 0.30 ml/min. The carrier gas was helium. The column temperature programme was 80°C for 8 min increased at 1°C/min to 230°C and held at 230°C for 16 min. The injector and detector temperatures were 250°C. The volume of oil injected was 0.5 μl and the volume of pure sample injected was 0.2 μl. The splitting ratio was 1:20.

Standard compounds were obtained from Fluka (Buchs, Switzerland). Essential oil of cypress was extracted from fresh leaves and twigs by hydrodistillation in the laboratory in March 1989 (d_{20}^{20} = 0.8795, n_D^{20} = 1.4719, α_D^{20} = 5.6°). The oil was analysed by fused-silica capillary GC either alone (25-m OV-101 and 25-m FFAP columns) or coupled with mass spectrometry (GC–MS) (50-m FFAP column) and with Fourier transform IR spectrometry (GC–FT-IR) (25-m column BP 21). Ninety-five compounds have been identified by these techniques [1].

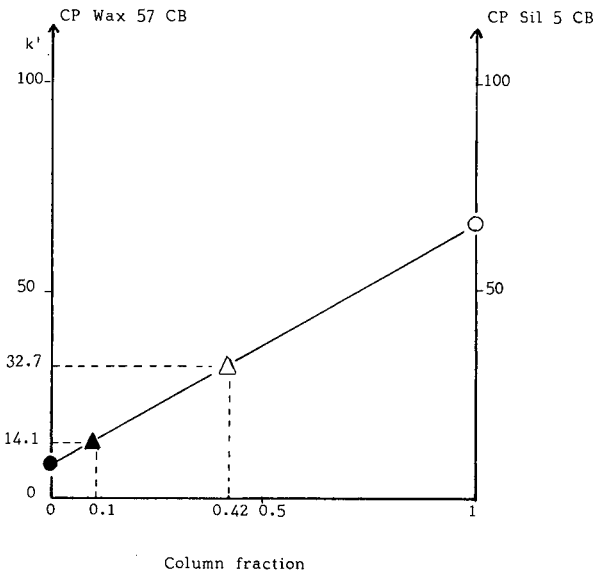

Fig. 1. k' Values *versus* column fraction. ○ = CP-Sil 5 CB; ● = CP-Wax 57 CB; △ = CP-Sil 5 CB–CP-Wax 57 CB; ▲ = CP-Wax 57 CB–CP-Sil 5 CB.

RESULTS AND DISCUSSION

The characteristics of the individual columns and of the columns connected in the two different orders are reported in Table I. The number of theoretical plates of the serially linked columns is about 65% of the sum of the values for the single columns.

The values of $k'_{C_{10}}$, $\alpha_{C_{11}/C_{10}}$ and TZ on series-coupled columns are between those given by the individual columns. The plot of the capacity factor $k'_{C_{10}}$ *versus* column fraction is shown in Fig. 1. The contribution of each column to the coupled system is not equal to 0.5 as one would have expected. The contribution of the CP-Sil 5 CB column, for example, is 0.42 for order 1 (NON → POL) and 0.10 for order 2 (POL → NON).

Moreover, the Van den Dool retention indices I were calculated for temperature programming [14–16] of standards that are not well separated either on OV-101 (25 m) [1] or Carbowax 20M (25 m) columns [17] or by GC–MS (FFAP, 50 m) [1]. We also calculated the increments ΔI relative to OV-101 and to Carbowax 20M. The results are reported in Table II.

All the retention indices are situated between

TABLE I

CHARACTERISTICS OF COLUMNS (C_{10} at 100°C)

NON→POL = CP-Sil 5 CB–CP-Wax 57 CB; POL→NON = CP-Wax 57 CB–CP-Sil 5 CB.

Column	N	$k'_{C_{10}}$	$\alpha_{C_{11}/C_{10}}$	U (cm/s)	TZ
CP-Wax 57 CB	24 118	8.3	1.1	55	1.60
CP-Sil 5 CB	30 945	65.7	1.4	362	11.37
NON→POL	37 398	32.7	1.3	100	7.08
POL→NON	36 260	14.1	1.3	44	8.17

TABLE II

RETENTION INDICES (I) AND THEIR INCREMENTS (ΔI)

$\Delta I_a = I_{NON \rightarrow POL} - I_{OV\text{-}101}$; $\Delta I_b = I_{NON \rightarrow POL} - I_{CBWax\ 20M}$; $\Delta I_c = I_{POL \rightarrow NON} - I_{OV\text{-}101}$; $\Delta I_d = I_{POL \rightarrow NON} - I_{CBWax\ 20M}$.

Compound	$I_{OV\text{-}101}$	$I_{CBWax\ 20M}$ [17]	$I_{NON \rightarrow POL}$	$I_{POL \rightarrow NON}$	ΔI_a	ΔI_b [17]	ΔI_c	ΔI_d [17]
Myrcene[a]	982	1156	1006	1128	24	−150	146	−28
Octanal	991	1278	1051	–	60	−227	–	–
p-Cymene[a]	1010	1272	1064	1153	54	−208	143	−119
Limonene[a]	1019	1206	1048	1123	29	−158	104	−83
1,8-Cineole[a]	1020	1228	1061	1137	41	−167	117	−91
β-Phellandrene[a]	1013	1216	1068	1152	55	−148	139	−64
α-Phellandrene[a]	994	1177	1015	1166	21	−162	172	−11
Terpin-4-en-1-ol[a]	1160	1628	1260	1651	100	−368	491	+23
Borneol[a]	1147	1698	1311	1758	164	−387	611	+60
Isoborneol	1137	1660	1280	1705	143	−380	568	+45
α-Terpineol	1185	1661	1332	1552	147	−329	367	−109
Bornyl acetate[a]	1283	1580	1395	1558	112	−185	275	−22
Thymol[a]	1277	2100	1661	–	384	−439	–	–
α-Cedrene[a]	1409	1600	1440	1550	31	−160	141	−50

[a] Constituents of Algerian cypress essential oil.

those given by the individual columns except for borneol, isoborneol and the terpin-4-en-1-ol. For limonene as an example, $I_{OV\text{-}101} = 1030 < I_{NON \rightarrow POL} = 1048$, $I_{POL \rightarrow NON} = 1123 < I_{CBWax\ 20M} = 1206$.

These results depend also on the column sequence and advantage can be taken of coupling columns with large polarity differences in series. Indeed, the most retained compounds in one column are the least retained in the other column. Consequently, there are no great changes in the total analysis times when using serially linked columns [10].

The observed values of the retention indices for both coupling sequences 1 and 2 are close to the values given by the first column of the coupled system, *e.g.* for *p*-cymene, $I_{NON \rightarrow POL} = 1064$, $I_{OV\text{-}101} = 1020$, $I_{CBWax\ 20M} = 1272$, $I_{POL \rightarrow NON} = 1153$, $\Delta I_a = (I_{NON \rightarrow POL} - I_{OV\text{-}101}) = 54$. $\Delta I_b = (I_{NON \rightarrow POL} - I_{CBWax\ 20M}) = -208$, $\Delta I_c = (I_{POL \rightarrow NON} - I_{OV\text{-}101}) = 143$, $\Delta I_d = (I_{POL \rightarrow NON} - I_{CBWax\ 20M}) = -119$. In other words, the first column of the couple imposes its polarity on the coupled system, as has been confirmed by Cartoni *et al.* [13]. Thus, the polarity of the system increases in the direct OV-101, NON→POL, POL→NON and Carbowax 20M.

In Table III are reported the ΔI values for some previously poorly separated pairs and their resolutions, $R_{A/B}$, for both orders of column coupling. The sequence POL→NON (Table III) includes some of the problem pairs, *e.g.*, *p*-cymene–β-phellandrene ($\Delta I = 1$, $R_{A/B} = 0.3$) and α-cedrene–α-terpineol ($\Delta I = 2$, $R_{A/B} = 0.4$). For this reason, we chose the order NON→POL for the analysis of cypress essential oil.

Application of serial coupling of capillary columns to the analysis of Algerian cypress essential oil

Essential oils are a typical example of very complex mixtures containing many constituents of different nature, polarities and relative amounts. To optimize the resolution for the cypress oil, we used serial coupling of two columns. First, different temperature programmes have been used, as reported in Table IV. Programme A gave the largest number of peaks with both coupling sequences and was therefore adopted.

Fig. 2 shows the chromatogram obtained with the column order NON→POL. A better separation was achieved for the previously poorly resolved pairs: limonene (No. 16)–1,8-cineole (No. 17) (OV-101, 25 m), 1,8-cineole (No. 17)–β-phellandrene (No. 18) (OV-101, 25 m; GC–MS, FFAP, 50 m). However, the use of the serially coupled capillary system to provide optimized separations can

TABLE III

RESOLUTION ($R_{A/B}$) OF PAIRS OF COMPOUNDS AND THEIR RETENTION INCREMENTS (ΔI)

NON→POL = CP-Sil 5 CB–CP-Wax 57 CB; POL→NON = CP-Wax 57 CB–CP-Sil 5 CB; ΔI: $I_A - I_B$.

Compound pairs A/B	$\Delta I_{OV\text{-}101}$	$\Delta I_{CBWax\ 20M}$ [17]	$\Delta I_{NON\rightarrow POL}$	$\Delta I_{POL\rightarrow NON}$	$R\ (A/B)_{NON\rightarrow POL}$	$R\ (A/B)_{POL\rightarrow NON}$
Limonene[a]/1,8-cineole[a]	1	22	13	14	2.8	5.2
1,8-Cineole[a]/β-phellandrene[a]	7	12	7	15	2.9	7.7
Myrcene[a]/octanal	9	122	45	–	72.7	–
Octanal/*p*-cymene[a]	19	6	13	–	11.1	–
β-Caryophyllene[a]/β-cedrene[a,b]	11	9	8	16	4.9	6.5
Terpenyl acetate[a]/verbenone[a,b]	252	43	88	–	80.3	–
Isoborneol/α-terpineol	48	1	52	153	6	40
Bornel[a]/α-terpineol [18][b,c]	38	37	21	206	3.9	33.9
p-Cymene[a]/β-phellandrene[a]	3	56	4	1	3.2	0.3
α-Cederene[a]/α-terpineol	224	61	108	2	42.9	0.4

[a] Constituents of Algerian cypress essential oil.
[b] Bad resolution by GC–MS (50-m FFAP column).
[c] Ref. 18: GC–MS (50-m FFAP column).

TABLE IV

DIFFERENT TEMPERATURE PROGRAMMES

NON→POL = CP-Sil 5 CB–CP-Wax 57 CB; POL→NON = CP-Wax 57 CB–CP-Sil 5 CB. Explanation: *e.g.*, 80°(8)1°/min 230°(16) means initial temperature 80°C held for 8 min, then increased at 1°C/min to 230°C, the final temperature being maintained for 16 min.

Programme	NON→POL	No. of peaks	POL→NON	No. of peaks
A	80°(8)1°/min230°(16)	107	80°(4)1°/min230°(8)	99
B	80°(0)1°/min230°(16)	94	80°(0)1°/min230°(8)	96
C	80°(4)2°/min230°(16)	74	40°(0)4°/min100°(0)1°/min230°(8)	94
D	60°(4)2°/min230°(16)	79	70°(0)2°/min230°(32)	92
E	60°(8)2°/min230°(16)	76	60°(0)2°/min230°(16)	96

include some new problem pairs, *e.g.*, peaks Nos. 68/69, 89/90 (Fig. 2).

CONCLUSIONS

The proposed method allows some interesting possibilities for the separation of complex mixtures where the various temperature programmes, the order of column coupling and the polarities of the two columns are chosen according to the constitution of each sample mixture.

This technique can be used as a complementary method, in either qualitative or quantitative analysis of essential oils where the titration of an important constituent can be easily made, *e.g.*, 1,8-cineole in eucalyptus oil.

Finally, it is generally preferable to use serial coupling of capillary columns with different polarities than to use only one column with the same length as the total length of the coupled columns but with only one stationary phase, *e.g.*, a 50-m FFAP column in GC–MS [1]. However, in certain circumstances, a single capillary GC column provides a more convenient solution than serially linked capillary columns. For example, limonene, β-phellandrene and 1,8-cineole are completely separable on a column of intermediate polarity, such as RSL 300.

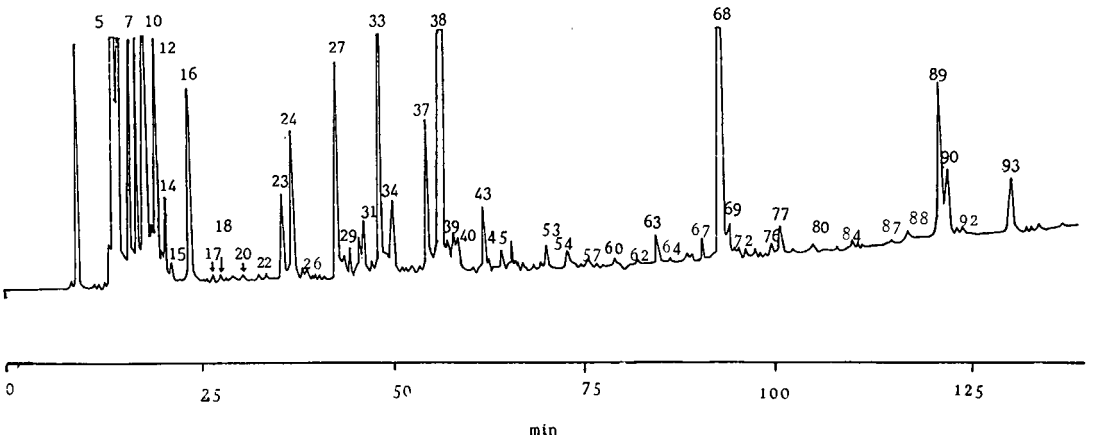

Fig. 2. Chromatogram of Algerian cypress essential oil obtained with the CP-Sil 5 CB–CP-Wax 57 CB (NON→POL) coupled column system. 5 = α-Pinene; 10 = Δ^3-carene; 12 = myrcene; 16 = limonene; 17 = 1,8-cineole; 18 = β-phellandrene; 38 = terpenyl acetate; 39 = β-caryophyllene; 40 = β-cedrene; 68 = cedrol; 89 = sandaracopimaradiene; 93 = dehydroabietane.

REFERENCES

1 N. Chanegriha, *Magister Thesis*, Université des Sciences et de la Technologie Houari Boumediene, Algiers, 1991.
2 G. P. Hildebrand and C. N. Reilley, *Anal. Chem.*, 36 (1964) 47.
3 T. S. Buys and T. W. Smuts, *J. High Resolut. Chromatogr. Chromatogr. Commun.*, 3 (1980) 461.
4 J. Krupcik, G. Guiochon and J. M. Schmitter, *J. Chromatogr.*, 213 (1981) 189.
5 D. F. Ingraham, C. F. Shoemaker and W. Jennings, *J. Chromatogr.*, 239 (1982) 39.
6 J. H. Purnell and P. S. Williams, *J. High Resolut. Chromatogr. Chromatogr. Commun.*, 6 (1983) 569.
7 J. H. Purnell and P. S. Williams, *J. Chromatogr.*, 292 (1984) 197.
8 H. T. Mayfield and S. N. Chesler, *J. High Resolut. Chromatogr. Chromatogr. Commun.*, 8 (1985) 595.
9 J. H. Purnell and P. S. Williams, *J. Chromatogr.*, 321 (1985) 249.
10 G. P. Cartoni, G. Goretti, B. Monticelli and M. V. Russo, *J. Chromatogr.*, 370 (1986) 93.
11 J. H. Purnell, J. R. Jones and M. H. Wattan, *J. Chromatogr.*, 399 (1987) 99.
12 R. J. Jeffrey and J. H. Purnell, *Anal. Chem.*, 62 (21) (1990) 2300.
13 G. P. Cartoni, G. Goretti and M. V. Russo, *Chromatographia*, 23 (1987) 790.
14 Association Française de Normalisation, *Recueil des Normes Françaises des Huiles Essentielles*, AFNOR, Paris, 1982.
15 H. Van den Dool and P. D. Kratz, *J. Chromatogr.*, 11 (1963) 453.
16 H. Van den Dool, *Doctorate Thesis*, University of Groningen, Groningen, 1974.
17 W. Jennings and T. Shibamoto, *Qualitative Analysis of Flavors and Fragrance Volatiles by Glass Capillary Gas Chromatography*, Academic Press, New York, 1980.
18 G. Vernin, J. Metzger, C. Ghiglione, A. Hammoud, K. N. Suon, D. Fraisse and C. Parkanyis, *Phytochemistry*, 27 (1988) 1061.

Journal of Chromatography, 633 (1993) 169–176
Elsevier Science Publishers B.V., Amsterdam

CHROM. 24 766

Automatic determination of N-methylcarbamate pesticides by using a liquid–liquid extractor derivatization module coupled on-line to a gas chromatograph equipped with a flame ionization detector

E. Ballesteros, M. Gallego and M. Valcárcel*

Department of Analytical Chemistry, Faculty of Sciences, University of Córdoba, Córdoba 14004 (Spain)

(First received July 17th, 1992; revised manuscript received November 18th, 1992)

ABSTRACT

A continuous extraction system for the continuous introduction of carbamate pesticide derivatives into a gas–liquid chromatograph was developed. The hydrolysis products of aryl N-methylcarbamates (phenols) were extracted with or without derivatization in a continuous fashion by using ethyl acetate or acetic anhydride in *n*-hexane, respectively. The acetylated phenolic portion of N-methylcarbamates is highly selective, which was taken advantage of to identify six pesticides (propoxur, carbofuran, carbaryl, aminocarb, benthiocarb and methiocarb). The chromatographic responses obtained were linear between 0.2 and 160 mg/l of the different N-methylcarbamates, and the relative standard deviation was 1.9–3.9%.

INTRODUCTION

Carbamate pesticides have become increasingly important in recent years on account of their broad spectrum of biological activity. Gas–liquid chromatography (GLC) is by far the most commonly used technique for the determination of carbamates [1,2]. Direct GLC causes most N-methylcarbamates to be decomposed into their respective phenols to different extents. However, GLC analysis for carbamate phenols is not a widely accepted practice, because the determination of phenols is hindered by the low sensitivity of flame ionization detectors; nevertheless, on derivatization to their ethers [3] or acetates [4], these substances can be readily determined. Chemical derivatization offers some advantages for the determination of carbamates including improved thermal stability, increased sensitivity and the possibility of implementing multi-residue analysis. There are two general approaches to the determination of derivatized N-methylcarbamates, namely with derivatization of the intact pesticide or of one of its hydrolysis products, which include the volatile methylamine. Methods for the derivatization and extraction of pesticides have been the subject of excellent reviews [5,6]. Reagents such as heptafluorobutyric anhydride [7,8], pentafluoropropionic anhydride [9] and pentafluorobenzyl bromide [10,11] have been employed for this purpose. However, chemical derivatization involves additional steps that result in analyte losses through manipulation. Moreover, many derivatizing reagents are toxic, carcinogenic or explosive. Alternative techniques used for the determination of N-methylcarbamates include spectrophotometry [12], TLC [13] and HPLC [14–17].

Flow-injection analysis (FIA) has also been employed for the determination of carbamates [18]. Various continuous separation systems have been used in combination with chromatographic techniques for this purpose. Thus, one method using a

* Corresponding author.

0021-9673/93/$06.00

continuous-flow extraction system for the determination of organophosphorus pesticides was developed by Farran and co-workers, who used HPLC and UV detection [19] plus MS characterization [20]. Two GC methods for the determination of a variety of phenols in water samples by use of a continuous liquid–liquid extraction–derivatization system were also recently developed; quantification with a flame ionization detector was done with manual injection [21] or via an injection valve allowing 4 μl of vaporized sample to be introduced directly via the instrument's injection port [22]. Also, a continuous gas-diffusion separation system was combined with an electron-capture detection system [23] for the continuous generation and determination of volatile species such as chlorine and sulphur dioxide.

The aim of this work was to reduce human involvement in the determination of N-methylcarbamate pesticides, particularly as regards sample treatment, reaction development and transfer of the treated sample to the detector. This was accomplished by using a continuous liquid–liquid extractor for the simultaneous extraction, with or without derivatization, of various N-methylcarbamates, which was connected on-line to a gas chromatograph. The acetate esters of the hydrolysis products of six N-methylcarbamates were formed by adding acetic anhydride to the *n*-hexane extractants used.

EXPERIMENTAL

Apparatus

The flame ionization detector used was built into a Hewlett-Packard Model 5890 A gas chromatograph. Chromatographic assays were performed on a cross-linked 50% phenyl–50% methylpolysiloxane (film thickness 2.0 μm) fused-silica column (10 m × 0.53 mm I.D.) supplied by Hewlett-Packard (HP-17). Nitrogen was used as the carrier gas at a flow-rate of 35 ml/min. The injector and detector temperatures were kept at 150 and 220°C, respectively, throughout. The temperature programme of the chromatographic oven was either (a) 100°C (held for 2 min), increased at 35°C/min to 175°C (held for 1 min), at 25°C/min to 210°C (held for 1 min) and at 50°C/min to 250°C (held for 3 min) or (b) increased at 8°C/min from 100 to 130°C (held for 3 min), at 15°C/min to 170°C (held for 1 min) and at 30°C/min to 250°C (held for 3 min), to separate the hydrolysis products and their acetates, respectively. Peak areas were measured by using a Hewlett-Packard 3392 A integrator. The flow extraction–derivatization system consisted of a Gilson Minipuls-2 peristaltic pump, a Tecator A-10 T solvent segmenter and a custom-made phase separator furnished with a Fluoropore membrane (1.0 μm pore size, FALP; Millipore) [24]. Poly(vinyl chloride) and Solvaflex pump tubing for aqueous and *n*-hexane solutions, respectively, displacement bottles for pumping ethyl acetate and PTFE tubing for coils were used. A Knauer 6332000 six-port switching valve and a thermostated water-bath were also employed.

Standards and reagents

N-Methylcarbamates were purchased from Dr. Ehrenstorfer (Augsburg), at 97–99% purity. Phenanthrene (internal standard) and all other reagents (acetic anhydride, sodium hydroxide, *n*-hexane and ethyl acetate) were supplied by Merck.

Preparation of test solutions

Stock standard solutions of propoxur, carbofuran and carbaryl (I) or propoxur, benthiocarb, carbofuran, aminocarb, carbaryl and methiocarb (II) for extraction and extraction–derivatization, respectively, were prepared at a concetration of 2 g/l of each pesticide in 99.9% acetone and stored in PTFE bottles at 4°C. Appropriate volumes of these stock solutions were diluted with doubly distilled water to prepare 25 ml of solutions containing between 0.2 and 160 mg/l of each pesticide in $4 \cdot 10^{-3}$ *M* (I) or $1.2 \cdot 10^{-2}$ *M* (II) sodium hydroxide (hydrolysis reagent). Ethyl acetate containing 100 mg/l of phenanthrene (internal standard) for extraction, and *n*-hexane containing the same concentration of phenanthrene plus 8% (v/v) of acetic anhydride (derivatization reagent) for extraction–derivatization, were used as extractants.

Sample introduction system

The system used to introduce the extracted samples into the gas chromatograph is depicted in Fig. 1. The interface between the extraction system and the gas chromatograph has been described elsewhere [22]. The injection interface was constructed by using an injection valve originally designed for

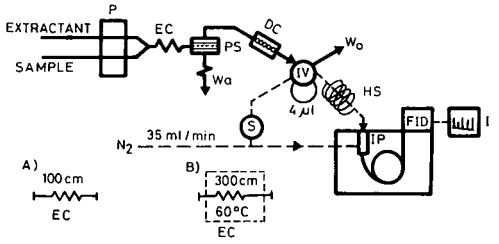

Fig. 1. Flow-injection system for the extraction and extraction–derivatization of N-methylcarbamate pesticides. EC = extraction coil (A for extraction and B for extraction–derivatization); PS = phase separator; DC = desiccating column; IV = injection valve; HS = heating system; S = tube stopcock; IP = injection port; FID, flame ionization detector; I = integrator.

HPLC; the large volume of the valve loop was reduced to 4 µl and a 25-cm stainless-steel tube was fitted to the carrier outlet of the valve. The tube had a stainless-steel needle soldered on one end, which allowed direct fitting of the valve to the injection port of the gas chromatograph by inserting its needle into the septum of the instrument port. This tube linking the valve and the injection port was heated by means of a wire coiled helically around a hollow ceramic tube that could be heated between 25 and 175 °C. The inlet for the carrier gas (nitrogen at 35 ml/min) of the chromatograph was split into two parts that were connected directly to the carrier inlet of the valve (flow-rate 25 ml/min) and the chromatograph injection port (flow-rate 10 ml/min), respectively. The inlet was shut by a stopcock so that the instrument could be used for manual injections by allowing the nitrogen stream to follow its normal pathway through the instrument.

Procedure

Fig. 1 depicts the combined extraction analyser–chromatographic system used. The aqueous sample, containing sodium hydroxide, was continuously mixed with a stream of ethyl acetate (for extraction of the hydrolysis products) or *n*-hexane (for simultaneous extraction–derivatization). The extracts were used to load the loop of the injection valve. The loop contents (4 µl) were transferred to the chromatograph port by the nitrogen carrier gas. The section of the tube valve port was heated at 120 or 125 °C for extraction and extraction–derivatization of the pesticides, respectively, in order to prevent samples from being adsorbed on the tube walls during transfer. A desiccating column (5 cm × 3 mm I.D.) packed with sodium aluminosilicate pellets (pore diameter 4 Å) was used prior to the injection valve to prevent any water from reaching the column.

RESULTS AND DISCUSSION

Four organic solvents (ethyl acetate, toluene, *n*-hexane and dichloromethane) were tried as extractants for the N-methylcarbamates. Ethyl acetate was found to be the most efficient for hydrolysable pesticides (extraction yields ranged between 60 and 80%). On the other hand, simultaneous acylation with acetic anhydride and extraction with *n*-hexane, toluene and dichloromethane was similar in efficiency. Toluene and dichloromethane were discarded as they caused the PTFE membrane of the phase separator to deteriorate rapidly, so *n*-hexane was finally chosen for extraction–derivatization of the hydrolysis products. Extracted underivatized hydrolysis products could not be fully resolved; in fact, the peaks of benthiocarb, aminocarb and methiocarb were markedly overlapped. Conversion of the hydrolysis products into their esters allowed the sequential separation of the above-mentioned pesticides plus carbaryl, carbofuran and propoxur.

Optimization of the extraction unit

The experimental conditions studied included the sodium hydroxide, ethanol and acetic anhydride concentrations, the flow-rates of the aqueous and organic phases, the temperature and the extraction coil length. Thus, a sample solution containing 10 mg/l of each N-methylcarbamate from standard solutions I or II for extraction and extraction–derivatization, respectively, were prepared in doubly distilled water. Table I gives the optimum conditions for the preparation of the samples and extractants and operation of the flow extraction system.

According to the literature, the hydrolysis of N-methylcarbamates is best accomplished in alkaline ethanol media [12]. The influence of the sodium hydroxide concentration was studied over the range $0–2 \cdot 10^{-2}$ *M*. In the absence of alkali, the peaks in the gas chromatogram obtained corresponded to intact N-methylcarbamates and their hydrolysis products because the carbamates were partially

TABLE I

OPTIMUM CONDITIONS FOR THE DETERMINATION OF N-METHYLCARBAMATES

Parameter	Range studied	Optimum range	Selected value
NaOH[a] (*M*)	$0–2 \cdot 10^{-2}$	$2 \cdot 10^{-3}–5 \cdot 10^{-3}$	$4 \cdot 10^{-3}$
NaOH[b] (*M*)	$0–2 \cdot 10^{-2}$	$8 \cdot 10^{-3}–2 \cdot 10^{-2}$	$1.2 \cdot 10^{-2}$
Ethanol[a] (%)	0–4	0–2.4	–
Acetic anhydride[b] (%)	0–12	6–12	8
Reactor temperature[b] (°C)	20–100	50–70	60
Extraction coil length[a] (cm)	20–300	50–300	100
Extraction coil length[b] (cm)	20–500	125–500	300
Flow-rate[a,b] (ml/min):			
aqueous phase	0.4–2.8	1.0–2.8	2.7
organic phase	0.2–1.6	0.3–0.8	0.7
Nitrogen flow-rate[a,b] (ml/min)	15–65	25–50	35
Tube valve port temperature[a] (°C)	25–160	110–125	120
Tube valve port temperature[b] (°C)	25–160	100–150	125

[a] Extraction method.
[b] Extraction–derivatization method.

transformed into their corresponding phenols, which rendered quantitative interpretation of the results difficult. In the presence of sodium hydroxide, however, only the peaks of the hydrolysis products (phenols) were obtained. In order to ensure complete hydrolysis of the pesticides, different amounts of ethanol were added to the samples. Reaction development did not seemingly depend on the ethanol concentration because the N-methylcarbamates were instantaneously hydrolysed to their corresponding phenols by sodium hydroxide alone. The ionic strength, which was adjusted with potassium nitrate, did not affect the signal in the extraction or extraction–derivatization method up to 1.5 *M*. The influence of the acetic anhydride concentration on the yield of acetate derivatives of the hydrolysis products was investigated by using several solutions in *n*-hexane. A 6% solution was found to be adequate for derivatization purposes (Fig. 2); lower concentrations resulted in incomplete derivatization of the phenols and in chromatograms including the peaks of both the underivatized and the derivatized hydrolysis products.

The effect of the extraction coil temperature was studied over the range 15–100°C. This variable affected the extraction yield only when extraction and derivatization were performed simultaneously as a result of ester formation being favoured by heating. Below 50°C, the chromatograms showed the peaks of both the underivatized and the derivatized hydrolysis products. The extraction coil was maintained at room temperature or heated at 60°C for extraction and extraction–derivatization, respectively (Fig. 1).

The flow-rates of the sample and extractant were also optimized. Increasing the sample flow-rate (at a constant organic phase flow-rate) resulted in increased peak areas through increased preconcentration ratios. Obviously, the peak areas also increased with decreasing organic phase flow-rate (at a con-

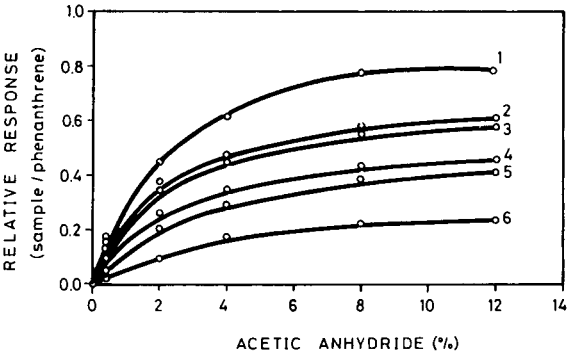

Fig. 2. Effect of the acetic anhydride concentration (%) on the derivatization reaction. 1 = Aminocarb; 2 = methiocarb; 3 = benthiocarb; 4 = carbofuran; 5 = propoxur; 6 = carbaryl. For GC conditions, see text.

stant sample flow-rate) for the same reason. Flow-rates were chosen as a compromise between adequate reproducibility, preconcentration ratio and sampling frequency. Thus, we chose sample and organic phase flow-rates of 2.7 and 0.7 ml/min, respectively. The influence of the residence time was studied at different extraction coil lengths between 20 and 500 cm and the aforementioned sample and extractant flow-rates. The peak area of the underivatized hydrolysis products was not significantly affected by the coil length; however, if the compounds were extracted and derivatized simultaneously, the coil length was somehow influential as esters required some time to form. As shown in Fig. 3, a reaction coil longer than 125 cm was required for the simultaneous extraction–derivatization of all the pesticides. A derivatization–extraction coil length of 300 cm, which resulted in a residence time of 10.5\s, was chosen.

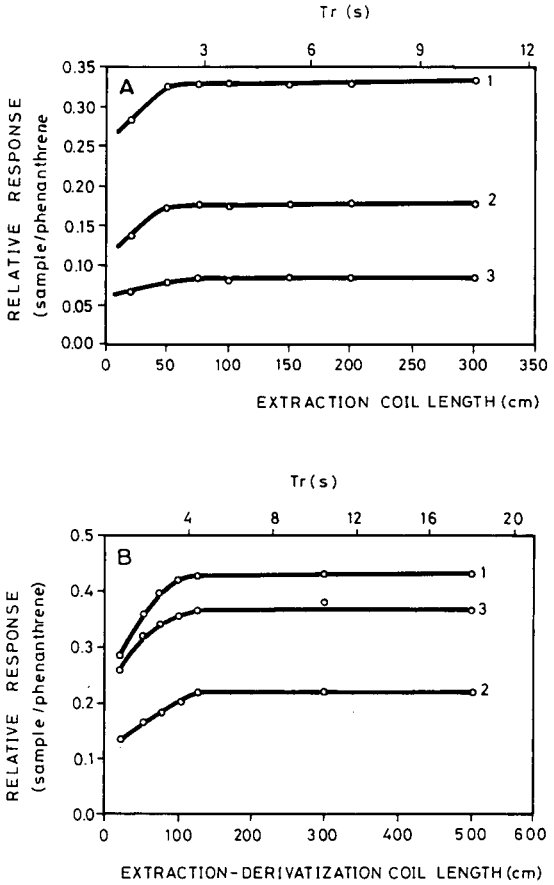

Fig. 3. Effect of the coil length through the residence time (Tr) on (A) the extraction and (B) the extraction–derivatization of (1) propoxur, (2) carbofuran and (3) carbaryl. For GC conditions, see text.

Optimization of the sample introduction device

The extraction unit described above was fitted to the chromatograph via a modified injection valve (see Experimental). Earlier experiments [22] showed that coupling a liquid–liquid extractor to a gas chromatograph required that the carrier gas stream (nitrogen) be split into two: one to be passed through the loop of the injection valve in order to flush the sample into the chromatograph and other to be circulated through the gas inlet of the instrument. Also, the tube linking the valve and the injection port must be heated in order that the sample may reach the chromatograph in vaporized form. The overall flow-rate of carrier gas passed through the valve and the injection port was varied between 15 and 65 ml/min. A flow-rate higher than 25–30 ml/min was required to offset the background signal. An overall gas flow-rate of 35 ml/min (flow-rates through the valve and injection port 25 and 10 ml/min, respectively) was found to be optimum. Higher flow-rates resulted in diminished signals through sample dispersion on the gas side and in the risk of extinction of the detector flame. By using the heating system described under Experimental, the tube valve port was heated at different temperatures (Table I). Fig. 4 shows the chromatograms obtained by injecting extracts of the six derivatized pesticides in *n*-hexane. The first chromatogram (Fig. 4A) was recorded with automatic injection at room temperature and the third (Fig. 4C) with heating at 125 °C. As can be seen, injection at room temperature (Fig. 4A) provided overlapped peaks, so no individual pesticides could be identified. In addition, the background signal was tall owing to adsortion of the pesticides on the walls of the tube valve port, which resulted in sluggish passage through the column and analyte losses. On heating at 125°C (Fig. 4C), the analytes reached the injection port in the vapour phase, so they were readily flushed trough the valve port connecting tube, thereby avoiding clogging the tube and dilution of the analytes in the carrier gas prior to reaching the chromatographic column. Similar results were obtained by extracting the hydrolysis products into ethyl acetate.

TABLE II

FEATURES OF THE CALIBRATION GRAPHS AND DETERMINATION OF HYDROLYSED AND ACETYLATED N-METHYLCARBAMATES

Compound	Regression equation[a]	Correlation coefficient	Linear range (mg/l)	Detection limit (mg/l)	R.S.D. (%)
Propoxur[b]	$y = 8.1 \cdot 10^{-3} + 3.96 \cdot 10^{-2}x$	0.999	0.2–4	0.2	3.80
Carbofuran[b]	$y = -2.4 \cdot 10^{-3} + 4.02 \cdot 10^{-2}x$	0.999	0.2–4	0.2	3.92
Carbaryl[b]	$y = -6.9 \cdot 10^{-3} + 1.23 \cdot 10^{-2}x$	0.997	0.8–4	0.4	3.88
Propoxur[b]	$y = 1.9 \cdot 10^{-2} + 2.97 \cdot 10^{-2}x$	0.999	2–40		2.52
Carbofuran[b]	$y = -1.7 \cdot 10^{-2} + 1.92 \cdot 10^{-2}x$	0.999	2–40		3.00
Carbaryl[b]	$y = 6.3 \cdot 10^{-3} + 7.50 \cdot 10^{-3}x$	0.999	2–40		3.53
Propoxur[c]	$y = 2.3 \cdot 10^{-2} + 4.23 \cdot 10^{-2}x$	0.995	0.2–4	0.2	3.48
Benthiocarb[c]	$y = 3.3 \cdot 10^{-2} + 6.90 \cdot 10^{-2}x$	0.997	0.2–4	0.2	2.97
Carbofuran[c]	$y = 2.8 \cdot 10^{-2} + 3.81 \cdot 10^{-2}x$	0.999	0.4–4	0.2	3.52
Aminocarb[c]	$y = -1.3 \cdot 10^{-2} + 7.20 \cdot 10^{-2}x$	0.997	0.4–4	0.4	2.47
Carbaryl[c]	$y = 2.2 \cdot 10^{-2} + 2.17 \cdot 10^{-2}x$	0.996	0.4–4	0.4	3.00
Methiocarb[c]	$y = 4.5 \cdot 10^{-3} + 4.71 \cdot 10^{-2}x$	0.997	0.4–4	0.4	3.50
Propoxur[c]	$y = -2.8 \cdot 10^{-2} + 4.05 \cdot 10^{-2}x$	0.998	4–40		3.15
Benthiocarb[c]	$y = -3.6 \cdot 10^{-2} + 6.00 \cdot 10^{-2}x$	0.998	4–40		3.20
Carbofuran[c]	$y = -4.2 \cdot 10^{-2} + 4.62 \cdot 10^{-2}x$	0.997	4–40		2.95
Aminocarb[c]	$y = -1.2 \cdot 10^{-2} + 7.86 \cdot 10^{-2}x$	0.998	4–40		2.15
Carbaryl[c]	$y = -1.0 \cdot 10^{-1} + 3.24 \cdot 10^{-2}x$	0.994	4–40		2.15
Methiocarb[c]	$y = -9.0 \cdot 10^{-2} + 6.60 \cdot 10^{-2}x$	0.998	4–40		2.94

[a] y = Analyte peak area/internal standard peak-area ratio; x = concentration (mg/l).

[b] Extraction method.

[c] Extraction–derivatization method.

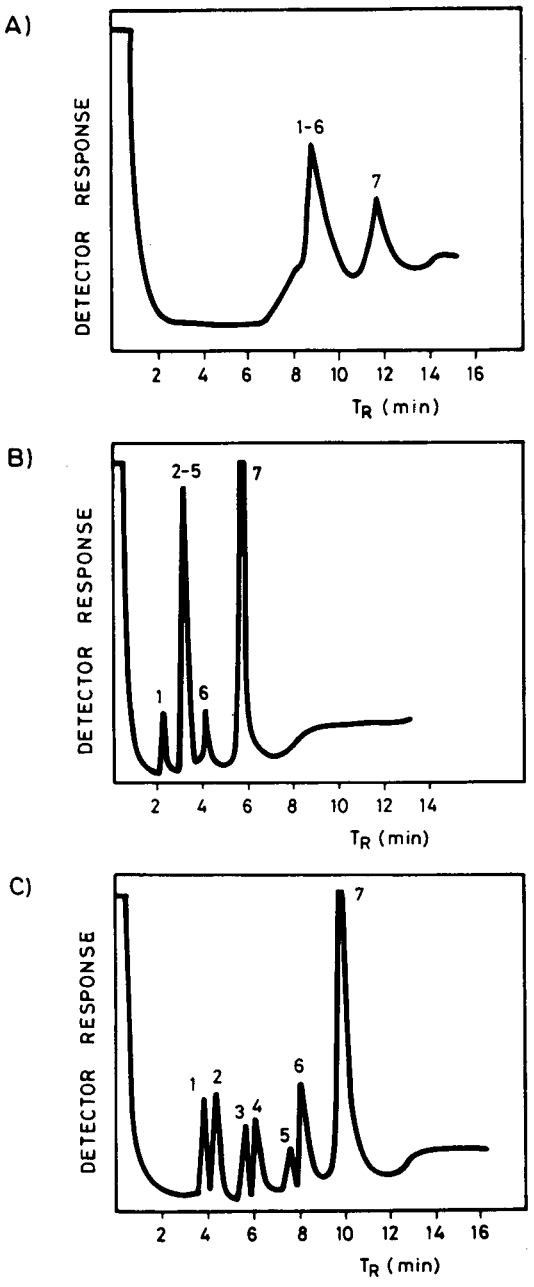

Fig. 4. Gas chromatograms of extracted N-methylcarbamates pesticides. (A) Acetate derivatives without heating the tube valve port. (B) Underivatized hydrolysis products. (C) Acetate derivatives with heating of the tube valve port at 125°C. Concentration of N-methylcarbamates in the aqueous sample, 8 mg/l. Extractants, 6% acetic anhydride in (A,C) *n*-hexane or (B) ethyl acetate. Peaks: 1 = propoxur; 2 = benthiocarb; 3 = carbofuran; 4 = aminocarb; 5 = methiocarb; 6 = carbaryl; 7 = internal standard (phenanthrene).

Determination of N-methylcarbamates

The GC separation of the underivatized and acetylated hydrolysis products (carbamate phenols) is illustrated in Figs. 4B and C, respectively. As can be seen, the peaks of the hydrolysis products of benthiocarb, aminocarb, methiocarb and carbofuran extracted into ethyl acetate were completely overlapped, so derivatization of these pesticides was essential for identification.

The calibration graphs for extracted and extracted–derivatized carbamates were linear throughout the concentration range studied (0.2–160 mg/l). The figures of merit of these graphs at two integrator sensitivities, and those of the analytical procedure, are summarized in Table II. The detection limit was calculated as the concentration yielding the minimum detectable signal in the chromatogram. The relative standard deviation (R.S.D.) was calculated from eleven samples containing intermediate concentrations (1, 20 or 80 mg/l) of each pesticide in the linear range assayed (0.2–4, 2–40 and 40–160, respectively). It ranged between 1.9 and 2.6% for concentrations between 40 and 160 mg/l. Reproducibility was measured by injecting a sample containing also intermediate concentrations of the analytes eleven times; the R.S.D. values thus obtained ranged between 0.4 and 0.7%.

CONCLUSIONS

The two proposed continuous methods for extraction and extraction–derivatization of the phenolic portion of N-methylcarbamates prior to introduction into a gas chomatograph yield better analytical results in terms of precision, throughput and economy than their manual counterparts, which are more laborious (and hence prone to analyte losses) and consume greater amounts of reagents. The sample introduction system used allows the complete introduction of small volumes of low-volatility samples into the instrument injection port, which simplifies on-line coupling of the extractor and the chromatograph without the need to alter the latter in any way.

The sensitivity (slope of the calibration graph) of both methods (extraction and extraction–derivatization) is similar for propoxur and carbofuran. Carbaryl differs in that it results in a low sensitivity when extracted from the phenolic portion (1-naph-

thol). Formation of the carbamate derivative (acetylated 1-naphthol) not only prevents on-column decomposition, but also facilitates detection through increased sensitivity. Excess of acetic anhydride (the derivatizing reagent) causes no disturbance as its peaks overlapped with those of the extractant. Finally, the derivatives of the phenolic portion of the carbamates allow the identification of aminocarb, benthiocarb and methiocarb, which is impossible without derivatization under the chromatographic conditions used.

ACKNOWLEDGEMENT

This work was financially supported by the Spanish CICYT (Grant No. PB90-0925).

REFERENCES

1 B. D. Ripley and A. S. Y. Chau, in A. S. Y. Chau and B. K. Afghan (Editors), *Analysis of Pesticides in Water. Vol III. Nitrogen-Containing Pesticides*, CRC Press, Boca Raton, FL, 1982.
2 D. Bullock, in G. Zweig (Editor), *Analytical Methods for Pesticides and Plant Growth Regulators*, Vol. 6, Academic Press, London, 1972, pp. 478–482.
3 L. Ogierman, *J. Assoc. Off. Anal. Chem.*, 65 (1982) 1452.
4 R. T. Coutts, E. E. Hargesheimer and F. M. Pasutto, *J. Chromatogr.*, 195 (1980) 105.
5 J. F. Lawrence, *J. Chromatogr. Sci.*, 17 (1979) 113.
6 K. G. Furton and J. Rein, *Anal. Chim. Acta*, 236 (1990) 99.
7 J. F. Lawrence, D. A. Lewis and H. A. McLeod, *J. Chromatogr.*, 138 (1977) 143.
8 K. Nagasawa, H. Uchiyama, A. Ogamo and T. Shinozuka, *J. Chromatogr.* 144 (1977) 78.
9 T. Talbi, *Grasas Aceites (Seville)*, 32 (1981) 381.
10 G. H. Tjan and T. A. Jansen, *J. Assoc. Off. Anal. Chem.*, 62 (1979) 769.
11 R. E. Cline, G. D. Todd, D. L. Ashley, J. Grainger, J. M. McCraw, C. C. Alley and R. H. Hill, *J. Chromatogr. Sci.*, 28 (1990) 167.
12 M. C. Quintero, M. Silva and D. Perez-Bendito, *Analyst*, 114 (1989) 497.
13 H. De la Vigne and D. Janchen, *J. Planar Chromatogr.–Mod. TLC*, 3 (1990) 6.
14 A. Di Corcia and M. Marchetti, *Anal. Chem.*, 63 (1991) 580.
15 C. H. Marvin, I. D. Brindle, R. P. Singh, C. D. Hall and M. Chiba, *J. Chromatogr.*, 518 (1990) 242.
16 M. E. Leon-Gonzalez and A. Townshend, *J. Chromatogr.*, 539 (1991) 47.
17 W. Blad, *Fresenius' J. Anal. Chem.*, 339 (1991) 340.
18 R. Kindervater, W. Kuennecke and R. D. Schmid, *Anal. Chim. Acta*, 234 (1990) 113.
19 A. Farran, J. De Pablo and S. Hernández, *Anal. Chim. Acta*, 221 (1988) 123.
20 A. Farran, J. L. Cortina, J. De Pablo and D. Barcelo, *Anal. Chim. Acta*, 234 (1990) 119.
21 E. Ballesteros, M. Gallego and M. Valcárcel, *J. Chromatogr.*, 518 (1990) 59.
22 E. Ballesteros, M. Gallego and M. Valcárcel, *Anal. Chem.*, 62 (1990) 1587.
23 M. Novic, L. Zupancic-Kralj and B. Pihlar, *Anal. Chim. Acta*, 243 (1991) 131.
24 M. Gallego, M. Silva and M. Valcárcel, *Anal. Chem.*, 58 (1986) 2265.

Journal of Chromatography, 633 (1993) 177–183
Elsevier Science Publishers B.V., Amsterdam

CHROM. 24 741

Determination of toxaphene in soil by electron-capture negative ion mass spectrometry after fractionation by high-performance gel permeation chromatography

William C. Brumley* and Cynthia M. Brownrigg

US Environmental Protection Agency, Environmental Monitoring Systems Laboratory, P.O. Box 93478, Las Vegas, NV 89193-3478 (USA)

Andrew H. Grange

Lockheed Engineering and Sciences Company, Environmental Program Office, 980 Kelly Johnson Drive, Las Vegas, NV 89119 (USA)

(First received September 2nd, 1992; revised manuscript received November 3rd, 1992)

ABSTRACT

Toxaphene is extracted from soil by standard procedures using Soxhlet or sonication methods. The extract is fractionated by high-performance gel permeation chromatography (HPGPC), which separates toxaphene from the bulk of co-extractives including polychlorinated biphenyls. This HPGPC fractionation has broad application to many problems of environmental analysis. A solid-phase extraction cleanup with silica gel further removes any polar components present in the collected fraction. Determination of toxaphene is accomplished by electron-capture negative ion mass spectrometry (ECNI-MS) after introduction by capillary gas chromatography. Levels down to 100 μg/kg in soil are obtainable. Brief mention is made of high-resolution ECNI-MS carried out at a resolution of 10 000.

INTRODUCTION

Toxaphene is a multi-component mixture of chlorinated terpenes, primarily based on the C_{10} structure of bornane [1–5]. Hundreds of individual compounds make up the commercial pesticide. Although toxaphene is now limited in use, interest in its analysis continues because of its persistence and widespread transport in the environment [4,6–10].

Current US Environmental Protection Agency (EPA) methodology (SW-846) [11] consists of electron ionization mass spectrometry (MS) and gas chromatography (GC)–electron-capture detection methods (8270 and 8080) [11], both of which are greatly affected by interferences such as polychlorinated biphenyls (PCBs), chlordane and other pesticides. Swackhamer *et al.* [4] published an electron-capture negative ion (ECNI) method that was selective and lowered detection limits for toxaphene in fish. Their work was based, in part, on previous studies indicating the advantages of negative ion approaches [2,3,12]. Currently, no negative ion methods are recommended in SW-846, despite recent examinations that suggest the technique is useful [13–15] when due caution is exercised [16].

In our work, the negative ion approach is extended to soil matrices with the use of high performance gel permeation chromatography (HPGPC) [17,18] and solid-phase extraction cartridges [19,20]. Results obtained with high-resolution ECNI-MS [21,22] at a resolution of 10 000 are briefly discussed

* Corresponding author.

in the context of resolving potentially interfering ions that contain oxygen [4] from those of the same nominal mass that come from toxaphene.

EXPERIMENTAL

Chemicals

Toxaphene, chlordane, other pesticides, and PCB reference standards were obtained from the EPA Repository (Research Triangle Park, NC, USA). The following solutions from the Repository are defined: Pesticides II: aldrin, α-benzene hexachloride (BHC), β-BHC, γ-BHC, 4,4′-DDD, 4,4′-DDE, 4,4′-DDT, dieldrin, α-endosulfan, β-endosulfan, endosulfan sulfate, endrin, endrin aldehyde, heptachlor and heptachlor epoxide; Acid Extractables II: benzoic acid, *p*-chloro-*m*-cresol, 2-chlorophenol, *o*-cresol, *p*-cresol, 2,4-dichlorophenol, 2,4-dimethylphenol, 4,6-dinitro-*o*-cresol, 3,4-dinitrophenol, 2-nitrophenol, 4-nitrophenol, pentachlorophenol, phenol, 2,4,5-trichlorophenol and 2,4,6-trichlorophenol; Basic Extractables: 4-chloroaniline, 2-nitroaniline, 3-nitroaniline and 4-nitroaniline. Additional pesticide standards were purchased from Supelco (Bellefonte, PA, USA). Chem Service (West Chester, PA, USA) was the source of 2,2′,3,4,4′,5,6,6′-octachlorobiphenyl (OCB). [$^{13}C_1$]Chlordane (CHL) was obtained from Cambridge Isotope Laboratories (Woburn, MA, USA). Methylene chloride, methanol, diethyl ether and hexane were obtained from Burdick & Jackson (Muskegon, MI, USA).

Extraction/cleanup

Soils consisted of Nevada soil obtained locally; soil from Eagle Harbor, Puget Sound, Washington; organic potting soil purchased locally; and clay of unknown origin. The soils were weighed out and then spiked with the appropriate amount of toxaphene standard in hexane at a concentration of 50 ng/μl. The spiked soil was throroughly mixed after spiking.

Extraction was accomplished according to standard methods (3540 and 3550) [11]. Micro-Soxhlet extractions of 2-g samples were performed with a Wheaton micro-Soxhlet apparatus using methylene chloride. Sonication extraction of 20–30-g soil samples used a methylene chloride–acetone (1:1, v/v) solvent with a Heat Systems-Ultrasonic sonicator, Model XL2020 (Farmingdale, NY, USA).

Extracts were concentrated to about 0.5 ml for injection into a GPC system consisting of a guard column (50 × 7.8 mm) and two standard columns (250 × 22.5 mm) in tandem packed with Phenogel 10-μm particles of 100 Å pore size. The system was equipped with a Valco (Houston, TX, USA) injector, Isco (Lincoln, NE, USA) UA-5 detector, Isco 260D syringe pump, and Isco Foxy 200 fraction collector. The flow was 7 ml/min [17] and fractions 29–31 (14:00–15:30 min:s) were collected for toxaphene (12-mm diameter tubes, 30 s per tube) with a retention time of about 15 min using methylene chloride as solvent.

Solid-phase extraction cleanup used Supelco 3-g silica cartridges that were pre-rinsed with 6 ml of hexane, 6 ml of hexane–diethyl ether (50:50, v/v), and 6 ml of hexane. The sample was applied in 0.5 ml of hexane followed by elution with 0.4 ml of hexane, and 4 ml of diethyl ether–hexane (5:95). The eluent was concentrated to a 1.0–0.1-ml volume as appropriate and spiked with internal standards at 0.5 mg/kg level for unknowns or at a ratio of approximately 80 pg OCB and 1.2 ng CHL to 50 ng toxaphene standard. The CHL internal standard was primarily used for retention time reference.

GC–MS

A J&W DB-5 column (Folsom, CA, USA) 30 m × 0.25 mm I.D. (0.25-μm film thickness) was used with a flow-rate of 38 cm/s at 60°C. The initial temperature was 60°C for 3 min followed by a program rate of 20°C/min to 300°C. A Finnigan-MAT (San Jose, CA, USA) 4021 was operated in the negative ion mode at a source temperature setting of 170°C and 0.50 mA filament emission current with an electron energy of 70 eV; methane was used as the moderator gas for electron capture (0.40 Torr source pressure reading; 1 Torr = 133.322 Pa).

The following ions were monitored: *m/z* 309, 311, 326, 341, 342, 343, 345, 377, 379, 381, 410, 411, 413, 415, 430, 444, 447 and 449; dwell time was 0.05 s/ion with a total cycle time of 1.025 s. Only the areas of the ions at *m/z* 341, 343, 345, 377, 379, 381, 411, 413, 415, 447 and 449 with appropriate scan ranges were summed (with an area threshold) to determine response factors and to quantify toxaphene in extracts.

The standard glass GC injector insert of the Finnigan 9610 GC system was modified by a glass-

blower (Supelco) to have a restriction that passed a 26-gauge syringe needle for injection but not a 0.53 mm I.D. capillary inserted from the oven side as a retention gap. A standard 10-μl Hamilton syringe (Reno, NV, USA) fitted with 13-cm needle was then used for on-column injections with the modified insert acting as a needle guide.

High-resolution ECNI-MS

A DB-5 column 30 m × 0.25-mm I.D. (0.25-μm film thickness) was used with on-column injections using a retention gap on a Hewlett-Packard 5890A gas chromatograph. The temperature program was that of Swackhamer *et al.* [4]: 80°C for 1 min; 10°C/min to 200°C; 1.5°C/min to 230°C; 10°C/min to 250°C. The mass spectrometer was a Fisons/VG 70-250SE operated in the negative ion mode with filament current of 0.200 μA at an electron energy of 50 eV, source temperature of 110°C, −8 kV accelerating voltage, and methane as moderator gas at a source housing pressure of about $1 \cdot 10^{-4}$ mbar. Fomblin (Ultramark 1600; PCR, Gainesville, FL) was used as calibrant. Resolutions were determined using peak widths displayed by the selected ion recording software.

RESULTS AND DISCUSSION

Quantitation procedure

The ions monitored for toxaphene consist of the $(M-Cl^{\bullet})^-$ ions resulting from $C_{10}H_{12}Cl_6$ through $C_{10}H_8Cl_{10}$ elemental compositions (bornanes) and overlapping contributions from $(M-Cl^{\bullet})^-$ ions resulting from $C_{10}H_{10}Cl_6$ through $C_{10}H_6Cl_{10}$ (bornenes). We have found that ion pairs at *m/z* 309 and 311 and *m/z* 447 and 449 contribute little to the overall toxaphene response and were eliminated from consideration. In addition, the *m/z* 309–311 range was also subject to matrix contributions. The areas of the 11 ions given in the experimental section were integrated by automated procedures and summed to obtain a response for toxaphene. The response of the internal standard was obtained from the area of *m/z* 430 of OCB. An average response factor based on at least five runs of toxaphene standards spiked with OCB was used in quantitating toxaphene in soil extracts. As a control measure, the response factor was checked daily to confirm that it fell within ± 15% of the average response factor.

Previous work [4] included correction factors due to the presence of coextractives in quantitating toxaphene. In our work, no corrections were necessary for the presence of chlordane. Nevertheless, its presence (along with heptachlor and nonachlor) was monitored by the responses at *m/z* 342, 410 and 444 in order to assess potential contributions to ions indicative of toxaphene.

Responses of PCBs, which are also potential interferences, were monitored at *m/z* 326 (pentachlorobiphenyls) and 430 (octachlorobiphenyls). PCBs constitute an interference due to the oxygen reaction producing $(M - Cl + O)^-$ ions that are of the same nominal mass as ions monitored for toxaphene. We suspect that it is common for operators not to be able to completely eliminate the oxygen reaction in certain instruments. Our HPGPC cleanup, however, eliminates PCBs prior to determination of toxaphene by ECNI-MS and no correction for their presence is needed.

Results of the determination of toxaphene in soil

Table I provides results of analyses of unspiked (blank) soils (samples 4, 6, 11, 13, 15, 17 and 19) and spiked soils (samples 1–3, 5, 7–10, 12, 14, 16, 18 and 20) for toxaphene ranging from spiking levels of 100 μg/kg (samples 3 and 16) to 10.0 mg/kg (sample 10). Samples spiked with chlordane and other pesticides, PCBs, anilines and phenols were analyzed as well as soils already contaminated with polynuclear aromatics (PNAs) (samples 11 and 12). Fig. 1A and B gives example chromatograms of *m/z* 377 from a standard and from a cleaned-up extract (sample 18) at a spiked level of 0.5 μg/kg, respectively. Fig. 1C shows an example of a toxaphene standard taken through the cleanup. Chromatographic patterns and relative ion abundances remain largely consistent between standards and extracts. There are, however, some changes in the pattern caused by the cleanup.

For spiked samples, one could assess comparisons of ion chromatographic patterns using a standard taken through the cleanup. For real samples, however, weathering [23] could alter relative contributions of specific components of toxaphene that could vary on a case-by-case basis. This possibility and the results discussed later led us to rely solely on quantitations obtained using the toxaphene standard directly. We found, for example, that for a

TABLE I

DETERMINATION OF TOXAPHENE IN SOILS BY ECNI-MS

Soil origin	Sample No.	Spike level toxaphene (mg/kg)	Spike level chlordane (mg/kg)	Spike level PCBs (mg/kg)[a]	Spike level phenols/anilines (mg/kg)[b]	Toxaphene level (mg/kg), ECNI-MS
Nevada	1	1.0	–	–	–	0.823
						0.862
Nevada	2	0.5	–	–	–	0.394
						0.396
Nevada	3	0.1	–	–	–	0.111
						0.137
						0.103
Nevada	4	Blank	–	–	–	0.046
Nevada	5	0.5	1.0	–	–	0.467
Nevada	6	Blank	–	1.0	–	0.017[c]
Nevada	7	0.5	–	1.0	–	0.423
Nevada	8	0.5	–	1.0	–	0.360
Nevada	9	0.5	–	–	1.0	0.474
						0.549
						0.421
Nevada	10	10.0	–	–	–	1.83[d]
Eagle Harbor	11	Blank	–	–	–	0.032[c]
Eagle Harbor	12	0.125	–	–	–	0.083
Clay	13	Blank	–	–	–	0.069
Clay	14	0.5	–	–	–	0.703
Organic	15	Blank	–	–	-	0.025[c]
Organic	16	0.1	–	–	–	0.082
CH_2Cl_2	17	Blank	–	–	–	0.021[c]
CH_2Cl_2	18	0.5	–	–	–	0.459
Nevada	19	Blank	–	–	–	0.016[c]
Nevada	20	0.5	1.0	1.0	1.0[e]	0.450

[a] PCB 1242, 1248 and 1254 each 1 mg/kg.
[b] 1 ppm of Basic Extractables and Acid Extractables II.
[c] Not confirmable as toxaphene.
[d] Weathered 6 months.
[e] 1 ppm of Pesticides II.

soil spiked at 10 mg/kg (sample 10) and weathered for 6 months, only slight changes in ion chromatographic patterns were evident compared with standards.

The detection limit for toxaphene is actually lower than 100 μg/kg as evidenced, for example, by results for sample 16 (80 μg/kg). Quantitative results for blanks reflect reagent and matrix contributions integrated by the automated procedure and do not indicate the presence of toxaphene-like compounds. A reagent blank (sample 17) taken through the cleanup gave a result of 0.021 mg/kg (not confirmable as toxaphene), so that laboratory contamination involving toxaphene is not at issue. The higher-level blanks (samples 4 and 13) were a result of carry-over from calibration of the HPGPC with toxaphene standards. Once proper precautions were taken in rinsing the injector, a background level of about 0.02 mg/kg resulted. This response was not confirmable as toxaphene. Hence, a 0.100 mg/

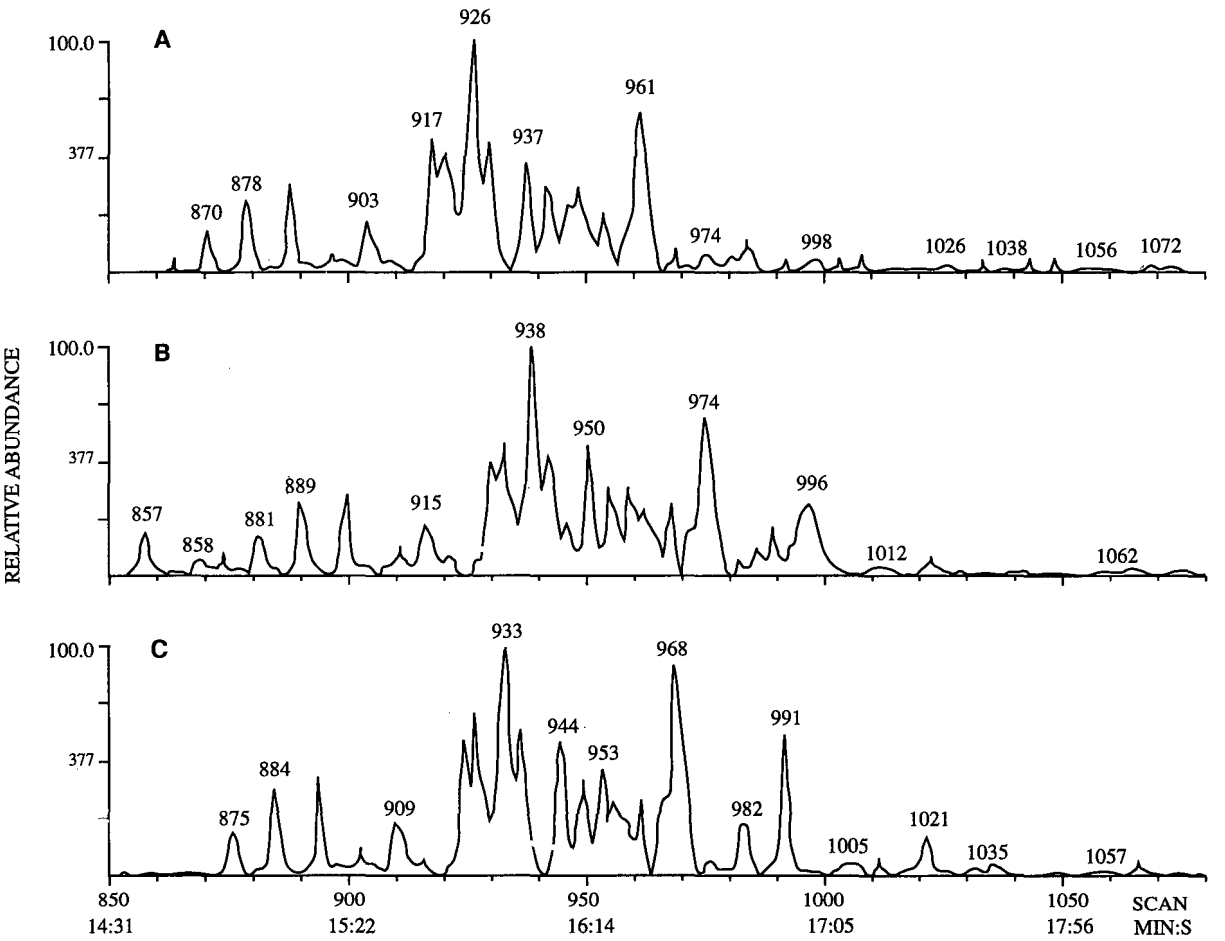

Fig. 1. Ion chromatograms of m/z 377 of (A) a standard of toxaphene; (B) sample 18, 0.5 mg/kg toxaphene taken through the cleanup; and (C) a standard of toxaphene taken through the cleanup.

kg limit seems reasonable in view of apparent unidentified background contributions at this level of cleanup.

The effects of PCBs, chlordane and other pesticides are considered in the spiking studies reported in Table I (samples 5–9 and 20). In general, quantitation of 0.5 mg/kg levels are unaffected by these compounds. This substantiates the improvement of this approach over existing methodology [11]. As an indication of the presence of PCBs, ions monitored at m/z 326 and 430 correspond to molecular anions of pentachlorobiphenyls and octachlorobiphenyls and serve as a check on the efficiency of the HPGPC cleanup. Without the HPGPC cleanup, a 1.0 mg/kg spike of PCBs would result in a "toxaphene-like" response quantitated as 3–6 mg/kg toxaphene in our instrument.

Because PCBs create an interference when oxygen is present in the ion source, the question arises as to the contribution of the internal standard OCB in producing a toxaphene-like response due to the oxygen reaction. No corrections were found necessary at the levels studied and the retention time of this compound.

A blank soil spiked at 1.0 mg/kg PCBs (sample 6) establishes the efficiency of the HPGPC cleanup in removing PCBs (compare 0.017 mg/kg to other blank levels in samples 4, 11, 15 and 19). The 1.0

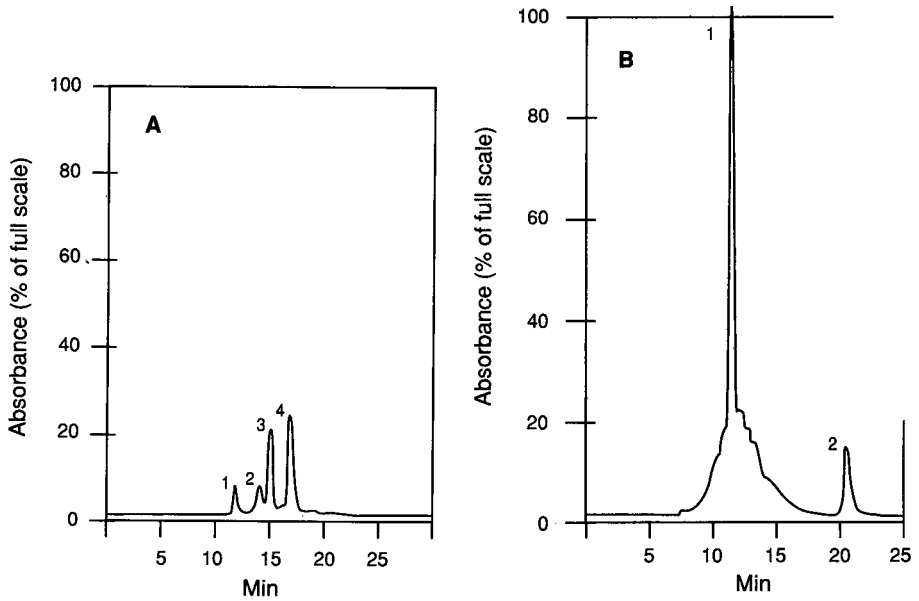

Fig. 2. HPGPC separations. (A) Standards of (1) bis(2-ethylhexyl)phthalate, retention time 12 min 20 s; (2) toxaphene, retention time 14 min 50 s; (3) Arochlor, retention time 15 min 40 s; and (4) perylene, retention time 17 min 30 s. (B) Soil extract with (1) main matrix components centered at retention time 11 min 30 s, and (2) sulfur at retention time 21.0 min.

mg/kg spikes of PCBs and chlordane and other pesticides (*e.g.*, sample 20) do not generate interferences either because they are not collected in the fraction with toxaphene or because they do not afford ions that can interfere. Chlordane is collected in the fraction with toxaphene but does not interfere at levels comparable to those of toxaphene, as evidenced by the results in Table I (samples 5 and 20). By monitoring chlordane response at m/z 342, one can assess whether the chlordane level is of such magnitude as to require any of the corrections suggested by Swackhamer *et al.* [4].

Selective fractionation by HPGPC has broad implications for cleanup of environmental samples. Fig. 2 illustrates the chromatography and separations obtained with HPGPC for standrds (Fig. 2A) and for a typical soil extract (Fig. 2B). HPGPC, unlike most adsorption chromatography, separates toxaphene, a multi-component mixture, as one peak rather than separated into multicomponents over a broad retention range. Since HPGPC is operated in an automatic fractionation mode, other analytes such as PCBs are also collected in individual fractions as a first cleanup step. This approach seems to be an obvious advantage in PCB analysis since the usual subsequent cleanup steps are spent isolating PCBs from interferences. Other target analytes found in the window from bis(2-ethylhexyl)phthalate to beyond perylene but before sulfur can be collected separately or taken as a whole by combining fractions if desired [17,18].

Finally, the solid-phase extraction cleanup step with silica removes polar components (sample 9) that might be present. The main benefit is an extract free from relatively non-volatile components that could cause problems in the injection port or retention gap.

The precision of determination for a given sample extract is about 10% as seen, for example, at the 0.5 mg/kg level with sample 9. Precision of recovery (reproducibility) at the same spiking level is also about 10% (samples 2, 5 and 7–9). The relative response factor for toxaphene *versus* the internal standard (OCB) exhibited a 13% R.S.D. over a 3-month period. Linearity of the relative response of toxaphene to the internal standard was demonstrated for levels of toxaphene from 0.1 to 1.0 mg/kg with OCB levels at 0.5 mg/kg. The recovery of toxaphene from spiked samples is summarized as follows from the data in Table I. At the 0.5 mg/kg level

for spiked soils for which extensive data are available, the average recovery was 85% ±10% (7 determinations). At the 1.0 and 0.1 mg/kg levels the recoveries were similar but are based on fewer determinations.

High-resolution ECNI-MS

Although a variety of soils were analyzed in developing the ECNI-MS methodology, potential exists in environmental analysis for unexpected difficulties or interferences. A high-resolution ECNI-MS determination could present an alternative or tiered approach that would give the analyst a more selective determinative technique without having to resort immediately to further sample cleanup.

In the early stages of this work, high-resolution ECNI-MS was examined to explore its ability to eliminate interferences caused by the reaction of oxygen with PCBs and the potential interference posed by polychorinated diphenyl ethers (PCDPEs) [4]. High-resolution ECNI-MS at 10 000 resolution can eliminate responses from oxygen-containing ions that are isobaric in nominal mass with toxaphene ions regardless of whether they arise from PCDPEs or from oxygen reactions with PCBs (*e.g.* *m/z* 342.8646 for $C_{12}H_4OCl_3{}^{37}Cl_2$ and 342.8962 for $C_{10}H_{11}Cl_5{}^{37}Cl$).

Potential also exists for the presence of *m/z* 342.8776 from $C_{10}H_9Cl_4{}^{37}Cl$ in toxaphene, which would require a resolution of about 26 000 to resolve from the interfering ion. Studies of ratios of toxaphene standards to PCBs of 1:0, 1:10, 1:100 and 1:1000 at resolutions of 1000, 5000, 10 000 and 15 000 were made. Results indicated that a resolution of 10 000 was sufficient to give reliable quantitations in the presence of PCBs.

Despite these apparent advantages, high-resolution ECNI-MS has not been widely adopted, even though reports of its applications [21,22] and calibration procedures [22] have appeared. Some additional effort by instrument manufacturers may be necessary to deal with arcing and beam instability problems.

NOTICE

Although the research described in this article has been funded wholly or in part by the US Environmental Protection Agency through contract No. 68-C0-0049, it has not been subjected to Agency review. Therefore, it does not necessarily reflect the views of the Agency, and no official endorsement should be inferred. Mention of trade names or commercial products does not constitute endorsement or recommendation for use.

REFERENCES

1 R. L. Holmstead, S. Khalifa and J. E. Casida, *J. Agric. Food Chem.*, 22 (1974) 939.
2 M. A. Saleh, *J. Agric. Food Chem.*, 31 (1983) 748.
3 B. Jansson and V. Wideqvist, *J. Environ. Anal. Chem.*, 13 (1983) 309.
4 D. L. Swackhamer, M. J. Charles and R. A. Hites, *Anal. Chem.*, 59 (1987) 913.
5 M. A. Saleh and J. E. Casida, *J. Agric. Food Chem.*, 26 (1978) 583.
6 P. Fuerst, C. Fuerst and W. Groebel, *Dtsch. Lebensm.-Rundsch.*, 85 (1989) 273.
7 F. Becker, G. Lach and H. Parlar, *Toxicol. Environ. Chem.*, 20 (1989) 203.
8 G. Lach and H. Parlar, *Toxicol. Environ. Chem.*, 31–32 (1991) 209.
9 H. Parlar, F. Becker, R. Mueller and G. Lach, *Fresenius' Z. Anal. Chem.*, 331 (1988) 804.
10 F. I. Onuska and K. A. Terry, *J. Chromatogr.*, 471 (1989) 161.
11 *Test Methods for Evaluating Solid Waste (SW-846)*, Vol. 1B, US Environmental Protection Agency, Washington, DC, 3rd ed., November 1986.
12 M. A. Ribick, G. R. Dubay, J. D. Petty, D. L. Stalling and C. J. Schmitt, *Environ. Sci. Technol.*, 16 (1982) 310.
13 M. Oehme, D. Stöckl and H. Knöppel, *Anal. Chem.*, 58 (1986) 554.
14 E. A. Stemmler and R. A. Hites, *Biomed. Environ. Mass Spectrom.*, 15 (1989) 659.
15 E. A. Stemmler, R. A. Hites, B. Arbogast, W. L. Budde, M. L. Deinzer, R. C. Dougherty, J. W. Eichelberger, R. L. Fultz, C. Brimm, E. P. Grimsrud, C. Sakashita and L. J. Sears, *Anal. Chem.*, 60 (1988) 781.
16 S. Erhardt-Zabik, J. T. Watson and M. J. Zabik, *Biomed. Environ. Mass Spectrom.*, 19 (1990) 101.
17 M. M. Krahn, C. A. Wigren, R. W. Pearce, L. K. Moore, R. G. Bogar, W. D. MacLeod, Jr., S.-L. Chan and D. W. Brown, *NOAA Technical Memorandum NMFS FINWC-153*, US Department of Commerce, October 1988.
18 G. J. Fallick, R. Cotter, R. Foster and R. L. Wellman, *Proceedings of the 7th Annual Waste Testing and Quality Assurance Symposium, Washington DC, July 8-12, 1991*, p. II-232.
19 V. Lopez-Avila, J. Milanes, N. S. Dodhiwala, and W. F. Beckert, *J. Chromatogr. Sci.*, 27 (1989) 209.
20 P. R. Loconto, *LC · GC*, 9 (1991) 460.
21 A. H. Grange and W. C. Brumley, *Proceedings of the 39th ASMS Conference on Mass Spectrometry and Allied Topics, Nashville, TN, May 19–24*, 1991.
22 G. M. Brillis and W. C. Brumley, *Anal. Chim. Acta*, 229 (1990) 163.
23 J. N. Seiber, S. C. Madden, M. M. McChesney and W. L. Winterlin, *J. Agric. Food Chem.*, 27 (1979) 284.

Journal of Chromatography, 633 (1993) 185–193
Elsevier Science Publishers B.V., Amsterdam

CHROM. 24 737

Static headspace gas chromatographic determination of fault gases dissolved in transformer insulating oils

Yves Leblanc

Département de Chimie, Université de Montréal, P.O. Box 6128, Montréal, Québec H3C 3J7 (Canada)

Roland Gilbert and Michel Duval

Institut de Recherche d'Hydro-Québec, 1800 Montée Ste-Julie, Varennes, Québec J3X 1S1 (Canada)

Joseph Hubert*

Département de Chimie, Université de Montréal, P.O. Box 6128, Montréal, Québec H3C 3J7 (Canada)

(First received August 6th, 1992; revised manuscript received November 4th, 1992)

ABSTRACT

The analysis of dissolved gases in power transformer oils is an efficient diagnostic tool for routine performance monitoring of power transformers. A static headspace gas chromatographic method has been developed to automate the analysis. The parametric study showed that initial equilibration time is about 200 min at 70°C and set the sample volume to 15 ml of oil. Distribution coefficient values were determined under these optimized headspace conditions, avoiding the need of subsequent calibration from oil standards. The precision of the method was better than 5% and detection limits for hydrogen, carbon monoxide and methane, carbon dioxide, and hydrocarbons were 7, 10, 5 and 1 ppm (v/v), respectively. The response is linear over 3 decades up to 1000 ppm. A comparison study between the headspace and the currently used ASTM D3612 method using on-line transformer oil samples showed a good agreement. The headspace method permits an increased number of analysis per day, as much as four times, compared to the ASTM method.

INTRODUCTION

Analysis of dissolved gases in power transformer oils is widely performed by public utilities worldwide for routine performance monitoring. The presence of faults such as arcing, local overheating and partial discharges in the equipment always results in the chemical decomposition of the insulating materials, which are composed of mineral oil and cellulose [1]. The main degradation products are gases (H_2, CO, CO_2, CH_4, C_2H_2, C_2H_4, C_2H_6 and C_3H_8) which partially or totally dissolve in the insulating oil. Other gases, such as O_2 and N_2 along with CO_2, are also dissolved by contact of ambient air with a limited surface of oil inside the oil expansion chamber of conservator-type transformers. A normally operating transformer may contain as much as 10% (v/v) dissolved gas, consisting mostly of air as well as fault gases at concentration up to 100 ppm (v/v)☆. Since correlations between the nature and proportion of the gases and the types of faults have been established, it is possible to diagnose the presence of faults at an early stage and take corrective actions before they lead to unexpected failure of the unit [1,2]. Dissolved gas analysis (DGA) is thus an efficient diagnostic tool that cuts costs and improves service reliability.

Various approaches exist for DGA in transformer oils and differ mainly through the gas extrac-

* Corresponding author.

☆ All the concentrations are given in ppm (v/v).

0021-9673/93/$06.00

tion technique rather than the component gas chromatographic separation step. Vacuum gas extraction, widely used in North America [3], is the basis of a method approved by the American Society for Testing and Materials (ASTM) [4]. The oil sample is introduced into a degassing flask attached to a vacuum glassware maintained at less than $1 \cdot 10^{-3}$ Torr (1 Torr = 133.322 Pa). The extracted gases are then compressed by a mercury column into a burette and a sample is injected into a gas chromatograph. This method is tedious, requiring the operation of many valves, and has limited sensitivity when the total gas content is very low (<2%). A second method, described in International Electrotechnical Commission Publication 567 and mainly used in Europe, involves gas stripping [5]. The system consists of a carrier gas sweeping through a U-shaped glass tube containing the oil sample and connected to the chromatographic system. However, due to peak broadening resulting from a loss of the pin-point feature of the injection, the detection limits are around the same as with the preceding method. A variant of the stripping method involves a straight tube filled with stainless steel beads providing a greater surface area which accelerates the extraction process [6]. However, the detection limit for hydrogen is too high for early fault warning [7]. All these methods have a common drawback: the possibilities for automation are limited, which increases manpower costs in DGA laboratories, reduces their ability to fully optimize the use of the chromatographic equipment, and limits the number of DGA that could be achieved in a regular day shift.

This paper describes an automated method for the analysis of dissolved gases in power transformer oils. The static headspace gas chromatographic method (HSP-GC) allows more samples to be analyzed with minimal supervision, and offers analytical performances comparable to those of the vacuum extraction method. A parametric study on equilibration time, temperature and sample volume will be presented. The performances of the method will be estimated using the optimized headspace parameters. The results obtained with this method and the ASTM method on in-service transformer oil samples will be compared to assess the validity and performances of the HSP-GC approach.

EXPERIMENTAL

Instrumentation

A schematic of the chromatographic system is presented in Fig. 1. An HP-5890 gas chromatograph equipped with a thermal conductivity detection (TCD) system, a nickel catalyst unit to convert CO and CO_2 into CH_4 and a flame ionization detection (FID) system, was used for all analyses (Hewlett-Packard, Palo Alto, CA, USA). The methanizer was maintained at 350°C and fed with pure hydrogen serving both as reactant for the catalytic reactor and fuel for the FID system. A pneumatic 6-port valve (Valco, Houston, TX, USA) with 1/16-in. (1

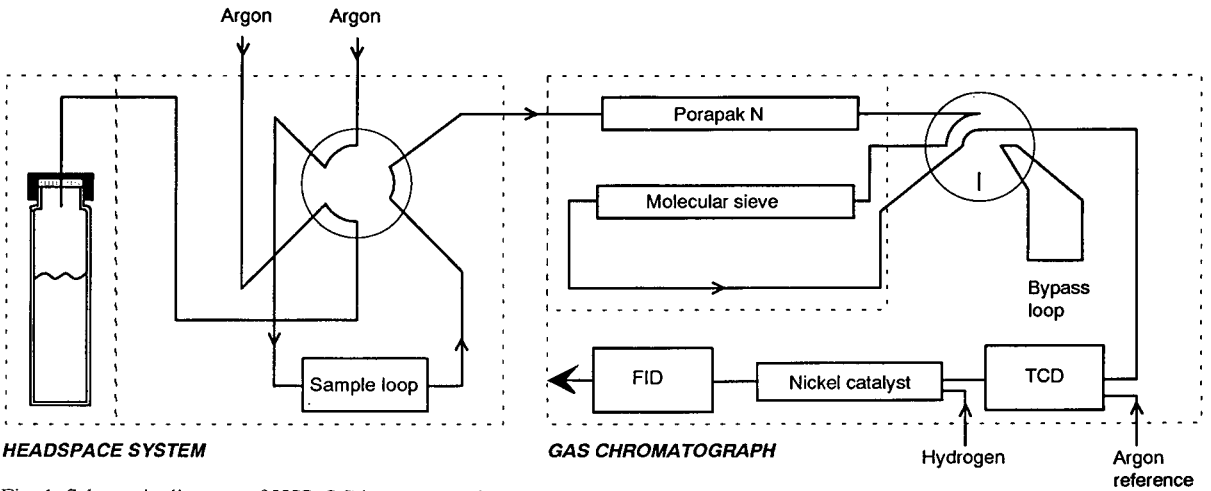

Fig. 1. Schematic diagram of HSP-GC instrumentation.

TABLE I

INSTRUMENTAL CONDITIONS

Headspace system	
Auxiliary pressure	0.4 bar
Valve timing	0 s, probe needle down 3–13 s, argon pressurization 43–53 s, venting 54–64 s, injection 65 s, probe needle up
Sample loop temperature	3°C above bath temperature
Gas chromatograph	
Carrier gas	Ar, 40 ml/min
Catalytic gas	H_2, 70 ml/min
Valve operation	0–7 min, column in series 7–18 min, molecular sieve bypassed
Oven program	40°C for 4 min 40 to 180°C at 20°C/min 180°C for 7 min
Detector temperature	TCD at 250°C FID at 350°C

in. = 2.54 cm) fittings installed on the gas chromatograph and maintained at 150°C was used for column selection. An HP molecular sieve column 13X (0.8 m × 1/8 in., 45–60 mesh) was connected at the outlet of an HP Porapak N column (4 m × 1/8 in., 80–100 mesh) through the GC valve to separate the lighter gases (H_2, O_2, N_2, CH_4 and CO) that were poorly resolved on the Porapak. Once the lighter gases have been eluted, the valve is switched automatically so that the CO_2 and C_2 and C_3 hydrocarbons separated by the porous polymer column bypass the molecular sieve to end up in the detectors. TCD and FID signals were recorded simultaneously using the HP-3365 Chemstation software. The valve was activated by an HP-19405A event controller. The headspace sampling unit was an HP-19395A equipped with a 1-ml injection loop. This unit consists of a rotating temperature-controlled sample carousel able to load up to 24 vials and a control unit for programming the time and temperature of the sampling. The 20-ml glass vials purchased from Wheaton (Millville, NJ, USA) were hermetically sealed by PTFE-lined septa. The 10-, 30- and 100-ml glass syringes used for oil manipulations were from Perfectum (Thomas Scientific, Swedesboro, NJ, USA). Table I gives the instrumental conditions.

Chemicals and standards

The absolute response of the detectors was calibrated with standard gas mixtures of H_2, O_2, N_2, CO, CO_2, CH_4, C_2H_2, C_2H_4, C_2H_6 and C_3H_8 at concentration levels of 100, 1000, and 5000 ppm (v/v) in argon (Scott Specialty Gases, Plumsteadville, PA, USA). Dissolved-gas oil standards were prepared using Voltesso 35 (Esso Imperial Oil Company, Sarnia, Canada) transformer insulating oil and gases at least 99.9% pure (Matheson Gas Products, Secaucus, NJ, USA). Argon used as carrier gas and hydrogen were 99.999% pure (Union Carbide, Toronto, Canada).

Procedure

The preparation of the dissolved-gas oil standard used for calibration was done according to Duval and Giguère [8]. Sub-standards were obtained by diluting the dissolved-gas oil standard with degassed oil in the headspace vials. The dilution factor was determined by weighting. Preparation of headspace vials for analysis was done as follows: after being sealed, the vials were purged with argon; oil sample was then introduced into the vial, releasing pressure buildup through a 0.5 mm O.D. needle. The vials were weighed before and after filling to control the volume injected. A 30-ml syringe with a 1.2 mm O.D. stainless-steel needle was used for this transfer.

RESULTS AND DISCUSSION

Parametric study

Equilibration time. Fig. 2 shows typical variations in the gas phase concentration as a function of time at 50°C for ethane and ethylene. For each curve, a set of vials filled with 5 ml of dissolved-gas standard containing 354 ppm of both ethane and ethylene was loaded into the thermostated bath at time zero and analyzed sequentially. The time elapsed between two data point measurements corresponds to the time required to perform a chromatographic run. The signals measured at time zero are the result of the partial phase equilibration that occurs during the few min elapsed between the end of the filling and the gas-phase injection of the first vial. In order to obtain consistent results from one vial to another, the sample must be thermostated for a minimum amount of time to bring the oil and gas phases into

equilibrium. The time required to reach such an equilibrium is about 500 min at 50°C. Similar curves were obtained with all the other fault gases studied and gave approximately the same equilibration time, although the volatility and solubility levels were quite different. This suggests that the equilibration time is governed by the matrix viscosity rather than the nature of the gases. The gas concentrations in the phases at equilibrium depend on the solubility of the analyte in oil at a given temperature. As can be seen in Fig. 2, for an oil standard of equimolar concentration of gases, ethane has a higher solubility which gives a lower maximum headspace concentration at 50°C.

Temperature. The same set of analyses was repeated for temperatures at 35, 60, 70, 80 and 90°C. As shown in Fig. 3, for ethylene a similar trend is observed for the variation of gas phase concentrations as a function of time. However, the first segment of the curves is steeper with increased temperature, which can be explained by an increase of the analyte liquid–gas exchange rates associated with the decrease in matrix viscosity. Fig. 4 shows the effect of the temperature on the equilibration time averaged over the ten gases studied; the time required to reach 90% of the asymptotic value is used for that comparison. Based on these results, it seems obvious that in order to minimize thermostating time, the highest temperature allowed by the matrix will be required. However, the solubility changes with temperature are different from one gas to another: H_2, N_2, O_2 and CO have a lower solubility

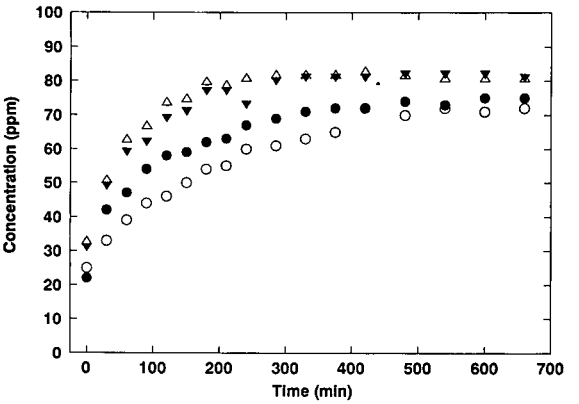

Fig. 3. Influence of the temperature on the gas phase concentration and equilibration time for ethylene. ○ = 35°C; ● = 50°C; ▼ = 70°C; △ = 80°c.

when the temperature is raised, whereas CH_4, CO_2 and C_2 and C3 hydrocarbons have higher solubility [9]. For O_2 and N_2 present in relatively high concentrations, the temperature is not a limitation since their determination can tolerate a loss in analytical sensitivity. Also, carbon monoxide is not specific enough to be solely associated to cellulose degradation. It can also appear as a result of long term oxidation of the oil [10]. Therefore, in DGA, CO is not a key compound in determining a transformer's internal state from correlation rules. On the other hand, hydrogen is important for fault diagnosis and a low detection limit is highly desirable. This would normally be achieved by lowering the temperature so that hydrogen is less soluble in oil. A compro-

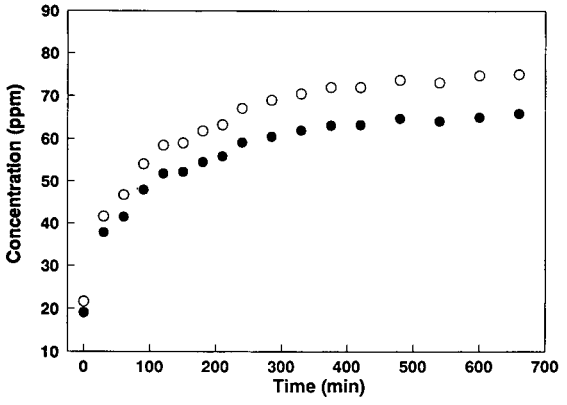

Fig. 2. Gas phase concentration in headspace as time allowed to equilibrate (50°C). ○ = C_2H_4; ● = C_2H_6.

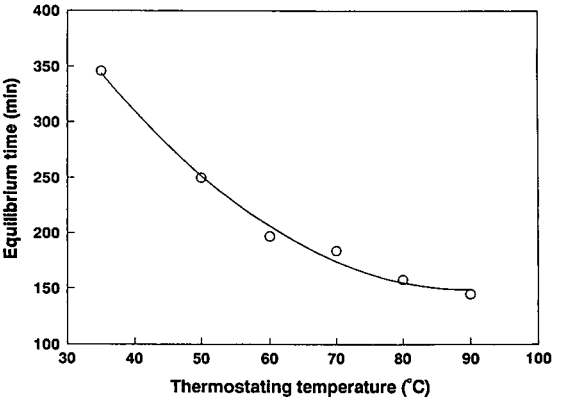

Fig. 4. Temperature effect on equilibration time considering 90% maximum value (5 ml of oil).

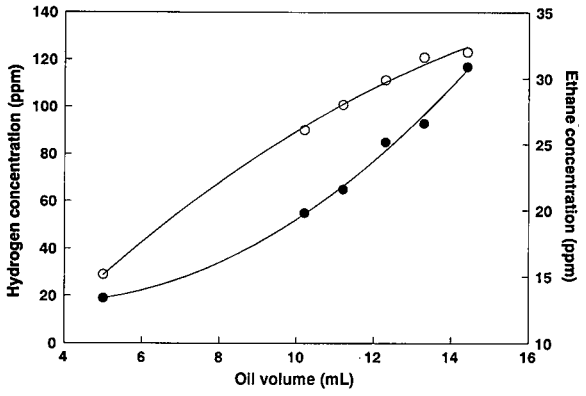

Fig. 5. Effect of volume V_L on equilibrium gas concentration in volume V_G. ● = H_2; ○ = C_2H_6.

mise between sensitivity and equilibration time is achieved by setting the temperature at 70°C. At this temperature, partial vaporization of certain oil components which could produce subsequent chromatographic ghost peaks will be minimized.

Sample volume. The sensitivity of the headspace method is also strongly affected by the ratio V_G/V_L as indicated by the relation:

$$C_G = \frac{C_L^0}{K + \left(\frac{V_G}{V_L}\right)} \quad (1)$$

where C_G is the concentration of the analyte in the gas phase at equilibrium, C_L^0 the initial concentration of the analyte in the liquid phase, K the distribution coefficient of the analyte between the two phases in equilibrium, and V_G, V_L the volumes of the gas and liquid phases in the headspace vials, respectively [11]. Since the total volume is fixed ($V_{total} = V_G + V_L$), only the liquid volume V_L can be varied and optimized. Fig. 5 shows the variation of the gas phase concentration C_G with the volume of oil for H_2 and C_2H_6. For gases with a K lower than unity, C_G increases with a positive curvature, whereas gases with a K greater than unity have a negative curvature. The greater the difference between the K value and unity, the more pronounced the curvature. This observation agrees with eqn.1 and suggests that V_L should be set to the highest volume allowed by the headspace system. However, the expression obtained after differentiation of eqn. 1 indicates that the error in the determination of C_L^0 increases as V_G/V_L decreases:

$$\frac{\Delta C_L^0}{C_L^0} = \frac{\Delta C_G}{C_G} + \frac{\Delta K}{K + \frac{V_G}{V_L}} \quad (2)$$

Under our conditions, $\Delta K/K$ usually exceeds $\Delta C_G/C_G$, so that V_L should be increased while maintaining precision within acceptable values. Table II gives the relative standard deviations obtained from ten replicates of the same standard for each of the three sample volumes studied. The variation in the sample volume from one vial to another (0.1 ml for a 15-ml injection) had a negligible contribution to these values. As expected from eqn. 2, the precision is generally improved by lowering V_L so that a good compromise is obtained by setting the sample volume at 15 ml. The precision for H_2 is less than expected at V_L = 10 ml; in this case, the analytical conditions are close to the detection limit and the contribution of $\Delta C_G/C_G$ becomes more important.

The final set of conditions retained for the headspace unit is 70°C and 15 ml sample volume with an equilibration time of 200 min.

Analytical performances

Calibration. The calibration curves were established over a concentration range of 5 to 400 ppm generally encountered in transformer oils, and their linearity verified to a concentration of up to 1000 ppm. An example of the chromatograms is shown

TABLE II

INFLUENCE OF V_L ON ANALYTICAL PRECISION

Gas	Precision (R.S.D.) (%)[a]		
	V_L = 10 ml	V_L = 15 ml	V_L = 18 ml
H_2	4	3	4
CO	2	2	4
CH_4	1	2	4
CO_2	14	14	10
C_2H_4	1	2	3
C_2H_6	1	3	3
C_2H_2	5	4	7

[a] Measured with a standard of 70 ppm H_2 and C_2 hydrocarbons, 141 ppm CO and CH_4, and 220 ppm CO_2

in Fig. 6. Table III lists the calibration curve parameters of the first-order regressions used. The detection limits for a signal-to-background noise ratio of 3 are listed in Table IV together with the ASTM D3612 values determined under identical chromatographic conditions. The detection limits using the HSP-GC technique are slightly higher than those using the ASTM method but still sufficiently low to allow the use of the method for the diagnosis on in-service transformers. As expected, both techniques have better detection limits for the FID-detected hydrocarbons even though these analytes are far more soluble than permanent gases.

Generally it is not necessary to use dissolved-gas oil standards to calibrate the chromatographic response provided that the analyte distribution coefficients (K values) are known and a linear relation exists between C_L^0 and C_G in the range of concentrations of interest. As expressed by eqn. 1, if K and the ratio V_G/V_L are known, then C_L^0 can be calculated from the chromatographic determination of C_G. Subsequently, the only response necessary for cali-

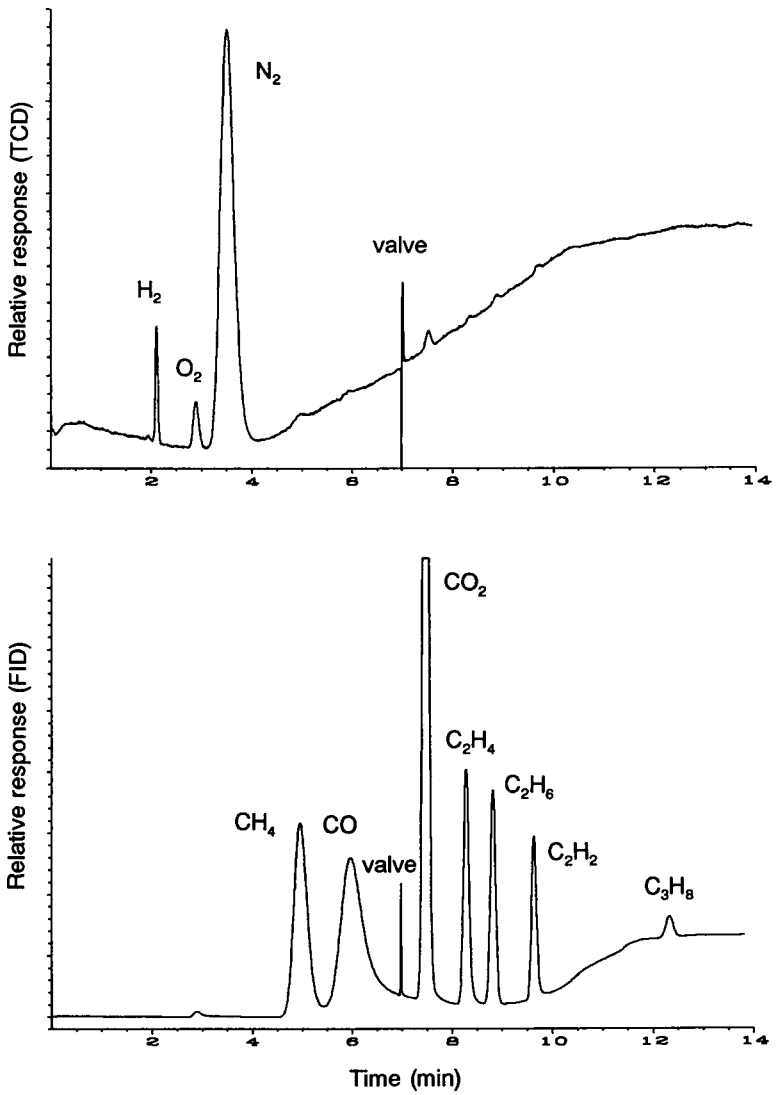

Fig. 6. Typical chromatograms of the headspace of a dissolved-gas-in-oil sample.

TABLE III

CALIBRATION CURVE PARAMETERS

Gas	Regression coefficients[a]		Correlation coefficient	Number of datapoints
	b	*m*		
H_2	10.7	1.7693	0.9991	9
CH_4	1.0	1.1450	0.9940	10
CO	42.7	1.4418	0.9691	10
CO_2	0.0	0.7219	0.9856	10
C_2H_4	0.0	0.5315	0.9986	10
C_2H_6	1.1	0.4370	0.9992	10
C_2H_2	−4.9	0.6659	0.9981	10
C_3H_8	0.0	0.1799	0.9988	10

[a] $y = mx + b$.

bration would be C_G through direct introduction of gas mixtures in headspace vials. The experimental distribution coefficients K shown in Table V were obtained from the determination of an equilibrium gas phase concentration of a dissolved-gas oil standard. These values evaluated for Voltesso 35 were used for the calculations of C_L^0 under the final headspace conditions. Negligible changes are expected when using a different type of oil, especially as modern transformer oils do not vary widely in chemical composition. However, if an oil significantly different in composition is used (aromatics, aliphatics, synthetics, etc.) or if high precision analysis is required, recalculating K values with an oil standard might be advisable.

Precision and accuracy. Table VI gives the accuracy and precision of the HSP-GC and ASTM D3612 techniques for the determination of fault gases. These parameters were estimated by analyzing an oil sample of known gas composition prepared by the technique of Duval and Giguère [8]. A slight improvement of the precision is noted with the headspace. The difference in R.S.D. between the headspace and the ASTM method can be explained by a contamination of the sample by the injection of the oil into the vial. Five gases out of the seven listed in Table VI were measured with greater accuracy with the headspace method compared to the ASTM method.

In-service oil samples analysis. Since the HSP-GC method was developed as an alternative to the ASTM method, a series of comparisons were made between these two methods on real transformer oil samples. A total of 20 syringes were collected from on-line units. Fig. 7 show the correlation obtained for two of the gases studied. The slopes and correlation factors for all gases studied given in Table VII show that good correlation exists between the two methods. Most of the points are well within the 95% confidence range. The deviation noted for the total gas content is due to the difference in its determination: with the ASTM method, the volume compressed in the burette at atmospheric pressure is used whereas the HSP-GC total gas content is the numerical summation of the individual gases measured by chromatography. Thus, headspace extraction allows quantitative analysis of dissolved gases to be performed in transformer insulating oil with analytical performances similar to the currently used ASTM D3612 vacuum method.

TABLE IV

DETECTION LIMITS OF THE HEADSPACE AND ASTM EXTRACTION METHODS (ppm)

Signal-to-background noise ratio = 3

Gas	Headspace[a]	ASTM D3612
H_2	7	1
CO,CH_4	10	5
CO_2	5	2
Hydrocarbons	1	0.5

[a] 70°C, V_L = 15 ml of oil.

TABLE V

DISTRIBUTION COEFFICIENTS OF FAULT GASES IN VOLTESSO 35 OIL–ARGON SYSTEM AT 70°C

Gas	Distribution coefficient K (Ostwald)[a]
H_2	0.074 ± 0.003
O_2	0.20 ± 0.04
N_2	0.11 ± 0.04
CO	0.20 ± 0.02
CH_4	0.40 ± 0.01
CO_2	0.90 ± 0.03
C_2H_4	1.40 ± 0.04
C_2H_6	1.80 ± 0.04
C_2H_2	1.01 ± 0.02
C_3H_8	5.1 ± 0.5

[a] (V_G/V_L = 0.4913).

TABLE VI

ACCURACY AND PRECISION OF HEADSPACE AND ASTM EXTRACTION METHODS

Gas	Reference value (ppm)	Measured value (ppm)	Precision (%)	Accuracy (%)	Extraction method
H_2	71	66	3	−6	HSP
		82	4	+16	ASTM
CH_4	141	129	3	−9	HSP
		170	3	+20	ASTM
CO	142	119	2	−16	HSP
		150	3	+6	ASTM
CO_2	220	234	4	+6	HSP
		266	7	+21	ASTM
C_2H_4	71	76	3	+8	HSP
		79	5	+12	ASTM
C_2H_6	72	66	3	−8	HSP
		83	5	+16	ASTM
C_2H_2	67	57	4	−14	HSP
		69	4	+3	ASTM

[a] ± 1% [8].

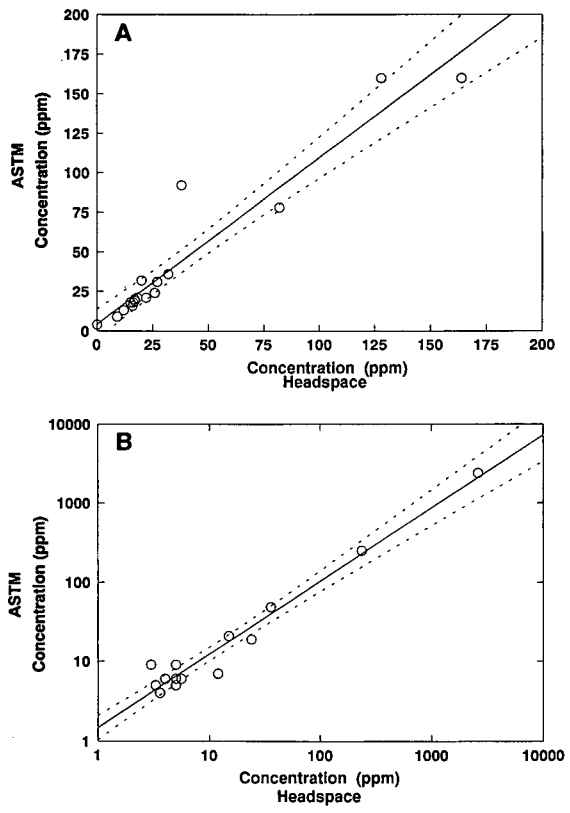

Fig. 7. Correlation between analysis results from ASTM D3612 and headspace extraction method for hydrogen and ethylene. (A) H_2; (B) C_2H_4.

CONCLUSIONS

The fact that the HSP-GC sampling can be automated allows for the possibility of achieving a higher number of analyses daily with minimal supervision. As much as 41 samples can be analyzed daily as compared to nine using the ASTM method over

TABLE VII

CORRELATION BETWEEN DISSOLVED GAS ANALYSIS RESULTS FROM HEADSPACE AND ASTM D3612 EXTRACTION METHODS FOR IN-SERVICE TRANSFORMER OILS

Gas	Slope	Correlation factor
H_2	1.05	0.9556
	1.05[a]	0.9862[a]
O_2	0.85	0.9561
N_2	0.88	0.9714
CH_4	0.99	0.9997
CO	0.94	0.9857
CO_2	0.96	0.9887
C_2H_4	0.92	0.9999
C_2H_6	1.00	0.9990
C_2H_2	0.64[b]	0.9992[b]
C_3H_8	0.81	0.9661
Total gas content	1.30	0.9572

[a] Without erroneous point on Fig. 7.

[b] Detected in five samples only.

a regular day shift. The major drawback of this method is the long initial equilibration time (200 min) necessary before the chromatographic analysis. However, once the batch of vials is at equilibrium, the time elapsed between two successive analyses will depend only on the length of the chromatographic run which is approximately 35 min.

ACKNOWLEDGEMENTS

The authors would like to thank Hydro–Québec's Direction Appareillage for funding this project. We wish to express our thanks to Michel Pilon of Laboratoire Jeanne D'Arc d'Hydro–Québec for his cooperation. We are grateful to the Fonds FCAR of Québec for a Graduate Fellowship awarded to Y. L.

REFERENCES

1 J. Galand, M. Thibault, F. Viale, J. Samat and P. Vuarchex, *Rev. Gen. Elect.*, 81 (1972) 727.
2 M. Duval, F. Langdeau, G. Bélanger and P. Gervais, *Minutes of the 55th International Conference of Doble Clients*, Doble Engineering Co., Watertown, MA, 1988, Section 10-7.1.
3 M. Duval, *IEEE Electr. Insul. Mag.*, 5 (1989) 22.
4 *Annual Book of ASTM Standards*, American Society for Testing and Materials, Philadelphia, PA, 1988, method D3612.
5 *Publication 567*, International Electrotechnical Commission, Geneva, 1977.
6 D. J. Fisher, *US Pat.*, 4 587 834 (1986).
7 S. J. Ferrito, *IEEE Trans. Power Delivery*, 5 (1990) 220.
8 M. Duval and Y. Giguère, *Minutes of the 51st International Conference of Doble Clients*, Doble Engineering Co., Watertown, MA, 1984, Section 10-1.
9 *Annual Book of ASTM Standards*, American Society for Testing and Materials, Philadelphia, PA, 1988, method D2779.
10 P. J. Burton, M. Carballeira, M. Duval, C. W. Fuller, J. Graham, J. A de Pablo, J. Samat and E. Spicar, *Conférence Internationale des Grands Résaux Electriques à Haute Tension*, CIGRE, Paris, 1988, Paper 15-08.
11 B. Ioffe and A. G. Vitenberg, *Head-Space Analysis Methods in Gas Chromatography*, Wiley, Toronto, 1982, Ch. 1.

Journal of Chromatography, 633 (1993) 195–205
Elsevier Science Publishers B.V., Amsterdam

CHROM. 24 746

Utilization of a benchtop mass spectrometer with capillary supercritical fluid chromatography

Balasingam Murugaverl and Kent J. Voorhees*

Department of Chemistry and Geochemistry, Colorado School of Mines, Golden, CO 80401 (USA)

Stephan J. DeLuca

Leybold Inficon, 2 Technology Place, E. Syracuse, NY 13057 (USA)

(First received May 19th, 1992; revised manuscript received November 11th, 1992)

ABSTRACT

Direct coupling of a capillary supercritical fluid chromatograph to a benchtop electron ionization (EI) mass spectrometer using a GC–MS interface with minor modification is described. The SFC–EI-MS of the thermally labile pesticides aldicarb, diuron, methiocarb, alachlor, bendiocarb, and carbaryl plus other analytes have been obtained with good chromatographic integrity and sensitivity. This system routinely provided low nanogram level detection in the full scan mode for the pesticides as well as picogram levels for some selected analytes. The highest %R.S.D. for repeated injections of naphthalene over a two-week period using this benchtop SFC–EI-MS system was 6.4. The EI-mass spectra have been successfully searched using conventional mass spectral libraries.

INTRODUCTION

The viability of supercritical fluid chromatography with mass spectrometry (SFC–MS) has been demonstrated by many researchers [1–15]. These investigations have produced reliable methods for conducting chemical ionization (CI), atmospheric pressure ionization (API) and electron ionization (EI) with both capillary and packed-column SFC. A majority of these investigators have employed CI since it generally provided lower detection limits than EI at high source pressures typical for SFC. Most of the mass spectrometers used for these studies have been research grade instruments.

The use of benchtop mass spectrometers in conjunction with gas chromatography has made GC–MS accessible to most laboratories. These instruments have not been applied to SFC primarily because of their pumping limitations, low mass range, and integrated design. The mass range limitation is critical for analysis of high-molecular-mass compounds, but does not limit the use of benchtop instruments for the analysis of lower-molecular-mass thermally labile or highly polar compounds. The sophistication involved in the reported interfacing techniques is also a problem and is often too complex to implement in a routine analytical instrument.

There are only three papers thus far cited in the literature on SFC with a benchtop mass spectrometer. Two of these research groups resorted to chemical ionization to accommodate the high source pressures of SFC. One, by Lee and Henion [16], described the marriage of capillary SFC to a HP 5970 mass selective detector modified with the addition of 330 L/s turbo pump and a HP 5995 CI ion source. This system detected low nanogram levels of some selected volatile compounds. The CI mass spectra of these compounds showed an abundance of (M + 1) ions, but lacked the structurally

* Corresponding author.

0021-9673/93/$06.00

important fragmentation ions typical of EI conditions. This same instrument was later successfully used to generate pseudo-electron ionization spectra by charge exchange ionization [17]. Saunders *et al.* [18] on the other hand showed the feasibility of coupling micro-packed columns to a benchtop thermospray mass spectrometer. These authors utilized a HP 5970 mass-selective detector equipped with a Vestec 101 thermospray unit and a modified ion source designed to operate at higher pressures. Good chromatographic separation and CI mass spectra for a mixture of ureas were reported. Todd *et al.* [19] have reported the use of an EI-ion trap detector; however, the sensitivity was in the microgram range for a butylbenzene standard.

The ideal SFC–MS interface for routine analytical use should be as simple as the GC–MS interface and also capable of operating with electron ionization to provide spectra that are reproducible and can be searched against existing EI libraries. The present paper describes the development and evaluation of such a benchtop SFC–MS system employing electron ionization. The mass spectrometer used in this study was a commercially available Leybold Inficon benchtop MS equipped with an EI source. Minor modifications were made to the original stainless steel GC–MS interface to convert it into a SFC–MS interface. The compounds investigated were primarily thermally labile; however, other analytes commonly reported in other SFC–MS papers are also described.

EXPERIMENTAL

Samples

Aldicarb, diuron, methiocarb, alachlor, bendiocarb and carbaryl pesticide reference standards were obtained from the Environmental Protection Agency (Research Triangle Park, NC, USA). Other chemicals were purchased from Aldrich (Milwaukee, WI, USA).

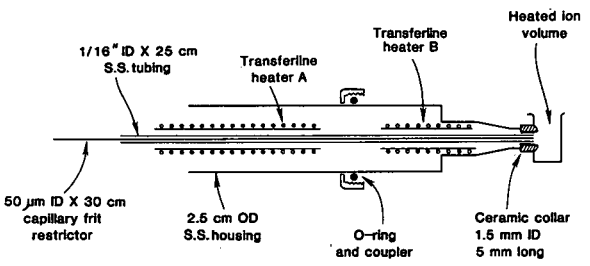

Fig. 1. Schematic diagram of the SFC–MS Interface. " = Inch; S.S. = stainless steel.

Instrumentation

A Leybold Inficon (E. Syracuse, NY, USA) benchtop quadrupole mass spectrometer was modified for SFC work by altering the standard GC interface and adding increased pumping. This instrument comes from the manufacturer with an open heated EI source, a 50 L/s turbo pump and a scan range of 10–650 u. Fig. 1 shows the modified interface as used for SFC applications. The major change to the original interface was the introduction of an extra heater and thermocouple to allow for differential heating of the transfer line.

The principal modification to the mass spectrometer involved removing the existing pumping manifold from the integrated system and replacing it with a new larger diameter manifold with a 4-in. (1 in. = 2.54 cm) flange for the pump. A new 150 L/s Leybold (Export, PA, USA) turbo pump replaced the existing 50 L/s pump. This turbo pump provides adequate vacuum to allow use of the SFC in the pressure range of 100–350 atm (1 atm = 101 325 Pa). Although not tested, it is expected that the system can handle the effluents to the syringe pump's upper range of 400 atm. One additional modification involved adding a 1-in. Cajon fitting to the new vacuum manifold which allowed the addition of an ion gauge. Fig. 2 presents a drawing of the manifold. Because of the added size of the pump, an external stand was constructed to hold the manifold, pump, and pump controller. The existing ionizer and rod assembly were used with no modifications; no changes were made to the electronics.

A Lee Scientific (Salt Lake City, UT, USA) Model 600 syringe pump with a dedicated pump controller and a Hewlett-Packard (Palo Alto, CA, USA) Model 5720A gas chromatograph were used as the basic supercritical fluid chromatograph. A Valco (Houston, TX, USA) Model C14W.1 injection valve with an internal volume of 0.06 µl allowed for direct injection of samples. Both a 1.5 m × 0.05 mm I.D. SB-Biphenyl 30 and a 1.5 m × 0.05 mm I.D. SB-Octyl 30 column, purchased from Lee Scientific, were used for the study. The pressures were maintained in the column by a Lee Scientific

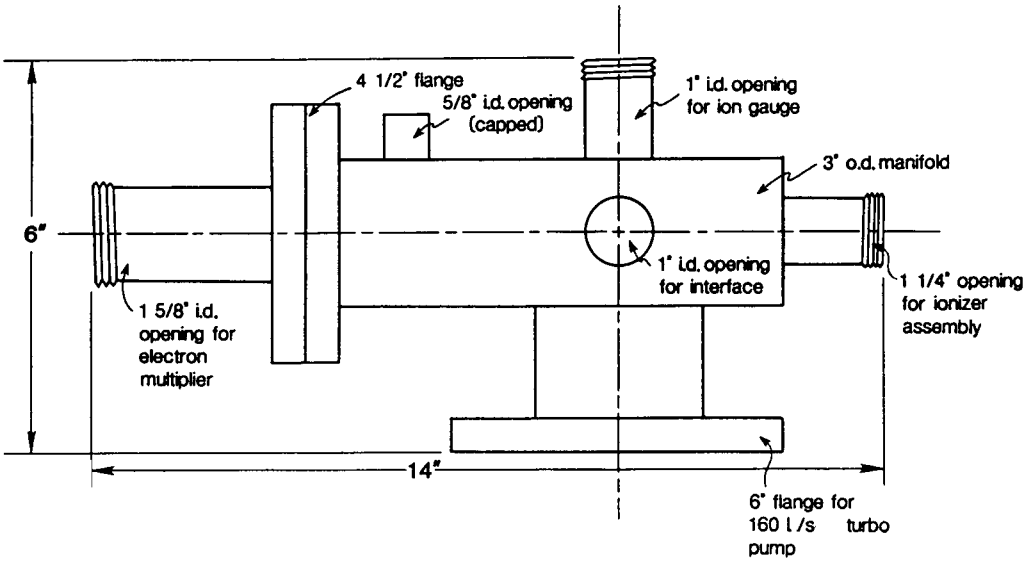

Fig. 2. Schematic diagram of the pumping manifold.

frit restrictor (rated at 0.5 cm/s at 102 atm) cut to allow for an approximate 1 ml/min gas equivalent flow (measured by allowing the carbon dioxide to expand into a bubble meter) at a head pressure of 102 atm into the mass spectrometer. Carbon dioxide was used as the mobile phase throughout this study, while the SFC conditions varied according to the analytes being analyzed. Conditions are listed under each chromatogram.

Interface design

The interface shown in Fig. 1 consists of a 30 cm × 1/16 in. I.D. stainless-steel differentially heated transfer line and a 40 cm × 50 μm I.D. capillary frit restrictor, all contained in a 1 in. O.D. stainless-steel tube. The tip of the probe was heated by the ion volume via the ceramic collar which also prevented shorting of the ion volume and the interface. The transfer line heater A was maintained at the SFC oven temperature while heater B was maintained at about 155°C. The ion volume was maintained at 290°C. The connection of the frit restrictor to the analytical column was accomplished using a fused-silica coupler obtained from Lee Scientific. The restrictor tip was positioned flush with the tip of the transfer line to allow the supercritical fluid to expand inside the ion volume. Nominal flow at the restrictor was about 1 ml/min of carbon dioxide gas at a head pressure of 102 atm. The pressure in the manifold ranged from $2 \cdot 10^{-5}$ Torr (1 Torr = 133.322 Pa) at a SFC pressure of 100 atm to about $8 \cdot 10^{-5}$ Torr at 250 atm.

RESULTS AND DISCUSSION

The primary objective of this study was to develop an inexpensive benchtop electron ionization mass spectrometer as a detector for an on-line supercritical flow system that was previously developed for the trace analysis of pesticides in complex sample matrices [20]. The initial studies were focused on coupling the SFC apparatus to the benchtop mass spectrometer using a simple interface. The existing stainless steel GC–MS interface that came with the mass spectrometer was ideal for use with SFC. Initially, this interface was used without any modification. An integral tapered restrictor [21] was attached to the analytical column to obtain desired flow-rates of the decompressed gas (typically 1–5 ml/min). A few problems were encountered with this early system. One of the problems was the differences in sensitivity between solid and liquid analytes (at room temperature and pressure). Liquid samples could be detected at low nanogram levels while reproducible spectra for solid analytes were unattainable at these levels. Varying parameters

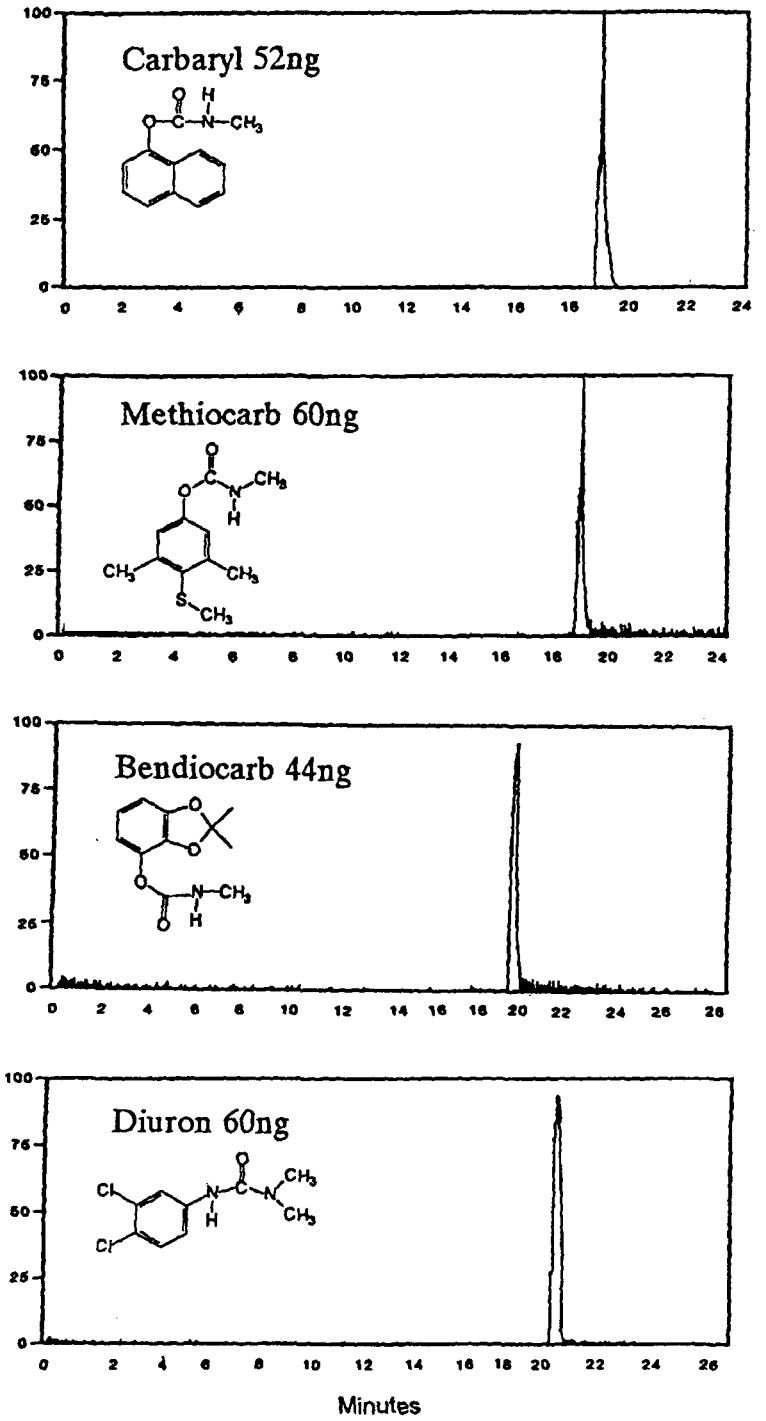

Fig. 3. The SFC–EI-MS total ion chromatograms of four thermally labile pesticides using a 1.5 m × 0.05 mm I.D. SB-octyl 30 column at 90°C and 0.45 g/ml.

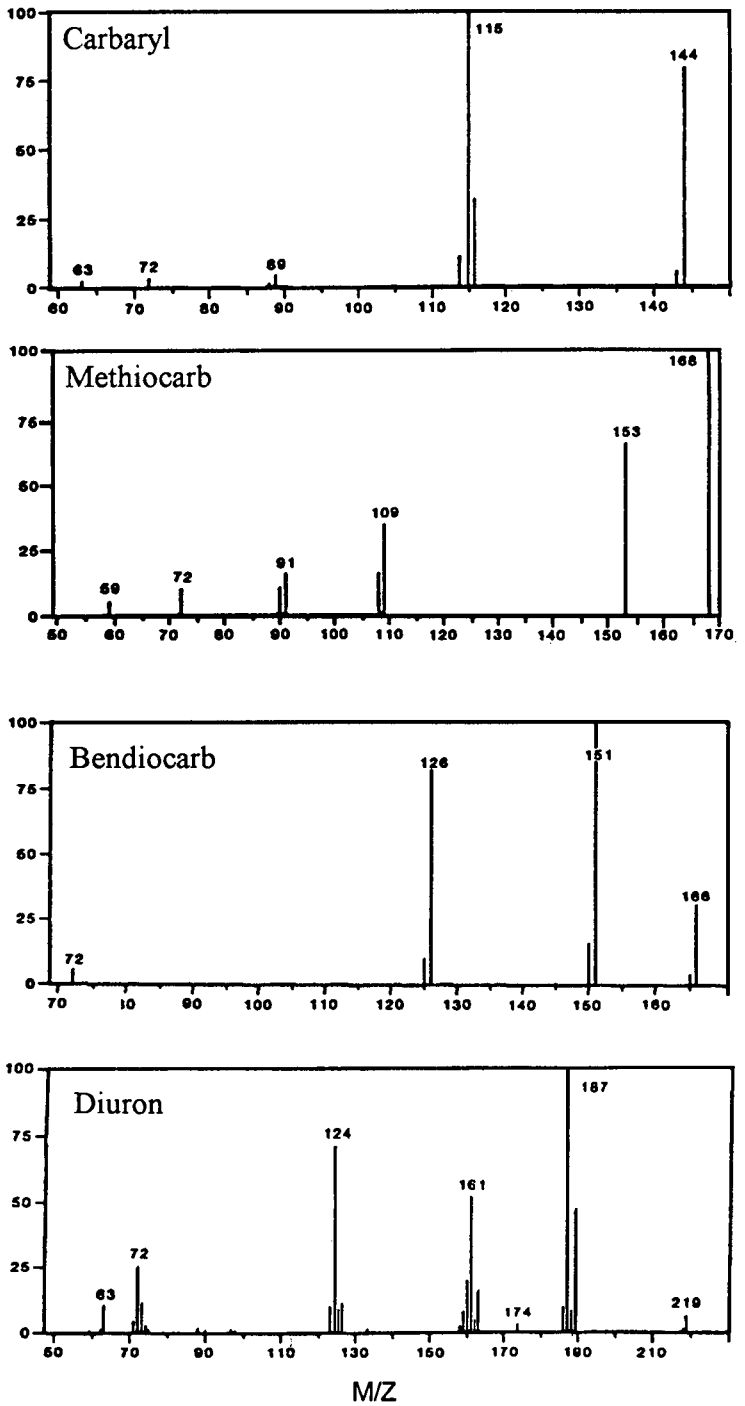

Fig. 4. The EI-mass spectra of the four pesticides in Fig. 3.

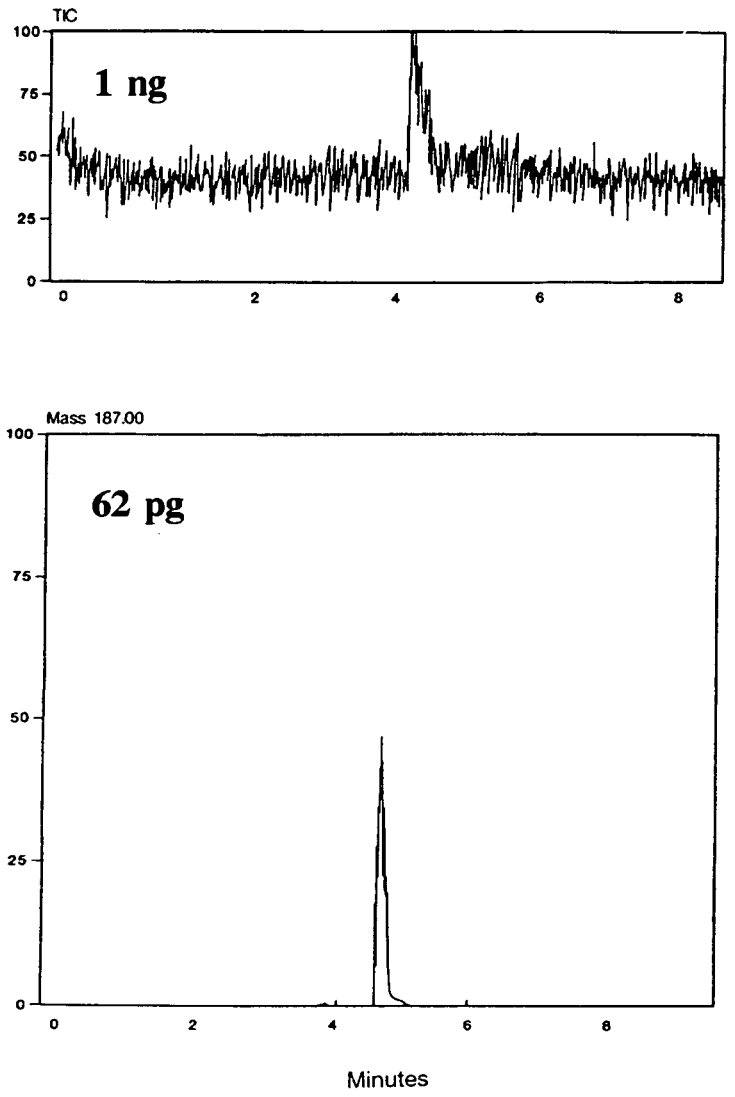

Fig. 5. Full-scan detection of 1 ng diuron and 62 pg in the selected-ion mode using a 1.5 m × 0.05 mm I.D. SB-octyl 30 column at 100°C and 0.6 g/ml.

such as the temperatures of the transfer line and ion volume, flow-rate, and the position of the tip of the restrictor had no effect. Modifying the interface to allow differential heating of the transfer line also had no effect. The problem was solved by adjusting the temperature of the probe tip and ion source to 290°C. Two other shortcomings of the SFC–MS apparatus were the short life of the thoriated tungsten filament in the ionizer and clogging of the tapered restrictor tip. These problems were eliminated by replacing the tungsten filament with a rhenium filament and using a capillary frit restrictor in place of the integral restrictor. The design and evaluation of the interface and mass spectrometer are presented in the following discussion.

Evaluation of the SFC–MS apparatus

Capillary SFC–MS is an attractive tool for polar thermally labile compounds such as carbamate pesticides [22–25] that are not amenable to GC–MS

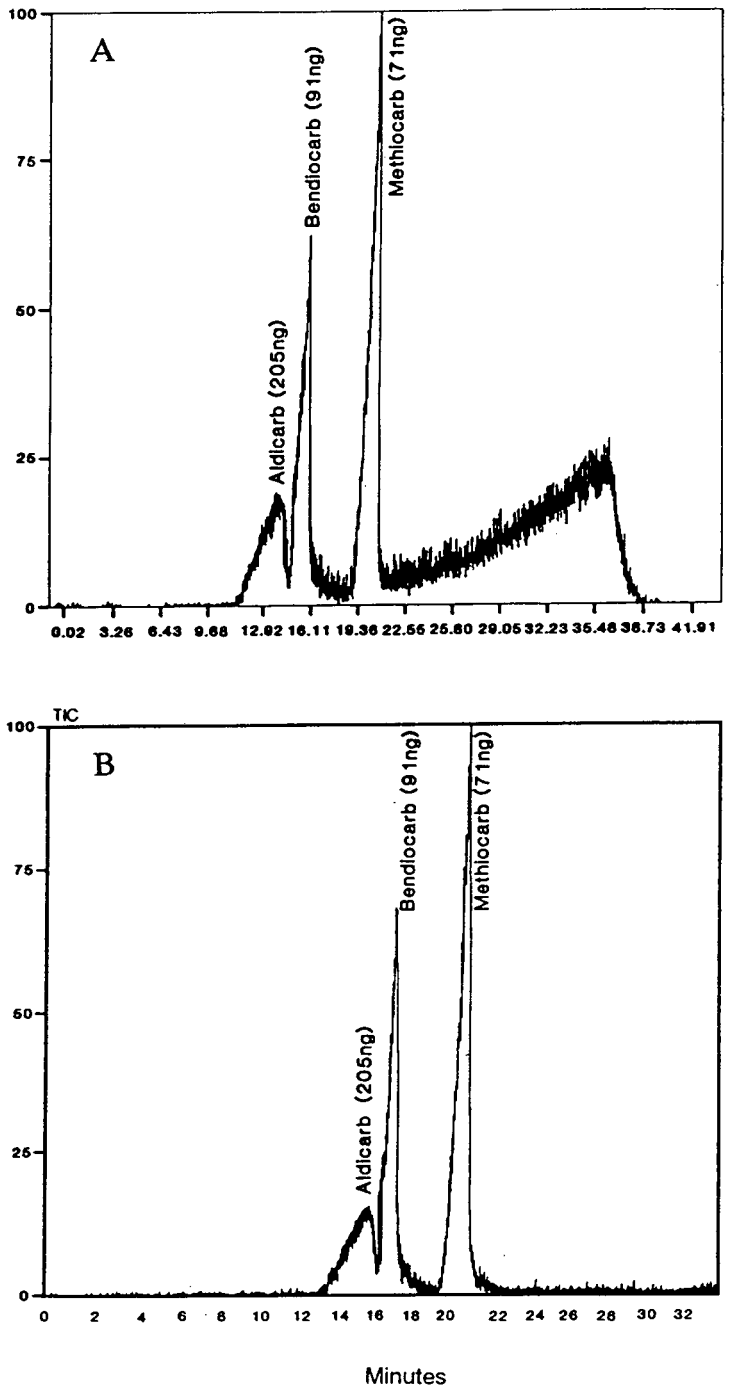

Fig. 6. The total ion chromatograms of a mixture of three carbamate pesticides obtained at different scan ranges using a 1.5 m × 0.05 mm I.D. SB-octyl 30 column at 80°C with density programming of carbon dioxide from 0.1 g/ml to 0.6 g/ml at 0.012 g/ml per min. (A) Scan range 50–250 u; (B) scan range 75–250 u.

methods. The SFC–EI-MS total ion chromatograms of four thermally labile pesticides including carbaryl (52 ng), methiocarb (60 ng), bendiocarb (44 ng) and diuron (60 ng) are shown in Fig. 3. Typical EI mass spectra of these pesticides are shown in Fig. 4 which compared favorably with the reference EI spectra obtained by other introduction methods. The chromatograms in Fig. 5 show the detection of 1 ng of diuron in the full scan mode ($S/N = 5$) and 63 pg of diuron in the selected-ion mode ($S/N > 100$), demonstrating the detection capability of this system. Separation and detection of a standard solution containing three carbamate pesticides using density programming are shown in Fig. 6. The two chromatograms A and B were obtained under identical conditions except for the scan range. Chromatogram A was obtained by scanning between 50 and 250 u, while chromatogram B was obtained between 75 and 250 u. There is a substantial reduction in the noise and baseline drift in the TIC scanned above m/z 75, since predominant ions in the noise part of the TIC in Fig. 6A were m/z 71 and 72. The poor peak shape for the aldicarb in these figures was due to the stationary phase employed. The chromatograms shown in Fig. 7 are another example of the detection capability of

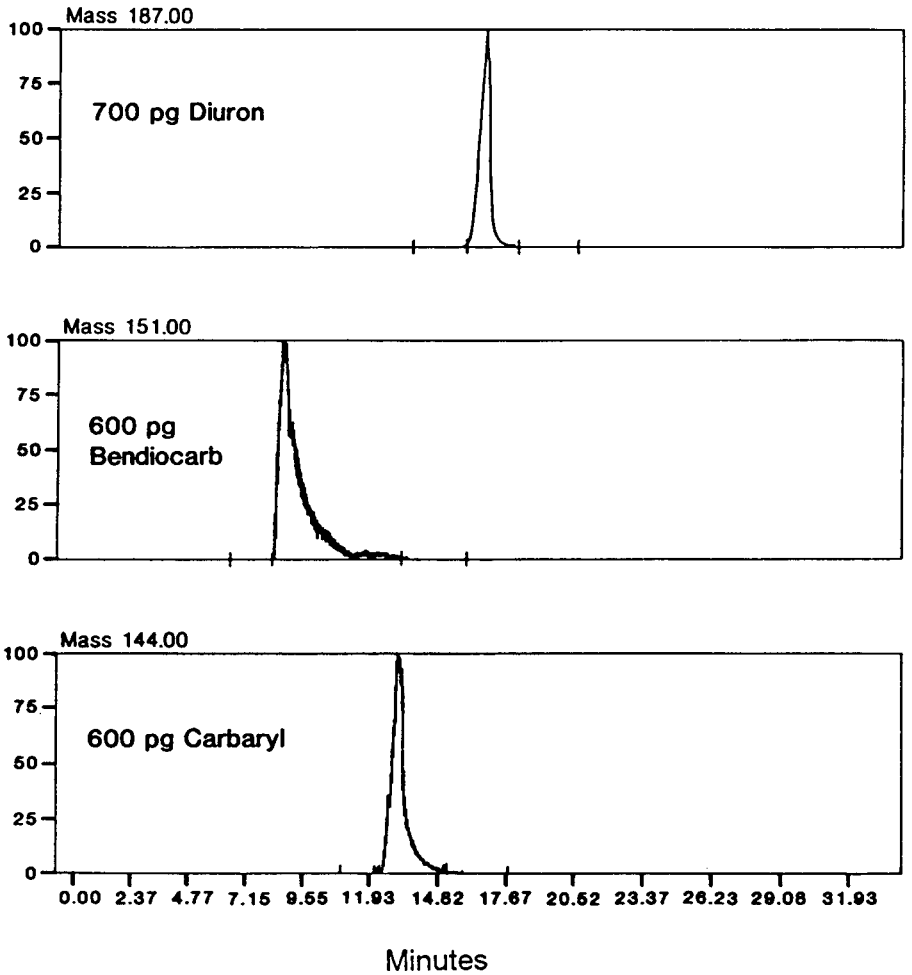

Fig. 7. Separation and detection of a pesticide mixture containing picogram levels of three thermally labile pesticides in the selected-ion mode. SFC conditions: 1.5 m × 0.05 mm I.D. SB-biphenyl 30 column at 100°C with density programming of carbon dioxide from 0.1 to 0.6 g/ml at 0.012 g/ml per min.

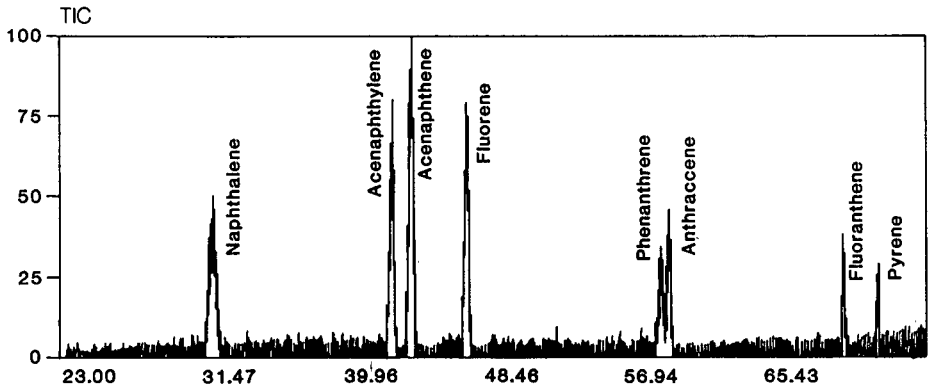

Fig. 8. Total ion chromatograms of a mixture containing eight polynuclear aromatic hydrocarbons using 5 m × 0.05 mm I.D. SB-biphenyl 30 column at 100°C with density programming from 0.2 to 0.3 g/ml at 0.01 g/ml per min then to 0.7 g/ml at 0.015 g/ml per min.

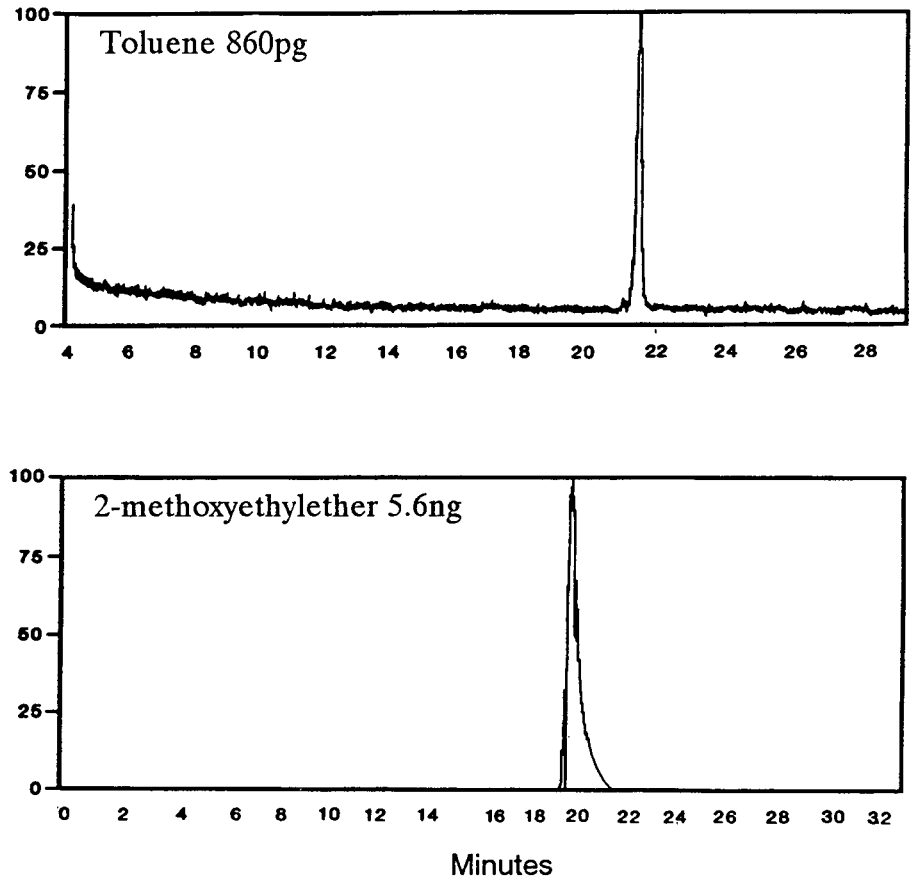

Fig. 9. Total ion chromatograms of 860 pg of toluene and 5.6 ng of 2-methoxyethyl ether using a 5 m × 0.05 mm I.D. SE-52 column at 100°C at 0.2 g/ml of carbon dioxide.

this system as a routine analytical tool. These chromatograms were obtained in the selected-ion monitoring mode for a standard pesticide solution containing diuron (700 pg), bendiocarb (600 pg), and carbaryl (600 pg) in methanol. The *S/N* ratios for these selected ion peaks were calculated to be 2700, 297, and 606 for diuron, bendiocarb and carbaryl, respectively.

The application of SFC–EI-MS to polynuclear aromatic hydrocarbons (PAHs) is shown in Fig. 8. The total ion chromatogram shows the separation and detection of a standard solution containing 15 ng each of eight PAHs.

Fig. 9 shows the total ion chromatogram for 860 pg of toluene and 5.6 ng of 2-methoxyethyl ether. Toluene has shown the lowest detectable level. There remains a significant difference in sensitivity and chromatographic peak shape between the solid pesticide and polynuclear aromatic compounds and the liquid analytes such as toluene and 2-methoxyethyl ether. Our best explanation for the observed differences is the insufficient atomization of the solid analytes at the restrictor end.

The SFC–EI-MS system has been evaluated for reproducibility and linearity of the detector response. Repeated injections of different standard naphthalene solutions were analyzed over a period of two weeks. The peak area results are shown in Fig. 10 for samples ranging from 50.7 ng to 126 ng.

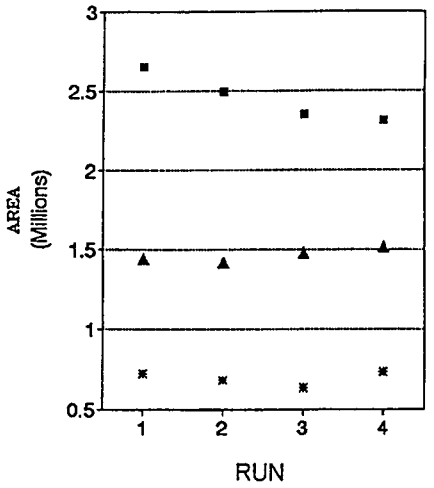

Fig. 10. The reproducibility of peak areas from the SFC–EI-MS for various amounts of naphthalene in methanol injected over two weeks. Symbols: ■ = 126 ng, ▲ = 76 ng, * = 50.7 ng.

The calculated %R.S.D. (5 replicates for each point) was from 2.9 to 6.4. It is evident from this graph that the response of this system is quite consistent.

The effect of the SFC column pressure on sensitivity and the signal-to-noise ratio has been evaluated using hexachlorobenzene as a standard. For column pressure between 219 and 347 atm, the chromtographic peak area of *m/z* 284 for a 100-ng injection of hexachlorobenzene changed from 50 841 to 10 750 for a decrease in sensitivity of 4.7. The *S/N* ratio decreased from 16 to 6 with the increase in pressure. Table I summarizes the peak areas and *S/N* for *m/z* 284 for three replicate 100-ng hexachlorobenzene injections at four different pressures. The best sensitivity is obtained at low pressure. The mass spectra obtained from the SFC–MS scanned above *m/z* 75 have been computer searched against the NIST/EPA/MSDC Version 3.02 Mass Spectral Database. For spectra that contained a low number of peaks below *m/z* 75, similarity indexes greater than 75 (perfect match = 100) have been obtained for comparison against the full library. Compounds which produce mass spectra with major peaks below *m/z* 75 do not provide good matches. Improved searching results have been achieved using an in-house library containing SFC mass spectra (start mass *m/z* 75). Similarity indexes of greater than 75 are common for spectra searched against this library.

CONCLUSIONS

The data presented in this paper clearly demonstrate the ease and feasibility of converting a commercially available benchtop GC–MS system into a SFC–EI-MS system for routine analytical work. The described instrument represents the most sensitive SFC–EI-MS reported yet. Traditional GC–MS techniques are not suitable for thermally labile pesticides, for which HPLC is the recommended analytical technique. The preliminary results reported here show that the analysis of these compounds are possible using SFC–MS with carbon dioxide as the mobile phase. The EI mass spectra can be seached against the conventional mass spectral library for compound identification. Further work is in progress in optimizing the detection capabilities of this system.

TABLE I

PEAK AREAS (*m/z* 284) AND SIGNAL-TO-NOISE RATIOS FOR A 100-ng HEXACHLOROBENZENE INJECTION AS A FUNCTION OF COLUMN PRESSURE

Values for the peak areas and *S/N* ratios are averages from three measurements.

Pressure (atm)	Peak area	*S/N*	R.S.D. (%)
219	50 841	16	1.4
250	28 804	22	2.2
305	14 088	10	5.6
347	10 750	6	2.1

ACKNOWLEDGEMENT

The authors wish to thank the US Department of Agriculture, the Environmental Protection Agency and Leybold Inficon for support of this work.

REFERENCES

1 L. G. Randall and A. L. Wahrhaftig, *Anal. Chem.*, 50 (1978) 1703.
2 J. R. Chapman, *Rapid Commun. Mass Spectrom.*, 5 (1991) 149.
3 J. D. Pinkston, T. E. Delaney, K. L. Morland and R. G. Cooks, *Proc. 39th ASMS Conf. on Mass Spectrom. and Allied Topics, Nashville, TN, May 19–25, 1991*, 1991, p. 160.
4 J. F. D. Todd, I. C. Mylchreest, A. J. Berry, D. E. Games and R. D. Smith, *Rapid Commun. Mass Spectrom.*, 2 (1988) 55.
5 H. L. Chung, J. C. Aldridge and D. S. Moore, *Anal. Instrum.*, 9 (1990) 99.
6 P. O. Edlund and J. D. Henion, *J. Chromatogr. Sc.*, 27 (1989) 274.
7 E. D. Ramsey, J. R. Perkins, D. E. Games and J. R. Startlin, *J. Chromatogr.*, 464 (1989) 353.
8 E. R. Baumeister, C. D. West, C. F. Ijmes and C. L. Wilkins, *Anal. Chem.*, 63 (1991) 251.
9 H. T. Kalinosky and R. D. Smith, *Anal. Chem.*, 60 (1988) 529.
10 S. M. Musser and P. S. Callery, *Biomed. Environ. Mass Spectrom.*, 19 (1990) 348.
11 J. F. Anacleto, L. Ramaley, R. K. Boyd, S. Pleasance, M. A. Quilliam, P. G. Sim and F. M. Benoit, *Rapid Commun. Mass Spectrom.*, 5 (1991) 149.
12 B. W. Wright, H. R. Udseth, E. K. Chess and R. D. Smith, *J. Chromatogr. Sc.*, 26 (1988) 228.
13 A. J. Berry, D. E. Games, I. C. Mylchreest, J. R. Perkins and S. Pleasance, *J. High Resolut. Chromatogr. Chromatogr. Commun.*, 11 (1986) 61.
14 R. D. Smith, W. D. Felix, J. C. Fjelsted and M. L. Lee, *Anal. Chem.*, 54 (1982) 1883.
15 S. D. Zaugg, S. J. DeLuca, G. U. Holzer and K. J. Voorhees, *J. High Resolut. Chromatogr. Chromatogr. Commun.*, 10 (1987) 100.
16 E. D. Lee and J. D. Henion, *J. High Resolut. Chromatogr. Chromatogr. Commun.*, 9 (1986) 173.
17 E. D. Lee, S-H. Hsu and J. D. Henion, *Anal. Chem.*, 60 (1988) 1990.
18 C. W. Saunders, L. T. Taylor, J. Wilkes and M. Vestal, LC GC, (1990) 46.
19 J. F. J. Todd, I. C. Mylchreest, A. J. Berry, D. E. Games and R. D. Smith, *Rapid Commun. Mass Spectrom.*, 2 (1988) 55.
20 B. Murugaverl and K. J. Voorhees, *J. Microcol. Sep.*, 3 (1991) 11.
21 E. J. Guthrie and H. E. Schwartz, *J. Chromatogr. Sci.*, 24 (1986) 236.
22 B. W. Wright and R. D. Smith, *J. High Resolut. Chromatogr. Chromatogr. Commun.*, 8 (1985) 8.
23 H. T. Kalinoski, B. W. Wright and R. D. Smith, *Biomed. Environ. Mass Spectrom.*, 13 (1986) 33.
24 B. W. Wrigth, H. T. Kalinoski, H. R. Udseth and R. D. Smith, *J. High Resolut. Chromatogr. Chromatogr. Commun.*, 9 (1986) 145.
25 A. J. Berry, D. E. Games, I. C. Mylchreest, J. R. Perkins and S. Pleasance, *Biomed. Environ. Mass Spectrom.*, 15 (1988) 105.

Journal of Chromatography, 633 (1993) 207–211
Elsevier Science Publishers B.V., Amsterdam

CHROM. 24 745

On-column detection in capillary zone electrophoresis with ion-selective microelectrodes in conical capillary apertures

André Nann* and Wilhelm Simon☆

Department of Organic Chemistry, Swiss Federal Institute of Technology (ETH), CH-8092 Zurich (Switzerland)

(Received September 21st, 1992)

ABSTRACT

In capillary zone electrophoresis with an ion-selective microelectrode (ISME) as detector in an on-column position, drift and noise problems are encountered, mainly because the ISME is not decoupled from the electrophoretic field and because temporary instabilities in its position give rise to potential changes, which are superimposed on the Nernstian response. To stabilize the position of the ISME with a precision of at least ±10 nm would be very costly. This paper describes a procedure for drastically reducing drift and noise by etching the detector-side capillary end with hydrofluoric acid to a conical aperture. The field strength at the tip of the ISME is considerably reduced compared with that of the remaining capillary.

INTRODUCTION

In the past few years, the use of capillary zone electrophoresis (CZE) has greatly increased, but so far only UV and fluorescent detectors are commercially available. In contrast to optical and conductivity detectors, electrochemical and potentiometric [ion-selective microelectrodes (ISMEs)] [1,2] on-column detectors must be decoupled from the electrophoretic field, otherwise meaningless or noisy signals are obtained. Decoupling from the electrophoretic current was first achieved by means of a porous glass joint [3], which allowed catecholamines to be detected amperometrically with a carbon fibre inserted in the capillary end and an external reference electrode. The major drawback of amperometric detectors is that they are applicable only to electroactive analytes. For electrochemically inert systems and very small detection volumes, ISMEs have certrain advantages. In a single run, it is possible to detect widely different ions, *e.g.*, of neurotransmitters and inorganic electrolytes [4]. It could even be possible to detect individually two co-migrating ions with the help of two ISMEs showing adequate selectivity behaviour. In addition, the detection limits for specially designed ISMEs may be lower than those for conductivity detectors.

When first using ISMEs as CZE detectors [1,2] the microelectrode tip was positioned several micrometres behind the capillary end (post-column) to avoid drifting and noisy potentials due to the electrophoretic field inside the capillary. If the buffer vessel is considered as a sphere of infinite radius, r with its surface as the common electrode and the capillary end at its centre, the electrophoretic field decreases with r^3. Owing to irreproducible (thermal) turbulence, post-column detection leads to distorted peak shapes, so that conditions for quantitative analysis and maximum resolution are not fulfilled. With the aim of using ISMEs as on-column detectors in CZE, the capillary end was etched to a conical aperture in which the field strength is lower and thus allows the accurate measurement of ions.

* Corresponding author.
☆ Author deceased November 17th, 1992.

THEORY

For the following theoretical treatment, a system consisting of an ISME inserted in a buffer-filled capillary (Fig. 1) is considered electrically as a voltage divider with the capillary as a potentiometer and the ISME as its wiper. This allows a simple description of potential drift and noise of the ISME caused by instabilities in its position.

The resistance, R_l, of a cylindrical volume element with length l and radius r is given by

$$R_l = \rho l/\pi r^2 \quad (1)$$

where ρ is the specific resistance of the buffer solution. If a voltage V is applied over the total length, L, of a buffer-filled capillary (resistance R_L) and the ISME is inserted to a length l, the potential, U_l, sensed by the ISME corresponds to

$$U_l = V(R_l/R_L) \quad (2)$$

Substitution of eqn. 2 with eqn. 1 gives

$$U_l = V(l/L) \quad (3)$$

Discrete values of U_l are of interest only in so far as they are superimposed on the Nernstian response of the ISME, thus falsifying the e.m.f. values. Much more important are changes in U_l as a function of l, which describe the potential drift and noise caused by variations in l. On the other hand, the derivative dU/dl, corresponding to the field strength, E, is proportional to drift and noise at the tip of the ISME. Derivative of eqn. 3 leads to

$$dU/dl = V/L = E \quad (4)$$

which means that E at any point in the capillary is independent of l. This relationship is expected for a cylindrical conductor, but does not hold if the capillary has a conical aperture (Fig. 2). This aperture geometrically has the form of a frustum of a cone with height K and radii g and r of the base and top area, respectively. The corresponding cone is characterized by its height, H, and slope, m:

$$m = g/H \quad (5)$$

The resistance, dR, of a volume element with infinitesimal height, dh (h being the distance between the tip of the cone and any point on the axis of the frustum), is calculated as follows:

$$dR = \frac{\rho}{\pi m^2 h^2} \cdot dh \quad \text{with } (H - K) \leqslant h \leqslant H \quad (6)$$

Definite integration of eqn. 6 between the limits a and b leads to

$$R = \frac{\rho}{\pi m^2}\left[-\frac{1}{h}\right]_a^b \quad \text{with } (H - K) \leqslant a \leqslant b \leqslant H \quad (7)$$

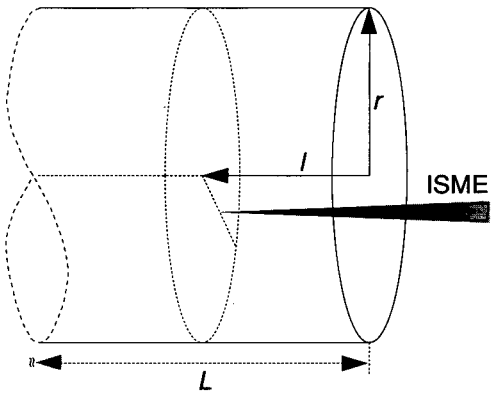

Fig. 1. On-column positioning of an ISME in a cylindrical capillary aperture. L = Total length of the capillary, l = distance from capillary end to ISME tip; r = inner radius of the capillary.

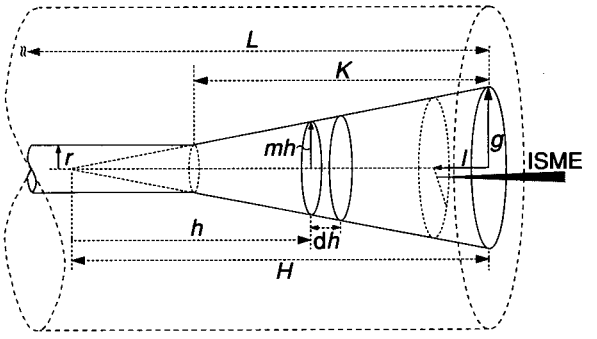

Fig. 2. On-column positioning of an ISME in a conical capillary aperture. g = Aperture radius at capillary end; H = height of conical aperture; h = distance from tip of the cone to any point on its axis; dh = infinitesimal element of h; K = height of conical frustum; L = total length of capillary; l = distance between tip of the ISME and capillary end; mh = radius of aperture at any point on cone axis; r = inner radius of unetched capillary.

Hence, the resistance R_l of a volume element of length l at the end of the capillary is given by

$$R_l = \frac{\rho}{\pi m^2}\left[\frac{1}{H-l} - \frac{1}{H}\right] \quad \text{with } 0 \leqslant l \leqslant K \quad (8)$$

Eqn. 8 only holds if $l < K$; if not, inaccurate values of R_l will result.

Using for R_L the same definition as for a cylindrical conductor (which entails an error $\ll 1\%$), U_l at the tip of the ISME in a capillary with a conical apertune is obtained by substituting eqn. 2 with eqns. 1 and 8:

$$U_l = \frac{Vr^2}{m^2 L}\left[\frac{1}{H-l} - \frac{1}{H}\right] \quad \text{with } 0 \leqslant l \leqslant K \quad (9)$$

Again, the derivative dU/dl yields the field strength, E_l:

$$E_l = \frac{Vr^2}{m^2 L} \cdot \frac{1}{(H-l)^2} \quad \text{with } 0 \leqslant l \leqslant K \quad (10)$$

Obviously, in this instance, the field strength is no longer independent of l, but decreases with $(H - l)^2$. This means that positioning the tip of the ISME in a conical aperture at a length, l from the end of the capillary yields lower field strengths than in a cylindrical aperture.

EXPERIMENTAL

Reagents

Chemicals of the highest purity available (Fluka, Buchs, Switzerland) and doubly quartz-distilled water were used.

CZE system and data acquisition

The CZE system used was similar to that described previously [1]. The electrophoretic field was generated by a Model 225-50 R high-voltage power supply (Bertan Associates, Hicksville, NY, USA). Fused-silica capillaries of I.D. 10 μm were purchased from Scientific Glass Engineering (Ringwood, Australia). Potentials were measured differentically, *i.e.*, the potential difference between the ISME and a reference electrode [Ag | AgCl | $MgCl_2$ (20 m*M*); tip diameter 1 mm] was determined with the aid of a platinum cathode as a common electrode. The platinum cathode, ISME, reference electrode and capillary end were placed in a small plastic vessel filled with buffer solution. On-column positioning of the ISME was achieved with micromanipulators and an inverse microscope (Narishige and Diaphot; Nikon, Chiyoda-ku, Tokyo, Japan). Capillaries were filled under pressure (80 bar) with buffer solution passed through a microfilter (0.2 μm Prep-Disk sample filter; Bio-Rad Labs., Richmond, CA, USA). For stabilizing the electrophoretic system, a high voltage was applied to the capillaries until a constant current was reached. The reference and the ion-selective electrodes were directly connected to Type AD 515 KH operational amplifiers (Analog Devices, Norwood, MA, USA), wired as voltage followers. Potentials were amplified with a laboratory-made electrode monitor.

Data were acquired with an Apple Macintosh IIx computer (Apple Computer, Cupertino, CA, USA) through a 16-bit NuBus A/D converter card (MacAdios II; GW Instruments, Somerville, MA, USA). Analysis of the electropherograms was performed with the program LabView (National Instruments, Austin, TX, USA).

Etching of capillaries

Conically shaped apertures were prepared by immersing the buffer-filled capillaries over a length of 3 mm in 40% hydrofluoric acid for 25 min. The dimensions (see Fig. 2) of the conical aperture were determined with a microruler under a microscope and typically were $g = 25$ μm and $H = 500$ μm.

Ion-selective microelectrodes

Preparation, pulling and silanization of the ISMEs have been described previously [5,6]. Under a microscope, tips were broken to a diameter of *ca.* 4 μm against a polished glass rod. By applying a slight overpressure with a syringe, the micropipettes were back-filled with 20 m*M* $MgCl_2$. The tips were then front-filled to a height of *ca.* 150 μm by dipping them into the ion-selective membrane phase, which consisted of potassium tetrakis(4-chlorophenyl)borate (10 mg) in 2-nitrophenyl octyl ether (500 mg). The ISMEs were conditioned on-column for 3 h, applying an electrophoretic voltage of 30 kV.

RESULTS AND DISCUSSION

Using unetched capillaries (see Fig. 1) of length 50 cm with an applied voltage of 30 kV, the field strength, E, at the tip of the ISME is 60 mV/μm according to eqn. 4. Through a microscope, it was observed that the ISME tip suffered slight variations of up to 5 μm/h in its axial position. Theoretically, this would lead to a drift of up to 50 mV in the time necessary for running an electropherogram (*ca.* 10 min). Accordingly, a noise of ± 0.4 mV would correspond to axial vibrations of about ± 7 nm, which of course are too small to be detected under the light microscope. On the other hand, theory shows that positional instabilities perpendicular to the capillary axis do not induce significant potential drift. This was confirmed experimentally by varying, within a single run, the position of the ISME perpendicularly to the capillary axis. The axial stabilization of the ISME within the maximum required range of ± 7 nm would be very costly and the use of such a detection system cumbersome. According to eqn. 10, E_l is expected to decrease significantly if on-column potentiometric detection is performed in a conically shaped capillary end. By inserting the ISME in the capillary aperture to a length of l = 10 μm (see Fig. 2), the field strength at the tip is only 2.5 mV/μm, which means that potential drift and noise are reduced by a factor of *ca.* 25.

TABLE I

TYPICAL POTENTIAL DRIFT AND NOISE VALUES FOR DIFFERENT CAPILLARY APERTURES

Parameter	Capillary aperture		Improvement factor
	Cylindrical	Conical	
Drift	≤5.0 mV/min	<0.17 mV/min	≈30
Noise [7]:			
Short-term	±0.4 mV	±0.06 mV	6
Long-term	±2.0 mV	±0.25 mV	8

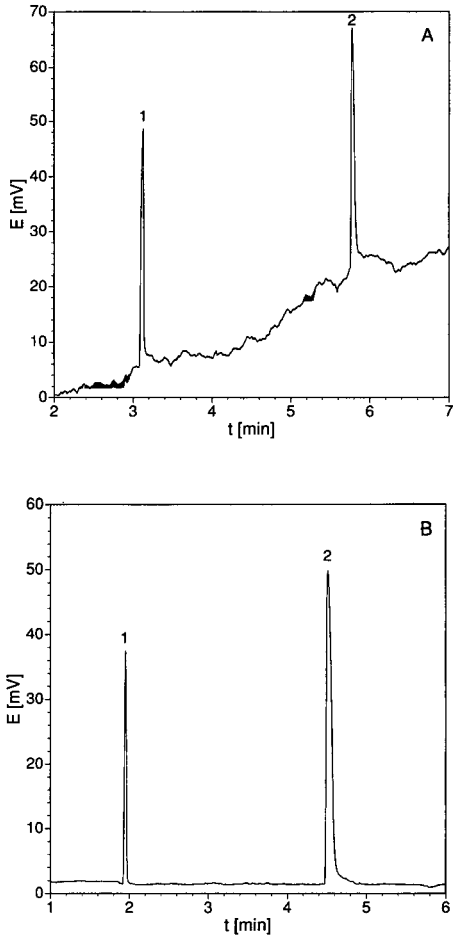

Fig. 3. CZE on a 50-cm capillary. Buffer, 20 mM magnesium acetate solution; voltage, 30 kV; injection, electrokinetic, 5 kV for 5 s. (1) 1 mM potassium chloride and (2) 3 mM dopamine hydrochloride in 10 mM magnesium acetate solution. (A) Cylindrical aperture, with ISME inserted 1 μm; (B) conical aperture, with ISME inserted 10 μm.

Fig. 3 shows two electropherograms obtained on CZE capillaries with a cylindrial and a conical aperture. The improvements in the baseline stability and the drift reduction are obvious. Table I gives typical results obtained with both detection systems. For the drift, the improvement factor is in agreement with the above theoretical calculation, whereas for the noise it is much lower. This could be due, *e.g.*, to noise from the electronic set-up or to environmental disturbances. Nevertheless, a straight baseline is achieved, which is of utmost importance for accurate peak integration and analyte quantification.

ACKNOWLEDGEMENTS

We are grateful to Prof. Dr. E. Pretsch and Dr. D. Wegmann for helpful suggestions. Part of this work was supported by the Swiss National Science

Foundation and by Ciba-Corning Diagnostic Corp.

REFERENCES

1 C. Haber, I. Silvestri and S. Röösli, *Chimia*, 4 (1991) 117.
2 C. Haber, *Dissertation*, No. 9713, ETH, Zurich, 1992.
3 R. A. Wallingford and A. G. Ewing, *Anal. Chem.*, 59 (1987) 1762.
4 I. Silvestri, C. Haber and W. Simon, in preparation.
5 F. Lanter, *Dissertation*, No. 7076, ETH, Zurich, 1982.
6 T. Bührer, *Dissertation*, No. 8984, ETH, Zurich, 1989.
7 R. P. W. Scott, *Liquid Chromatography Detectors* (*Journal of Chromatography Library*, Vol. 33), Elsevier, Amsterdam, 2nd ed., 1986.

Journal of Chromatography, 633 (1993) 213–220
Elsevier Science Publishers B.V., Amsterdam

CHROM. 24 798

Two-dimensional protein separation by microcolumn size-exclusion chromatography–capillary zone electrophoresis

Anthony V. Lemmo and James W. Jorgenson*

Department of Chemistry, University of North Carolina, Chapel Hill, NC 27599-3290 (USA)

(First received September 30th, 1992; revised manuscript received December 4th, 1992)

ABSTRACT

A two-dimensional separation system for the study of proteins consisting of size-exclusion chromatography (SEC) and capillary zone electrophoresis (CZE) is presented. The SEC separation was carried out in a 1 m × 250 μm I.D. microcolumn. The effluent from this SEC microcolumn filled a sample loop on a computer controlled 6-port valve. The contents of this loop were swept past the grounded end of the CZE capillary for electromigration injection. Detection was by on-line UV detection at 214 nm. The system was initially tested with protein test mixtures, then was used to analyze human, horse and bovine sera. Data are presented as three-dimensional chromatoelectropherograms and grayscale images.

INTRODUCTION

The realization that in many cases no single separation technique is capable of completely resolving all the components in a complex mixture has spawned considerable interest in the area of two-dimensional (2D) separation techniques. Although the general theory underlying these 2D systems has been fully explained [1–4] and is widely accepted, the reduction to practice of this theory into viable 2D separation systems has been relatively slow. Bushey and Jorgenson [5] realized that capillary zone electrophoresis (CZE) was well suited as a second dimension separation due to its potential for high speed while maintaining high separation efficiency. They introduced the first automated "comprehensive" 2D system that coupled column liquid chromatography (LC) with CZE [5]. The focus of this work was the study of peptides by reversed-phase HPLC–CZE. Previous approaches to 2D coupled column techniques involved analysis of only certain regions of interest from the first dimension by the second dimension of separation. In the comprehensive 2D approach of Bushey and Jorgenson, all sample components from the first dimension are analyzed by the second dimension (although the entire volume is not re-injected). Since the inception of this 2D system, our research group has become increasingly interested in expanding the scope of 2D separations. Part of our interest lies in constructing a 2D system for separating proteins.

One of the major tasks facing bioanalytical chemistry is the separation of complex mixtures of biopolymers. Novotny [6] has outlined the recent advances in biomacromolecular separations and forecasts some of the new technology required to further the advancement in this area. He points out that HPLC, particularly when employing microcolumn separations, along with CZE, holds considerable promise for separation and microisolation of protein mixtures due to the high selectivity and efficiency these techniques provide. To address this point, we have constructed an automated 2D separation system for proteins based on microcolumn size-exclusion chromatography (SEC) and CZE.

As a first-dimension separation, SEC is particularly well suited for protein separation because it provides easily interpretable qualitative informa-

* Corresponding author.

0021-9673/93/$06.00

tion: the molecular weight distribution of a mixture. In addition, SEC is run under non-denaturing conditions. This allows any biological activity that a protein might possess to be maintained. The relative merits of using microcolumns rather than conventional size columns has been previously discussed [7]. The major advantage —increased separation efficiency— is particularly important in SEC. In SEC, separation is based primarily on size, and as a result, is not noticably enhanced by the addition of mobile phase modifiers. Resolution in SEC is therefore essentially a sole function of separation efficiency. CZE, also run under non denaturing conditions, provides information on overall molecular charge. When operating in tandem in a 2D system, SEC–CZE can provide an estimate of overall charge within a certain molecular mass range of a mixture. This type of information may prove to be valuable in studies of biopolymers.

EXPERIMENTAL

Reagents

Protein standards, sera samples and buffer reagents were purchased from Sigma (St. Louis, MO, USA). Formamide was obtained from Fisher Scientific (Raleigh, NC, USA). All chemicals were used as received.

The buffer used for both separations was 10 m*M* tricine, 25 m*M* Na_2SO_4, 0.005% (w/v) sodium azide adjusted to pH 8.23 with NaOH. Buffer solutions were made with deionized water purified with a Barnstead Nanopure system (Boston, MA, USA) and were filtered with 0.2-μm nylon membrane filters from Alltech (Deerfield, IL, USA).

Sample preparation

A protein standard mixture was made from thyroglobulin (THYRO), bovine serum albumin (BSA), chicken egg albumin (OVA), and horse heart myoglobin (MYO) each present at 2% (w/v). This mixture also contained 5% (w/v) formamide (FA). Human serum (lyophilized powder) and bovine serum (lyophilized powder) were reconstituted in 500 μl of buffer containing 8% (w/v) formamide (1 ml was the original volume according to Sigma). Horse serum (lyophilized powder) was reconstituted in 1000 μl of buffer containing 7.5% (w/v) formamide (2 ml was the original volume). The protein standard mixture and the sera samples were subjected to centrifugation at 16 000 *g* for 2 min. After centrifugation, the supernatants were drawn off and stored at 4°C. Centrifugation removes any undissolved particulate matter from the samples. This approach was used rather than filtering due to the small volumes being used.

Column packing procedure

The size exclusion column used was a 250 μm inner diameter (I.D.) fused-silica capillary with length 105 cm (Polymicro Technologies, Phoenix, AZ, USA). The capillary was slurry packed in our laboratory with 6-μm, spherical, Zorbax GF450 particles (Rockland Technologies, Newport, DE, USA). The packing procedure has been described previously [7] and was followed with slight modification to the fritting process. A frit is constructed by tapping one end of the fused-silica capillary into a vial containing 100 μm diameter borosilicate glass beads (Sigma). Once a band of glass beads approximately 200 μm in length has been formed in the capillary, the beads are sintered by an arcing device built in the laboratory [8]. Prior to packing, frits are tested by placing the inlet end of the column in a reservoir of methanol and applying 3 bar (50 p.s.i.) of helium pressure for 30 s. Any unstable frits will dislodge during this process. The inlet end is next placed in a high pressure slurry reservoir containing a slurry of 1:10 (w/v) packing material to methanol. Methanol is forced into the reservoir at 200 bar (3000 p.s.i.) by an Altex model 110A pump. Columns are typically packed in 8–10 h and allowed to settle overnight under pressure. The pump is then turned off and the pressure allowed to bleed out through the column for 4 h. The column is then rinsed with deionized water for 4 h, followed by the running buffer which is allowed to rinse overnight.

Instrumentation

Fig. 1 is a schematic of the entire instrumental setup.

Chromatographic system. The chromatographic injection system has been modified from a static split injection system which had been developed for open-tubular LC in our laboratory [9]. Rather than performing a static split injection which requires several hundred microliters of sample per injection, injections were made from a pressure reservoir con-

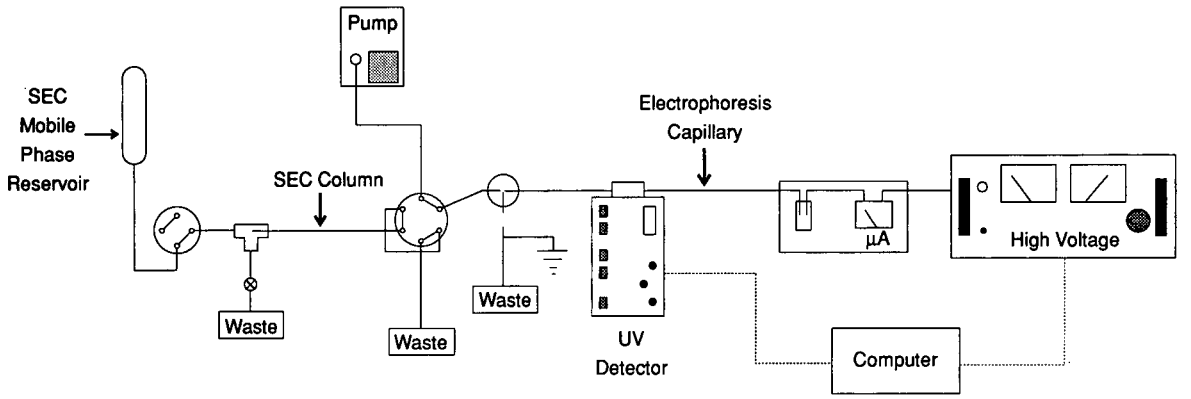

Fig. 1. Schematic of instrumental setup for 2D SEC–CZE.

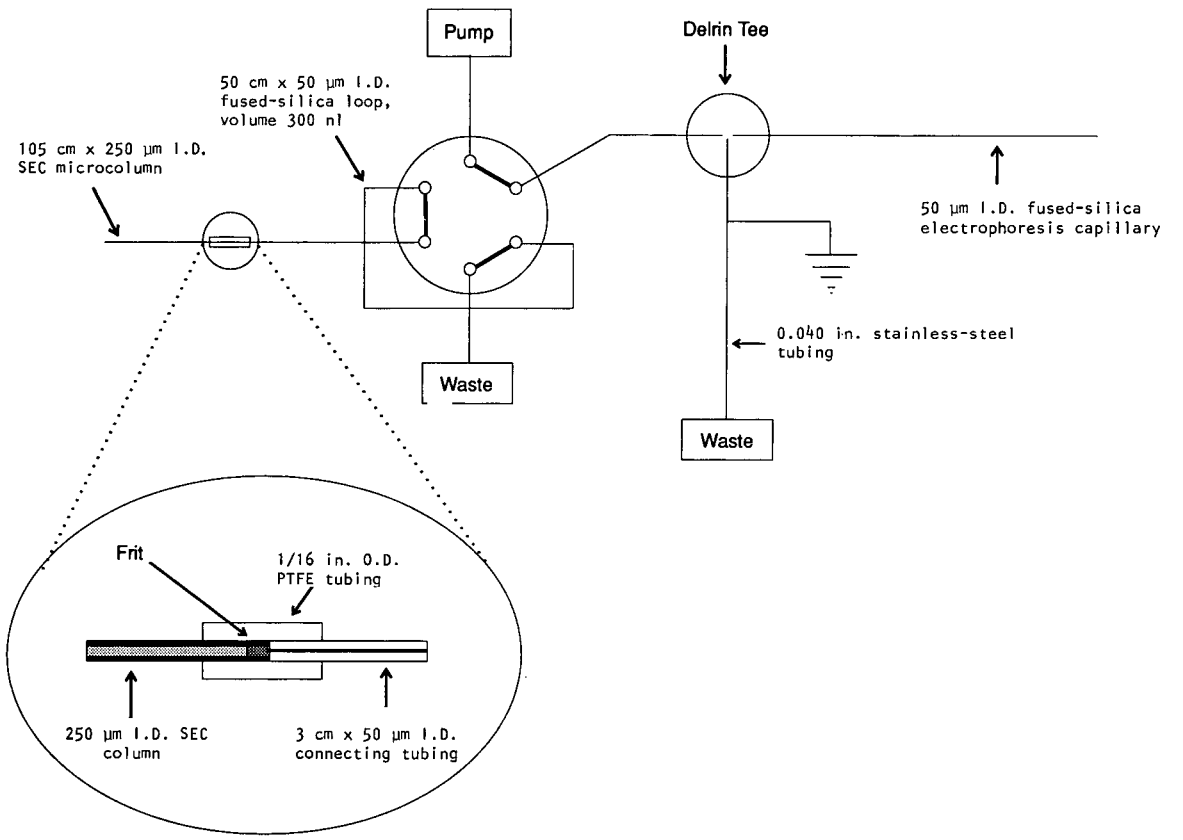

Fig. 2. Expanded view of the 6-port valve used to interface the SEC microcolumn with the CZE capillary. The inset shows the union between the SEC microcolumn and the fused-silica connecting tubing used to interface the microcolumn to the 6-port valve. Details are given in the text.

taining a small vial of sample. The microcolumn was removed from the static split injection tee and inserted into the pressure reservoir where head pressure of 7 bar (100 p.s.i.) was applied for a predetermined time to inject the desired volume of sample. For the protein standards sample, a 10-min injection was performed. A shorter injection time of 6 min was used for the sera samples. After the injection was complete the microcolumn was returned to the static split injection tee where 55 bar (800 p.s.i.) of head pressure was applied to begin chromatography. This head pressure generates an SEC flow-rate of approximately 360 nl/min.

Electrophoresis system. Capillary electrophoresis was performed in untreated fused-silica capillary with inner diameter of 50 μm. Capillary lengths and distance to the detection window varied and are reported in the figure captions. A ± 30 kV high-voltage power supply (Spellman High Voltage Electronics Corp., Plainview, NY, USA) was used in the negative high-voltage mode. Electromigration injections were done at −3 kV for 5 s. Typical run conditions were 4 min at −8 kV and 28 μA. Any changes in CZE operating conditions are provided in figure captions.

SEC–CZE Interface. The SEC microcolumn was interfaced to the CZE system through a 6 port electrically actuated valve. Fig. 2 shows a schematic of this interface. The 6-port valve (Valco, Houston, TX, USA) was fitted with a 300-nl collection loop fabricated in-house from a 15 cm long piece of 50 μm I.D. × 350 μm O.D. fused-silica capillary. Each end of the fused-silica loop was held in place in the valve by sleeving through polyether ether ketone (PEEK) tubing "liners". The liners were made from 2-cm lengths of 0.020 in. I.D. × 1/16 in. O.D. (1 in. = 2.54 cm) PEEK tubing (Upchurch Scientific, Oak Harbor, WA, USA). Each of these liners has a "Light-Touch" removable ferrule system (Upchurch Scientific) and a standard 1/16-in. stainless-steel nut for fittings.

Rather than directly exposing the relatively fragile fritted end of the microcolumn to the fittings necessary to hold the capillary in place within the valve, the microcolumn was coupled to a 3 cm long section of 50 μm I.D. × 350 μm O.D. fused-silica capillary. The union between these capillaries was made by sleeving the capillaries with a 1 cm piece of 0.007 in. I.D. × 1/16 in. O.D. PTFE tubing. When heated, the PTFE tubing expands and allows insertion of the capillaries. Upon cooling, a snug fit is obtained between the capillaries and the tubing. The 3-cm fused-silica connecting tube is also held in place within the valve by a PEEK tubing liner. Protecting the delicate frit in this manner increases column lifetime and allows easy insertion and removal of the SEC microcolumn from the valve.

The electrophoresis capillary was coupled to the valve through a Delrin tee (Alltech) which was connected to the valve by a 5-cm section of 0.005 in. I.D. × 1/16 in. O.D. PEEK tubing (Upchurch Scientific). The capillary extended in to the tee and was held in place near the center of the tee with a PEEK tubing liner. A 20-cm section of 0.040 in. I.D. stainless-steel tubing was also inserted into the Delrin tee. This tubing serves as both a waste line and as the ground electrode (anode) for the CZE system. A microammeter was placed between the tubing and the connection to ground to allow for current monitoring. The height of this stainless-steel waste line was kept level with the cathodic buffer reservoir to minimize hydrodynamic flow within the CZE capillary. The general operation and timing sequence of the valve have been previously described [5]. A flush rate of 100 μl/min was provided by a Hewlett-Packard 1050 pump (Hewlett-Packard, Palo Alto, CA, USA).

Detection. A Linear model 200 variable-wavelength UV–VIS detector outfitted with an on-column capillary flowcell was used for UV detection (Linear Instruments, Reno, NV, USA). Detection was done at 214 nm with a sensitivity of 0.05 absorbance units full scale (AUFS) and a rise time of 0.1 s.

Instrument control. A Hewlett-Packard Vectra 386/25 computer with 25 MHz clock speed and math coprocessor was used to control the 6-port valve, high-voltage power supply and data collection system. The computer was outfitted with a Labmaster multifunction data acquisition board (Scientific Solutions, Solon, OH, USA). Details concerning data collection with this interface board were previously described [5]. The data collection rate for all experiments was 2 points per second.

Data analysis and display. Laboratory-written software with QuickBasic 4.5 (Microsoft Corp, Redmond, WA, USA) provided control over experimental parameters and allowed for data processing

and analysis. The primary means of data display are provided by two commercial software packages. Three-dimensional (3D) chromatoelectropherograms are provided by Surfer 4.0 (Golden Software, Golden, CO, USA). This software allows for viewing 3D data plots from any angle of observation or rotation. These plots are useful for showing peak profile characteristics such as peak symmetry and extent of tailing. Spyglass Transform and Spyglass Format (Spyglass, Champaign, IL, USA), imaging software for the Apple Macintosh, provide grayscale images. There are built in mathematical functions within Spyglass that allow data manipulation (*e.g.* logarithms) and interpolation to be performed.

System preparation. Prior to a 2D separation, samples are run by CZE alone in order to gauge the performance of the electrophoretic system. This ensures that any change in electroosmotic flow can be compensated for by adjusting CZE voltage. This testing is done by manually injecting sample into the collection loop. This is accomplished by inserting a syringe adaptor into the valve port where the microcolumn normally resides. Injections are made with a 25-μl injection syringe. After manual injections are complete, fresh buffer is aspirated into the capillary prior to 2D operation.

RESULTS

Fig. 3A is a Surfer-generated 3D chromatoelectropherogram of the separation of the protein standards mixture. The 360 nl/min SEC flow-rate yields a 2-h run time for the entire 2D separation. Fig. 3B shows a Spyglass-generated grayscale image of the same separation. Unlike the 3D view which requires several observation angles for total viewing, the grayscale image provides easy observation of all separated sample components. The peak assignments indicated were confirmed by independently running each protein with formamide by CZE. Formamide plays two important roles in the 2D separation. Being a small molecule it serves as a totally included marker for SEC. As such, it indicates when the SEC separation is complete. This is useful for initial testing of the system because its elution time sets the upper limit on run time for any given set of conditions. Any peak elution after formamide indicates that a mechanism in addition to size exclusion is occuring. Also, because formamide is a neutral species, it serves as an electroosmotic flow marker in the CZE separation. Any variation in migration time for formamide can be attributed to changing electroosmotic flow. More importantly, neutral species do not tend to undergo adsorptive interactions with the fused-silica capillary surface and therefore usually yield symmetric peaks. Evidence of peak tailing in CZE for formamide is an

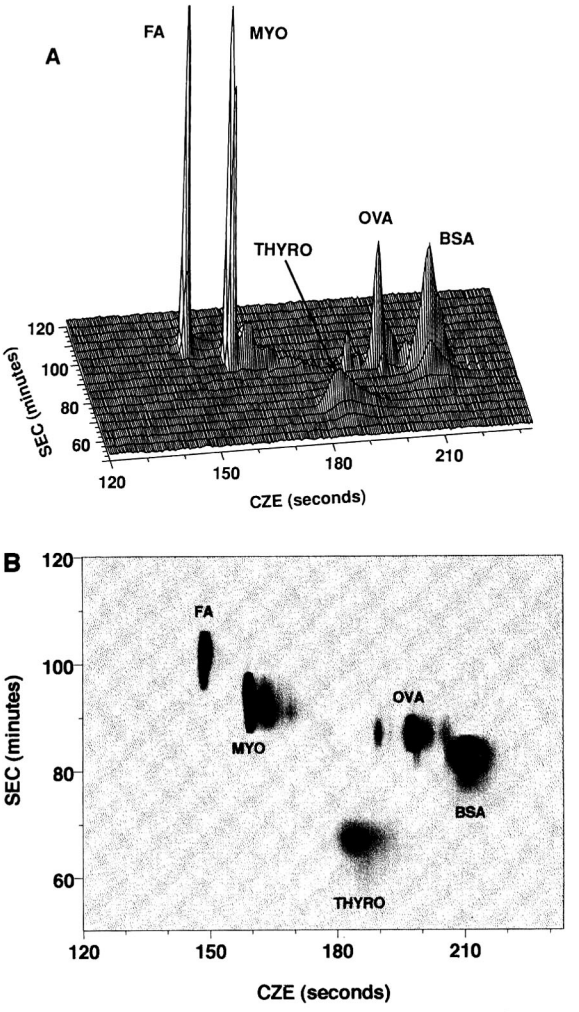

Fig. 3. Separation of protein standards by 2D SEC–CZE. SEC injection was 10 min at 7 bar (100 p.s.i.). Head pressure of 55 bar (800 p.s.i.) was applied to generate a flow-rate of 360 nl/min for the chromatographic separation. The electrophoresis capillary was 38 cm long, 20 cm to the detection window. CZE conditions are 5-s electromigration injection at −3 kV and 4-min runs at −8 kV. Data collection was 2 points/s. Shown here: (A) Surfer-generated 3D chromatoelectropherogram and (B) Spyglass-generated grayscale image.

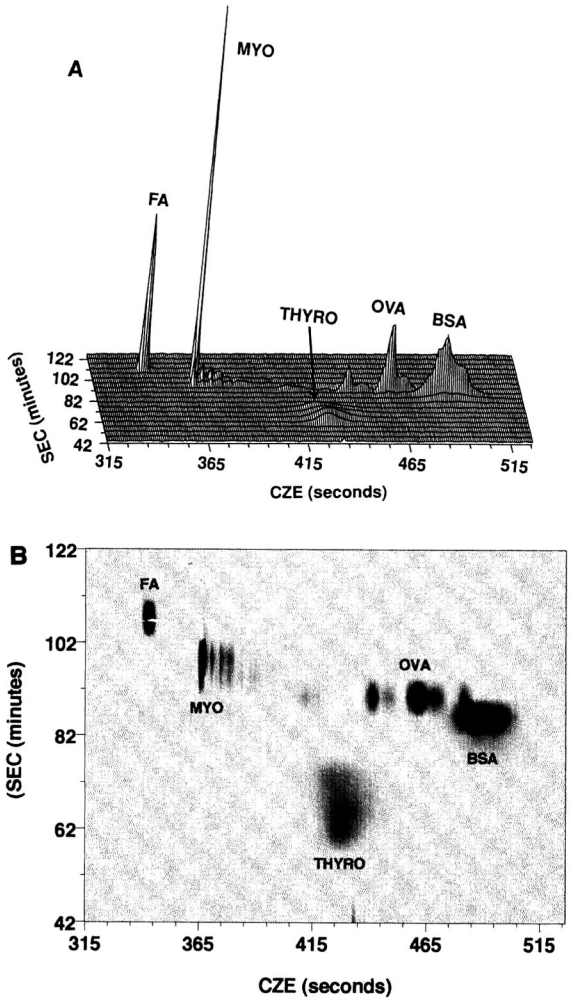

Fig. 4. Separation of protein standards by 2D SEC-CZE with overlapping CZE runs. SEC conditions as in Fig. 3. The electrophoresis capillary was 58 cm long, 40 cm to the detection window. CZE conditions are 5-s electromigration injection at −5 kV and 4.5-min runs at −11 kV. The actual required run time is 9 min. Data collection was 2 points/s. Shown here: (A) Surfer-generated 3D chromatoelectropherogram and (B) Spyglass-generated grayscale image. Data are in logarithm (base 10) scale.

indicator of an injection problem or poor interface washout characteristics.

In taking a closer look at Fig. 3B it becomes evident that the time span in which all the sample components migrate in the CZE dimension does not make full use of the entire separation time available. Although the CZE run time is 4 min long, all sample components migrate within a 1-min span. More importantly, detection of the first sample component does not begin until after half of the CZE run time has passed. This means that the entire first 2 min of the CZE run is analytically "wasted" time. One way to make use of this separation time is to overlap one CZE run onto the empty time of the next CZE run. In doing so, two samples reside in the capillary at any point in time prior to detection. Fig. 4 shows a separation of the proteins standards mixture obtained by overlapping the CZE runs. The capillary length was increased from 38 cm overall, 20 cm to the window, to 58 cm overall, 40 cm to the window. The run time now increased from 4 min to 9 min. The overlap was achieved by performing an injection every 4.5 min. There is a noticable increase in CZE resolution as a result of the added capillary length. The faint band after the main component of myoglobin in Fig. 3B has been clearly resolved into 3 distinct bands in Fig. 4B. Clearly, under separation conditions which allow for its use, overlapping CZE runs is a simple means of enhancing overall 2D resolution.

The combined resolving power of SEC and CZE is evident in separations involving complex sample mixtures. Fig. 5 contains grayscale images of 2D SEC–CZE separations of human serum (A), horse serum (B) and bovine serum (C). It is clearly evident that neither separation run independently could have resolved all the components that the combined use of 2D SEC–CZE was able to resolve. There are distinct pattern differences between the three sera samples shown in Fig. 5. Human serum seems to contain more higher-molecular-mass species than either the horse or bovine sera. All three samples show the presence of a high albumin constituent concentration.

DISCUSSION

We have presented what we believe is the first "comprehensive" 2D system to couple two capillary separation techniques that both use liquid mobile phases. The system provides greater resolving power than either dimension alone could running under the same conditions. The current system generates run times on the order of 2 h. If the SEC separation was being operated at an optimal mobile phase velocity for a mid-range molecular-mass protein (*e.g.*

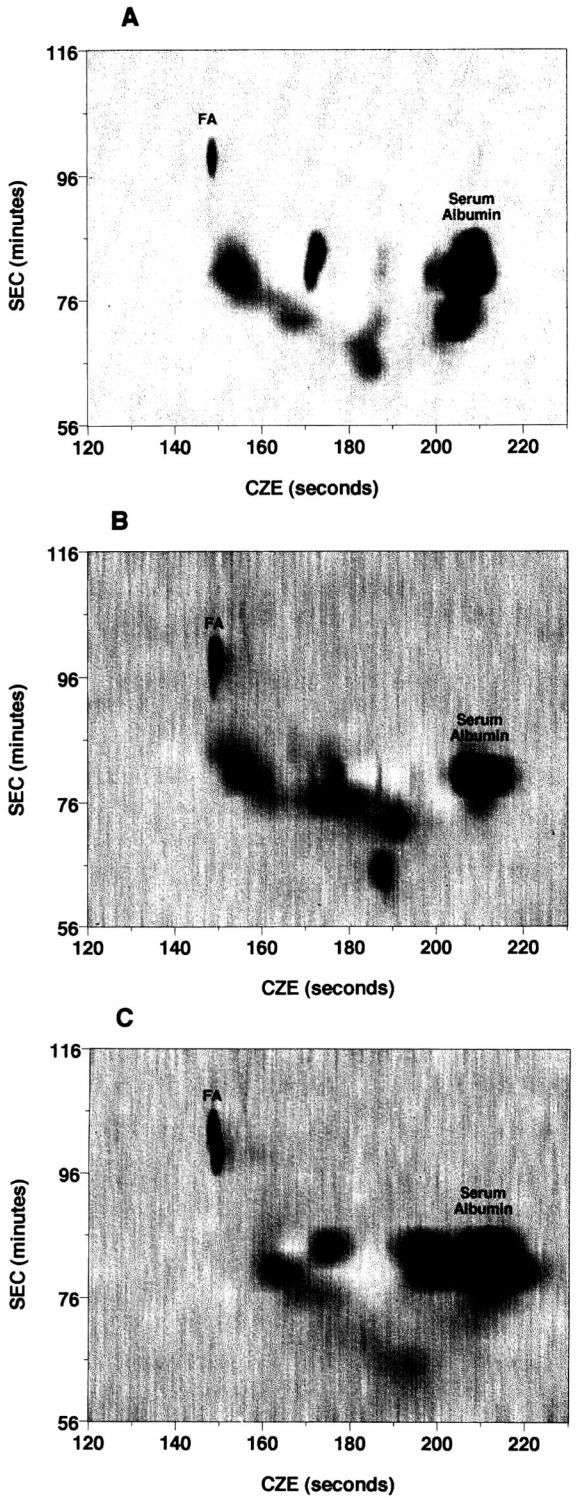

Fig. 5. Separation of sera samples by 2D SEC–CZE. Conditions as in Fig. 3. Spyglass-generated grayscale images are shown for : (A) human serum, (B) horse serum and (C) bovine serum. Data are in logarithm (base 10) scale.

ovalbumin), the run time would approach 12 h. Run times on the order of h are necessary in order to approach the maximum separation efficiency attainable from the chromatographic separation. This arises out of the slow diffusion rates associated with protein species. Although these run times might seem long, they are typical of many of the separation techniques used in protein analysis.

One area of major concern in constructing this 2D separation system was the compatibility of the operating conditions for each separation. Traditional silica-based SEC is performed under conditions of high salt concentration, often approaching 0.5 *M*. Salt concentrations of this magnitude are needed due to the excess residual surface charge associated with the silica. In marked contrast, CZE is typically carried out under salt concentrations around 50 m*M*. Clearly, a compromise in operating conditions must be made in order to allow the two systems to be effectively coupled. The Zorbax GF450 packing material used in this work was chosen because it has the desirable quality of relatively low excess surface charge. The end result of this lowering of surface charge is that we are able to perform SEC in a buffer with a salt concentration compatible with CZE. We are, however, restricted to separating proteins with a p*I* less than the buffer pH of 8.23. If this is not the case, strong protein adsorption to both the SEC silica stationary phase and the fused-silica capillary results. The second area of concern in the construction of the system was the means of achieving the interface between the SEC microcolumn and the CZE system.

The characteristics of the type of interface used to couple the SEC microcolumn to the CZE capillary ultimately determines the operating conditions of the entire system. In the work presented here this serves to set the minimum SEC column size and flow-rate able to be used. This limit arises primarily out of the extra (non-loop) volumes contained within the valve itself. For the 6-port valve used here, each port provides 160 nl of extra volume. The valve rotor, used to make the internal connections between ports, has three engravings that each provide an additional 220 nl of volume. These volumes are in addition to the volume of the sample loop. Regarding the sample loop itself, the minimum distance to connect any two ports (in the proper configuration) and allow for fittings is 15 cm. The

smallest I.D. tubing (of 15 cm length) that could be used without generating excessively high back pressure upon flushing was determined to be 50 μm. A 15 cm long section of 50 μm I.D. fused-silica capillary provides 300 nl of volume. With the extra volume of the valve taken into account, the valve/loop assembly shown in Fig. 2 requires approximately 900 nl of sample volume to enter the valve in order to fill the 300-nl loop with sample. This fixed volume of 900 nl must be generated within the time of one CZE run. This relationship imposes severely limiting restrictions on SEC and CZE operating conditions.

An ideal 2D SEC–CZE system would allow SEC operation near the optimum flow-rate with a CZE injection frequency great enough to prevent recombination of components separated by SEC. To meet these ideal conditions with the system presented here would require an SEC flow-rate near 50 nl/min and CZE runs 2–3 min long. Under these conditions, only 100–150 nl of sample would be generated in the time for one CZE run. This is nearly six times less volume than the 900 nl required to fill the valve/loop assembly. Collection of 900 nl would take 18 min at an SEC flow-rate of 50 nl/min. Although an 18-min CZE run time would provide the ability for very high CZE resolution, gross undersampling of the SEC dimension would result. The operating conditions chosen for the work presented here provided an acceptable trade-off between the factors of resolution (in both SEC and CZE) and sampling frequency. A new interface design is required if lower SEC flow-rates are to be used, or if a smaller I.D. microcolumn is desired. The combination of lower SEC flow-rates, approaching optimum conditions, and higher performance smaller I.D. microcolumns is an important consideration for maximizing the overall performance of 2D SEC–CZE. It has been shown that a 1 m × 50 μm I.D. SEC microcolumn run under optimum conditions for a protein sample can generate nearly 100 000 theoretical plates [7]. A column with this separation efficiency, coupled with the separation efficiency of CZE, would certainly be a powerful system for protein separations. In addition to a new type of interface, improvements in CZE performance will be necessary to further develop the potential of 2D SEC–CZE.

We did not investigate using any type of capillary coating technique to improve the CZE protein separation. Several coating procedures have been developed to provide CZE separation efficiencies near 100 000 theoretical plates for a wide range of proteins [10,11]. Unfortunately, as a result of the capillary coating process, many of these techniques greatly reduce or even eliminate electroosmotic flow. In a 2D scheme, where fast CZE runs are required for frequent first dimension sampling, loss of electroosmotic flow is detrimental to overall performance. Zwitterionic buffer additives have also been shown to be an effective means of reducing protein–capillary adsorptive interactions [12,13]. This approach is promising for use in a 2D system because electroosmotic flow is maintained. New interfacial schemes and methods of improving CZE performance are currently under investigation in our laboratory.

ACKNOWLEDGEMENTS

We thank Hewlett-Packard for the donation of the pump and computer used in this work, and Rockland Technologies Inc., for the donation of the Zorbax GF450 packing material. Support for this work was provided by the National Science Foundation under Grant CHE - 9215320.

REFERENCES

1 J. C. Giddings, *Anal. Chem.*, 56 (1984) 1258A.
2 J. M. Davis and J. C. Giddings, *Anal. Chem.*, 57 (1985) 2168.
3 J. M. Davis and J. C. Giddings, *Anal. Chem.*, 57 (1985) 2178.
4 J. C. Giddings, *J. High Resolut. Chromatogr. Chromatogr. Commun.*, 10 (1987) 319.
5 M. M. Bushey and J. W. Jorgenson, *Anal. Chem.*, 62 (1990) 978.
6 M. Novotny, *J. Microcolumn Sep.*, 2 (1990) 7.
7 R. T. Kennedy and J. W. Jorgenson, *J. Microcolumn Sep.*, 2 (1990) 120.
8 A. M. Hoyt Jr., S. C. Beale, J. P Larmann, Jr. and J. W. Jorgenson, *J. Microcolumn Sep.*, in press.
9 E. J. Guthrie and J. W. Jorgenson, *J. Chromatogr.*, 255 (1983) 335.
10 R. M. McCormick, *Anal. Chem.*, 60 (1988) 2322.
11 J. K. Towns and F. E. Regnier, *Anal. Chem.*, 63 (1991) 1126.
12 M. M Bushey and J. W. Jorgenson, *J. Chromatogr.*, 480 (1989) 301.
13 M. Merion, B. Bell-Alden, E. Grover, U. Neue and J. Peterson, presented at the *3rd International Symposium on High Performance Capillary Electrophoresis, San Diego, CA, February 4–6, 1991*, Poster PT-69.

Journal of Chromatography, 633 (1993) 221–225
Elsevier Science Publishers B.V., Amsterdam

CHROM. 24 794

Peak homogeneity determination and micro-preparative fraction collection by capillary electrophoresis for pharmaceutical analysis

K. D. Altria* and Y. K. Dave

Pharmaceutical Analysis, Glaxo Group Research, Park Road, Ware, Herts. (UK)

(First received April 7th, 1992; revised manuscript received October 28th, 1992)

ABSTRACT

This paper described the novel employment of micropreparative CE to a pharmaceutical analysis problem. Capillary zone electrophoresis (CZE) and HPLC are used separately to quantify drug related impurity levels. Good agreement was obtained between the two techniques. Peak homogeneity was determined for both fractions obtained by HPLC and CZE. This peak purity determination was achieved by analysing the appropriate fraction by the alternative technique. This work demonstrates that CZE and HPLC, used together, are a powerful analytical combination.

INTRODUCTION

The capillary electrophoretic (CE) methods of capillary zone electrophoresis (CZE) and micellar electrokinetic capillary chromatography (MECC) are finding increasing application [1–6] within the area of pharmaceutical analysis. Particular areas include the quantitative determination of drug content, drug related impurities and chiral analysis [5,6]. Due to the low sample volumes introduced into the capillary for analysis, typically of the order of a few nanolitres, CE is not routinely considered for preparative purposes.

Fluparoxan is a compound currently under development within Glaxo Group Research. The structure is shown in Fig. 1. Previously, we have reported [7] the use of CZE to separate fluparoxan from one of its related impurities. Having established the applicability of CZE for determination of fluparoxan related impurities the work was extended to the determination of other specific related impurites. For this purpose it was appropriate to employ micro-preparative CZE facilities.

In this report we demonstrate the micro-preparative use of CZE to collect fractions and to verify peak purity of fractions prepared by HPLC. This is the first report of the use of micro-preparative CZE for pharmaceutical analysis. Previous reports have centred on protein and nucleotide separations [8–12]. In addition, the complimentary nature of applying CZE and HPLC in combination is shown, and this novel parallel approach to method validation is discussed.

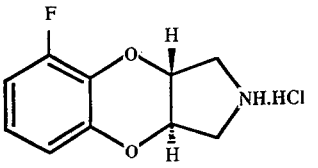

* Corresponding author.

0021-9673/93/$06.00

EXPERIMENTAL

Materials and instruments

Electrolyte reagents were obtained from Aldrich (Poole, UK). Water was obtained from a Millipore Milli-Q system (Watford, UK). CE was performed on a P/ACE 2000 CE instrument (Beckman, Palo Alto, CA, USA) which was connected to a Hewlett-Packard (Bracknell, UK) data collection system. Samples of fluparoxan (GR50360) were obtained from within Glaxo Group Research.

The fused-silica capillaries used in this study were purchased from Beckman.

Procedure

Automated fraction collection is possible with the CZE instrument available within our laboratory (Beckman P/ACE 2000). This collection is possible by suitable programming of a separation method into the personal computer controlling the CE instrument.

The separation method is a user-defined, stepwise control programme for the instrument. The separation method used for the micro-preparative CZE is given in Table I.

In step V a voltage is applied across the capillary causing migration of solutes through the detector. The low field end of the capillary is dipped into a vial containing electrolyte. When performing the micro-preparative CZE fraction collection step (step VI) this reservoir is replaced, at the selected time, by a microvial containing a few microlites of water. This switch is timed to be immediately prior to the elution of the solute peak from the capillary end. Following the migration of the selected peak from the capillary into the collection microvial the separation is stopped and the capillary rinsed.

The exact timing of the reservoir switch to the collection microvial in the selected example was calculated as given below. The migration time, to the detector, of the peak of interest was 7.8 min. The total length of the capillary used was 57 cm long; 50 cm to the detector. Therefore, the time taken for the peak to reach the tip of the capillary is calculated by:

$$57/50 \cdot 7.8 = 8.9 \text{ min}$$

In the separation method employed (step VI, Table I) the switch to the collection vial is timed to be after 8.3 min. The material eluted from the capillary after the switch contains the required impurity is collected for 30 s into the collection vial (step VI, Table I).

The volume of sample injected in CZE is in the order of a few nanolitres. Therefore the sample concentration was increased from 0.5 mg/ml, for the analytical separation, to 25 mg/ml for the micro-preparative separation. This was the maximum concentration that could be analysed whilst still obtaining suitable resolution of impurity I from the fluparoxan peak. In CZE (as in HPLC) there is a loss in both resolution and peak efficiency with increased sample loading.

TABLE I

CAPILLARY ELECTROPHORESIS SEPARATION METHOD

Step I	Rinse cycle 1: 0.5 *M* NaOH, 2 min
Step II	Rinse cycle 2: run buffer, 4 min
Step III	Set detector: 0.02 AUFS, 210 nm
Step IV	Sampling: 5.0 s pressure
Step V	Operating voltage: 30 kV Operating temperature: 25°C Run time: 8.3 min
Step VI	Operating voltage: 30 kV Operating temperature: 25 °C Run time: 0.5 min
	Electrolyte: 50 m*M* borax pH adjusted to 2.5 with conc. H_3PO_4 Capillary dimensions: 57 cm × 75 μm

RESULTS AND DISCUSSION

Determination of related impurities by CZE and HPLC

A fluparoxan drug substance sample, prior to purification (batch 1, Table II) containing high levels of related impurities was analysed by both CZE and HPLC. In addition, more purified drug substance batches (batches 2 and 3) were also analysed. Table II compares impurity levels as determined by both methods. The reasonable agreement achieved by two entirely different separative techniques suggests that all principal impurities are being quantified by both techniques.

Fig. 2 shows two replicate CZE separations of batch 1. The migration position of a selected syn-

TABLE II

IMPURITY LEVELS (%AREA/AREA) BY CZE AND HPLC

	Batch 1	Batch 2	Batch 3
HPLC total impurities	13.4	1.8	0.3
CZE total impurities	11.2	1.8	0.3
Impurity 1 content by HPLC	2.74	0.08	ND[a]
Impurity 1 content by CZE	2.41	0.09	ND

[a] ND = Not determined.

thetic impurity, termed "impurity 1" is indicated. The selectivity of the CE separation was markedly different to that of the HPLC analysis (Fig. 3). For example, impurity 1 is a late running peak by HPLC whilst it migrates before the main peak in CZE.

Determination of peak purity by CZE and HPLC

Peak purity is of concern when using electrophoretic or chromatographic techniques since it is possible that a minor component may be co-eluting/co-migrating with the principal component. This situation would lead to an underestimation of impurity levels. Accordingly, spectral purity of HPLC peaks are often determined to confirm peak purity using a diode array detector and comparing the spectra with an authentic sample. This method is however incapable of detecting minor component levels of less than about 1%. Since impurities are often present at lower levels a further means of peak homogenity testing should be considered. This is often the collection of main peak fractions and their subsequent analysis under different operating conditions, or by employing an alternative orthogonal analytical technique. In this example the orthogonal techniques of CZE and HPLC are employed to confirm peak homogeneity of fractions taken from preparative HPLC and CZE analysis.

A HPLC fraction was prepared containing impurity 1. This solution was analysed by CZE to confirm the presence of a major component. The CZE separation (Fig. 4) showed the sample to be a single component.

A sample of fluparoxan was spiked with the HPLC fraction to identify the CZE migration time of impurity 1. Levels of impurity 1 were quantified in batches 1–3 by both CZE and HPLC. Table II shows there to be good agreement between the levels quantified by HPLC and CZE.

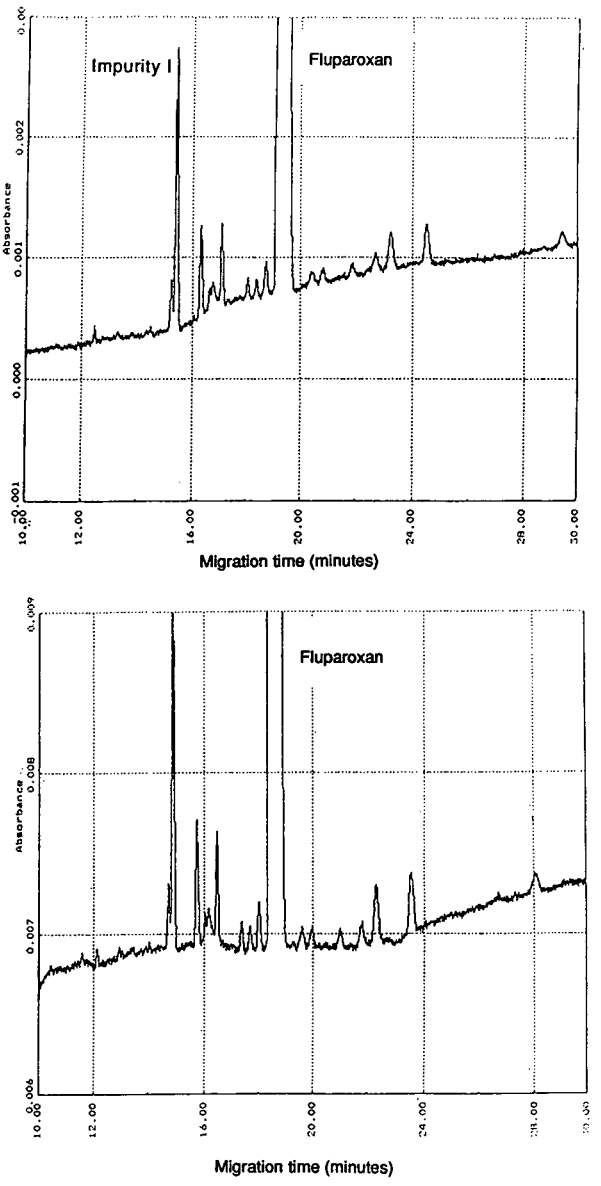

Fig. 2. Replicate CE analyses of a sample of batch 1. Separation conditions: 50 m*M* borax pH adjusted to 2.5 with conc. H_3PO_4, 5.0 s pressure sampling, +30 kV, 25°C, 57 cm (50 cm to detector) × 75 μm.

Fraction collection by CZE

Micro-preparative CZE has advantages over the preparative use of conventional electrophoresis. These are principally the ease of sample handling and the full automation of preparative CZE. In addition, the standard equipment can be used for both

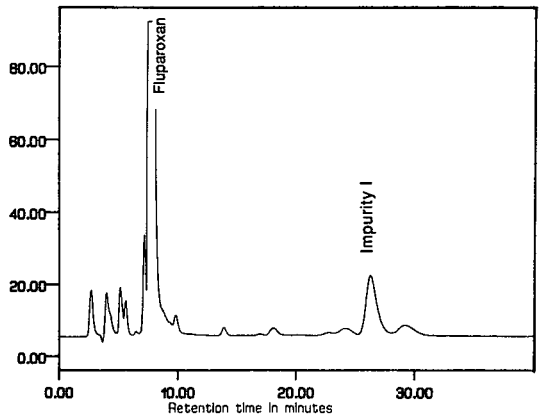

Fig. 3. HPLC analysis of batch 1. Separation conditions: 15 cm × 4.6 mm I.D. Spherisorb CN 5 μm, acetonitrile–0.005 *M* $NH_4H_2PO_4$–methanol (6:5:3, v/v/v), 0.8 ml min $^{-1}$, UV at 210 nm, 20 μl injection volume. Y-axis represents absorbance (arbitrary units).

analytical and micro-preparative CZE. The major disadvantage is that the sample volumes involved with CZE are relatively small.

Fraction collection by HPLC is an established technique and several automated fraction collection systems are commercially available. The operation of micro-preparative CZE is less common. Therefore, it is appropriate that the operation of CZE in a preparative mode should be discussed.

Using the method given in Table I, 27 fractions were collected overnight into the collection vial. This produced a 10 μg/ml solution of the impurity, the concentration was calculated as follows:

2 s pressure injection on a 57 cm × 75 μm capillary = 11.8 nl injection volume [13];
25 mg/ml solution, therefore injected 0.295 μg material;
impurity present at 2.5 % level therefore injection is 7.4 ng;
27 replicate injections = 198 ng collected into 20 μl of water;
concentration = 10 μg/ml in water.

Sample solutions of this concentration are suitable for submission for identification by mass spectrometry.

The CZE generated fraction was analysed by HPLC (Fig. 5) and the principal component of the chromatogram was confirmed as impurity 1 by retention time.

FUTURE DEVELOPMENTS

The small volumes injected in CZE, typically in the order of a few nanolitres remains the greatest limitation to development in this area. The two solutions that have been suggested are the use of wider bore capillaries [8] or to use bundles of capillaries [12,14]. The first approach is somewhat limited in that heat dissipation is significantly reduced with wider bore tubes making band broadening effects more appreciable. The alignment of capillary bundles is essential to retain the high efficiencies of a CE separation. This alignment would represent a serious mechanical challenge.

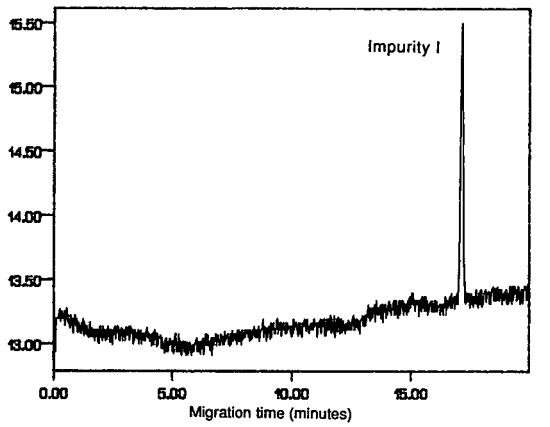

Fig. 4. CZE analysis of HPLC fraction containing impurity 1. Separation conditions as in Fig. 2. Y-axis represents absorbance (arbitrary units).

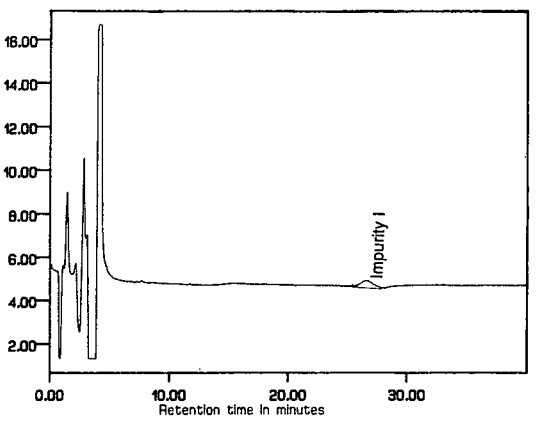

Fig. 5. HPLC analysis of CZE fraction containing impurity 1. Separation conditions as in Fig. 3. Y-axis represents absorbance (arbitrary units).

CONCLUSIONS

CZE has been shown to be useful for micro-preparative fraction collection of a drug related impurity. This facility allows the determination of the purity of CZE peaks by analysing appropriate fractions by an orthogonal separative method. In addition CZE has been used for the determination of HPLC peak homogeneity.

Good cross-correlation with results generated by both CZE and HPLC has also been shown with respect to total impurity content and for an individual impurity. This information could form part of the validation of either the HPLC or CZE method. This work demonstrates that CZE and HPLC, used together, are a powerful analytical combination.

Micro-preparative CZE is a viable option and should be considered for suitable applications.

REFERENCES

1 K. D. Altria and C. F. Simpson, *J. Pharm. Biomed. Anal.*, 6 (1988) 801.
2 K. D. Altria and M. M. Rogan, *J. Pharm Biomed. Anal.*, 8 (1990) 1005.
3 H. Nishi, T. Fukuyama, M. Matsuo and S. Terabe, *J. Pharm. Sci.*, 79 (1990) 519.
4 H. Nishi and S. Terabe, *Electrophoresis*, 11 (1990) 691.
5 K. D. Altria, D. M. Goodall and M. M. Rogan, *Chromatographia*, 34 (1992) 19.
6 S. Fanali, *J. Chromatogr.*, 545 (1991) 437.
7 K. D. Altria and N. W. Smith, *J. Chromatogr.*, 538 (1991) 506.
8 A. Guttman, A. S. Cohen, D. N. Heiger and B. L. Karger, *Anal. Chem.*, 62 (1990) 137.
9 A. S. Cohen, D. R. Najarian, A. Paulus, A. Guttman, J. A. Smith and B. L. Karger, *Proc. Natl. Acad. Sci. U.S.A.*, 85 (1988) 9660.
10 D. J. Rose and J. W. Jorgenson, *J. Chromatogr.*, 438 (1988) 23.
11 P. Camilleri, G. N. Okafo, C. Southan and R. Brown, *Anal. Biochem.*, 198 (1991) 36.
12 N. A. Guzman, L. Hernadez and B. G. Hoebel, *Biopharm.*, 2 (1989) 22.
13 G. McLaughlin, R. Biehler and H. E. Schwartz, *Application Datasheet TIBC-103*, Beckman, Palo Alto, CA, 1991.
14 K. D. Altria and C. F. Simpson, *Chromatographia*, 24 (1987) 527.

Journal of Chromatography, 633 (1993) 227–233
Elsevier Science Publishers B.V., Amsterdam

CHROM. 24 782

Determination of ester substituents in cellulose esters

G. W. Tindall* and R. L. Perry

Research Laboratories, Eastman Chemical Company, Eastman Kodak Company, P.O. Box 1972, Kingsport, TN 37662 (USA)

(First received August 5th, 1992; revised manuscript received November 23rd, 1992)

ABSTRACT

A method to determine most ester substituents in cellulose esters has been developed. The cellulose ester is first dissolved in dimethyl sulfoxide. The esters are rapidly hydrolyzed at room temperature by adding a mixture of methanol and sodium hydroxide. Acids in the resulting sample can be determined by gas chromatography, ion chromatography or capillary zone electrophoresis. Capillary zone electrophoresis provides a nearly universal way to determine the hydrolyzed acids and it is the preferred method.

INTRODUCTION

Cellulose esters are an important class of polymers used for the manufacture of fibers, films, plastics, paints and drug delivery systems. The properties of the polymer depend on the degree of substitution of the cellulose hydroxyls as well as the properties of the ester substituents. There are numerous methods to determine the degree of substitution. Most of these methods are specific to one type of ester [1]. For example, phthalate is determined in cellulose acetate phthalate by titration [2]. Acetate in cellulose acetate is determined by a saponification procedure [3]. A method applicable to all, or at least most, cellulose esters and mixed esters would be desirable.

A reagent was recently described that is particularly effective for the hydrolysis of esters for analytical purposes [4]. It consists of a mixture of a polar aprotic solvent, methanol and a strong base, for example sodium hydroxide. It can hydrolyze esters at extraordinary rates. For example, solid polyesters are routinely hydrolyzed in min. A major component of this reagent can be dimethyl sulfoxide (DMSO). DMSO is a solvent for most cellulose esters. A possible analytical scheme employing this reagent would involve dissolving the cellulose ester in DMSO followed by addition of base in methanol. Since the cellulose ester is in solution, the esters would be expected to hydrolyze very rapidly. The hydrolyzed acids could then be analyzed by various chromatographic procedures. This scheme was investigated for the analysis of some commercial cellulose esters. Several approaches for determining the acids in the hydrolysis mixture were investigated. Capillary zone electrophoresis (CZE) was the most versatile approach.

* Corresponding author.

EXPERIMENTAL

Sample preparation

Approximately 0.1 g of cellulose ester was placed in a 50-ml culture tube. An 8-ml volume (4 ml for GC analysis) of dry DMSO (Burdick & Jackson) were added to the tube. The tube was capped and the contents mixed to dissolve the ester. After the ester dissolved, 2 ml (1 ml for GC analysis) of 5 *M* sodium hydroxide in dry methanol (Burdick & Jackson) was added. During addition, the contents were swirled on a vortex mixer at medium speed. After the addition, the tube was capped and mixed at high speed for 2 min. After mixing, 15 ml of water (20 ml for GC analysis) was added and the tube capped. The contents were swirled at high speed for

2 min to extract the acids. A portion of the contents was filtered through a 0.45-μm Gelman PTFE filter. Final sample dilutions for each method are given below.

For GC analysis, 1 ml of filtrate was transferred to a 10-ml volumetric flask containing 15 μl of phosphoric acid. The flask was diluted to volume with an internal standard solution (300 μg/ml 2-methylbutyric acid in water). For ion chromatographic analysis, 0.1 ml of filtrate was transferred to a 10-ml volumetric flask. The flask was diluted to volume with water. For CZE analysis, 1 ml of filtrate was transferred to a 10-ml volumetric flask. The flask was diluted to volume with water. During standard preparation for CZE, the final dilution for each standard concentration included 1 ml of a sample blank (8 ml DMSO and 2 ml 5 *M* sodium hydroxide in methanol diluted to 25 ml with water).

Data were collected and processed on a PE Nelson Access*Chrom chromatography data system.

Gas chromatography operating conditions

All analyses were performed on a Perkin-Elmer Sigma 3B gas chromatograph. The isothermal separation was performed on a Quadrex Corporation 007-FFAP column, 25 m × 0.53 mm I.D., with a 1.0-μm film thickness. The injection temperature and oven temperature were 122°C. Detection was by flame ionization at 200°C. The on-column injection volume was 1 μl. High-purity helium was used as the carrier gas at a flow of 8 ml/min.

Ion chromatography operating conditions

The separation was performed on a Dionex IonPac AS10 analytical column, 25 cm × 4 mm, with an AG10 guard column in conjunction with an AMMS II micromembrane suppressor. The regenerant was 50 m*M* sulfuric acid at a flow-rate of 5 ml/min. The eluent was 3.5 m*M* sodium borate at a flow of 1 ml/min.

Capillary zone electrophoresis operating conditions

Analyses were performed on a Waters Quanta 4000 capillary electrophoresis system. The separation was performed on a 60 cm × 75 μm I.D., fused-silica column with an applied potential of 20 kV negative. The injector to detector distance was 52.7 cm. The electrolyte was 7 m*M* 3-nitrophthalic acid (Aldrich) with 0.5 m*M* myristyltrimethylammonium bromide (Aldrich) as the electroosmotic flow modifier, adjusted to pH 7.0 with sodium hydroxide. Detection was by indirect UV at 254 nm. Sample injection was by hydrostatic flow for 30 s.

RESULTS AND DISCUSSION

Before the utility of the hydrolysis reagent could be explored, a means of determining aliphatic acids in the hydrolysis mixture had to be developed. Chromatography of the hydrolysis solution is not trivial, particularly if a universal procedure is sought. The acids will be present as minor components in the DMSO–methanol mixture. Ion exclusion chromatography with a 300 × 7.8 mm Aminex HPX-87H (Bio-Rad) and dilute sulfuric acid eluent or reversed-phase liquid chromatography with a 150 × 4.7 mm C22 (ES Industries) column and methanol–0.1 *M* pH 2.2 phosphate buffer are preferred ways to determine aliphatic acids in our laboratories. However, DMSO is sufficiently retained in these methods to be a major interference in determining aliphatic acids in the hydrolysis mixture. These methods could be useful for the determination of some acids, but they are not broadly applicable.

Gas chromatography is adequate for the determination of acetic, propionic and butyric acids, but not aliphatic diacids, in the hydrolysis mixture. Methanol is not retained under the conditions used. DMSO elutes between propionic and butyric acid

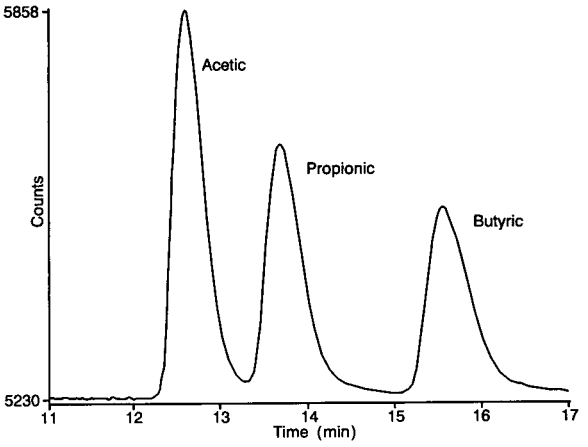

Fig. 1. Ion chromatographic separation of aliphatic acids. See Experimental for conditions; 20 μg/ml of each acid.

and it does not interfere with either component. Calibration of acetic acid is a problem if it is necessary to analyze it at low levels, for example 50 μg/ml. At 50 μg/ml it is necessary to condition the column with a duplicate injection to get reproducible data. Above 100 μg/ml there was no problem reproducing standards or samples. Repeated injection of hydrolysate eventually led to degraded column performance that could be restored by removing a short inlet section. This inconvenience and the inability to determine diacids were the only significant limitations encountered.

Ion chromatography provides a barely adequate separation between acetic and propionic acid (Fig. 1). DMSO and methanol are not retained so neither is an interference. Aliphatic diacids must be eluted with a gradient or determined with another column, for example a Dionex AS5 with NaOH eluent, or an AS10 guard column, which is an inexpensive equivalent to the AS5 analytical column for many applications. The most serious disadvantage of ion chromatography is the small linear range available when a conductivity detector is used. A typical calibration curve for acetic acid is shown in Fig. 2. The severe curvature is a result of the weak dissociation of aliphatic acids [5]. The acids generated by the suppressor column can be ion exchanged back to fully dissociated salts before detection, but the added complexity makes this approach impractical for many situations. While good nonlinear fits are possible, many more standards are necessary to achieve accuracy comparable to linear situations. In spite of these limitations, ion chromatography provides a robust method for the determination of acids in the hydrolysis mixture.

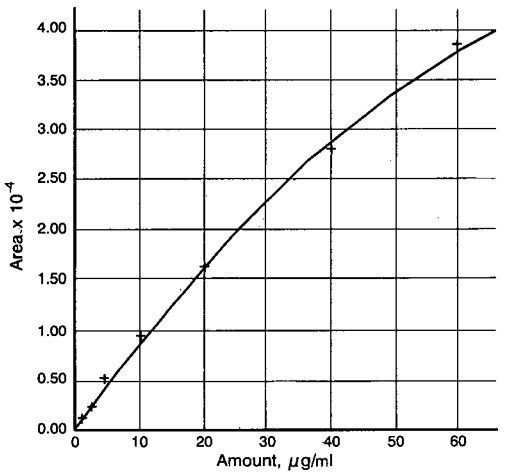

Fig. 2. Ion chromatography calibration curve for acetic acid.

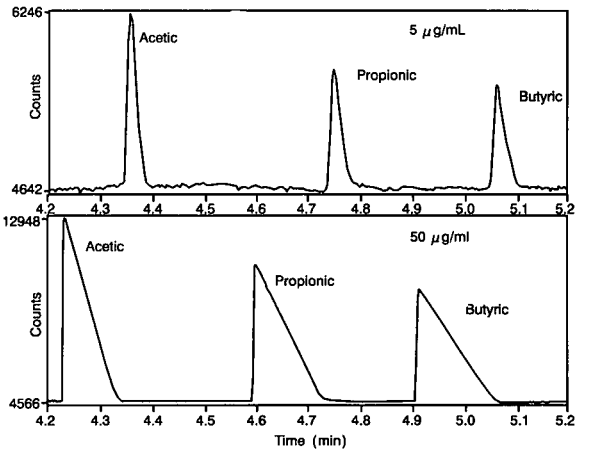

Fig. 3. Comparison of 5 and 50 μg/ml standard by CZE. See Experimental for conditions.

Altria and Simpson [6] proposed using CZE with an alkyl quaternary salt for anion analysis. Hjertén *et al.* [7] described the CZE separation and indirect detection of aliphatic acids and small anions. Several more recent papers [8–10] and a patent [11] describe the use of capillary zone electrophoresis for the determination of aliphatic acid anions. CZE would seem to be an ideal technique to apply to the problem of determining acids in the hydrolysis mixture. CZE provides a class separation of charged anions from neutral species, in this case DMSO and methanol, and within the charged species it offers the possibility of high resolution and fast separations of nearly any acid of interest, including aliphatic diacids and aromatic acids. In addition, consumables cost is insignificant compared to alternative methods.

In our investigation of CZE we encountered a limitation not emphasized in the above references. The conditions previously described result in a dynamic range of less than two decades for the determination of aliphatic acids. This range is too limited for many applications. The bottom of the dynamic range is set by the limit of quantitation; the top of the range is limited by resolution which is deter-

mined by peak shape at high concentration. Unless there is a good match between the mobility of the analyte and the electrolyte, the peaks severly broaden at high concentration. This phenomena was shown by Hjertén [12] and a mathematical description of the origin of peak broadening was provided by Mikkers *et al.* [13] and Poppe [14]. The problem is illustrated in Fig. 3. The criteria to achieve the best dynamic range in indirect detection have been discussed [15–20]. The chromophore for indirect detection should have the largest possible molar absorbtivity to achieve the best limit of quantitation. The mobility of the electrolyte should closely match the mobility of the analytes to preserve peak shape at high concentration. None of the chromophore-electrolytes previously used were optimized for aliphatic acid determination. The mobility of chromate and phthalate is too large; benzoate mobility is too small. Small aliphatic acids either severely tail, or front, with these electrolytes.

Chromophore-electrolytes were investigated that might provide a better mobility match to the aliphatic acids of interest and provide an anion with a large molar absorbtivity. These improvements would provide a more useful dynamic range. We discovered that hydroxy- or nitro-substituted phthalic, isophthalic or terephthalic acids provide a good mobility match for C_2 to C_4 aliphatic acids and these compounds have a large molar absorptivity. The phthalic acid derivatives were readily soluble and stock solutions were more convenient to prepare than the less soluble terephthalic acid derivatives.

With 3-nitrophthalic acid as the chromophore-electrolyte, two decades of useful concentration range could be quantitated with good precision, 1–100 μg/ml, at 254 nm. Calibration curves were slightly curved over this range, but accurate cali-

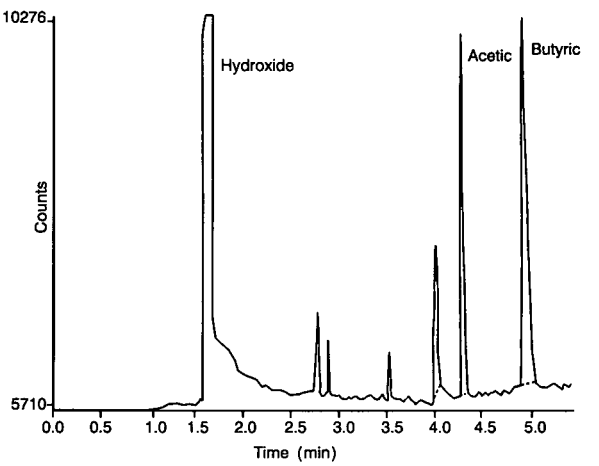

Fig. 5. Electropherogram of a typical hydrolysis solution. See Experimental for conditions.

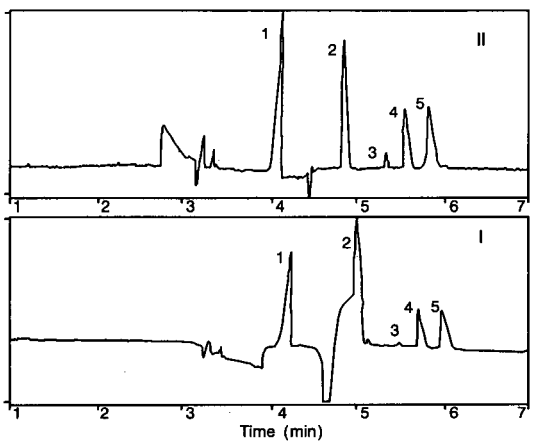

Fig. 4. Comparison of standards prepared from aliphatic acids (I) and aliphatic acids neutralized with sodium hydroxide (II). Peaks: 1 = formic; 2 = acetic; 3 = propionic; 4 = isobutyric; 5 = isovaleric acid. See Experimental for conditions.

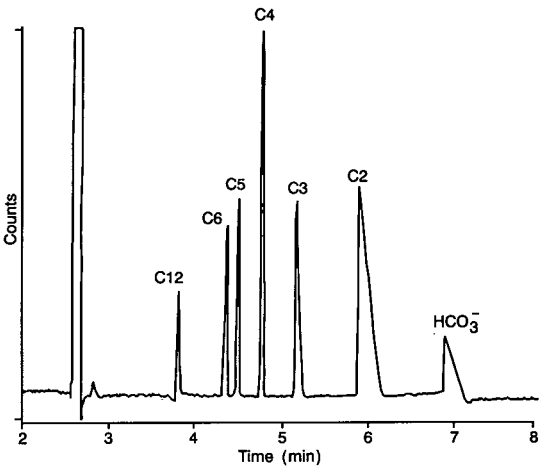

Fig. 6. Separation of C_2–C_{12} aliphatic acids. Conditions: 75 cm × 50 μm column, 30 kV, detection at 220 nm, 0.007 m*M* benzoate at pH 6. Separation performed on an ABI 270A-HT instrument.

brations could be made with five points. It is necessary to use acid salts for calibration. When the standard is acidic, a negative dip occurs which can interfere with acids of interest (see Fig. 4). The migration time of the dip is the same as for the electrolyte, so a plug of electrolyte is the likely cause. We do not know what causes this plug to form when an acidic standard is analyzed.

A typical electropherogram for a hydrolysis solution from a mixed acetate–butyrate ester is shown in Fig. 5. The mobility match of 3-nitrophthalate is not perfect for C_2 to C_4 aliphatic acids; they front at high concentrations. A slightly less mobile salt could extend the dynamic range even further, which could be an advantage for some applications. Without the constraint of detection at 254 nm, other chromophore-electrolyte possibilities are available. Electrolyte optimization for anion analysis will be the subject of a subsequent publication.

Recent work suggests the osmotic flow modifier may be unnecessary for separating many aliphatic and aromatic acids. Fig. 6 shows the separation of C_2–C_{12} aliphatic acids on a 50-μm column at high pH. Under these conditions the electroosmotic flow is fast enough to counter the high mobility of these ions. An investigation into the utility of this approach is in progress.

Validation of hydrolysis procedure

To be successful, the hydrolysis reagent must quantitatively hydrolyze the ester, the resulting acid salt must quantitatively extract from the cellulose, these acid salts must not be lost by decomposition or volatilization, and the reaction must not form interfering acids or other products. The hydrolysis procedure described meets these essential criteria.

Previous work has shown the reagent attacks ester bonds at extraordinary rates. When the methanol–NaOH solution is added to the cellulose ester solution, the cellulose formed after hydrolysis does not instantly precipitate. Undoubtably, this delay helps to achieve complete hydrolysis and extraction of the acid salts. Experiments were performed to measure the extent of hydrolysis as a function of hydrolysis temperature and time. A cellulose butyrate ester was hydrolyzed at temperatures between 20 and 120°C and times from 1 to 60 min. The amount of acid recovered was essentially the same for all conditions. At higher temperatures acidic components formed that could be an interference with some acids. Since the recovery was the same at room temperature there was no reason to use higher temperature for hydrolysis and the potential problem was avoided. Extraction times up to 24 h were investigated. There was no significant difference in the amount of acids recovered by increasing the extraction time. The insensitivity of recovery to hydrolysis and extraction conditions suggested these steps were quantitative. To prove this point cellulose recovered after hydrolysis was washed and hydrolyzed with dilute sulfuric acid to yield a completely soluble product. No aliphatic acids were detected in this hydrolyzate which proves they were quantitatively hydrolyzed and extracted by the original hydrolysis procedure.

Four commercial and one experimental cellulose ester were used to evaluate the proposed hydrolysis and analysis procedures. Five replicate samples of each ester were hydrolyzed and analyzed by each of the chromatography techniques described in the Experimental section, as well as traditional methods. These data are shown in Table I. In general there is good agreement between the various approaches for determining the ester substituents.

The precision of the gas and ion chromatography methods was typical for these techniques, about 2% relative standard deviation (R.S.D.). We were able to analyze standards with CZE with a precision of 1–2% R.S.D. Overall method precision, hydrolysis plus acid determination, was typically about 2% R.S.D. for the major component acids (10–50%). For the minor component acids (1–5%), R.S.D.s were in the range of 2–13%. The poorer precision results were always associated with the determination of low concentrations of acetic acid and may reflect inadequate precautions to prevent contamination by acetate. During the course of this work it was discovered that glassware used for processing samples was a significant source of acetate contamination. To reliably determine lower levels of acetate it was necessary to rinse glassware in deionized water just before use. Acetic acid is used as a solvent in our laboratory and we speculate that it adsorbs from the air onto the relatively basic surface of some glassware, particularly autosampler vials.

The main advantage of this sample preparation procedure is speed and convenience. Traditional methods involve refluxing the sample to achieve hy-

TABLE I

WEIGHT % SUBSTITUENTS IN VARIOUS CELLULOSE ESTERS

Cellulose ester	Method	Substituent (%, w/w)			
		Acetyl	Propionyl	Butryl	Succinyl
CAB-171-15S	GC[a]	28.7		18.3	
	NMR[b]	28.1		19.1	
	GC[c]	31.3		19.6	
	IC[d]	30.0		19.3	
	CZE[e]	29.4		19.1	
CAB-381-20	GC[a]	13.6		36.8	
	NMR[b]	12.9		38.2	
	GC[c]	16.4		38.3	
	IC[d]	15.1		37.5	
	CZE[e]	13.8		37.5	
CAP-482-0.5	GC[a]	1.3	44.6		
	NMR[a]	0.7	45.8		
	GC[c]		42.0		
	IC[d]	1.3	43.0		
	CZE[e]	1.6	45.8		
CAB-500-5	GC[a]	3.3		50.9	
	NMR[b]	2.8		53.4	
	GC[c]	3.7		51.6	
	IC[d]	3.7		52.5	
	CZE[e]	4.2		49.5	
CABSU 160	GC[a]	1.9		40.8	10.5[f]
	IC[d]				10.1
	CZE[e]	1.9		40.7	9.8

[a] Internal method. Sample is hydrolyzed in pyridine–methanol–KOH and hydrolyzed acids determined by GC.
[b] Internal method. Substituents determined by integration of proton NMR spectrum.
[c] Hydrolysis as described in Experimental section. Acid determination by GC.
[d] Hydrolysis as described in Experimental section. Acid determination by ion chromatography.
[e] Hydrolysis as described in Experimental section. Acid determination by CZE.
[f] Determined by titration with base.

drolysis. Reflux times are typically 30 min or more and sample sizes are large. The proposed hydrolysis is nearly instantaneous and it can be done in a test tube. We have performed the analysis on as little as one milligram of material.

CONCLUSIONS

Cellulose esters can be rapidly hydrolyzed at room temperature in a mixture of DMSO, methanol and sodium hydroxide. Acids in the resulting sample can be determined by GC, ion chromatography, or CZE. CZE provides a nearly universal way to determine the hydrolyzed acids and it is the preferred method.

ACKNOWLEDGEMENT

We are grateful to the Waters Corporation for the loan of a CZE instrument for much of the work reported.

REFERENCES

1 American Society for Testing and Materials, Philadephia, PA. 1983. method D 817.
2 *US Pharmacopeia National Formulary*, Rockville, MD, 1980, p. 1219.
3 American Society for Testing and Materials, Philadelphia, PA, 1983, method D 871.
4 G. W. Tindall, R. L. Perry, J. L. Little and A. T. Spaugh, *Anal. Chem.*, 63 (1991) 1251.

5 H. Small, *Ion Chromatography*, Plenum Press, New York, 1989, p. 175.
6 K. D. Altria and C. F. Simpson, *Chromatographia*, 24 (1987) 527.
7 S. Hjertén, K. Elenbring, F. Kilár, J. Liao, A. J. C. Chen, C. J. Siebert and M. Zhu, *J. Chromatogr.*, 470 (1989) 299.
8 X. Huang, J. A. Luckey, M. J. Gordon and R. N. Zare, *Anal. Chem.*, 61 (1989) 766.
9 B. F. Kenney, *J. Chromatogr.*, 546 (1991) 423.
10 T. Wang and R. A. Hartwick, *J. Chromatogr.*, 589 (1992) 307.
11 W. R. Jones, P. Jandik and M. Merion, *US Pat.*, 5 104 506 (1990).
12 S. Hjertén, in D. Glick (Editor), *Methods of Biochemical Analysis*, Vol. 18, Wiley, New York, 1970, p. 55–79.
13 F. E. P. Mikkers, F. M. Everaerts and Th. P. E. M. Verheggen, *J. Chromatogr.*, 169 (1979) 1.
14 H. Poppe, *Anal. Chem.*, 64 (1992) 1908.
15 H. Small and T. E. Miller, *Anal. Chem.*, 54 (1982) 462.
16 F. Foret, S. Fanali and L. Ossicini, *J. Chromatogr.*, 470 (1989) 299.
17 M. W. F. Nielen, *J. Chromatogr.*, 588 (1991) 321.
18 V. Šustáček, F. Foret and P. Boček, *J. Chromatogr.* 545 (1991) 239.
19 M. T. Ackermans, F. M. Everaerts and J. L. Beckers, *J. Chromatogr.*, 549 (1991) 345.
20 P. Jandik and W. R. Jones, *J. Chromatogr.*, 546 (1991) 431.

Journal of Chromatography, 633 (1993) 235–244
Elsevier Science Publishers B.V., Amsterdam

CHROM. 24 781

Capillary zone electrophoresis and packed capillary column liquid chromatographic analysis of recombinant human interleukin-4

John Bullock

Sterling-Winthrop Pharmaceuticals Research Division, Malvern, PA 19355 (USA)

(First received September 29th, 1992; revised manuscript received November 24th, 1992)

ABSTRACT

Capillary zone electrophoresis (CZE) and packed capillary column liquid chromatography (micro-LC) have been applied to the analysis of the recombinant human protein interleukin-4 (rhIL-4). Separations for both the parent protein and its enzymatic digest were developed for the purpose of characterizing protein purity and identity. CZE separations of the intact protein were investigated over the pH range of 4.5 to 8.0 using uncoated fused silica capillaries. Gradient reversed-phase micro-LC was performed using 0.32 mm packed capillary columns at flow-rates of 5–6 μl/min. Emphasis was placed on the ability of these methods to separate close structural variants and degradation products of the protein. Peptide mapping of the tryptic digest of rhIL-4 using a combination of CZE and micro-LC provided complimentary high resolution methods for establishing protein identity. Reproducible separations were achieved using sub-picomol amounts of sample. The advantages and problems encountered with these two techniques for characterizing rhIL-4 were assessed.

INTRODUCTION

The characterization of recombinant DNA derived protein products intended for therapeutic purposes has created significant challenges in the field of bioanalytical chemistry. The need to detect subtle structural differences such as posttranslational modification of individual amino acid residues, genetic variants, degradation products and other protein impurities places significant demands on the efficiency and quality of analytical separations. In many cases, an additional constraint is imposed by a limited quantity of sample available for analysis, a situation that is often encountered in characterizing low-level impurities or new protein species. In such instances, the amount of sample available may be in the low microgram to nanogram range.

HPLC and electrophoresis have attained prominent positions as analytical tools for characterizing proteins and peptides [1,2].The potential for higher-resolution separations along with the reduced sample requirements associated with the capillary analogues of these techniques, capillary zone electrophoresis (CZE) and packed capillary liquid chromatography (micro-LC), has resulted in a greater utilization of these reduced-scale separation techniques in bioanalytical chemistry. The separation mechanisms associated with these techniques (charge-based for CZE and hydrophobicity-based for reversed-phase micro-LC) are quite different providing complementary methods for separating close structural protein analogs or complex protein digests. A added advantage of these reduced-scale separation techniques is their compatibility with a mass spectrometer [3,4], which can provide additional selectivity and structural information for the analysis of unknowns.

Investigations comparing the utility of RP-HPLC and CZE for characterizing biopolymers have been demonstrated for recombinant proteins [5], small peptides [6] and tryptic digests of proteins [7]. However, in most cases the investigations in-

0021-9673/93/$06.00

volved the comparison of CZE with conventional HPLC using 4.6 mm I.D. columns with a notable exception being the work by Cobb and Novotny [8] in which a comparison was made using packed capillary columns for peptide mapping. The rapid development and influx of commercial CZE instrumentation in the last couple of years has resulted in a dramatic increase in the utilization of this technology. However, the commercialization of micro-LC instrumentation and packed capillary LC columns has lagged behind the developments in CZE instrumentation. This has hindered this technique from achieving the same level of acceptance in bioanalytical chemistry. Nevertheless, the advantages of micro-LC enumerated earlier makes this an attractive technique, in many instances, for biopolymer analysis.

The present work focuses on the use of CZE and micro-LC for characterizing the recombinant human protein interleukin-4 (rhIL-4), a cytokine which has been investigated for cancer therapy. This M_r 15 400 monomeric protein contains three intra-chain disulfide bonds and possesses a p*I* value of 9.2. Separations of structural variants and degradation products of the parent protein as well as peptide mapping on its tryptic digest have been accomplished using both techniques. The relative merits of these techniques in terms of selectivity, efficiency and reproducibility for the analysis of rhIL-4 have been assessed. The utilization of the complimentary nature of these techniques to improve the quality of tryptic digest separations will also be demonstrated.

EXPERIMENTAL

Materials

Trifluoroacetic acid (TFA) was HPLC/Spectro grade (Pierce, Rockford, IL, USA). 1,3-Diaminopropane was purchased from Aldrich (Milwaukee, WI, USA). Perchloric acid, *n*-propanol and acetonitrile (HPLC grade) were obtained from EM Science (Cherry Hill, NJ, USA). Trypsin (sequencing grade) was from Boehringer Mannheim (Indianapolis, IN, USA). rhIL-4 was from Immunex/Sterling. Water was purified by a Milli-Q system (Millipore, Bedford, MA, USA). All other chemicals were reagent grade and obtained from J. T. Baker (Phillipsburg, NJ, USA).

Preparation of tryptic digest of rhIL-4

To 370 μg of rhIL-4 in 40 μl of 100 m*M* pH 7.4 Tris buffer were added 7.4 μg of trypsin (20 μl) plus 63 μl of 100 m*M* pH 8.6 Tris buffer. The sample was incubated at 37°C for 20 h after which the pH was adjusted below 3 with dilute HCl. The sample was stored frozen.

Instrumentation

Micro-LC analyses were conducted using an Isco (Lincoln, NE, USA) microbore HPLC system composed of two Micro-LC-500 pumps connected to a ChemResearch interface box and controlled using a Compaq Desk Pro 286E PC. Several modifications to the standard system were made to improve gradient performance at the low flow-rates used in this work. The standard 3-μl Upchurch mixing tee was replaced by a 10-μl Lee (Westbrook, CT USA) micro-mixer tee followed immediately by a second inline Lee 10-μl micro-mixer. All tubing connections downstream of the mixers were made using minimum lengths of 0.004 in. (1 in. = 2.54 cm) I.D. stainless-steel tubing. All tubing, mixers, injector and column were insulated with 1 cm thick foam insulation. A 30 cm × 0.32 mm Delta Pack C_{18}, 5 μm, 300 Å packed capillary column (LC Packings, San Francisco, CA, USA) was connected directly to a Valco Model C14W injector with a 200-nl injector rotor. The outlet of the column was connected directly to an Isco Micro-LC-10 UV detector equipped with a 2-mm microbore flow cell. Data were collected and analyzed with a PENelson Model 6000 data system (PENelson, Cupertino, CA, USA) operated off a VAX computer system.

Three different CZE systems were used for this work. System A was a modular system constructed in-house which has been described elsewhere [9]. System B was a Pace 2000 from Beckman (Palo Alto, CA, USA) and system C was a Spectra-Phoresis 1000 from Spectra-Physics (San Jose, CA, USA). All capillary tubing (50 μm I.D. × 375 μm O.D.) was purchased from Polymicro Technologies Phoenix, AZ, USA). Capillary cartridges for the commercial systems were prepared in-house using the respective manufacturers' cartridge kits. Capillaries were conditioned by rinsing with 1 *M* NaOH for 30 min followed by operating buffer for about 10 h. All samples were injected from 100-μl vials. In between injections, capillaries were rinsed with the operating

buffer. All data was collected and analyzed using the PENelson Model 6000 data system.

RESULTS AND DISCUSSION

Purity analysis of rhIL-4

One of the more critical tasks in characterizing a protein pharmaceutical is the determination of purity. This has typically been achieved using a variety of techniques including electrophoresis, chromatography and immunoassays. While no one technique is able to detect all possible impurities that might be encountered, HPLC and more recently CZE, have proven to be particularly effective in detecting close structural analogues and protein degradation products due to the high resolving power of these techniques.

As a result of the basic character of rhIL-4 (p*I* 9.2) [10], the development of suitable CZE separations for this protein using uncoated fused-silica capillaries was problematic. Irreversible protein adsorption occurred when working in the pH range 2.5–10 using standard separation protocols. Although analysis could be performed below pH 2.5 or above pH 10, resolution was limited at low pH values and protein stability was poor at high pH values. We have found that a combination of an amine modifier with alkali metal salts to be effective in reducing protein–capillary wall interactions for basic proteins [11]. Using this strategy, several useful separations were developed for rhIL-4 in the pH range from 4.5 to 8.0.

Fig. 1 shows a series of electropherograms obtained at pH 7.0 on 3 different samples of rhIL-4 possessing different impurity profiles (typical bulk drug substance sample, acid-stressed sample and sample stressed at room temperature/neutral pH). The high resolution of this technique is evident from an examination of the electropherogram of the acid stressed sample. As many as 24 components are partially to totally resolved in this sample. Although the exact nature of all of these peaks has not been elucidated, experiments were conducted to demonstrate that these are real components rather than separation artifacts. Since aggregation/oligomerization has been identified as a major degradation pathway for rhIL-4 drug product [12] it is possible that this is, in part, responsible for some of these peaks. The sample of rhIL-4 bulk drug substance and the sample stressed at pH 7.4/room temperature for several months were found to contain several percent oligomeric impurities using size exclusion HPLC. The peak labeled 2 (analogue 1) in

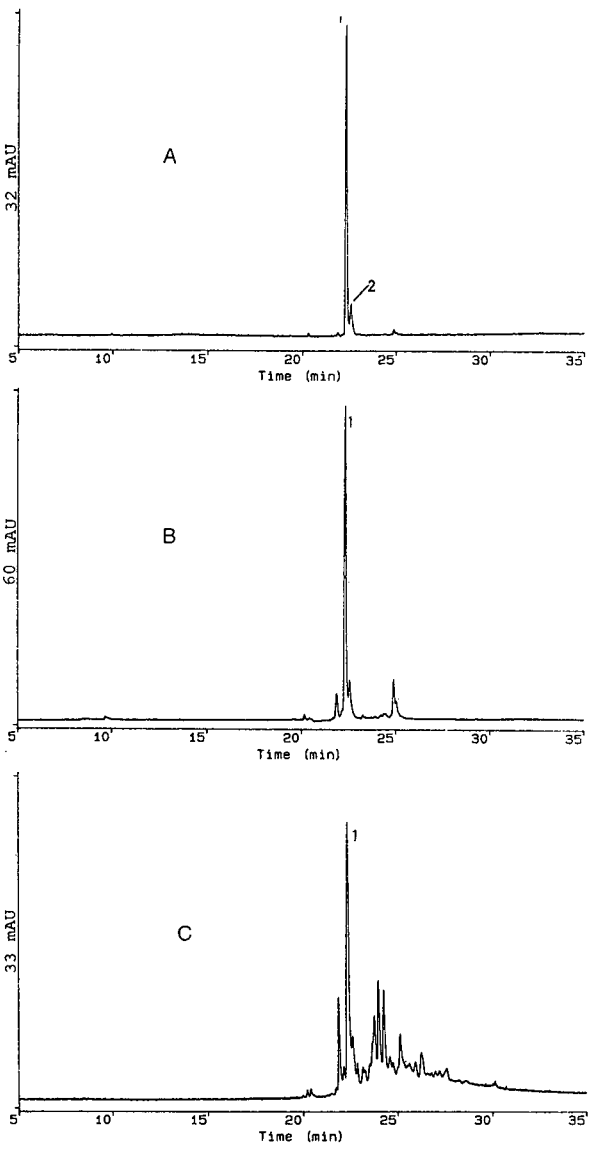

Fig. 1. CZE separations of (A) rhIL-4 bulk drug substance, (B) rhIL-4 degraded at pH 7.4/room temperature and (C) rhIL-4 degraded at pH 2. CZE system B: Capillary, 57 cm (50 cm separation distance) × 50 μm I.D.; buffer, 50 m*M* 1,3-diaminopropane, 0.04 *M* Na_2SO_4, pH 7.0 with H_3PO_4; voltage, 17 kV (70 μA); temperature, 25°C; detection, 200 nm, 3 s pressure injection of a 0.8 μg/μl protein solution. Peaks: 1 = rhIL-4; 2 = analogue 1.

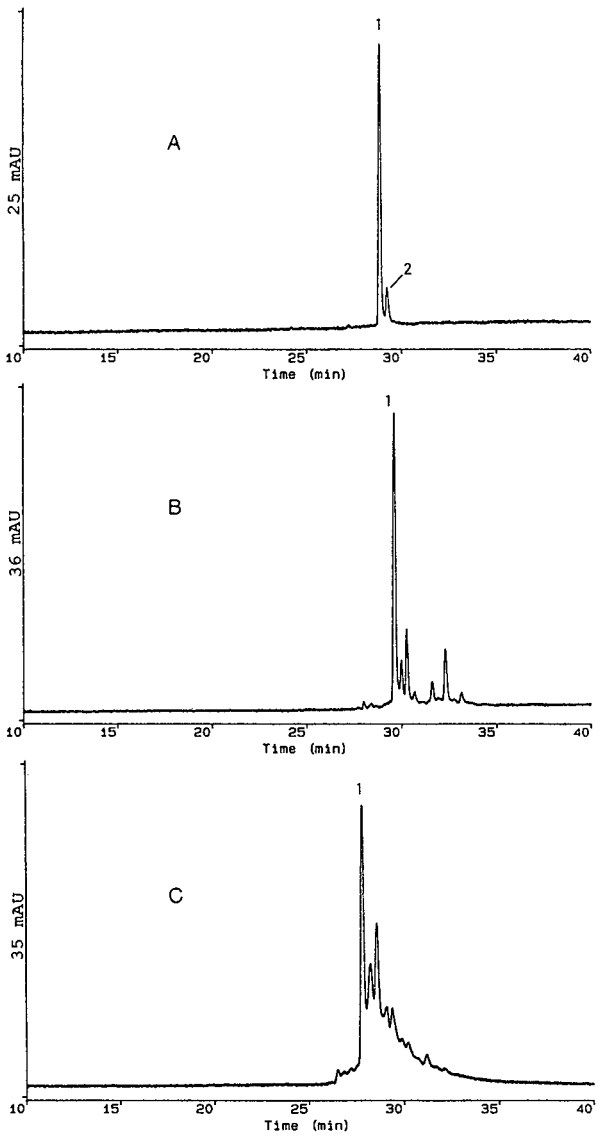

Fig. 2. CZE separations of rhIL-4 in a pH 4.5 buffer, CZE conditions and sample identities as in Fig. 1 with the following changes: Buffer, 50 m*M* 1,3-diaminopropane, 0.04 *M* Na_2SO_4, 10 m*M* formic acid, 0.01 *M* NaH_2PO_4, pH 4.5 with H_2SO_4; voltage, 15 kV (68 μA). Peaks: 1 = rhIL-4; 2 = analogue 1.

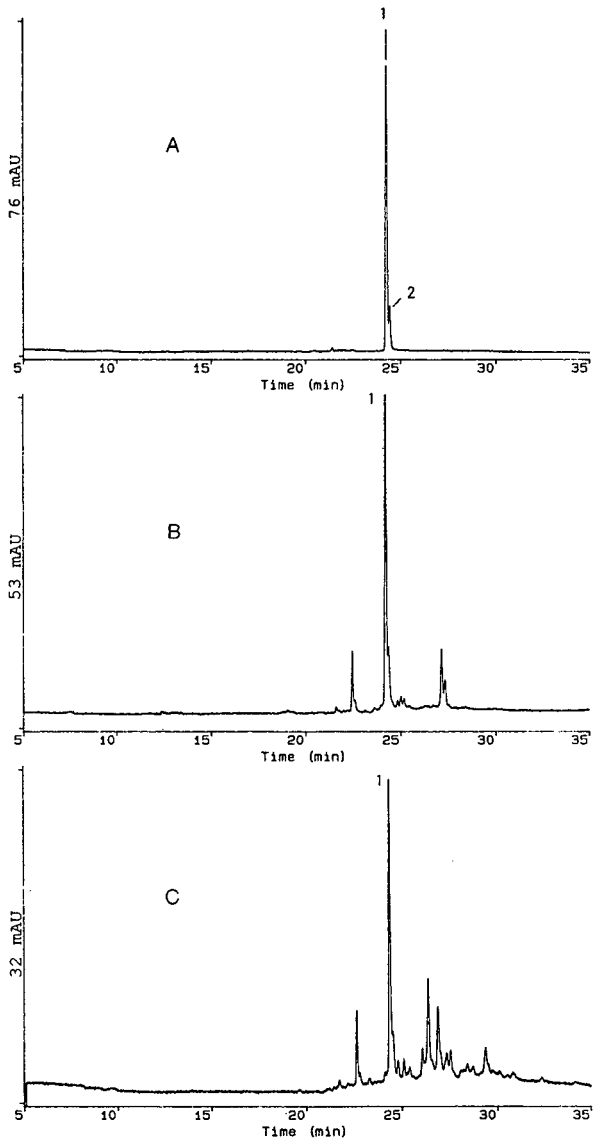

Fig. 3. CZE separations of rhIL-4 in a pH 8.0 buffer. CZE conditions and sample identities as in Fig. 1 with the following changes: Buffer, 50 m*M* 1,3-diaminopropane, 0.08 *M* NaH_2PO_4 pH 8.0; voltage, 17 kV (59 μA). Peaks: = rhIL-4; 2 = analogue 1.

the typical bulk drug substance sample has been identified as an active analogue of rhIL-4 in which one of the three intrachain disulfide linkages has been cleaved. Several impurities are resolved in a sample of rhIL-4 stressed at pH 7.4/room temperature for several months, clearly demonstrating the utility of CZE for detecting likely degradation products formed under normal storage or handling conditions.

The flexibility of CZE for optimizing or altering the selectivity of a separation is demonstrated with Figs. 2 and 3. These electropherograms were obtained at two different pH values (4.5 and 8.0) using the same set of three samples depicted in Fig. 1.

Both resolution and selectivity (peak migration order) could be altered by changing the buffer pH and composition. This flexibility of CZE is clearly an advantage when attempting to resolve a series of close structural analogues. While separations at pH 7.0 and 8.0 were highly reproducible within day and over different days, separations at pH 4.5 were more variable from day to day. This is apparently due to the pronounced pH hysteresis exhibited by fused-silica in the pH range from 4–6 [9]. Thus, although there is an apparent better overall resolution of impurities in sample B when analyzed at pH 4.5, this is at the expense of the precision of the separation.

Fig. 4 contains a series of reversed-phase micro-LC chromatograms of these same samples of rhIL-4. A 0.32-mm column packed with a 5-μm C_{18} phase was used at a flow-rate of 5 μl/min. A perchloric acid–acetonitrile gradient was used in an attempt to reduce background absorbance typically encountered with TFA at low wavelengths.

Although there are examples in the literature demonstrating the successful separation of close structural analogues of other interleukins using HPLC [13,14], for the present application, RP-HPLC was not able to provide anywhere near the same quality of separation achieved using CZE. Only in the acid stressed sample were any significant impurities separated and detected. Using a very shallow gradient, the active analogue 1 of rhIL-4 could be partially resolved from the main peak (data not shown). Since the peak response of the intact rhIL-4 peak decreases after stressing, it is possible that the decomposition products are selectively and irreversibly adsorbed to the column. In addition to the poorer resolution and/or lack of recovery of impurities, these chromatograms tended to be contaminated with several "blank" peaks (peaks marked by an asterisk in Fig. 4) and a rising baseline resulting from the gradient process. These artifacts tend to reduce sensitivity and can possibly obscure impurity peaks.

While the gradient elution process is responsible for the problems documented above, it is also an advantage of HPLC that the elution strength can conveniently be varied using a solvent gradient. This fact is demonstrated in Fig. 5 which compares a reveresed-phase micro-LC chromatogram with a CZE electropherogram of a crude sample of rhIL-4.

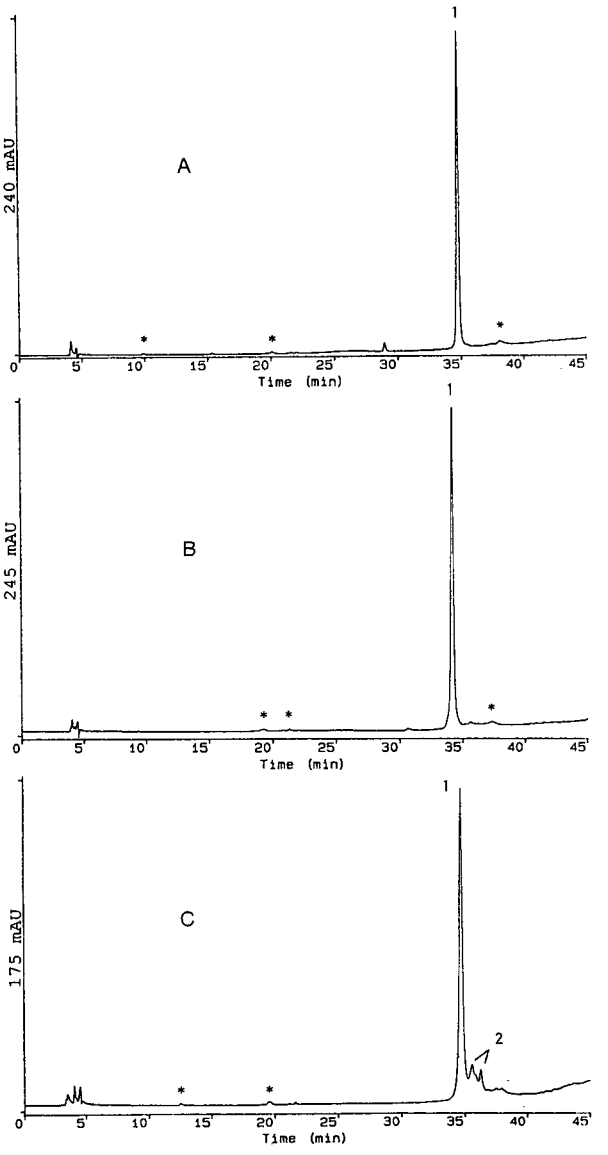

Fig. 4. Reversed-phase micro-LC chromatograms of rhIL-4. Sample identities as in Fig. 1. Column, 30 cm × 0.32 mm Deltabond C_{18}; 300 Å; flow-rate, 5 μl/min; mobile phase, (A) water–acetonitrile–*n*-propanol (92:5:3)–0.05 *M* $HClO_4$–$NaClO_4$ pH 2.0, (B) water–acetonitrile–*n*-propanol (15:82:3)–0.05 *M* $HClO_4$–$HClO_4$; linear gradient from 10–80% B over 40 min; injection volume, 200 nl (100 ng) rhIL-4; detection, 214 nm. Peaks: 1 = rhIL-4; 2 = degradation peaks; for peaks marked *, see text.

Here, gradient elution allows for the separation of many impurity peaks of widely differing hydrophobicities in a reasonable amount of time. CZE also provides good resolution of these impurities. How-

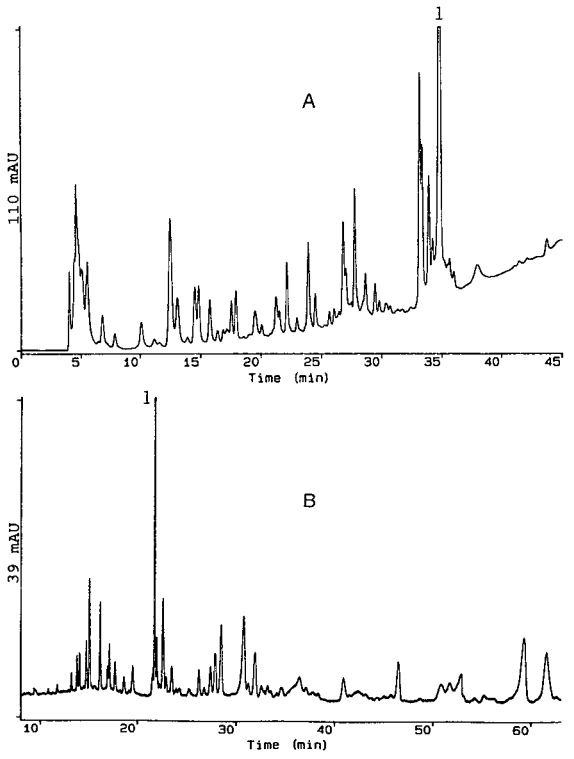

Fig. 5. Comparison of (A) reversed-phase micro-LC and (B) CZE separations of a crude sample of rhIL-4. CZE conditions as in Fig. 1. Reversed-phase micro-LC conditions as in Fig. 4 with a gradient of 5–80% B over 45 min and detection at 200 nm. Peak 1 = rhIL-4.

ever, due to the apparent wide variation in charge to size ratios for these components, the electropherogram is spread out over a longer time window. The orthogonality of these two techniques is evidenced from the difference in the relative position of the main rhIL-4 peak in each separation pattern. By HPLC rhIL-4 is nearly the last peak to elute while in CZE it is one of the earlier peaks to elute.

Quantitation

The relative quantitative aspects of these techniques were evaluated by measuring peak migration/retention time and area responses for multiple injections of a typical sample of rhIL-4 drug substance. For CZE (pH 7.0 buffer) hydrodynamic injections were made using a 0.8 ng/nl protein solution. For the hydrodynamic injections (3 s) the amount of protein injected was estimated to be 3.6 nl [15] or 2.88 ng. For the micro-LC evaluation, a 200-nl injection of a 0.5 ng/nl solution, corresponding to 100 ng, was used.

TABLE I

PRECISION OF rhIL-4 PEAK MIGRATION TIMES AND AREA RESPONSES BY CZE

CZE conditions as in Fig. 1 (sample A).

	Migration time	Peak area
Mean (n = 8)	22.67 min	34 620
S.D.	0.06468 min	1 061
R.S.D. (%)	0.285	3.06

Table I contains the CZE data and Table II the analogous reversed-phase micro-LC data. The precision of peak migration times was slightly better by CZE whereas the precision of peak area responses was comparable for the two techniques. The strategy used in developing the CZE separation was to carefully optimize the buffer composition to eliminate protein adsorption. By eliminating protein adsorption, highly reproducible separations were achieved at pH 7.0 and 8.0. The absence of temperature control and the difficulty in delivering gradients at 5 μl/min flow-rates is responsible for the poorer precision in retention times by micro-LC compared to what is typically achieved using standard-bore LC. It is possible that the precision of the micro-LC system could be improved by operating the pumps at a somewhat higher flow-rate where the precision of solvent delivery is better and splitting the flow at a tee prior to the injector to achieve

TABLE II

PRECISION OF rhIL-4 PEAK RETENTION TIMES AND AREA RESPONSES BY REVERSED-PHASE MICRO-LC

Chromatographic conditions as in Fig. 4 (sample A).

	Retention time	Peak area
Mean (n = 7)	34.68 min	4847
S.D.	0.2002 min	142.7
R.S.D. (%)	0.577	2.94

TABLE III

PRECISION DATA FOR THE PURITY DETERMINATION OF rhIL-4 BY CZE

CZE conditions as in Fig. 1 (sample A).

	rhIL-4	Impurity 1	Impurity 2	Impurity 3	Impurity 4
Mean (n = 8) (peak area %)	79.75%	1.16%	1.72%	11.95%	5.42%
S.D. (peak area %)	0.6724	0.132	0.457	0.651	0.815
R.S.D. (%)	0.843	11.4	26.6	5.45	15.0

the desired flow-rate through the column, although the precision was deemed suitable for this application.

Since the ultimate goal of these methods is the determination of purity, the peak responses for the impurities were determined for the CZE experiments using a typical sample of rhIL-4 bulk drug substance (Fig. 1A). The data compiled in Table III shows fairly good precision for overall purity estimation (R.S.D. 0.843%), although R.S.D.s for individual impurity peaks were much higher. This is due to the fact that some of the impurities are at or just above the limit of detection. Improvements in the concentration sensitivity and dynamic linear range of the detection scheme are needed to realize improvements here. No comparison can be made with micro-LC in this instance since no significant impurity peaks were resolved in this sample with this method.

The estimated limit of detection (mass sensitivity) for rhIL-4 by CZE (pH 7.0 buffer system) of 18 pg ($1.2 \cdot 10^{-15}$ mol) is more than an order of magnitude better than that found by micro-LC (400 pg, $2.6 \cdot 10^{-14}$ mol). Poor recovery of low concentrations of rhIL-4 from the reversed-phase column (a problem that is typically encountered with proteins and is not unique to rhIL-4), the presence of blank peaks and the gradient induced rising baseline contributed to the poorer sensitivity by micro-RP-HPLC. However, this detection limit considers only the amount of sample actually being injected onto the columns. With micro-LC a much greater percentage of the available sample could be injected (approximately 50%) compared to CZE where several microliters of solution were required to make an injection of a few nanoliters. Thus, while CZE exhibits a much lower mass sensitivity, in a true sample limited situation this advantage is offset by the poorer concentration sensitivity and the fact that a much larger volume of sample can be loaded onto the micro-LC column.

The sensitivities achieved here do not approach those obtained for other compounds by other investigators using modified UV detection [16,17] or alternative detection schemes such as laser-induced fluorescence [18,19]. Instead, the results reported here reflect what might typically be achieved for underivatized proteins using presently available commercial instrumentation with UV detection.

Tryptic mapping

Peptide mapping of enzymatic digests of proteins is a well established technique for confirming protein identity and potentially detecting protein modifications. Fig. 6 shows a reversed-phase micro-LC

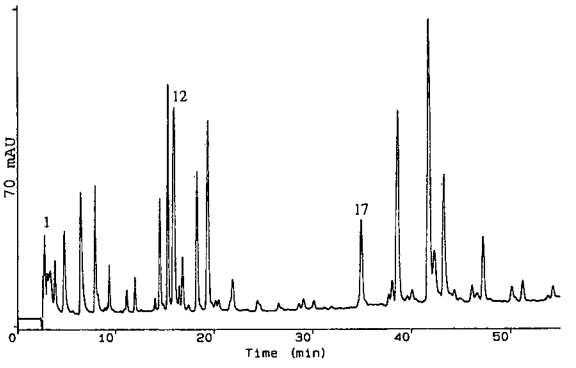

Fig. 6. Reversed-phase micro-LC map of tryptic digest of rhIL-4. Flow-rate, 5 μl/min; (A) 0.05% TFA in water, (B) 0.05% TFA in acetonitrile–water (50:50); gradient, 2–30% B in 10 min, 30 to 70% B at 50 min; detection, 210 nm; sample, 200 nl of a 1 ng/nl solution of rhIL-4 tryptic digest. For numbered peaks, see text.

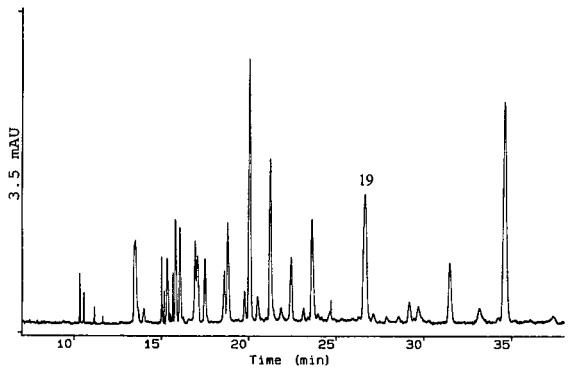

Fig. 7. CZE map of rhIL-4 tryptic digest. CZE system A: Capillary, 100 cm (80 cm separation distance) × 50 μm I.D.; buffer, 20 m*M* 1,3-diaminopropane–phosphate, pH 3.20; voltage, 30 kV (8 μA); detection, 200 nm; sample, 3 mg/ml rhIL-4 tryptic digest, hydrodynamic injection by raising the inlet capillary a height of 7 cm for 5 s. For numbered peak, see text.

map of a tryptic digest of rhIL-4 and Fig. 7 a CZE of the same digest. Due to the different separation mechanisms, the selectivity of these separations are quite different, a point that has been demonstrated by other investigators applying CZE to peptide separations [6–8]. This difference can be used as an aid in developing a suitable separation by either technique. By isolating RP-HPLC peaks and subsequent analysis by CZE, it was determined that HPLC peak 12 contained two peptides. Similarly, two peptides that were well separated by HPLC (peaks 1 and 17) coeluted by CZE (peak 19). Using

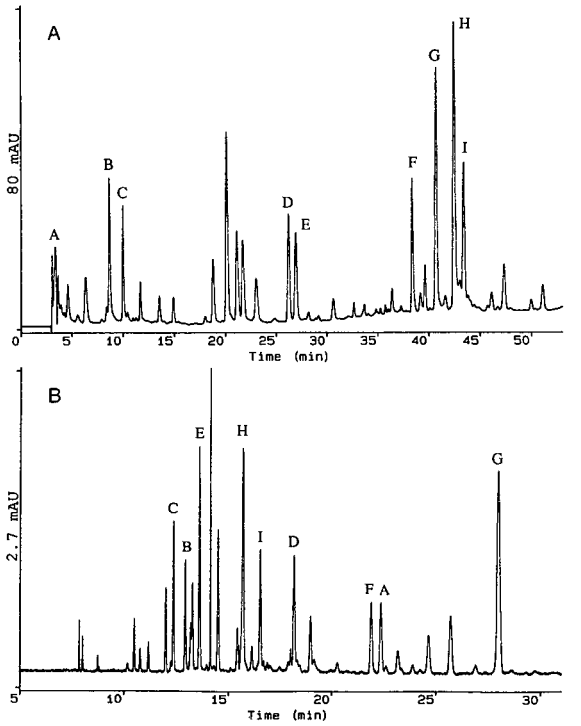

Fig. 8. Optimized reversed-phase micro-LC (A) and CZE (B) maps of rhIL-4 tryptic digest. Micro-RP-HPLC conditions as in Fig. 7 with a flow-rate of 6 μl/min, (a) 0.05% TFA in water, (B) 0.05% TFA in acetonitrile–water (50:50); linear gradient from 0–18% B in 8 min, 18–38% B at 25 min, 38–53% B at 30 min, 53–70% B at 50 min. CZE conditions: CZE system C: Capillary, 70 cm (63 cm separation distance) × 50 μm I.D.; buffer, 25 m*M* 1,3-diaminopropane–phosphate, pH 3.35; temperature, 25°C; voltage 25 kV (31 μA); detection, 200 nm; sample 1-s vacuum injection of a 2.3 mg/ml solution of rhIL-4 tryptic digest. For peaks, see text.

TABLE IV

PRECISION OF rhIL-4 TRYPTIC PEPTIDE MIGRATION TIMES BY CZE

CZE conditions as in Fig. 8.

	Peak migration times of tryptic peptides (min)									
	1	2	3	4	5	6	7	8	9	10
Mean (n = 8)	10.50	11.97	12.91	13.61	14.51	15.73	18.24	22.02	25.95	28.26
S.D.	0.0226	0.0774	0.0421	0.0362	0.0325	0.0484	0.0456	0.0880	0.123	0.142
R.S.D. (%)	0.216	0.647	0.326	0.266	0.224	0.308	0.250	0.399	0.476	0.502

TABLE V

PRECISION OF rhIL-4 TRYPTIC PEPTIDE RETENTION TIMES BY REVERSED-PHASE MICRO-LC

Chromatographic conditions as in Fig. 6.

	Peak retention times of tryptic peptides (min)									
	1	2	3	4	5	6	7	8	9	10
Mean (n = 6)	6.59	10.55	12.38	18.45	23.28	38.42	41.96	44.89	46.29	54.22
S.D.	0.365	0.3263	0.2657	0.2265	0.3206	0.3845	0.3619	0.3415	0.3262	0.2973
R.S.D. (%)	5.54	3.09	2.15	1.23	1.38	1.00	0.863	0.761	0.705	0.548

this information, the two methods were further optimized resulting in the separations depicted in Fig. 8. As an indication of the complementary separation mechanisms, letters have been assigned to some of the peaks indicating identical peptides separated by the two techniques. The overall resolution and efficiency of CZE and reversed-phase micro-LC were found to be comparable for this particular application. A notable exception is the ability of CZE to better resolve the most hydrophilic peptides, some of which elute in or just after the void volume in reversed-phase micro-LC.

Precision of tryptic maps

The reproducibility of rhIL-4 tryptic peptide migration times by CZE and retention times by reversed-phase micro-LC was evaluated for replicate injections made over the course of a day. Table IV contains the CZE data and Table V the reversed-phase micro-LC data for selected peaks in these maps. Overall, precision of migration times were better by CZE (mean R.S.D. of 0.361% *versus* 1.73% by micro-LC). It should be noted that to obtain this level of precision by CZE, a new buffer vial was required for each injection. If the same buffer vial was used for multiple injections, peak migration times and in some cases migration orders changed significantly from injection to injection. This was attributed to ion depletion/pH changes that occurred in the buffer vial during the course of a run. The precision of the peptide retention times using micro-LC improved steadily over the course of a single run. Apparently, the gradient process tends to compensate for minor flow-rate differences that occur from run to run leading to better precision for later eluting peaks. Peptides eluting in the first 10 min are being eluted under near isocratic conditions and the retention times are more susceptible to flow-rate fluctuations in either pump. The overall poorer precision by reversed-phase micro-LC could be traced, in part, to a lack of suitable column and solvent temperature control. In fact, changes in retention times from injection to injection correlated to changes in the laboratory temperature over the course of the day. It is anticipated that improvements in this aspect of the micro-LC instrumentation will improve the overall precision.

CONCLUSIONS

CZE and micro-LC were evaluated for characterizing the purity and identity of rhIL-4. CZE was found to be superior to reversed-phase micro-LC for separating close structural analogues and degradation products from the parent protein due to its high efficiency and ability to manipulate the selectivity and resolution of the separation by changing the buffer composition/pH. Reversed-phase micro-LC, due to its gradient elution capabilities, may have advantages when separating sample components of widely differing structures and properties such as in crude protein isolates. The quantitative aspects of these techniques, in terms of precision, approach what can typically be achieved using standard-scale HPLC with the added advantage of improved mass sensitivity. The combination of these two techniques provides a powerful set of tools for characterizing protein purity and identity. This is

especially apparent for the analysis of protein digests, where the complementary nature of the separation mechanisms can be utilized to aid in the development process for peptide mapping.

REFERENCES

1 R. L. Garnick, N. J. Solli and P. A. Papa, *Anal. Chem.*, 60 (1988) 2546.
2 V. R. Anicetti, B. A. Keyt and W. S. Hancock, *Trends Biotechnol.*, 70 (1989) 342.
3 E. C. Huang and J. D. Henion, *Anal. Chem.*, 63 (1991) 732.
4 M. A. Moseley, L. J. Deterding, K. B. Tomer and J. W. Jorgenson, *Rapid Commun. Mass Spectrom.*, 3 (1989) 87.
5 J. Frenz, S. W. Wu and W. S. Hancock, *J. Chromatogr.*, 480 (1989) 379.
6 T. A. A. M. van de Goor, P. S. L. Janssen, J. W. van Nispen, M. J. M. van Zeeland and F. M. Everaerts, *J. Chromatogr.*, 545 (1991) 379.
7 P. D. Grossmann, J. C. Colburn, H. H. Lauer, R. G. Nielsen, R. M. Riggin, G. S. Sittampalam and E. C. Rickard, *Anal. Chem.*, 61 (1989) 1186.
8 K. A. Cobb and M. Novotny, *Anal. Chem.*, 61 (1989) 2226.
9 W. J. Lambert and D. L. Middleton, *Anal. Chem.*, 62 (1990) 1585.
10 J. Snider, personal communication.
11 J. A. Bullock and L. C. Yuan, *J. Microcol Sep.*, 3 (1991) 241.
12 L. C. Yuan, D. M. Forde, J. Snider, W. Fenderson, E. Wanner and J. A. Bullock, *Pharm. Res.*, submitted for publication.
13 M. Kunitani, P. Hirtzer, D. Johnson, R. Halenbeck, A. Boosman and K. J. Korths, *J. Chromatogr.*, 371 (1986) 391.
14 M. Kunitani, D. Johnson and L. R. Snyder, *J. Chromatogr.*, 359 (1986) 313.
15 *Technical Information Bulletin No. TIBC-103*, Beckman Instruments, Palo Alto, CA, 1990.
16 J. P. Chervet, R. E. J. van Soest and M. Ursem, *J. Chromatogr.*, 543 (1991) 439.
17 T. Tsuda, J. V. Sweedler and R. N. Zare, *Anal. Chem.*, 62 (1990) 2149.
18 J. Liu, Y. Z. Hsieh, D. Wiesler and M. Novotny, *Anal. Chem.*, 63 (1991) 408.
19 M. Novotny, *J. Microcol. Sep.*, 2 (1990) 7.

Journal of Chromatography, 633 (1993) 245–250
Elsevier Science Publishers B.V., Amsterdam

CHROM. 24 756

Measurement of vitamin C by capillary electrophoresis in biological fluids and fruit beverages using a stereoisomer as an internal standard

Edward V. Koh, Michael G. Bissell and Ralph K. Ito*

Nichols Institute, Nutrition and Metabolism Biochemistry Department, 33608 Ortega Highway, San Juan Capistrano, CA 92690-6130 (USA)

(First received June 11th, 1992; revised manuscript received November 13th, 1992)

ABSTRACT

Ascorbic acid (or vitamin C) is an important component of many biological systems and various physiological roles have been described for it. A rapid and simple capillary electrophoresis method for ascorbic acid measurements in biological fluids as well as in beverages was developed. A stereoisomer of ascorbic acid, isoascorbic acid, not normally found in nature, was used as the internal standard for this assay. The analysis was performed in a 30 cm × 75 μm I.D. fused-silica capillary with 100 m*M* tricine buffer, pH 8.8, and measured by UV absorbance at 254 nm. The method was sensitive to 1.6 μg/ml and linear to 480.1 μg/ml. Within-run R.S.D. was 3.2% (93.5 ± 3.0 μg/ml, mean ± S.D., $n = 18$) and run-to-run R.S.D. was 3.3% (35.6 ± 1.2 μg/ml, mean ± S.D., $n = 10$) and 1.9% (149.4 ± 2.8 μg/ml, mean ± S.D., $n = 10$). Average spiked recovery from human plasma samples was 98.0%. The technique has been demonstrated to be suitable for assay of vitamin C in biological samples and some fruit juices.

INTRODUCTION

Ascorbic acid is the most abundant biologically active form of vitamin C in humans. Analysis of ascorbic acid by present techniques is both time consuming and complicated [1–4]. High-performance liquid chromatography (HPLC) methods have been used for vitamin C analysis. Examples are cation-exchange chromatography [5], ion-exclusion chromatography [6], and reversed-phase chromatography [7–13]. Some minor problems with ascorbic acid measurement have been observed when using amperometric detectors [6] and ultraviolet detectors [14]. These problems have been related to working electrode contamination of amperometric detectors and ultraviolet interfering components in biologic fluids.

Capillary electrophoresis (CE) is a useful analytical separation technique known for its high resolution and small sample volume. The number of CE applications is rapidly growing and includes some interesting applications in the clinical field [15]. The analysis of urinary components by CE also has been reported [16–18]. More recently, several papers have demonstrated the usefulness of micellar electrokinetic capillary chromatography (MECC) for separation of various groups of compounds, including water and fat-soluble vitamins [19]. These reports on vitamins were focused on the separation techniques and did not reach low detection limits of 1.6 μl/ml for clinical applications where < 2.0 μg/ml is considered deficient [3].

The main objective of this investigation was to develop a simple and rapid method for vitamin C analysis in biological fluids using a commercially available CE apparatus. By developing a CE method using isoascorbic acid as an internal standard, a fully automated quantitative analysis of vitamin C in plasma, serum, urine and some beverages has been developed.

* Corresponding author.

0021-9673/93/$06.00

EXPERIMENTAL

Instrumentation

A Model 2100 high-performance capillary electrophoresis system (Beckman Instruments, Fullerton, CA, USA) was used for CE studies. A personal integrator system (Model 1020; Perkin-Elmer, Norwalk, CT, USA) was used for data handling. A refrigerated centrifuge (Model J-6B; Beckman Instruments, Palo Alto, CA, USA), and a multitube vortexer (VWR Scientific, Philadelphia, PA, USA) were used for sample extractions.

The capillary (Polymicro Technologies, Scottsdale, AZ, USA) size was 37 cm × 75 μm I.D. and length to the detector was 30 cm. The polyimide coating at the detector window was removed by flaming followed by methanol wash. After installing the capillary column into a capillary cartridge, the capillary was conditioned by pressuring with 1 *M* sodium hydroxide for 10 min, water for 10 min, and the run buffer for 10 min.

Reagents

The following reagents were purchased from Sigma (St. Louis, MO, USA): EDTA, trichloroacetic acid, L-ascorbic acid; D-isoascorbic acid; uric acid standard solution and tricine. Sodium hydroxide was purchased from Fisher Scientific (Fair Lawn, NJ, USA), Ascorbic acid oxidase from Boehringer Mannheim (Indianapolis, IN, USA), and metaphosphoric acid from Aldrich (Milwaukee, WI, USA). Reagent-grade deionized water from EM Science (Gibbstown, NJ, USA) was used to prepare all buffers. Biocell plasma (Biocell Labs., Rancho Dominguez, CA, USA) lots were screened and those deficient in ascorbic acid were used to make plasma standard and controls.

Procedures

Fresh urine and whole blood were collected and treated to obtain plasma (EDTA, 0.1 m*M*) or serum (after clotting) from volunteers. Volunteers were asked to fast overnight prior to sample collection. All the urine samples were preserved by adding metaphosphoric acid (MPA, 100 g/l) and then stored at −80°C. Samples were stored up to 4 weeks and were run in batches. Urine and beverage samples for the analysis were prepared by diluting 0.2 ml of sample with 0.1 ml of MPA (100 g/l) in a 75 × 12 mm test tube which also contained 0.1 ml isoascorbic acid (100 μg/ml) as an internal standard. Samples were vortex-mixed for 15 s and filtered through a 0.45-μm filter by centrifugation (3000 *g*, 10 min, 5°C). The filtrate was transferred to a Beckman CE microvial and analyzed. Aliquots of plasma or serum (0.5 ml) were mixed with 0.5 ml of 12% trichloroacetic acid (TCA) to deproteinate sample and extract analytes into the aqueous phase. The TCA also preserves the ascorbic acid. The solution was vortexed for 30 s. After centrifugation for 5 min at 5°C, the supernatants (0.7 ml) were filtered and 100 μl of isoascorbic acid (81.5 μg/ml) were added to 0.4 ml of filtrate for analysis.

Two lots of urine and plasma controls were prepared by supplementation of known amounts of ascorbic acid such that the final concentration of ascorbic acid in each lot was 35.6 and 149.4 μl/ml of urine, and 3.5 and 20.0 μg/ml of plasma (low end and high end of expected adult reference range, respectively).

Samples were injected into the separation capillary by the pressure injection method. Separation voltage was set at 11 kV (297 V/cm) across the capillary and on-column UV absorption at 254 nm was used for measurement. After each separation, the capillary was rinsed sequentially with 0.1 *M* NaOH, distilled water, and buffer, for 1 min each, between successive electrophoretic runs.

RESULTS AND DISCUSSION

Mobility (migration time) can change during CE separation and this is noted to occur from run-to-run [20]. It is important to minimize migration time variation in the sample analysis for proper peak identification. Sample pretreatment and extraction methods are often used to resolve sample-to-sample variation and retention time drift problems with HPLC [5,6,7–13]. This can be done by traditional methods such as solid-phase or liquid–liquid phase extractions then followed by sample analysis. Plasma samples for CE analysis were processed using TCA as the liquid–liquid extraction method which also served as a preservative for ascorbic acid. The samples became homogenous by extraction and the procedure reduced the sample's matrix effects on migration time and improved means of peak identification by reducing interference. For CE analysis

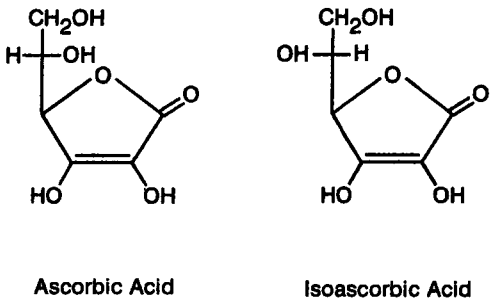

Fig. 1. Structure of ascorbic acid and one of its stereoisomers, isoascorbic acid.

in urine and beverage samples, concentrated metaphosphoric acid (100 g/l) was added as a preservative for ascorbic acid. Additional sample pretreatment was not found to be necessary. All the analytical results after these sample pretreatment procedures showed significant improvement in sample-to-sample variation and reduced retention time drift.

It is most desirable to use a suitable internal standard for quantitative analysis when possible. Ascorbic acid is the biologically important analyte to measure [21]. One of its stereoisomers, isoascorbic acid, which does not naturally exist in humans or other natural products, was selected as an internal standard. Manufacturers of some foods or beverages may add isoascorbic acid to products as an additive. The addition of isoascorbic acid as an internal standard for ascorbic acid analysis in foods or beverages which may contain isoascorbic acid as an antioxidant will result in erroneous values for ascorbic acid. In this case, the native level of isoascorbic acid must be established by testing the sample prior to addition of the isoascorbic acid. Ascorbic acid and isoascorbic acid differ from each other only in the way the atoms are oriented in space (Fig. 1). These physical properties of stereoisomers make them difficult to distinguish by usual analytical methods. Several interesting MECC techniques have been reported which include the separation of stereoisomers [22].

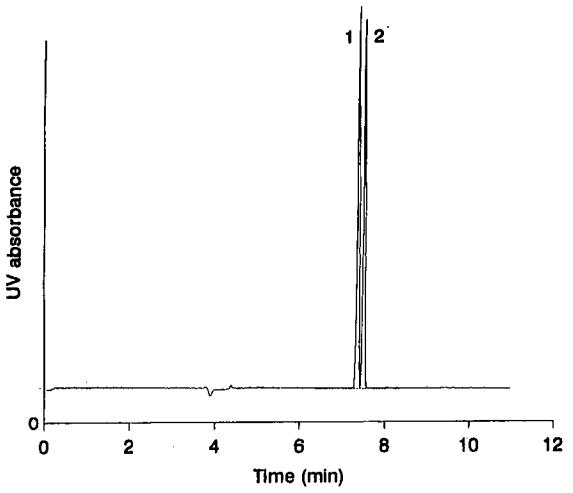

Fig. 2. Electropherogram of ascorbic acid (a) and isoascorbic acid (2) using 100 μg/ml each in metaphosphoric acid solution (100 g/l). Procedure conditions: buffer, 100 m*M* tricine (pH 8.8); capillary, uncoated 37 cm × 75 μm I.D. (30 cm to detector); applied voltage, 11 kV.

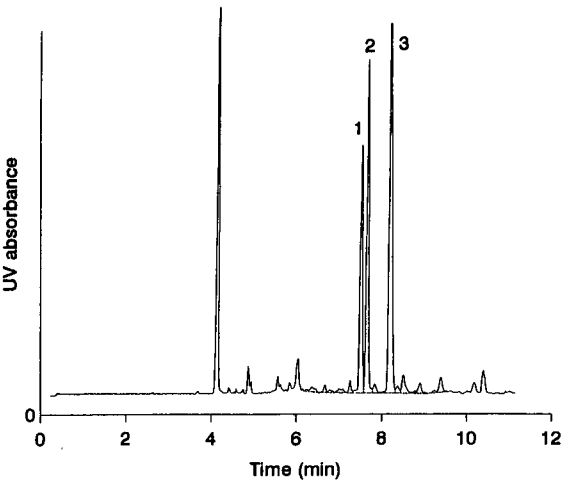

Fig. 3. Electropherogram of a human urine. Peaks: 1 = ascorbic acid (17.5 μg/ml); 2 = isoascorbic acid (85.0 μg/ml); 3 = uric acid. CE separation conditions as in Fig. 2.

The method we report here is a novel CE procedure (not MECC), which separates these two stereoisomers with baseline resolution as shown in Fig. 2. It is favorable to have an internal standard migrating near the analyte peak for CE applications. The use of a stereoisomer as an internal standard is highly desirable as conditions that effect the analyte peak, similarly effect the internal standard peak. We have observed that the effect of changing electrophoretic conditions (*i.e.*, pH, ionic strength) has little influence on quantifying or identifying the ascorbic acid peak [22]. Some useful assay applications

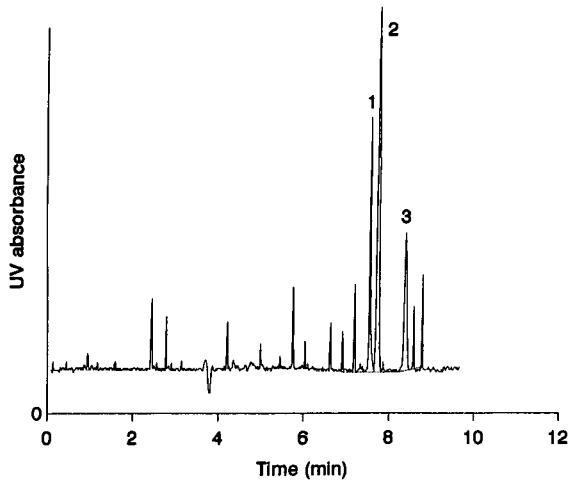

Fig. 4. Electropherogram of a human plasma which was extracted with 12% trichloroacetic acid. Peaks: 1 = ascorbic acid (5.8 μg/ml); 2 = isoascorbic acid (16.3 μg/ml); 3 = uric acid. CE separation conditions as in Fig. 2.

are shown for ascorbic acid measurements in urine (Fig. 3), plasma (Fig. 4), and fruit juice (Fig. 5). In addition, the uric acid peak (Figs. 3 and 4) which was consistently observed in urine and plasma was identified using a uric acid standard solution by standard recovery studies and retention times. These applications show that CE is a useful analytical method for the quantitative analysis of ascorbic

TABLE I

REPRODUCIBILITY OF ASCORBIC ACID IN URINE FOR BOTH INTRA-RUN AND INTER-RUN

	n	Mean ± S.D. (μg/ml)		R.S.D. (%)
Intra-run	18	93.5	3.0	3.2
Inter-run				
Level 1	10	35.6	1.2	3.3
Level 2	10	149.4	2.8	1.9

acid and the selection of rare isomers can be ideal internal standards for analysis.

Metaphosphoric acid was previously reported to be used as preservative for ascorbic acid [5]. We have found that both urine samples can be preserved with MPA and plasma with TCA without interfering with the CE method. These preservatives maintained reproducibility of ascorbic acid in both intra-run and inter-run analysis (Table I). As shown in Table I, excellent relative standard deviations were recorded from run-to-run (*i.e.*, intra-run, R.S.D. = 3.2%) and day-to-day (*i.e.*, inter-run, level 1, R.S.D. = 3.3% and level 2, R.S.D. = 1.9%).

We examined interference due to the biological sample matrix by standard recovery studies. A known amount of ascorbic acid standard (34.5 μg/ml) was spiked into serum samples (n = 5). Recovery of the added standard averaged 98% which shows excellent analytical accuracy in a complex

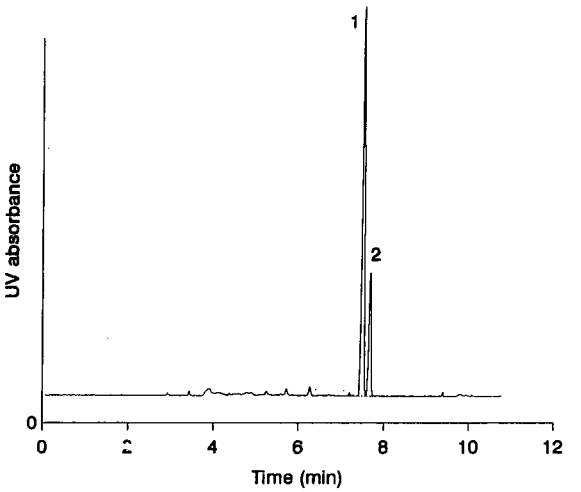

Fig. 5. Electropherogram of a name brand juice. Peaks: 1 = ascorbic (329.9 μg/ml); 2 = isoascorbic acid (100.0 μg/ml). CE separation conditions as in Fig. 2.

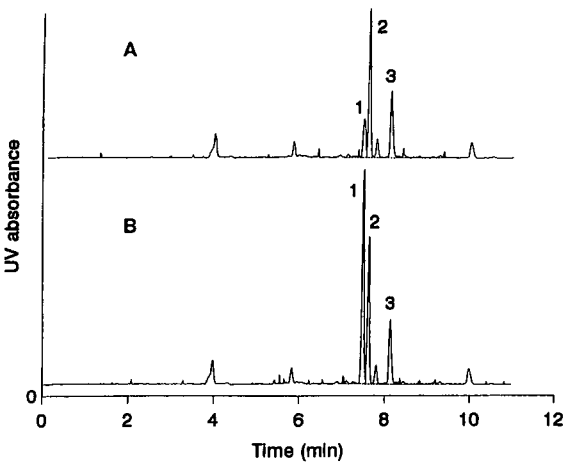

Fig. 6. Electropherogram of human urine (A) and spiked human urine (B). Peaks: 1 = ascorbic acid; 2 = isoascorbic acid; 3 = uric acid. CE separation conditions as in Fig. 2.

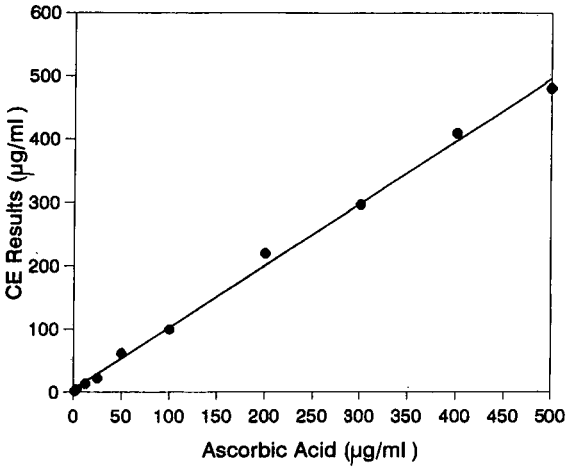

Fig. 7. Linearity curve obtained with a CE assay and a known ascorbic acid standard. The linear regression equation found was $y = 1.0149x - 4.2632$, $r = 0.9984$.

matrix. Similar results were obtained in urine matrix. The spiked electropherogram is shown in Fig. 6. In addition, we further demonstrate analytical specificity with use of ascorbate oxidase to remove ascorbic acid from sample solution. We added 17 U ascorbic acid oxidase to 3.0 ml of urine and incubated at 23°C for 6.0 min. This results in a smaller ascorbic acid peak as the ascorbic acid in the sample solution is oxidized to dehydroascorbic acid.

Linearity and sensitivity of the assay is shown in Fig. 7 using an aqueous standard. The method was sensitive to 1.6 µg/ml (lowest measurable level above background) and linear to 480.0 µg/ml. The linear regression and correlation equation with known ascorbic acid standard samples was $y = 1.0149x - 4.2632$, $r = 0.9984$. Satisfactory signal-to-noise ratios were observed at sensitive levels needed to cover the vitamin C deficiency cases in plasma or serum (less than 2.0 µg/ml) [3]. In addition, those patients that supplemented themselves with large oral dosages of vitamin C also can be evaluated.

We tested the application of this assay to measure vitamin C in several different types of fruit juices and a wine sample. The measurements were accomplished with use of the same electrophoretic system as described previously for the analysis of vitamin C in plasma and urine. The concentration of vitamin C in these beverages is shown in Table II. It is of interest to note that a considerable difference of vitamin C concentration was found between beverages.

TABLE II

ASCORBIC ACID DETERMINATION IN BEVERAGES

Sample	Ascorbic acid (µ/ml)
Orange juice	329.9
Apple juice	356.1
Grapefruit juice	103.8
Vegetable juice	344.4
Cranberry cocktail	>1.6
White wine	>1.6

The open-tube CE system is an excellent and powerful analytical system when considering that only a simple buffer solution was used to separate ascorbic acid from its stereoisomer, isoascorbic acid. It is applicable to a large variety of biological samples, many of which have been accomplished with HPLC [5–13,23,24] but are more labor intensive. This application of CE demonstrates excellent separation characteristics between ascorbic acid and isoascorbic acid and appears to be an improvement over HPLC means of stereoisomer separation and analysis. From the data we presented, this separation technique is well suited for clinical evaluation of human vitamin C status. Vitamin C has been reported to be an important antioxidant and nutrient which has been shown to increase longevity 6 years in men and 2 years in women [25]. The simplicity of this method suggests that vitamin C levels and distribution (ingestion, absorption and excretion) can now be easily monitored in body fluids.

REFERENCES

1 M. R. H. Lowik, J. Schrijver and M. Wedel, *Int. J. Vit. Nutr.*, 61 (1991) 43.
2 J. M. Kim, K. Huang and R. D. Schmid, *Anal. Lett.*, 23 (1990) 2273.
3 N. W. Tietz, *Clinical Guide to Laboratory Tests*, Saunders, Philadelphia, PA, 1990.
4 A. J. Pesce and L. A. Kaplan, *Methods in Clinical Chemistry*, Mosby, St. Louis, MO, 1987.
5 S. A. Margolis and T. P. Davis, *Clin. Chem.*, 34 (1988) 2217.
6 H. P. Wagner and M. J. McGarrity, *J. Chromatogr.*, 546 (1991) 119.
7 M. A. Kutnink, J. H. Skala, H. E. Sauberlich and S. T. Omaye, *J. Liq. Chromatogr.*, 8 (1985) 31.

8 M. C. Gennaro and C. Abrigo, *Fresenius J. Anal. Chem.*, 340 (1991) 422.
9 J. Cammack, A. Oke and R. H. Adams, *J. Chromatogr.*, 565 (1991) 529.
10 N. Bilic, *J. Chromatogr.*, 543 (1991) 367.
11 G. B. de Quinga, M. Lopez-Torres, R. Perez Campo and C. Rojas, *Anal. Biochem.*, 199 (1991) 81.
12 K. P. Dhariwal, W. O. Hartizell and M. Levine, *Am. J. Clin. Nutr.*, 54 (1991) 712.
13 C. S. Tsau and S. D. Salimi, *J. Chromatogr.*, 245 (1982) 355.
14 G. Lazzarino, D. D. Pierro, B. Tarazzi, L. Gerroni and B. Giardina, *Anal. Biochem.*, 197 (1991) 191.
15 W. G. Kuhr, *Anal. Chem.*, 62 (1990) 403R.
16 N. A. Guzman, M. A. Trebelcock and J. P. Adris, *J. Liq. Chromatogr.*, 14 (1991) 997.
17 I. Z. Atamna, G. M. Janini, G. H. Muschik and H. J. Issaq, *J. Liq. Chromatogr.*, 14 (1991) 427.
18 W. Thormann, P. Meier, C. Marcolli and F. Binder, *J. Chromatogr.*, 545 (1991) 445.
19 C. P. Ong., C. L. Ng., H. K. Lee and S. F. Y. Li, *J. Chromatogr.*, 547 (1991) 419.
20 T. Tsuda, K. Nomura and G. Nakagawa, *J. Chromatogr.*, 264 (1983) 385.
21 N. W. Tietz, *Fundamentals of Clinical Chemistry*, Saunders, Philadelphia, PA, 1987.
22 S. Terabe, M. Shibata and Y. Miyashita, *J. Chromatogr.*, 480 (1989) 403.
23 M. C. Gennaro, C. Abrigo and E. Marengo, *Chromatographia*, 30 (1990) 311.
24 S. A. Margolis, R. C. Paule and R. G. Ziegler, *Clin. Chem.*, 36 (1990) 1750.
25 G. Cowley and V. Church, *Newsweek*, May 18 (1992) 60.

Journal of Chromatography, 633 (1993) 251–259
Elsevier Science Publishers B.V., Amsterdam

CHROM. 24 752

Bidirectional isotachophoresis

I. Verification of bidirectional isotachophoresis and simultaneous determination of anionic and cationic components

Takeshi Hirokawa*, Kazuhiko Watanabe, Yasuro Yokota and Yoshiyuki Kiso☆

Applied Physics and Chemistry, Faculty of Engineering, Hiroshima University, Kagamiyama 1, Higashi-hiroshima 724 (Japan)

(First received June 16th, 1992; revised manuscript received November 10th, 1992)

ABSTRACT

Bidirectional isotachophoretic migration was confirmed by the direct measurement of the pH profiles and the boundary velocities of the separated zones. The anolyte used was 10 m*M* HCl–β-alanine (pH 3.6) and the catholyte was 10 m*M* KOH–acetic acid (pH 4.8). It was shown that bidirectional isotachophoresis could be achieved with an electrolyte system consisting of a leading electrolyte for an anionic analysis and one for a cationic analysis. The combination was not arbitrary but the pH difference between the anolyte and the catholyte was restricted to keep the effective mobility of the terminating ion not too small. The simultaneous separation and determination of anions and cations in a test mixture were demonstrated on the basis of the time-based zone length measured by the use of a dual detection system.

INTRODUCTION

As electrophoretic phenomena are bidirectional in principle, isotachophoretic migration must be also bidirectional. In fact, as pointed out by Thormann *et al.* [1], isotachophoretic stacking zones can be formed simultaneously for anionic and cationic components in a sample when a suitable electrolyte system is chosen. They demonstrated bidirectional isotachophoretic migration under an electrolyte system of sodium acetate and HCl. However, no practical separation utilizing bidirectional isotachophoresis has been reported in spite of its utility in the simultaneous determination of anions and cations.

In this work, bidirectional isotachophoretic migration was verified by the direct measurement of the pH profile and the boundary velocities of the separated zones. In the pH profile measurement, a free-flow apparatus (Bender and Hobein, Elphor Vap 22) was used and the pH values of the fractions were measured. For boundary velocity measurements, a capillary-type ITP analyser equipped with a position scanning ultraviolet detector was used.

The practical simultaneous determination of anions and cations was demonstrated for a test mixture by the use of a dual potential gradient detector system applied from two Shimadzu IP-2A ITP analysers.

Although the selection of the operational electrolyte system for bidirectional isotachophoresis is not very difficult, the difference between the pH of an anolyte and that of a catholyte is restricted. In the next section we outline how bidirectional iso-

* Corresponding author.
☆ Present address: Hijiyama Women's College, Ushita-shinmachi, Hiroshima 732, Japan.

0021-9673/93/$06.00

tachophoresis works and how the restriction comes about.

THEORETICAL

Configuration of an operational electrolyte system

Fig.1 illustrates the configuration of a bidirectional operational electrolyte system in a separation tube. In bidirectional isotachophoresis, the leading electrolyte for anions must be simultaneously the terminating electrolyte for cations, and the leading electrolyte for cations must be the terminating electrolyte for anions. That is, the pH-buffering cations coexisting with the leading anion play the role of the terminating cation, and the pH-buffering anions coexisting with the leading cation plays the role of the terminating anion.

Fig.1 also shows an example of the electrolyte system. The anolyte [a 10 m*M* HCl solution buffered by adding 20 m*M* β-alanine (pH 3.6)] is a typical leading electrolyte for anionic analysis, where the leading ion is Cl^-. This solution can be the terminating electrolyte for a cationic analysis in the pH range 4–5, because β-alanine has a suitably small effective mobility in this pH range. On the other hand, the catholyte [a 10 m*M* KOH solution buffered by adding 20 m*M* acetic acid (pH 4.8)] is a typical leading electrolyte for a cationic analysis (leading ion K^+). Acetic acid in this solution is an acceptable terminator in the pH range 3–4. When these electrolytes are used in combination, bidirectional isotachophoretic migration will occur.

Limitation on the electrolyte combination

There are several typical leading electrolytes for a cationic analysis and for an anionic analysis, where the pH ranges from 3 to 10 [2–4]. However, these electrolyte systems cannot be combined arbitrarily, because the pH difference between the anolyte and the catholyte is restricted, as discussed below.

The pH of each electrolyte should be selected to ensure the pH-buffering ability as follows:

$$pK_{QA} - 0.5 < pH_{LA} < pK_{QA} + 0.5 \quad (1)$$

$$pK_{QC} - 0.5 < pH_{LC} < pK_{QC} + 0.5 \quad (2)$$

where pK_{QA} and pK_{QC} are the pK_a values of the pH buffer of an anolyte and that of a catholyte, respectively, and pH_{LA} and pH_{LC} are the pH_L of an anolyte and a catholyte, respectively.

Fig. 2 shows the simulated R_E of model cations and anions of weak electrolytes at the isotachophoretic steady state. R_E is one of the qualitative indices of isotachophoresis [3] defined for a sample S as follows:

$$R_{E,S} = E_S/E_L = \bar{m}_L/\bar{m}_S \quad (3)$$

where E_S and E_L are the potential gradient of the sample (S) and the leading (L) zones and $\bar{m}$ is the effective mobility. The leading anion used in the simulation was 10 m*M* Cl^- and the leading cation was 10 m*M* K^+. The simulated effective mobility of the leading ion ($\bar{m}_L$) was $74.7 \cdot 10^{-5}$ cm^2 V^{-1} s^{-1} for Cl^- and $71.4 \cdot 10^{-5}$ cm^2 V^{-1} s^{-1} for K^+. The absolute mobilities of the model samples were var-

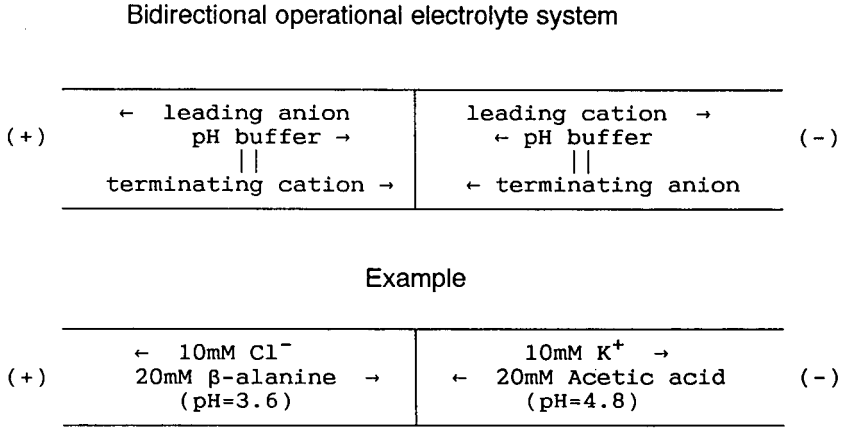

Fig. 1. Configuration of a bidirectional operational electrolyte system in a separation tube and an example.

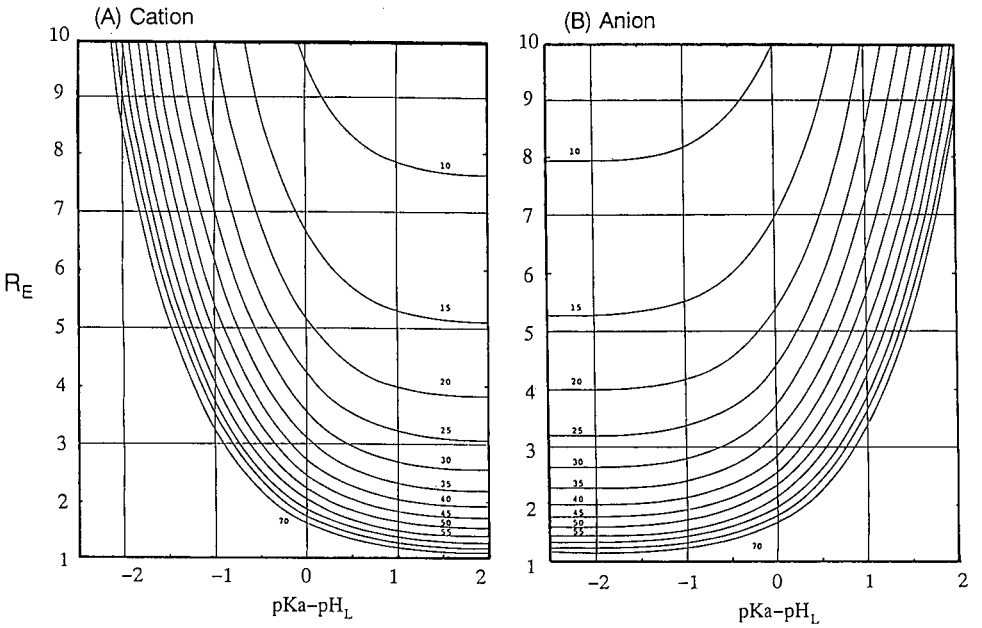

Fig. 2. Simulated R_E of model cations and anions of weak electrolytes. The leading anion was 10 mM Cl^- and the leading cation was 10 mM K^+. The absolute mobilities of the model samples were in the range $10 \cdot 10^{-5}$–$70 \cdot 10^{-5}$ cm^2 V^{-1} s^{-1}.

ied in the range of $10 \cdot 10^{-5} - 70 \cdot 10^{-5}$ cm^2 V^{-1} s^{-1}. The maximum buffering ability ($pH_{LA} = pK_{QA}$ and $pH_{LC} = pK_{QC}$) was assumed in the simulation and this is just the case for the electrolyte system illustrated in Fig.1.

As the effective mobility of a sample ($\bar{m}_S$) decreases with decrease in the degree of dissociation, R_E increases with decrease in $pK_a - pH_L$ for cations, and *vice versa* for anions, as shown in Fig. 2. If the pK_a value of the terminator used is different from the pH of the leading electrolyte, it is not a suitable terminator from the practical view point because the terminator should have an adequately small effective mobility.

In the bidirectional electrolyte system, the anionic terminator is the pH buffer for a cationic analysis and the cationic terminator is the pH buffer for an anionic analysis. Even if the selected pH buffers satisfied eqns. 1 and 2, they might not be suitable as terminators. The pK_a values of the pH buffer and the pH_L of the bidirectional electrolyte system should satisfy the following conditions:

$$0.5 \leqslant pK_{QC} - pH_{LA} \leqslant 1.5 \quad (4)$$

$$0.5 \leqslant pH_{LC} - pK_{QA} \leqslant 1.5 \quad (5)$$

The upper limiting value in eqns. 4 and 5 is to keep the effective mobility not too small as the terminator. If it is too small, the operational system is not practically useful owing to the limitation of the high-voltage power supply. It should be noted that the limiting values in the above equations depend on the absolute mobility of the terminator ion (the larger absolute mobility, the larger is the limiting value, and *vice versa*). Suppose a typical terminator of an anionic analysis, acetic acid ($pK_a = 4.756$), is used in combination with a leading electrolyte of 10 mM HCl–20 mM β-alanine ($pK_a = 3.55$, $pH_{LA} = 3.6$). In this instance, $pK_{QC} - pH_{LA} \approx 1.2$. According to our simulation, the effective mobility and R_E value of acetate ion were $12.5 \cdot 10^{-5}$ cm^2 V^{-1} s^{-1} and 5.99 at the steady state. Similarly, when a typical terminator β-alanine ($pK_a = 3.55$) is used in combination with a leading electrolyte of 10 mM KOH–20 mM acetic acid ($pH_{LC} = 4.8$), $pH_{LC} - pK_{QA} \approx 1.3$. The simulated effective mobility and R_E value of β-alanine were $12.5 \cdot 10^{-5}$ cm^2 V^{-1} s^{-1} and 5.73. The large value of $pK_{QC} - pH_{LA}$ or $pH_{LC} - pK_{QA}$ means a small effective mobility as the terminating ion.

On the other hand, the lower limiting value of 0.5

in eqns. 4 and 5 is to avoid an unnecessarily large mobility as the terminator. If the effective mobility is too large, the mobility range of analysable samples becomes narrow.

When eqns. 1 and 2 are satisfied as $pH_{LA} = pK_{QA}$ and $pH_{LC} = pK_{QC}$, eqns. 4 and 5 can be rewritten as follows:

$$0.5 \leqslant pH_{LC} - pH_{LA} \leqslant 1.5 \quad (6)$$

The above relationship expresses the adequate range of the pH difference between the catholyte and the anolyte: the pH of a catholyte should be appropriately higher than that of an anolyte.

EXPERIMENTAL

Samples

The cationic samples used were toluidine blue (TB), tris(hydroxymethylamino)methane (Tris), astrazone pink (AP), ethanolamine (EA), creatinine (CR) and ε-aminocaproic acid (AMC). The anionic samples were 4,5-dihydroxy-3-(*p*-sulfophenylazo)-2,7-naphthalenedisulphonic acid (SPADNS), monochloroacetic acid (MCA), picric acid (PA), *o*-chlorobenzoic acid (CB) and benzoic acid (BZA). Except for Tris and MCA, these samples absorb visible and/or UV light. The sodium salt of SPADNS was purchased from Dojin (Kumamoto, Japan) in the purest form. The other chemicals were guaranteed-grade reagents from Tokyo Kasei (Tokyo, Japan).

Three-component mixtures of SPADNS, MCA and PA and of TB, Tris and AP were used for the observation of the boundary velocities in the bidirectional electrolyte system. A six-component mixture of EA, CR, AMC, MCA, CB and BZA was used for the observation of bidirectional isotachopherograms.

Operational electrolyte system

Table I shows the operational electrolyte systems used. Electrolyte systems 1 and 2 (abbreviated as ES1 and ES2) were used for free-flow isotachophoresis. ES1 is a bidirectional electrolyte system. The pH of the ES1 anolyte was adjusted to 3.6 by adding β-alanine to 10 m*M* HCl and the pH of the ES1 catholyte was adjusted to 4.8 by adding acetic acid to 10 m*M* KOH solution. ES2 is a unidirectional electrolyte system for a cationic analysis and the pH of the anolyte was also adjusted to 3.6 by adding acetic acid to 20 m*M* β-alanine. Electrolyte systems 3, 4 and 5 were used for the boundary velocity measurements. ES3 is a bidirectional electrolyte system and ES4 and ES5 are unidirectional electrolyte systems for a cationic analysis and an anionic analysis, respectively. The use of 5 m*M* leading electrolyte was to avoid saturation of the UV detection system due to a high concentration of the sample in each zone. Hydroxypropylcellulose (HPC) (0.1%) was added to all of the operational electrolytes to suppress electroendosmosis.

pH measurements were carried using a Horiba (Tokyo, Japan) Model F7ss expanded pH meter.

TABLE I

OPERATIONAL ELECTROLYTE SYSTEMS

Electrolyte systems 1 and 3 are bidirectional and the others are the usual unidirectional electrolyte systems. Hydroxypropylcellulose (0.1%) was added.

No.	Anolyte[a]	Catholyte[a]
1	10 m*M* HCl–β-Ala (pH 3.6)	10 m*M* KOH–Ac (pH 4.8)
2	20 m*M* β-Ala–Ac (pH 3.6)	10 m*M* KOH–Ac (pH 4.8)
3	5 m*M* HCl–β-Ala (pH 3.6)	5 m*M* KOH–Cap (pH 4.8)
4	10 m*M* β-Ala–Cap (pH 4.5)	5 m*M* KOH–Cap (pH 4.8)
5	5 m*M* HCl–β-Ala (pH 3.6)	10 m*M* Cap–β-Ala (pH 3.6)

[a] β-Ala = β-Alanine; Ac = acetic acid; Cap = caproic acid.

Apparatus

Three different types of apparatus were used. The first was a free-flow isotachophoretic analyser (Bender and Hobein, Elphor Vap 22), which was used for pH profile measurements. The separation chamber was 50 cm high 10 cm wide and 0.5 mm thick. The sample and operational electrolytes were supplied continuously to the separation chamber and the sample was separated owing to the electric field applied perpendicular to the flow. The separated sample zones were fractionated at the end of the sample chamber using a 90-fold peristaltic pump. The total flow-rate of the operational electrolytes through the separation chamber was 160 ml/h. The migration current applied was 15 mA and the separation chamber was thermostated at 15°C. The anolyte and catholyte used were 2 l in volume and they were circulated by pumps through the electrode compartments during migration.

The second was a capillary-type ITP analyser equipped with a position-scanning UV spectrophotometric detector [5], which was used for the observation of separation process and boundary velocities. It was operated at λ_{max} = 330 nm. The separation tube used was a fused-silica capillary (32 cm × 0.7 mm O.D. × 0.53 mm I.D.). All experiments were carried out at 25°C. A single cycle to scan the 32-cm tube took 7.025 s and the number of data in a single scan was 5333. The resolution was 0.06 mm per datum, which was sufficient to trace the separation process accurately. Data were acquired by the use of a NEC (Tokyo, Japan) PC9801VX microcomputer (80286-80287, clock 10 MHz) and were processed for boundary velocity evaluation.

The last type was two Shimadzu isotachophoretic analysers (IP-2A), which were used in combination, on each side of the sample injection port, for the measurement of bidirectional isotachopherograms. The other components necessary for isotachophoresis such as the separation tube and high-voltage power supply were single units. Potential gradient detectors were used. The PTFE separating tube used was 40 cm × 0.5 mm I.D. The driving current applied was 50 μA.

For the simulations of steady-state isotachophoresis, our program SIPS was used on an NEC PC-9801RA2 (CPU 80386, coprocessor 80387, clock 20 MHz). SIPS permits the precise simulation of qualitative and quantitative indices [3] and isotachopherograms. A small database of mobility and pK_a values for *ca.* 500 samples can be used for sample data input.

RESULTS AND DISCUSSION

Verification of bidirectional isotachophoresis

As the steady state of an isotachophoretic zone is usually not affected by the counter ion contained in the terminating zone, there is no fundamental difference between the steady state of bidirectional isotachophoresis and that of unidirectional isotachophoresis. Therefore, bidirectional isotachophoretic migration can be simulated as the combination of the respective simulations for an anionic analysis and a cationic analysis.

Fig. 3 shows the configuration of the bidirectional electrolyte system studied and the sample zone properties simulated for the steady state (the pH of the zones, the total concentration of acetic acid and β-alanine and R_E). The anolyte was 10 m*M* HCl buffered by 20 m*M* β-alanine (pH 3.6) and the catholyte was 10 m*M* KOH solution buffered by 20 m*M* acetic acid (pH 4.8). It should be noted that the components of the anionic terminating zone developed (TA in Fig. 3B) were the same as those of the cationic terminating zone developed (TC in Fig. 3B), but according to our simulation the concentrations were different from each other, as shown in Fig.3C.

Fig. 3B shows the pH of zones simulated for the steady state. The values were significantly different from each other and this simulation was proved experimentally by measuring the pH of fractions obtained by the use of a free-flow isotachophoretic apparatus: 90 fractions were obtained in 2.5 h using two different electrolyte systems, 1 and 2 in Table I (ES1 and ES2). Three adjacent fractions were mixed to increase the volume for convenience, and the pH values of the solutions were measured. Fig. 4 shows the results of pH measurement under three conditions: (A) no migration current and the electrolyte system unidirectional (ES2), (B) migration current 15 mA and ES2 was used, and (C) migration current 15 mA and the electrolyte system bidirectional (ES1). As shown in Fig. 4B, the observed pH profile was simple when a unidirectional electrolyte system was used. Fractions 45–55 corresponded to the cationic terminating zone of S0163TbS0180T-alanine and the average pH was 3.9, in good agreement with the simulated value of 3.83. There was no pH change in the fractions from 1 to 40.

On the other hand, when the bidirectional electrolyte system was used, as shown in Fig. 4C, another zone was seen from fractions 25 to 40. It was definitely assigned to the developed terminating zone of acetic acid. The observed pH value (4.4) was again in good agreement with the simulated pH value (4.38), confirming bidirectional isotachophoretic migration.

Fig. 5 shows the migration process of picric acid and astrazone pink with the bidirectional electrolyte system (3 in Table I) observed with the use of the position-scanning UV detection system. Each component was injected into the separation tube individually to prevent precipitation by ion pairing. They were pushed towards the centre of the separation capillary by the flow of the anolyte. Appar-

(A)Before migration

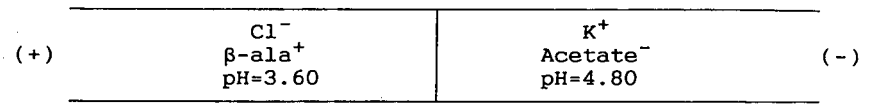

(B)Steady state configuration and pH (Blank run)

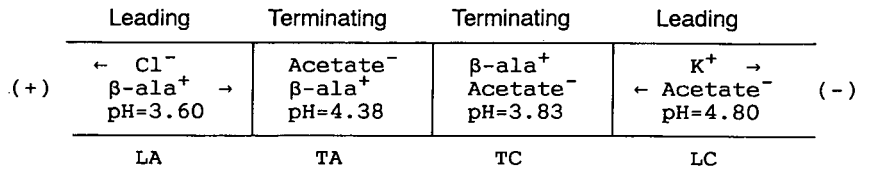

(C)Total concentration of acetic acid(Ac) and β-alanine

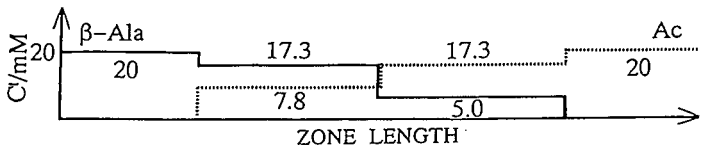

(D)Potential gradient ratio R_E

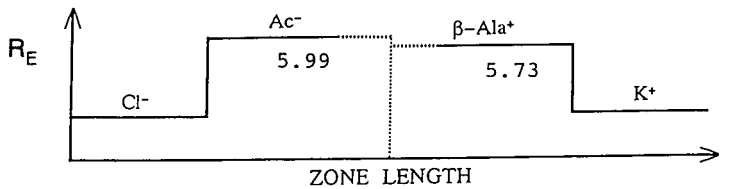

Fig. 3. Configuration of a bidirectional electrolyte system and simulation at the steady state.

ently from Fig. 5, the boundary velocity of rectangular zones was constant after 500 s, confirming isotachophoretic migration in both directions. The initial velocity change was due to mixing of samples with the operational electrolytes.

The boundary velocity was then measured exactly for three-component samples. Fig. 6 shows the observed transient isotachopherograms for a three-component mixture of SPADNS, MCA and PA. The amount of each sample was 60 nmol. The boundaries between the leading and the SPADNS zones in Fig. 6 were rearranged at the same abscissa position. Table II summarizes the boundary velocities observed with unidirectional and bidirectional electrolyte systems. For cations, only the steady-state boundaries are shown, because a mixed zone between the leading ion and toluidine blue was formed. Apparently from Table II and Fig. 6, the boundary velocity of the separated zones and the resolution time of each mixed zone agree well with each other, confirming that the separated zones migrated isotachophoretically and there was no significant difference between the migration behaviours of a bidirectional and a unidirectional system.

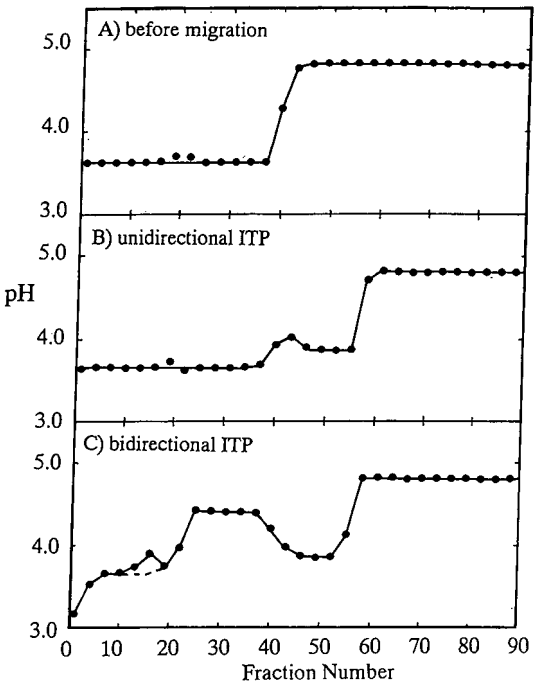

Fig. 4. pH of fractions obtained by the use of a free-flow isotachophoretic apparatus. (A) No migration current and electrolyte system unidirectional (electrolyte system 2 in Table I); (B) migration current = 15 mA and electrolyte system 2 was used; (C) migration current = 15 mA and electrolyte system bidirectional (electrolyte system 1). Cathode, right-hand side; anode, left-hand side.

Analysis of a test mixture

Lastly, isotachopherograms of anionic and cationic components in a sample were obtained simultaneously using a dual detection system (two potential gradient detectors) to demonstrate the analytical utility. Fig. 7 shows the observed isotachopherograms of an equimolar six-component mixture with electrolyte system 1. The ordinate scale of each detection system was not normalized. The total sample amount was 120 nmol and the migration current was 100 μA. The time-based zone lengths were measured varying the sample amount. The calibration lines evaluated for the sample components are shown in Fig. 8. The linearity is good, as usual, suggesting that bidirectional isotachophoresis is useful in practical analyses using conventional detectors such as the potential gradient detector.

In conclusion, we have confirmed bidirectional isotachophoretic separation by direct measurement of the pH of separated zones and the boundary velocity using a position-scanning detector. Bidirectional isotachophoresis is possible when the anolyte is a leading electrolyte for anions and the catholyte is a leading electrolyte for cations, and the pH-buffering ions in each electrolyte also play the role of the terminating ions. The one demerit of bidirectional isotachophoresis is that a dual detection sys-

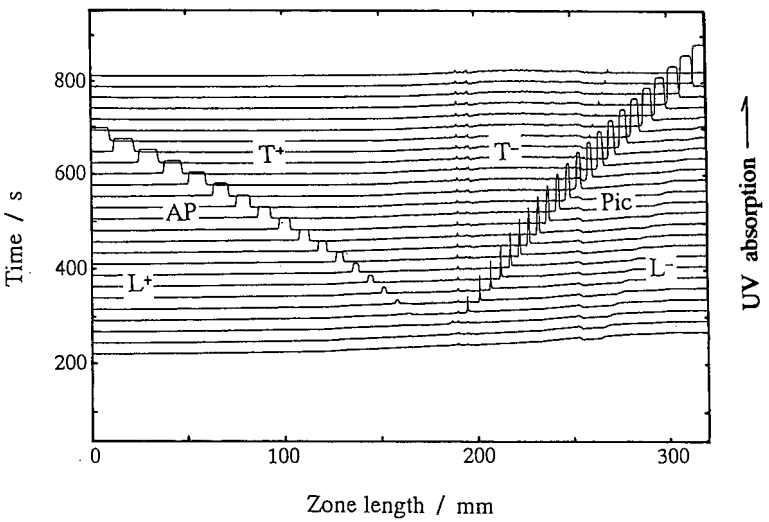

Fig. 5. Bidirectional isotachophoresis of picric acid and astrazone pink observed with the use of a position-scanning UV detection system. Electrolyte system 3 in Table I was used. Migration current, 50 μA.

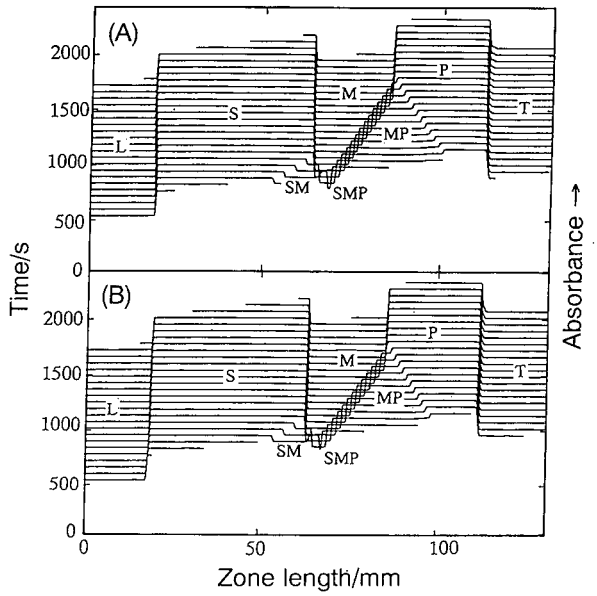

Fig. 6. Transient isotachopherogram of SPADNS (S), monochloroacetic acid (M) and picric acid (P) obtained with the use of a position-scanning UV spectrophotometric detector. The amount of each sample was 60 nmol. (A) Unidirectional electrolyte system; (B) bidirectional system (see Table I). Migration current, 50 μA.

TABLE II

BOUNDARY VELOCITIES OBSERVED BY THE USE OF A POSITION-SCANNING UV DETECTION SYSTEM

Electrolyte system No. 3; migration current, 50 μA. L = leading; S = SPADNS; M = monochloroacetic acid; P = picric acid; B = toluidine blue; R = Tris; A = astrazone pink; SM = mixed zone of SPADNS and monochloroacetic acid; MP = mixed zone of monochloroacetic acid and picric acid; SMP = mixed zone of SPADNS, monochloroacetic acid (M) and picric acid.

Boundary	Velocity (mm/s)		Difference (%)
	Unidirectional	Bidirectional	
Anions			
L/S	0.254	0.253	−0.4
S/M	0.254	0.253	−0.4
M/P	0.253	0.252	−0.4
P/T	0.254	0.253	−0.4
S/SM	0.203	0.201	−1.0
SM/M	0.291	0.292	0.3
M/MP	0.232	0.231	−0.4
MP/P	0.274	0.272	−0.7
SM/SMP	0.185	0.181	−2.2
SMP/MP	0.314	0.314	0.0
Cations			
L/B	0.315	0.319	1.3
B/R	0.314	0.318	1.3
R/A	0.315	0.319	1.3
A/T	0.315	0.319	1.3

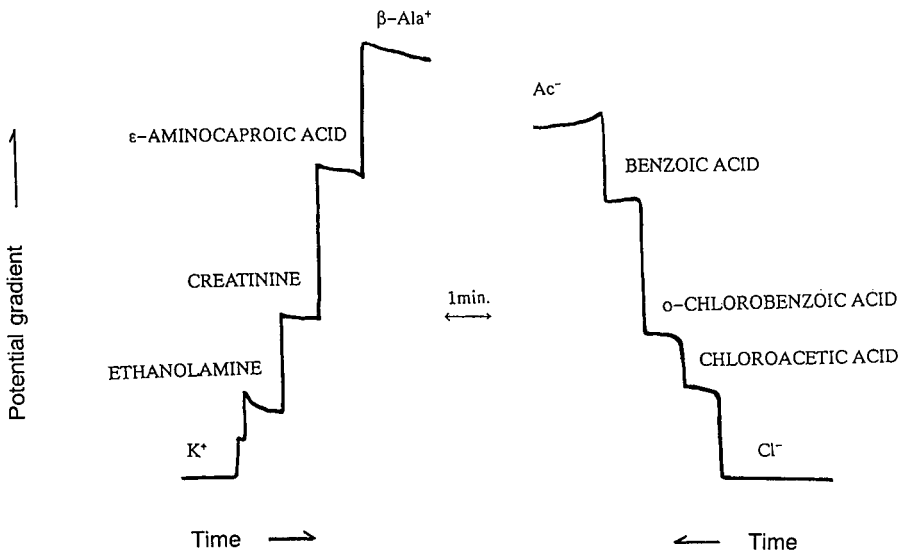

Fig. 7. Observed isotachopherograms from an equimolar six-component mixture of ethanolamine, creatinine, ε-aminocaproic acid, monochloroacetic acid, picric acid, *o*-chlorobenzoic acid and benzoic acid using electrolyte system 1. The total sample amount was 120 nmol. Migration current, 100 μA.

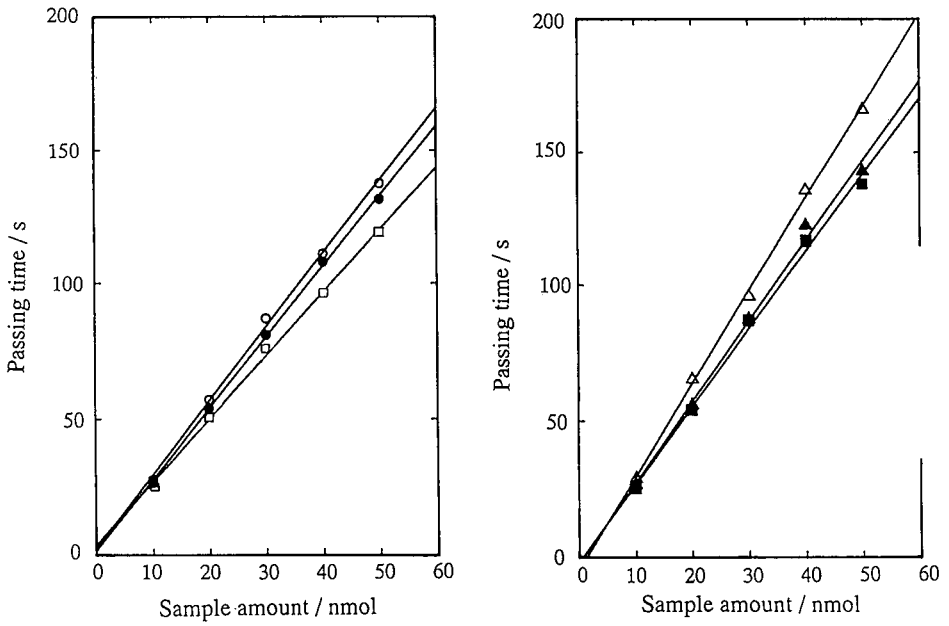

Fig. 8. Calibration line for a six-component mixture of (▲) ethanolamine, (■) creatinine, (△) ε-aminocaproic acid, (□) monochloroacetic acid, (○) *o*-chlorobenzoic acid and (●) benzoic acid with electrolyte system 1. Migration current, 100 μA.

tem is necessary. Bidirectional isotachophoresis can be utilized in practice by the use of two leading electrolytes for anionic and cationic analyses in the pH range 3–11 as usual, although one must take care of the pH difference of the anolyte and the catholyte, as discussed. The possible combination of the electrolyte systems and the predicted migration behaviour will be reported in due course.

ACKNOWLEDGEMENTS

The authors express their thanks to Power Reactor and Nuclear Fuel Development (Tokyo, Japan) for providing the free-flow apparatus for this study.

REFERENCES

1 W. Thormann, D. Arn and E. Schumacher, *Electrophoresis*, 6 (1985) 10.
2 F. M. Everaerts, J. L. Beckers and Th. P. E. M. Verheggen, *Isotachophoresis*, Elsevier, Amsterdam, 1976.
3 T. Hirokawa, M. Nishino, N. Aoki, Y. Kiso, Y. Sawamoto, T. Yagi and J. Akiyama, *J. Chromatogr.*, 271 (1983) D1.
4 P. Boček, M. Deml, P. Gebauer and V. Dolnik, *Analytical Isotachophoresis*, VCH, Weinheim, 1988.
5 T. Hirokawa, Y. Yokota and Y. Kiso, *J. Chromatogr.*, 538 (1991) 403.

Journal of Chromatography, 633 (1993) 261–272
Elsevier Science Publishers B.V., Amsterdam

CHROM. 24 759

Study of isotachophoretic separation behaviour of metal cations by means of particle-induced X-ray emission

IV. Separation of metal ions in a non-radioactive model solution of a high-level liquid waste

Takeshi Hirokawa*, Miki Ueda, Akihiko Ijyuin, Satoshi Yoshida, Fumitaka Nishiyama and Yoshiyuki Kiso☆

Applied Physics and Chemistry, Faculty of Engineering, Hiroshima University, Kagamiyama 1, Higashi-hiroshima 724 (Japan)

(First received July 13th, 1992; revised manuscript received November 16th, 1992)

ABSTRACT

The isotachophoretic separation behaviour of metal ions in a model soluition of a high-level liquid waste (HLLW) was investigated by means of the isotachophoresis–particle-induced X-ray emission (ITP–PIXE) method for the purpose of fractionation of useful elements contained in the HLLW. The leading electrolyte used was 20 m*M* ammonia solution buffered by acetic acid (pH 4.8), in which a complex-forming agent (10 m*M* α-hydroxyisobutyric acid) was contained. The migration order of the cationic components was (Rb^+, Cs^+), NH_4^+, Ba^{2+}, Sr^{2+}, Na^+, Mn^{2+}, Fe^{2+}, (Cr^{2+}, Rh^{2+}, Cd^{2+}), Ni^{2+}, La^{3+}, Ce^{3+}, Pr^{3+}, Nd^{3+}, Sm^{3+}, Eu^{3+}, Gd^{3+} and Y^{3+}, where the ions in parentheses could not be separated from each other. The separation efficiency of rare earth elements was 178 nmol/C and it was decreased to 96 nmol/C when $NaNO_3$ coexisted as the matrix. Part of the Fe^{3+}, $Zr^{IV}O^{2+}$, $Mo^{VI}O_4^{2-}$ and platinum group elements formed a cationic colloidal zone. Although the cationic recovery was 100% for most of the components, a substantial part of Fe, $Te^{VI}O_3$, $Zr^{IV}O$, Ru, Rh and Pd did not migrate, suggesting the formation of non-ionic hydrolysis species. Although ITP was not suitable for their analysis, platinum group metals in the HLLW might be partitioned efficiently as non-ionic components.

INTRODUCTION

In coupled isotachophoresis–particle-induced X-ray emission (ITP–PIXE), isotachophoretically fractionated zones are analysed off-line by PIXE. As PIXE is a sensitive, non-destructive and rapid method with multi-elemental capacity, it is useful as a detection method for the components in the micro-fractions obtained using a capillary isotachophoretic apparatus.

A PIXE detector permitted a detailed investigation of the isotachophoretic separation behaviour of metal ions [1,2], such as the migration order, the separability and the recoveries. Also, its high sensitivity allowed the determination of trace metal ions in a sample solution. In a previous paper [3], we demonstrated the determination of trace heavy lanthanoids in a crude rare earth chloride: the number of cationic components was fifteen and their abundance varied over four orders of magnitude.

This paper deals with the separation behaviour of another sample of complex composition, a model solution of a high-level liquid waste (HLLW). HLLW is generated in the reprocessing of nuclear fuels after recovering Pu and U. It contains 30 or more elements of the fission products of U, cladding

* Corresponding author.
☆ Present address: Hijiyama Women's College, Ushita-shinmachi, Hiroshima 732, Japan.

0021-9673/93/$06.00

materials of the fuel and the extracting agent for Pu and U (sodium tributylphosphate). Moreover, a large amount of $NaNO_3$ may be added for solidification. The abundances of the components differ widely.

HLLW is chemically heterogeneous, as it contains almost all of the chemical groups. Representative components are light lanthanoids, Cs, Sr, Fe^{III}, $Zr^{IV}O$ and platinum group elements, such as Ru, Rh and Pd.

We have already reported low cationic recoveries of Fe^{III} and $Zr^{IV}O$, probably owing to the formation of hydrolysis species, suggesting that ITP was not useful for the measurement of these ions [1]. The leading electrolyte used contained a useful complex-forming agent for lanthanide separation, α-hydroxyisobutyric acid. As summarized in a comprehensive review on the isotachophoretic separation of inorganic compounds [4], transition metals form complicated mixtures of hydrolysis species and the reaction rate of the complex-forming equilibria is not rapid enough that the complexes formed may split into different zones (zone splitting). Although this is an unfavourable feature for analytical use, from a preparative viewpoint the formation of a non-ionic zone is not always a negative feature, that is, high efficiency can be expected for the fractionation of non-ionic substances from mobile ions.

In this work, the isotachophoretic separation of the HLLW components was investigated for the purpose of elucidating the separation behaviour of platinum group elements. Two non-radioactive model waste solutions were analysed by the ITP–PIXE method. The most significant difference between the two models was the abundance of Na^+. From our previous study on the effect of composition on separation efficiency [5], low separability was estimated for the components of the model solution containing a large amount of Na^+. Taking account of the zone splitting problem and the composition effect, the recoveries, the migration order and the separation efficiency of the HLLW components were studied in detail. In addition to the above-mentioned complex-forming electrolyte system, non-buffered electrolyte systems were also used to evaluate the effect of counter ions on the recoveries.

EXPERIMENTAL

Samples

The composition of the fission products in the following two model waste solutions was determined according to computer simulation appropriately taking into account the burn-up and cooling time of the actual fuel. One of the model waste solutions (MW-1) was of low Na^+ abundance, which was prepared in our laboratory. MW-1 contained twenty metal ions and it was prepared from stock solutions of chloride salts obtained from Katayama Kagaku (Tokyo, Japan). They were dissolved in high-purity deionized water obtained by using a Puric-R ion exchanger (Japan Organo, Tokyo, Japan). The specific resistance of the water used was $18.3 \cdot 10^6$ Ω cm. The concentrations of the sample components are summarized in Table I.

The other model waste solution (MW-2) contained 27 metal ions. The composition was simulated by Power Reactor and Nuclear Fuel Development (Tokyo, Japan). Table I also shows the constituents of MW-2. Obviously the concentration of Na^+ was very high. As the original solution was strongly acidic (a 2.5 *M* nitric acid solution), it was not suitable as the sample for isotachophoresis. Therefore, the solution was dried by using an evaporator to remove nitric acid, and the residue was dissolved in deionized water. This process was repeated three times. The pH of the stock solution obtained was 1.5. Just before migration experiments, it was diluted with deionized water to 2% of the concentration of the original solution and this diluted solution (pH 2.74) was used as the ITP sample.

Small amounts of cationic dyes, toluidine blue (TB) and astrazon pink (AP), were added to the above model solutions in order to monitor the migration process and determine the timing of fractionation appropriately. Extra-pure grade dyes were purchased from Tokyo Kasei (Tokyo, Japan).

Electrolyte system

Table II summarizes the operational electrolyte systems used. WNH_4Ac–HIB is the abbreviation for the leading electrolyte in which the solvent used was water (W), the leading ion was NH_4^+, the pH buffer was acetic acid (Ac) and the complex-forming agent was α-hydroxyisobutyric acid (HIB). The

TABLE I

COMPOSITIONS OF SAMPLES MW-1 AND MW-2

Element (Z)	Concentration (m*M*)		Form[a]	Element (Z)	Concentration (m*M*)		Form
	MW-1	MW-2			MW-1	MW-2	
11 Na	0.901	19.6198	$NaNO_3$	46 Pd	0.214	0.1732	$Pd(NO_3)_2$
13 Al	0.00901	0.00901	Al	47 Ag	–	0.0068	$AgNO_3$
15 P	–	0.2538	P	48 Cd	0.0102	0.0092	$Cd(NO_3)_2$
24 Cr	0.108	0.0788	$Cr(NO_3)_3$	50 Sn	–	0.0066	Sn
25 Mn	–	0.2622	$Mn(NO_3)_2$	52 Te	–	0.0714	TeO_2
26 Fe	0.451	1.5538	$Fe(NO_3)_3$	55 Cs	–	0.322	$CsNO_3$
28 Ni	0.0715	0.1874	$Ni(NO_3)_2$	56 Ba	0.246	0.1944	$Ba(NO_3)_2$
34 Se	–	0.0110	Na_2SeO_3	57 La	0.174	0.1642	$La_2(CO_3)_3$
37 Rb	–	0.0728	$RbNO_3$	58 Ce	0.391	1.1780	$Ce(CO_3)_2$
38 Sr	0.196	0.175	$Sr(NO_3)_2$	59 Sr	0.163	0.1492	Pr_6O_{11}
39 Y	0.0996	0.1256	Y_2O_3	60 Nd	0.515	0.5000	Nd_2O_3
40 Zr	0.818	0.722	$ZrO(NO_3)_2$	62 Sm	0.102	0.1020	Sm_2O_3
42 Mo	–	0.612	Na_2MoO_4	63 Eu	0.0255	0.0160	Eu_2O_3
44 Ru	0.403	0.338	$Ru(NO_3)_3$	64 Gd	0.0119	0.0078	Gd_2O_3
45 Rh	0.0949	0.06789	$Rh(NO_3)_3$				

[a] Chemicals used for the preparation of MW-2. Chloride salts were used for MW-1.

pH of the leading electrolyte (pH_L) was 4.8. Hydroxypropylcellulose (HPC) was added to the leading electrolyte (0.1%, w/w) to suppress electroosmotic flow. HPC was obtained from Tokyo Kasei and the viscosity of a 2% aqueous solution was given as 1000–4000 cP at 20°C.

Ammonia solution was used because NH_4^+ was inactive in a PIXE analysis. The conventional leading ion K^+ was highly sensitive and it affected the rapid acquisition of spectral data. The electrolyte system WNH_4Ac–HIB is compatible with WKAc–HIB, as the mobilities of NH_4^+ and K^+ are almost the same. The terminating electrolyte used was a 10 m*M* carnitine hydrochloride solution. This operational electrolyte system permits bidirectional isotachophoresis [6,7]: both cations and anions in a sample migrate isotachophoretically in the opposite direction to each other when these operational electrolytes are used in combination. The leading anion is 10 m*M* Cl^- and the terminating ion is 10 m*M* HIB.

The other two leading electrolyte systems were

TABLE II

ELECTROLYTE SYSTEMS USED FOR ISOTACHOPHORETIC SEPARATION

HIB = α-Hydroxyisobutyric acid; HPC = hydroxypropylsellulose.

Parameter	WNH_4Ac–HIB	WHCl	$WHClO_4$
Leading electrolyte	20 m*M* NH_3	10 m*M* HCl	10 m*M* $HClO_4$
Complexing agent	10 m*M* HIB	–	–
pH buffer	Acetic acid	–	–
pH	4.80	2	2
Additive	0.1% HPC	0.1% HPC	0.1% HPC
Terminating electrolyte	10 m*M* carnitine hydrochloroide		
pH	2.5		

non-buffered systems of WHCl and $WHClO_4$, which were simply 10 m*M* HCl and 10 m*M* $HClO_4$ solution, respectively. The terminating electrolyte was 10 m*M* carnitine hydrochloride solution. All the reagents used for the operational electrolytes were purchased from Tokyo Kasei. pH measurements were carried using a Horiba (Tokyo, Japan) Model F7ss expanded pH meter.

Preparative isotachophoretic analyser

The micro-preparative analyser used was of the capillary type as reported previously [8]; the separation tube used was of 0.5 mm I.D. Separated sample zones migrating towards the leading electrolyte compartment were fractionated dropwise by a counter-flow of the leading electrolyte. A syringe pump was used to make the counter-flow. One drop (*ca.* 5 μl) constituted one fraction, which contained *ca.* 5 nmol of components. The amount in the fraction can be controlled by varying the velocity of the counter-flow and the migration current. In the present experiment, the interval of fractionation was *ca.* 10 s and the migration current was 150 μA. The migration of the zones was monitored by a potential gradient detector placed before the fractionating compartment. In addition to the separation unit, a Shimadzu (Kyoto, Japan) IP-2A isotachophoretic analyser was used.

PIXE analysis

A Model AN-2500 Van der Graaff accelerator (Nisshin High Voltage, Tokyo, Japan) was used for PIXE measurements. The energy of the H^+ beam was 2.0 MeV and the beam current was 50 nA. A typical single run for an ITP fraction took 200 s. The detector used was a highly pure Ge detector (Ortec Model GLP-10180); the multi-channel analyser used was a Laboratory Equipment (Tokyo, Japan) Model AMS-1000. The elements analysable using this system were those with atomic numbers greater than 16. The detection limit of a conventional PIXE analysis was of the order of nanograms and the amount of sample necessary was as small as a few micrograms or less.

The Nuclepore filter used as the target backing was of thickness 5 μm and pore size 0.1 μm. The diameter of the fraction spot was *ca.* 3 mm on the filter. The PIXE spectrum of each fraction was measured after drying in a desiccator.

In order to calibrate the PIXE sensitivities for quantification, 5 μl of standard sample solution was spotted on the Nuclepore filter and the PIXE spectrum was measured (1000 ppm (w/w) solution for atomic absorption spectrometry, Tokyo Kasei).

As the volume of one fraction was *ca.* 5 μl, a few or more components were contained in the fraction when the abundances were small. Our data reduction software PIXS [9] was used to analyse the PIXE spectrum. A least-squares fitting was applied for spectrum deconvolution, in which an X-ray relative intensity database optimized to our measurement system was utilized. Calculations were carried out on an NEC (Tokyo, Japan) PC-9801RA microcomputer (CPU 80386, co-processor 80387, clock 20 MHz).

RESULTS AND DISCUSSION

As the present model samples contained significant amount of rare earth elements, first WNH_4Ac–HIB was used as the operational electrolyte system as it is well known that this system gives good separation for rare earth elements [1–4].

Separation behaviour of MW-1 using WNH_4Ac–HIB

The model waste solution MW-1 contained twenty metal ions. The main components were the fission products of U and cladding materials of the fuel. As shown in Table I, the composition was essentially the same as for the other model waste (MW-2) except for the number of elements contained and the abundance of Na^+. Na^+ was present to simulate the counter ion of tributylphosphate but tributylphosphate ion itself was not present.

Fig. 1 shows the isotachopherogram obtained by using a potential gradient detector. The sample volume was 60 μl, which contained 300 nmol of metal ions. The amounts of major components injected were, in decreasing order, 54 nmol Na, 49 nmol ZrO, 31 nmol Nd, 27 nmol Fe, 24 nmol Ru, 23 nmol Ce, 15 nmol Ba, 13 nmol Pd, 12 nmol Sr and 10 nmol La. The amount of total rare earth elements was 89 nmol.

Fig. 2 shows the PIXE results for the 37 fractions obtained for the same sample. The observed migration order was NH_4^+, Ba^{2+}, Sr^{2+}, Na^+, (Cd^{2+}, Cr^{2+}), Ni^{2+}, La^{3+}, Ce^{3+}, Pr^{3+}, Nd^{3+}, Sm^{3+},

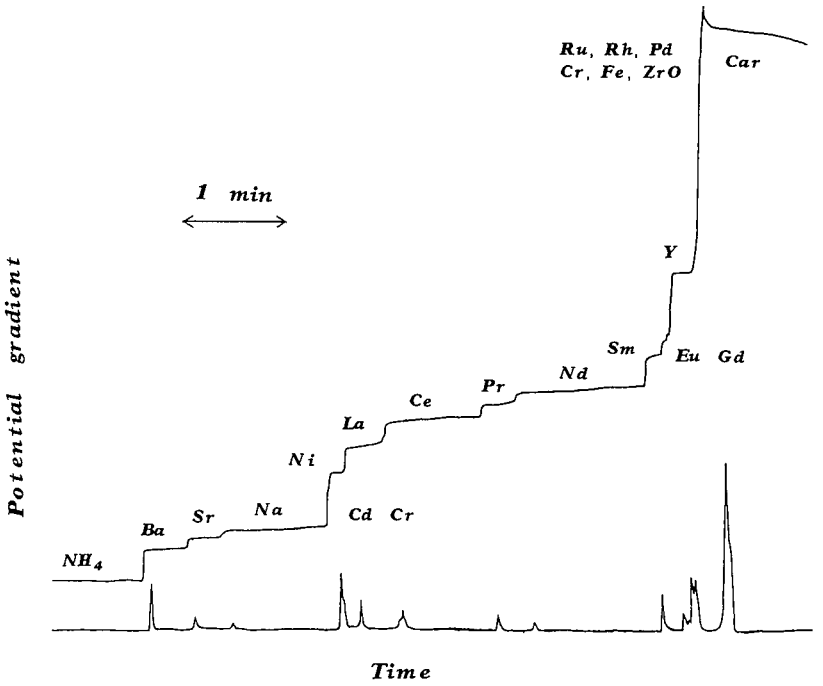

Fig. 1. Observed isotachopherogram of MW-1 model solution under the WNH_4Ac–HIB system. The injected sample amount was 60 μl (300 nmol of metal ions). For electrolyte conditions, see Table II. Migration current, 150 μA; amount of electricity, 0.5 C.

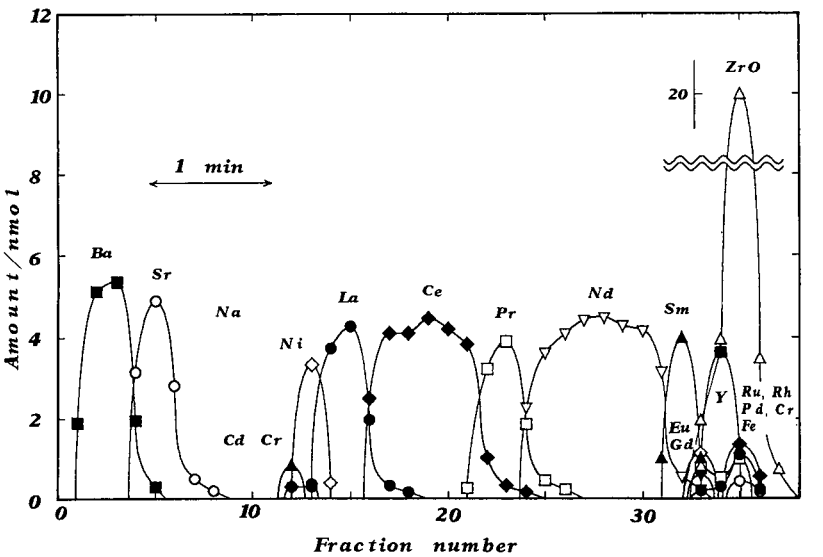

Fig. 2. Analytical results for cations for the 37 fractions of MW-1 obtained by PIXE. The corresponding isotachopherogram is shown in Fig. 1. Operational conditions as in Fig. 1.

Eu^{3+}, Gd^{3+}, Y^{3+}, ($Zr^{IV}O^{2+}$, Fe^{3+}, Ru^{3+}, Rh^{3+} and Pd^{3+}), where the ions in parentheses could not be separated from each other. Although Eu (1.5 nmol) and Gd (0.7 nmol) were found in the same fraction (No.33), they had been separated in the separation tube, as shown in Fig.1. Among the components of MW-1, Na and Al were inactive to our PIXE detection system. Fractions 7–12 were analysed by ITP and it was found that the main component was Na^+. The Al zone could not be assigned.

The amount of electricity applied was 0.5 C (300 μA for 18 min + 150 μA for 20 min). The separability was 178 nmol/C for the separation of rare earth elements and 600 nmol/C for the whole sample. When the amount of electricity was decreased, a mixed zone of Pr and Nd developed.

An interesting observation was that $Zr^{IV}O^{2+}$ formed a concentrated zone (fraction 35) with small amounts of Ru, Rh, Pd, Cr and Fe. According to Kohlrausch's regulating function, the equivalent concentration of the isotachophoretically steady-state zones should decrease from the leading towards the terminating zone with decrease in effective mobility. The concentration irregularity of fraction 35 suggested that $Zr^{IV}O^{2+}$ formed positively charged colloidal particles of hydrolysis species including Fe, Ru and Rh. From a PIXE analysis, it was found that *ca.* 60% of the $Zr^{IV}O^{2+}$ injected contributed to forming the cationic colloid (zone splitting).

This anomalous migration of the colloidal zone might affect the recoveries of the other components. The recoveries of the other components were evaluated using the following equation:

$$\text{Recovery (\%)} = \frac{\text{amount of element in fractions}}{\text{amount of element injected}} \cdot 100 \quad (1)$$

where the amount in fractions denotes the amount determined by the PIXE method and the amount injected was calculated from the composition shown in Table I. The recoveries of cations are summarized in Table III. The error of the evaluated recoveries was less than 5%, which was mainly due to the error in the PIXE analysis. Obviously from Table III the recoveries can be regarded as 100% for Ba^{2+}, Sr^{2+}, Cd^{2+}, Cr^{2+}, Ni^{2+}, La^{3+}, Ce^{3+}, Pr^{3+}, Nd^{3+}, Sm^{3+}, Eu^{3+}, Gd^{3+} and Y^{3+}. The recovery of Na^+ might be also 100% although it was not measured. Although we have already confirmed

TABLE III

RECOVERIES OF CATIONS (%) FOR MW-1 AND MW-2 USING WNH_4Ac–HIB, WHCl AND $WHClO_4$ SYSTEMS

Element (*Z*)	MW-1: HIB[a]	MW-2			Element (*Z*)	MW-1: HIB[a]	MW-2		
		HIB[a]	HCl[b]	$HClO_4$[c]			HIB[a]	HCl[b]	$HClO_4$[c]
24 Cr	93	50	29	23	47 Ag	nc	–	–	–
25 Mn	nc[d]	100	22	23	48 Cd	100	99	–	–
26 Fe	6	22	49	33	50 Sn	nc	–	–	–
28 Ni	98	101	25	24	52 Te	nc	45	36	15
34 Se	nc	42	29	0	55 Cs	nc	nf	103	98
37 Rb	nc	nf[e]	104	75	56 Ba	97	nf	100	98
38 Sr	101	nf	99	100	57 La	100	99	102	100
39 Y	100	100	102	100	58 Ce	102	101	102	102
40 Zr	64	56	48	17	59 Pr	101	100	99	97
42 Mo	nc	33	32	10	60 Nd	98	98	102	99
44 Ru	12	61	40	13	62 Sm	99	100	–	–
45 Rh	54	51	0	0	63 Eu	101	97	–	–
46 Pd	1	17	3	0	64 Gd	98	97	–	–

[a] WNH_4Ac–HIB.
[b] WHCl.
[c] $WHClO_4$.
[d] Not contained in MW-1.
[e] Not fractionated.

the 100% recovery of these metal ions [1], an important conclusion was that the recoveries of these ions were not affected by the coexistence of excess of Fe^{III} and $Zr^{IV}O$, the recoveries of which were low: most of the Fe^{3+}, Ru^{3+}, Rh^{3+} and Pd^{3+} and half of the $Zr^{IV}O^{2+}$ and Rh^{2+} did not migrate as cations. These elements with unrecovered chemical forms migrated as anions or did not migrate, forming non-ionic substances of hydrolysis species.

Separation behaviour of MW-2 using WNH_4Ac–HIB

The model waste solution MW-2 was similarly separated and the fractions were analysed. A remarkable difference between MW-1 and MW-2 was that the Na^+ concentration in MW-2 added as $NaNO_3$ was twenty times as large as that of MW-1. The separability of rare earth elements might be smaller than for MW-1 because of the coexistence of a large amount of Na^+ (effect of composition on separability [5]).

The sample was 60 μl of the preprocessed MW-2, which contained 1619 nmol of metal ions. The amount of Na^+ was 1177 nmol and those of the other major components were 93 nmol Fe, 71 nmol Ce, 43 nmol ZrO, 37 nmol MoO_4, 30 nmol Nd, 20 nmol Ru, 16 nmol Mn, 12 nmol Ba, 11 nmol Ni, 11 nmol Sr, 10 nmol Pd and 10 nmol La. After a steady state had been reached, most of the Na^+ zone was discarded and the zones behind the Na^+ zone were fractionated; the fractions were analysed by PIXE. Among the components of MW-2, Na, Al and P were inactive to PIXE.

Fig. 3 shows the isotachopherogram for rare earth zones and Fig. 4 shows the analytical results for the 46 fractions. The amount of electricity necessary for complete separation of the rare earth elements was 1.4 C (300 μA for 68 min + 150 μA for 20 min). The separability of the rare earth elements was calculated as 96 nmol/C, *i.e.*, about half that for MW-1. This decrease was due to the composition effect[5] caused by a large amount of coexisting Na^+. The separability for the whole sample was 1156 nmol/C. The observed migration order was essentially the same as that for MW-1.

A concentrated colloidal zone containing Fe^{3+}, $Zr^{IV}O^{2+}$, $Mo^{VI}O_4^{2-}$ and platinum group elements was also observed at fraction 40 just before the terminating zone. It seems that $Mo^{VI}O_4^{2-}$ formed ion pairs with Fe^{3+} and/or $Zr^{IV}O^{2+}$ Although Fe

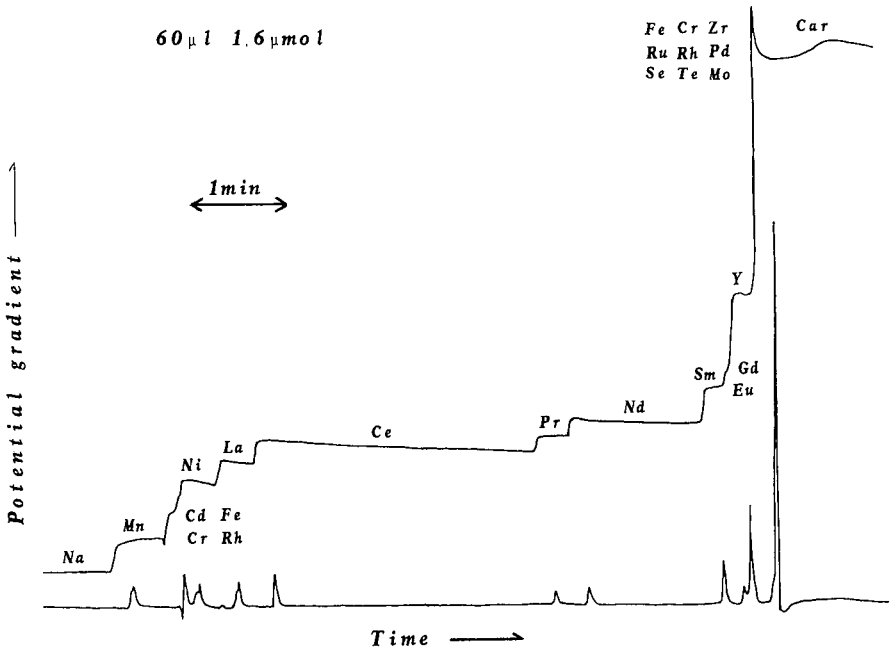

Fig. 3. Observed isotachopherogram of MW-2 using the WNH_4Ac–HIB system. The injected sample amount was 60 μl (1619 nmol of metal ions). Amount of electricity, 1.4 C. Other operational conditions as in Fig. 1.

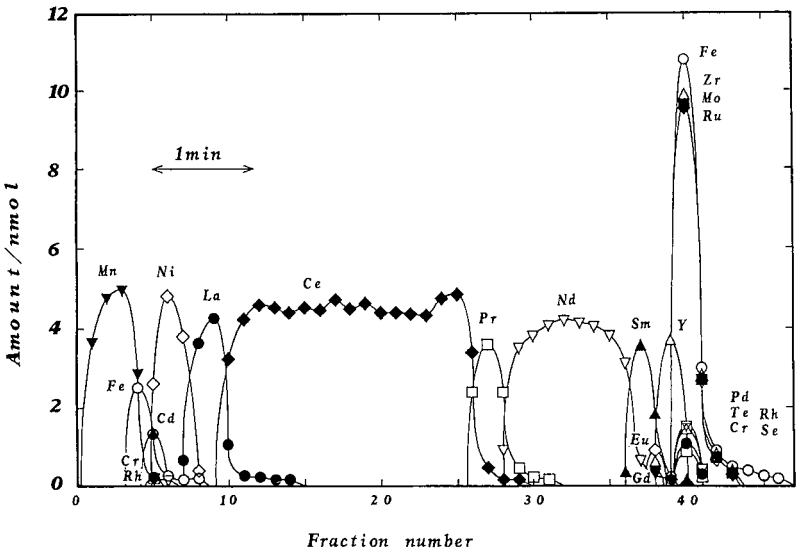

Fig. 4. Analytical results for cations for the 46 fractions of MW-2 obtained by PIXE. The corresponding isotachopherogram is shown in Fig. 3. Operational conditions as in Fig. 1.

$(NO_3)_3$ was used in the sample preparation, a considerable amount of Fe^{2+} was found in fraction 4. Rh and Cr split into two zones (5 and 40). Although Ag was analysable, it was not found in the cationic fractions. Fraction 40 also contained small amounts of Pd and Sn. Table III also summarizes the recoveries of the cationic components of MW-2: obviously, Mn, Ni, Y, La, Ce, Pr and Nd were recovered completely as cations. However, about 50% recoveries were obtained for Cr, Se, Zr, Ru, Rh and Te and very low recoveries of *ca.* 20% were obtained for Fe and Pd; most of them did not migrate as cations.

In order to clarify whether the unrecovered components in the cationic fractionation had anionic or non-ionic forms, the anionic zones of MW-2 were fractionated in the same manner using the same electrolyte system. The electrolyte system used in this work was bidirectional [6,7]: the leading electrolyte was carnitine hydrochloride and the terminating electrolyte was the WNH_4Ac–HIB system. The leading anion was Cl^- and the terminating ion was HIB^-, which migrated faster than acetate ion. Fig. 5 shows the analytical results for the anionic fractions. The components migrating as anions were $Mo^{VI}O_4^{2-}$, $Se^{IV}O_3^{2-}$ and a Zr anion. The chemical species of the Zr anion was not identified. The concentration profile in Fig. 5 suggests that these components migrated isotachophoretically. A small amount of Fe was observed, which had a triangle zone profile: the migration of Fe was not isotachophoretic but zone electrophoretic [10]. Although migration of $Mo^{VI}O_4^{2-}$ as an anion was natural, an interesting observation was that small amounts of Zr and Fe were detected as anions. It seemed that these ions formed ion pairs with abundant counter ions.

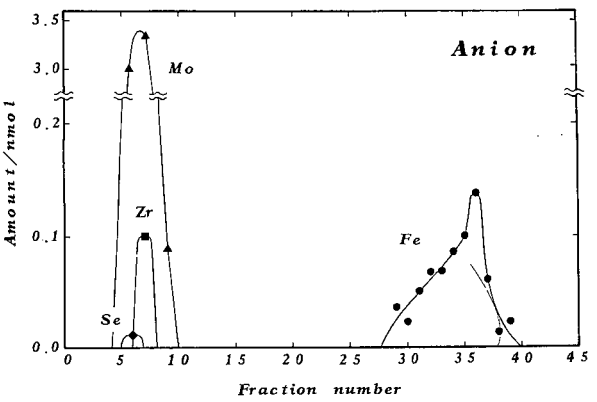

Fig. 5. Analytical results for anions for the 31 fractions of MW-2 obtained by PIXE. Amount of electricity, 1.4 C. Other operational conditions as in Fig. 1.

TABLE IV

RECOVERIES OF CATIONS, ANIONS AND NON-IONIC COMPONENTS (%) FOR MW-2 USING THE WNH_4Ac–HIB SYSTEM

Element (Z)	Cation	Anion	Non-ionic[a]	Element	Cation	Anion	Non-ionic[a]
24 Cr	50	0	50	47 Ag	–	–	–
25 Mn	100	0	0	48 Cd	100	–	–
26 Fe	22	1	77	50 Sn	–	–	–
28 Ni	101	0	0	52 Te	45	0	55
34 Se	42	3	55	55 Cs	100	0	0
37 Rb	100	0	0	56 Ba	100	0	0
38 Sr	100	0	0	57 La	99	0	0
39 Y	100	0	0	58 Ce	108	0	0
40 Zr	56	4	44	59 Pr	110	0	0
42 Mo	33	16	51	60 Nd	98	0	0
44 Ru	61	0	39	62 Sm	97	0	0
45 Rh	51	0	49	63 Eu	112	0	0
46 Pd	17	0	83	64 Gd	100	0	0

[a] Calculated values: 100 − (cation recovery + anion recovery). These values contain errors from the two observed values.

The recoveries of anions are summarized in Table IV together with the recoveries of cations and the calculated recoveries of non-ionic substances. Obviously Fe, Se, Zr, Mo, Ru, Rh, Pd and Te split into two or three zones. Most of the Fe and Pd formed non-mobile species, but the chemical species are unknown. The other possibility was that their mobilities were very small and they migrated zone electrophoretically in the terminating zone like the Fe zone in Fig. 5.

Fig. 6 summarizes the migration order of the MW-2 components using the WNH_4Ac–HIB system; the components in a particular box could not be separated.

Separation behaviour of MW-2 using WHCl and $WHClO_4$ systems

The low cationic recoveries of platinum group metals and Fe^{III} ions is due to the formation of hydrolysis species. The formation might be suppressed

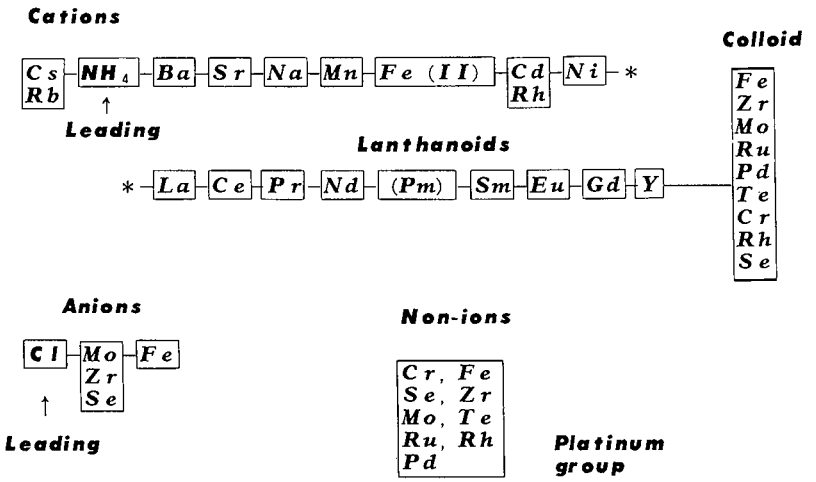

Fig. 6. Migration order of MW-2 using the WNH_4Ac–HIB system. The sample components in a particular box could not be separated.

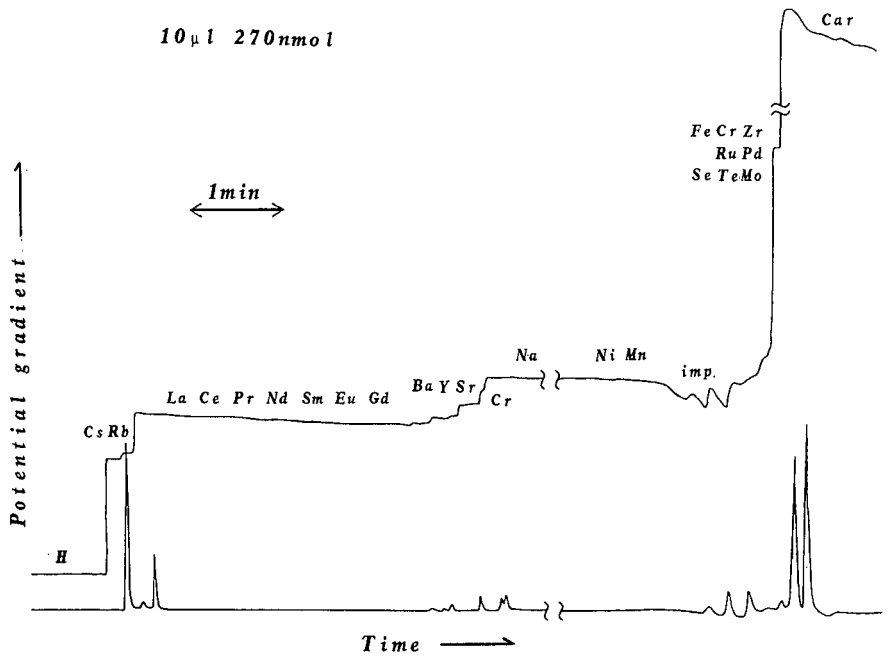

Fig. 7. Observed isotachopherogram of MW-2 using the WHCl system. The injected sample amount was 10 μl (270 nmol of metal ions). Amount of electricity, 1.1 C.

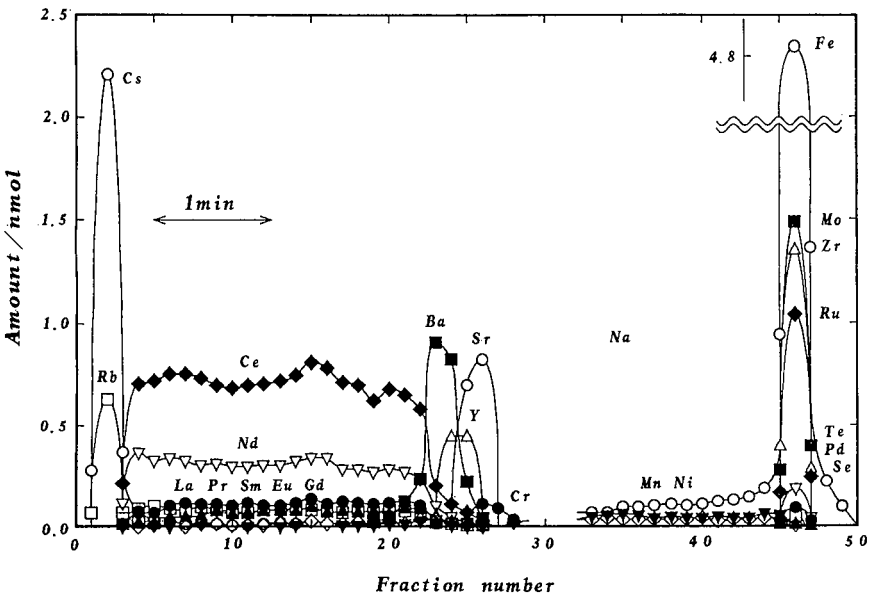

Fig. 8. Analytical results for cations for the 50 fractions of MW-2 using the WHCl system. The corresponding isotachopherogram is shown in Fig. 7.

to some extent by using a leading electrolyte of a low pH and consequently the cationic recoveries might be improved. MW-2 was analysed by using the non-buffered leading electrolytes WHCl and $WHClO_4$ where the leading ion was 10 m*M* H^+ (pH 2). The terminating electrolyte used was 10 m*M* carnitine hydrochloride solution.

Fig. 7 shows the isotachopherogram with the WHCl system obtained by using a potential gradient detector. The sample volume was 10 μl, which contained 270 nmol of metal ions. The amount of electricity applied was 1.1 C (300 μA for 28 min + 150 μA for 51 min). Fig. 8 shows the analytical results for 50 fractions evaluated by PIXE. Most of Na^+ zone was not fractionated. Obviously from Fig. 8, the separability was poor and the observed migration order was (Cs^+,Rb^+),(La^{3+}, Ce^{3+}, Pr^{3+}, Nd^{3+}, Sm^{3+}, Eu^{3+}, Gd^{3+}), Ba^{2+}, Y^{3+}, Sr^{3+}, Cr^{2+}, (Na^+, Mn^{2+}, Ni^+), (Fe^{3+}, MoO_4^-, Ru^{3+}, Rh^{3+}, $Zr^{IV}O^{2+}$, Pd^{3+}, Sn^{2+}), where the ions in parentheses were not separated from each other. The separability with the $WHClO_4$ system was almost the same as that with the WHCl system.

Table III shows the recoveries of cations for MW-2 using the WHCl and $WHClO_4$ systems. The recoveries of Mn^{2+} and Ni^{2+} were estimated as 100% but they could not be evaluated because they formed a mixed zone with Na^+ as shown in Fig. 7 and the mixed zone was not fractionated.

Among the transition elements in MW-2, only the recovery of Fe^{3+} was improved slightly by using non-buffered systems (pH 2). The recovery of $Zr^{IV}O^{2+}$ using WHCl was almost the same as that with the WNH_4Ac–HIB system (pH 4.8), but it became worse when $WHClO_4$ was used. Similarly, the recoveries of Ru, Rh and Pd could not be improved by using non-buffered electrolyte systems. These observations suggested that the recoveries of Fe, Zr and platinum group elements were affected by both the formation of hydrolysis species and the ion pairing with the other counter ions, in this instance Cl^- and ClO_4^-. As the rate of complex-forming equilibrium is small, the pH of the sample solution and the reaction time before measurement are presumably important factors affecting the recoveries of cations, as exemplified in the isotachophoretic separation of Al^{3+} [11]. However, this problem was not investigated in further detail.

As far as the present electrolyte systems are concerned, the isotachophoretic analysis of Fe^{3+}, $Zr^{IV}O^{2+}$ and platinum group elements cannot be recommended owing to the formation of a colloidal zone and the low recoveries of cations. However, from a preparative viewpoint platinum group elements will be fractionated as non-mobile substances very efficiently by using continuous free-flow equipment. For example, 80% of Pd in MW-2 might be recovered as non-ionic substances with the WNH_4Ac–HIB (pH_L 4.8) system. Among the actual HLLW components of unfavourably long-lived and highly radioactive nuclides, the activity of the platinum group metals is very low and if they could be separated from the others they might be useful as industrial catalysts, for example.

The present model wastes did not contain transuranium elements, which are inevitable in real HLLW samples. However, the successful separation of transuranium elements and rare earth elements has already been reported by Bilal *et al.* [12] using a counter-flow technique. The separation behaviour of a model HLLW using continuous free-flow equipment is now under investigation and will be reported in due course.

ACKNOWLEDGEMENTS

The authors express their thanks to Power Reactor and Nuclear Fuel Development (Tokyo, Japan) for financial support of part of this work.

REFERENCES

1 T. Hirokawa, J. Hu, S. Eguchi, F. Nishiyama and Y. Kiso, *J. Chromatogr.*, 538 (1991) 413.
2 J. Hu, T. Hirokawa, F. Nishiyama and Y. Kiso, *J. Chromatogr.*, 589 (1992) 339.
3 J. Hu, T. Hirokawa, F. Nishiyama, Y. Kiso, K. Ito and E. Shoto, *J. Chromatogr.*, 594 (1992) 371.
4 P. Boček and F. Foret, *J. Chromatogr.*, 313 (1984) 189.
5 T. Hirokawa, A. Omori, Y. Yokota, J. Hu, and Y. Kiso, *J. Chromatogr.*, 585 (1991) 297.
6 W. Thormann, D. Arn and E. Schumacher, *Electrophoresis*, 6 (1985) 10.
7 T. Hirokawa, K. Watanabe, Y. Yokota and Y. Kiso, *J. Chromatogr.*, 633 (1993) 251.
8 T. Hirokawa, J. Hu, K. Umeda, G. Kimura, H. Ikeda, F. Nishiyama and Y. Kiso, *J. Chromatogr.*, 513 (1990) 297.
9 T. Hirokawa, F. Nishiyama and Y. Kiso, *Nucl. Instrum. Methods*, B31 (1988) 525.
10 F. E. P. Mikkers, F. M. Everaerts and Th. P. E. M. Verheggen, *J. Chromatogr.*, 169 (1979) 11.

11 S. Schmid, W. Kordel, H. Kloppel and W. Klein, *J. Chromatogr.*, 470 (1989) 289.
12 B. A. Bilal, F. Herrmann, K. Metscher, B. Muhig, C. Reuchmuth and B. Schwartz, in J. D. Narvatil and W. Schulz (Editors), *Actinide Separations* (*ACS Symposium Series*, No. 117), American Chemical Society, Washington, DC, 1980, p. 561.

Journal of Chromatography, 633 (1993) 273–280
Elsevier Science Publishers B.V., Amsterdam

CHROM. 24 758

Short Communication

Evaluation of several affinity chromatographic supports for the purification of maltose-binding protein from *Escherichia coli*

Yolande Kroviarski

INSERM U 76, INTS, 6 Rue Alexandre Cabanel, 75739 Paris Cedex 15 (France) and Centre de Recherche sur les Enzymopathies de l'Association Claude Bernard, Hôpital Beaujon, 92118 Clichy (France)

Sylvie Cochet

INSERM U 76, INTS, 6 Rue Alexandre Cabanel, 75739 Paris Cedex 15 (France)

Pierre Martineau

CNRS URA 1444, Institut Pasteur, 25 Rue de Docteur Roux, 75015 Paris (France)

Jean Pierre Cartron and Olivier Bertrand*

INSERM U 76, INTS, 6 Rue Alexandre Cabanel, 75739 Paris Cedex 15 (France)

(Received October 6th, 1992)

ABSTRACT

To obtain affinity adsorbents with good mechanical resistance, suitable for the purification of maltose-binding protein (MBP) from *Escherichia coli* and genetically engineered proteins fused to MBP, a series of supports were prepared by grafting amylose on to agarose by different chemistries. Their capacities for MBP and their abilities to be used at relatively high flow-rates were examined. Efficient supports were most conveniently prepared by coupling amylose to epoxy-activated agarose in an aqueous–organic mixture.

INTRODUCTION

Gene fusion can provide an elegant solution to some purification problems [1]: if the gene for the protein of interest is fused to a DNA sequence coding for a protein or a peptide endowed with a particular property, such as a peculiar charge pattern [1–3], the propensity to make hydrophobic interactions [4,5] or an affinity for a specific ligand [6–9], the fusion protein can be rapidly purified by taking advantage of this property.

Fusion to maltose-binding protein (MBP) [10–14], for example, has the advantage that the fusion protein can be purified on reticulated amylose, for

* Corresponding author.

0021-9673/93/$06.00

which MBP has a significant affinity [15]. Fusion to the periplasmic MBP allows the recombinant protein to be exported to the periplasmic space. Targeting recombinant proteins to the periplasmic space has the following advantages: the periplasmic space is favourable to protein folding and disulphide bond formation, whereas cytoplasmic compartment is not [16,17]; it has been demonstrated that (pre) proinsulin was more stable when secreted in the periplasm than when expressed in cytoplasm, suggesting that proteolysis was lower in periplasm [18]; and periplasmic space contains no DNA, fewer proteins at lower concentrations than does the cytoplasm, periplasmic contents can be easily recovered by osmotic shock [19], hence export of the protein of interest to the periplasmic space provides for easier protein purification.

Despite its obvious advantages, the fusion of recombinant proteins to MBP seems to be confined to the research laboratory. One cause of this apparent lack of success in the large-scale production of recombinant proteins could be the poor mechanical resistance of the reticulated amylose which is generally used as the chromatographic support for MBP purification. Reticulated amylose can be used only at low flow-rates, and in fact often has to be used in a batch mode.

This study was carried out to prepare and test supports for MBP affinity chromatography that had better mechanical properties than reticulated amylose.

EXPERIMENTAL

Chemicals

Maltose, amylose from potato (Ref. No. A-0512) or from corn (Ref. No. A-7043) were purchased from Sigma (St. Louis, MO, USA), Sepharose 6B from Pharmacia (Uppsala, Sweden) and epichlorohydrin (gold label), hydrazine hydrate, and dimethyl sulphoxide (DMSO) from Aldrich (Milwaukee, WI, USA). Other chemicals were purchased from Merck (Darmstadt, Germany).

Enzyme-linked immunosorbent assay (ELISA) for MBP

ELISA was performed using a standard protocol for sandwich-type assays. Plates were coated with a monoclonal antibody directed against MBP and serial dilutions of MBP-containing material were incubated in the plate wells. The plates were washed and the bound MBP was determined using either an in-house prepared or a commercial (New England Biolabs, Beverly, MA, USA) rabbit anti-MBP antiserum. MBP purified by affinity chromatography was used as a standard.

Amylase assay

Amylase was measured using a chromogenic *p*-nitrophenyl maltoheptaoside substrate, according to the vendor's recommendations (Sigma).

Gel electrophoresis

Gel electrophoresis was performed according to Laemmli [20] using 10% gels. They were stained with Coomassie Brilliant Blue.

Preparation of reticulated amylose

The procedure of Ferenci and Klotz [15] was followed exactly.

Grafting of amylose to agarose by epoxide coupling

Activation of agarose with epichlorohydrin. The activation procedure of Porath and Larsson [21] was used, with minor modifications. Sepharose 6B (10 ml) was exhaustively rinsed with water, transferred into a vessel with a minimum amount of water and 5 ml of 2 *M* NaOH were added, followed by 0.5 ml of epichlorohydrin and 20 mg of $NaBH_4$. Further aliquots of 1.2 ml of 2 *M* NaOH and 0.6 ml of epichlorohydrin were added every 30 min (five times) and the gel suspension was tumbled for 16 h at room temperature. This epoxide-activated gel was immediately used for coupling.

Coupling of amylose to epichlorohydrin-activated agarose in aqueous medium. A 2% (w/v) amylose solution in water was prepared by adding hot water to the amylose in small portions and warming the suspension carefully in a microwave oven until it had completely dissolved.

A 10-ml aliquot of epoxy-activated gel was rinsed with water on a fritted disc and transferred into a vessel with a minimum amount of water, then 80 ml of the 2% amylose solution, 2.3 g of Na_2CO_3 and 55 mg of $NaBH_4$ were added and the gel suspension was shaken for 36 h at 37°C.

Coupling of amylose to epichlorohydrin-activated agarose in aqueous–organic mixture. A 10-ml ali-

quot of epoxide-activated gel was rinsed with water on a fritted disc and then with 20 ml of DMSO–water (20:80, v/v) and with 100 ml of DMSO–water (50:50, v/v). It was then transferred into a vessel with a minimum amount of DMSO–water (50:50, v/v) and 40 ml of amylose solution in DMSO were added (several amylose concentrations were used; see Results and Discussion), then 30 ml of water and 48 mg of $NaBH_4$ were sequentially added. The pH of the gel suspension was increased to 12 with 2 *M* NaOH and the gel suspension was incubated at 37°C with gentle mechanical agitation for 36 h. The gel was then rinsed with DMSO–water (70:30, v/v), DMSO–water mixtures of decreasing DMSO concentration and finally with water alone.

Preparation of a hydrazide derivative of agarose. A 10-ml volume of epoxide-activated gel was rinsed with water and incubated with 15 ml of hydrazine hydrate and 0.3 mg of $NaBH_4$ for 90 min at 40°C, and finally rinsed exhaustively with water.

Coupling of amylose to a hydrazide derivative of agarose in aqueous medium. The technique was derived from the procedures of Wilchek and Lamed [22] as follows: A 10-ml volume 2 *M* of sodium acetate buffer (pH 5) was added to 200 ml of a 2% aqueous solution of amylose, followed by 10 ml of the hydrazide derivative of agarose (prepared as above). The gel suspension was tumbled for 36 h at room temperature. The gel was then washed on a Büchner funnel with 1 *M* NaCl solution and water (using prewarmed solution and glassware), and finally with 0.5 *M* Tricine–HCl buffer (pH 8.0). The gel was suspended in the latter buffer and four additions of 100 mg of $NaBH_4$ were made at 60 min intervals. The gel was finally rinsed with water.

Coupling of amylose to a hydrazide derivative of agarose in aqueous–organic mixture. A 4-g amount of amylose was added to 40 ml of DMSO and dissolved by briefly warming at 60°C. The hydrazide of agarose was gradually brought to DMSO–water (50:50, v/v) by successive 30-min incubations in solutions of increasing DMSO content and filtering through a Büchner funnel. A 10-ml portion of the gel was added to the amylose solution in DMSO. Water and 2 *M* sodium acetate buffer (pH 5.0) were then added to bring the final concentrations of sodium acetate and DMSO to 0.1 *M* and 50%, respectively. The gel to total reaction volume ratio was 1:8.

Gels were incubated for 60 h at 40°C with gentle mechanical agitation and rinsed on a prewarmed Büchner funnel with successively DMSO–water (70:30, 50:50 and 25:75, v/v), with distilled water and 1 *M* NaCl solution.

Determination of substitution levels of the various chromatographic supports

The amount of grafted amylose was determined by first hydrolysing amylose to glucose, by incubating an aliquot of gel in 1 *M* HCl for 60 min in a boiling water-bath. Sodium phosphate was added (final concentration 50 m*M*) to the hydrolysate and the pH was adjusted to 7.2 with 4 *M* NaOH. Glucose was then assayed using a commercial glucose oxidase kit (Merck).

Bacteria fermentation and preparation of MBP-containing crude extract

Bacteria of the ED9 *Escherichia coli* strain [23], harbouring a multicopy plasmid pPD1 (carrying a functional MalE gene coding for MBP [24]) were cultivated at 30°C in Luria broth. They were induced with 0.2% maltose and thereafter submitted to the osmotic shock procedure [19]. The osmotic fluid was made 20 m*M* in Tris–HCl (pH 8.0) and ammonium sulphate was added to 100% saturation. It was stored at 4°C. An aliquot of the suspension was centrifuged at 40 000 *g* for 30 min and the pellet was dissolved in 50 m*M* Tris containing 150 m*M* NaCl adjusted to pH 7.5 with HCl (buffer A). This solution was chromatographed on a Sephadex G-25 column equilibrated in the same buffer, to give the starting material for affinity chromatographic experiments.

Evaluation of the MBP capacity of the various supports by chromatography under overload conditions

The supports were sedimented in 1.1 cm I.D. columns to a height of 1 cm. The columns were equilibrated in buffer A. Several flow-rates were used (see Results and Discussion). Starting material was assayed for MBP by ELISA and diluted to 0.1 mg/ml MBP. A volume of 20 ml was loaded on to the column and the column was rinsed with 30 column volumes of buffer A. The retained MBP was eluted with 0.2 *M* maltose in buffer A. The amount of eluted MBP was determined by measuring the absorbance at 280 nm using $E = 14.7\ cm^{-1}\ (g/100\ ml)^{-1}$ [12].

Chromatography of MBP-containing extracts in normal (non-overload) conditions

Several supports were also used under normal conditions. The load was chosen (from data obtained under overload conditions) so as not to saturate the column. The procedure was otherwise the same as above. The amounts of MBP in pooled fractions (flow-through and rinse, and eluted proteins) were measured by ELISA.

RESULTS AND DISCUSSION

Substitution levels and capacities of the various preparations

Flow-rate capabilities. The degrees of amylose substitution of each chromatographic support are shown in Table I together with their capacities for MBP. Table I demonstrates that a series of efficient chromatographic supports for MBP purification were prepared. The capacities were similar to or better than those of the reference support, reticulated amylose, with a single exception.

As the ligand grafted on to the agarose is a high-molecular-mass polymer, it could possibly hinder diffusion of the solutes to the inside volume of beads. For this reason we carefully checked the effect of flow-rate on capacity using gels to which the amylose had been grafted by either reductive amination or epoxide coupling. The capacities of both types of gels for MBP did not decrease appreciably when the flow-rate was increased from 15 to 45 ml/h. Reticulated amylose is a very soft and compressible medium which cannot be used in large-volume columns or at high flow-rates (we could not pump at a flow-rate above 5 ml/h in our 1.1 cm I.D. column, of bed height 1 cm. In contrast, agarose can be used in columns and at flow-rates sized to the needs of the industrial production of proteins. The

TABLE I

CHARACTERISTICS OF VARIOUS AFFINITY CHROMATOGRAPHIC SUPPORTS FOR PURIFYING MBP

Column 1 shows the final amylose concentration in the coupling medium. Column 2: RAm indicates that the support was prepared by grafting amylose on to a hydrazide derivative of agarose and Epox that it was grafted on to epoxy-activated agarose. Aq. indicates that the coupling medium was purely aqueous and Aq.Org. that it contained DMSO. Column 3: figures given in parentheses are those obtained after further thorough washing of the gel with DMSO. The capacities for MBP were measured under overload conditions.

Amylose concentration in coupling medium (%, w/v)	Activation method	Substitution (mg/ml gel)	MBP capacity (mg/ml gel)		
			5 ml/h[d]	15 ml/h[d]	45 ml/h[d]
	Reticulated amylose		0.68		
1.8[a]	Aq./RAm	31.3 (12.0)	0.90	0.94	0.60
1.8	Aq./RAm	26.7 (12.7)		0.81	
1.8	Aq./Epox	21		0.61	
5	Aq.Org./RAm	4.5		0.67	
5	Aq.Org./RAm	2.7		0.90	
5[b]	Aq.Org./RAm	3.9		0.70	
0.5	Aq.Org./Epox	3.0		1.17	
1	Aq.Org./Epox	2.5		1.05	
2[a]	Aq.Org./Epox	10.8	0.51	1.21	1.0
2	Aq.Org./Epox	10.2		0.54	
2	Aq.Org./Epox	9.9		0.82	
3	Aq.Org./Epox	11.4		0.86	
5[c]	Aq.Org./Epox	n.d.		n.d.	

[a] Support used for experiments illustrated by Table II and Fig. 1.
[b] Amylose from corn.
[c] At the end reaction the beads had coalesced into an intractable mass.
[d] Flow-rates.

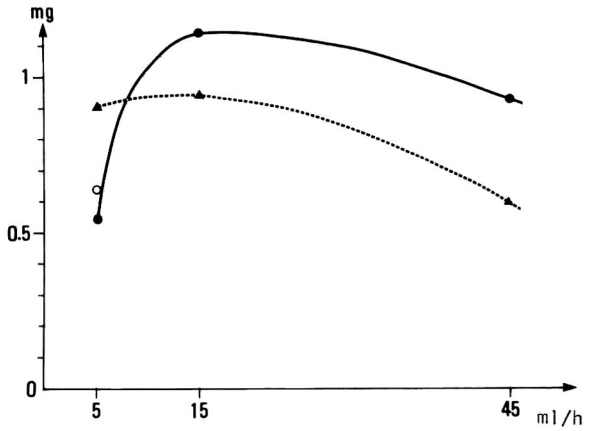

Fig. 1. Capacity of amylose–agarose for MBP. Capacities were measured under overload conditions at various flow-rates. Solid line = Support prepared by grafting amylose on to epoxide-activated gel in aqueous–organic medium. ● = Results obtained with periplasmic extract; ○ = obtained with purified MBP. Dotted line = support prepared by grafting amylose on to a hydrazide derivative of agarose in aqueous medium.

results in Fig. 1 demonstrate that full benefit can be taken of the mechanical resistance of agarose to purify MBP at relatively high flow-rates.

Fig. 1 shows that the capacity of the amylose epoxy agarose gel was higher at a flow-rate of 15 ml/h than at 5 ml/h. This paradoxical result is not related to the presence of amylase in the starting material. It was confirmed by activity measurements that some amylolytic activity was effectively present in the starting material for chromatography, but the same value for the gel capacity was found when purified MBP (devoid of any amylase activity) was used (Fig. 1).

The capacities shown in Table I were obtained under overload conditions, but satisfactory performance was obtained under conditions closer to the usual operating conditions (Table II). About one tenth of the MBP loaded was found in the breakthrough fractions with all three supports tested. Others have also noticed that small, but definite, amounts of MBP-containing fusion proteins were released from the column during sample loading on to reticulated amylose [12,14]. These supports allowed pure MBP [as shown by sodium dodecyl sulphate polyacrylamide gel electrophoresis (SDS PAGE)] to be prepared in a single chromatographic step (Fig. 2).

Purely aqueous vs. aqueous–organic synthesis mixtures. Amylose is poorly soluble in water; the solubility varies from batch to batch of amylose, purchased from the same supplier, and having the same reference number. It is extremely difficult to remove unbound amylose by filtration, because the fritted discs rapidly become clogged by amylose coming out of solution, even when prewarmed solutions and glassware are used. This problem is worse when the resin is prepared on a larger scale.

We suspected that the high glucose figures obtained with the gels prepared by reductive amination of a hydrazide derivative of agarose were in fact due to incomplete rinsing of the supports,

TABLE II

MBP CAPACITIES OF THREE PREPARATIONS OF AFFINITY CHROMATOGRAPHIC SUPPORTS

The amounts of MBP in the starting material and in the collected pools were determined by ELISA. The flow-rate was 5 ml/h for the reticulated amylose column and 15 ml/h for the others. Column dimensions: I.D. 1.1 cm and bed height 1 cm.

Preparation	MBP loaded (μg)	MBP found in breakthrough (μg)	MBP in maltose eluate (μg)
Reticulated amylose	250	19	220
Amylose agarose (Aq./Ram)[a]	250	27	220
Amylose agarose (Aq.Org./Epox)[a]	250	27	220

[a] See definitions in Table I.

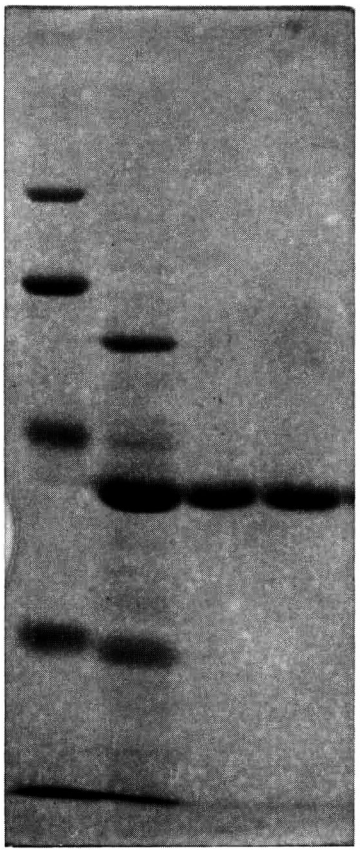

Fig. 2. SDS gel showing, from left to right molecular mass standards (from top to bottom, 94 000, 67 000, 43 000, 30 000), periplasmic extract and purified MBP obtained by chromatography on supports used to collect the data in Table II and Fig. 1.

which probably contained some precipitated amylose. One such gel was examined under a light microscope and it was found to contain both agarose beads and clumps of insoluble amylose (Fig. 3A). This gel sample was incubated in DMSO followed by careful rinsing in the same solvent on a Büchner funnel. It was then rinsed with DMSO–water mixtures of increasing water content and finally with water alone. This treatment significantly reduced the amylose content (Table I) with the loss of the peculiar appearance of the gel under the light microscope (Fig. 3B).

The difficulties associated with the low aqueous solubility of amylose led us to perform the coupling reaction in DMSO–water. The results (Table I) demonstrate that this method can be used to prepare satisfactory supports.

Grafting of amylose on to a hydrazide derivative of agarose vs. grafting on to epoxide-activated support

Several batches were prepared by reductive amination of amylose using a hydrazide derivative of agarose. The substitution levels routinely obtained using aqueous–organic coupling mixture were *ca.* 3 mg of amylose per ml of gel. The capacity for MBP was similar to that of the reticulated amylose, but, as already discussed, with much better flow-rate capabilities.

Satisfactory results were also obtained by simply grafting amylose on to an epoxide-activated gel. The highest capacities were obtained with these gels. The capacity for MBP is not correlated with the degree of amylose substitution. Although we have no proved satisfactory explanation, the amylose coverage of each support may be not equally accessible to MBP present in the mobile phase. Amylose can have either a random coil or a helical conformation, and it is not known if both conformations are satisfactory ligands for MBP. If they are not, a difference in the relative proportions of helix or random coil from batch to batch could explain variations of capacities for MBP. These possibilities will be tested in the near future. Nevertheless, most of the supports prepared were at least as efficient as, and some were much better than, the reticulated amylose reference support with regard to their capacities for MBP. However, the epoxy-activated agarose beads agglomerated into a single intractable mass if the amylose concentrations in coupling mixture was too high (*e.g.*, 5%).

CONCLUSIONS

Affinity chromatography on amylose or on starch can be traced back to the very early days of affinity chromatography. Ambard [25] used insoluble starch to adsorb amylase selectively from biological fluids and eluted the enzyme with glycogen or soluble starch. More recently, cross-linked starch has been used to purify amylases of bacterial and insect origin [26,27] and a glycosyl transferase from *Bacillus circulans* [28,29]. An amylose agarose composite has been used to purify lectins [30]. Amylose was immobilized on amino-silica and used to purify

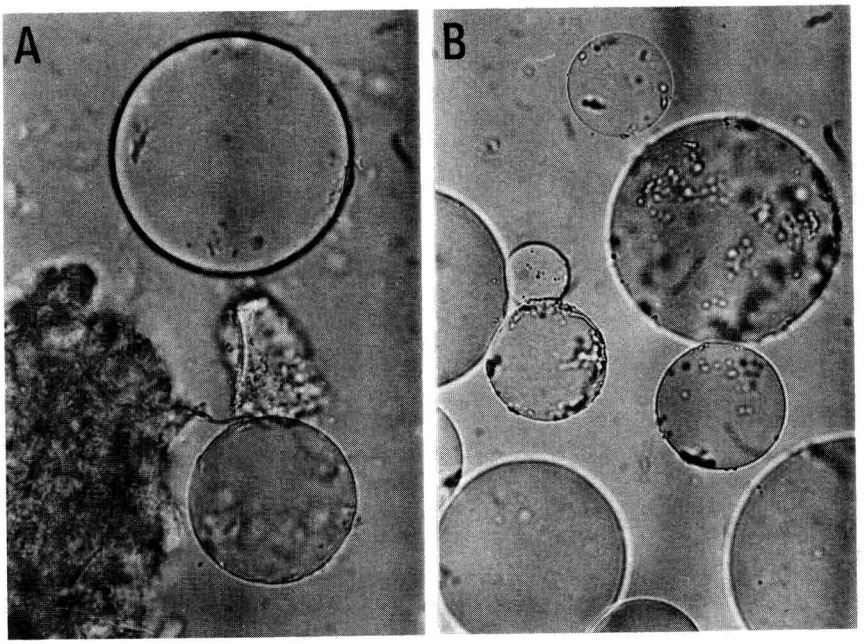

Fig. 3. Light microscope photographs of amylose–agarose prepared by reductive amination in purely aqueous medium. (A) The gel was washed only with aqueous solutions; (B) the gel was also rinsed with DMSO.

a bacterial amylase [31]. Cross-linked amylose has also been used to purify MBP and fusion proteins [10–15,32]. A reticulated composite containing both agarose and amylose and also amylose-coated silica have also been used to purify MBP but no details of their preparation are available [32].

Amylose was covalently grafted on to agarose and used to separate, in a population of *E. coli*, bacteria deficient for LamB (the outer membrane maltose transporter) from wild-type bacteria [33,34], but no attempt has been made to use it to purify MBP [33].

These results clearly demonstrate that amylose covalently grafted to agarose can be used to purify MBP efficiently. Unpublished results suggest that this support can also be used to purify recombinant fusion proteins to MBP. The relatively satisfactory mechanical resistance of agarose will make such supports suitable for production-scale chromatography. Several routes for synthesizing these supports have been evaluated. Epoxy activation of the agarose support, followed by coupling of amylose in aqueous–organic conditions, appears to be the most convenient and effective procedure.

ACKNOWLEDGEMENTS

We thank Professor Boivin and D. Dhermy (Hôpital Beaujon) for their interest and support and Professor Hofnung, S. Szmelcman and J. M. Clement for illuminating discussions.

REFERENCES

1 H. M. Sassenfeld, *Tibtech*, 8 (1990) 88.
2 H. M. Sassenfeld and S. J. Brewer, *Biotechnology*, 2 (1984) 76.
3 D. E. Parker, C. E. Glatz, C. F. Ford, S. M. Gedel, I. Duominen and M. A. Rougvie, *Biotechnol. Bioeng.*, 36 (1990) 467.
4 K. Köhler, C. Ljungquist, A. Kondo, A. Veide and B. Nilsson, *Biotechnology*, 9 (1991) 642.
5 M. Persson, M. G. Bergstrand, L. Bulow and K. Mosbach, *Anal. Biochem.*, 172 (1988) 330.
6 A. Ullman, *Gene*, 29 (1984) 27.
7 T. Moks, L. Abrahmsen, B. Osterlof, S. Josephson, M. Ostling, S. O. Enfors, I. Persson, B. Nilsson and M. Uhlen, *Biotechnology*, 5 (1987) 379.
8 D. B. Smith and K. S. Johnson, *Gene*, 192 (1991) 262.
9 M. E. Taylor and K. Drickamer, *Biochem. J.*, 274 (1991) 575.
10 H. Bedouelle and P. Duplay, *Eur. J. Biochem.*, 171 (1988) 541.
11 C. di Guan, P. Li, P. D. Riggs and H. Inouye, *Gene*, 67 (1988) 21

12 A. Blondel and H. Bedouelle, *Eur. J. Biochem.*, 193 (1990) 325.
13 J. M. Clement, S. Szmelcman, M. Jehanno, P. Martineau, O. Schwartz and M. Hofnung, *C.R. Acad. Sci.*, 308 (1989) 401.
14 S. Szmelcman, J. M. Clement, M. Jehanno, O. Schwartz, L. Montagnier and M. Hofnung, *J. AIDS*, 3 (1990) 859.
15 T. Ferenci and U. Klotz, *FEBS Lett.*, 94 (1978) 213.
16 G. W. Becker and H. S. Hsiung, *FEBS Lett.*, 204 (1986) 145.
17 A. I. Derma and J. Beckwith, *J. Bacteriol.*, 173 (1991) 7719.
18 K. Talmagde and W. Gilbert, *Proc. Natl. Acad. Sci. U.S.A.*, 79 (1982) 1830.
19 H. C. Neu and L. A. Heppel, *J. Biol. Chem.*, 240 (1965) 3685.
20 U. K. Laemmli, *Nature*, 227 (1970) 680.
21 J. Porath and B. Larsson, *J. Chromatogr.*, 155 (1978) 47.
22 M. Wilchek and R. Lamed, *Methods Enzymol.*, 34 (1974) 475.
23 P. Martineau, S. Szmelcman, J. C. Spurlino, F. A. Quiocho and M. Hofnung, *J. Mol. Biol.*, 214 (1990) 337.
24 P. Duplay, H. Bedouelle, A. Fowler, I. Zabin, W. Saurin and M. Hofnung, *J. Biol. Chem.*, 259 (1984) 10806.
25 L. Ambard, *Bull. Soc. Chim. Biol.*, 3 (1921) 230.
26 H. Rozie, W. Somers, K. van 't Riet, F. M. Rombouts and J. Visser, *Carbohydr. Polym.*, 15 (1991) 349.
27 M. Weber, C. Coulombel, D. Darzens J. M. Foglibtil and J. F. Percheron, *J. Chromatogr.*, 355 (1986) 456.
28 E. Norberg and D. French, *J. Am. Chem. Soc.*, 72 (1950) 1302.
29 S. Schwimmer, *Arch. Biochem. Biophys.*, 43 (1953) 108.
30 S. Y. Sawhney, U. N. Nandedkar, S. V. Bhide and N. R. Kale, *Starch*, 40 (1988) 254.
31 H. Li and X. Cheng, *J. Liq. Chromatogr.*, 15 (1992) 707.
32 J. M. Clement and O. Popescu, *Bull. Inst. Pasteur Paris*, 89 (1991) 243.
33 T. Ferenci and K. S. Lee, *J. Mol. Biol.*, 160 (1982) 431.
34 J. W. Roos and M. A. Hjortso, *Biotechnol. Bioeng.*, 38 (1991) 380.

Journal of Chromatography, 633 (1993) 281–286
Elsevier Science Publishers B.V., Amsterdam

CHROM. 24 757

Short Communication

Analysis of lysosomal degradation of fluorescein isothiocyanate-labelled proteins by Toyopearl HW-40 affinity chromatography

Takeyuki Ohshita*

Division of Enzyme Chemistry, Institute for Enzyme Research, University of Tokushima, Tokushima 770 (Japan)

Nobuhiko Katunuma

Institute for Health Science, Tokushima Bunri University, Tokushima 770 (Japan)

(Received October 5th, 1992)

ABSTRACT

Fluorescein isothiocyanate (FITC) was found to have a strong affinity to Toyopearl gel, which is used for gel filtration. FITC-labelled amino acids also showed affinity to Toyopearl gel, their elution from a Toyopearl HW-40 column being retarded. On the other hand, FITC-labelled proteins had no affinity to the gel and were recovered in the flow-through fractions. These findings were applied to the analysis of the degradation of various FITC-labelled proteins by lysosomal enzymes *in vitro*. FITC-labelled degradation products were easily separated from FITC-labelled substrate proteins on a small Toyopearl HW-40 column. Their production increased with the incubation time and was markedly suppressed by the proteinase inhibitor leupeptin. The FITC-labelled degradation product was identified to be mainly lysine with a FITC-labelled ε-amino group by its different elution position to those of lysine with a FITC-labelled α-amino group and other various FITC-labelled amino acids.

INTRODUCTION

Lysosomes degrade various species of proteins sequestered by autophagy and/or heterophagy. As the final degradation products of proteins by total lysosomal proteinases are amino acids, measurements of the release of amino acids are important for examining the total proteolytic activity of lysosomes. Isotope-labelled proteins have been used as substrates, but their use is limited quantitatively and requires facilities to prevent environmental radioactive contamination. Fluorescein isothiocyanate (FITC) has been used for the fluorimetric labelling of proteins and amino acids [1–5]. Protein degradation has been analysed by measurements of acid-soluble materials from fluorescently labelled proteins [6–8]. Acid-soluble materials, however, do not always consist only of free amino acids. We found that FITC has a strong affinity to Toyopearl gel, which is used in gel filtration, and that FITC-labelled amino acids retain affinity to this gel, showing retarted elution from a Toyopearl HW-40 column, whereas FITC-labelled proteins have no affinity to the gel. In this study, we developed a method

* Corresponding author.

0021-9673/93/$06.00

for the analysis of protein degradation based on these differences in interactions of FITC-labelled amino acids and proteins with Toyopearl HW-40 gel. In this way, lysine with an FITC-labelled ε-amino group was identified as the main FITC-labelled degradation product of FITC-labelled proteins by lysosomal enzymes *in vitro*.

EXPERIMENTAL

Reagents

Fluorescein isothiocyanate (FITC) was obtained from ICN Biomedicals, Toyopearl HW-40 (Fine) from Tosoh, Sephacryl S-200, Sepharose 4B and Percoll from Pharmacia, fetuin (from foetal calf serum), myoglobin (from horse heart) and bovine serum albumin (BSA) from Sigma and neuraminidase (from *Arthrobacter ureafaciens*), 4-nitrocatechol sulphate and leupeptin from Nacalai Tesque.

Labelling of amino acids with FITC and Toyopearl HW-40 column chromatography

FITC was dissolved in 0.25 *M* hydrogencarbonate buffer (pH 8.0) and stored at 0°C. This stock solution was stable for at least 5 h. Amino acids were dissolved in water and stored at −20°C until used.

The reaction mixture (0.2 ml) containing 100 nmol of each amino acid, 5 μg of FITC and 0.25 *M* hydrogencarbonate buffer (pH 9.0) was allowed to stand for 1 h at room temperature in the dark. Its pH was then decreased by addition of 0.3 ml of 0.5 *M* hydrogencarbonate buffer (pH 8.0). Samples were applied to a Toyopearl HW-40 column (20 ml bed volume) equilibrated with 10 m*M* phosphate buffer (pH 8.0) containing various concentrations of NaCl. The running buffer was introduced with a peristaltic pump at 0.8 ml/min. Fractions of 2 ml of eluate were collected and their fluorescence intensities were measured with excitation and emission wavelengths of 490 and 520 nm, respectively in a Hitachi Model F-2000 spectrofluorimeter.

Purification of substrate proteins and their labelling with FITC

Asialofetuin was prepared by treating fetuin with neuraminidase as described [9], except that desialylated fetuin was purified by gel filtration on a Sephacryl S-200 column. L-Lactate dehydrogenase (EC 1.1.1.27) (LDH) was purified from the cytosol fraction of rat liver by the method of Scopes [10]. BSA and myoglobin, obtained commercially, were purified further on a Sephacryl S-200 column. Proteins were labelled with FITC as described [11], and stored at −20°C in the presence of 25% glycerol until used.

Preparation of lysosomes

Lysosomes were prepared from rat liver by Percoll density gradient centrifugation as described [9]. The final precipitate of lysosomes was suspended in 20 m*M* sodium acetate buffer (pH 5.0), mixed with an equal volume of 50% glycerol and stored at −20°C until used. Arylsulphate was assayed with 4-nitrocatechol sulphate as substrate [12]. Protein was determined by the microbiuret method of Itzhaki and Gill [13].

Analysis of degradation of FITC-labelled proteins in vitro

For degradation of FITC-labelled proteins by disrupted lysosomes, the incubation mixture (100 μl) contained 50 m*M* acetate buffer (pH 5.0), 10 m*M* 2-mercaptoethanol, 1 m*M* EDTA, 10 or 20 μg of FITC-labelled substrate protein and disrupted lysosomes containing 50 mU of arylsulphatase and was incubated at 37°C for the indicated times. The reaction was stopped by adding 0.3 ml of 0.5 *M* hydrogencarbonate buffer (pH 8.5) and the mixture was applied to a small Toyopearl HW-40 column (20-ml bed volume) equilibrated with the running buffer described in the text. The running buffer was introduced with a peristaltic pump at 0.8 ml/min. Fractions of 2 ml of eluate were collected and their fluorescence intensities were measured with excitation and emission wavelengths of 490 and 520 nm, respectively.

RESULTS AND DISCUSSION

Interaction of FITC and FITC-labelled compounds with Toyopearl HW-40

FITC and FITC-labelled glycine and BSA were each applied to a small Toyopearl HW-40 column (20-ml bed volume) and their elution positions were compared (Fig. 1). Elution of FITC from the column was much delayed with running buffer containing 0.2 *M* NaCl, but was fast when the running

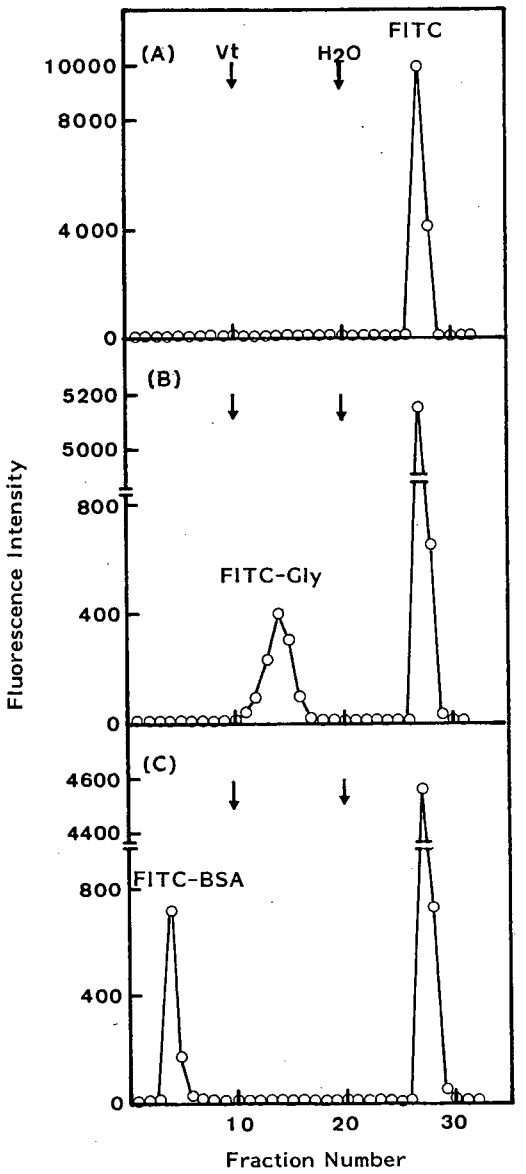

Fig. 1. Comparison of the elution behaviours of FITC and FITC-labelled glycine and BSA on a Toyopearl HW-40 column. Glysine (100 nmol) and BSA (100 μg) were each treated with FITC (5 μg) in 0.2 ml of 0.25 *M* hydrogenbicarbonate buffer (pH 9.0) for 1 h at room temperature. Solutions of FITC (5 μg) in 0.2 ml of 0.25 *M* hydrogencarbonate buffer (pH 9.0) and FITC-treated glycine and BSA were each mixed with 0.3 ml of 0.5 *M* hydrogencarbonate (pH 8.0) and applied to a small Toyopearl HW-40 column (20-ml bed volume) equilibrated with 0.2 *M* NaCl–10 m*M* phosphate buffer (pH 8.0). Materials were eluted with the same running solution and deionized water, both introduced at 0.8 ml/min with a peristaltic pump. Fractions of 2 ml of eluate were collected and their fluorescence intensities were measured with excitation and emission wavelengths of 490 and 520 nm, respectively. The elution profiles of (A) FITC, (B) FITC-labelled glycine and (C) FITC-labelled BSA are shown. The arrows labelled Vt and H_2O show the positions of the bed volume and the change of the running solution to deionized water, respectively.

buffer was changed to deionized water (Fig. 1A) as FITC has a strong affinity to Toyopearl HW-40 in the presence but not the absence of salt. FITC-labelled glycine was eluted much faster than FITC but had affinity to the gel, its elution being retarted with running buffer containing 0.2 *M* NaCl (Fig. 1B). FITC-labelled BSA had no affinity to the gel and was mainly eluted in the flow-through fractions (Fig. 1C). These results show that FITC-labelled amino acids can easily be separated from FITC-labelled proteins on a small Toyopearl HW-40 column. Therefore, we next applied these findings to the analysis of the degradation of FITC-labelled proteins by lysosomal enzymes *in vitro*.

Analysis of degradation of FITC-labelled proteins using a Toyopearl HW-40 column

Using a small Toyopearl HW-40 column (20-ml bed volume), we examined the degradations of various FITC-labelled proteins by disrupted lysosomes *in vitro*. Fig. 2A and B show results for the degradation of FITC-labelled asialofetuin by disrupted lysosomes. FITC-labelled degradation products, elution of which from the column was much delayed, were clearly separated from undegraded or partially degraded FITC-labelled compounds eluted in the flow-through fractions. Their formation increased with time during incubations and was suppressed strongly by leupeptin.

The FITC-labelled degradation product of FITC-labelled proteins by disrupted lysosomes seems to be mainly lysine, the ε-amino group of which is labelled with FITC, but Fig. 1A gives no direct evidence. We therefore compared the elution positions of the FITC-labelled degradation product and lysine and other various amino acids all labelled with FITC. The elution profile of FITC-labelled lysine shows that it contains two components, one major and one minor (Fig. 3A). As the pK_a values of its α-amino and ε-amino groups are 8.95 andf 10.53, respectively, its α-amino group should mainly be labelled with FITC. Hence the main component should be lysine with an FITC-labelled α-amino group. The FITC-labelled degradation product of FITC-labelled asialofetuin was eluted in the same fractions as the minor component of FITC-labelled lysine (Fig. 3B). Therefore, the minor component should be lysine with an FITC-labelled ε-amino group. The amino terminal

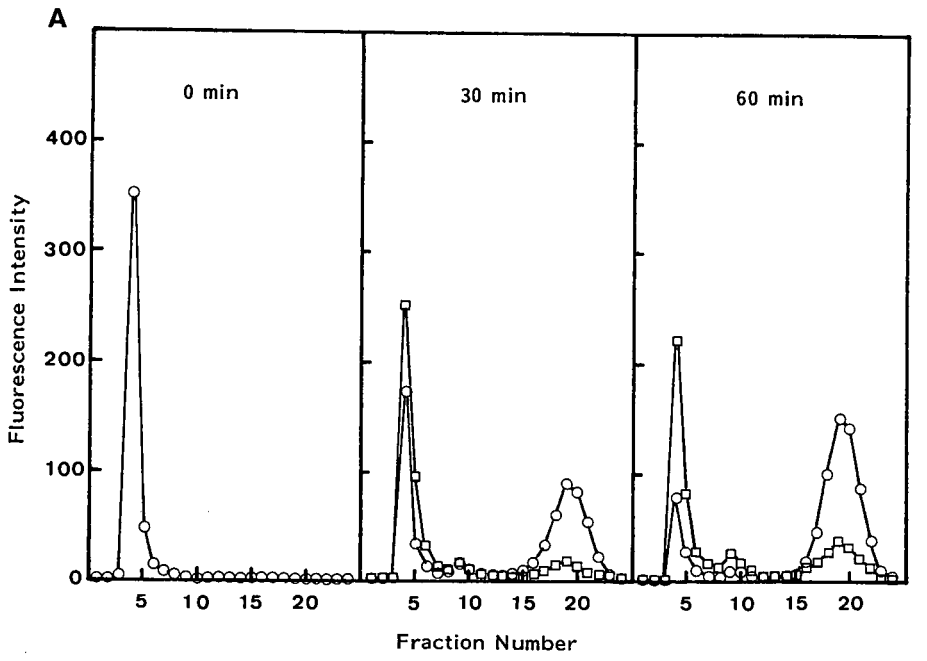

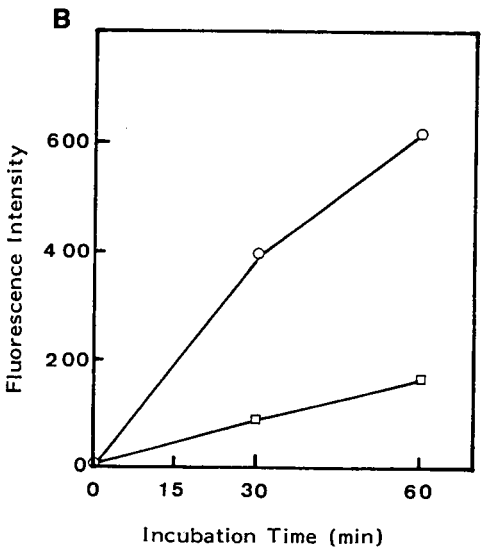

Fig. 2. (A) Analysis of degradation of FITC-labelled asialofetuin on a Toyopearl HW-40 column. FITC-labelled asialofetuin (10 μg) was incubated with disrupted lysosomes in the (□) presence or (○) absence of leupeptin (100 μg) for the indicated times at 37°C, then its degradation was analysed using a Toyopearl HW-40 column (20-ml bed volume) equilibrated with 0.2 *M* NaCl–10 m*M* phosphate buffer (pH 8.0). Fractions of 2 ml of eluate were collected and their fluorescence intensities were measured as described under Experimental. (B) Degradation of FITC-labelled asialofetuin by disrupted lysosomes with time. Eluate fractions 16–23 were pooled and their total fluorescence intensity (□) with and (○) without leupeptin was plotted against incubation time.

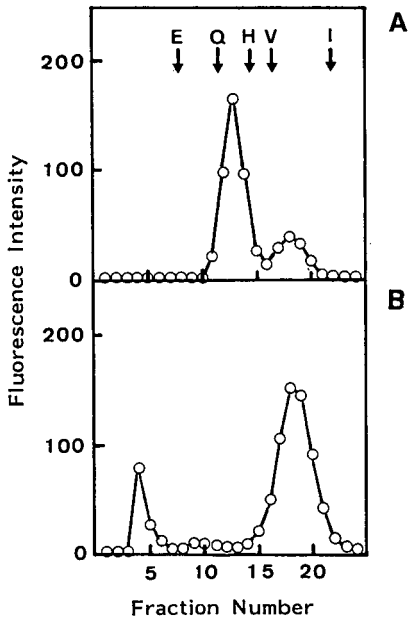

Fig. 3. Comparison of the elution profiles of FITC-labelled lysine and degradation products of FITC-labelled asialofetuin. Amino acids (100 nmol each) were treated with FITC (5 μg) as described under Experimental. They were then mixed with 0.3 ml 0.5 *M* hydrogencarbonate (pH 8.0) and applied to a Toyopearl HW-40 column (20-ml bed volume) equilibrated with 0.2 *M* NaCl–10 m*M* phosphate buffer (pH 8.0). Elution profiles of (A) FITC-labelled lysine and (B) FITC-labelled degradation products of FITC-labelled asialofetuin by disrupted lysosomes (60 min degradation shown in Fig. 2) are compared. The arrows show the elution positions of the peak of various FITC-labelled amino acids (one-letter symbols).

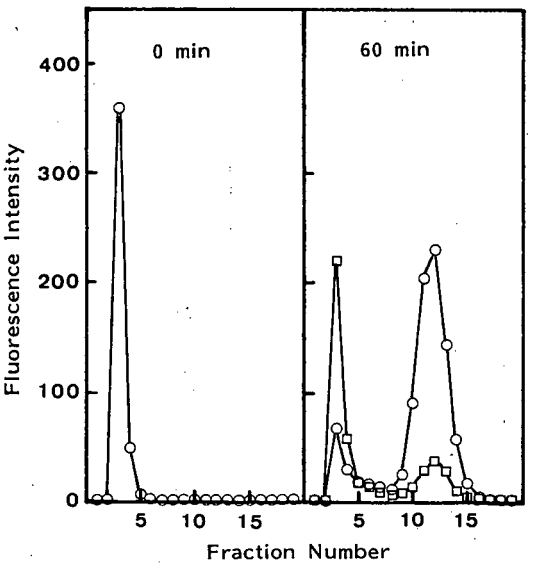

Fig. 4. Degradation of FITC-labelled LDH by disrupted lysosomes. FITC-labelled LDH (10 μg) was incubated with disrupted lysosomes in the (□) presence or (○) absence of leupeptin (100 μg) for the indicated times at 37°C, then the degradation was analysed with a small Toyopearl HW-40 column (10-ml bed volume). Other details as in Fig. 2.

residue of fetuin is isoleucine [14] and may be labelled with FITC. However, the elution positions of FITC-labelled isoleucine and various other amino acids were different from that of the FITC-labelled degradation product (Fig. 3A), the FITC-labelled degradation product being mainly lysine with an FITC-labelled ε-amino group. We also analysed the degradation of FITC-labelled LDH, myoglobin and BSA by disrupted lysosomes using a Toyopearl HW-40 column. In each instance lysine with an FITC-labelled ε-amino group was the main degradation product identified. A smaller column of Toyopearl HW-40 (10-ml bed volume) was available for separating FITC-labelled degradation products from undegraded FITC-labelled substrate protein eluted in the flow-through fractions (Fig. 4).

Toyopearl HW-40 has been used for gel filtration. However, the separation of FITC-labelled compounds on Toyopearl HW-40 is based not on the principle of gel filtration, but on differences in the affinities of the compounds to the gel. The gel filtration effect was negligible, if present at all, because of the small size of the column used (10–20-ml bed volume), the fast flow-rate of the running buffer (0.8 ml/min) and the large fraction size (2 ml per fraction). The presence of salt in the elution solution was necessary for affinity of FITC to Toyopearl HW-40. The affinity of FITC to Toyopearl HW-40 is completely lost on elution with deionized water, suggesting the hydrophobic interaction of FITC with the gel. This method is similar to a method of Sephadex G-25 affinity chromatography that we recently developed for analysing the degradation of FITC-labelled proteins [11], but it gives a better separation of the FITC-labelled amino acids because the differences in the affinities of different amino acids to Toyopearl HW-40 are greater than those to Sephadex G-25. Further, lysine with an FITC-labelled ε-amino group can be clearly separated from lysine with an FITC-labelled α-amino

group on a Toyopearl HW-40 column but not on a Sephadex G-25 column. The Toyopearl HW-40 column chromatography described here is very simple and also inexpensive, because a small column is effective and it can be used repeatedly after simple washing with deionized water.

REFERENCES

1 J. D. Marshall, W. C. Eveland and C. W. Smith, *Proc. Soc. Exp. Biol. Med.*, 98 (1958) 898–900.
2 H. Maeda, N. Ishida, H. Kawauchi and K. Tuzimura, *J. Biochem. (Tokyo)*, 65 (1969) 777–783.
3 H. Kawauchi, K. Tuzimura, H. Maeda and N. Ishida, *J. Biochem. (Tokyo)*, 66 (1969) 783–789.
4 V. E. Duffy, P. A. Stockwell, D. M. Warrington and B. C. Monk, *Anal. Biochem.*, 179 (1989) 291–298.
5 J. Tuls, L. Geren and F. Millett, *J. Biol. Chem.*, 264 (1989) 16421–16425.
6 B. O. De Lumen and A. J. Tappel, *Anal. Biochem.*, 36 (1970) 22–29.
7 R. Wiesner and W. Troll, *Anal. Biochem.*, 121 (1982) 290–294.
8 S. S. Twining, *Anal. Biochem.*, 143 (1984) 30–34.
9 T. Ohshita, E. Kominami, K. Ii and N. Katunuma, *J. Biochem. (Tokyo)*, 100 (1986) 623–632.
10 R. K. Scopes, *Biochem. J.*, 161 (1977) 253–263.
11 T. Ohshita and N. Katunuma, *Anal. Biochem.*, 202 (1992) 400–404.
12 D. W. Milson, F. A. Rose and K. S. Dodgson, *Biochem. J.*, 128 (1972) 331–336.
13 R. F. Itzhaki and D. M. Gill, *Anal. Biochem.*, 9 (1964) 401–410.
14 K. M. Dziegielewska, W. M. Brown, S. J. Casey, R. C. Christie, R. M. Hill and N. R. Saunders, *J. Biol. Chem.*, 265 (1990) 4354–4357.

Journal of Chromatography, 633 (1993) 287–294
Elsevier Science Publishers B.V., Amsterdam

CHROM. 24 763

Short Communication

2,3,4,6-Tetra-O-benzoyl-β-D-glucopyranosyl isothiocyanate: an efficient reagent for the determination of enantiomeric purities of amino acids, β-adrenergic blockers and alkyloxiranes by high-performance liquid chromatography using standard reversed-phase columns

Mario Lobell and Manfred P. Schneider*

Fahrbereich 9, Bergische Universität–Gesamthochschule Wuppertal, Postfach 100127, W-5600 Wuppertal 1 (Germany)

(First received September 9th, 1992; revised manuscript received November 18th, 1992)

ABSTRACT

The use of the chiral derivatization reagent 2,3,4,6-tetra-O-benzoyl-β-D-glucopyranosyl isothiocyanate (BGIT) is described for the conversion of a variety of amino acids and β-adrenergic blockers into diastereomeric thioureas, which can be separated on achiral RP-18 HPLC columns. In comparison with the established reagent 2,3,4,6-tetra-O-acetyl-β-D-glucopyranosyl isothiocyanate (AGIT), BGIT shows increased sensitivity owing to the higher molar absorptivity on the BGIT derivatives. Also a series of monosubstituted alkyloxiranes was transformed with 2-propylamine into the corresponding amino alcohols, which were then further reacted with BGIT, 2,3,4,6-tetra-O-pivaloyl-β-D-galactopyranosyl isothiocyanate (PGIT) or AGIT, leading to the corresponding thiourea derivatives. The diastereomers derived from BGIT could be separated with excellent resolution on a standard RP-18 column, whereas the PGIT and AGIT derivatives showed less or no resolution.

INTRODUCTION

One of the most widely used chiral reagents for the derivatization of enantiomeric amines to form diastereomeric thioureas is 2,3,4,6-tetra-O-acetyl-β-D-glucopyranosyl isothiocyanate (AGIT), introduced by Kinoshita and co-workers [1–3]. As a derivative of natural glucose it is optically pure. The conditions for the derivatizations are mild, thus minimizing possible racemization during the reactions. AGIT has been used for the separation of α-amino acids [1,2,4], amphetamines [5], norepinephrine [3,6], epinephrine [7], propranolol [8], amino alcohols [9,10], mexiletine [11] and oxiranes [12]. It was pointed out by Scott *et al.* [13] and Nambara and co-workers [14,15] that the degree of separation of diastereomers should depend strongly on the rigidity of their conformation and Kinoshita *et al.* [2] suggested that the conformations of their thioureas derived from AGIT and amino acids are rigidly fixed owing to the bulky acetylglycosyl residues. It was to be expected that this effect would be amplified by the introduction of even more bulky benzoyl or pivaloyl groups into the carbohydrate moiety. We therefore decided to investigate whether 2,3,4,6-

* Corresponding author.

0021-9673/93/$06.00

tetra-O-benzoyl-β-D-glucopyranosyl isothiocyanate (BGIT) and 2,3,4,6-tetra-O-pivaloyl-β-D-galactopyranosyl isothiocyanate (PGIT) would be suitable for the separation of amino derivatives that can be analysed only with difficulty using AGIT.

Enantiomerically pure, monosubstituted alkyloxiranes are important chiral building blocks for the synthesis of pheromones [16–19], δ-lactones [20–22] and other important naturally occurring compounds [23], and for polyoxiranes [24] and ferroelectric liquid crystals [25–27]. In contrast to oxiranes carrying chromophores (*e.g.*, aromatic substituents), there is no simple and general method available for the determination of their optical purities. Schurig and co-workers described the resolution of methyl- [28–32], ethyl- [29–32], 2-propyl- [29–31], *tert.*-butyl- [30,31] and vinyloxirane [32] using optically active bis[(1*R*)-3-(heptafluorobutyryl)-camphorates] of nickel(II) [28,29,31,32], manganese (II) [30,31] and cobalt(II) [31] as stationary phases in capillary gas–liquid chromatographic columns. Low separation factors (α = 1.02–1.04, resolution data not given) were reported by Li *et al.* [33] in the resolution of *n*-butyl-, *n*-hexyl-, *n*-octyl-, *n*-decyl- and *n*-dodecyloxirane using 2,6-di-O-pentyl-3-O-trifluoracetyl-α-cyclodextrin (DP-TFA-α-CD) as liquid stationary phase in capillary gas chromatography. Better results in the resolution of *n*-butyloxirane were obtained by Li *et al.* [33] using DP-TFA-γ-CD (α = 1.10) and König [34] employing a modified β-cyclodextrin. The best results so far were obtained by Gal [12] employing a two-step derivatization procedure involving ring opening of the corresponding oxiranes (methyl-, *tert.*-butyl- and *n*-hexyloxirane) using a variety of primary amines, followed by derivatization of the resulting amino alcohols with AGIT. The obtained separation factors (α = 1.15–1.23) and resolutions (R_s = 2.14–2.29) are acceptable. Unfortunately, the times required for the first derivatization step using cyclohexylamine [68 h], *n*-butylamine [24 h] and isobutylamine [2 h] are frequently much too long.

In order to facilitate the whole procedure and reduce the times required for derivatization we chose 2-propylamine for the ring opening of the oxiranes. Using this procedure the time required for the preparation of amino alcohols is only 2 h. Results obtained in the resolution of the oxirane-derived amino alcohols were compared using BGIT, PGIT and AGIT as reagents for the second derivatization step.

In addition to improved resolutions due to increased steric bulk (benzoate and pivaloate *versus* acetate), it was expected that the use of BGIT derivatives would result in higher detection sensitivities for the resulting diastereomeric thioureas as compares with AGIT. Therefore, the UV absorbance spectra of BGIT, AGIT and their thiourea derivatives of L-leucine were recorded and compared.

In order to demonstrate the versatile applicability of BGIT, it was also used for the separation of β-adrenergic blockers and a variety of natural and unnatural amino acids.

EXPERIMENTAL

2,3,4,6-Tetra-O-acetyl-α-D-glucopyranosyl bromide, 2,3,4,6-tetra-O-pivaloyl-β-D-galactopyranosylamine, thiophosgene, 1,2-alkenes, racemic oxiranes, (*R*)-(+)-methyloxirane, amino acids, β-adrenergic blockers and other reagents including 67 m*M* phosphate buffer (pH 7.0) were obtained from Aldrich, Fluka, Lancaster and Merck. Racemic *n*-propyl-, *n*-pentyl- and *n*-heptyloxirane were synthesized from the corresponding 1,2-alkenes according to the procedure of Terao *et al.* [35]. Enantiomerically pure oxiranes except (*R*)-(+)-methyloxirane were synthesized via the enzymatic route reported by Goergens and Schneider [36]. BGIT and AGIT were prepared by treatment of 2,3,4,6-tetra-O-benzoyl-α-D-glucopyranosyl bromide and 2,3,4,6-tetra-O-acetyl-α-D-glucopyranosyl bromide with silver thiocyanate according to the procedure of Van de Kamp and Micheel [37]. 2,3,4,6-Tetra-O-benzoyl-α-D-glucopyranosyl bromide was prepared from D-glucose in two steps as described by Ness *et al.* [38]. PGIT was prepared by treatment of 2,3,4,6-tetra-O-pivaloyl-β-D-galactopyranosylamine with thiophosgene according to the procedure of Fuentes Mota *et al.* [39]. AGIT, BGIT and PGIT are also commercially available from Fluka (product numbers 86550, 86729 and 88102, respectively).

Equipment

The UV absorbance spectra were recorded with a UV-160A UV–Vis recording spectrophotometer (Shimadzu). The chromatographic system consisted

of an L-6200 intelligent pump (Merck–Hitachi), L-4200 UV–Vis Detector (Merck–Hitachi), D-2500 chromato-integrator (Merck–Hitachi) and a LiChrospher 100 RP-18 column (25 × 4 mm I.D., particle size 5 μm) (Merck). An L-6210 intelligent pump (Merck–Hitachi) was used if the mobile phase contained phosphate buffer.

Derivatization of amino acids and β-adrenergic blockers

A 5-mg amount of the corresponding amino acid or 0.1 mmol of the β-adrenergic blocker was dissolved in 50% (v/v) aqueous acetonitrile containing 0.55% (v/v) triethylamine in order to give a final volume of 10 ml. To 50 μl of this stock solution 50 μl of 0.66% (w/v) BGIT in acetonitrile were added. The resulting mixture was shaken on a laboratory shaker for 30 min, then 10 μl of 0.26% (v/v) ethanolamine in acetonitrile were added and shaking was continued for another 10 min. Ethanolamine reacts with any excess of BGIT and the resulting thiourea derivative is eluted well behind any of the amino acid derivatives. The mixture was then diluted with acetonitrile to a final volume of 1 ml and a 10-μl aliquot was used for HPLC.

Derivatization of oxiranes

Aliquots of 50 μl of the oxiranes were placed in 1-ml vials, to which 200 μl of 2-propylamine were added. The vials were tightly closed with a Teflon-lined cap and heated at 100°C for 2 h. Excess of 2-propylamine was evaporated in a stream of air, 950 μl acetonitrile were added and 50-μl aliquots were placed in a 1-ml Eppendorf vial. A 50-μl volume of 0.66% (w/v) BGIT, 0.56% (w/v) PGIT or 0.4% (w/v) AGIT in acetonitrile was added and the mixtures were allowed to stand at room temperature for 30 min. The resulting mixtures were diluted with acetonitrile to a final volume of 1 ml and a 7-μl aliquot was used for HPLC.

RESULTS

AGIT shows maximum UV absorption at 250 nm (π–π^* transition of the carbon–sulphur double bond), whereas BGIT has a maximum absorption at 231 nm (π–π^* transition in the benzoyl groups). The maximum molar absorptivity of BGIT is 60 times higher than that of AGIT (Table I). After derivatization with an α-amino acid (L-leucine), the molar absorptivity of the BGIT thiourea derivative decreases slightly in comparison with the underivatized reagent. In contrast, the corresponding thiourea derivative of AGIT displays a molar absorptivity ten times higher than that of AGIT itself, owing to the formation of the thiourea group (Table I). In summary, molar absorptivities of BGIT thiourea derivatives are about five times higher than those of AGIT thiourea derivatives.

TABLE I

MOLAR ABSORPTIVITIES OF BGIT, AGIT AND THEIR THIOUREA DERIVATIVES OF L-LEUCINE AT THEIR WAVELENGTHS OF MAXIMUM ABSORPTION

Absorbances were measured at concentrations between 10^{-5} and 10^{-4} mol/l in acetonitrile; λ_{max} = wavelength of maximum absorption; $\varepsilon(\lambda_{max})$ = molar absorptivity at λ_{max}.

Compound	λ_{max} (nm)	$\varepsilon(\lambda_{max})$ (l mol^{-1} cm^{-1})
BGIT	231	$5.79 \cdot 10^4$
AGIT	250	$9.57 \cdot 10^2$
BGIT–L-leucine	231	$5.05 \cdot 10^4$
AGIT–L-leucine	250	$1.03 \cdot 10^4$

Seventeen chiral amino acids (eleven natural and six non-natural) and seven β-adrenergic blockers were derivatized using BGIT. With the exception of adrenaline, conditions were found that allowed complete baseline separation of the corresponding diastereomers. Also mixtures of α-amino acids can be analysed and an example of the simultaneous

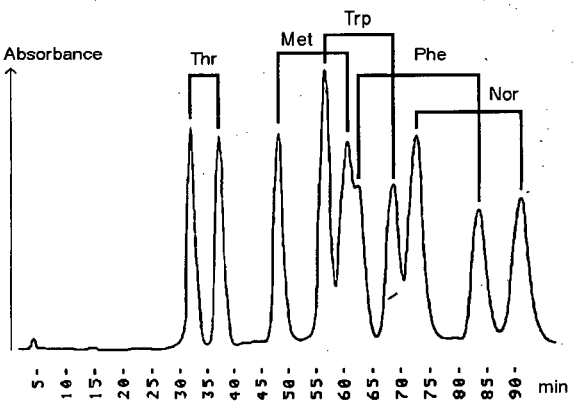

Fig. 1. Separation of ten diastereomeric thiourea derivatives formed from amino acids with BGIT. Mobile phase, methanol–water–67 m*M* phosphate buffer (pH 7.0) (68:27:5); flow-rate, 0.45 ml min^{-1}; 2 nmol of each derivative were injected.

TABLE II

SEPARATION OF DIASTEREOMERIC THIOUREA DERIVATIVES FORMED BY DERIVATIZATION OF RACEMIC AMINO ACIDS WITH BGIT

Column: LiChrospher 100 RP-18 (5 μm). Conditions: (A) mobile phase = methanol–water–67 m*M* phosphate buffer (pH 7.0) (65:27:8), flow-rate = 0.42 ml min^{-1}, t_0 = 4.1 min; (B) mobile phase = methanol–water–67 m*M* phosphate buffer (pH 7.0) (70:25:5), flow-rate = 0.45 ml min^{-1}, t_0 = 3.7 min; (C) mobile phase = methanol–water–67 m*M* phosphate buffer (pH 7.0) (80:15:5), flow-rate = 0.50 ml min^{-1}, t_0 = 3.1 min. k', α and R_s are defined in the text.

Amino acid	k'_L	k'_D	α	R_s	Conditions
Alanine	18.00	20.85	1.16	2.72	A
Isoleucine	9.27	12.35	1.33	3.08	B
Leucine	9.51	12.65	1.33	3.74	B
Lysine	13.48	15.32	1.14	2.28	C
Methionine	8.08	10.24	1.27	4.55	B
Phenylalanine	10.54	13.81	1.31	4.84	B
Proline	6.41	5.19	1.23	2.50	B
Threonine	5.35	6.24	1.17	2.28	B
Tryptophan	9.43	12.03	1.27	4.36	B
Tyrosine	6.22	7.41	1.19	2.00	B
Valine	7.22	9.16	1.27	3.00	B
2-Aminobutyric acid	6.24	7.57	1.21	2.97	B
3-Aminobutyric acid	16.88	18.95	1.12	2.74	A
Norleucine	12.89	16.81	1.30	5.92	B
Ornithine	11.94	13.90	1.16	2.54	C
Penicillamine	7.37	10.05	1.33	4.00	B
Phenylglycine	6.38	7.86	1.23	2.20	B

analysis of five racemic amino acids is shown in Fig. 1. Retention and resolution parameters of the diastereomeric BGIT derivatives are given in the Tables II and III (k', α and R_s refer to the capacity factor, separation factor and resolution, respectively, for a given pair of diastereomers).

Also thirteen monosubstituted racemic alkyloxiranes were converted with 2-propylamine into the

TABLE III

SEPARATION OF DIASTEREOMERIC THIOUREA DERIVATIVES FORMED BY DERIVATIZATION OF RACEMIC β-ADRENERGIC BLOCKERS WITH BGIT

Column: LiChrospher 100 RP-18 (5 μm). Conditions: (A) mobile phase = methanol–water (70:30), flow-rate = 1 ml min^{-1}, t_0 = 1.55 min; (B) mobile phase = methanol–water (80:20), flow-rate = 1 ml min^{-1}, t_0 = 1.55 min; (C) mobile phase = methanol–water (85:15), flow-rate = 0.5 ml min^{-1}, t_0 = 3.1 min; (D) mobile phase = methanol–water (90:10), flow-rate = 0.5 ml min^{-1}, t_0 = 3.1 min. k'_1 = capacity factor of the faster eluting derivative: α and R_s are defined in the text.

β-Adrenergic blocker	k'_1	k'_2	α	R_s	Conditions	Configuration of amine yielding faster eluting BGIT derivative
Adrenaline	22.61	25.67	1.14	1.44	A	
Phenylephrine	33.96	40.07	1.18	3.16	A	*S*
5-(2-N-Benzylamino-2-hydroxyethyl)salicylamide	8.86	11.66	1.32	2.72	B	
Atenolol	5.68	6.66	1.17	2.17	B	
Sotalol	5.01	6.53	1.30	5.88	B	
Pindolol	3.00	3.71	1.24	3.16	C	
Propranolol	2.65	3.65	1.38	4.43	D	

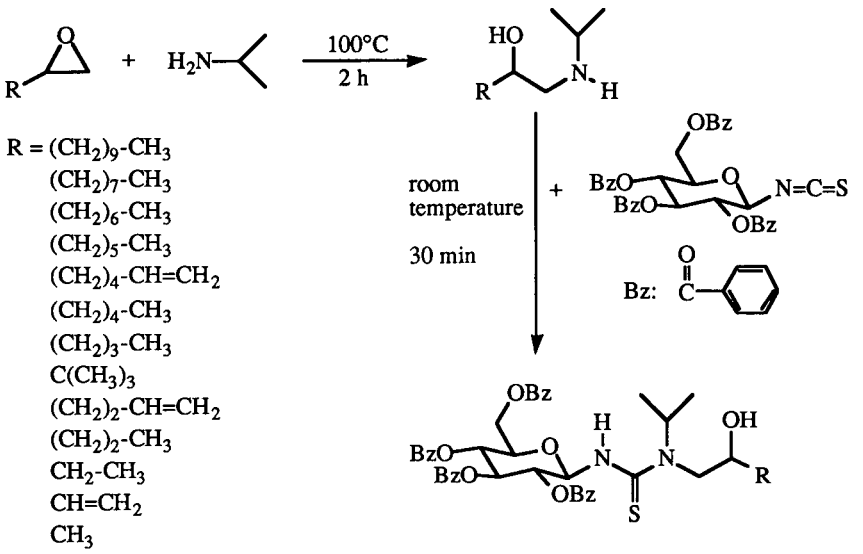

Fig. 2. Derivatization sequence using 2-propylamine and BGIT.

corresponding amino alcohols, which were then derivatized with BGIT, PGIT or AGIT, leading to the corresponding thioureas. The chromatographic analysis was carried out on an RP-18 column with detection at 231 nm (BGIT derivatives) or 250 nm (PGIT and AGIT derivatives).

Retention and resolution parameters of the diastereomeric BGIT, PGIT and AGIT derivatives are summarized in Tables IV–VI. As shown in Table IV and demonstrated in Fig. 3, all diastereomeric BGIT derivatives could be resolved very well and with short retention times. Baseline separations

TABLE IV

SEPARATION OF DIASTEREOMERIC BGIT DERIVATIVES OBTAINED FROM OXIRANE-DERIVED β-AMINO ALCOHOLS

Column: LiChrospher 100 RP-18 (5 μm); flow-rate = 0.50 ml min^{-1}; t_0 = 3.1 min; wavelength of detection = 231 nm. R = substituent as described in Fig. 2. k', α and R_s are defined in the text.

R	Mobile phase (MeOH–H_2O)	k'_R	k'_S	α	R_s	Mobile phase (MeOH–H_2O)	k'_R	k'_S	α	R_s
$(CH_2)_9CH_3$	90:10	9.38	11.35	1.21	4.34	95:5	3.16	3.62	1.15	4.70
$(CH_2)_7CH_3$	90:10	5.58	6.71	1.20	3.51	95:5	1.91	2.17	1.14	2.70
$(CH_2)_6CH_3$	90:10	4.17	5.00	1.20	3.66					
$(CH_2)_5CH_3$	90:10	3.06	3.63	1.19	2.92					
$(CH_2)_4CH=CH_2$	90:10	2.52	2.95	1.17	2.66	85:15	6.99	8.77	1.26	4.62
$(CH_2)_4CH_3$	90:10	2.62	3.06	1.17	2.30	85:15	7.10	8.88	1.25	4.26
$(CH_2)_3CH_3$	90:10	2.19	2.54	1.16	2.16	85:15	5.53	6.83	1.24	4.03
$C(CH_3)_3$	90:10	2.77	2.43	1.14	1.75	85:15	5.29	4.51	1.17	3.01
$(CH_2)_2CH=CH_2$	90:10	1.92	2.23	1.16	1.58	85:15	4.47	5.53	1.24	3.64
$(CH_2)_2CH_3$	90:10	1.96	2.27	1.16	1.58	85:15	3.71	4.50	1.21	3.27
CH_2CH_3	90:10	1.60	1.82	1.14	1.36	85:15	3.46	4.16	1.20	2.73
$CH=CH_2$	90:10	1.55	1.78	1.15	1.73	85:15	3.14	3.78	1.20	2.86
CH_3	90:10	1.45	1.65	1.14	1.55	85:15	2.57	3.06	1.19	2.55

TABLE V

SEPARATION OF DIASTEREOMERIC PGIT DERIVATIVES OBTAINED FROM OXIRANE-DERIVED β-AMINO ALCOHOLS

Column: LiChrospher 100 RP-18 (5 μm); flow-rate = 0.50 ml min^{-1}; t_0 = 3.1 min; wavelength of detection = 250 nm. R = substituent as described in Fig. 2. k', α and R_s are defined in the text.

R	Mobile phase (MeOH–H_2O)	k'_R	k'_S	α	R_s
$(CH_2)_9CH_3$	90:10	17.05	19.41	1.14	2.92
$(CH_2)_7CH_3$	90:10	9.18	10.37	1.13	2.45
$(CH_2)_6CH_3$	90:10	7.06	7.95	1.13	1.97
$(CH_2)_5CH_3$	90:10	5.85	6.50	1.11	1.85
$(CH_2)_4CH=CH_2$	90:10	4.39	4.86	1.11	1.83
$(CH_2)_4CH_3$	90:10	4.73	5.23	1.11	1.73
$(CH_2)_3CH_3$	90:10	3.72	4.03	1.08	1.37
$C(CH_3)_3$	90:10	4.35	3.92	1.11	1.64
$(CH_2)_2CH=CH_2$	90:10	2.95	3.17	1.07	0.96
$(CH_2)_2CH_3$	90:10	2.92	3.10	1.06	0.73
CH_2CH_3	90:10	2.61	2.76	1.06	0.69
$CH=CH_2$	90:10	2.20	2.39	1.09	0.98
CH_3	90:10	2.17	2.28	1.05	–

were achieved in all instances. Owing to the widely different retention times, it was possible to analyse a mixture of five different racemic oxiranes (corresponding to ten diastereomers) in a single experiment (Fig. 3). In contrast less or unsatisfactory separations were observed when PGIT was used as reagent for the second derivatization step (Table V). No or unsatisfactory separations were observed if AGIT was used for derivatization (Table VI).

TABLE VI

SEPARATION OF DIASTEREOMERIC AGIT DERIVATIVES OBTAINED FROM OXIRANE-DERIVED β-AMINO ALCOHOLS

Column: LiChrospher 100 RP-18 (5 μm); flow-rate = 0.50 ml min^{-1}; t_0 = 3.1 min; wavelength of detection = 250 nm, R = substituent as described in Fig. 2. k', α and R_s are defined in the text.

R	Mobile phase (MeOH–H_2O)	k'_R	k'_S	α	R_s
$(CH_2)_9CH_3$	85:15	5.19	5.54	1.07	1.33
$(CH_2)_7CH_3$	85:15	2.78	2.96	1.06	0.92
$(CH_2)_6CH_3$	85:15	2.04	2.16	1.06	–
$(CH_2)_5CH_3$	85:15	1.57	1.66	1.06	–
$(CH_2)_4CH=CH_2$	85:15	1.19	1.25	1.05	–
$(CH_2)_4CH_3$	85:15	1.25	1.30	1.04	–
$(CH_2)_3CH_3$	85:15	1.01	1.01	–	–
$C(CH_3)_3$	85:15	0.99	0.99	–	–
$(CH_2)_2CH=CH_2$	85:15	0.86	0.86	–	–
$(CH_2)_2CH_3$	85:15	0.80	0.80	–	–
CH_2CH_3	85:15	0.68	0.68	–	–
$CH=CH_2$	85:15	0.64	0.64	–	–
CH_3	85:15	0.59	0.59	–	–

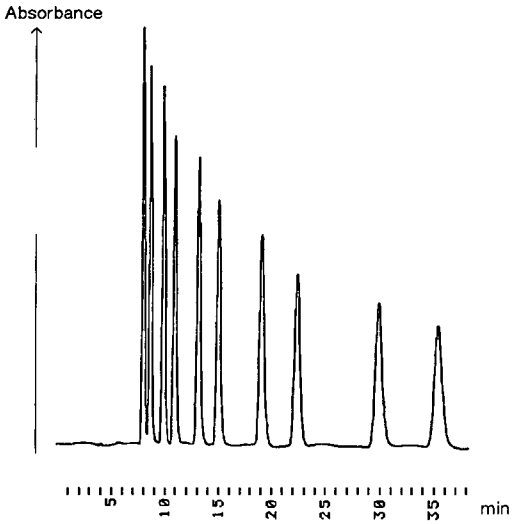

Fig. 3. Separation of a mixture of ten oxirane-derived β-amino alcohols as diastereomeric thiourea derivatives in a single experiment. Mobile phase, methanol–water (90:10); flow-rate, 0.50 ml min^{-1}; 0.7 nmol of each derivative was injected. Components were eluted in the following order: (*R*)-ethyloxirane, (*S*)-ethyloxirane, (*R*)-butyloxirane, (*S*)-butyloxirane, (*R*)-hexyloxirane, (*S*)-hexyloxirane, (*R*)-octyloxirane, (*S*)-octyloxirane, (*R*)-decyloxirane and (*S*)-decyloxirane.

DISCUSSION

The described methods using BGIT as derivatization reagent are very suitable for the determination of enantiomeric purities of chiral amines. BGIT can be prepared easily in optically pure form. It reacts readily with primary and secondary amines under mild conditions without the formation of undesirable by-products. Derivatizations are easy to carry out and separations can be achieved on normal, inexpensive reversed-phase HPLC columns. Owing to the high molar absorptivities of BGIT derivatives small enantiomeric impurities can easily be detected.

The separations achieved for amino acids and β-adrenergic blockers are comparable to the results obtained by Kinoshita *et al.* [2] and Sedman and Gal [10] using AGIT for derivatization. In contrast to AGIT, however, excellent results were obtained in the analysis of amino alcohols derived from chiral alkyloxiranes using BGIT. The method proved to be an excellent tool for the determination of enantiomeric purities in numerous representatives of this class of molecule, regardless of the chain length of the alkyl substituents. Moreover, the described procedure is simple and rapid and the times required for derivatization are greatly reduced in comparison with previous methods.

The assumption that there is a strong relationship between the bulkiness of the derivatization agent and the quality of resolution was not confirmed. In fact PGIT, containing the most bulky pivaloyl groups, did not turn out to induce the best separations, which were achieved using BGIT. Nevertheless, using PGIT the observed resolutions were satisfactory ($R_s > 1.6$) for the determination of enantiomeric purities in seven out of thirteen cases, whereas none of the AGIT derivatives was resolved satisfactorily.

ACKNOWLEDGEMENT

We thank Boehringer Mannheim GmbH for financial support of this work.

REFERENCES

1 N. Nimura, H. Ogura and T. Kinoshita, *J. Chromatogr.*, 202 (1980) 375.
2 T. Kinoshita, Y. Kasahara and N. Nimura, *J. Chromatogr.*, 210 (1981) 77.
3 N. Nimura, Y. Kasahara and T. Kinoshita, *J. Chromatogr.*, 213 (1981) 327.
4 N. Nimura, A. Toyama and T. Kinoshita, *J. Chromatogr.*, 316 (1984) 547.
5 K. J. Miller, J. Gal and M. Ames, *J. Chromatogr.*, 307 (1984) 335.
6 J. F. Allgire, E. C,. Juenge, C. P. Damo, G. M. Sullivan and R. D. Kirchhoefer, *J. Chromatogr.*, 325 (1985) 249.
7 J. Gal, *J. Chromatogr.*, 307 (1984) 220.
8 J. Gal and R. C. Murphy, *J. Liq. Chromatogr.*, 7 (1984) 2307.
9 J. Gal, *J. Liq. Chromatogr.*, 9 (1986) 673.
10 A. J. Sedman and J. Gal, *J. Chromatogr.*, 278 (1983) 199.
11 O. Grech-Bélanger and J. Turgeon, *J. Chromatogr.*, 337 (1985) 172.
12 J. Gal, *J. Chromatogr.*, 331 (1985) 349.
13 C. G. Scott, M. J. Petrin and T. McCorkle, *J. Chromatogr.*, 125 (1976) 157.
14 T. Nambara, S. Ikegawa, M. Hasegawa and J. Goto, *Anal. Chim. Acta*, 101 (1978) 111.
15 J. Goto, M. Hasegawa, S. Nakamura, K. Shimada and T. Nambara, *J. Chromatogr.*, 152 (1978) 413.
16 K. Mori, M. Sasaki, S. Tamada, T. Suguro and S. Masuda, *Tetrahedron*, 35 (1979) 1601.
17 K. Mori, M. Sasaki, S. Tamada, T. Suguro and S. Masuda, *Heterocycles*, 10 (1978) 111.
18 B. D. Johnston and K. N. Slessor, *Can. J. Chem.*, 57 (1979) 233.

19 B. D. Johnston and A. C. Oehlschlager, *J. Org. Chem.*, 51 (1986) 760.
20 J. L. Coke and A. B. Richon, *J. Org. Chem.*, 41 (1976) 3516.
21 S. Takano, M. Setoh and K. Ogasawara, *Tetrahedron: Asymmetry*, 3 (1992) 533.
22 U. Goergens and M. P. Schneider, *Tetrahedron: Asymmetry*, 3 (1992) 831.
23 Y. Masaoka, M. Sakakibara and K. Mori, *Agric. Biol. Chem.*, 46 (1982) 2319.
24 N. Spassky, P. Dumas, M. Sepulchre and P. Sigwalt, *J. Polym. Sci.*, 52 (1975) 327.
25 S. Arakawa and H. K. Tomimuro, *Ger. Pat.*, 3 836 855 A1 (1989).
26 K. Sakaguchi, T. Kitamura, Y. Shiomi, M. Koden and T. Kuratate, *Chem. Lett.*, (1991) 1383.
27 T. Kusumoto, K. Sato, T. Hiyama, S. Takehara, M. Osawa, K. Nakamura and T. Fujisawa, *Chem. Lett.*, (1991) 1623.
28 V. Schurig, B. Koppenhöfer and W. Bürkle, *Angew. Chem., Int. Ed. Engl.*, 17 (1978) 937.
29 H. B. Kagan, H. Mimoun, C. Mark and V. Schurig, *Angew. Chem., Int. Ed. Engl.*, 18 (1979) 485.
30 V. Schurig and R. Weber, *J. Chromatogr.*, 217 (1981) 51.
31 V. Schurig and W. Bürkle, *J. Am. Chem. Soc.*, 104 (1982) 7573.
32 V. Schurig and D. Wistuba, *Angew. Chem., Int. Ed. Engl.*, 23 (1984) 796.
33 W.-Y. Li, H. L. Jin and D. W. Armstrong, *J. Chromatogr.*, 509 (1990) 303.
34 W. A. König, *Gas Chromatographic Enantiomer Separation with Modified Cyclodextrins*, Hüthig, Heidelberg, 1991.
35 S. Terao, M. Shiraishi, K. Kato, S. Ohkawa, Y. Ashida and Y. Maki, *J. Chem. Soc., Perkin Trans. 1*, (1982) 2909.
36 U. Goergens and M. P. Schneider, *Tetrahedron: Asymmetry*, 3 (1992) 1149.
37 F.-P. van de Kamp and F. Micheel, *Chem. Ber.*, 89 (1956) 133.
38 R. K. Ness, H. G. Fletcher and C. S. Hudson, *J. Am. Chem. Soc.*, 72 (1950) 2200.
39 J. Fuentes Mota, R. Babiano Caballero and J. A. Galbis Perez, *Carbohydr. Res.*, 154 (1986) 280.

Journal of Chromatography, 633 (1993) 295–299
Elsevier Science Publishers B.V., Amsterdam

CHROM. 24 772

Short Communication

Characterization and separation of oxidized derivatives of pheophorbide *a* and *b* by thin-layer and high-performance liquid chromatography

M. Isabel Mínguez-Mosquera*, Lourdes Gallardo-Guerrero and Beatriz Gandul-Rojas

Unidad Estructural de Biotecnología de Alimentos, Instituto de la Grasa y sus Derivados (CSIC), Avenida Padre García Tejero 4, 41012 Seville (Spain)

(First received August 7th, 1992; revised manuscript received November 10th, 1992)

ABSTRACT

The separation and purification of the main oxidized derivatives of pheophorbide *a* and *b* by reversed-phase TLC afforded their characterization by physical and spectroscopic properties. Their subsequent separation and identification by reversed-phase HPLC was achieved using a system of gradient elution. Under these conditions the separation of rhodin g_7, chlorin e_6, pheophorbide *b*, pheophorbide *a*, purpurin *b*, pyropheophorbide *b*, pyropheophorbide *a* and purpurin *a* was achieved in 15 min.

INTRODUCTION

The process of lactic fermentation during the preparation of table olives involves the degradation of the chlorophylls to their corresponding pheophytins and pheophorbides in the final product [1]. However, it has been observed that during the subsequent conservation of these fruits in brine, another series of reactions takes place that may involve the oxidation of chlorophyllic compounds.

In numerous studies [2,3] HPLC has been used to follow the colour transformation from bright green to olive green in processed vegatables. This change is due mainly to the degradation of chlorophylls to pheophytins and pheophorbides. Nevertheless, there may be a reaction involving C-10 decarbomethoxylation or the opening of the isocyclic ring, giving rise to compounds with a higher degree of oxidation, whose control, by either TLC or HPLC, has not been sufficiently studied.

Hynninen [4] described the preparation and purification of some oxidized derivatives of chlorophylls (chlorines, rhodines and purpurins) by different alkaline treatments. These compounds were separated by TLC on cellulose plates with *n*-heptane–pyridine (7:3) as eluent [5].

In this work we investigated different conditions for the separation of pheophorbide derivatives by in normal- and reversed-phase TLC and ion-pair HPLC.

EXPERIMENTAL

Sample preparation

The study was carried out on olives, *Olea europaea* (L.), of Hojiblanca variety (*arolensis*). The

* Corresponding author.

0021-9673/93/$06.00

fruits were processed using the traditional method of Spanish-style fermentation in brine [1]. The fat-free extract pigment was prepared by extraction with N,N-dimethylformamide. Details of the extraction process have been published previously [3,6].

Standards

Chlorophyll *a* and *b* were supplied by Sigma (St. Louis, MO, USA) (chlorophyll *a*, No. C-6144, and chlorophyll *b*, No. C-3878). Chlorophyllides *a* and *b* were produced by enzymatic deesterification of chlorophylls: a protein precipitate of *Ailanthus altissima* (Mill.) leaves was incubated with acetone–Tris–HCl buffer (pH 8) (1:1) [7]. Pheophorbide *a* and *b* were obtained from their respective chlorophyllides by acidification with 0.01 *M* HCl [8]. Pyropheophorbide *a* and *b* were prepared by heating the corresponding pheophorbides in pyridine under reflux at 100°C for 24 h [2].

The remaining standards were prepared according to the method described by Hynninen [4], which is summarized as follows. Methyl esters of chlorin e_6 and rhodin g_7 were formed by saponification of pheophorbide *a* and pheophorbide *b*, respectively, with 0.5% KOH in methanol. Free chlorine e_6 and rhodin g_7 were obtained from their respective methyl esters by saponification with KOH (30%) at ambient temperature and under a nitrogen atmosphere. Purpurin *a* was obtained by alkaline oxidation of pheophorbide *a* with 30% KOH in methanol in the presence of atmospheric oxygen, and purpurin *b* from pheophorbide *b* using the same procedure.

Separation of pigments by TLC

Reversed-phase TLC was carried out on commercial aluminium plates of 20 × 20 cm covered with a 0.1-mm layer of cellulose (CE F_{254}; Sharlau, Barcelona, Spain), Kieselguhr plates 20 × 20 cm with a 0.25-mm layer of fluorescent indicator (Macherey–Nagel, Düren, Germany) of impregnated with 14% (v/v) of maize oil in light petroleum (b.p. 65–110°C) by vertical immersion up to 18 cm (spotting was done on the non-impregnated area) and plates of 10 × 10 cm covered with a 0.2-mm layer of silica gel C_{18} (Nano SI F_{254} C_{18}-100; Sharlau). The mobile phases used were *n*-heptane–pyridine (7:3), methanol–acetone–water (20:4:6) and methanol–acetone–water (20:4:3), respectively. The chromatography was performed in a normal saturated tank with detection using a Desaga UV-Vis lamp providing with white light and UV radiation of 254 and 366 nm.

Separation of pigments by HPLC

HPLC analysis was performed using a Waters Model 600 E chromatograph fitted with a Waters Model 994 photodiode-array detector and a Waters Model 5200 register–integrator.

The pigment extract (20 μl) was filtered through a 0.45-μm nylon membrane and injected into the liquid chromatograph. Separation was performed on a 25 x 0.4 cm I.D. C_{18} Spherisorb ODS-2 analytical column of 5-μm particle size (Supelco, Bellefonte, PA, USA). The column was protected by a cartridge (5 × 0.4 cm I.D.) packed with the same material. Pigments were separated using a linear gradient system at a flow-rate of 2 ml/min. The eluents used were (A) water–ion-pair reagent–methanol (1:1:8, v/v/v) and (B) acetone–methanol (1:1, v/v). The ion-pair reagent was 0.05 *M* tetrabutylammonium acetate and 1 *M* ammonium acetate in water. Elution was from 100% A linearity to 100% B in 15 min, returning to the initial conditions in 5 min. Multiple detection was performed at 400 and 430 nm. Pigments were identified by comparing the retention times with those of authentic standards and from their spectral characteristics.

Reagents

All reagents were of analytical-reagent grade, except acetone and methanol, which were of HPLC grade. Water was deionized and filtered through a 0.45-μm nylon membrane (Supelco).

RESULTS AND DISCUSSION

Separation of pigments by TLC

Different systems of sorbents and mobile phases were examined. The separation on cellulose plates using *n*-heptane–pyridine (7:3) as mobile phase [5] did not afford the expected results. The pigments advanced to the front of the chromatogram, except chlorin and rhodin, which remained at the base. Development in the reversed-phase mode with Kieselguhr plates impregnated with maize oil, and methanol–acetone–water (20:4:6) as mobile phase [9],

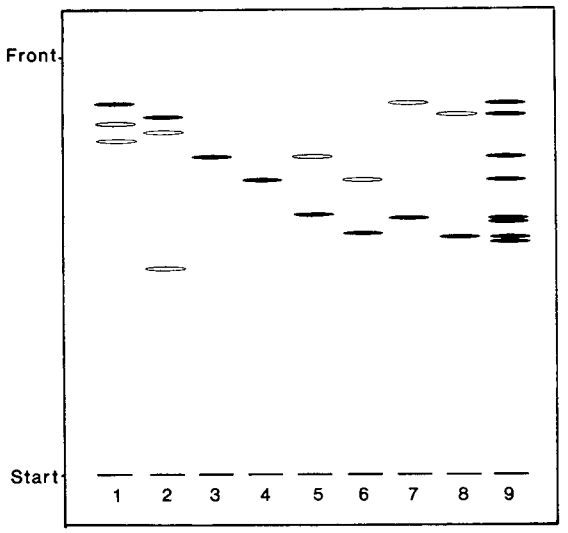

Fig. 1. Thin-layer chromatogram on silica gel C_{18} eluted with methanol–acetone–water (20:4:3): 1 = rhodin g_7; 2 = chlorin e_6; 3 = pheophorbide *b*; 4 = pheophorbide *a*; 5 = pyropheophorbide *b*; 6 = pyropheophorbide *a*; 7 = purpurin *b*; 8 = purpurin *a*; 9 = mixture of all purified standard pigments. Black spots, main pigment; white spots, traces of precursors.

gave similar results, with the pigments moving to the front of the elution. Using this mobile phase, decreasing the amount of water to give a ratio of 20:4:3, and cellulose plates as support, the pigments were well separated but poor resolution was obtained because the tails of the bands quite overlapped. To reduce this effect, the cellulose support was changed for commercial plates of silica gel C_{18} (HPTLC). This modification gave optimum results. A chromatogram was obtained in which the bands were sharp and well defined, permitting complete separation and purificaton of all the pigments under study. All the compounds were separated from the standard mixture of pheophorbide *a* and *b*, chlorin,

TABLE I

RESULTS OF TLC ON SILICA GEL C_{18} OF PURE STANDARD PIGMENTS

Solvent system: methanol–acetone–water (20:4:3).

Pigment	R_F value	Colour on plate	
		White light	UV radiation
Rhodin g_7	0.88	Brown-green	Red fluorescence
Chlorin e_6	0.84	Green-grey	Red fluorescence
Pheophorbide *b*	0.75	Brown-green	Red fluorescence
Pheophorbide *a*	0.69	Grey	Red fluorescence
Pyropheophorbide *b*	0.62	Brown-green	Red fluorescence
Purpurin *b*	0.61	Lemon-green	No fluorescence
Pyropheophorbide *a*	0.58	Grey	Red fluorescence
Purpurin *a*	0.56	Brown	No fluorescence

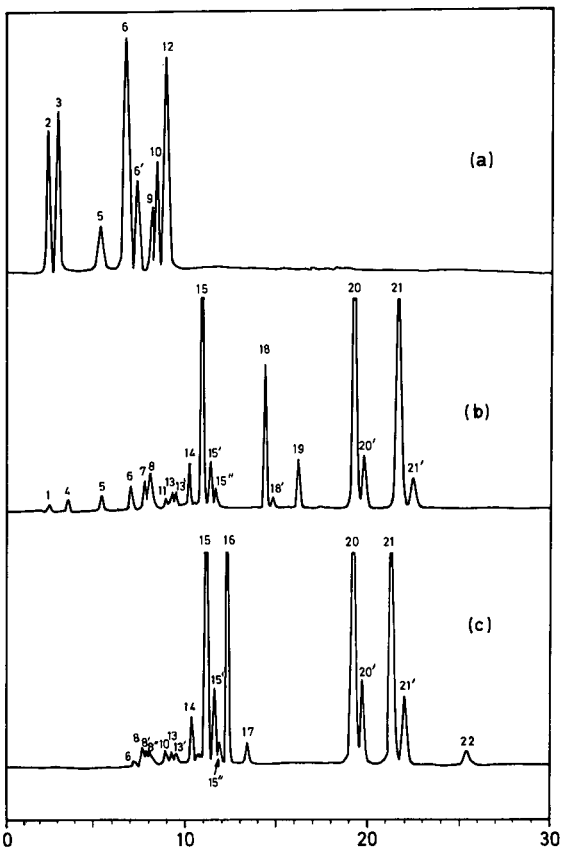

Fig. 2. HPLC: (a) standards obtained from the oxidation of pheophorbides; (b) pigments present in fermenting olives; (c) pigments present in fruits conserved in brine. Peaks: 1 = chlorophyllide *b*; 2 = rhodin g_7; 3 = chlorin e_6; 4 = chlorophyllide *a*; 5 = pheophorbide *b*; 6 = pheophorbide *a*; 6′ = pheophorbide *a*′ and purpurin *b*′ mixture; 7 = neoxanthin; 8 = neocrome; 8′ and 8″ = neocrome isomers; 9 = pyropheophorbide *b*; 10 = pyropheophorbide *a*; 11 = luteoxanthin; 12 = purpurin *a*; 13 = auroxanthin; 13′ = auroxanthin isomer; 14 = mutatoxanthin; 15 = lutein; 15′ and 15″ = lutein isomers; 16 and 17 = unknown pigments; 18 = chlorophyll *b*; 18′ = chlorophyll *b*′; 19 = chlorophyll *a*; 20 = pheophytin *b*; 20′ = pheophytin *b*′; 21 = pheophytin *a*; 21′ = pheophytin *a*′; 22 = pyropheophytin *a*. Gradient system described in ref. 3.

rhodin and purpurin *a* and *b*, including pheophorbides from their corresponding pyro derivatives. Only the mixture of purpurins and pyropheophorbides offered any resistance to separation, but as this situation does not occur very frequently, it is not a real problem. Therefore, there conditions were chosen to achieve individually purified pigments and to obtain standards that were used later in HPLC.

Fig. 1 shows the chromatogram of the standards obtained from the oxidation of pheophorbides. Small amounts of pheophorbides which had not undergone decarbomethoxylation were separated from the pyro derivatives. At the same time, purpurin *a* and purpurin *b* were accompanied by remains of chlorin and rhodin, respectively, and these in turn by traces of these esterified compounds. Once the pure standards had been obtained, a mixture of them was developed and successfully separated. Table I shows the chromatographic characteristics found for each pure component studied.

Separation of pigments by HPLC

Fig. 2a, b and c show the chromatograms for the separation, applying the gradient system described by Mínguez-Mosquera *et al.* [3], of the mixture of all purified standard pigments, of the pigments present in fermenting olives and of pigments present in fruits conserved in brine, respectively. In the last instance it can be seen that peaks 16 and 17 corresponding to the new pigments, possibly formed during the conservation in brine of table olives, do not correspond to any of the studied chlorophyll derivatives. At first they were identified incorrectly as isomers of pheophorbide *b* and *a*, respectively [3]. However, it was later shown that the localization of the maxima and the peak ratios in the absorption spectra of these compounds do not coincide exactly with those of pheophorbide *a* and *b*, but are identical with those of chlorin and rhodin. This result and the fact that the unknown pigments were eluted later than chlorin and rhodin, which means that they must be compounds of lower polarity, suggested that they might be esters of rhodin and chlorin, respectively. They could not be identified and at present it is not known when they were formed.

A detailed study of the standard separation by HPLC showed that all the pigments were eluted during the first 10 min of the 30-min gradient and that peak 6′ corresponded to a mixture of purpurin *a* and pheophorbide *a*. To improve the performance and reduce the separation time, different new gradient systems were tested. The optimum results were achieved with that given under Experimental, with which the total elution time was only 15 min. Using these conditions, the mixture of all the standards was separated by HPLC as shown in Fig. 3. Table II shows the spectroscopic and chromato-

TABLE II

SEPARATION OF STANDARD PIGMENTS BY HPLC

Capacity factor $k'_c = (t_r - t_m)/t_m$, where t_r = retention time of the pigment peak and t_m = retention time of an unretained component.

Peak No.	k'_c	Pigment	Spectral data in the eluent									
			Maxima (nm)[b]									Peak ratio[a]
			I	II	III	IV	V	VI	VII	VIII	IX	
1	0.76	Rhodin g_7	–	(408)	426	–	–	(530)	(570)	596	648	6.54
2	1.61	Chlorin e_6	–	–	400	–	500	532	–	602	660	3.86
3	4.13	Pheophorbide *b*	374	418	438	–	–	532	–	600	654	4.25
4	5.15	Pheophorbide *a*	(380)	(400)	410	–	504	536	–	608	666	2.48
5	5.36	Purpurin *b*	–	(420)	436	–	–	522	560	622	674	5.10
6	5.57	Pheophorbide *a*	(380)	(400)	410	–	504	536	–	608	666	2.48
7	6.08	Pyropheophorbide *b*	374	418	438	–	–	532	–	600	654	4.25
8	6.25	Pyropheophorbide *a*	(380)	(400)	410	–	504	536	–	608	666	2.48
9	6.60	Purpurin *a*	358	–	410	474	503	544	–	638	698	2.74

[a] Soret band (peak III) absorbance divided by the maximum absorbance in the red region (peak IX).

[b] The values in parentheses indicate inflection points in the absorption spectrum.

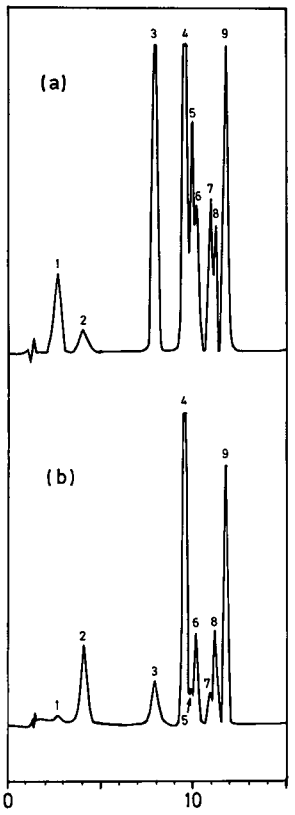

Fig. 3. HPLC of standard pigments mixture (20 μl). Detection by absorbance at (a) 430 and (b) 400 nm. Peaks: 1 = rhodin g_7; 2 = chlorin e_6; 3 = pheophorbide *b*; 4 = pheophorbide *a*; 5 = purpurin *b*; 6 = pheophorbide *a* isomer; 7 = pyropheophorbide *b*; 8 = pyropheophorbide *a*; 9 = purpurin *a*. Linear gradient system: 100% water–ion-pair reagent–methanol (1:1:8, v/v/v) to 100% acetone–methanol (1:1, v/v) in 15 min.

graphic characteristics of the pigments separated, including the capacity factors, absorption maxima in the eluent and peak ratios.

CONCLUSIONS

The study carried out on highly oxidized derivatives of pheophorbides permitted the development of a rapid HPLC method for the separation of these compounds. The method is of interest for easily detecting oxidation reactions that are undesirable during green table olive fermentation and for stricter control of this process. Equally, this method could be applied to detect these anomalous compounds in other feed products with chlorophylls as constituents and which have been processed, *e.g.*, canned vegetables, pickles and virgin olive oil.

ACKNOWLEDGEMENTS

The authors express their sincere gratitude to CICYT for supporting this research project, ALI91-1166-C03-02. Thanks are also due to M. Bodineau-Bada for technical assistance.

REFERENCES

1 M. I. Mínguez-Mosquera, J. Garrido-Fernández and B. Gandul-Rojas, *J. Agric. Food Chem.*, 37 (1989) 8.
2 S. J. Schwartz, S. L. Woo and J. H. Von Elbe, *J. Agric. Food Chem.*, 29 (1981) 533.
3 M. I. Mínguez-Mosquera, B. Gandul-Rojas, A. Montaño-Asquerino and J. Garrido-Fernández, *J. Chromatogr.*, 585 (1991) 259.
4 P. H. Hynninen, *Acta Chem. Scand.*, 27 (1973) 1771.
5 G. Sievers and P. H. Hynninen, *J. Chromatogr.*, 134 (1977) 359.
6 M. I. Mínguez-Mosquera and J. Garrido-Fernández, *J. Agric. Food Chem.*, 37 (1989) 1.
7 M. I. Mínguez-Mosquera, B. Gandul-Rojas and J. Garrido-Fernández, *Grasas Aceites*, 40 (1989) 114.
8 T. Watanabe, A. Hongu, K. Honda, M. Nakazato, M. Konno and S. Saitoh, *Anal. Chem.*, 56 (1984) 251.
9 I. D. Jones, L. S. Butler, E. Gibbs and R. C. White, *J. Chromatogr.*, 70 (1972) 87.

Journal of Chromatography, 633 (1993) 300–304
Elsevier Science Publishers B.V., Amsterdam

CHROM. 24 792

Short Communication

Quantitation of azadirachtins in insecticidal formulations by high-performance liquid chromatography

Clifford J. Hull, Jr.*, Walter R. Dutton and Barbara S. Switzer

Research Division, W. R. Grace & Company, Washington Research Center, 7379 Route 32, Columbia, MD 21044 (USA)

(First received September 25th, 1992; revised manuscript received December 2nd, 1992)

ABSTRACT

A sensitive high-performance liquid chromatographic procedure for the quantitative determination of azadirachting A and estimates of other azadirachtins in insecticidal formulations is described. The procedure utilizes reversed-phase chromatography with detection by UV absorption at 215 nm. The quantitative method described has been found to be accurate to within ±10% relative between the concentrations of 0.005 and 0.75% (w/w) azadirachtin A in insecticidal formulations of neem kernel extract. The lower limit of detection is 0.001% (w/w).

INTRODUCTION

Azadirachtin is a limonoid of the tetranortriterpenoid type found in the neem (*Azadirachta indica*) and chinaberry (*Melia azedarach*) trees [1,2]. The Indian neem tree is a fast growing robust tree found throughout India, Pakistan and parts of Africa as well as other parts of the world (*e.g.*, Australia and Haiti) [3]. Nearly the entire tree —roots, leaves and fruits— can potentially be used for agricultural, industrial and commercial products [4]. In particular, formulations made from neem kernel extract hold promise for use as plant protection products.

Since its isolation by Butterworth and Morgan [5], much world-wide interest, both academic and industrial, has developed in azadirachtin and related compounds due primarily to its powerful antifeedant and growth-disruptive activity toward a variety of insect pests [6,7]. In fact, azadirachtin is one of the most powerful naturally occurring insect-feeding deterrents known [8] from a botanical source. In spite of its powerful insecticidal activity, azadirachtin is non-mutagenic [9] and does not appear to exhibit any mammalian toxicity [10,11]. With increasing awareness of the hazards of chemical insecticides, the availability of a safe, natural product for insect and pest control is very attractive.

Azadirachtin is only one of many tetranortriterpenoids present in neem kernel which exhibit some degree of insecticidal properties. Others include salannin [12], nimbidin [13], and meliantriol [14]. Nevertheless, azadirachtin appears to be the most active of any of the limonoids studied. Recent work has demonstrated that azadirachtin itself should be designated azadirachtin A, since there exist at least six other compounds isolated from neem kernels that are structurally very similar to azadirachtin (designated B–G) [7,15]. Commercial products made

* Corresponding author.

0021-9673/93/$06.00

from seed extract, then, will have a multitude of natural products present in addition to azadirachtin A. Formulations from neem kernels may contain additional constitutents such as triglycerides, fatty acids and surfactants which can interfere with chromatographic analysis. A rapid and reliable method for determining azadirachtin A concentration is needed in order to determine the quality and potency of such complex insecticidal formulations.

Several HPLC methods have described reversed-phase methodology for the purification or analysis of azadirachtin [15–19] as well as an supercritical fluid chromatography (SFC) method [20]. However, these methods have been applied to relatively "clean" matrices at the end of an isolation procedure or have used a technique such as SFC which is not routine instrumentation. No reports have described the routine separation of azadirachtin A from azadirachtin B in insecticidal formulations. Here we present a sensitive and rugged HPLC method capable of quantifying azadirachtin A in stable, commercial formulations of neem kernel extract.

EXPERIMENTAL

Reagents and materials

Acetonitrile, methanol and tetrahydrofuran (THF) were from Baker (Phillipsburg, NJ, USA). Eluents were prepared with water purified by a Milli-Q water purification system (Millipore). Solid-phase extraction (SPE) tubes (C_{18}, 3 ml, 500 mg adsorbant) were from Baker and used without conditioning. Azadirachtin A was isolated essentially according to the procedure of Schroeder and Nakanishi [21]. From 11 kg of neem kernels, approximately 8 g of 77% pure azadirachtin A were isolated. Approximately 500 mg of this were further purified by preparative HPLC to 200 mg of >95% purity. The purity of azadirachtin A was determined using quantitative NMR and optical rotation measurements [22].

Equipment

The chromatographic system consisted of Waters Model 510 pumps, a WISP autosampler, Model 680 gradient controller and Model 480 variable-wavelength detector; all from Waters Associates (Milford, MA, USA). Data collection and handling was accomplished using LCI-100 integrators and a Chromatographics 3 Data System (Perkin-Elmer, Norwalk, CT, USA). A Supelcosil RP-8 column (15 cm × 4.6 mm, 3 μm)(Supelco, Bellefonte, PA, USA) with a guard column (2 cm, 40 μm) was used for all reversed-phase work and the azadirachtins were monitored at 215 nm. The neem components were eluted isocratically with acetonitrile–water (28:72, v/v) followed by a column wash using THF–acetonitrile (90:10). A 10-μl injection size was used at a flow-rate of 1.0 ml/min. For preparative-scale work, a Supelcosil RP-8 column (25 cm × 2.5 cm) was used.

The NMR spectra were collected with a Bruker AC 300 or AM 400. Azadirachtin was prepared in deuterated chloroform or deuterated methanol. ^1H NMR spectra were collected with a relaxation time of 15 s. Azadirachtin spectra were referenced against two internal standard spikes of quinoxiline and trimethoxybenzene for the purposes of quantitation.

Standard preparation

Azadirachtin A was prepared at approximately 1.0 mg/ml concentrations in methanol and stored at −20°C. This preparation was found to be stable for at least 6 months. From this stock standard appropriate dilutions are made into methanol to cover the concentration range 0.010 to 0.150 mg/ml azadirachtin A. These calibration standards are stable for at least 2 months when kept refrigerated.

Sample preparation

Samples of the insecticide formulation (Margosan-O Botanical Insecticide Concentrate) were prepared by carefully weighing (± 0.1mg) 500 μl of a vortexed aliquot into 9.5 ml of methanol–water (90:10). This diluted sample was then vortexed for 30 s before application of 2 ml to a C_{18} SPE tube (unconditioned) in order to retain unwanted materials which fouled the HPLC column. The liquid was eluted at < 2 ml/min, the first 0.5 ml was discarded and the remainder was dispensed into an autosampler vial.

Different sample diluents for SPE were evaluated to determine optimal retention of column fouling compounds (triglycerides) while maintaining 100% azadirachtin A recovery. SFC was employed to detect triglyceride levels in the SPE filtrates. A metha-

nol–water (90:10) mixture resulted in greater than 98% adsorption of triglycerides and fatty acids with full recovery of azadirachtin A and B.

Internal standards were occasionally used in storage stability studies. Several candidates were evaluated including benzyl alcohol, phenyl ethanol and phenyl propanol. Phenyl propanol was judged to be the most suitable internal standard based on its elution in an area free of other components.

RESULTS AND DISCUSSION

The two major challenges associated with the development of this chromatographic procedure were the separation of azadirachtin A from azadirachtin B and the effective gradient washing of trigylcerides, fatty acids and other components from the reversed-phase column. This washing procedure resulted in substantial extension of the column lifetime.

Chromatographic separation

Since a multitude of other limonoids and natural products are present in neem kernel extract, an efficient chromatographic method is required to obtain resolution of azadirachtin A from these other constitutents. The nearest eluting neighbor to azadirachtin A was azadirachtin B as confirmed by liquid chromatography–mass spectrometry of both standards and formulations. Initial chromatographic separations did not resolve the A and B azadirachtins. Several different columns were tested including C_{18} and C_8 materials from different manufacturers. Several different blends of methanol, acetonitrile and tetrahydrofuran with water were examined. Modifiers such as trifluoroacetic acid and acetic acid were examined as well as buffered mobile phases. The conclusion was that a 15 cm 3 μm C_8 column (Supelco) was found to give the best resolution between azadirachtin A and B with an acetonitrile-water mobile phase. Though a 25 cm column (5 μm) would give slightly better resolution, the equilibration time after the wash would have incurred a long turnaround time for each analysis ($>$ 50 min). The shorter column provided adequate resolution with a minimum turnaround time. Though the method is reliable and rugged, care must be taken when preparing the mobile phase as a small error in acetonitrile concentration gave a significant shift in azadirachtin A retention.

Since the chromatographic run was isocratic and the insecticidal formulation contains significant amounts of triglycerides and other components, carryover peaks were observed in subsequent chromatographic runs. To alleviate this problem, a suitable washing procedure was required. After investigation of several organic modifiers including methanol, isopropanol and acetonitrile, THF was found to be most effective. After elution of the azadirachtins (typically 19–24 min) the THF mobile phase was introduced and held for 5 min before returning to the acetonitrile–water (28:72). After an equilibration time of 10 min, the next injection was made. Total run time was thus 38 min. The THF washing protocol resulted in extending the column lifetime from an average of 150 injections to over 2000 injections. Representative chromatograms of purified azadirachtin A and of formulation containing azadirachtin A and B are shown in Fig. 1.

Estimation of concentration of azadirachtin B and other limonoids

Based on the structures of azadirachtin A and B and other limonoids such as salannin, one can estimate that the extinction coefficients of these compounds are similar. Chromatographic separations using a photodiode array detector revealed that the spectra for azadirachtin A and B were very similar. Most of the contribution to absorbance at 215 nm is from the α,β-unsaturated carbonyl chromophore in the tiglate ester and the vinyl ether. For limonoids that have similar types and numbers of such moieties this estimation should be reasonable. By assigning an extinction coefficient to azadirachtin B equivalent to that of azadirachtin A, one can generate estimates of the concentration of azadirachtin B. A similar procedure can be used to estimate other identifiable azadirachtin analogs and limonoids whose structures are sufficiently similar to that of azadirachtin A.

Precision and recovery

Precision was determined by analysis of six preparations of a neem kernal extract formulation. The precision of the method was 3.5% relative standard deviation.

Recovery was determined by spiking two preparations of the formulation at two different levels of azadirachtin A before analysis. Formulations con-

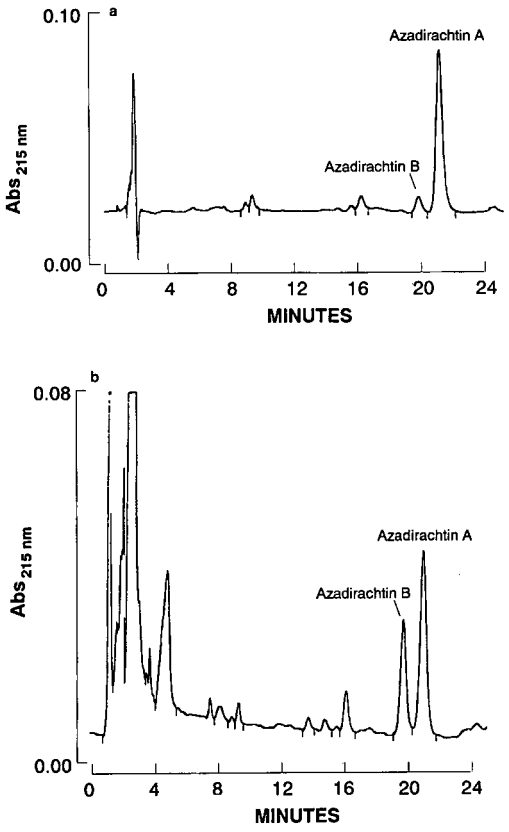

Fig. 1. (a) HPLC separation of purified azadirachtins A and B. The injection represents 0.08 mg/ml of azadirachtin A. (b) HPLC separation of azadirachtins A and B in Margosan-O. The injection represents a 50 mg/ml preparation of the formulation and 0.07 mg/ml of the azadirachtins.

taining approximately 0.126 mg/ml azadirachtin A were spiked at levels of 0.164 mg/ml and 0.302 mg/ml. Recovery ranged from 93 to 106%.

CONCLUSIONS

A procedure for the accurate quantification of azadirachtin A in insecticidial formulations has been presented. In addition, an estimation of azadirachtin B concentration can be derived from the method. The chromatography gives excellent resolution of azadirachtin A from azadirachtin B. The method is rugged and accurate and capable of quantifying azadirachtin A in the complex matrix containing oils, surfactants and other limonoids.

ACKNOWLEDGEMENTS

The authors wish to thank Charles G. Carter and Deborah Peru for isolation of azadirachtin A, Steven R. Prescott and James F. Walter for helpful discussions, James Cushman and Mark Brickhouse for NMR support, Patrica Gill and Raymond Rose for technical assistance, Jack Stuff for SFC support and Bret Jurd for preparative HPLC support.

REFERENCES

1 H. Schmutterer, K. R. S. Ascher and H. Rembold (Editors), *Natural Pesticides from the Neem Tree (Azadirachtia indica A. Juss); Proceedings of the 1st International Neem Conference, Rottach-Egern, 1980*, German Agency for Technical Cooperation, Eschborn, 1982.
2 H. Schmutterer and K. R. S Ascher (Editors), *Natural Pesticides from the Neem Tree (Azadirachtia indica A. Juss) and other Tropical Plants; Proceedings of the 2nd International Neem Conference, Rauischholzhausen, 1983*, German Agency for Technical Cooperation, Eschborn, 1984.
3 N. Veitmeier (Editor), *Firewood Crops —Shrub and Tree Species for Energy Production*, National Academy of Sciences, Washington, DC, 1980, p. 7.
4 S. S. Radwanski and G. E. Wickens, *Econ. Bot.*, 35 (1981) 398.
5 J. H. Butterworth and E. D. Morgan, *J. Insect Physiol.*, 17 (1971) 969.
6 J. D. Warthen, Jr., *Agric. Res. Results (Northeast Ser.)*, 4 (1979) 21.
7 H. Rembold, H. Wagner and R. Norman (Editors), *Economic and Medicinal Plant Research*, Vol. 3, Academic Press, New York, 1989, p. 57.
8 I. Kubo and J. A. Klocke, *Agric. Biol Chem. 46 (1982) 1951–1953.*
9 M. Jacobson, H. Schmutter, K. R. S. Ascher and H. Rembold (Editors), *Natural Pesticides from the Neem Tree (Azadirachtia indica A. Juss); Proceedings of the 1st International Neem Conference, Rottach-Egern*, 1980, German Agency for Technical Cooperation, Eschborn, 1982 pp. 33–42.
10 K. Nakanishi, *Rec. Adv. Phytochem.*, 9 (1975) 283–298.
11 E. D. Morgan, H. Schmutter, K. R. S. Ascher and H. Rembold (Editors), *Natural Pesticides from the Neem Tree (Azadirachtia indica A. Juss); Proceedings of the 1st International Neem Conference, Rottach-Egern, 1980*, German Agency for Technical Cooperation, Eschborn, 1982, pp. 43–52.
12 J. D. Warthen Jr., E. C. Uebel, S. R. Dutky, W. R. Lusby and H. Finegold, *Agric. Res. Results (Northeast. Ser.)*, 2 (1978) 11.
13 S. Radwanski, *World Crops Livestock*, 29 (1977) 167–168.
14 D. Lavie, M. K. Jain and S. R. Shpan-Gabrielith, *Chem. Commun.*, (1967) 910–911.
15 T. R. Govindachari, G. Sandhya and S. P. Ganeshraj, *Chromatographia*, 31 (1991) 303.
16 J. D. Warthen, J. B. Stokes, M. Jacobson and M. F. Kozempel, *J. Liq. Chromatogr.*, 7 (1984) 591.

17 R. B. Yamasaki, J. A. Klocke, S. M. Lee, G. A. Stone and M. V. Darlington, *J. Chromatogr.*, 356 (1986) 220.
18 T. R. Govindachari, G. Sandhya and S. P. Ganeshraj, *J. Chromatogr.*, 513 (1990) 389.
19 E. C. Uebel, J. D. Warthen, Jr. and M. Jacobson, *J. Liq. Chromatogr.*, 2 (1979) 875.
20 H.-P. Huang and E. D. Morgan, *J. Chromatogr.*, 519 (1990) 137–143.
21 D. R. Schroeder and K. Nakanishi, *J. Mat. Prod.*, 50 (1987) 241.
22 W. Kraus, M. Bokel, A. Bruhn, R. Cramer, I. Klaiber, A. Klenk, G. Nagl, H. Pohnl, H. Sadlo, and B. Vogler, *Tetrahedron*, 43 (1987) 2817.

Journal of Chromatography, 633 (1993) 305–310
Elsevier Science Publishers B.V., Amsterdam

CHROM. 24 755

Short Communication

Ion interaction chromatography with nonylamine reagent for the determination of nitrite and nitrate in natural waters

Ewa Pobozy, Beata Sweryda-Krawiec and Marek Trojanowicz*

Department of Chemistry, University of Warsaw, Pasteura 1, 02-093 Warsaw (Poland)

(First received July 21st, 1992; revised manuscript received November 10th, 1992)

ABSTRACT

An ion interaction chromatography method for the determination of nitrate and nitrite using a reversed-phase C_{18} column is described. The eluent was 2.0 m*M* nonylammonium phosphate of pH 6.5 and the UV detection wavelength was 205 nm. For a sample volume of 200 μl detection limits of 2.0 and 1.5 μg/l were obtained for nitrite and nitrate, respectively. The change of the detection wavelength to 190 nm enables also the quantitative detection of chloride. Results obtained for natural waters have been correlated with those obtained using standard spectrophotometric procedures.

INTRODUCTION

Among commonly used high-performance ion-chromatographic methods such as eluent-suppressed or single-column ion-exchange chromatography, ion exclusion chromatography or ion interaction chromatography, the last technique exhibits several advantages. Numerous examples of the use of all these techniques for nitrate and nitrite determination can be found in the literature [1]. The use of non-polar stationary phases covered with suitable ion-pairing reagents provides a wider variability of chromatographic parameters than other methods. In the past this method was widely employed for the separation of ionic and ionizable organic solutes, including biomolecules, and recently for the separation of inorganic ions. Because reversed-phase columns are readily available this approach is attractive. Ion interaction chromatography can be carried out using conventional HPLC instrumentation with most common phases and with numerous detection methods, including UV detection.

In ion interaction chromatography of inorganic anions, the most frequently used ion interaction reagents (column modifiers) are quaternary ammonium salts with hydrophobic long-chain aliphatic or aromatic groups [2–6]. As was shown for the first time by Skelly [7], with the use of different reversed-phase columns salts of long-chain primary aliphatic amines can also be very satisfactory column modifiers. Among butylamine, hexylamine, octylamine and decylamine, the best results were obtained with octylamine. This reagent was subsequently used by several workers in ion interaction chromatography with direct UV detection [8–10]. In a comparative study of different amines as ion

* Corresponding author.

0021-9673/93/$06.00

interaction reagents, an increase in the retention of inorganic anions with an increase in the length of the aliphatic chain was observed [11,12]. A comparison of heptylamine and octylamine indicated an increase in sensitivity of determination with the larger alkyl group [9].

In spite of preliminary modification of the column, the presence of an ion interaction reagent in the eluent was found to be necessary [7]. As counter ions in the amine salts used as column modifiers, perchlorate [11], salicylate [9] and most often weakly UV-absorbing phosphate [7,8,10] have been applied. The use of sulphonate as the eluting anion allows the indirect spectrophotometric detection of anions that do not absorbing UV radiation as chloride or sulphate [11].

Nonylamine has been used as a column modifier only by Dreux *et al.* [11]. Owing to the possibility of decreasing its concentration in the eluent in comparison with heptylamine or octylamine, better detectability with conductivity detection can be obtained. Using this ion interaction reagent a better sensitivity of UV detection at 204 nm than with conductivity was demonstrated.

The aim of this study was to optimize the ion interaction chromatographic determination of inorganic anions with the use of reversed-phase C_{18} columns modified with nonylamine with special emphasis on nitrite and nitrate, which are of significant importance for environmental protection. Results obtained for natural waters were verified using standard spectrophotometric procedures. Numerous other methods for nitrite and nitrate determination can be also found [12].

EXPERIMENTAL

Apparatus

The 3D HPLC system consisted of a Perkin-Elmer (Norwalk, CT, USA) Series 100 pump, a Rheodyne Model 7125 injection valve and a Tridet detector (Bacharach, Pittsburgh, PA, USA). For detection in the UV range a Knauer (Bad Homburg, Germany) variable-wavelength Type 87.00 monitor equipped with a 10-mm path-length flow-through cuvette of 10-μl volume was used. A PR-18 (5 μm) reversed-phase C_{18} column (250 × 4.0 mm I.D.) from ZOCh (Lublin, Poland) was employed. For pH measurements a Radelkis (Budapest, Hungary) OP-265 pH meter equipped with a combined glass–calomel electrode was used.

Reagents

As ion interaction reagents nonylamine and cetyltrimethylammonium bromide (CTAB) from Koch-Light and tetrabutylammonium bromide (TBAB) from Fluka were used. All other reagents used were of analytical-reagent grade from POCh (Gliwice, Poland). Deionized water obtained using a Milli-Q system (Millipore) was used for preparing solutions.

Mobile phases consisted of the ion interaction reagent with the pH was adjusted with concentrated orthophosphoric acid or 0.1 *M* sodium dihydrogenphosphate solution.

The column was washed with 500 ml of acetonitrile–water (1:1) and then with 100 ml of deionized water pumped at 1 ml/min before use. Preliminary modification of the column was carried out using 500 ml of 10 m*M* nonylammonium orthophosphate solution of pH 6.5 delivered at 1.0 ml/min.

Reference determinations of nitrate and nitrite

As reference methods for the determination of nitrate and nitrite widely accepted standard spectrophotometric procedures were used. Determination of nitrate was based on reaction of nitrate with sodium salicylate in concentrated sulphuric acid [13]. Nitrosalicylic acid formed in this reaction gives in alkaline solution an ionized yellow product, the absorbance of which is measured at 410 nm. For determination of nitrite a highly sensitive and specific modified Griess method was employed, involving the formation of an azo dye by reaction of nitrite with sulphanilic acid and 1-naphthylamine at pH 2.0–2.5, with spectrophotometric detection at 520 nm [14].

RESULTS AND DISCUSSION

Optimization of chromatographic parameters

Owing to their strong absorption in the UV region, for the chromatographic detection of nitrite and nitrate direct UV detection can be utilized if the eluent does not contain too high concentrations of UV-absorbing species. In an earlier report on the use of columns, UV detection was used in the wavelength range 204–254 nm [7–11]. It was found in this study that maximum absorption of nonylamine

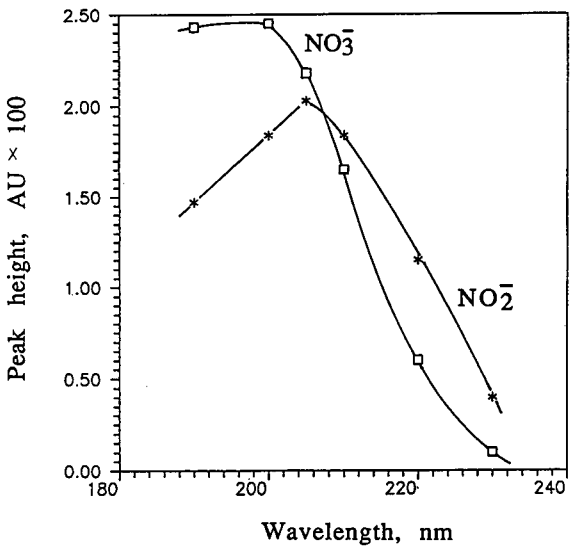

Fig. 1. Effect of wavelength on the detection of nitrite and nitrate by ion interaction chromatography using as eluent 2.0 m*M* nonylammonium phosphate (pH 6.5). Injection volume, 10 μl of 10 mg/l nitrite and nitrate solutions; flow-rate, 1 ml/min.

occurs at 220 nm, and the dependence of the peak height for nitrite and nitrate on wavelength was examined (Fig. 1). For nonylammonium phosphate solution as eluent the optimum wavelength for determination of nitrite and nitrate was taken to be 205 nm, where the best detectability is observed for nitrite, usually present at much lower levels than nitrate in natural samples. Under those conditions almost 90% of maximum sensitivity can be obtained for nitrate. The same wavelength has been already applied by other workers with the use of octylamine as modifier [8,11].

The concentration of modifier in the eluent and the concentration of the eluting anion have a substantial influence on the resolution of anions by ion interaction chromatography. The latter can be adjusted by changing the total concentration of the anion in the eluent solution or, for anions of weak acids, by changing the pH of the eluent. In this study the optimization of the eluent composition was carried out at a constant pH of 6.5 and as orthophosphate was used as the counter anion (Table I). From examination of a wide range of nonylamine concentrations, 2.0 m*M* was adopted as the optimum at the same total concentration of phosphate in the eluent solution. Under those conditions, the detection limits for a signal-to-noise ratio of 2 were calculated to be 2.0 μg/l for nitrite and 1.5 μg/l for nitrate for a sample volume of 200 μl. A further improvement in detectability can be obtained by increasing the

TABLE I

EFFECT OF ELUENT COMPOSITION ON SEPARATION OF NITRITE AND NITRATE AT ELUENT pH 6.5

Injected sample volume, 20 μl; detection wavelength, 205 nm.

Concentrations of eluent components (m*M*)		Retention time (min)	
Nonylamine	Phosphate	Nitrite	Nitrate
10	2	9.5	16.5
2	2	5.5	6.6
	3.5	3.8	4.8
0.5	2	4.6	5.8

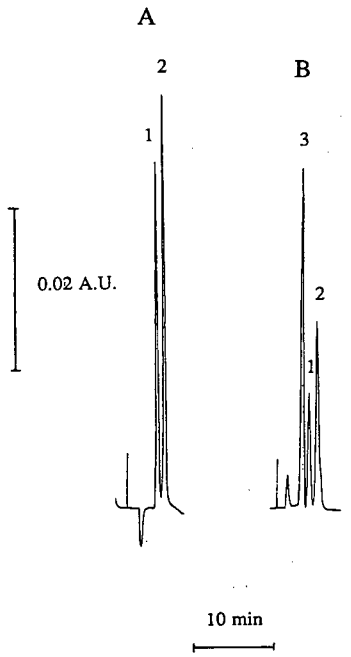

Fig. 2. Ion chromatograms obtained for injection of 200 μl of a mixture of 0.5 mg/l nitrite and nitrate and 20 mg/l chloride solutions, obtained (A) at 205 nm using as eluent 2.0 m*M* nonylamine solution (pH 6.5) containing 3.5 m*M* orthophosphate and (B) at 190 nm using as eluent 2.0 m*M* nonylammonium phosphate (pH 6.5). Peaks: 1 = nitrite; 2 = nitrate; 3 = chloride.

TABLE II

CHARACTERISTICS OF ION INTERACTION CHROMATOGRAPHY OF NITRITE AND NITRATE USING DIFFERENT ION INTERACTION REAGENTS IN ELUENTS UNDER OPTIMIZED CONDITIONS

Separation parameter	Ion interaction reagent[a]		
	CTAB	TBAB	Nonylamine
Resolution (R_s)	1.0	2.2	3.7
Theoretical plate number (N) for nitrate	280	2800	2800
Eluent	0.25 m*M* KHP–0.1 m*M* CTAB (pH 6.5)	5.0 m*M* KPH–0.2 m*M* TBAB (pH 6.5)	2.0 m*M* NPH (pH 6.5)
Detection wavelength (nm)	254	215	205
Retention time (min)			
Nitrite	3.7	3.8	5.5
Nitrate	5.8	4.3	6.6
Chloride			4.1
Bromide			4.8
Iodide			7.2
Thiocyanate			13.3
Sulphate			19.7

[a] CTAB = Cetyltrimethylammonium bromide; TBAB = tetrabutylammonium bromide; KHP = potassium hydrogenphthalate; KPH = potassium orthophosphate; NPH = nonylammonium orthophosphate.

phosphate concentration in the eluent, but it is accompanied by a loss of baseline resolution of the nitrite and nitrate peaks.

For the modifier used in this study it was confirmed that a single preliminary modification of the non-polar stationary phase is not sufficient for obtaining long-term stable values of retention times. For eluents containing nonylamine the deviations of the retention times during 5 days did not exceed ± 0.2 min. The precision of determination based on peak-height measurements, expressed as relative standard deviation for $n = 10$, was 1.5% for 0.5 mg/l of nitrate and 1.1% for 0.5 mg/l of nitrite.

Because of planned environmental application of the developed method, the effect of the presence of excess of chloride and sulphate on the determination of nitrite and nitrate was also examined. A 100 mg/l concentration of those two anions did not affect results. It was found, however, changing the detection wavelength from 205 to 190 nm permits the determination of chloride, as illustrated in Fig. 2.

The results obtained by ion interaction chromatography with nonylamine as modifier were compared with those obtained under optimum conditions and with the same instrumental set-up for other frequently used modifiers, CTAB and TBAB (Table II). This comparison illustrates well the effectiveness of the method developed in this study. In order to complete the characteristics of the system in Table II, retention times are included for several other anions.

Determination of nitrite and nitrate in natural waters

The chromatographic literature contains already several examples of the use of ion interaction chromatography with direct UV detection for the determination of nitrite and nitrate in waters with the use of tetraalkylammonium salts as modifiers [4–6] and long-chain primary amines [7–10]. Using tetrapentylammonium fluoride, satisfactory results for nitrate determination in the range 21–134 mg/l in well waters were obtained [4]. In the determination of nitrate using tetramethylammonium phosphate, the results obtained differed from those given by the standard UV method [5]. Using a C_{18} column modified with cetyltrimethylammonium chloride with UV detection for nitrate and amperometric detection for nitrite, satisfactory recovery results

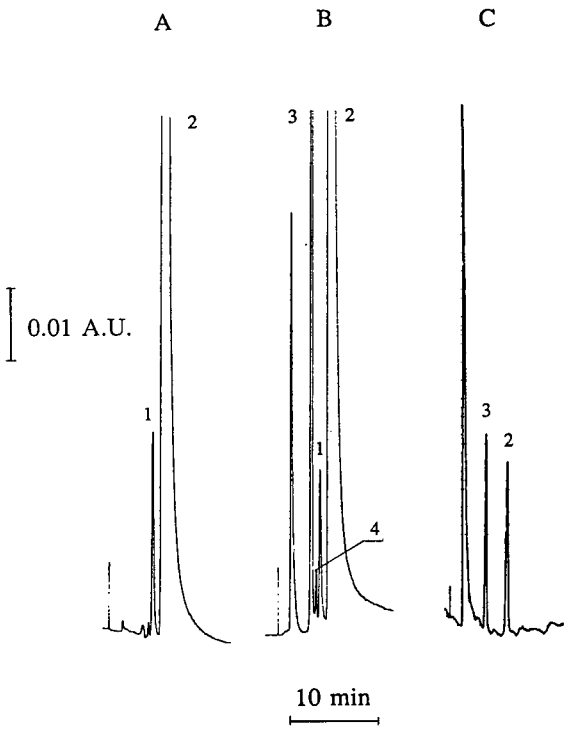

Fig. 3. Ion chromatograms obtained for a well water sample using direct UV detection at (A) 205 and (B) 190 nm and (C) conductivity detection. Eluent, 2.0 m*M* nonylammonium phosphate (pH 6.5). Sample volume, 10 μl. Peaks: 1 = nitrite; 2 = nitrate; 3 = chloride; 4 = bromide.

were obtained for the determination of both species in sea water [6].

In earlier studies in which octylamine was used as a modifier and chromatograms of natural waters [9,10] or plant extracts [7,8] were shown, the correlation with standard reference methods was not reported, hence it seemed to be valuable to carry out such a study for the present system with nonylamine as stationary phase modifier.

The reference spectrophotometric methods used for the determination of nitrate and nitrite were outlined under Experimental. Natural water samples were analysed soon after collection and filtered using a 0.45-μm filter. Fig. 3 shows chromatograms obtained for a well water sample at different detection wavelengths. For comparison, a chromatogram obtained with the same eluent with conductivity detection is shown. These results clearly demonstrate the much better detectability of UV detection under given chromatographic conditions.

The results given in Table III demonstrate satisfactory agreement between the results obtained by ion interaction chromatography and the reference spectrophotometric methods.

REFERENCES

1 P. R. Haddad and P. E. Jackson, *Ion Chromatography: Principles and Applications*, Elsevier, Amsterdam, 1990.
2 R. M. Cassidy and S. Elchuk, *Anal. Chem.*, 54 (1982) 1558.
3 W. E. Barber and P. W. Carr, *J. Chromatogr.*, 260 (1983) 89.
4 Z. Iskandarni and D. J. Pietrzyk, *Anal. Chem.*, 54 (1982) 2601.
5 S. H. Kok, K. A. Buckle and M. Wootton, *J. Chromatogr.*, 260 (1983) 189.
6 K. Ho, A. Ariyoshi, F. Tanabiki and H. Sunahara, *Anal. Chem.*, 63 (1991) 273.
7 N. E. Skelly, *Anal. Chem.*, 54 (1982) 712.
8 B. Luckas, *Fresenius' Z. Anal. Chem.*, 320 (1985) 519.

TABLE III

RESULTS OF ION INTERACTION CHROMATOGRAPHIC DETERMINATION OF NITRITE AND NITRATE IN NATURAL WATER SAMPLES AT 205 nm USING AS ELUENT 2 m*M* NONYLAMMONIUM ORTHOPHOSPHATE (pH 6.5)

Injected sample volume, 10 μl.

Sample	Nitrite found (mg/l)		Nitrate found (mg/l)	
	Ion interaction chromatography	Spectrophotometry	Ion interaction chromatography	Spectrophotometry
River water I	0.082	0.081	10.8	11.5
River water II	0.27	0.26	10.4	11.4
Lake water	ND[a]	0.009	1.4	1.4
Tap water	ND	ND	5.5	5.3

[a] ND = Not detected.

9 M. C. Gennaro and P. L. Bertolo, *Ann. Chim. (Rome)*, 80 (1990) 13.
10 M. C. Gennaro, P. L. Bertolo and A. Cordero, *Anal. Chim. Acta*, 239 (1990) 203.
11 M. Dreux, M. Lafosse and M. Pequignot, *Chromatographia*, 15 (1982) 653.
12 W. J. Williams, *Handbook of Anion Determination*, Butterworths, London, 1979.
13 *Polish Standard*, PN-81/C-04576.08, Polski Komitet Normalizacji, Miar i Jakosci, Warsaw, 1981.
14 *British Standard*, 2690: Part 7, British Standards Institution, London, 1968.

Journal of Chromatography, 633 (1993) 311–314
Elsevier Science Publishers B.V., Amsterdam

CHROM. 24 767

Short Communication

Determination of ammonia as its benzenesulphonyldimethylaminomethylene derivative in environmental water samples by gas chromatography with flame photometric detection

Hiroyuki Kataoka*, Satoshi Ohrui, Akiko Kanemoto and Masami Makita

Faculty of Pharmaceutical Sciences, Okayama University, Tsushima, Okayama 700 (Japan)

(First received September 22nd, 1992; revised manuscript received November 18th, 1992)

ABSTRACT

A selective and sensitive method for the determination of ammonia by gas chromatography (GC) was developed. Ammonia was converted into its benzenesulphonyldimethylaminomethylene derivative by a convenient procedure involving benzenesulphonylation with benzenesulphonyl chloride and subsequent reaction with dimethylformamide dimethyl acetal, and was determined by GC with flame photometric detection (FPD) using a DB-1 capillary column. The derivative was very stable on standing in ethyl acetate, eluted as a single peak and provided an excellent response in the flame photometric detector. A linear calibration graph was obtained in the range 2–40 nmol of ammonia. The detection limit of ammonia was about 1.5 pmol injected. Ammonia in environmental water samples could be measured without interference from co-existing substances. The recoveries of ammonia added to environmental water samples were 95.0–97.5% and the relative standard deviations were 3.3–6.0%. Ammonia contents in several environmental water samples were 0–119.3·nmol/ml.

INTRODUCTION

Ammonia arises mainly from natural sources by decomposition of organic matter containing nitrogen and from manufacturing processes for industrial chemicals. Ammonia is irritant to the skin, respiratory tract and mucous membranes. Water pollution by ammonia often has a toxic influence on aquatic species.

The determination of ammonia in environmental water samples has been carried out by spectrophotometric methods [1–3], ammonia-selective electrode methods [4,5], gas chromatography (GC) [6–8] high-performance liquid chromatography (HPLC) [9] and flow-injection methods [10–12]. However, colour and turbidity in the sample interfere with spectrophotometric methods based on the indophenol blue reaction [1,2] or Nessler's reaction [3], and therefore a time-consuming preliminary distillation is required before analysis. The electrode methods are susceptible to intereferences from amines. GC methods based on headspace sampling give tailing peaks. HPLC and flow-injection methods based on spectrophotometric or fluorimetric detection are suitable methods, but some of them require preliminary clean-up of the sample by

* Corresponding author.

0021-9673/93/$06.00

using an ion-exchange column or a PTFE membrane before reaction with *o*-phthalaldehyde.

In this work, ammonia was analysed as its benzenesulphonyldimethylaminomethylene derivative by GC with flame photometric detection (FDP). Using this method, the content of ammonia in environmental waters was also studied.

EXPERIMENTAL

Reagents

Ammonium chloride (Nacalai Tesque, Kyoto, Japan) was dissolved in distilled water to make a stock standard solution of concentration 2 m*M*. *p*-Toluenesulphonamide (Tokyo Kasei Kogyo, Tokyo, Japan) as an internal standard (I.S.) was dissolved in 0.01 *M* potassium hydroxide solution to make a stock standard solution of concentration 2 m*M*. Benzenesulphonyl chloride (BSC) and N,N-dimethylformamide dimethyl acetal (DMF-DMA) were purchased from Nacalai Tesque. BSC was used a 20% solution in dioxane. All other chemicals were of analytical-reagent grade.

Gas chromatography

GC analysis was carried out with a Shimadzu 12A gas chromatograph equipped with a flame photometric detector (S-filter). A fused-silica capillary column (15 m × 0.53 mm I.D., film thickness 1.5 μm) of cross-linked DB-1 (J & W, Folsom, CA, USA) was used. The column temperature was 230°C, the injection and detector temperatures 260°C and the nitrogen flow-rate 10 ml/min.

Gas chromatography–mass spectrometry (GC–MS)

A Hewlett-Packard Model 5890A gas chromatograph was operated in conjunction with a VG Analytical Model 70-SE mass spectrometer and a VG-250J mass data system. The GC column was of the same type as used for GC, with an ionizing voltage of 40 eV, an ion-source temperature of 250°C and a helium flow-rate of 10 ml/min.

Derivatization procedure

An aliquot of the sample solution containing 2–40 nmol of ammonia was pipetted into a 10-ml Pyrex glass tube with a PTFE-lined screw-cap. To this solution were added 0.1 ml of 0.2 m*M* I.S. solution, 0.75 ml of dioxane and 0.1 ml of 2.5% sodium carbonate solution and the total reaction volume was made up to 1.5 ml with distilled water. After addition of 0.05 ml of BSC, the mixture (pH > 10) was shaken up and down at 3000 rpm for 5 min at room temperature. The reaction mixture was extracted twice with 3 ml of *n*-hexane in order to remove the excess of reagent. The aqueous layer was acidified to pH 1–2 with 2 *M* hydrochloric acid and then extracted twice with 3 ml of diethyl ether. To the pooled ethereal extracts were added 20 μl of DMF-DMA and the mixture was stood for 10 min in a hot-block bath at 80°C without a cap. After the solvent had evaporated to dryness, the residue was dissolved in 0.2 ml of ethyl acetate and then 0.5–1 μl of this solution was injected into the gas chromatograph. The derivatization process is shown in Fig. 1.

Preparation of reference compound

A reference sample of the benzenesulphonyldimethylaminomethylene derivative of ammonia, m.p. 131–132°C, was prepared from benzenesulphonamide (Tokyo Kasei Kogyo) in essentially the same manner as in the derivatization procedure. The elemental analysis was as follows: calculated for $C_9H_{12}N_2O_2S$: C 50.93, H 5.70, N 13.20; found: C 51.17, H 5.83, N 13.13%.

RESULTS AND DISCUSSION

In a previous paper on the determination of aliphatic primary amines [13], we reported that the benzenesulphonamide derived from ammonia overlapped with the benzenesulphonyl derivatives of methylamine on the chromatogram, but these derivatives could be separated by reaction with DMF-

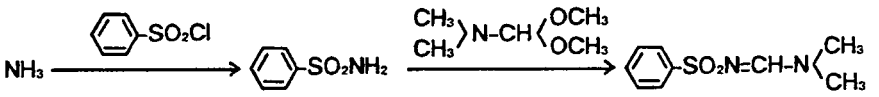

Fig. 1. Ammonia derivatization process.

DMA. The benzenesulphonamide was converted into the dimethylaminomethylene derivative, which has a longer retention time, but the benzenesulphonyl derivatives of primary amines did not react with DMF-DMA. These results indicate that ammonia could be selectively determined in samples containing low-molecular-mass primary amines such as methylamine and ethylamine. Experiments were conducted to find suitable reaction conditions for the preparation of the ammonia derivative. The benzenesulphonylation of ammonia with BSC was accomplished by shaking within 2 min at room temperature in aqueous alkaline media containing 50–70% of dioxane. By washing with hexane after benzenesulphonylation, excess of BSC and benzenesulphonyl derivatives of secondary amines were removed. The benzenesulphonyl derivative of ammonia reacted completely with DMF-DMA within 5 min at 80°C. The mean derivatization yield throughout the procedure established above was determined to be 94.6 ± 3.6% (n = 4) by comparison with the synthetic reference derivative.

The structure of the derivative was confirmed by both GC–MS and elemental analysis. As shown in Fig. 2, a molecular ion peak (M^+) with the postulated m/z 212 ion and prominent fragment ion peaks at m/z 141 [$M^+ - N{=}CHN(CH_3)_2$], 77 (C_6H_5), 71 [$N{=}CHN(CH_3)_2$] and 44 [$N(CH_3)_2$] were observed, and these peaks were useful for structure elucidation. The elemental analysis data agreed with the theoretical values calculated for the expected structure. These results supported the structure for the derivative shown in Fig. 1. The derivative was found to be very stable under normal laboratory conditions; no decomposition was observed even after standing in ethyl acetate for 2 weeks at room temperature.

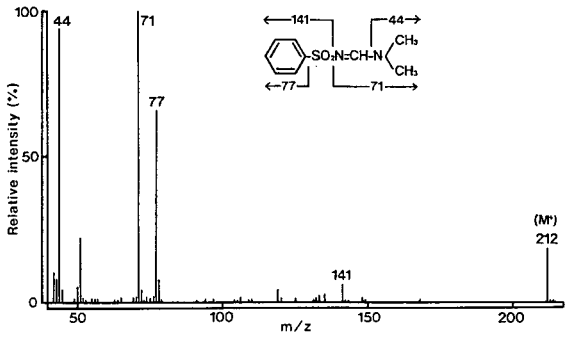

Fig. 2. Mass spectrum obtained by GC–MS of the benzenesulphonyldimethylaminomethylene derivative of ammonia.

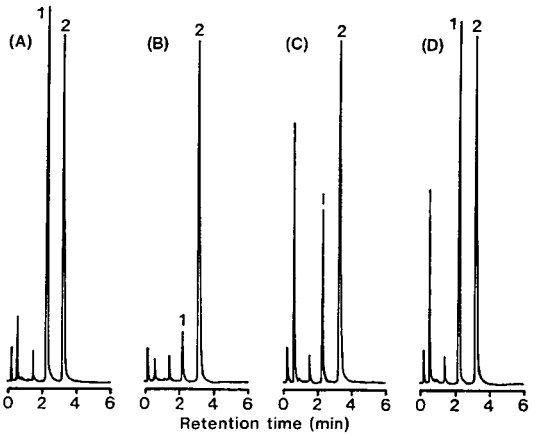

Fig. 3. Gas chromatograms obtained from a standard solution and river water samples. (A) Standard solution (containing 20 nmol of ammonia); (B–D) river waters. GC conditions are given under Experimental. Peaks: 1 = ammonia; 2 = p-toluenesulphonamide (I.S.).

As shown in Fig. 3A, the ammonia derivative was eluted as a single peak and provided an excellent response in the flame photometric detector. The minimum detectable amount of ammonia required to give a signal three times as high as the noise under our instrumental conditions was *ca.* 1.5 pmol injected. To test the linearity of the calibration graph, various amounts of ammonia ranging from 2 to 40 nmol were derivatized and aliquot representing 5–100 pmol were injected. A linear relationship was obtained from both logarithmic plots, and the regression line was $\log y = 1.064 \log x - 1.369$

TABLE I

RECOVERIES OF AMMONIA ADDED TO RIVER WATER SAMPLES

Sample	Ammonia added (nmol/ml)	Amount found[a] (nmol/ml)		Recovery (%)
		Without addition	With addition	
A	10	5.9 ± 0.3	15.4 ± 0.6	95.0
B	20	42.0 ± 1.4	61.4 ± 2.1	97.0
C	40	191.3 ± 11.4	230.3 ± 9.7	97.5

[a] Mean ± S.D. (n = 3).

TABLE II

AMMONIA CONCENTRATIONS FOUND IN ENVIRONMENTAL WATER SAMPLES

Sample	Concentration[a] (nmol/ml)
Subterranean water	ND[b]
River water (middle reaches)	5.9 ± 0.3
River water (lower reaches)	42.0 ± 1.4
Sewerage	119.3 ± 11.4
Irrigation water	39.9 ± 0.4
Pool water	34.6 ± 0.8
Lake water	29.4 ± 0.2
Sea water	55.6 ± 2.5

[a] Mean ± S.D. (n = 3).
[b] Not detectable.

(r = 0.9982, n = 15), where y is the peak-height ratio and x is the amount of ammonia.

The method developed was successfully applied to environmental water without prior clean-up of the samples. As shown in Fig. 3B–D, ammonia in the river water samples could be detected without any interferences from co-existing substances. As shown in Table I, the overall recoveries of ammonia added to river water samples were 95.0–97.5% and the relative standard deviations were less than 6%, indicating that the method is accurate and precise. The ammonia contents found in several environmental water samples are given in Table II.

In conclusion, these experiments have conclusively demonstrated that trace amounts of ammonia can be successfully determined by GC–FPD as its benzenesulphonyldimethylaminomethylene derivative. The method is selective and sensitive, and complex environmental samples can be analysed directly without any interference from other substances.

REFERENCES

1 C. J. Patton and S. R. Crouch, *Anal. Chem.*, 49 (1977) 464.
2 T. T. Ngo, P. H. D. Phan, C. F. Yan and H. M. Lenhoff, *Anal. Chem.*, 54 (1982) 46.
3 *Standard Methods for the Examination of Water and Waste Water*, American Public Health Association, Washington DC, 16th ed., 1985.
4 D. Midgley and K. Torrance, *Analyst*, 97 (1972) 626.
5 M. E. Lopez and G. A. Rechnitz, *Anal. Chem.*, 54 (1982) 2085.
6 E. H. Gruger, *J. Agric. Food Chem.*, 20 (1972) 781.
7 S. Uchiyama, T. Kondo and M. Uchiyama, *Nippon Shokuhin Eiseigaku Zasshi*, 17 (1976) 345.
8 Y. Tonogai, Y. Ito and M. Harada, *Nippon Shokuhin Eiseigaku Zasshi*, 25 (1984) 149.
9 S. S. Goyal, D. W. Rains and R. C. Huffaker, *Anal. Chem.*, 60 (1988) 175.
10 T. Aoki, S. Uemura and M. Munemori, *Anal. Chem.*, 55 (1983) 1620.
11 H. Mikasa, S. Motomizu and K. Toei, *Bunseki Kagaku*, 34 (1985) 518.
12 Z. Genfa and P. K. Dasgupta, *Anal. Chem.*, 61 (1989) 408.
13 H. Kataoka, S. Ohrui, Y. Miyamoto and M. Makita, *Biomed. Chromatogr.*, 6 (1992) 251.

Journal of Chromatography, 633 (1993) 315–319
Elsevier Science Publishers B.V., Amsterdam

CHROM. 24 784

Short Communication

Capillary electrophoresis with laser fluorescence detection for profiling damage to fluorescein-labeled deoxyadenylic acid by background, ionizing radiation and hydrogen peroxide

Wenni Li[☆], Adel Moussa[☆☆] and Roger W. Giese*

Department of Pharmaceutical Sciences in the Bouve College of Pharmacy and Health Sciences, and Barnett Institute of Chemical Analysis and Materials Science, Northeastern University, Boston, MA 02115 (USA)

(First received July 21st, 1992; revised manuscript received November 17th, 1992)

ABSTRACT

Fluorescein–ethylenediamine–deoxyadenosine-5′-monophosphate, as an aqueous solution (including 10% acetonitrile), was exposed, as separate aliquots, to ^{60}Co and H_2O_2. Analysis of the resulting samples by capillary electrophoresis with laser fluorescence detection showed a complex but significantly resolved array of peaks for each, even when a relatively concentrated sample was injected (the peak for the parent compound was 100 × off-scale). The pattern of peaks was qualitatively similar for both samples, and also for a "non-exposed" sample, but much more intense for the exposed sample. This indicated the predominant role of degradation by oxidation in both exposures as well as from background. At least one peak was caused only by the ^{60}Co exposure. The technique therefore may lead to a specific biomarker for exposure of DNA to ionizing radiation.

INTRODUCTION

We are interested in combining fluorescence labeling and capillary electrophoresis (CE) with laser fluorescence detection to study chemical damage to DNA. One strategy, investigated here, is to first label a nucleotide (X) with fluorescein (F) yielding the conjugate F–X. Due to the high separation efficiency and sensitivity of CE, even subtle chemical degradation of the X part of F–X can be readily visualized as resolved new peaks.

For this purpose, it is attractive to form an F–X conjugate in which the fluorescein moiety, F, is attached via an alkyldiamine spacer, such as ethylenediamine (ED), to the phosphate moiety of the nucleotide, X. This opens up a mechanism to differentiate damage to the nucleobase, which is our concern, from uninteresting damage to the F moiety: since a phosphoramidate linkage undergoes facile hydrolysis at low pH, damaged F–ED can be removed in this way, followed by replacement with fresh, undamaged F–ED. Damage to F can also be sorted out by the more severe change in fluorescence characteristics of F–X, or, ideally, goes un-

* Corresponding author.

☆ Present address: American Cyanamide Co., Agriculture Research Division, Princeton, NJ 08540-0400, USA.

☆☆ Present address: Covalent Associates, Inc., Woburn, MA 01801, USA.

0021-9673/93/$06.00

detected because of the significant loss in fluorescence.

Here we demonstrate some promise for the first part of this technique by comparing background, radiation and oxidative damage to a fluorescein–ethylenediamine–deoxyadenylic acid conjugate by CE. While F–X also might be subjected to HPLC with laser fluorescence detection for this purpose, HPLC is a surface-intensive technique, increasing the likelihood of band broadening, losses and interferences, which can complicate this kind of analysis.

EXPERIMENTAL

Chemicals and reagents

Trizma base [tris(hydroxymethyl)aminomethane, or Tris] and catalase (C-100) were purchased from Sigma (St. Louis, MO, USA). Hydrogen peroxide (30%) was from Aldrich (Milwaukee, WI, USA). Boric acid, HPLC-grade acetonitrile and 0.22-μm MSI Cameo filters were from Fisher Scientific (Bedford, MA, USA). The fluorescein–ethylenediamine–deoxyadenosine-5′-monophosphate (F–ED–dAMP) was prepared as described [1] using Isomer II FITC (fluorescein-6-isothiocyanate) from Molecular Probes (Eugene, OR, USA). All solution compositions were v/v unless indicated otherwise.

Capillary electrophoresis with laser fluorescence detection

A laboratory-built apparatus was used for CE. The laser fluorescence detector was designed and built by Dr. Edward S. Yeung at Iowa State University. It utilized an argon ion laser (Model 2211-30SL; Cyonics, CAS, USA) to give excitation at 488 nm. A Model PS/EH60R01.5 regulated high-voltage d.c. power supply (Glassman High Voltage, NJ, USA) was used. Capillary electrophoresis was performed in a 95 cm long fused-silica capillary (75 μm I.D.; PolyMicro Technologies, Phoenix, AZ, USA). The polyimide coating of the capillary was burned off to form a flow cell 50 cm from the injection end (grounded anode end) of the capillary. Samples were injected hydrodynamically: anode end 5 cm higher for 20 s.

New capillary columns were cleaned initially by syringe-filling (until 4 drops emerged, which was done for all syringe steps) with methanol–water (1:1), followed by 0.1 *M* NaOH, with standing for 30 min each. The buffer of interest was then subjected to 30 min of electrophoresis followed by standing overnight. Periodically (about once a week) the capillary was cleaned by syringe injection of 0.1 *M* NaOH, standing for 30 min, similarly injecting buffer, and then operating the electrophoresis for one hour before samples were injected.

Solutions

pH 8.7 Buffer. This was prepared by combining 0.8 ml of stock buffer (0.5 *M* Tris, 0.5 *M* boric acid, stored at room temperature), 35 ml of water, and 4 ml of acetonitrile, giving pH 8.7. This buffer (10 m*M* Tris–borate, 10% acetonitrile) was filtered (0.22 μm) and degassed (bubbling with helium for 15 min) prior to use as diluent to prepare solutions for injection. The other buffers were prepared by titrating the 10 m*M*, pH 8.7 solution to the desired pH with 2 *M* NaOH.

F–ED–dAMP Stock. The stock solution of F–ED–dAMP was obtained as an HPLC peak from a C_{18}-silica column in a mobile phase of 5 m*M* acetic acid with an acetonitrile gradient. Immediately after collection, the pH was adjusted to 8.7 by the addition of 0.5 *M* Tris–borate. The concentration of F–ED–dAMP was 90.7 μM based on the absorbance of the solution at 486 nm relative to that of a standard solution of fluorescein in the same solvent. This solution was kept in a polypropylene tube, and all dilutions, unless indicated otherwise, were made in polypropylene tubes comprising Corning Brand 15- and 50-ml polypropylene tubes, and Fisher Brand 1.5-ml polypropylene snap cap tubes. All dilutions were made using polypropylene tips. All solutions were kept dark by wrapping the tubes with aluminum foil.

^{60}Co Irradiation of F–ED–dAMP

F–ED–dAMP Stock was diluted 1:10 with pH 8.7 buffer into a glass vial and exposed at a dose rate of 830 rad/min to a Gammacell 220 ^{60}Co γ-ray source (Atomic Energy of Canada Ltd.). The solution was injected directly (or after dilution with pH 8.7 buffer) into the CE system.

H_2O_2 Reaction of F–ED–dAMP

F–ED–dAMP Stock was diluted 1:10 with pH 8.7 buffer and 97 μl were treated with 3 μl of 0.03% H_2O_2 (prepared by diluting 30% H_2O_2 with water).

After 5 min the solution was treated with 5 μl (as supplied) of catalase followed by vortexing, to quench the residual H_2O_2, and then injected directly into the CE system. A control experiment showed that the catalase did not modify the CE profile.

RESULTS AND DISCUSSION

To demonstrate this technique for studying chemical damage to DNA nucleobases, we prepared a F–ED conjugate of deoxyadenosine-5′-monophosphate (dAMP). An electropherogram by CE of the resulting compound, F–ED–dAMP, is shown in Fig. 1A, where the peak for the F–ED–dAMP is kept on scale. Injecting a 100 × more concentrated solution of the compound, under the same instrumental conditions, gives the "off-scale" electropherogram shown in Fig. 1B. It is impressive that the base of the peak for F–ED–dAMP is so narrow given that the actual height of this peak is 100 × the part that is observed. The extreme sharpness for this peak in turn, makes it possible to observe multiple trace impurities in the sample.

Exposure of a portion of the sample to a ^{60}Co source, and a second portion to H_2O_2, and similarly injecting in the off-scale mode for the parent compound, yields the electropherograms in Fig. 1C and D, respectively. Aside from much stronger peak intensities in Fig. 1C and D, the three patterns of peaks (Fig. 1B–D) are seen to be very similar. This was confirmed by injecting combined samples (data not shown). The profiles were reproducible, aside from the absolute migration times for the peaks (which can vary in CE due to fluctuations as in elec-

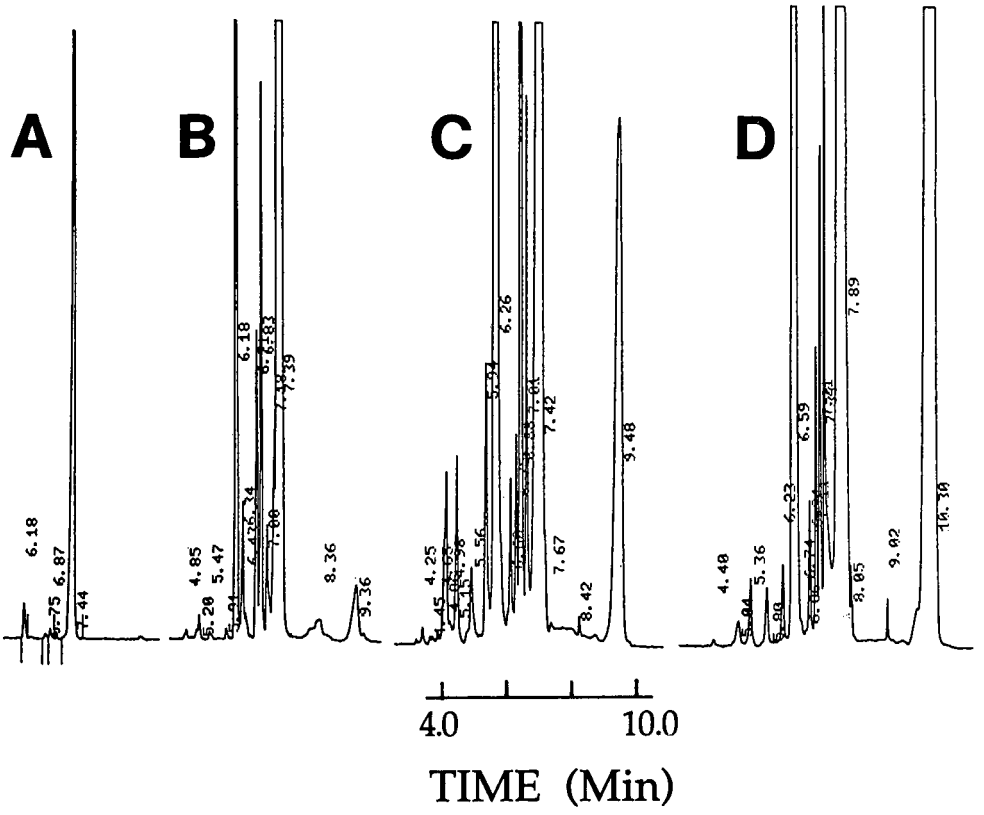

Fig. 1. Electropherograms from capillary electrophoresis at pH 8.7 with laser fluorescence detection of F–ED–dAMP samples: (A, B) unexposed; (C) after exposure to 581 Gy from a ^{60}Co source; (D) after reaction with H_2O_2. Sample (A) was 100 × more dilute than the other samples. The values give the migration times in minutes for the peaks; the major peak at 7.39–7.89 min (depending on the injection) corresponds to F–ED–dAMP. Injection time: 15 s; applied voltage: 30 kV.

troendosmosis and column temperature) throughout the period (one week) for the overall experiment.

The qualitative similarity of the three patterns of peaks (Fig. 1B–D) is interesting, especially the close resemblance of the Fig. 1B profile to the other two. It is reported that both ionizing radiation and H_2O_2 produce similar base products from aqueous DNA, apparently via attack especially by hydroxyl radicals [2–4]. Based on our data, such oxidative degradation apparently is important for this compound (or the precursors for its formation) as well under ordinary storage conditions, where H_2O, H_2O_2 and background radiation all exist. Of course, one cannot claim at this stage that all of the co-eluting peaks among the three electropherograms represent the same products. Some of the products probably correspond to those observed when polyadenylic acid [5], adenosine-5′-monophosphate [6], or DNA [2] are irradiated.

There is interest in establishing a specific biomarker for human exposure to ionizing radiation [7]. To examine the damage to F–ED–dAMP in this context by ^{60}Co *vs.* H_2O_2, we subjected samples of this exposed compound to CE at a higher pH to enhance the resolution. A higher pH was selected since molecules differing in charge tend to separate in CE, and oxidation of adenine is anticipated to form products having pK_a values more in the alkaline range. For example, deoxyguanosine-5′-monophosphate, possessing a purine base that is more highly oxidized than adenine, has a pK_a of 9.7 [8], and 8-oxoadenosine has a pK_a of 8.7 [9]. No pK_a exists for deoxyadenosine-5′-monophosphate throughout the pH range of 8–12 [8,10,11].

Separate ^{60}Co and H_2O_2 exposures of F–ED–dAMP, followed by off-scale CE separation at pH 10.4, yields the electropherograms shown in Fig. 2A and B, respectively. A combined sample was injected to obtain the profile shown in Fig. 2C. As before, similar patterns are observed aside from some of the relative peak ratios. Highlighted in Fig. 2A (and also in Fig. 2C from the combined injection) is a peak that is caused by ^{60}Co but not H_2O_2 exposure.

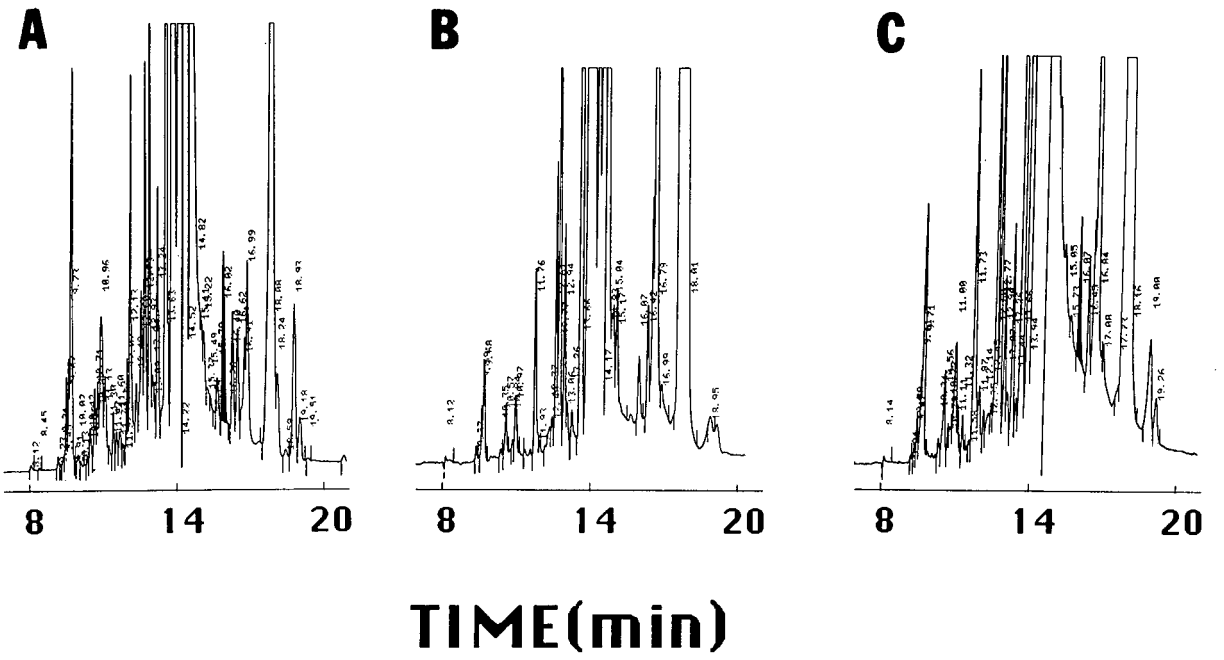

Fig. 2. Electropherograms by capillary electrophoresis at pH 10.4 with laser fluorescence detection of F–ED–dAMP after exposure to (A) ^{60}Co (166 Gy; the 581 Gy-exposed sample was exhausted); (B) H_2O_2; (C) combined injection of (A) and (B) samples. Injection time: 20 s; applied voltage: 15 kV.

It will therefore be interesting to elucidate the structure of this compound.

ACKNOWLEDGEMENT

This work was funded by the Office of Health and Environmental Research Division, Department of Energy, as Grant DE-FG02-90ER60964. Publication No. 566 from the Barnett Institute. We thank Dr. Jacquelyn C. Yanch at MIT for arranging the ^{60}Co experiment.

REFERENCES

1 A. N. Al-Deen, D. C. Cecchini, S. Abdel-Baky, N. M. Abdel Moneam and R. W. Giese, *J. Chromatogr.*, 512 (1990) 409–414.
2 E. Gajewski, G. Rao, Z. Nackerdien, M. Dizdaroglu, *Biochemistry*, 29 (1990) 7876–7882.
3 F. Hutchinson, *Progr. Nucl. Acid Res. Molec. Biol.*, 32 (1985) 115–154.
4 L. Packer and A. N. Glazer (Editors), *Methods in Enzymology, Vol. 186, Oxygen Radicals in Biological Systems*, Academic Press, New York, 1990.
5 A. J. Alexander, P. Kebarle, A. F. Fuciarelli and J. A. Raleigh, *Anal. Chem.*, 59 (1987) 2484–2491.
6 J. A. Raleigh and A. F. Fuciarelli, *Radiat. Res.*, 102 (1985) 165–175.
7 S. M. Fischer, R. A. Floyd and E. S. Copeland, *Cancer Res.*, 48 (1988) 3882–3887.
8 G. D. Fasman (Editor), *Handbook of Biochemistry and Molecular Biology*, CRC Press, Boca Raton, Fl, 3rd ed., 1975.
9 B. P. Cho, F. E. Evans, *Nucleic Acids Res.*, 19 (1991) 1041–1047.
10 T. Hirokawa, S. Kobayashi and Y. Kiso, *J. Chromatogr.*, 318 (1985) 195–210.
11 W. Saenger, *Principles of Nucleic Acid Structure*, Springer, New York, 1984.

Journal of Chromatography, 633 (1993) 320
Elsevier Science Publishers B.V., Amsterdam

CHROM. 24 721

Book Review

Modern chromatographic analysis of vitamins (*Chromatographic Science Series*, Vol. 60) edited by A. P. De Leenheer, W. E. Lambert and H. J. Nelis, Marcel Dekker, New York, Basle, Hong Kong, 2nd ed., 1992, IX + 575 pp., price US$ 175.00, ISBN 0-8247-8626-2.

The first edition of this book was published in 1985, and this second edition constitutes an update of the state of the art of vitamin analysis and highlights new and important chromatographic trends (GC, GC–MS, HPLC and TLC) in this area. The authors have expended a great deal of effort to compile relevant data and methodological details.

This book reviews thirteen vitamins or groups of vitamins which are described in individual chapters. The first part (233 pages) deals with the fat-soluble vitamins A (retinoids and carotenoids), D, E and K and the second part (326 pages) covers the water-soluble vitamins and coenzyme forms of ascorbate, folate, nicotinate, vitamin B_1, flavins, vitamin B_6, biotin, cobalamins and panthothenate. Panthothenic acid is reviewed in an additional chapter in this new edition.

The major aim of this book is obviously to present detailed information on the quantitative analysis of each vitamin or vitamin group using chromatographic methods, in particular on sample preparation and chromatographic conditions. In addition, the information concerning chemical properties, metabolism and biochemical functions of each compound is reviewed. Such information can be valuable for a researcher new to the field.

Unfortunately, the data on the concentrations of the compounds in biological fluids and diagnostic values are not always clearly arranged and it is difficult to find a general scheme in the review. Although the review on the different approaches (*e.g.*, saturation analysis and biological assay) to the analyses of these compounds are beyond the scope of this book, an abstract of these methods and a comparison with chromatographic methods would have been helpful in understanding the analysis in this area (*e.g.*, the chapters on vitamins D and B_6). The abolute configurations of the structures of the compounds shown are not always represented and data on the recent coupled technique HPLC–MS should also be reviewed in the next edition.

In conclusion, in spite of the above-mentioned shortcomings, the book contains much valuable information and it can be recommended not only to those who have an acquaintance with the different chromatographic techniques but also to researchers new to this field.

Kanazawa (Japan) K. Shimada

Author Index

Erratum

J. Chromatogr., 629 (1993) 97–122

Page 103, 9th line and eqn. I.6: "$\nu\Delta_{c_i}$" should read "$\nu_{\Delta c_i}$".

Vol. 633, Nos. 1 + 2

Journal of Chromatography

NEWS SECTION

CALL FOR NOMINATIONS

Chromatography Forum of the Delaware Valley

Stephen Dal Nogare Award for Excellence and Significant Contributions in the Field of Chromatography

This award will be given to the recipient during the 1994 calendar year. All nominations should consist of one or more letters of nomination and a biographical sketch listing experience and significant contributions to the advancement of the chromatographic field.

The deadline for nominations is March 31, 1993. Previous year nominations can be renewed or appended with an updating letter of nomination.

Nominations should be sent to:
Mary Ellen McNally, Ph.D.,
E.I. du Pont de Nemours and Company,
Du Pont Agriculture Products,
Experimental Station,
Wilmington, DE 19880-0402
USA

Hyphenated Techniques in Supercritical Fluid Chromatography and Extraction

edited by **K. Jinno,** Toyohashi University of Technology, Toyohashi, Japan

Journal of Chromatography Library Volume 53

This is the first book to focus on the latest developments in hyphenated techniques using supercritical fluids. The advantages of SFC in hyphenation with various detection modes, such as, FTIR, MS, MPD and ICP and others are clearly featured throughout the book. Special attention is paid to coupling of SFE with GC or SFC.

In this edited volume, chapters are written by leading experts in the field. The book will be of interest to professionals in academia, as well as to those researchers working in an industrial environment, such as analytical instrumentation, pharmaceuticals, agriculture, food, petrochemicals and environmental.

Contents:

1992 x + 334 pages
Price: US $ 157.00/ Dfl. 275.00
ISBN 0-444-88794-6

ORDER INFORMATION

For USA and Canada
ELSEVIER SCIENCE PUBLISHERS
Judy Weislogel
P.O. Box 945
Madison Square Station,
New York, NY 10160-0757
Tel: (212) 989 5800
Fax: (212) 633 3880

In all other countries
ELSEVIER SCIENCE PUBLISHERS
P.O. Box 211
1000 AE Amsterdam
The Netherlands
Tel: (+31-20) 5803 753
Fax: (+31-20) 5803 705

US$ prices are valid only for the USA & Canada and are subject to exchange fluctuations; in all other countries the Dutch guilder price (Dfl.), is definitive. Books are sent postfree if prepaid.

ELSEVIER
SCIENCE PUBLISHERS

711/414\141\0001-00

Capillary Electrophoresis

Principles, Practice and Applications

by **S.F.Y. Li**, *National University of Singapore, Singapore*

Journal of Chromatography Library Volume 52

Capillary Electrophoresis (CE) has had a very significant impact on the field of analytical chemistry in recent years as the technique is capable of very high resolution separations, requiring only small amounts of samples and reagents. Furthermore, it can be readily adapted to automatic sample handling and real time data processing. Many new methodologies based on CE have been reported. Rapid, reproducible separations of extremely small amounts of chemicals and biochemicals, including peptides, proteins, nucleotides, DNA, enantiomers, carbohydrates, vitamins, inorganic ions, pharmaceuticals and environmental pollutants have been demonstrated. A wide range of applications have been developed in greatly diverse fields, such as chemical, biotechnological, environmental and pharmaceutical analysis.

This book covers all aspects of CE, from the principles and technical aspects to the most important applications. It is intended to meet the growing need for a thorough and balanced treatment of CE. The book will serve as a comprehensive reference work and can also be used as a textbook for advanced undergraduate and graduate courses. Both the experienced analyst and the newcomer will find the text useful.

Contents:

1992 xxvi + 586 pages
Price: US$ 225.50 / Dfl. 395.00
ISBN 0-444-89433-0

TO ORDER

Contact your regular supplier or:

ELSEVIER SCIENCE PUBLISHERS
P.O. Box 211
1000 AE Amsterdam
The Netherlands

Customers in the USA & Canada:
ELSEVIER SCIENCE PUBLISHERS
Attn. Judy Weislogel
P.O. Box 945
Madison Square Station
New York, NY 10160-0757, USA

No postage will be added to prepaid book orders. US $ book prices are valid only in the USA and Canada. In all other countries the Dutch guilder (Dfl.) price is definitive. Customers in The Netherlands please add 6% BTW. In New York State please add applicable sales tax. All prices are subject to change without prior notice.

ELSEVIER
SCIENCE PUBLISHERS

Chromatography, 5th edition

Fundamentals and Applications of Chromatography and Related Differential Migration Methods

edited by **E. Heftmann**, *Orinda, CA, USA*

These are completely new books, organized according to the successful plan of the previous four editions. While avoiding repetition of material covered in the previous editions, the authors have succeeded in presenting a coherent and comprehensive picture of the state of each topic. The books provide beginners as well as experienced researchers with a key to understanding current activities in various separation methods. They will also serve as textbooks for graduate courses in technical, medical and engineering schools as well as all universities offering science courses.

Part A: Fundamentals and Techniques

Journal of Chromatography Library Volume 51A

Part A covers the theory and fundamentals of such methods as column and planar chromatography, countercurrent chromatography, field-flow fractionation, and electrophoresis. Affinity chromatography and supercritical-fluid chromatography are covered for the first time. Each topic is treated by one of the most eminent authorities in the field.

Contents Part A: 1. Theory of chromatography *(L.R. Snyder)*. 2. Countercurrent chromatography *(Y. Ito)*. 3. Planar chromatography *(S. Nyiredy)*. 4. Column liquid chromatography *(H. Poppe)*. 5. Ion-exchange chromatography *(H.F. Walton)*. 6. Size-exclusion chromatography *(L. Hagel and J.-C. Janson)*. 7. Affinity chromatography *(T.M. Phillips)*. 8. Supercritical-fluid chromatography *(P.J. Schoenmakers and L.G.M. Uunk)*. 9. Gas chromatography *(C.F. Poole and S.K. Poole)*. 10. Field-flow fractionation *(J. Janca)*. 11. Electrophoresis *(P.G. Righetti)*. Manufacturers and dealers of chromatography and electrophoresis supplies. Subject Index.

1992 xxxvi + 552 pages
Price: US $ 179.50 / Dfl. 350.00
ISBN 0-444-88236-7

Parts A & B Set
Set price: US $ 333.50 / Dfl. 650.00
ISBN 0-444-88404-1

Part B: Applications

Journal of Chromatography Library Volume 51B

Part B presents various applications of these methods. New developments are reviewed and summarized. Important topics such as environmental analysis and the determination of synthetic polymers and fossil fuels, are covered for the first time.

Contents Part B: 12. Inorganic species *(P.R. Haddad and E. Patsalides)*. 13. Amino acids and peptides *(C.T. Mant, N.E. Zhou and R.S. Hodges)*. 14. Proteins *(F.E. Regnier and K.M. Gooding)*. 15. Lipids *(A. Kuksis)*. 16. Carbohydrates *(S.C. Churms)*. 17. Nucleic acids, their constituents and analogs *(N-I Jang and P.R. Brown)*. 18. Porphyrins *(K. Jacob)*. 19. Phenolic compounds *(J.B. Harborne)*. 20. Drugs *(K. Macek and J. Macek)*. 21. Fossil fuels *(R.P. Philp and F.X. de las Heras)*. 22. Synthetic polymers *(T.H. Moury and T.C. Schunk)*. 23. Pesticides *(J. Sherma)*. 24. Environmental analysis *(K.P. Naikwadi and F.W. Karasek)*. 25. Amines from environmental sources *(H.A.H. Billiet)*. Manufacturers and dealers of chromatography and electrophoresis supplies. Subject Index.

1992 xxxii + 630 pages
Price: US $ 189.50 / Dfl. 370.00
ISBN 0-444-88237-5

Elsevier Science Publishers

P.O. Box 211, 1000 AE Amsterdam, The Netherlands
P.O. Box 882, Madison Square Station, New York, NY 10159, USA

PUBLICATION SCHEDULE FOR THE 1993 SUBSCRIPTION

Journal of Chromatography and *Journal of Chromatography, Biomedical Applications*

MONTH	O 1992	N 1992	D 1992	J	F	M	
Journal of Chromatography	623/1 623/2 624/1 + 2	625/1 625/2	626/1 626/2 627/1 + 2	628/1 628/2 629/1 629/2	630/1 + 2 631/1 + 2 632/1 + 2 633/1 + 2	634/1 634/2	The publication schedule for further issues will be published later.
Cumulative Indexes, Vols. 601–650							
Bibliography Section						649/1	
Biomedical Applications				612/1	612/2	613/1	

INFORMATION FOR AUTHORS

(Detailed *Instructions to Authors* were published in Vol. 609, pp. 437–443. A free reprint can be obtained by application to the publisher, Elsevier Science Publishers B.V., P.O. Box 330, 1000 AH Amsterdam, The Netherlands.)

Types of Contributions. The following types of papers are published in the *Journal of Chromatography* and the section on *Biomedical Applications:* Regular research papers (Full-length papers), Review articles, Short Communications and Discussions. Short Communications are usually descriptions of short investigations, or they can report minor technical improvements of previously published procedures; they reflect the same quality of research as Full-length papers, but should preferably not exceed five printed pages. Discussions (one or two pages) should explain, amplify, correct or otherwise comment substantively upon an article recently published in the journal. For Review articles, see inside front cover under Submission of Papers.

Submission. Every paper must be accompanied by a letter from the senior author, stating that he/she is submitting the paper for publication in the *Journal of Chromatography*.

Manuscripts. Manuscripts should be typed in **double spacing** on consecutively numbered pages of uniform size. The manuscript should be preceded by a sheet of manuscript paper carrying the title of the paper and the name and full postal address of the person to whom the proofs are to be sent. As a rule, papers should be divided into sections, headed by a caption (*e.g.*, Abstract, Introduction, Experimental, Results, Discussion, etc.). All illustrations, photographs, tables, etc., should be on separate sheets.

Abstract. All articles should have an abstract of 50–100 words which clearly and briefly indicates what is new, different and significant. No references should be given.

Introduction. Every paper must have a concise introduction mentioning what has been done before on the topic described, and stating clearly what is new in the paper now submitted.

Illustrations. The figures should be submitted in a form suitable for reproduction, drawn in Indian ink on drawing or tracing paper. Each illustration should have a legend, all the *legends* being typed (with double spacing) together on a *separate sheet*. If structures are given in the text, the original drawings should be supplied. Coloured illustrations are reproduced at the author's expense, the cost being determined by the number of pages and by the number of colours needed. The written permission of the author and publisher must be obtained for the use of any figure already published. Its source must be indicated in the legend.

References. References should be numbered in the order in which they are cited in the text, and listed in numerical sequence on a separate sheet at the end of the article. Please check a recent issue for the layout of the reference list. Abbreviations for the titles of journals should follow the system used by *Chemical Abstracts*. Articles not yet published should be given as "in press" (journal should be specified), "submitted for publication" (journal should be specified), "in preparation" or "personal communication".

Dispatch. Before sending the manuscript to the Editor please check that the envelope contains four copies of the paper complete with references, legends and figures. One of the sets of figures must be the originals suitable for direct reproduction. Please also ensure that permission to publish has been obtained from your institute.

Proofs. One set of proofs will be sent to the author to be carefully checked for printer's errors. Corrections must be restricted to instances in which the proof is at variance with the manuscript. "Extra corrections" will be inserted at the author's expense.

Reprints. Fifty reprints will be supplied free of charge. Additional reprints can be ordered by the authors. An order form containing price quotations will be sent to the authors together with the proofs of their article.

Advertisements. The Editors of the journal accept no responsibility for the contents of the advertisements. Advertisement rates are available on request. Advertising orders and enquiries can be sent to the Advertising Manager, Elsevier Science Publishers B.V., Advertising Department, P.O. Box 211, 1000 AE Amsterdam, Netherlands; courier shipments to: Van de Sande Bakhuyzenstraat 4, 1061 AG Amsterdam, Netherlands; Tel. (+31-20) 515 3220/515 3222, Telefax (+31-20) 6833 041, Telex 16479 els vi nl. *UK*: T. G. Scott & Son Ltd., Tim Blake, Portland House, 21 Narborough Road, Cosby, Leics. LE9 5TA, UK; Tel. (+44-533) 753 333, Telefax (+44-533) 750 522. *USA and Canada*: Weston Media Associates, Daniel S. Lipner, P.O. Box 1110, Greens Farms, CT 06436-1110, USA; Tel. (+1-203) 261 2500, Telefax (+1-203) 261 0101.